LEABHARLANN CHOLÁISTE NA TRÍONÓIDE, BAILE ÁTHA CLIATH | TRINITY COLLEGE LIBRARY DUBLIN
Ollscoil Átha Cliath | The University of Dublin

Terms and Conditions of Use of Digitised Theses from Trinity College Library Dublin

Copyright statement

All material supplied by Trinity College Library is protected by copyright (under the Copyright and Related Rights Act, 2000 as amended) and other relevant Intellectual Property Rights. By accessing and using a Digitised Thesis from Trinity College Library you acknowledge that all Intellectual Property Rights in any Works supplied are the sole and exclusive property of the copyright and/or other IPR holder. Specific copyright holders may not be explicitly identified. Use of materials from other sources within a thesis should not be construed as a claim over them.

A non-exclusive, non-transferable licence is hereby granted to those using or reproducing, in whole or in part, the material for valid purposes, providing the copyright owners are acknowledged using the normal conventions. Where specific permission to use material is required, this is identified and such permission must be sought from the copyright holder or agency cited.

Liability statement

By using a Digitised Thesis, I accept that Trinity College Dublin bears no legal responsibility for the accuracy, legality or comprehensiveness of materials contained within the thesis, and that Trinity College Dublin accepts no liability for indirect, consequential, or incidental, damages or losses arising from use of the thesis for whatever reason. Information located in a thesis may be subject to specific use constraints, details of which may not be explicitly described. It is the responsibility of potential and actual users to be aware of such constraints and to abide by them. By making use of material from a digitised thesis, you accept these copyright and disclaimer provisions. Where it is brought to the attention of Trinity College Library that there may be a breach of copyright or other restraint, it is the policy to withdraw or take down access to a thesis while the issue is being resolved.

Access Agreement

By using a Digitised Thesis from Trinity College Library you are bound by the following Terms & Conditions. Please read them carefully.

I have read and I understand the following statement: All material supplied via a Digitised Thesis from Trinity College Library is protected by copyright and other intellectual property rights, and duplication or sale of all or part of any of a thesis is not permitted, except that material may be duplicated by you for your research use or for educational purposes in electronic or print form providing the copyright owners are acknowledged using the normal conventions. You must obtain permission for any other use. Electronic or print copies may not be offered, whether for sale or otherwise to anyone. This copy has been supplied on the understanding that it is copyright material and that no quotation from the thesis may be published without proper acknowledgement.

Molecular Characterisation of Region A of FnBPA from *Staphylococcus aureus*

A thesis submitted for the degree of Doctor of Philosophy

By

Fiona Mary Keane

Moyne Institute of Preventive Medicine

Department of Microbiology

Trinity College Dublin

May 2007

TRINITY COLLEGE
2 7 MAY 2008
LIBRARY DUBLIN
THESIS
8380

Declaration

I hereby declare that this thesis has not previously been submitted for a degree at this or any other university and that it is my own work except where it is duly acknowledged in the text.

I agree that this thesis may be lent or copied at the discretion of the Librarian, Trinity College Dublin.

Fiona Keane

Fiona M. Keane

May, 2007

Acknowledgements

First and foremost, I would like to thank Prof. Tim Foster for the opportunity to work in his laboratory. His help and guidance throughout the years of lab work and during the writing of this thesis have been invaluable. Thanks also to the members of my thesis committee for their help and advice. I would also like to thank Prof. Tony Weiss at the University of Sydney for the great opportunity to work in his lab and for all his support in the later stages of this project. Thank you also to all the members of his lab, especially Adam and Lisa for their help and friendship. Thanks to Marian at RCSI for helping me with the structural and docking studies in this project. I would also like to thank all the members of the Moyne prep room for all the materials they provided and for their willingness to help at a moments notice.

A big thank you to all the members of the TJF lab, both past and present including Mary, Louise, Rob, Fiona, Evelyn, Deirdre, Orla, Ross, Naoko, Jenny, Judy, Tony, Maghnus, Helen, Joan, Rebecca and Fiona. Working with you all over the past few years has been thoroughly enjoyable. Thanks to Dee for constantly keeping us stocked up with everything we may need and ensuring that the lab runs smoothly. Thanks in particular to Louise, Rob, Mary, Evelyn and Tony for answering my endless questions! Thanks also to the other members of the West Bunker lab for all the help and craic and for reminding us that there's more to life than MSCRAMMs!

A special word of thanks to my good friends in the Moyne for their company, advice and help, including Marie, Arlene and Libby for the often-extended coffee breaks; to Eithne, Matthew, Brian, Gwen and Enda for all the lunchtime chats, various coffee and other breaks and Friday nights out! You've all been fantastic friends and I'll miss working with you. Thanks also to Julie for all her computer knowledge and for keeping me sane through too many hours of p-values and confidence intervals!

Thanks also to my other friends, Catriona, Caitrin, Helen, Helena, Karin, Marie, Niamh, Sarah, and Sinead for all the nights out and trips away. Thanks for cheering me up when I needed it and distracting me from science.

Finally, I'd like to thank my family. Thanks to my two sisters Claire and Orla for their help and support. You warned me Orla, and now I know why! Thanks Claire for always being so kind on your poor little sister! Thanks to my parents for all their support and making me be grateful for not working on elephants!

Summary

The surface-expressed fibronectin-binding proteins, FnBPA and FnBPB, of *Staphylococcus aureus* promote attachment to immobilised fibrinogen and elastin via the N-terminal A region. The N2N3 subdomains of region A were found to contain the minimum ligand-binding activity. A model of the 3D structure of the N2N3 subdomains of FnBPA was created based on the crystal structure of a similar fibrinogen-binding protein, ClfA. This model allowed C-terminal truncates of rAFnBPA to be constructed. Those lacking the latching peptide and preceding hinge region were defective in binding both fibrinogen and elastin indicating that both ligands bind to FnBPA in a similar manner. Further support for this theory was the inhibition of bacteria expressing FnBPA from binding immobilised fibrinogen and elastin by using a monoclonal anti-rAFnBPA antibody and a peptide comprising the C-terminal residues of the γ chain of fibrinogen.

Recombinant proteins of rAFnBPA containing substitutions of residues located around the hydrophobic trench were tested for fibrinogen and elastin binding. Two residues in particular, N304 and F306, were found to be crucial in the interaction with both ligands. This is further evidence that fibrinogen and elastin bind to rAFnBPA in the same way, possibly by the dock, lock and latch mechanism.

A recombinant protein spanning the N2 and N3 subdomains of rAFnBPA from strain P1 was purified and shown to bind to immobilised fibrinogen and elastin. Despite retaining ligand-binding ability, rAFnBPA (P1) reacted poorly with polyclonal antibodies raised against rAFnBPA (8325-4). In addition, binding of several monoclonal anti-rAFnBPA (8325-4) antibodies to rAFnBPA (P1) was not detectable, demonstrating that antigenic variation occurred between two FnBPA proteins from different *S. aureus* strains.

Tropoelastin is the monomeric precursor of elastin fibres. Truncates of rAFnBPA, lacking subdomain N1 and C-terminal fibronectin-binding residues, bound strongly to full-length tropoelastin. The binding of recombinant rAFnBPA proteins, bearing alanine substitutions of residues known to be important in the α-elastin interaction indicates that FnBPA binds to tropoelastin and to α-elastin by different mechanisms. The binding to tropoelastin is proposed to occur through ionic surface interactions between the two proteins.

Publications

Keane, F. M., Loughman, A., Valtulina, V., Brennan, M., Speziale, P., and Foster, T. J. (2007) Fibrinogen and elastin bind to the same region within the A domain of fibronectin binding protein A, an MSCRAMM of *Staphylococcus aureus*. *Mol Microbiol* **63**: 711-723

Keane, F. M., Clarke, A. W., Foster, T. J., and Weiss, A. S. (2007) The N-terminal A domain of *Staphylococcus aureus* fibronectin binding protein A binds to the elastin monomer, tropoelastin. Manuscript accepted to *Biochemistry*.

Fitzgerald, J. R., Loughman, A., Keane, F., Brennan, M., Knobel, M., Higgins, J., Visai, L., Speziale, P., Cox, D., and Foster, T. J. (2006) Fibronectin-binding proteins of *Staphylococcus aureus* mediate activation of human platelets via fibrinogen and fibronectin bridges to integrin GPIIb/IIIa and IgG binding to the FcγRIIa receptor. *Mol Microbiol* **59**: 212-230.

Roche, F. M., Downer, R., Keane, F., Speziale, P., Park, PW., and Foster, T. J. (2004) The N-terminal A domain of fibronectin binding proteins A and B promotes adhesion of *Staphylococcus aureus* to elastin. *J Biol Chem* **279**: 38433-38440.

Contents

Declaration ii

Acknowledgements iii

Summary iv

Publications v

List of Figures xiii

List of Tables xx

Key to Abbreviations xxi

Chapter 1 Introduction

1.1 Biology of staphylococci 1

1.1.1 Classification and identification 1

1.1.2 Colonisation and disease 1

1.2 *S. aureus* virulence factors 2

1.2.1 Cell wall components 3

1.2.2 Surface proteins 4

1.2.2.1 Sorting 4

1.2.2.2 Protein A 5

1.2.2.3 Fibrinogen-binding surface proteins 6

1.2.2.3.1 ClfA 7

1.2.2.3.2 ClfB 9

1.2.2.3.3 Other fibrinogen-binding proteins 10

1.2.2.4 Fibronectin-binding proteins 10

1.2.2.4.1 Fibronectin-binding proteins binding to fibronectin 11

1.2.2.4.2 Fibronectin-binding proteins binding to fibrinogen/elastin 13

1.2.2.4.3 Role of fibronectin-binding proteins in pathogenesis 14

1.2.2.5 Collagen-binding protein 16

1.2.2.6 Iron-regulated surface proteins 17

1.2.2.7 Other surface proteins 19

1.2.2.7.1 Other LPXTG-containing proteins 19

1.2.2.7.2 Non-covalently attached cell wall proteins 20

1.2.3 Capsule 21

1.2.4 Extracellular proteins 22
1.2.4.1 Extracellular fibrinogen-binding protein, Efb 22
1.2.4.2 Extracellular adherence protein, Eap 23
1.2.4.3 Coagulase 24
1.2.4.4 Extracellular Proteases 25
1.2.4.4.1 Metalloprotease 25
1.2.4.4.2 Serine protease 26
1.2.4.4.3 Cysteine proteases (staphopains) 26
1.2.4.5 Other secreted proteins/toxins 27
1.2.5 Immune evasion by *S. aureus* 28
1.2.5.1 Host defences against infection 28
1.2.5.2 Inhibition of chemotaxis 29
1.2.5.3 Toxins that kill leukocytes 29
1.2.5.4 Resistance to opsonophagocytosis 30
1.2.5.5 Resistance to killing by antimicrobial peptides 31
1.2.5.6 Superantigens 32
1.3 Mechanism of ligand binding by staphylococcal surface proteins 33
1.3.1 Crystal structures of staphylococcal surface proteins 33
1.3.2 Proposed dynamic model of ligand binding 35
1.4 Prevention and treatment of staphylococcal infections 36
1.4.1 Capsular polysaccharide vaccine – StaphVax 36
1.4.2 Immunotherapies targeting ClfA 37
1.4.3 Potential targets for immunotherapy 37
1.5 Elastin 39
1.5.1 Tropoelastin 39
1.5.2 Coacervation and crosslinking of tropoelastin 41
1.5.3 Structure of elastin 42
1.5.4 Diseases affecting elastic fibres 44
1.5.5 Degradation and repair of elastin 44
1.6 Rationale for this study 46

Chapter 2 Materials and Methods

2.1 Bacterial strains and growth conditions 48
2.2 Plasmids 48

2.3 DNA manipulation 48
2.3.1 Polymerase Chain Reaction (PCR) 49
2.3.2 Isolation of plasmid DNA 49
2.4 Cloning of FnBPA truncates and alanine substitutions 50
2.4.1 rAFnBPA$_{37-511}$ 50
2.4.2 rAFnBPA$_{194-511}$ 50
2.4.3 rAFnBPA$_{194-509}$ 50
2.4.4 rAFnBPA$_{194-498}$ 50
2.4.5 rAFnBPA$_{194-483}$ 51
2.4.6 rAFnBPA$_{194-336}$ 51
2.4.7 rAFnBPA$_{337-511}$ 51
2.4.8 Site-directed mutagenesis of pQE30 and pNZ8037 51
2.4.9 rAFnBPA$_{194-511}$ (P1) 52
2.5 Purification of recombinant proteins by metal chelate affinity chromatography 52
2.6 Antibodies to *S. aureus* surface proteins 53
2.7 Isolation of *S. aureus* surface proteins 53
2.8 Protein electrophoresis and immunoblotting 54
2.8.1 SDS-PAGE 54
2.8.2 Western immunoblotting 54
2.8.3 Whole cell and recombinant protein dot immunoblotting 55
2.9 Protease treatment of recombinant FnBP proteins 55
2.10 Analysis of FnBPA and FnBPB expressed on the surface of *L. lactis* 55
2.10.1 Preparation and transformation of electrocompetent *L. lactis* NZ9800 55
2.10.2 Induction of *L. lactis* strains carrying pNZ8037 derivatives with nisin 56
2.11 Bacterial adherence assays 56
2.11.1 Bacterial adherence to immobilised elastin 56
2.11.2 Bacterial adherence to immobilised fibrinogen and fibronectin 57
2.12 ELISA assays 58
2.12.1 Antibody ELISA 58

2.12.2 Ligand ELISA 58
2.13 Inhibition assays 59
2.13.1 Inhibition of bacterial adherence to immobilised ligands with soluble inhibitor 59
2.13.2 Inhibition of recombinant protein binding to immobilised ligands with soluble inhibitor 59
2.14 *In silico* analysis of ligand binding by *S. aureus* surface proteins 60
2.14.1 Generation of a 3D structural model for the N2N3 domains of FnBPA 60
2.14.2 Docking of a fibrinogen ligand into the structural model of FnBPA 60
2.14.3 Viewing ClfA and SdrG crystal structures 61
2.15 Circular Dichroism (CD) Spectroscopy 61
2.16 Surface Plasmon Resonance (SPR) 61
2.16.1 Surface Plasmon Resonance Analysis of Molecular Interactions 61
2.16.2 Surface plasmon resonance analysis of rAFnBPA$_{194-511}$, rAFnBPA$_{37-511}$ wt and rAFnBPA$_{37-511}$ site-directed mutants binding to tropoelastin 62
2.17 Statistical analysis 62
Chapter 3 Adhesion of *S. aureus* to elastin is promoted by the fibronectin-binding proteins, FnBPA and FnBPB
3.1 Introduction 63
3.2 Results 67
3.2.1 *S. aureus* adheres to immobilised elastin peptides 67
3.2.2 Anti-fibronectin antibodies inhibit FnBP-mediated adhesion to immobilised fibronectin but not to immobilised elastin..... 68
3.2.3 Adherence of *L. lactis* expressing full-length FnBPA, FnBPB and truncates of FnBPA to immobilised elastin 69
3.2.4 Expression of recombinant region A of FnBPA and FnBPB 70
3.2.5 Titration of anti-rAFnBPA and anti-rAFnBPB antibodies 72
3.2.6 Binding of rAFnBPA$_{37-544}$ and rAFnBPB$_{37-540}$ to immobilised elastin and fibrinogen 73

3.2.7 Inhibition of rAFnBPA$_{37-544}$ and rAFnBPB$_{37-540}$ binding to immobilised elastin using soluble elastin peptides 74
3.2.8 Re-defining the A domain of FnBPA 75
3.2.9 The N2N3 subdomains of FnBPA contain the ligand-binding function 76
3.2.10 Modelling the 3D structure of rAFnBPA$_{194-511}$ 77
3.2.11 Construction of A domain truncates of FnBPA lacking C-terminal residues 78
3.2.12 Individual N2 and N3 subdomains of FnBPA cannot bind elastin or fibrinogen 79
3.2.13 Inhibition of FnBPA binding to immobilised elastin and fibrinogen 80
3.3 Discussion 82
Chapter 4 Site-directed mutagenesis of DNA encoding region A of FnBPA
4.1 Introduction 89
4.2 Results 93
4.2.1 Modelling the 3D structure of rAFnBPA$_{194-511}$ 93
4.2.2 Rationale for choosing residues of rAFnBPA$_{37-511}$ to be altered by site-directed mutagenesis 93
4.2.3 Expression of alanine-substituted variant proteins of rAFnBPA$_{37-511}$ 94
4.2.4 Circular dichroism (CD) spectroscopy of rAFnBPA$_{37-511}$ wild-type, rAFnBPA$_{37-511}$ N304A, rAFnBPA$_{37-511}$ F306A and rAFnBPA$_{37-511}$ N304A/F306A 95
4.2.5 Binding of polyclonal anti-rAFnBPA antibodies to rAFnBPA$_{37-511}$ wild-type and variant proteins 96
4.2.6 Binding of monoclonal anti-rAFnBPA antibodies to rAFnBPA$_{37-511}$ wild-type and variant proteins 96
4.2.7 Binding of rAFnBPA$_{37-511}$ wild-type and variant proteins to immobilised elastin and fibrinogen 97
4.2.7.1 Binding of rAFnBPA$_{37-511}$ G222A to immobilised elastin and fibrinogen 97
4.2.7.2 Binding of rAFnBPA$_{37-511}$ R224A to immobilised elastin and fibrinogen 98

4.2.7.3 Binding of rAFnBPA$_{37-511}$ N304A to immobilised elastin and fibrinogen 98
4.2.7.4 Binding of rAFnBPA$_{37-511}$ F306A to immobilised elastin and fibrinogen 98
4.2.7.5 Binding of rAFnBPA$_{37-511}$ F355A to immobilised elastin and fibrinogen 99
4.2.7.6 Binding of rAFnBPA$_{37-511}$ K357A to immobilised elastin and fibrinogen 99
4.2.7.7 Binding of rAFnBPA$_{37-511}$ G497A to immobilised elastin and fibrinogen 100
4.2.7.8 Binding of rAFnBPA$_{37-511}$ L498A to immobilised elastin and fibrinogen 100
4.2.7.9 Binding of rAFnBPA$_{37-511}$ N304A/F306A to immobilised elastin and fibrinogen 101
4.2.7.10 Binding of rAFnBPA$_{37-511}$ T354A/N356G to immobilised elastin and fibrinogen 101
4.2.7.11 Binding of rAFnBPA$_{37-511}$ A415G/T417A to immobilised elastin and fibrinogen 102
4.2.8 Construction and analysis of *L. lactis* NZ9800 (pNZ8037 FnBPA-NF) 103
4.3 Discussion 104

Chapter 5 Sequence diversity of region A of FnBPA from *S. aureus* strains 8325-4 and P1

5.1 Introduction 108
5.2 Results 111
5.2.1 Antibodies raised against FnBPA and FnBPB from *S. aureus* strain 8325-4 react poorly with strain P1 111
5.2.2 rAFnBPA$_{194-511}$ (P1) binding to immobilised elastin and fibrinogen 111
5.2.3 Reactivity of rAFnBPA$_{194-511}$ (P1) to polyclonal anti-rAFnBPA antibodies 112
5.2.4 Reactivity of rAFnBPA$_{194-511}$ (P1) to monoclonal anti-rAFnBPA (8325-4) antibodies 113

5.2.5 Examination of the locations of variant residues between rAFnBPA of strains 8325-4 and P1 113
5.2.6 Binding of function-blocking monoclonal antibody 7C5 to rAFnBPA 114
5.2.7 Ability of monoclonal antibody 7C5 to bind to rAFnBPA$_{194-511}$ already bound to immobilized fibrinogen 115
5.3 Discussion 117
Chapter 6 Region A of FnBPA binds to the elastin monomer, tropoelastin
6.1 Introduction 121
6.2 Results 125
6.2.1 rAFnBPA truncates bind to immobilised tropoelastin 125
6.2.1.1 rAFnBPA$_{37-511}$ binds to immobilised tropoelastin 125
6.2.1.2 rAFnBPA$_{194-511}$ binds to immobilised tropoelastin 125
6.2.1.3 rAFnBPA$_{37-511}$ alanine-substituted proteins bind to immobilised tropoelastin 126
6.2.2 Inhibition of rAFnBPA$_{37-511}$ binding to immobilised elastin peptides using soluble desmosine/isodesmosine 127
6.3 Discussion 128
Chapter 7 Discussion
7.1 Discussion 132
References 140
Supplementary Material ..... On CD

List of Figures

Following page

Figure 1.1 Comparative structure of staphylococcal surface proteins 4

Figure 1.2 Surface protein anchoring in *S. aureus* 4

Figure 1.3 Structure of fibrinogen 6

Figure 1.4 Fibronectin and the fibronectin-binding proteins of *S. aureus* 12

Figure 1.5 Tandem β-zipper mechanism of fibronectin binding by *S. aureus* 12

Figure 1.6 Topology of the DEv-IgG fold 34

Figure 1.7 Apo structures of the N2N3 domains of ClfA, ClfB and SdrG and the SdrG-peptide complex 36

Figure 1.8 Diagramatic structure of human elastin 40

Figure 1.9 Primary amino acid sequence of human tropoelastin 40

Figure 1.10 Formation of crosslinks in elastin 42

Figure 1.11 Desmosine crosslinks of elastin 42

Figure 3.1 Ribbon diagram representation of the structure of ClfA and SdrG N2N3 proteins 66

Figure 3.2 Adherence of *S. aureus* strain MSSA476 to human and bovine elastin 68

Figure 3.3 Adherence of *S. aureus* 8325-4 and P1 strains to human elastin 68

Figure 3.4 Adherence of *S. aureus* P1 strains to human elastin 68

Figure 3.5 Inhibition of *S. aureus* P1 strains adhering to immobilised elastin and fibronectin by preincubation with anti-fibronectin antibodies 68

Figure 3.6 Adherence of *L. lactis* strains to human elastin 70

Figure 3.7 Adherence of *L. lactis* strains to human fibrinogen 70

Figure 3.8 Adherence of *L. lactis* strains to immobilised elastin and fibrinogen 70

Figure 3.9 Adherence of *L. lactis* FnBPA to human elastin 70

Figure 3.10 Adherence of *L. lactis* FnBPA to human fibrinogen 70

Figure 3.11 Production of recombinant $FnBPA_{37-544}$ 70
Figure 3.12 Stability of $rAFnBPA_{37-544}$ and $rAFnBPB_{37-540}$ 72
Figure 3.13 Susceptibility of $rAFnBPA_{37-544}$ and $rAFnBPB_{37-540}$ to V8 serine protease 72
Figure 3.14 Susceptibility of $rAFnBPA_{37-544}$ and $rAFnBPB_{37-540}$ to aureolysin 72
Figure 3.15 Susceptibility of $rAFnBPA_{37-544}$ and $rAFnBPB_{37-540}$ to aureolysin over time 72
Figure 3.16 Titre of anti-rAFnBPA and anti-rAFnBPB antibodies for recombinant proteins 72
Figure 3.17 Affinity of anti-rAFnBPA and anti-rAFnBPB antibodies for full-length proteins released from cell wall extracts 72
Figure 3.18 Cross-reactivity of anti-rAFnBPA and anti-rAFnBPB antibodies for recombinant proteins 74
Figure 3.19 Inhibition of *S. aureus* P1 *fnbAfnbB* (pFnBA4) adherence to elastin by preincubation with antibodies 74
Figure 3.20 Inhibition of *L. lactis* pNZ8037*fnbA* adherence to elastin by preincubation with anti-rAFnBPA antibodies 74
Figure 3.21 Binding of $rAFnBPA_{37-544}$, $rAFnBPB_{37-540}$ and $rAClfA_{40-559}$ to immobilised elastin and fibrinogen 74
Figure 3.22 Binding of anti-rAFnBP antibodies to immobilised rAFnBP 74
Figure 3.23 Binding of anti-elastin antibodies to immobilised elastin 74
Figure 3.24 Inhibition of $rAFnBPA_{37-544}$ and $rAFnBPB_{37-540}$ binding to immobilised elastin using soluble elastin peptides 76
Figure 3.25 Re-defining the A domain of FnBPA 76
Figure 3.26 Binding of anti-fibrinogen antibodies to immobilised human fibronectin 76
Figure 3.27 Binding of $rAFnBPA_{37-544}$ and $rAFnBPA_{37-511}$ to immobilised human fibronectin and collagen 76
Figure 3.28 Binding of $rAFnBPA_{37-511}$ and $rAFnBPA_{194-511}$ to immobilised elastin and fibrinogen 76
Figure 3.29 Predicted 3D structure of $rAFnBPA_{194-544}$ 78
Figure 3.30 Truncates of the A domain of FnBPA 80

Figure 3.31 Binding of rAFnBPA$_{194-511}$ and rAFnBPA$_{194-509}$ to immobilised elastin and fibrinogen 80
Figure 3.32 Binding of rAFnBPA$_{194-511}$ and rAFnBPA$_{194-498}$ to immobilised elastin and fibrinogen 80
Figure 3.33 Binding of rAFnBPA$_{194-511}$ and rAFnBPA$_{194-483}$ to immobilised elastin and fibrinogen 80
Figure 3.34 Binding of rAFnBPA$_{194-511}$ and rAFnBPA$_{194-336}$ to immobilised elastin and fibrinogen 80
Figure 3.35 Binding of rAFnBPA$_{194-511}$ and rAFnBPA$_{337-511}$ to immobilised elastin and fibrinogen 80
Figure 3.36 Inhibition of rAFnBPA$_{37-511}$ binding to immobilised elastin and fibrinogen using soluble fibrinogen 80
Figure 3.37 Inhibition of rAFnBPA$_{37-511}$ binding to immobilised elastin and fibrinogen using fibrinogen γ chain peptides 80
Figure 3.38 Inhibition of *L. lactis* expressing FnBPA binding to immobilised elastin and fibrinogen using fibrinogen γ chain peptides 80
Figure 3.39 Inhibition of *L. lactis* expressing FnBPA binding to immobilised elastin and fibrinogen using monoclonal antibodies 81
Figure 3.40 Comparison of the structural models of N2N3 of FnPBA based on ClfA and SdrG 87
Figure 4.1 Sequence alignment of the N2N3 subdomains of ClfA and FnBPA 92
Figure 4.2 3D structural model of N2N3 of FnBPA 94
Figure 4.3 Hydrophobic trench of 3D structural model of N2N3 of FnBPA 94
Figure 4.4 Site-directed mutagenesis of region A of FnBPA 94
Figure 4.5 Alanine-substituted variants of rAFnBPA$_{37-511}$ 96
Figure 4.6 CD scan of recombinant proteins rAFnBPA$_{37-511}$ wt, N304A, F306A and N304A/F306A 96
Figure 4.7 Affinity of polyclonal anti-rAFnBPA antibodies for immobilised rAFnBPA$_{37-511}$ wt and site-directed mutants 96

Figure 4.8 Binding of monoclonal antibodies 1E6 and 1F9 to immobilised rAFnBPA$_{37-511}$ wt and site-directed mutants 96
Figure 4.9 Binding of monoclonal antibodies 1G8 and 7B7 to immobilised rAFnBPA$_{37-511}$ wt and site-directed mutants 96
Figure 4.10 Binding of monoclonal antibodies 8G3 and 11F6 to immobilised rAFnBPA$_{37-511}$ wt and site-directed mutants 98
Figure 4.11 Location of monoclonal antibody 8G3 epitope 98
Figure 4.12 Position of the G222A substitution in rAFnBPA 98
Figure 4.13 Binding of recombinant proteins rAFnBPA$_{37-511}$ wt and rAFnBPA$_{37-511}$ G222A to immobilised human elastin and fibrinogen 98
Figure 4.14 Position of the R224A substitution in rAFnBPA 98
Figure 4.15 Binding of recombinant proteins rAFnBPA$_{37-511}$ wt and rAFnBPA$_{37-511}$ R224A to immobilised human elastin and fibrinogen 98
Figure 4.16 Position of the N304A substitution in rAFnBPA 98
Figure 4.17 Binding of recombinant proteins rAFnBPA$_{37-511}$ wt and rAFnBPA$_{37-511}$ N304A to immobilised human elastin and fibrinogen 98
Figure 4.18 Position of the F306A substitution in rAFnBPA 100
Figure 4.19 Binding of recombinant proteins rAFnBPA$_{37-511}$ wt and rAFnBPA$_{37-511}$ F306A to immobilised human elastin and fibrinogen 100
Figure 4.20 Position of the F355A substitution in rAFnBPA 100
Figure 4.21 Binding of recombinant proteins rAFnBPA$_{37-511}$ wt and rAFnBPA$_{37-511}$ F355A to immobilised human elastin and fibrinogen 100
Figure 4.22 Position of the K357A substitution in rAFnBPA 100

Figure 4.23 Binding of recombinant proteins rAFnBPA$_{37\text{-}511}$ wt and rAFnBPA$_{37\text{-}511}$ K357A to immobilised human elastin and fibrinogen 100
Figure 4.24 Position of the G497A substitution in rAFnBPA 100
Figure 4.25 Binding of recombinant proteins rAFnBPA$_{37\text{-}511}$ wt and rAFnBPA$_{37\text{-}511}$ G497A to immobilised human elastin and fibrinogen 100
Figure 4.26 Position of the L498A substitution in rAFnBPA 102
Figure 4.27 Binding of recombinant proteins rAFnBPA$_{37\text{-}511}$ wt and rAFnBPA$_{37\text{-}511}$ L498A to immobilised human elastin and fibrinogen 102
Figure 4.28 Position of the N304A/F306A substitutions in rAFnBPA 102
Figure 4.29 Binding of recombinant proteins rAFnBPA$_{37\text{-}511}$ wt and rAFnBPA$_{37\text{-}511}$ N304A/F306A to immobilised human elastin and fibrinogen 102
Figure 4.30 Position of the T354A/N356G substitutions in rAFnBPA 102
Figure 4.31 Binding of recombinant proteins rAFnBPA$_{37\text{-}511}$ wt and rAFnBPA$_{37\text{-}511}$ T354A/N356G to immobilised human elastin and fibrinogen 102
Figure 4.32 Position of the A415G/T417A substitutions in rAFnBPA 102
Figure 4.33 Binding of recombinant proteins rAFnBPA$_{37\text{-}511}$ wt and rAFnBPA$_{37\text{-}511}$ A415G/T417A to immobilised human elastin and fibrinogen 102
Figure 4.34 Site-directed mutangenesis of plasmid pNZ8037 FnBPA 103
Figure 4.35 FnBPA and FnBPA-NF expression at the same concentration of nisin 103
Figure 4.36 Adherence of *L. lactis* strains expressing full-length FnBPA or FnBPA-NF to immobilised elastin and fibrinogen 103
Figure 4.37 Adherence of *L. lactis* strains expressing full-length FnBPA or FnBPA-NF to immobilised fibronectin 103
Figure 4.38 Proposed model of ligand binding for rAFnBPA 107
Figure 5.1 Detection of FnBPs in cell wall extracts of *S. aureus* P1 and its derivative strains 110

Figure 5.2 Sequence alignment of region A of FnBPA from *S. aureus* strains 8325-4 and P1 112
Figure 5.3 Diversity in the amino acid sequences of region A of FnBPA from *S. aureus* strains 8325-4 and P1 112
Figure 5.4 Cloning of rAFnBPA$_{194-511}$ (P1) 112
Figure 5.5 Binding of rAFnBPA$_{194-511}$ (8325-4) and rAFnBPA$_{194-511}$ (P1) to immobilised elastin and fibrinogen 112
Figure 5.6 Binding of anti-rAFnBPA polyclonal antibodies to immobilised rAFnBPA$_{194-511}$ (8325-4) and rAFnBPA$_{194-511}$ (P1) 112
Figure 5.7 Binding of anti-histidine monoclonal antibodies to immobilised rAFnBPA$_{194-511}$ (8325-4) and rAFnBPA$_{194-511}$ (P1) 112
Figure 5.8 Coomassie and Western blot analysis of rAFnBPA$_{194-511}$ from *S. aureus* strains 8325-4 and P1 114
Figure 5.9 Coomassie and Western blot analysis of rAFnBPA$_{194-511}$ from *S. aureus* strains 8325-4 and P1 114
Figure 5.10 Position of variant residues between rAFnBPA from strains 8325-4 and P1 114
Figure 5.11 Binding of monoclonal antibody 7C5 to immobilised rAFnBPA$_{194-511}$ (8325-4) and rAFnBPA$_{194-511}$ (P1) 114
Figure 5.12 Binding of monoclonal antibody 7C5 to immobilised rAFnBPA$_{37-511}$ and rAFnBPA$_{194-511}$ 116
Figure 5.13 Analysis of *E. coli* strains expressing rAFnBPA truncates 116
Figure 5.14 Binding of monoclonal antibody 7C5 to immobilised rAFnBPA$_{194-336}$ and rAFnBPA$_{337-511}$ 116
Figure 5.15 Binding of monoclonal antibody 7C5 to rAFnBPA$_{194-511}$ (8325-4) bound to immobilised fibrinogen 116
Figure 6.1 Elastin in various forms 122
Figure 6.2 Formation of crosslinks in elastin 122
Figure 6.3 rAFnBPA binding to tropoelastin truncates 124
Figure 6.4 Effect of pH on interaction between rAFnBPA$_{37-544}$ and tropoelastin 124
Figure 6.5 Biacore procedure 124

Figure 6.6 Biacore sensogram 124
Figure 6.7 Structural organisation of FnBPA and recombinant truncated derivatives 126
Figure 6.8 SDS PAGE analysis of rAFnBPA proteins and recombinant human tropoelastin 126
Figure 6.9 SPR analysis of $rAFnBPA_{37-511}$ wt binding to immobilised full-length tropoelastin at pH 7.0 126
Figure 6.10 SPR analysis of $rAFnBPA_{194-511}$ wt binding to immobilised full-length tropoelastin at pH 7.0 126
Figure 6.11 Site of amino acid substitutions of rAFnBPA 126
Figure 6.12 SPR analysis of $rAFnBPA_{37-511}$ F306A binding to immobilised full-length tropoelastin at pH 7.0 126
Figure 6.13 SPR analysis of $rAFnBPA_{37-511}$ N304A/F306A binding to immobilised full-length tropoelastin at pH 7.0 126
Figure 6.14 SPR analysis of $rAFnBPA_{37-511}$ R224A binding to immobilised full-length tropoelastin at pH 7.0 127
Figure 6.15 SPR analysis of $rAFnBPA_{37-511}$ L498A binding to immobilised full-length tropoelastin at pH 7.0 127
Figure 6.16 SPR analysis of $rAFnBPA_{37-511}$ N304A binding to immobilised full-length tropoelastin at pH 7.0 127
Figure 6.17 Inhibition of $rAFnBPA_{37-511}$ binding to immobilised elastin and fibrinogen using soluble desmsoine 127
Figure 7.1 Ligand binding by FnBPA 137

List of Tables

		Following page
Table 1.1	Diseases of the elastic fibre	44
Table 2.1	Bacterial strains	49
Table 2.2	Plasmids	49
Table 2.3	Primers	49
Table 2.4	Antibodies	53
Table 3.1	Half maximum binding values for rAFnBPA proteins binding to immobilised elastin and fibrinogen	80
Table 4.1	The relative affinities of rAFnBPA$_{37\text{-}511}$ wt and 11 amino acid-substituted proteins for immobilised elastin and fibrinogen	102
Table 6.1	Binding of rAFnBPA constructs to immobilised tropoelastin	127

Key to Abbreviations

Amino acids

Name	Three letter code	One letter code
Alanine	Ala	A
Arginine	Arg	R
Asparagine	Asn	N
Aspartic Acid	Asp	D
Cysteine	Cys	C
Glutamine	Gln	Q
Glutamic Acid	Glu	E
Glycine	Gly	G
Histidine	His	H
Isoleucine	Ile	I
Leucine	Leu	L
Lysine	Lys	K
Methionine	Met	M
Phenylalanine	Phe	F
Proline	Pro	P
Serine	Ser	S
Threonine	Thr	T
Tryptophan	Trp	W
Tyrosine	Tyr	Y
Valine	Val	V

Nucleotides

A	Adenosine
C	Cytidine
G	Guanosine
T	Thymidine

Antibiotics

Amp	Ampicillin
Cm	Chloramphenicol
Em	Erythromycin
Tet	Tertracycline
Kan	Kanamycin

Other

agr	accessory gene regulator
BSA	bovine serum albumin
CD	circular dichroism
CHIPS	chemotaxis inhibitory protein of staphylococci
ClfA	clumping factor A
ClfB	clumping factor B
Cna	collagen-binding protein
DNA	deoxyribonucleic acid
dNTP	deoxy nucleoside triphosphate
Eap	extracellular adherence protein
EbpS	elastin-binding protein of staphylococci
ECM	extracellular matrix

EDTA	ethylenediaminetetraacetic acid
Efb	extracellular fibrinogen-binding protein
EGFR	epidermal growth factor receptor
ELISA	enzyme linked immunosorbent assay
El	elastin
Fab	fragment of antibody
Fc	crystallisable fragment of IgG
Fg	fibrinogen
Fn	fibronectin
FnBP	fibronectin-binding protein
h	hour(s)
HRP	horseradish peroxidase
Ig	immunoglobulin
IPTG	isopropyl-β-D-thiogalactopyranoside
Isd	iron surface determinant
kb	kilobase pair
kDa	kilodalton
min	minute(s)
mRNA	messenger ribonucleic acid
MRSA	methicillin resistant *S. aureus*
MSCRAMM	microbial surface component recognising adhesive matrix molecules
NEAT	near transporter
nt	nucleotides
OD	optical density

PBS	phosphate buffered saline
PCR	polymerase chain reaction
PVDF	polyvinylidene diflouride
PVL	Panton-Valentine leukocidin
rpm	revolutions per minute
Sar	staphylococcal accessory regulator
SCIN	staphylococcal complement inhibitor
SCV	small colony variant
Sdr	serine-aspartate repeat
SDS	sodium dodecyl sulphate
SDS-PAGE	sodium dodecyl sulphate polyacrlyamide gel electrophoresis
Spa	staphylococcal protein A
TNFR-1	tumor necrosis factor receptor 1
Tris	trishydroxymethylaminomethane
TSA	tripticase soy agar
TSB	tripticase soy broth
TSST-1	toxic shock syndrome toxin 1
v/v	volume per volume
w/v	weight per volume
wt	wild-type

Chapter 1

Introduction

1.1 Biology of staphylococci

1.1.1 Classification and identification

Spherical bacterial cells were seen in pus by Robert Koch in 1878 and cultivated by Louis Pasteur in 1880. The genus *Staphylococcus* had thus been discovered and first described. Its members are non-motile, spherical, gram-positive cocci that often occur in irregular grape-like clusters. The current number of staphylococcal species extends to approximately 30, comprising commensals and pathogens of both humans and animals. They may be divided into two groups, those that produce the enzyme coagulase and those that do not. Coagulase is a secreted protein that binds fibrinogen and also activates prothrombin to initiate the host blood coagulation pathway (Section 1.2.4.3). It is produced by *S. aureus* and the animal pathogens, *Staphylococcus intermedius*, *Staphylococcus schleiferi subsp. coagulans* and, usually, *Staphylococcus hyicus*. All other staphylococci are negative for coagulase production. Phylogenetically, the genus *Staphylococcus* belongs to the broad *Bacillus-Lactobacillus-Streptococcus* cluster of the gram-positive bacteria *Micrococcaceae* (Ludwig *et al.*, 1985; Schleifer and Kroppenstedt, 1990; Stackebrandt and Teuber, 1988) with the G + C content of their genomic DNA ranging from 30 – 40 %. The staphylococci are extremely halotolerant (growing at up to 3.5 M NaCl) and are resistant to desiccation.

1.1.2 Colonisation and disease

The habitats of the staphylococci are the skin, skin glands and mucous membranes of humans and warm-blooded animals. Coagulase-negative *Staphylococcus epidermidis* are ubiquitous organisms of humans present on the nares, skin and mucous membranes of the gastrointestinal and respiratory tracts. *S. epidermidis* is now recognized as an important opportunistic agent of human disease. *S. aureus* is also an important human pathogen. Its natural habitat is the moist squamous epithelium of the anterior nares. Approximately 20% of healthy adults are persistently colonized by *S. aureus* and another 20% never carry the bacterium (Foster, 2004; Lowy, 1998). The remainder may or may not carry *S. aureus* at any given time. Persistent carriage is more common in children than in adults, and many people change their pattern of carriage between the age of 10 and 20 years (Armstrong-Esther, 1976). The anterior nares are lined by fully keratinized epidermal cells along with hairs, sebaceous glands and sweat glands (Kluytmans *et al.*, 1997). Staphylococci flourish here amid a complex interplay between bacterial and host factors. Carriage of *S. aureus* has been

identified as a risk factor for the development of infection. *S. aureus* causes a wide variety of diseases including superficial infections such as abscesses, boils and impetigo. If the host's natural barriers such as skin and mucous membranes are damaged, *S. aureus* can infect host tissue and cause a localized infection from where it can disseminate via the bloodstream to internal organs and cause a wide variety of invasive diseases resulting in high morbidity and mortality. Such infections include those of the bone (osteomyelitis), lungs (pneumonia), joints (septic arthritis) and heart valves (infective endocarditis). The source of ~80% of *S. aureus* bacteraemias is endogenous since infecting bacteria have been shown by genotypic analysis to be identical to organisms recovered from the nasal mucosa (von Eiff *et al.*, 2001a), although it has been noted that bacteraemia-related death was significantly higher in infected non-carriers compared to infected carriers, suggesting that carriers could be immunologically adapted to the strain of *S. aureus* that they carry (Wertheim *et al.*, 2004).

1.2 *S. aureus* virulence factors

The disease-causing potential of *S. aureus* highlights the extent of the virulence factors possessed by this bacterium. These virulence factors may be classified into three main categories, adhesins, evasins and toxins. Adhesins are ligand-binding surface proteins, attached covalently to the cell wall peptidoglycan, that are co-ordinately expressed to promote adherence to damaged tissue by binding to components of the extracellular matrix (ECM). These proteins have been termed MSCRAMMs (microbial surface components recognizing adhesive matrix molecules) and many have been shown to be important in the initiation of bacterial infection. Evasins are proteins that help the bacterium to evade the host's immune system. They may be associated with the bacterial cell wall or secreted into the extracellular environment. The functions of evasins include the inhibition of neutrophil chemotaxis by the chemotaxis inhibitory protein of staphylococci (CHIPS) and extracellular adherence protein (Eap), resistance to phagocytosis by staphylococcal protein A (Spa), capsular polysaccharide, and complement binding proteins and resistance to antimicrobial peptides by staphylokinase and proteases. Secreted toxins of *S. aureus* are virulence factors that facilitate tissue destruction and bacterial spreading. Toxic shock syndrome toxin -1 (TSST-1) and Panton-Valentine leukocidin (PVL) are associated with particular staphylococcal conditions such as toxic shock syndrome and severe skin infections, respectively. These virulence factors will be described individually in subsequent sections.

1.2.1 Cell wall components

The bacterial cell wall is the point of contact between *S. aureus* and its surrounding environment. It functions as a physical barrier protecting bacteria from cell lysis in environments of low osmolarity. It consists mainly of peptidoglycan (approximately 60%), the remainder comprising wall teichoic acids, lipoteichoic acids and small amounts of protein. The peptidoglycan is made up of a glycan backbone consisting of repeating disaccharide units of N-acetlyglucosamine and N-acetylmuramic acid which are β1 → 4 linked (GlcNAc – (β1 → 4) – MurNAc) (Ghuysen and Strominger, 1963). Short tetrapeptides (L-Ala – D-Glu – L-Lys – D-Ala) are linked to MurNAc moieties in the glycan chains (Ghuysen *et al.*, 1965; Tipper and Strominger, 1965). Cross-linking of nascent peptidoglycan strands, a reaction known as transpeptidation, generates a rigid three dimensional molecular network that maintains the integrity of the bacterium (Tipper and Strominger, 1965). A characteristic feature of *S. aureus* peptidoglycan is the presence of pentaglycine interpeptide bridges that link the tetrapeptide units on neighbouring glycan chains and renders *S. aureus* peptidoglycan susceptible to cleavage by the glycyl-glycyl endopeptidase lysostaphin (Schleifer and Kandler, 1972).

Teichoic acids are another major component of the *S. aureus* cell wall. Wall teichoic acids are made up of ribitol-phosphate polymers substituted with N-acetylglucosamine and D-alanine residues (Collins *et al.*, 2002; Endl *et al.*, 1983; Ward, 1981). Wall teichoic acids are covalently linked to peptidoglycan. In contrast, lipoteichoic acids (glycerol phosphate polymers substituted with D-alanine (Fischer *et al.*, 1990) are attached to glycolipids in the plasma membrane. Peptidoglycan and teichoic acids together make up a polyanionic matrix that functions in cation homeostasis and trafficking of proteins and nutrients across the cell wall. Wall teichoic acids may be an important factor in promoting *S. aureus* nasal colonization (Weidenmaier *et al.*, 2004) and may play a role in infective endocarditis (Weidenmaier *et al.*, 2005). The degree of D-alanyl esterification of teichoic acids regulates the net anionic charge of the bacterial cell surface and is thought to play a role in resistance to antimicrobial peptides (Collins *et al.*, 2002; Peschel *et al.*, 1999). The remainder of the cell wall consists of a variety of proteins that are displayed on the cell surface and mediate the interaction of *S. aureus* with its surroundings.

1.2.2 Surface proteins

1.2.2.1 Sorting

S. aureus produces a diverse array of cell wall-associated ligand-binding surface proteins. These proteins are collectively known as MSCRAMMs and function in binding to components of the host's extracellular matrix. The binding of MSCRAMMs to their respective ligands in vertebrate tissues is a fundamental process required for colonization, invasion and ultimately for causing disease. A number of MSCRAMMs of *S. aureus* have been characterized both structurally and functionally. These include the immunoglobulin- and von Willebrand factor-binding protein A, Spa (Hartlieb *et al.*, 2000; Moks *et al.*, 1986), fibrinogen-binding proteins, clumping factors ClfA (McDevitt *et al.*, 1994) and ClfB (Ni Eidhin *et al.*, 1998), the fibronectin-binding proteins, FnBPA and FnBPB (Jonsson *et al.*, 1991; Signas *et al.*, 1989) and the collagen-binding protein, Cna (Switalski *et al.*, 1989) (Figure 1.1).

The staphylococcal MSCRAMMs are covalently attached to the uncrosslinked pentaglycine bridge that is incorporated into the growing peptidoglycan via the transpeptidation and transglycosylation reactions of cell wall synthesis (Perry *et al.*, 2002). This occurs at the C-terminus where the proteins contain conserved features required for cell wall sorting. These include a positively-charged tail at the extreme C-terminus, a membrane-spanning domain, an LPXTG motif and a wall-spanning domain either rich in proline and glycine residues or composed of serine and aspartate dipeptide repeats (Navarre *et al.*, 1998; Schneewind *et al.*, 1993). The membrane-bound enzyme sortase A (SrtA) cleaves the proteins between the threonine and glycine residue of the LPXTG motif, thus releasing the proteins from their membrane anchor (Ton-That *et al.*, 1999). SrtA then catalyses the covalent linkage of the carboxy end of the threonine residue to the amino end of glycine in the nascent pentaglycine cross bridge by transpeptidation (Mazmanian *et al.*, 1999; Ton-That *et al.*, 1999) (Figure 1.2). Both the cleavage function and the transpeptidation function of SrtA require a conserved cysteine residue at position 184 in the catalytic domain of the protein (Ton-That *et al.*, 1999; Ton-That *et al.*, 2000). Residue Arg197, which is located in close proximity to the active site Cys184 is also crucial for catalysis (Marraffini *et al.*, 2004). Calcium has recently been shown to be important in promoting substrate binding by SrtA by altering the mobility and structure of an active site loop (Naik *et al.*, 2006). A mutant of *S. aureus* in which the *srtA* gene was disrupted by allelic replacement failed to process and display surface proteins and had reduced virulence in a mouse peritoneal infection model (Mazmanian *et al.*, 2000). A

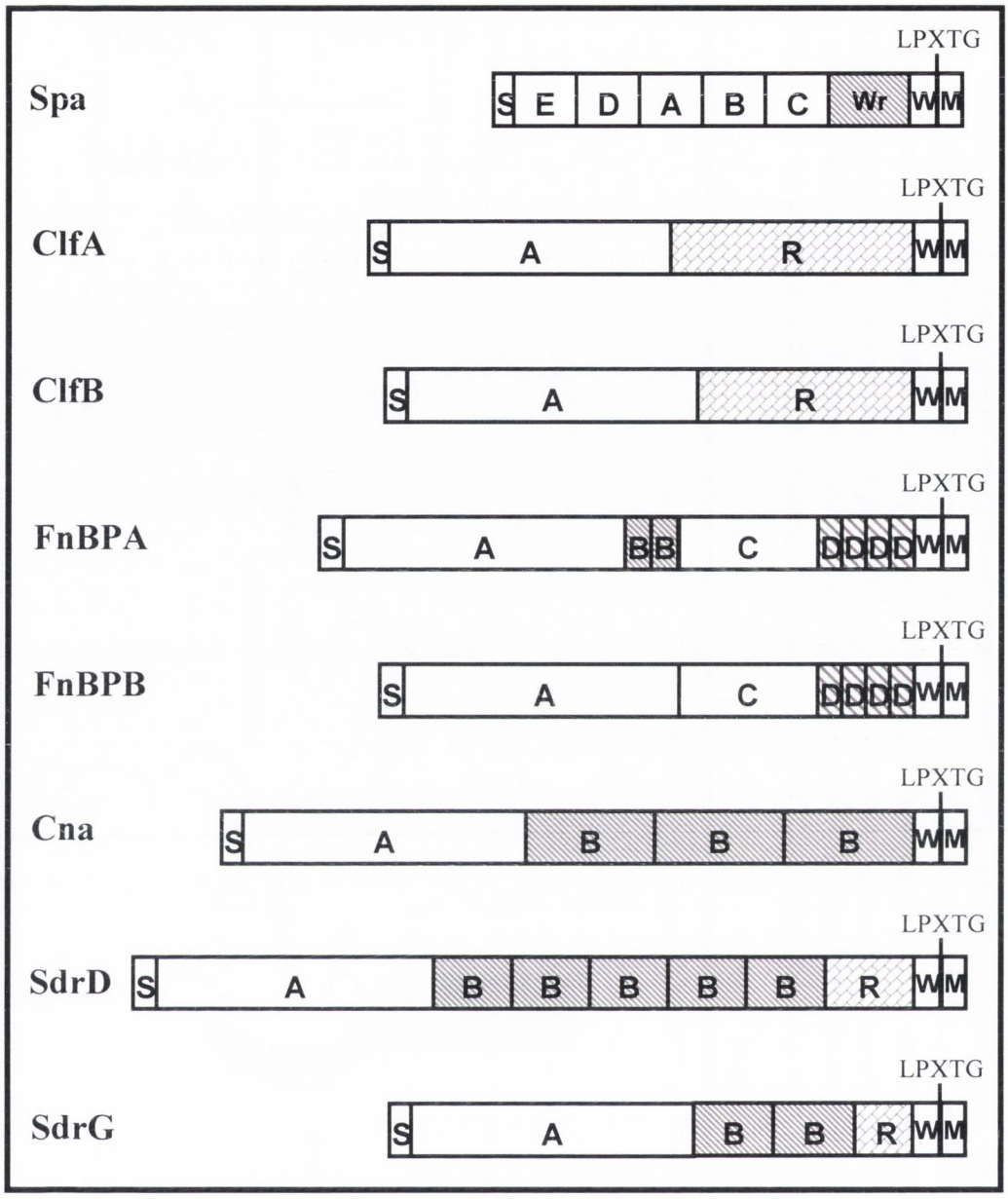

Figure 1.1 Comparative structural organisation of staphylococcal surface proteins

Schematic diagram of the structural organisation found in surface proteins from *S. aureus* (Spa, ClfA, ClfB, FnBPA, FnBPB, Cna and SdrD) and *S. epidermidis* (SdrG). The signal sequence (S), ligand-binding and repeat regions A, B, C, D, E and R as well as wall/membrane spanning regions (WM) are shown. LPXTG motifs are also indicated.

second sortase protein, StrB has also been identified. The *strB* gene is transcribed as part of an iron-regulated operon and the StrB protein catalyses the cleavage and cell wall sorting of IsdC, a cell wall protein that is cleaved by the enzyme at an NPQTN motif (Mazmanian *et al.*, 2002). StrB appears to be involved in the process of iron acquisition during bacterial infection and is required for bacterial persistence in infected tissue (Mazmanian *et al.*, 2002). The crystal structures of both SrtA (Zong *et al.*, 2004a) and SrtB (Zong *et al.*, 2004b) have been solved which provides insight into substrate specificity and suggests a universal sortase-catalyzed mechanism of bacterial surface protein anchoring in gram-positive bacteria. The role of sortase enzymes in bacterial virulence has been examined using a murine septic arthritis model. This showed that sortase B plays a contributing role during the pathogenesis of the infection, whereas sortase A is an essential virulence factor for the establishment of septic arthritis (Jonsson *et al.*, 2003).

1.2.2.2 Protein A

Staphylococcal Protein A (Spa) is the archetypal LPXTG-anchored cell wall protein. It is a prime example of the multi-functionality shown by *S. aureus* surface proteins. It was first noted for its ability to bind the Fc region of mammalian IgG (Moks *et al.*, 1986; Uhlen *et al.*, 1984). It was then discovered to bind to the Fab heavy chain of V_H3 class antibodies, in particular to subsets of IgM molecules (Hillson *et al.*, 1993) and also to von Willebrand factor (Hartleib *et al.*, 2000) and tumour necrosis factor receptor-1 (TNFR-1) (Gomez *et al.*, 2004). The *spa* gene is transcribed during the mid-exponential phase of growth but expression is repressed as cultures enter stationary phase (Vandenesch *et al.*, 1991).

Protein A is composed of tandem repeats of four or five domains of 58-62 residues, designated E, D, A, B and C (Sjodahl, 1977) (Figure 1.1) each of which is capable of binding immunoglobulin (Moks *et al.*, 1986). Both the Spa-Fc and Spa-Fab interactions have been investigated at the molecular level (Gouda *et al.*, 1998; Graille *et al.*, 2000). Each of the Ig-binding domains forms a three-helix bundle. One face comprising residues from helices I and II binds IgG Fc whereas residues from helices II and III on the other face of the molecule bind IgM. This explains why the binding of protein A to Fc and Fab is non-competitive. Protein A has been shown to bind to von Willebrand factor, which is a large multifunctional glycoprotein, released constitutively or upon stimulation of endothelial cells or platelets (Hartleib *et al.*, 2000). Von Willebrand factor is important in mediating platelet adhesion to endothelial cells at the sites of vascular damage and protein A has been shown to bind to both

soluble and immobilised forms, making it a true MSCRAMM. The binding site for protein A within von Willebrand factor has been narrowed down to the A and D'-D3 domains (O'Seaghdha *et al.*, 2006). Protein A also binds directly to the gC1qR/p33 receptor on activated platelets (Nguyen *et al.*, 2000). Both of these interactions may promote bacterial colonization of damaged endovascular tissue and establish a focus of infection during infective endocarditis. Protein A can also act directly as an immune effector through its ability to bind and activate TNFR-1. Residues in the Spa D domain that are important in the binding to Fc regions of IgG were shown to be involved in the binding to TNFR-1 (Gomez *et al.*, 2006). Recently, it has been shown that protein A also interacts with the epidermal growth factor receptor (EGFR) to activate the TNF-α converting enzyme (TACE) which results in cleavage of TNFR-1 and its shedding from the epithelial cell surface. This prevents proinflammatory host cell signalling and neutralises the effect of free TNF-α (Gomez *et al.*, 2007).

Protein A binds to IgG in such a way that it prevents the Fc receptors on phagocytic cells binding to the Fc region of bound IgG. This is an effective method of resistance to opsonisation by *S. aureus* cells, thereby evading the host's immune response (Section 1.2.5.4). Spa has been shown to be a virulence factor in staphylococcal arthritis and septic death, whereby inoculation of an *S. aureus* wild-type strain gave rise to more severe arthritis and higher mortality than the isogenic *spa* mutant strain (Palmqvist *et al.*, 2002). The ability of protein A to bind a diverse set of ligands highlights its role in the pathogenesis of *S. aureus* infections.

1.2.2.3 Fibrinogen-binding surface proteins

S. aureus expresses several proteins, both covalently and non-covalently attached to the cell wall, that interact with fibrinogen. Fibrinogen is a blood glycoprotein of 340 kDa that is involved in plasma clot formation through its polymerization to form fibrin and in platelet aggregation at sites of vascular damage. It is also one of the main proteins deposited on implanted prostheses and medical devices. This provides an adhesive surface allowing *S. aureus* colonization (Cheung and Fischetti, 1990). The protein is composed of three pairs of non-identical polypeptide chains, two α chains, two β chains and two γ chains. These chains are assembled by their N-termini through a number of disulphide bonds to form a symmetrical dimeric structure (Doolittle, 1984). The fibrinogen molecule has three distinct domains, two terminal D domains and a central E domain (Figure 1.3). Fibrinogen is cleaved by thrombin to form insoluble fibrin, a major component of blood clots. Following fibrin formation the clot is

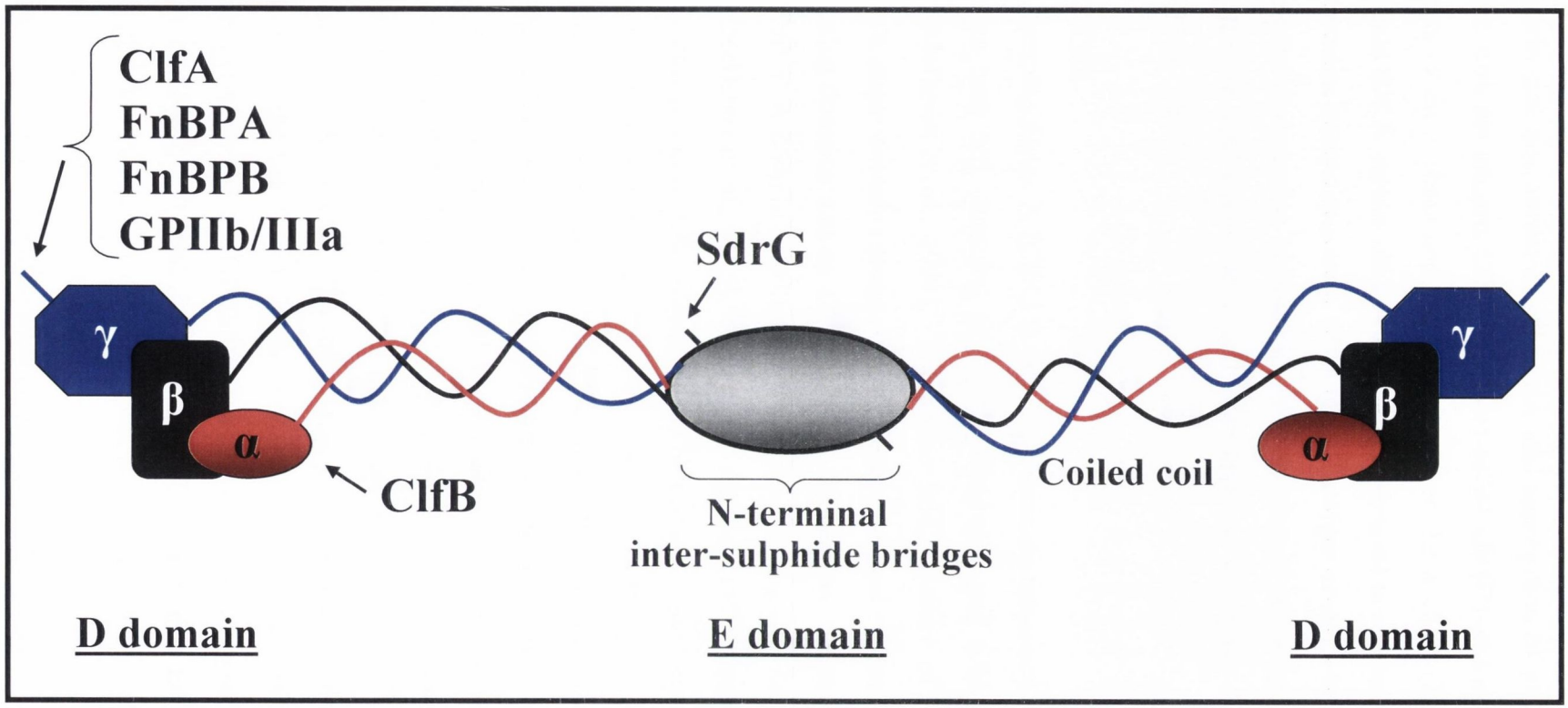

Figure 1.3 Structure of fibrinogen

Fibrinogen is composed of two α, two β and two γ chains arranged in a coiled coil manner. The binding sites for *S. aureus* (ClfA, ClfB, FnBPA and FnBPB), *S. epidermidis* (SdrG) and platelet (GPIIb/IIIa) proteins are indicated with arrows.

stabilized by the covalent linkage of the α and γ chains at their C-termini by the enzyme Factor XIII. Fibrinogen also mediates adherence and aggregation of platelets at sites of injury by interaction with the integrin GPIIb/IIIa (also called αIIbβ3) on the surface of platelets via the C-terminus of the γ chain and the RGD motif on the α chain (Hawiger *et al.*, 1982). The phenomenon that *S. aureus* cells clump when suspended in plasma is now known to occur via surface protein interactions with fibrinogen (Hawiger *et al.*, 1983). Fibrinogen and fibrin cleavage products are also involved in the regulation of cell adhesion and spreading, display vasoconstrictive and chemotactic activities and are mitogens for a variety of cell types (Herrick *et al.*, 1999).

1.2.2.3.1 ClfA

Clumping factor A (ClfA) is one of the best characterized MSCRAMMs of *S aureus.* It promotes both cell clumping in soluble fibrinogen and adherence to fibrinogen-coated surfaces (McDevitt *et al.*, 1994). The amino acid sequence of this protein was shown to contain two major domains along with the required signal sequence, cell membrane and cell wall spanning domains and an LPXTG motif, all required for efficient sorting (Figure 1.1). The N-terminal A domain contains the fibrinogen binding site, located between residues 221 and 559 (McDevitt *et al.*, 1995). The serine-aspartate (SD) dipeptide repeat region R, was deemed to function as a stalk, projecting the N-terminal ligand-binding A domain away from the surface of the cell wall (Hartford *et al.*, 1997). The R region of ClfA varies from 193 to 440 residues in length between *S. aureus* isolates (McDevitt and Foster, 1995).

The binding site for ClfA in fibrinogen has been localized to the 15 residues at the C-terminus of the γ chain, a site that is also recognized by the platelet integrin GPIIb/IIIa (McDevitt *et al.*, 1997) (Figure 1.3). Similar to GPIIb/IIIa, the binding of ClfA to fibrinogen is inhibited by divalent calcium ions. It has been shown that Ca^{2+} ions bind to an inhibitory site within the A domain of ClfA and induce a conformational change that is incompatible with binding to the C-terminus of the γ chain of fibrinogen (O'Connell *et al.*, 1998). The binding of fibrinogen to the GPIIb/IIIa integrin receptor is required for platelet aggregation (Farrell *et al.*, 1992). Indeed, recombinant ClfA is a potent inhibitor of both fibrinogen-mediated platelet aggregation and adherence of platelets to immobilised fibrinogen *in vitro* (McDevitt *et al.*, 1997). The mechanism of platelet activation and aggregation by bacteria expressing ClfA on the cell surface has been elucidated. A model has been proposed whereby both the bridging of ClfA to the GPIIb/IIIa platelet receptor via fibrinogen along with the

bridging of ClfA to the platelet antibody receptor FcγRIIa via ClfA A domain specific antibodies are both necessary in platelet activation and subsequent aggregation (Loughman *et al.*, 2005). In studies with a non-fibrinogen-binding mutant of ClfA, (ClfA PY), a less efficient fibrinogen-independent mechanism was also shown to occur. This mechanism involved the binding of ClfA A domain specific antibodies to ClfA and the platelet FcγRIIa receptor along with the bridging of ClfA PY to the platelet via complement proteins (Loughman *et al.*, 2005).

The A domain of ClfA is divided into three subdomains termed N1, N2 and N3. The minimum ligand-binding segment is contained within subdomains N2 and N3 (McDevitt *et al.*, 1995). Further investigation indicated that the C-terminus of this protein was crucial in the fibrinogen interaction as antibodies raised against ClfA residues 500-559 blocked the interaction of both *S. aureus* and recombinant ClfA with immobilised fibrinogen (Hartford *et al.*, 2001). In addition, it was noted that the substitution of two adjacent residues in this area, Glu526 and Val527 caused a severe defect in fibrinogen binding (Hartford *et al.*, 2001). However the precise role for the C-terminal residues 500-559 including Glu526 and Val527 was not known at that time. Further insight into the mechanism of fibrinogen binding came with the resolution of the crystal structure of the N2N3 subdomains of ClfA (Deivanayagam *et al.*, 2002). Both N2 and N3 domains were folded into a similar DE-variant immunoglobulin fold (DE-v IgG fold). A synthetic fibrinogen γ chain peptide was docked *in silico* into a hydrophobic trench situated between N2 and N3 proposed to be the binding site for fibrinogen. Substitution of residues located around this trench resulted in proteins with markedly reduced affinities for fibrinogen. The details of the structure of ClfA will be discussed further in Section 1.3.1.

ClfA has been shown to be an important virulence factor in several models. In a rat endocarditis model, a lower infection rate of a *clfA* mutant strain was observed compared to the parental strain (Moreillon *et al.*, 1995). ClfA expressed on the surface of the heterologous host *Lactococcus lactis* is sufficient to produce endocarditis in rats with catheter induced aortic vegetations (Que *et al.*, 2001). ClfA is also a virulence factor in murine models of septic arthritis and septic death (Josefsson *et al.*, 2001), however it has since been shown that this may be due to the anti-phagocytic properties of ClfA (Higgins *et al.*, 2006). ClfA is one of the major factors involved in staphylococcal adherence to ventricular assist devices (VADs), posing a threat to the survival of patients with congestive heart failure (Arrecubieta *et al.*, 2006). ClfA is expressed by almost all *S. aureus* strains tested from healthy blood donors

(98%) and in 100% of those with invasive disease (Peacock *et al.*, 2002). This makes ClfA an ideal target for the development of novel immuno prophylactic or therapeutic agents to combat *S. aureus* infection (Section 1.4.2).

1.2.2.3.2 ClfB

Clumping factor B (ClfB) is another cell surface MSCRAMM responsible for the clumping of *S. aureus* cells when suspended in soluble fibrinogen and for bacterial adherence to immobilised fibrinogen *in vitro* (Ni Eidhin *et al.*, 1998). In contrast to ClfA which is expressed maximally in stationary phase of growth, transcription of *clfB* ceases before the end of the exponential phase in a manner that does not involve the staphylococcal global regulatory genes, *agr* or *sar* (McAleese *et al.*, 2001). ClfB has a similar domain organization to ClfA (Figure 1.1); a unique A domain, an SD dipeptide repeat region (R) and typical cell wall attachment regions including an LPXTG motif, cell wall spanning domain and a positively-charged C-terminus. Sequence alignment of the A domains of ClfA and ClfB shows only 26% amino acid identity and in contrast to ClfA, ClfB binds to the α chain of fibrinogen (Ni Eidhin *et al.*, 1998). Inhibition of bacterial cells binding to immobilised fibrinogen using polyclonal antibodies revealed that the ligand-binding activity of the protein is located in the A domain, between residues 44 and 542 (Ni Eidhin *et al.*, 1998). Two forms of the ClfB protein occur on the bacterial cell surface, the smaller of which is generated by the proteolytic degradation at the SLAVA motif in the A domain by the *S. aureus* metalloprotease, aureolysin (Section 1.2.4.4.1). The proportion of the smaller form of the protein, which cannot bind fibrinogen, increases as cells enter stationary phase (McAleese *et al.*, 2001). Studies on recombinant A domain of ClfB showed that it is composed of three independently folded subdomains, N1, N2 and N3 (Perkins *et al.*, 2001). The form of N2N3 generated by aureolysin cleavage of the A domain of ClfB is unable to bind fibrinogen, however an extended N-terminus of this protein regains ligand-binding ability (Perkins *et al.*, 2001). A mechanism similar but slower to that of ClfA has been elucidated for platelet activation by cells expressing ClfB. It requires a fibrinogen bridge between ClfB on the surface of bacterial cells and GPIIb/IIIa on the platelet surface along with specific antibody binding to both the ClfB protein and the FcγRIIa platelet receptor. Similar to ClfA, the fibrinogen independent mechanism of ClfB platelet activation requires complement proteins to bridge the bacterial surface with platelet complement receptors (Miajlovic *et al.*, 2007). The increased lag time

for ClfB activation is thought to be due to the lower affinity of this MSCRAMM for fibrinogen.

S. aureus colonises the moist squamous epithelium of the anterior nares. It was demonstrated that adhesion of staphylococci to squamous cells was, in part, mediated by ClfB binding to cytokeratin 10 (O'Brien *et al.*, 2002b; Walsh *et al.*, 2004). Unlike ClfA, the A domain of ClfB was shown to bind specifically to a glycine loop region of the tail domain of keratin 10 where there may be multiple binding sites (Walsh *et al.*, 2004). Both fibrinogen and the glycine loop peptide binds to the same region in ClfB (Walsh *et al.*, 2004). The adherence of *S. aureus* to squamous epithelia via ClfB is likely to be important in nasal colonization. A study showing that anti-ClfB antibodies were more prevalent in non-carriers compared to those individuals who have *S. aureus* present in the nares (carriers) supports the notion that high ClfB antibody levels may contribute to prevention of infection (Dryla *et al.*, 2005). *S. aureus* strains defective in ClfB expression exhibited reduced nasal colonization in mice. In addition, immunization with recombinant ClfB, either subcutaneously or intranasally, showed a rapid serum antibody response in mice and a subsequent reduction in nasal colonization. A specific anti-ClfB monoclonal antibody that inhibited the interaction of this protein with cytokeratin 10 was also shown to be protective against nasal colonization when used in passive immunization studies. These data show that ClfB is an attractive component for inclusion in a vaccine to reduce *S. aureus* nasal colonization. As nasal colonization correlates with susceptibility to staphylococcal infection, such a vaccine might therefore reduce infections by this pathogen.

1.2.2.3.3 Other fibrinogen-binding proteins

Other surface proteins that can bind fibrinogen, including the fibronectin-binding proteins FnBPA and FnBPB, the iron surface determinant, IsdA, the extracellular fibrinogen-binding protein, Efb and the *S. epidermidis* protein SdrG, will each be discussed in subsequent sections.

1.2.2.4 Fibronectin-binding proteins

The ability to bind immobilised fibronectin is a characteristic feature of many *S. aureus* strains (Peacock *et al.*, 2000). Fibronectin is a ubiquitous protein which mediates a wide variety of cellular processes, including tissue repair, embryogenesis, blood clotting, and cell migration/adhesion. Fibronectin exists in two main forms, as an insoluble glycoprotein

dimer that serves as a linker in the ECM and as a soluble disulphide-linked dimer found at a concentration of ~300 μg/ml in the plasma. The plasma form is synthesized by hepatocytes, and the ECM form is made by fibroblasts, chondrocytes, endothelial cells, macrophages, as well as certain epithelial cells. Fibronectin is rod-like and is composed of three different types of repeating homologous modules, designated type I (F1), type II (F2) and type III (F3) which are separated by connecting sequences (Bork *et al.*, 1996) (Figure 1.4). Two molecules of fibronectin are linked via a disulphide bridge at the C-terminus of the molecule forming a dimer of approximately 500 kDa found in plasma. In addition to its functions in cellular adhesion, differentiation and tissue repair after injury, fibronectin has adhesive sites for various molecules such as heparin, collagen, fibrin and specific integrins (Potts and Campbell, 1994).

1.2.2.4.1 Fibronectin-binding proteins binding to fibronectin

The binding of *S. aureus* to human fibronectin is mediated by the fibronectin-binding proteins, FnBPA and FnBPB (Figure 1.4). The expression of either FnBPA or FnBPB on the surface of *S. aureus* is sufficient to promote bacterial adhesion to immobilised fibronectin (Greene *et al.*, 1995). These proteins are related, cell wall-associated proteins encoded by two closely linked but independently transcribed genes, *fnbA* and *fnbB* (Jonsson *et al.*, 1991; Signas *et al.*, 1989) and are expressed predominantly in the exponential phase of growth (Saravia-Otten *et al.*, 1997). The domain organisation of both proteins allows for Sec-dependent secretion and sortase-dependent anchoring to the cell wall peptidoglycan via the LPETG motif. FnBPA contains two additional fibronectin-binding B repeats that are absent in FnBPB. The C-terminal D repeats of FnBPA and FnBPB were shown to share 95% identity while the N-terminal A domains are ~45% identical (Jonsson *et al.*, 1991). The proteins were first identified for their fibronectin-binding ability, a phenotype which is only abolished when regions B, C and D are deleted (Massey *et al.*, 2001).

The domain organisation of FnBPA has been recently revised with the mapping of the 11 fibronectin-binding motifs spanning residues 511 to 842 which encompasses the C-terminus of the A domain as well as the B, C and D domains (Schwarz-Linek *et al.*, 2003). The binding site in fibronectin for FnBPs is located in the N-terminal F1 modules (Figure 1.4) although another binding site towards the C-terminus has also been demonstrated (Bozzini *et al.*, 1992; Kuusela *et al.*, 1984). The structure of the B3 peptide of the SfbI fibronectin-binding adhesin of *Strep. dysgalactiae* in complex with two of the N-terminal F1 modules of

fibronectin has been solved (Schwarz-Linek *et al.*, 2003). It revealed a novel binding mechanism whereby motifs in the B3 peptide form an additional antiparallel β-strand on the triple-stranded β-sheet of sequential F1 modules. This mechanism was termed a tandem β-zipper (Figure 1.5). It was shown that homologous fibronectin-binding repeats of FnBPA from *S. aureus* bind to fibronectin in a similar manner (Pilka *et al.*, 2006). *Borrelia burgdorferi* also binds fibronectin by the tandem β-zipper, indicating that it is a common mechanism of fibronectin binding by microorganisms (Raibaud *et al.*, 2005). Furthermore it was shown that while the fibronectin modules do not undergo a significant change in conformation upon peptide binding, the FnBPA peptide undergoes a transition from a disordered conformation to an extended β-strand like conformation (Pilka *et al.*, 2006). This is in agreement with studies that have found that the C-terminus of FnBPA lacks discernable secondary structure and only takes on an ordered conformation upon binding to fibronectin (House-Pompeo *et al.*, 1996). In addition, it has been noted that an immune response directed against the C-terminus of FnBPA is predominantly against neo-epitopes created when this unfolded region binds fibronectin (Casolini *et al.*, 1998).

The binding of FnBPs to fibronectin promotes the internalization of *S. aureus* into host cells. *S. aureus* is capable of adhering to and invading a number of different cell types, including endothelial cells, epithelial cells, fibroblasts, osteoblasts and keratinocytes (Dziewanowska *et al.*, 1999; Hudson *et al.*, 1995; Kintarak *et al.*, 2004; Ogawa *et al.*, 1985; von Eiff *et al.*, 2001b). Fibronectin acts as a bridging molecule linking the bacterial cell to the host cell integrin $\alpha_5\beta_1$ (Fowler *et al.*, 2000; Massey *et al.*, 2001; Peacock *et al.*, 1999; Sinha *et al.*, 1999). Indeed the FnBPs have been shown to be sufficient for invasion of *S. aureus* into endothelial cells (Sinha *et al.*, 2000). Using live cell imaging, it has been recently shown that FnBPA-mediated uptake of *S. aureus* is relatively slow in comparison to the invasin protein of *Yersinia* (Schroder *et al.*, 2006a). It was proposed that the delay in inducing host cell actin rearrangement and eventual bacterial internalization was to allow time for *S. aureus* to produce critical amounts of cell damaging toxins (Schroder *et al.*, 2006b). The uptake of *S. aureus* by mammalian cells may provide a safe harbour for the bacterium from the immune response and most antimicrobials. The FnBPs, therefore, confer on the bacterium an ability to cross the endothelial lining and to disseminate through the bloodstream to infect other tissues. This may help to explain the persistent nature of some *S. aureus* infections.

After internalization, the subsequent fate of the endothelial cell varies between studies but appears to depend on the secretion of α- toxin, which is cidal to endothelial cells (Vann and

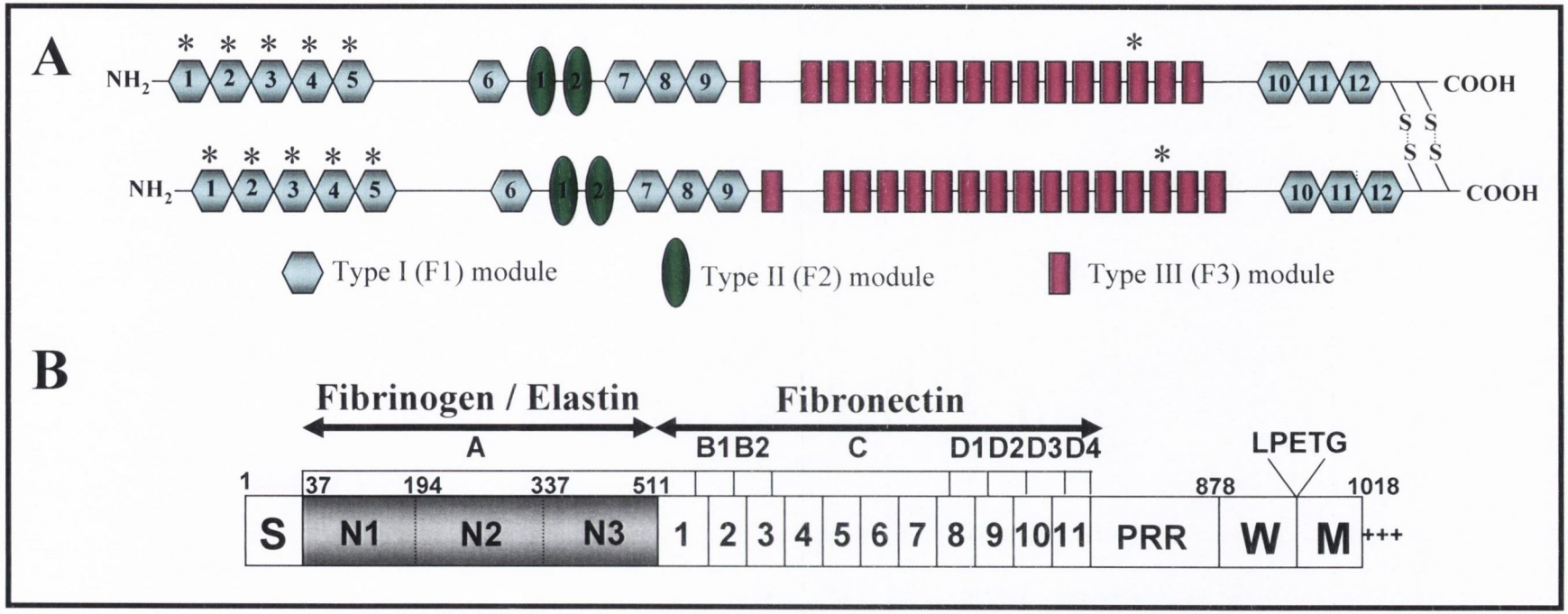

Figure 1.4 Fibronectin and the fibronectin-binding proteins of *S. aureus*

(A) Schematic diagram of human fibronectin. Fibronectin monomers are linked at their C-termini by a disulphide bond to produce the mature dimer of approximately 500 kDa found in plasma. *S. aureus* binding sites are indicated by an asterisk. (B) Structural organisation of the fibronectin-binding protein, FnBPA. A secretory signal sequence (S), region A (divided into subdomains N1, N2 and N3), regions B, C and D (now tandem repeats 1-11), proline rich region (PRR), cell wall- and membrane-spanning domains (W, M) are all indicated. Adapted from Schwarz-Linek *et al.*, 2003. The distinct binding domains for fibrinogen/elastin and fibronectin are also shown.

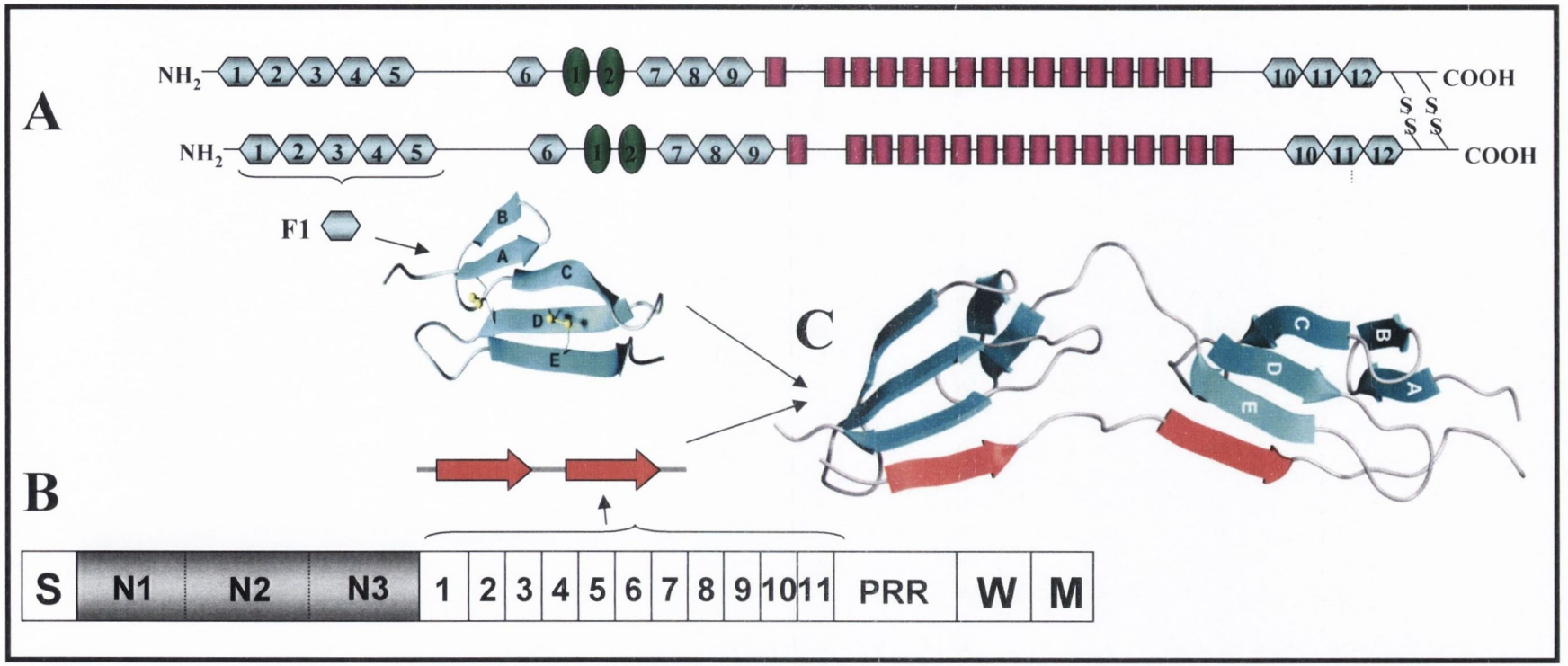

Figure 1.5 Tandem β-zipper mechanism of fibronectin binding by *S. aureus*

(A) The N-terminal F1 modules of fibronectin each consist of a β-sandwich of two antiparallel β-sheets; a double-stranded sheet (strands A and B) and a triple-stranded sheet (strands C, D and E). (B) The fibronectin-binding domains of FnBPA contain repeated motifs forming β-strands (red). **C** The tandem β-zipper mechanism whereby the bacterial peptide contributes a fourth β-strand to the triple stranded β-sheet of sequential F1 modules. Adapted from Schwarz-Linek *et al.*, 2003.

Proctor, 1988). An alternative to host cell lysis is the adaptation of *S. aureus* cells to become small colony variants (SCVs). SCVs have been isolated from patients with persistent, antibiotic-resistant and recurring infections (Proctor *et al.*, 1995). The majority of clinical *S. aureus* SCV isolates are characterized by defects in menadione and hemin biosynthesis, resulting in defective electron transport (Balwit *et al.*, 1994). SCVs persist in cells due to their slow growth, intracellular location and decreased antibiotic uptake (Proctor *et al.*, 1995; Proctor and Peters, 1998; von Eiff *et al.*, 1997a). They are also capable of resisting the bactericidal activity of host cell phagosome/lysosome fusion (Schroder *et al.*, 2006a). All aspects of the SCV phenotype, such as slower growth, reduced production of lytic toxins, no pigmentation, failure to ferment mannitol and resistance to aminoglycoside antibiotics and host antimicrobial peptides can be attributed to loss of one or another of the enzymes critical to the biosynthesis of the electron transport chain components. The resistance to aminoglycoside antibiotics and host antimicrobial peptides is due to the loss of membrane potential resulting from defects in electron transport (Lewis *et al.*, 1990; Vesga *et al.*, 1996). SCVs are able to persist within cultured endothelial cells because they do not lyse cells due to decreased α-toxin production (von Eiff *et al.*, 1997b). It has been shown that SCVs have higher expression of surface adhesins such as ClfA and FnBPA than their isogenic parent and therefore have increased virulence despite the slower growth (Vaudaux *et al.*, 2002). SCVs are associated with many disease states including cystic fibrosis, osteomyelitis and device-related infections and present a challenge for diagnosis and treatment. The altered colony morphology and biochemical profile may lead to the erroneous identification of *S. aureus* SCVs as streptococci or coagulase negative staphylococci. The slow growth and antibiotic resistance may lead to the belief that a new, rather than recurrent, infection is present.

1.2.2.4.2 Fibronectin-binding proteins binding to fibrinogen/elastin

The multifunctionality in ligand binding demonstrated by *S. aureus* MSCRAMMs such as protein A and ClfB is also apparent with FnBPA and FnBPB. In addition to binding fibronectin, they have also been shown to bind specifically to fibrinogen and elastin (Roche *et al.*, 2004; Wann *et al.*, 2000).

The A domains of FnBPA and FnBPB share 25% identity to the A domains of ClfA and ClfB. Indeed, the FnBPA and FnBPB A domains bind to the C-terminus of the γ chain of fibrinogen at the same site as ClfA (Wann *et al.*, 2000). In contrast, ClfB (Section 1.2.2.3.2) and SdrG (Section 1.3.1) are capable of binding the α and β chain of fibrinogen, respectively.

The integrity of the extreme C-terminus of the γ chain is important as substitution of the terminal 4 amino acids from AGDV to VRPE obliterated FnBPA binding (Wann *et al.*, 2000). The addition of Ca^{2+}, Mn^{2+} or Mg^{2+} ions did not affect the binding of recombinant A domain of FnBPA to fibrinogen (Wann *et al.*, 2000). This contrasts with the ClfA-fibrinogen interaction which is inhibited by both Ca^{2+} and Mn^{2+} (O'Connell *et al.*, 1998) (Section 1.2.2.3.1). Upon analysis of the N1, N2 and N3 subdomains of ClfA, it was proposed that a similar subdomain organization exists for region A of FnBPA and FnBPB (Deivanayagam *et al.*, 2002). The primary sequence of the C-terminal two thirds (N2 and N3) of the A regions of ClfA, ClfB, FnBPA and FnBPB were aligned and predictions of secondary structures showed that the A domains of the FnBPs were likely to contain a variant IgG-like fold similar to ClfA (Deivanayagam *et al.*, 2002) (Section 1.3.1). The SLAVA motifs at the junction of the N1 and N2 subdomains of region A of ClfA and ClfB have important roles in fibrinogen-binding. In contrast to ClfA, metalloprotease cleavage at the SLAVA site in ClfB renders the resulting truncate unable to bind fibrinogen (McAleese *et al.*, 2001). The role of a SLAVA-like motif in FnBPA and FnBPB however has not been investigated.

Unlike ClfA, the A domains of FnBPA and FnBPB can also mediate *S. aureus* adherence to immobilised elastin peptides (Roche *et al.*, 2004). Elastin, along with microfibrillar proteins, is a major component of the elastic fibre ECM. It is a hydrophobic protein that provides resilience and elasticity to tissues such as lung, aorta and skin (Section 1.5). *S. aureus* strains P1, MSSA and Cowan were shown to bind to immobilised elastin in exponential phase only (Roche *et al.*, 2004). The fibronectin-binding proteins FnBPA and FnBPB were shown to be necessary and sufficient for the adherence of *S. aureus* strain P1 to immobilised elastin peptides, a phenotype previously thought to be conferred by the elastin-binding protein, EbpS (Section 1.2.2.7.2). Furthermore, recombinant proteins of FnBPA and FnBPB, spanning residues 37-544 and 37-540, respectively, were shown to contain the elastin-binding function (Roche *et al.*, 2004).

1.2.2.4.3 Role of fibronectin-binding proteins in pathogenesis

The *fnbA* gene is present significantly more often in invasive isolates compared to carriage strains (Peacock *et al.*, 2002). Furthermore, 97% of clinical strains isolated from the airway of cystic fibrosis and pneumonia patients were shown to possess both *fnb* genes (Mongodin *et al.*, 2002). There is also evidence that individuals who have suffered invasive infection contain higher serum anti-FnBPA antibody levels than healthy individuals (Dryla *et*

al., 2005). Taken together, these data indicate that FnBPA is expressed *in vivo* during infection and suggests a role for FnBPA as a virulence factor. Several researchers have studied the role of FnBPA and FnBPB proteins in *S. aureus* pathogenesis with conflicting results (Flock *et al.*, 1996; Kuypers and Proctor, 1989). This can, in part, be explained by the use of FnBP-deficient *S. aureus* laboratory strains such as Newman which has been shown to contain a point mutation in both the *fnbA* and *fnbB* genes resulting in a premature stop codon (Grundmeier *et al.*, 2004). Strain Newman thus produces truncated FnBP proteins that are secreted rather than anchored to the cell wall peptidoglycan. Due to the a small deletion in a positive regulator of sigma factor B (RsbU), *S. aureus* strain 8325-4 produces low levels of FnBPs which results in weak adherence to immobilised fibronectin. The topic is further complicated by the ability of FnBPs to bind several ligands present in host tissue and by the functional redundancy between FnBPs and other *S. aureus* ligand-binding surface proteins.

Despite this, FnBPA has been shown to be a virulence factor in several models of *S. aureus* infection. In a large molecular epidemiological study, adherence to immobilised fibronectin was considerably greater for bacterial isolates associated with orthopaedic implant-associated infection than for isolates associated with nasal carriage, endocarditis, septic arthritis and osteomyelitis (Peacock *et al.*, 2000). FnBP mutants have greatly reduced uptake into host cells and antibodies directed against fibronectin reduce staphylococcal internalization (Dziewanowska *et al.*, 1999; Sinha *et al.*, 1999). In fact, FnBPA alone is sufficient for invasion of host cells without the need for other staphylococcal cofactors (Sinha *et al.*, 2000). The expression of serine protease, SspA, which specifically cleaves FnBPs (McGavin *et al.*, 1997) may aid in the detachment of bacterial cells from fibronectin-coated surfaces and allow dissemination of *S. aureus* to other tissues. A study employing the poorly pathogenic strain *L. lactis* for heterologous expression of *S. aureus* FnBPA showed a positive correlation between expression of FnBPA and the colonization of damaged heart valves in an experimental model of rats with catheter-induced aortic vegetations (Que *et al.*, 2001). The roles of ClfA and FnBPA were assessed in a mouse model of septic arthritis. Using a clinically relevant *S. aureus* strain LS-1, ClfA contributed to the arthritogenicity of *S. aureus* while FnBPA played an important role in the induction of systemic inflammation characterized by interleukin (IL)-6 secretion, severe weight loss and mortality (Palmqvist *et al.*, 2005). In another study using the surrogate *L. lactis* host, cells expressing ClfA successfully colonized damaged heart valves but were spontaneously eradicated over 48 hours. In contrast, FnBPA-positive lactococci increased bacterial titres and invaded adjacent endothelial cells (Que *et al.*, 2005). It was also

demonstrated that the fibrinogen- and fibronectin-binding ability of FnBPA could cooperate for *S. aureus* valve colonization and endothelial invasion (Que *et al.*, 2005).

It has recently been shown that both FnBPA and FnBPB are potent activators of human platelets (Fitzgerald *et al.*, 2006). Both the N-terminal fibrinogen-binding domains and the C-terminal fibronectin-binding domains of FnBPA and FnBPB are capable of activating platelets in a similar manner to that described for ClfA and ClfB (Section 1.2.2.3). Activation is mediated by fibrinogen or fibronectin bridges between the N- and C-termini, respectively, to the low affinity form of the GPIIb/IIIa integrin on resting platelets. Antibodies recognizing the A domain or the complex between the BCD domains and fibronectin bind to the FcγRIIa platelet receptor (Fitzgerald *et al.*, 2006). Bacteria such as *S. aureus* thus exploit circulating anti-MSCRAMM antibodies to cause platelet activation and induce thrombus formation.

1.2.2.5 Collagen-binding protein

Collagen is a major structural protein of mammals that provides tensile strength to connective tissues such as bone, ligament, cartilage and tendon, and to the fibrous matrices of skin and blood vessels. There are four distinct types of collagen, some of which display tissue tropism. Type I collagen is found in skin, bone, ligaments and tendons. Type II collagen is preferentially found in cartilage while type III collagen is associated with blood and skin. Type IV collagen is found almost exclusively in basement membranes. All collagen types are composed of a triple helix of polypeptide chains known as α chains. These chains wind around each other to form a right handed superhelical structure. Each chain contains multiple repeats of the sequence motif GXY, where X is often proline and Y is often hydroxyproline.

The *S. aureus* collagen-binding protein, Cna, promotes bacterial adherence to several types of collagen and to collagenous tissue such as cartilage (Switalski *et al.*, 1989; Switalski *et al.*, 1993). Expression of the *cna* gene occurs maximally during the exponential phase of growth and diminishes to almost undetectable levels during stationary phase (Gillaspy *et al.*, 1997). The global regulatory protein SarA binds directly to DNA sequences upstream of the *cna* gene and negatively regulates its expression (Blevins *et al.*, 1999). This *sar*-mediated regulation was shown to be independent of *agr* (Blevins *et al.*, 1999).

Cna possesses a similar domain organization to that of other *S. aureus* surface proteins (Figure 1.1). The N-terminal A domain comprises approximately 500 amino acids and contains the collagen-binding activity. This is followed by region B which is a tandem array of a 187-residue domain that is repeated one to four times depending on the strain (Gillaspy *et*

al., 1998). The precise ligand-binding region of Cna was localised to residues 151-318 (Patti *et al.*, 1993) and a recombinant protein spanning these residues was crystallised (Symersky *et al.*, 1997). The protein was shown to consist of two antiparallel β-sheets and two short α-helices. Recombinant proteins containing single amino acid substitutions designed to disrupt the surface of the putative binding site exhibited significantly lower affinities for collagen (Symersky *et al.*, 1997). The function of the B repeats in Cna remains unclear. They do not bind to collagen and do not affect the collagen-binding activity of region A (Rich *et al.*, 1998). Studies with capsule-containing strains of *S. aureus* have shown that the presence of a capsule can mask the collagen-binding activity of Cna (Gillaspy *et al.*, 1998). It was hypothesized that the B repeats may act as a stalk, projecting the ligand-binding A domain further away from the cell surface. However bacteria expressing multiple B repeats cannot overcome the inhibition of collagen binding associated with capsule production (Snodgrass *et al.*, 1999).

Cna may have an important role in the pathogenesis of infections involving collagen-rich tissue such as osteomyelitis and arthritis. Studies on *S. aureus*-induced septic arthritis have reported lower infectivity rates of mice injected with a *cna* mutant compared to those injected with a Cna expressing strain (Patti *et al.*, 1994). In another investigation, both active and passive immunization of mice with a recombinant fragment of Cna and anti-Cna antibodies, respectively, was shown to provide protection against *S. aureus*-mediated septic death (Nilsson *et al.*, 1998). Other studies have shown that Cna is involved in the pathogenesis of contact lens-associated bacterial keratitis (Rhem *et al.*, 2000). It has also been shown that the virulence potential of Cna is determined by the adhesin's affinity for its ligand, as well as its binding kinetics (Xu *et al.*, 2004). A recent study has shown that vaccination with a fusion protein containing Cna and the fibronectin-binding protein A (FnBPA) also induced a strong and specific humoral response in mice (Zhou *et al.*, 2006). Mice immunized with Cna-FnBP survived significantly longer following challenge with *S. aureus* than nonimmunized mice. Despite this, the *cna* gene is present in only approximately 30%-45% of strains tested (Arciola *et al.*, 2005; Peacock *et al.*, 2002), indicating that vaccine development targeting this adhesin alone is unlikely.

1.2.2.6 Iron-regulated surface proteins

The expression of a subset of staphylococcal genes is induced under iron-limiting conditions, which are likely to resemble growth conditions in serum and within the host during infection. Iron regulation in *S. aureus* involves Fur, an iron-responsive transcriptional

regulator. This repressor prevents transcription of a specific set of genes in the presence of iron. In the absence of iron, the repression is alleviated and transcription occurs. Inactivation of *fur* and *perR*, a homologue of *fur*, led to a reduction in virulence in a mouse model of *S. aureus* infection (Horsburgh *et al.*, 2001). The products of the iron-regulated surface determinant (*isd)* genes are involved in iron acquisition. The *isdA*, *isdB* and *isdC* genes are found in a locus encoding an iron transport system (Mazmanian *et al.*, 2003). The gene encoding IsdH is found outside the main *isd* cluster (Dryla *et al.*, 2003). All four proteins are covalently attached to the cell wall peptidoglycan. IsdA, IsdB and IsdH each contain the sortase A sorting signal (LPXTG), while IsdC contains the NPQTN signal for sortase B-mediated sorting (Dryla *et al.*, 2003; Mazmanian *et al.*, 2002). IsdA is involved in the uptake of iron across the bacterial cell envelope and binds to iron-containing ligand such as transferrin, hemin and haemoglobin, but not haptoglobin (Mazmanian *et al.*, 2003; Taylor and Heinrichs, 2002). Recombinant IsdA in solution was shown to exist as a monomer with each monomer capable of binding a single heme molecule (Vermeiren *et al.*, 2006). IsdB is effective at the removal of heme iron from hemoglobin and transport of this compound into staphylococcal cells. Importantly, mutants lacking *isdB* were shown to display a reduction in virulence in a murine model of abscess formation (Torres *et al.*, 2006). IsdH also interacts with iron-containing compounds such as haptoglobin and haptoglobin-hemoglobin complexes (Dryla *et al.*, 2003). Collectively these proteins bind human hemoproteins, remove the heme molecule, and transport heme through the cell wall and plasma membrane for accumulation in the bacterial cytoplasm. IsdA, IsdB and IsdH are all displayed on the bacterial cell surface but IsdC appears to be buried in the peptidoglycan layer and may function in the passage of iron through the cell wall (Skaar and Schneewind, 2004). The crystal structure of the heme-IsdC complex has recently been solved (Sharp *et al.*, 2007).

In addition to iron-containing compounds, Isd proteins have been shown to interact with other ligands. IsdA binds fibronectin and fibrinogen and acts as an adhesin when *S. aureus* is grown in iron-limiting conditions (Clarke *et al.*, 2004). IsdH has been shown to interact specifically with the complement protein C3 (Yanasigisawa, N. and Foster, T. J., manuscript in preparation). This may interfere with complement deposition on the cell surface thereby preventing bacterial lysis. The ligand-binding domains of IsdA and IsdH are called NEAT domains (near transporter) (Andrade *et al.*, 2002). These structural domains are found in proteins encoded by genes close to siderophore genes in Gram-positive bacteria, and are involved in binding to iron-containing molecules. Crystal structure analysis of the NEAT

domain shows it to adopt a β-sandwich fold that consists of two five-stranded antiparallel β-sheets. Although unrelated at the primary sequence level, the NEAT domains belong to the immunoglobulin superfamily (Pilpa *et al.*, 2006).

Antibodies to IsdA have been found in convalescent sera indicating that it is expressed *in vivo* (Clarke *et al.*, 2004; Morrissey *et al.*, 2002). In addition, significantly higher concentrations of antibodies to IsdA and IsdH were found in serum samples from healthy individuals who were not nasal carriers of *S. aureus*, compared with those in healthy carriers (Clarke *et al.*, 2006). IsdA is involved in adherence of *S. aureus* to human desquamated nasal epithelial cells and is required for nasal colonization in the cotton rat model. Indeed, vaccination of cotton rats with IsdA or IsdH protected against nasal carriage (Clarke *et al.*, 2006). In agreement with this a vaccine containing IsdB was highly immunogenic in mice and in rhesus macaques, inducing a five-fold increase in antibody titres after a single immunization (Kuklin *et al.*, 2006). IsdB therefore has excellent prospects for use as a vaccine against *S. aureus* disease in humans. Immunisation with a combined vaccine containing IsdA, IsdB and SdrD and SdrE (Section 1.2.2.7.1) generated significant immunity in a murine model of abscess formation. This vaccine induced the production of opsonophagocytic antibodies and afforded high levels of protection against invasive disease or lethal challenge with human clinical *S. aureus* isolates (Stranger-Jones *et al.*, 2006).

1.2.2.7 Other surface proteins

1.2.2.7.1 Other LPXTG-containing proteins

In addition to ClfA and ClfB, *S. aureus* expresses three other cell wall-associated surface proteins containing SD dipeptide repeats (Sdr proteins) (Josefsson *et al.*, 1998). The *sdrC*, *sdrD* and *sdrE* genes are tandemly arrayed in the bacterial chromosome, although some strains do not contain all three genes (Josefsson *et al.*, 1998; Sabat *et al.*, 2006). The three proteins have a structural organization similar to other surface-expressed ligand-binding proteins, including a secretion signal and C-terminal sorting motifs. Each protein has a similar domain structure to ClfA and ClfB, but includes additional B repeat sequences between region A and region R (Josefsson *et al.*, 1998). No biological activities have been attributed to SdrC or SdrD. SdrE was shown to promote platelet aggregation by *S. aureus* (O'Brien *et al.*, 2002a). Another member of the staphylococcal Sdr family with homology to SdrE was shown to bind to bone sialoprotein, which may be important in the localisation of bacteria to bone tissue, and thus might be of relevance in the pathogenicity of osteomyelitis (Tung *et al.*, 2000).

A family of Sdr proteins, designated SdrF, SdrG and SdrH, has also been found in *S. epidermidis* (McCrea *et al.*, 2000). SdrG binds to the β chain of fibrinogen and inhibits thrombin-induced fibrinogen clotting (Davis *et al.*, 2001). The A domain of this protein has been crystallised with and without its fibrinogen ligand (Ponnuraj *et al.*, 2003) giving new insight into the mechanism of ligand binding by staphylococcal surface proteins (Section 1.3).

Bioinformatic analysis of the genome sequences of six *S. aureus* strains revealed the presence of 10 novel genes encoding surface proteins belonging to the LPXTG family (Roche *et al.*, 2003a). These were designated Sas (*S. aureus* surface) and along with specific sorting signals, they contain a typical surface protein domain organization. Several of these proteins share similar structural organisation with the Clf-Sdr protein family with some having repeat regions (B repeats), rather than SD dipeptide repeats. SasE, Sas I and Sas J have been characterized and renamed as IsdA, IsdH and IsdB, respectively. SasG is homologous to the plasmin-sensitive cell wall-associated protein Pls of *S. aureus* which has been shown to have anti-adhesive properties by impairing adhesion to immobilised ligands (Savolainen *et al.*, 2001). SasG and Pls have also been shown to promote bacterial adherence to nasal epithelial cells (Roche *et al.*, 2003b) and may have a role to play in nasal colonisation. The expression of SasG on the surface of bacterial cells masks the ability of *S. aureus* expressing Spa, ClfB, FnBPA and FnBPB to bind to their respective ligands. The presence of the numerous B repeats of SasG played a crucial role in the masking phenotype. While SasG size variants with eight, six or five B repeats masked ligand-binding, variants with four, two or one repeats had no effect. In a similar manner, SasG variants with eight, six and five B repeats were capable of forming a biofilm whereas variants with four, two or one repeats were not (Corrigan *et al.*, 2007). SasA (also known as SraP) is encoded by a gene locus similar to that encoding the *Streptococcus gordonii* platelet adhesin GspB. Glycosylation of these proteins is required for solubility and secretion (Takamatsu *et al.*, 2004). SasA promotes adhesion to platelets and is a virulence factor in an animal model of endocarditis (Siboo *et al.*, 2005). No functions have been attributed to other Sas proteins (SasC, SasD, SasF, SasH and SasK). Antibodies to the Sas proteins have been recovered from convalescent sera, indicating that these proteins are expressed *in vivo* during infection (Roche *et al.*, 2003a).

1.2.2.7.2 Non-covalently attached cell wall proteins

S. aureus also possesses a number of non-covalently attached cell wall-associated proteins that bind to components of the host's ECM and plasma proteins.

Sbi is an IgG binding protein that has been identified on the surface of *S. aureus* cells. It is a 436-residue protein that binds to IgG via a single binding domain of approximately 52 residues that shares significant homology with the IgG binding domain of protein A (Zhang *et al.*, 1998). The protein contains a typical N-terminal secretion signal but lacks a cell sorting motif at the C-terminus. Sbi also bound another serum component identified as β2-glycoprotein I (β2-GPI), also known as apolipoprotein H. The minimal β2-GPI-binding domain is mediated by a region of 57 amino acids that is distinct from the IgG-binding domain (Zhang *et al.*, 1999). The amount of Sbi on the cell surface significantly increases when bacteria are grown in the presence of human serum and it is thought that the binding of IgG to Sbi upregulates its own synthesis (Zhang *et al.*, 2000).

The binding of *S. aureus* to the elastin monomer, tropoelastin and to soluble digested elastin fragments (Section 1.5) is mediated by the cell wall-associated elastin-binding protein, EbpS (Park *et al.*, 1991; Park *et al.*, 1996). The binding site in tropoelastin for EbpS was mapped to a 30 kDa segment in the N-terminus of the protein which is distinct from the mammalian receptor binding site (Park *et al.*, 1991). Subsequent investigation found that the elastin-binding domain of EbpS was contained within a segment spanning Gln14-Glu34 (Park *et al.*, 1999). In contrast to the LPXTG-anchored surface proteins EbpS is an integral membrane protein with two transmembrane domains and a third hydrophobic domain separating the N- and C-termini (Downer *et al.*, 2002). It was proposed that the N-terminus projected past the peptidoglycan layer to be expressed on the surface of the cell allowing interaction with elastin ligands (Downer *et al.*, 2002). However, EbpS was unable to promote bacterial adherence to immobilised elastin as an *S. aureus epbS* mutant still adhered to the immobilised ligand (Roche *et al.*, 2004). Thus, EbpS is not an MSCRAMM for elastin. *S. aureus* defective in the expression of the fibronectin-binding proteins FnBPA and FnBPB was unable to adhere to immobilised elastin (Roche *et al.*, 2004) implicating these proteins in the binding of *S. aureus* cells to this ligand. Expression of EbpS was correlated with the ability of cells to grow to a higher density in liquid culture, suggesting that EpbS may have a role in regulating cell growth (Downer *et al.*, 2002).

1.2.3 Capsule

More than 90% of *S. aureus* clinical isolates produce capsular polysaccharide (CP). These have been divided into 11 serogroups, which can be further divided into two distinct groups based on colony morphology. Mucoid-type capsule strains (serogroups 1 and 2) are

heavily encapsulated and colonies have a mucoid appearance on solid medium. Microcapsule strains (serogroups 3-11) possess a thin layer of capsular polysaccharide and are non-mucoid in appearance on solid medium. Serotypes 5 and 8 are most prevalent among clinical isolates of *S. aureus* (Hochkeppel *et al.*, 1987). Approximately 25% of human isolates express serotype 5 microcapsules and 50% express type 8, both of which are polymers of hexosaminuronic acids (O'Riordan and Lee, 2004). Capsular polysaccharide has antiphagocytic properties due to inhibition of binding of opsonising antibodies that recognise proteins, teichoic acids and peptidoglycan on the cell surface, thereby reducing killing by neutrophils (Thakker *et al.*, 1998).

1.2.4 Extracellular proteins

1.2.4.1 Extracellular fibrinogen-binding protein, Efb

The extracellular fibrinogen-binding protein Efb is a secreted 15.8 kDa protein produced by *S. aureus* mainly during the post-exponential phase of growth (Palma *et al.*, 1998). The protein binds the α chain of fibrinogen (Palma *et al.*, 2001) but does not support bacterial adherence to immobilised fibrinogen *in vitro* (Palma *et al.*, 1996). The binding of Efb to fibrinogen is divalent, with one binding site at the N-terminus of Efb and the other at the C-terminus of the protein which is dependent on the concentration of Ca^{2+} (Palma *et al.*, 1998; Wade *et al.*, 1998). The binding of Efb to the α chain of fibrinogen interferes with platelet activation (Palma *et al.*, 2001). The N-terminal domain of Efb contains two repeated regions that bear structural similarity to the fibrinogen-binding C-terminal domain of coagulase (Boden and Flock, 1992; Watanabe *et al.*, 2005). These regions of Efb and coagulase compete for the same binding domain on fibrinogen, which is close to an RGD sequence recognised by platelet receptor GPIIb/IIIa (Palma *et al.*, 2001). The binding of Efb to platelets can occur in a fibrinogen-dependent manner via GPIIb/IIIa or in a fibrinogen-independent manner, directly to the platelet surface (Shannon and Flock, 2004). Efb also has anti-opsonic activity due to its ability to bind to the α chain of complement protein C3 and inhibit both the classical and alternative pathways of complement activation (Lee *et al.*, 2004a). Efb thereby inhibits complement activity by blocking deposition of C3 or by preventing further complement activation beyond C3b. The C3b binding region of Efb is located within the C-terminus and has recently been crystallised (Hammel *et al.*, 2006; Lee *et al.*, 2004b). It was also shown that recombinant Efb could bind to both C3b and fibrinogen simultaneously, forming a trimolecular complex (Lee *et al.*, 2004b). This demonstrates that

Efb is a virulence factor involved in facilitating persistent *S. aureus* infections by interfering with complement activity *in vivo*.

Efb has been shown to be an important virulence factor in infection models. Pre-treatment with Efb resulted in a significant prolongation of bleeding time in a mouse model. Furthermore, Efb was capable of rescuing animals from death caused by the administration of potent platelet agonists (Shannon *et al.*, 2005). This anti-platelet effect may explain the retardation of wound healing associated with Efb in *S. aureus* wound infections. Antibodies against Efb blocked the binding of Efb to fibrinogen and prevented Efb-mediated inhibition of platelet aggregation (Shannon *et al.*, 2006). Furthermore, these antibodies cross-reacted with coagulase and blocked coagulase activity in plasma. Immunization of mice with Efb resulted in the generation of high titre specific antibodies and vaccinated animals developed significantly less severe wound infection than the unvaccinated controls (Shannon *et al.*, 2006).

1.2.4.2 Extracellular adherence protein, Eap

Extracellular adherence protein (Eap) is a 60 kDa protein secreted from *S. aureus* cells which is able to bind to the bacterial cell surface as well as to eukaryotic cells and several plasma and matrix proteins including fibronectin, the α chain of fibrinogen, and prothrombin (Palma *et al.*, 1999). While an *S. aureus eap* mutant bound equally well to fibronectin- and fibrinogen-coated surfaces, it adhered significantly less to cultured fibroblasts than the wild-type strain (Hussain *et al.*, 2002). Eap has also been shown to inhibit the recruitment of host leukocytes by binding intercellular adhesion molecule-1 (ICAM-1) (Chavakis *et al.*, 2002) and to enhance the internalisation of *S. aureus* cells into human eukaryotic cells (Haggar *et al.*, 2003). Eap consists of four to six tandemly repeated EAP domains. The crystal structure of the EAP domain reveals a core fold that is comprised of an α-helix lying diagonally across a five-stranded β-sheet which resembles the C-terminal domain of bacterial superantigens (Geisbrecht *et al.*, 2005). Eap can cause a significant inhibition of T cell proliferation induced by *S. aureus* toxic shock syndrome toxin-1 (Haggar *et al.*, 2005). In a mouse wound healing model, wound closure was prolonged in an *S. aureus* Eap-deficient strain (Athanasopoulos *et al.*, 2006). Eap can also bind to different collagen types such as the monomolecular form of collagen I but not collagen II (Hansen *et al.*, 2006). However, collagen I is not recognized by Eap when it is incorporated into banded fibrils. Eap only bound to banded fibrils after their partial disintegration by matrix-degrading metalloproteases (Hansen *et al.*, 2006). This shows

that adherence to matrix structures by *S. aureus* can be supported by inflammatory reactions. The anti-inflammatory activities of Eap such as inhibition of neutrophil recruitment have recently been exploited to suppress experimental autoimmune encephalomyelitis (EAE) in mice (Xie *et al.*, 2006) and indicate that this protein represents an attractive treatment for autoimmune inflammatory disorders such as multiple sclerosis.

1.2.4.3 Coagulase

During physiological blood coagulation, prothrombin is converted to thrombin through a specific cleavage by trypsin in response to tissue damage. Cleavage generates a new N-terminus that triggers folding of the thrombin molecule into an active conformation. Thrombin cleaves fibrinogen to yield fibrin, which creates the basis of a blood clot at the site of tissue damage. Coagulase is a secreted protein of *S. aureus* that activates the host blood coagulation pathway independently of tissue damage by complexing with and activating prothrombin (Hemker *et al.*, 1975; Kawabata *et al.*, 1986). It binds to human prothrombin in a 1:1 molar ratio to form a complex called staphylothrombin, which converts fibrinogen to fibrin in a process that does not involve proteolytic cleavage of prothrombin (Kawabata *et al.*, 1985). The coagulase molecule consists of two independently folded α-helical N-terminal domains, a C-terminal repeat region including between six and nine 27-amino acid repeats, and a highly conserved central domain. The N-terminal domains contain the prothrombin-binding and activation sites and the C-terminal repeat regions can bind fibrinogen (Boden and Flock, 1992; Friedrich *et al.*, 2003). The isoleucine and valine residues at positions 1 and 2 at the extreme N-terminus of coagulase insert into the trypsin activation pocket in prothrombin. This causes conformational changes which trigger the folding of the prothrombin activation domain. This mechanism has been defined as the prototype for a novel mechanism of zymogen activation (Friedrich *et al.*, 2003). The ability to bind both prothrombin and fibrinogen simultaneously may be involved in bringing coagulase-activated prothrombin into close proximity with fibrinogen, allowing the formation of fibrin.

Coagulase production is the main characteristic used to distinguish *S. aureus* from the less virulent coagulase-negative staphylococci in clinical laboratories. However, the role of coagulase in bacterial infection models is unclear. The ability to create a fibrin clot around bacterial cells may hinder phagocytosis. Although coagulase has been shown to be a virulence factor in animal models of pulmonary infection and murine mastitis (Jonsson *et al.*, 1985;

Sawai *et al.*, 1997) it is perhaps surprising that it did not contribute to the pathogenesis of *S. aureus* in a rat endocarditis model (Baddour *et al.*, 1994; Moreillon *et al.*, 1995).

Ten different serotypes of staphylococcal coagulase have been reported to date. A recent study examined the sequences of the ten serotypes and sequenced the upstream and downstream flanking regions of the *coa* gene (Watanabe *et al.*, 2005). The N-terminal signal sequence and the first seven amino acids of the D1 region are identical in all ten serotypes. The central regions and C-terminal sequence are also relatively conserved. In contrast, the remainder of D1 and the D2 region are the most diverged with average amino acid identities of 52.8% and 60.2%, respectively (Watanabe *et al.*, 2005). It is proposed that antigenic variation in coagulase may be useful to evade the host immune response and/or to adapt to the different coagulase-prothrombin binding sites of mammalian species. The flanking regions of *coa* were highly homologous indicating that the gene could be transmitted to *S. aureus* while sections of it, responsible for variable antigenicity, may have evolved independently.

1.2.4.4 Extracellular Proteases

S. aureus secretes an array of proteases that facilitate tissue destruction, provide defence against the host immune response, allow interception of bacterial and host enzymes and alteration of surface proteins. Three main classes of proteases are secreted from *S. aureus* cells: metalloproteases, serine proteases and cysteine proteases.

1.2.4.4.1 Metalloprotease

Aureolysin is an extracellular zinc-dependent metalloprotease produced by *S. aureus*. This enzyme, which binds one zinc and three calcium ions, comprises a single chain of 301 amino acids that consists of a β-strand-rich upper domain and an α-helix-rich lower domain (Banbula *et al.*, 1998). The gene encoding aureolysin, *aur*, occurs in two allelic forms and is highly conserved, implying that it has important functions in the cell, including the processing of other protease precursors (Sabat *et al.*, 2000). Aureolysin is produced as a proenzyme and is activated by post-translational processing (Chan and Foster, 1998). The global regulator, SarA has an important role in repressing the expression of extracellular proteases. In *sarA* mutant cells high amounts of proteases resulted in lower levels of cell-bound surface proteins such as FnBPA and protein A compared to wild-type cells, in spite of unaltered or even increased transcription of the corresponding genes (Karlsson *et al.*, 2001). Aureolysin is capable of degrading the human bactericidal peptide cathelicidin LL-37 contributing to the

resistance of *S. aureus* to the innate immune system (Sieprawska-Lupa *et al.*, 2004). Aureolysin also cleaves other substrates including the glutamyl endopeptidase (V8 serine protease, SspA) from its precursor form (Drapeau, 1978; Shaw *et al.*, 2004), lipase (Rollof and Normark, 1992) and ClfB (McAleese *et al.*, 2001). Aureolysin also affects the stimulation of B and T lymphocytes and inhibits immunoglobulin production (Prokesova *et al.*, 1991). However, despite numerous functions that influence staphylococcal virulence factors, an *aur* mutant is not attenuated in animal models of infection (Calander *et al.*, 2004; Shaw *et al.*, 2004).

1.2.4.4.2 Serine protease

The serine protease SspA (also called V8 protease) is secreted as a proenzyme that is activated by proteolytic cleavage by aureolysin (Drapeau, 1978). SspA cleaves peptide bonds exclusively on the carbonyl side of aspartate and glutamate residues. The crystal structure of SspA revealed that it contained no disulfide bridges, distinguishing it from human serine proteases (Prasad *et al.*, 2004). SspA possesses structural similarity with several other serine proteases, including the epidermolytic toxins A and B from *S. aureus* and trypsin, where the conformation of the active site is almost identical (Prasad *et al.*, 2004). SspA is also unique in that the positively-charged N-terminus is involved in determining the substrate-specificity of the enzyme.

SspA is produced in post-exponential phase (Shaw *et al.*, 2004) and is also repressed by SarA. It can cleave the staphylococcal surface proteins FnBPA and protein A (Karlsson *et al.*, 2001; McGavin *et al.*, 1997) which may facilitate detachment from ligand-coated surfaces or immune evasion by the removal of surface antigens. SspA is also capable of cleaving the heavy chains of human immunoglobulins (Prokesova *et al.*, 1992), the human α_1-protease inhibitor (Potempa *et al.*, 1986) and activates the staphylococcal cysteine protease, SspB (Rice *et al.*, 2001b). The *sspA* gene forms part of an operon. A polar mutation in *sspA* led to decreased virulence in a murine tissue abscess model, murine bacteraemia and wound infection, but not in murine septic arthritis (Calander *et al.*, 2004; Coulter *et al.*, 1998; Shaw *et al.*, 2004).

1.2.4.4.3 Cysteine proteases (staphopains)

Staphopain A (ScpA) and staphopain B (SspB) are important secreted proteases of *S. aureus*. ScpA is produced during the post-exponential phase of growth as a proenzyme that is

activated by proteolytic cleavage. Its maturation is independent of aureolysin, SspA and SspB. It has a very broad substrate range, relatively little specificity in cleavage site, and may undergo autocatalytic activation (Shaw *et al.*, 2004). It has elastinolytic activity and may be involved in tissue destruction (Potempa *et al.*, 1988). The *scpA* gene forms part of a bi-cistronic operon including *scpB*, which encodes a specific inhibitor of staphopain A, named staphostatin A (ScpB) that is exclusively expressed in the cytoplasm (Rzychon *et al.*, 2003). Staphostatins are very specific and form non-covalent 1:1 complexes with their corresponding enzymes or proenzymes, abolishing their cysteine protease activity (Dubin, 2003). Recombinant staphopain A is toxic to *E. coli* cells unless it is co-expressed with fully-functional staphostatin A (Wladyka *et al.*, 2005) suggesting that the role of staphostatins is to protect cytoplasmic proteins in the event of proteases becoming active prior to secretion.

The cysteine protease staphopain B (SspB) is encoded in an operon with the serine protease SspA (Rice *et al.*, 2001b) and the specific inhibitor of staphopain B, staphostatin B, SspC (Massimi *et al.*, 2002). SspB is cleaved from a secreted proenzyme by SspA (Chan and Foster, 1998; Rice *et al.*, 2001b) although the uncleaved proenzyme has some protease activity (Massimi *et al.*, 2002).

Deletion of *sspB* caused attenuation of virulence in a murine abscess model of infection (Shaw *et al.*, 2004) whereas non-polar deletion of *sspA* had no influence on virulence (Rice *et al.*, 2001b). Mutation of *sspC* caused a growth defect and changes in the production of secreted proteins due to the degradation of cytoplasmic proteins, presumably by the unprotected cysteine protease SspB (Shaw *et al.*, 2005). This implies that SspB is the protease that is most important for virulence in this operon.

1.2.4.5 Other secreted proteins/toxins

More than half of the actual or potential virulence determinants in *S. aureus* are secreted extracellular proteins (Kuroda *et al.*, 2001). These include specific proteins that interfere with the host's innate or adaptive immunity. Secreted proteins targeting the innate immune system include those responsible for the inhibition of neutrophil chemotaxis such as chemotaxis inhibitory protein of staphylococci (CHIPS), toxins that kill leukocytes such as Panton Valentine leukocidin (PVL) and proteins that inhibit complement fixation such as staphylococcal complement inhibitor (SCIN). In contrast, secreted superantigens, such as enterotoxins and toxic shock syndrome toxin thwart the host's adaptive immunity. Such secreted *S. aureus* proteins will be discussed in Section 1.2.5.

1.2.5 Immune evasion by *S. aureus*

1.2.5.1 Host defences against infection

The body's skin and mucous membranes constitute an important physical barrier to the microbiological flora. When *S. aureus* breaches these barriers through a wound, it encounters the innate and acquired immune system of the host. Infection by *S. aureus* triggers a strong inflammatory response, involving the migration of neutrophils and macrophages to the site of infection. These cells engulf and destroy the invading organism, aided by available antibodies and complement proteins present in the host's serum. The complement system is a family of proteins and proteolytic fragments that have varied roles in innate and acquired immunity, including direct killing of foreign cells and regulation of other effectors of the immune response. A major role of complement is to recruit effector molecules that label bacteria and target them for destruction by host phagocytes. The process of complement deposition on bacterial cell surfaces occurs in three ways, the classical pathway, the lectin pathway and the alternative pathway. In contrast to the classical and lectin pathway, the alternative pathway is part of the acquired immune system as it requires specific interactions with antibodies bound to antigens on target cells. The fixation of complement proteins on the surface of *S. aureus* promotes phagocytosis by professional phagocytes such as neutrophils and macrophages. Initially, phagocytes are attracted to the site of infection by formylated peptides released by growing bacteria and by chemoattractant molecules such as small peptide fragments (C3a and C5a) that are released during complement activation. The membranes of phagocytes have specific receptors for fragments of complement and formylated peptides that promote migration. Neutrophils also express specific receptors that recognise the Fc portion of IgG and complement proteins bound to the bacterial cell surface that facilitate efficient uptake and killing.

The initial response to invading organisms is their uptake into macrophages and other antigen-presenting cells and their subsequent transport to the lymph nodes. In the lymph, B cells are stimulated and differentiate to produce antibodies to neutralise toxins and to promote phagocytosis of bacterial cells. In the case of *S. aureus*, it is evident that this system does not work well. Antibodies to antigens of *S. aureus* are present in all humans and there is evidence that antibody titres rise following an infection (Dryla *et al.*, 2005; Roche *et al.*, 2003a). Despite this, antibodies and immunological memory seem to be insufficient to prevent a recurrent infection. *S. aureus* is now recognised as an invasive pathogen, promoting its uptake into non-professional phagocytes such as endothelial cells (Section 1.2.2.4.1). This pathogen

has many mechanisms to thwart the immune response to survive and proliferate inside the host. Some examples of these mechanisms are discussed below.

1.2.5.2 Inhibition of chemotaxis

Neutrophils reacting to invasion by microorganisms are attracted by complement peptide fragments and formylated peptides secreted by bacterial cells. Receptors on the surface of neutrophils are stimulated, activating intracellular signalling cascades which results in the migration of neutrophils from the blood to the site of infection.

The chemotaxis inhibitory protein of staphylococci (CHIPS). produced by 65% of clinical *S. aureus* strains, is a 14 kDa protein that blocks neutrophil chemotaxis by binding the formylated peptide receptor and the C5a receptor on neutrophils (de Haas *et al.*, 2004; Veldkamp *et al.*, 2000). The gene encoding CHIPS is on an immune evasion cluster which also encodes SCIN (Section 1.2.5.4) as well as staphylokinase (SAK) and staphylococcal enterotoxin A (SEA), which can modulate later steps of the immune response (van Wamel *et al.*, 2006). CHIPS is produced early in the growth phase of *S. aureus* in order to be an effective immune modulator (Rooijakkers *et al.*, 2006). Two distinct domains are present on the protein to facilitate binding to the formyl peptide receptor (FPR) and the C5a receptor (C5aR). This prevents binding of the respective agonists and results in potent inhibition of chemotaxis (Haas *et al.*, 2004; Postma *et al.*, 2004; Postma *et al.*, 2005). The structure of the N-terminus of CHIPS, containing the C5aR binding site shows resemblance to the staphylococcal superantigen proteins and to the extracellular adherence protein, Eap (Haas *et al.*, 2005). Its role as an anti-inflammatory agent, preventing leukocyte migration to the site of infection demonstrates the importance of this protein in disease pathogenesis.

1.2.5.3 Toxins that kill leukocytes

The ability of *S. aureus* to produce cytolytic toxins that damage leukocytes contributes to the development of an infection by killing neutrophils that are attempting to engulf and destroy bacteria. These toxins form β-barrel structures in the cytoplasmic membrane of host cells causing leakage and eventual lysis. Bicomponent leukotoxins comprise two subunits that are secreted separately and assemble into hexameric or heptameric oligomers in the cell membrane. There are four types of bicomponent leukotoxins, the γ toxin (Hlg), the Panton-Valentine leukocidin (PVL), leukocidin E/D and leukocidin M/F-PV-like toxins. γ toxin lyses both erythrocytes and leukocytes whereas PVL is toxic only for leukocytes. The *pvl* genes,

which are present in a lysogenic bacteriophage, are found in only 1-2% of *S. aureus* strains (Prevost *et al.*, 1995). There is a strong association between PVL expression and severe skin infections (Prevost *et al.*, 1995). Recently, community acquired methicillin resistant *S. aureus* (CA-MRSA) strains have emerged that cause severe necrotising pneumonia and contagious skin infections in previously healthy individuals (Gillet *et al.*, 2002; Said-Salim *et al.*, 2003). These strains are characterised by the carriage of type IV or type V staphylococcal cassette chromosome (SCCmec), encoding resistance to methicillin and other antibiotics, and often by expression of PVL. It is likely that these virulent strains have emerged as a result of horizontal transfer of PVL phages and SCCmec elements. However, not all CA-MRSA strains produce PVL (Moroney *et al.*, 2006). It has recently been shown that PVL expression induces global changes in transcriptional levels of genes encoding secreted and cell-wall-anchored proteins such as protein A (Labandeira-Rey *et al.*, 2007).

1.2.5.4 Resistance to opsonophagocytosis

Antibodies that recognise bacterial cell surface components such as teichoic acids, peptidoglycan and cell wall anchored proteins are present in sera of most individuals. *S. aureus* expresses surface-associated anti-opsonic proteins and a polysaccharide capsule that can interfere with the deposition of antibodies and complement formation by classical and alternative pathways, or interfere with their access to neutrophil complement receptors and Fc receptors. The ability of neutrophils to recognise bound complement and antibody is thus compromised, reducing the efficiency of phagocytosis. The extent to which *S. aureus* avoids opsonins in host serum is an important factor in the success of infection.

Cell wall anchored surface proteins have an important role to play in resistance of *S. aureus* to opsonophagocytosis. Protein A contains four or five domains, each capable of binding the Fc region of IgG (Section 1.2.2.2) which results in the bacterial surface being coated by IgG molecules that are in the incorrect orientation to be recognised by neutrophil Fc receptors. The finding that protein A-deficient strains of *S. aureus* are phagocytosed more efficiently by neutrophils *in vitro* and show decreased virulence in several animal infection models (Palmqvist *et al.*, 2002; Patel *et al.*, 1987) demonstrates the anti-phagocytic effect of protein A and its role in pathogenesis. ClfA also displays anti-phagocytic properties due to its fibrinogen-binding phenotype. When cells are densely packed together in suspension, the γ chain termini of fibrinogen, which are located at either end of the bivalent molecule (Figure 1.3), can bind simultaneously to two ClfA molecules on different cells which results in cell

clumping. *In vivo*, the cell density is too low for clumping to occur but instead, bacterial cells are coated with fibrinogen molecules. The coating of bacterial cells in host proteins prevents the targeting of these cells by circulating antibodies and complement proteins. Indeed, ClfA has been shown to inhibit phagocytosis by human polymorphonuclear leukocytes (Higgins *et al.*, 2006). This may be important in the pathogenesis of conditions such as sepsis and septic arthritis. Other fibrinogen-binding proteins such as ClfB, FnBPA and FnBPB may exhibit anti-phagocytic properties in a similar manner.

The majority of *S. aureus* isolates express one of three different serotypes of capsular polysaccharide on their cell surface (O'Riordan and Lee, 2004). Expression of type 5 and type 8 capsule is associated with increased virulence in animal models of infection and reduces phagocytosis in the presence of normal serum opsonins *in vitro* (Nilsson *et al.*, 1997; Thakker *et al.*, 1998). Capsular polysaccharide is likely to prevent access of phagocyte complement receptors to complement components assembled beneath the capsule layer, thus impairing phagocytosis (Cunnion *et al.*, 2003).

S. aureus also secretes a number of proteins that interfere with complement fixation on the bacterial surface and thus hinder killing by neutrophils. Extracellular fibrinogen-binding protein, Efb binds to the α chain of the complement component C3 inhibiting its deposition on the cell surface and subsequent complement-mediated opsonophagocytosis (Lee *et al.*, 2004a). Staphylococcal complement inhibitor (SCIN) specifically interacts with bacterium-bound C3 convertases thus efficiently preventing C3b deposition and phagocytosis (Rooijakkers *et al.*, 2005).

1.2.5.5 Resistance to killing by antimicrobial peptides

If *S. aureus* is successfully engulfed by host neutrophils, it is well equipped with surface modifications to help it survive in the phagosome. Natural modifications of wall teichoic acid, lipoteichoic acid and membrane phospholipids all contribute to resist killing by antimicrobial peptides. Antimicrobial peptides are important components of the innate immune system. They are produced in tissues and by platelets and neutrophils and are present on mucosal surfaces, in the airways and on skin. They function to disrupt the integrity of the lipid bilayer of bacterial cell membranes and can be classified into four categories, small anionic peptides (e.g. dermacidin), small cationic peptides (e.g. cathelicidin LL-37), cationic peptides that form disulphide bonds (e.g. α-defensins) and anionic/cationic peptide fragments derived from larger proteins (e.g. lactoferrin) (Brogden, 2005). The Dlt proteins of *S. aureus*

result in D-alanine substitutions of ribitol teichoic acid and lipoteichoic acid that partially neutralises the negative charge of the cell surface that attracts cationic peptides (Peschel *et al.*, 1999). Similarly, the MprF protein adds an L-lysine to phosphatidylglycerol exposed on the cell wall (Peschel *et al.*, 2001) to reduce the net negative charge of the bacterial surface.

In addition to D-Ala and lipid modifications, *S. aureus* also secretes proteins that neutralise cationic peptides. The metalloprotease aureolysin (Section 1.2.4.4.1) cleaves and inactivates the defensin peptide cathelicidin LL-37 (Sieprawska-Lupa *et al.*, 2004). Staphylokinase, which disrupts the formation of fibrin clots, also has potent defensin binding activity. It binds to defensins with a stoichiometry of approximately 1:6 and contributes to protection of bacteria *in vivo* (Jin *et al.*, 2004).

1.2.5.6 Superantigens

Clinical isolates of *S. aureus* often express several superantigens. Superantigens have the ability to bind the exterior surface of the major histocompatibility (MHC) class II protein on the surface of antigen-presenting cells and link it to T-cell receptors on the surface of a T helper cell (Proft and Fraser, 2003). Binding occurs without the requirement for the MHC class II molecule to present an antigenic peptide to a suitable T-cell receptor. Up to 30% of T-cells can become activated, leading to proliferation and massive release of cytokines which results in toxic shock, tissue damage and possible organ failure (Bone, 1994; Marrack and Kappler, 1990). Expression of superantigens in low levels can prevent development of a normal immune response (Llewelyn and Cohen, 2002). The local depletion of T-cells and failure to induce an appropriate antibody response causes immunosuppression. The binding of protein A to the V_H3 domains of IgM on B-lymphocytes also induces a similar mitogenic response. *S. aureus* also secretes numerous enterotoxins, designated SEA-O. These proteins cause stimulation of the emetic centre of the brain, hyper-stimulation of T lymphocyte proliferation and cytokine release, all resulting in staphylococcal food poisoning when such toxins are ingested (Dinges *et al.*, 2000).

1.3 Mechanism of ligand binding by staphylococcal surface proteins

1.3.1 Crystal structures of staphylococcal surface proteins

Analysis of the crystal structure of the minimum ligand-binding region of ClfA (N2N3) revealed that these domains each contain a novel variant of the immunoglobulin (Ig) fold (Deivanayagam *et al.*, 2002). Each subdomain is dominated by antiparallel β-strands with N2 and N3 each containing three short α-helices. While the primary sequence alignment of N2 and N3 domains of ClfA showed 13% amino acid identity and 36% amino acid similarity over their entire lengths, the secondary structural elements of these domains superimpose with a root mean square deviation of 0.97 Å, highlighting the near identity of their structural motifs (Deivanayagam *et al.*, 2002). The topology of the N2 and N3 subdomains of ClfA resembles that of the IgG fold whereby β-strands A, B, E, D and G, F, C are on opposite sides, respectively of the fold. In ClfA, the N2 and N3 subdomains follow the topological arrangement of the IgG fold from strands A through D, with the prominent variation occurring between strands D and E, with two additional β-strands (D' and D''). Resuming from strand E through G, the topology of N2 and N3 again conforms to the IgG fold (Deivanayagam *et al.*, 2002) (Figure 1.6). This slight variation of the IgG fold was termed a DEv-IgG fold. Searches for similar structures in the Protein Data Bank, indicated that the DEv-IgG fold could be assigned to numerous other crystal structures that were previously referred to as jelly roll barrels. Included in these structures is the collagen-binding adhesin of *S. aureus* (Cna), the receptor binding domain of α2-macroglobulin, the R domain of the diphtheria toxin, the cellulose-binding domain from the cellulosomal scaffolding protein and the Calf-1 and -2 domains of the extracellular region of the integrin $\alpha v\beta_3$. Sequence alignments of the N2 and N3 subdomains of other fibrinogen-binding MSCRAMMs of *S. aureus* indicated that the DEv-IgG fold was also likely to be present in ClfB, FnBPA and FnBPB, despite only 24% overall amino acid identity between the A domains of these four proteins. A peptide comprising the ClfA binding site within fibrinogen (C-terminal 14 residues of the γ chain) was docked *in silico* into the ClfA crystal structure. This peptide was found to dock into a hydrophobic pocket formed at the interface between N2 and N3 (Deivanayagam *et al.*, 2002). This pocket contains the glutamate and valine (E526, V527) residues previously found important for fibrinogen-binding by ClfA (Hartford *et al.*, 2001). In the ClfA-fibrinogen model, V527 was predicted to form a hydrophobic interaction with the C-terminal residue of the fibrinogen γ chain (V411) which may stabilize the complex. Other residues which were found to be in

contact with the terminal residues of the fibrinogen γ chain were targeted for amino acid substitution which led to the identification of several ClfA residues crucial in the interaction with fibrinogen such as proline 336 and tyrosine 338.

In the analysis of the crystal structure of ClfB, both N2 and N3 subdomains were deemed to contain a similar DEv-IgG fold as that of ClfA. It was also noted that the C-terminus of the N3 subdomain interacted extensively with neighbouring molecules (Deivanayagam, C. and Narayara, S., unpublished data). This had implications in the mechanism of ligand binding as discussed in Section 1.3.2.

Further insight into the structure of the A domains of staphylococcal surface proteins came with the crystallisation of the fibrinogen-binding domains of SdrG from *S. epidermidis* (Ponnuraj *et al.*, 2003). This protein was crystallised in its apo- and ligand-bound states. In the apo structure, there was a high degree of disorder observed at the C-terminus which extends out into the solvent medium. The rest of the protein adopted a fold similar to that of ClfA, with both the N2 and N3 subdomains each revealing a DEv-IgG fold as described above. In the ligand bound state, a cleft between N2 and N3 of approximately 30 Å in length was shown to accommodate the fibrinogen peptide. This peptide fits into the cleft in an extended conformation, interacting with both the N2 and N3 domains. The central region of the cleft was covered by residues 581-586 of SdrG, a segment corresponding to the loop region separating β-strands G' and G'' of N3, giving the binding region a tunnel like appearance (Ponnuraj *et al.*, 2003). A large number of contacts were identified with less than 4 Å between the SdrG protein and the fibrinogen peptide. These include interactions between both the backbone and side chains of SdrG residues with the peptide. Residues around the ligand-binding cleft predicted to be important in stabilizing the interaction were identified. Substitution of serine 338 and aspartate 339 to histidine and alanine, respectively, completely abolished the fibrinogen-binding ability of recombinant SdrG (Ponnuraj *et al.*, 2003).

In the solved crystal structure, the bound peptide contained an additional phenylalanine residue that is not present in the human fibrinogen sequence. This contaminating peptide however, had a higher affinity for SdrG than the native sequence. Similarly, it has been found that synthetic peptide analogues representing amino acid variants of the fibrinogen γ chain show higher affinity for ClfA than the native sequence (Hook, M. unpublished data). Peptides with higher affinities may aid in the co-crystallisation attempts of other *S. aureus* proteins. Thus, it is shown that structurally related MSCRAMMs containing repeated IgG like folds can accommodate linear peptides with a certain degree of sequence variability.

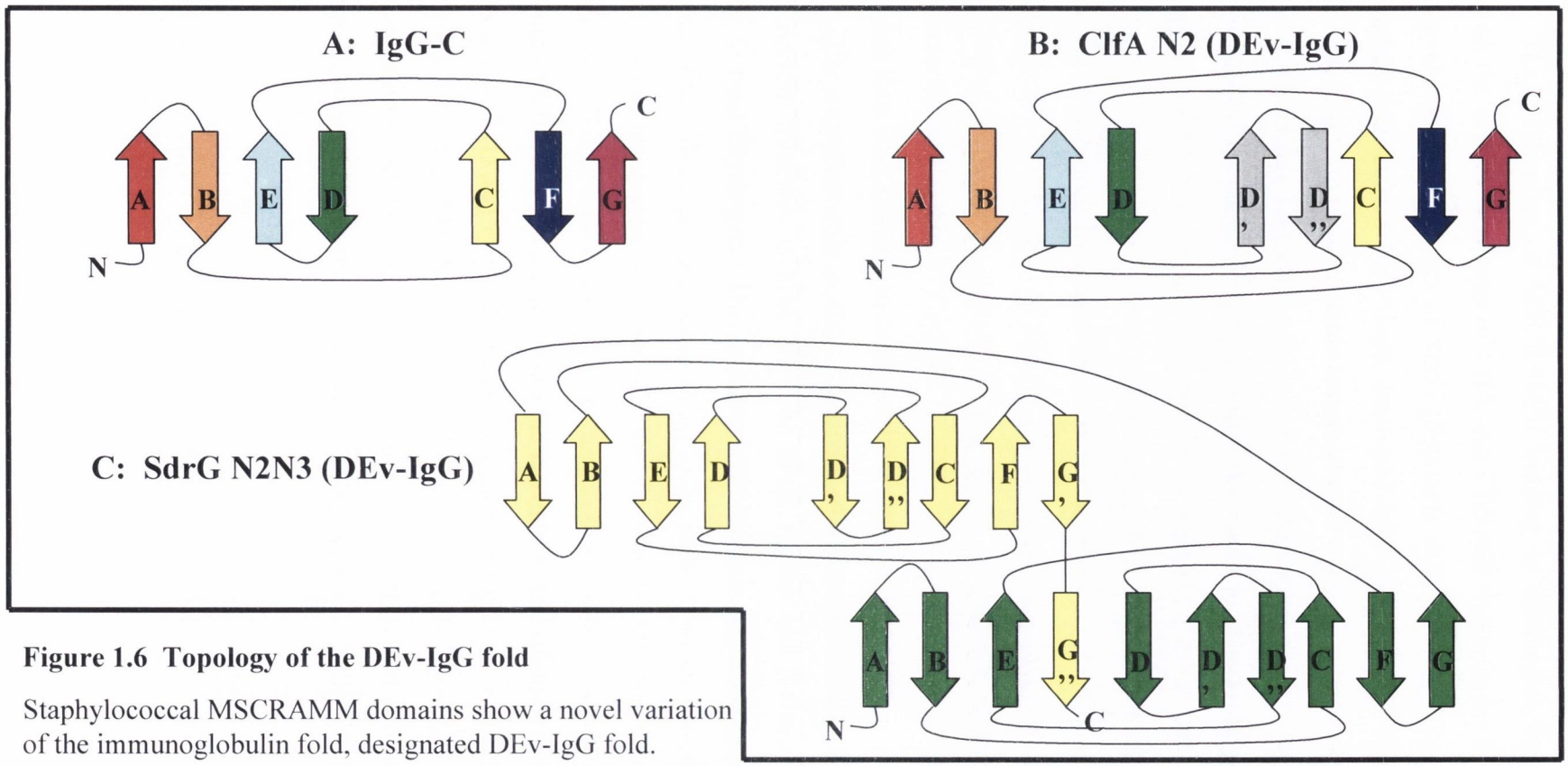

Figure 1.6 Topology of the DEv-IgG fold

Staphylococcal MSCRAMM domains show a novel variation of the immunoglobulin fold, designated DEv-IgG fold.
(A) The immunoglobulin IgG-C fold. (B) The DEv-IgG fold for the N2 subdomain of ClfA region A contains additional β-strands designated D' and D'' (coloured grey). (C) The N2 and N3 domains of the SdrG A domain each comprise a DEv-IgG fold similar to that observed for ClfA. Upon ligand binding, the latching peptide (G'') of the N3 domain (yellow) latches into the space created between strands E and D in the N2 domain (green). The β-strand complementation stabilises the SdrG-fibrinogen interaction. Nomenclature and colouration of the SdrG β-sheets and subdomains matches that of the SdrG peptide complex in Figure 1.7. Adapted from Deivanayagam *et al.*, 2002 and Ponnuraj *et al.*, 2003.

1.3.2 Proposed dynamic model of ligand binding

The mechanism of MSCRAMM binding to fibrinogen ligands has been proposed based on the crystal structures of ClfA and ClfB and in particular by analyzing both the apo and ligand-bound complexes of SdrG (Ponnuraj *et al.*, 2003). The common ligand-binding mechanism was coined the "dock, lock and latch" model. In this model, the fibrinogen peptide binds into the hydrophobic trench located between subdomains N2 and N3 (docking). Crucial interactions between residues of the fibrinogen peptide and MSCRAMM residues situated around the trench help to stabilize the binding. The hinge region between β-strands G' and G'' of N3 fastens onto the peptide by forming a cover over the hydrophobic trench (locking). This involves a structural rearrangement of the C-terminus which results in the formation of backbone hydrogen bonds between the bound peptide and the covering segment (isoleucine 581 – serine 586 of SdrG). Finally, the C-terminal β strand of N3 inserts into the cleft formed between β strands E and D of subdomain N2 and undergoes β strand complementation (latching) (Figure 1.7). This stabilizes the overall structure. The G'' strand of N3 has thus been referred to as the latching strand.

The important role of the C-terminus in fibrinogen binding by SdrG was highlighted when protein truncates lacking both the hinge region and β-strand G'' were shown to be unable to bind fibrinogen. This indicates that locking and latching events subsequent to the docking of the fibrinogen peptide are vital in the stability of the interaction. In the absence of bound ligand, the crystal structure of ClfA showed the latching strand to be in an upwards orientation. This is now suspected to be an artefact of crystallisation. In addition, the crystal structure of ClfB showed a dimer with the latching strand of one molecule located in the cleft between strands D and E of N2 of the other molecule (Figure 1.7), providing strong evidence for the dock, lock and latch model. The C-terminus of the apo-SdrG protein was also shown to be extending out into the solvent medium. The latching strand is therefore able to adopt several positions and its precise orientation in ligand-free MSCRAMMs is yet unknown.

1.4 Prevention and treatment of staphylococcal infections

S. aureus is the leading cause of surgical wound infections and hospital-acquired infections world wide. It is also responsible for a large number of community-acquired infections. Beginning with the use of the penicillin in the 1940's, drug resistance has developed in *S. aureus* within a very short time after introduction of an antibiotic into clinical use. *S. aureus* also exhibits resistance to antiseptics and disinfectants, such as quaternary ammonium compounds, which may aid its survival in the hospital environment. MRSA strains of *S. aureus* are usually resistant to a variety of different antibiotics and have emerged as significant pathogens in the community. Glycopeptide antibiotics such as vancomycin and teicoplanin are the first line treatment for MRSA isolates. *S. aureus* remained susceptible to vancomycin until recently. Clinical infections by *S. aureus* isolates harbouring the enterococcal *vanA* gene mediating high level vancomycin resistance have now been reported (Cosgrove *et al.*, 2004). There is concern at present that new antibiotics have not been forthcoming. Linelozid and quinupristin/dalfopristin are recent antibiotics that both inhibit bacterial protein synthesis and are active against MRSA isolates but instances of resistance to these agents have been documented (Hancock, 2005). The previous trend suggests that it is only a matter of time before resistance to these agents becomes widespread.

The complex immune evasion mechanisms of *S. aureus* have ensured that individuals are often prone to repeated infections. It is possible however to generate a robust antibody response to highly purified surface components of *S. aureus* and a great deal of research is focused upon developing new targets for novel anti-staphylococcal therapies and vaccines. Immunisation with staphylococcal capsule, toxins and matrix binding surface proteins have all recently been described (Clarke *et al.*, 2006; Cui *et al.*, 2005; Fattom *et al.*, 2004; Hu *et al.*, 2006; Zhou *et al.*, 2006).

1.4.1 Capsular polysaccharide vaccine - StaphVax

The expression of capsular polysaccharide by *S. aureus* inhibits phagocytosis in the presence of normal serum opsonins (Section 1.2.5.4). However, high levels of specific anti-capsular polysaccharide antibodies promote opsonophagocytosis and protect against infection (Lee *et al.*, 1997; O'Riordan and Lee, 2004; Thakker *et al.*, 1998). Capsular polysaccharide is generally poorly immunogenic but increased immunogenicity occurs with conjugation to a carrier protein (Fattom *et al.*, 1993). A bivalent vaccine comprising the most predominant

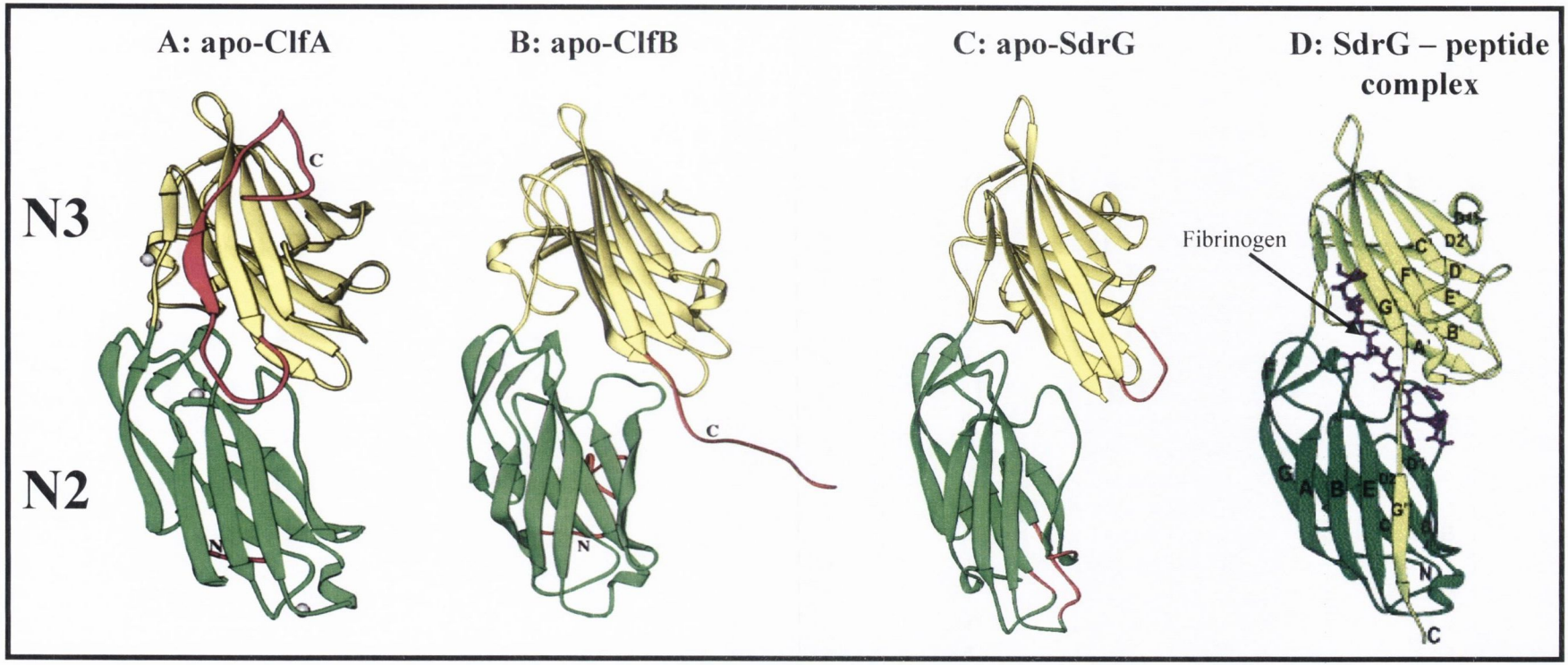

Figure 1.7 Apo structures of the N2N3 domains of ClfA, ClfB and SdrG and the SdrG-peptide complex

Ribbon representation of rAClfA$_{221\text{-}559}$, rClfB$_{282\text{-}542}$ and rSdrG$_{276\text{-}597}$. Regions of poor resolution are shown in red. Domains N2 and N3 are shown in green and yellow, respectively. (A) The C-terminus of rAClfA (latching strand shown in red) loops back and folds onto the N3 domain, partially blocking the ligand-binding trench. (B) In rClfB this strand is located in the latching cleft of another rClfB molecule. (C) In apo-SdrG the latching strand is free in solution. (D) Fibrinogen peptide in complex with rSdrG is shown in ball and stick format (taken from Ponnuraj, *et al.*, 2003). Strand designations and colours correspond to the DEv-IgG fold represented in Figure 1.6.

capsular polysaccharide serotypes (CP5 and CP8) conjugated to recombinant *Pseudomonas aeruginosa* exotoxin A (StaphVax) was developed by Nabi Inc. (Florida, USA). It has undergone Phase I, II and III clinical trials and immunisation of haemodialysis patients with StaphVax was successful in reducing the incidence of infection over an eight month period (Fattom *et al.*, 2004).

1.4.2 Immunotherapies targeting ClfA

ClfA is an important virulence factor in several animal models of infection and is expressed by 100% of invasive *S. aureus* strains (Peacock *et al.*, 2002). Both passive and active immunisation against ClfA is protective in animal models (Brouillette *et al.*, 2002; Josefsson *et al.*, 2001). High levels of anti-ClfA antibodies in serum may promote efficient phagocytosis of bacteria by neutrophils and inhibit ClfA-mediated adhesion to fibrinogen-coated surfaces.

Inhibitex Inc. (Georgia, USA) have developed a hyperimmunoglobulin, SA-IGIV (Veronate), derived from plasma donors with high titres of antibodies against ClfA and the *S. epidermidis* SdrG protein for the prevention of staphylococcal infections in very low weight neonates (Vernachio *et al.*, 2003). When used in conjunction with vancomycin, it was shown to be effective in a rabbit model of catheter-induced infective endocarditis caused by an MRSA strain (Vernachio *et al.*, 2003). Phase II trials yielded promising results in low birth weight neonates (Bloom *et al.*, 2005) but no success was achieved with Phase III trials and Inhibitex are currently reviewing all data in the Veronate clinical trial programme.

Another product in development by Inhibitex is a humanised monoclonal antibody against the fibrinogen-binding A domain of ClfA (Aurexis) (Patti, 2004). Aurexis inhibits bacterial adhesion to immobilised fibrinogen, enhances opsonophagocytosis and protects against intravenous challenge in a murine sepsis model (Hall *et al.*, 2003). Aurexis is intended for the treatment of serious *S. aureus* infections in hospitalised patients and is currently in Phase II trials.

1.4.3 Potential targets for immunotherapy

Attempts are ongoing to identify novel targets for anti-staphylococcal therapies. As nasal carriage of *S. aureus* is a risk factor for infection, studies into reducing bacterial colonisation of the nares are promising. A mouse model of nasal colonisation was used to demonstrate that *S. aureus* mutants deficient in sortase A or ClfB showed reduced nasal

colonisation. Immunisation with a recombinant vaccine composed of the A domain of ClfB exhibited lower levels of colonisation than control animals. Passive immunisation of mice with an anti-ClfB monoclonal antibody resulted in reduced nasal colonisation compared with the colonisation observed after immunisation with an isotype-matched control antibody (Schaffer *et al.*, 2006). This demonstrates that ClfB is an attractive component for inclusion in a vaccine to reduce *S. aureus* nasal colonisation in humans, which may reduce the risk of staphylococcal infection.

Vaccination of cotton rats with the iron surface determinants, IsdA or IsdH protected against nasal carriage (Clarke *et al.*, 2006). IsdA has been shown to be involved in adherence of *S. aureus* to human desquamated nasal epithelial cells and is required for nasal colonisation in the cotton rat model. Thus, vaccination with these antigens may prevent *S. aureus* carriage and reduce the prevalence of human disease. To develop a broadly protective vaccine, immunisation with four surface components of *S. aureus*, IsdA, IsdB, SdrD and SdrE, induced opsonophagocytic antibodies and afforded high levels of protection against invasive disease in a murine model of abscess formation (Stranger-Jones *et al.*, 2006). A vaccine comprising IsdB alone is highly immunogenic in rhesus macaques and resulted in increased survival in a murine *S. aureus* sepsis model (Kuklin *et al.*, 2006).

Recent studies have shown that a vaccine comprising a fusion protein of the collagen- and fibronectin-binding proteins (Cna-FnBP) showed good immunogenicity against *S. aureus* infections in a mouse model. Mice immunised with Cna-FnBP survived significantly longer following the challenge with *S. aureus* than non-immunised mice did (Zhou *et al.*, 2006). Other studies on mice vaccinated with a fusion protein containing mutant toxic shock syndrome toxin and glutathione S transferase (TSST-GST) and mice vaccinated with an *S. aureus* mutant defective in the production of two enterotoxins have shown that the survival rate of immunised group was higher and the bacterial counts in the organs were significantly lower than those of the non-immunised mice (Cui *et al.*, 2005; Hu *et al.*, 2006).

1.5 Elastin

Elastic fibres are found in the extracellular matrix of connective tissue, providing elasticity and resilience to tissues which require the ability to deform repetitively and reversibly. Fibres are organised into distinct morphologies in different tissues; small rope-like networks in lung, skin and ligament, thin concentric sheets in blood vessels and large three-dimensional honeycomb structures in elastic cartilage (Pasquali-Ronchetti and Baccarani-Contri, 1997). Elastic fibres are complex structures composed of two major components: an amorphous component consisting of the extensively crosslinked protein, elastin which makes up >90% of the fibre and a fibrillar component, the microfibrils which are rich in acidic glycoproteins and are organised into 8-16 nm fibrils of beaded appearance (Vrhovski and Weiss, 1998). The elastin protein is found in all vertebrates studied and is amongst the most hydrophobic proteins known. Although there is some species variation, elastin from higher vertebrates including humans contains over 30% glycine and approximately 75% of the entire sequence is made up of just four amino acids (glycine, valine, alanine and proline). Tissues rich in elastin include aorta and major blood vessels (28-32% dry weight), lung (3-7%), ligaments (50%), tendon (4%) and skin (2-3%) (Uitto, 1979). Mammalian tropoelastin, the soluble monomeric precursor of elastin is a moderately conserved protein consisting of alternating hydrophobic and hydrophilic (crosslinking) domains. A large amount of divergence is tolerated in the hydrophobic domains once overall hydrophobicity is maintained. The crosslinking domains, however are much more highly conserved (Boyd *et al.*, 1991).

1.5.1 Tropoelastin

A single elastin gene has been localised in the human genome to chromosome 7 (Fazio *et al.*, 1991), spanning 45 kb (Bashir *et al.*, 1989). The human gene has 34 exons with an intron:exon ratio of 20:1, indicating that relatively small exons are interspersed with large introns (Bashir *et al.*, 1989). Analysis of the gene in various species shows that hydrophobic and crosslinking domains of tropoelastin are encoded by separate exons that alternate. The human gene contains an unusually hydrophilic amino acid-encoding exon 26A which is not described in any other species. Exon 36 is highly conserved amongst species and codes for the basic C-terminus of tropoelastin in addition to a large 3' untranslated region (Indik *et al.*, 1987) (Figure 1.8 A). Expression of tropoelastin mRNA and elastic fibre synthesis is highest in foetal and infant development (Parks *et al.*, 1988). A study of elastin gene expression

during mouse lung development showed that expression increases rapidly at embryonic day 18 and reaches its highest peak at postnatal days 10-14. Levels then decrease rapidly between postnatal days 14-21 and remain low into adulthood (Mariani *et al.*, 2002). A strong correlation exists between tropoelastin mRNA levels and protein synthesis, indicating that tropoelastin expression is mainly under pre-translational control (Sephel *et al.*, 1987). The promoter region of the human gene has been analysed and found to contain both up and down-regulatory elements (Rosenbloom *et al.*, 1991). A positive transcriptional regulatory element has also been identified in exon 1 of the gene (Pierce *et al.*, 2006). The isolation of tropoelastin cDNAs shows significant variation in nucleotide sequence and size indicating alternative splicing of tropoelastin mRNA. The presence of different human tropoelastin splice variants is thought to be developmentally regulated.

Smooth muscle cells, endothelial and microvascular cells, chondrocytes and fibroblasts have all been demonstrated to synthesise tropoelastin which is secreted to the plasma membrane via secretory vesicles (Damiano *et al.*, 1981). Protein trafficking inhibitors can prevent the secretion of tropoelastin which results in the intracellular degradation of the protein by cysteine proteases (Davis and Mecham, 1996). Two major types of domain are found in tropoelastin,(a) hydrophobic domains rich in glycine, valine, alanine and proline often occurring in repeats of three to six residues such as GVGVP, GGVP and GVGVAP and (b) hydrophilic domains rich in lysine and alanine which are involved in crosslinking. These domains often consist of stretches of lysine separated by two or three alanines such as AAAKAAKAA. In general, the hydrophobic and hydrophilic domains alternate. The C-terminus of tropoelastin is highly basic and is very strongly conserved. It contains the only two cysteine residues in the entire protein and terminates with a positively-charged RKRK sequence both of which are strictly conserved (Figure 1.9). Tropoelastin is synthesised with an N-terminal 26 amino acid signal peptide and is secreted as an approximately 76 kDa protein in humans (Indik *et al.*, 1987) although there is some variation due to different isoforms. Tropoelastin undergoes very little post-translational modification and there is no evidence for glycoslyation. Deposition of tropoelastin into the extracellular space occurs only at specific regions on the cell surface and tropoelastin is then incorporated into the forming elastic fibre without any proteolysis (Bressan and Prockop, 1977). Microfibrils are secreted into the extracellular space as a molecular scaffold paving the way for the secretion of tropoelastin to be laid down in small clumps which gradually fuse to form amorphous fibres.

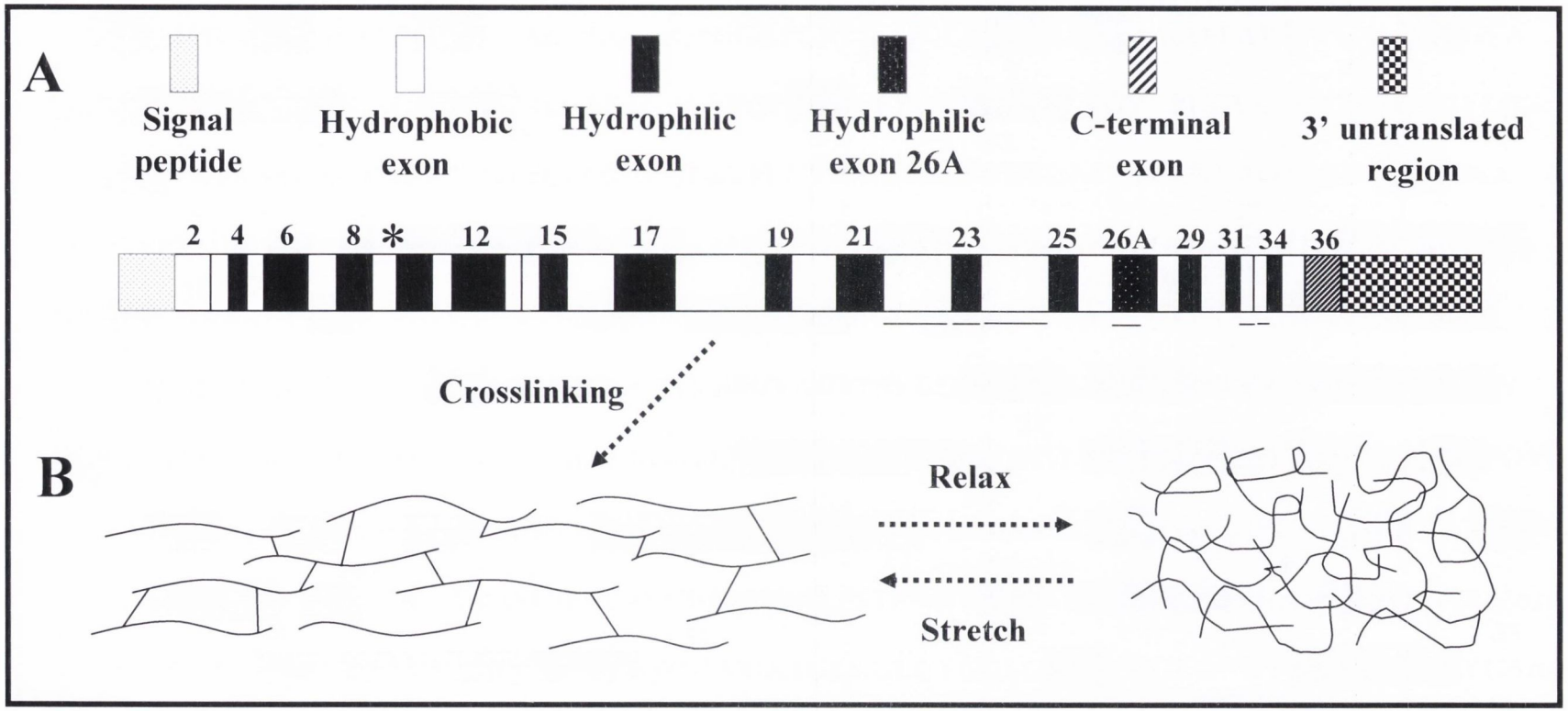

Figure 1.8 Diagrammatic structure of human elastin

(A) Domain organisation of human elastin complementary DNA. Selected exon numbers are given above the structure and lines underneath represent exons known to participate in alternative splicing. The EbpS binding site at exons 9 and 10 is shown with an asterisk. (B) Crosslinking of tropoelastin monomers results in a polymerised network of elastin capable of enduring repeated cycles of stretch and recoil.

1.5.2 Coacervation and crosslinking of tropoelastin

The initial step in elastin fibre assembly is the formation of small elastin aggregates on the cell surface (Kozel *et al.*, 2006). These aggregates then coalesce to form larger globules that are transferred to microfibrils already present in the ECM. The early organisation of tropoelastin monomers into aggregates most likely occurs through a self-association process. Tropoelastin is soluble in cold aqueous solutions of less than 20°C. However upon raising the temperature towards the physiological range the solution becomes cloudy as the tropoelastin molecules aggregate by interactions between hydrophobic domains in a process called coacervation. The process is thermodynamically controlled and can be reversed on cooling the solution. The inverse temperature phenomenon of coacervation can be explained in terms of the water molecules surrounding tropoelastin. Water molecules form hydrogen bonds and arrange themselves in an ordered configuration around the hydrophobic regions of the protein keeping it unfolded. Increasing the temperature results in breakage of the hydrogen bonds, the water molecules becoming more in contact with the surrounding water leaving the tropoelastin molecules free to fold and interact with other hydrophobic segments including those on other polypeptides forming a coacervate (Toonkool *et al.*, 2001; Urry *et al.*, 1995). The optimal conditions for coacervation are those mimicking the conditions in the extracellular matrix, 37°C, 150mM NaCl and pH 7-8. Coacervation is considered an important step in elastogenesis and is thought to both concentrate and align tropoelastin monomers prior to crosslinking.

After coacervation, tropoelastin is rapidly insolubilised by crosslink formation. The initial reaction is oxidative deamination of lysine residues in the hydrophilic domains by the enzyme lysyl oxidase to produce a δ-aldehyde called allysine (Figure 1.10 A). All subsequent reactions are spontaneous and involve the condensation of closely positioned lysine and allysine residues to produce bi- and tri- functional crosslinks such as allysine aldol, lysinonorleucine, merodesmosine and tetra-functional crosslinks unique to elastin, such as desmosine and isodesmosine (Reiser *et al.*, 1992) (Figure 1.10 B). Approximately 40 lysine residues in 16 hydrophilic domains of tropoelastin eventually participate in forming these crosslinks that help make the resulting product a polymer with reversible deformation and high resilience. Desmosine and isodesmosine are aromatic isomers (Figure 1.11 A) that are formed from three allysines and one lysine residue but only link two tropoelastin molecules (Foster *et al.*, 1974). Specific studies of elastin peptides have shown that domains 19 and 25 are linked by a desmosine crosslink while domain 10 bridges domains 19 and 25 through

lysinonorleucine crosslinks (Brown-Augsburger *et al.*, 1995) (Figure 1.11 B). Lysine residues in hydrophilic domains are in groups of two or three separated by either two or three alanine residues. These regions are likely to be α-helical and the separation of lysine by two or three alanines places the lysines near one another on the same side of the helix, resulting in a favourable conformation for desmosine/isodesmosine formation.

Lysyl oxidase is a copper-dependent, highly thermostable enzyme with a broad pH optimum. It initiates crosslink formation in both elastin and collagen (Kagan and Sullivan, 1982). When lysyl oxidase is inhibited, crosslinking is greatly reduced and tropoelastin accumulates in tissues, demonstrating the vital importance of this enzyme in elastogenesis. Nutritional deprivation of copper in humans and animals results in aberrant elastin synthesis which can lead to haemorrhage and aortic aneurysms. In fact the first purification of tropoelastin was from copper-deficient animals (Rucker, 1982; Sandberg and Wolt, 1982). The affinity of lysyl oxidase is higher for insoluble forms of tropoelastin and collagen than for monomers in solution, emphasising the importance of tropoelastin coacervation. Overexpression of lysyl oxidase has been shown to increase crosslinking and improve tissue strength and wound healing (Lau *et al.*, 2006). The enzyme has been localised to the mature elastin fibre, indicating that it may be incorporated into the growing fibre (Kagan *et al.*, 1986). Elastin monomers bind many proteins on the cell surfaces or in the ECM and specific interactions with fibrillin-1, microfibril associated glycoprotein 1 (MAGP-1), integrin αvβ3, lactadherin and matrix glycosaminoglycans have been described (Clarke and Weiss, 2004; Clarke *et al.*, 2005; Larsson *et al.*, 2006; Rodgers and Weiss, 2004; Wu *et al.*, 1999).

1.5.3 Structure of elastin

Microscopic studies of elastic fibres strongly suggest the presence of a filamentous or fibrillar structure. Transmission and scanning electron microscopy of purified elastin showed it to consist of interwoven and twisted fibrils (Gotte, 1977). In addition to crosslinking, hydrophobic interactions are thought to hold the structural units together. Elastin is proposed to be a three dimensional network of globular, regularly aligned tropoelastin molecules crosslinked with their neighbours and with themselves. The structure of each tropoelastin molecule consists of (a) rather rigid α-helical segments where the crosslinks are formed, (b) large hydrophobic domains which are responsible for the elastic properties of the polymer and whose conformation consists of β structures and undefined conformations continuously and rapidly changing and (c) a substantial amount of hydration water molecules which are tightly

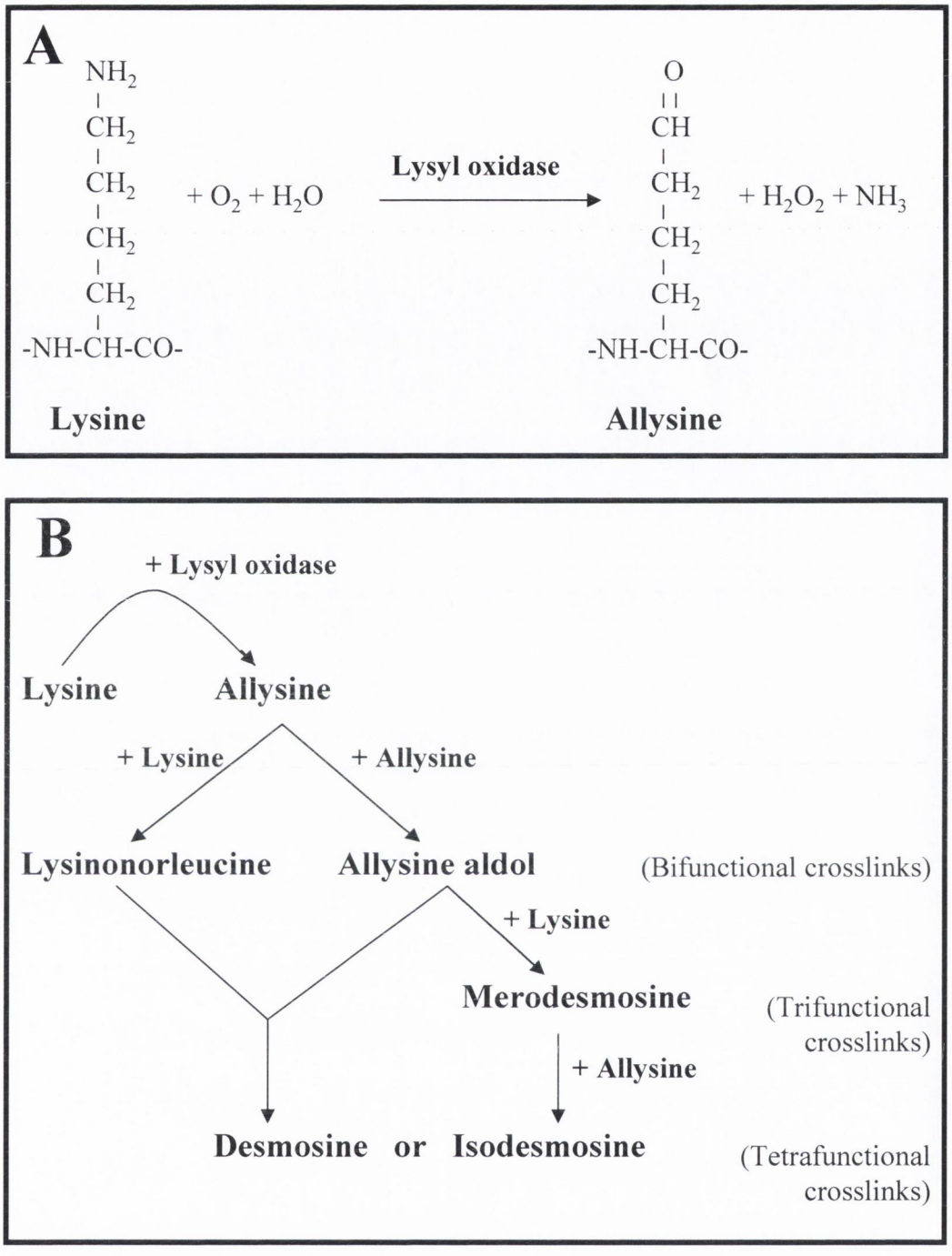

Figure 1.10 Formation of crosslinks in elastin

(A) Lysyl oxidase oxidatively deaminates a peptidyl lysine to generate a peptidyl α-aminoadipic-δ-semialdehyde (allysine). (B) Reactions of lysine in the biosynthesis of crosslinked elastin. Allysine undergoes spontaneous condensation reactions with corresponding aldehydes to form various di-, tri- or tetrafunctional cross-links. To simplify, intermediates in the reactions are not shown.

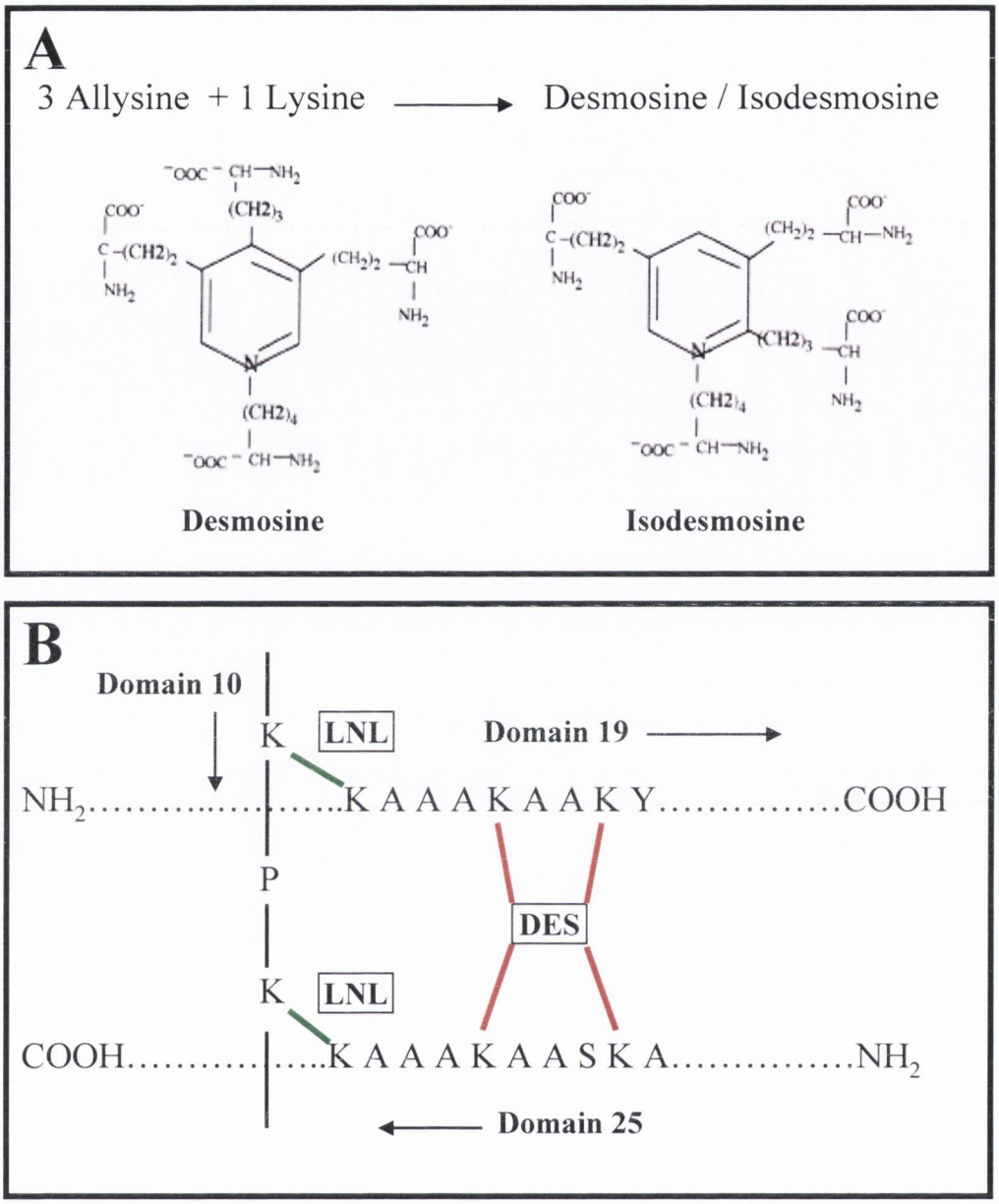

Figure 1.11 Desmosine crosslinks of elastin

(A) Desmosine and isodesmosine are rare isomeric amino acids found only in elastin and are formed by condensation of four molecules of lysine into a pyridinium ring. (B) Intramolecular crosslinking of tropoelastin. Domains 19 and 25, running antiparallel, are joined by a desmosine (DES) cross-link involving the last two lysines in domain 19 and the first two lysines in domain 25. The third lysine in each domain joins with a lysine in domain 10 to form lysinonorleucine (LNL) cross-links. Taken from Brown-Augsburger *et al*, 1995.

bound to polypeptide chains (Debelle and Alix, 1999). Dry elastin is known to be brittle while water swollen elastin is highly elastic (Gosline, 1978). In the relaxed state it appears that the elastin filaments are arranged randomly, but when the elastin fibre is stretched, filaments are orientated in the direction of the applied force showing the filamentous structure quite clearly (Figure 1.8 B). While several models for the mechanism of elasticity of elastin have been put forward, the basis of each mechanism is entropic, whereby stretching of the fibres decreases the entropy of the system and recoil is driven by a spontaneous return to maximum entropy (Gosline, 1978). Much research has been carried out into the viability of elastin biomaterials in tissue engineering. Synthetically engineered vascular replacements must incorporate an elastic component to ensure appropriate mechanical function (Patel *et al.*, 2006).

The insolubility of elastin and its resistance to many reagents has rendered it extremely difficult to study. To overcome this, two common forms of solubilised elastin are used in biological studies, namely α-elastin which is solubilised using hot oxalic acid and κ-elastin which is solubilised using potassium hydroxide. To produce α-elastin, elastic fibres are purified from human or animal tissue, boiled repeatedly in hot oxalic acid, cooled, precipitated, washed and dialysed. These elastin peptides are a heterogeneous mixture of partially crosslinked peptides with a wide molecular weight range. There is no intact tropoelastin molecule present but unique (iso)desmosine crosslinks are preserved. These peptides are used routinely in biological assays and are commercially available. Circular dichroism studies of α-elastin show high levels of disorder which increases in structural elements upon heating (Tamburro *et al.*, 1977). The elastin peptides themselves constitute an analytical challenge due to their hydrophobicity and low abundance of positively-charged amino acids which limits their efficient ionisation. Furthemore, the repetitive nature of the amino acid sequences in this biopolymer makes it difficult to assign the identified peptides to unique positions in elastin.

As tropoelastin is rapidly crosslinked *in vivo*, it does not exist in any appreciable quantities in normal animal tissues. To increase yields young animals have been raised on copper deficient diets which inhibits the crosslinking reaction of lysyl oxidase. These techniques can be very long and labour intensive and may result in some discomfort to animals as they often exhibit signs of deficiency and illness prior to sacrifice. Numerous steps are required to extract tropoelastin from tissues, including mincing, extensive salt solubilisation, coacervation, alcohol fermentation, ion exchange and gel filtration. In addition yields may be low and contamination with mixtures of splice variants often occurs. The

production of recombinant human tropoelastin in bacterial systems has greatly increased the availability of tropoelastin for biological studies. Due to the extreme amino acid usage in tropoelastin, a synthetic human tropoelastin gene has been constructed containing codons optimised for expression in *E. coli* (Martin *et al.*, 1995). Recombinant tropoelastin is a viable alternative to tissue-derived protein. It reacts with anti-elastin antibodies, is a chemotatic agent, demonstrates coacervation ability and has the same circular dichroic spectrum as naturally derived tropoelastin (Vrhovski *et al.*, 1997).

1.5.4 Diseases affecting elastic fibres

Loss of elasticity due to degradation of elastin is a major contributing factor in the ageing of connective tissues, in the development of aortic aneurysms and in lung emphysema. Various acquired and inherited diseases are known to affect the structure, distribution and abundance of elastic fibres (Table 1.1). Due to the complexity of the elastic fibre and the interplay of a variety of molecules in fibre formation, most of these diseases do not involve elastin as the primary defect, yet severely affect the elastic fibre integrity. Supravalvular aortic stenosis (SVAS) and William's syndrome have been directly linked with alterations in the elastin gene. Gene deletions and point mutations are responsible for the defects present in these conditions. Alterations of other proteins such as lysyl oxidase, elastases, microfibrillar proteins or a range of key molecules involved in elastic fibre synthesis can result in severe damage to the organ affected. It has also been shown in lung function studies that mice deficient for elastin have stunted development of airway branches and alveoli (Wendel *et al.*, 2000).

1.5.5 Degradation and repair of elastin

Insoluble elastin has a very slow turnover in normal tissues. In adult rat lung, turnover is estimated to be several years, approaching the lifetime of the animal (Dubick *et al.*, 1981). One of the reasons for this may be the high resistance of elastin to proteolytic degradation. The main group of proteases able to degrade insoluble elastin are collectively known as elastases and are generally active on a large number of substrates besides elastin. Serine elastases, which include pancreatic elastase, neutrophil elastase and cathepsin G are the most abundant elastases in mammals (Stone *et al.*, 1982). Blood monocytes also produce elastolytic matrix metalloproteases (Shapiro, 1994). An important regulator of serine elastase function, particularly in the lung, is α1-proteinase inhibitor (Shapiro, 1994).

Table 1.1 Diseases of the elastic fibre

Disease	Features
Atherosclerosis	Fragmentation of elastin in arteries, stiffness of arteries
Cutis laxa	Loose sagging skin, elastic fibre fragmentation
Emphysema	Increased compliance of lung, loss of elastin in lung
Marfan Syndrome	Widespread skeletal and cardiovascular defects, loose skin
Supravalvular Aortic Stenosis (SVAS)	Mutation in elastin gene causing narrowing of arteries, reduced elastin content, disruption of aorta architecture
William's Syndrome	Deletion of elastin gene and adjacent loci causing SVAS, mental retardation, premature ageing of skin and lax joints

Elastin degradation is important in many physiological processes such as growth, wound healing, pregnancy and tissue remodelling (Werb *et al.*, 1982). However, inappropriate and uncontrolled elastolysis can be destructive, contributing to disorders such as emphysema in the lung, atherosclerosis in arteries and cutis laxa in the skin. Increased elastolysis is also a feature of the normal ageing process demonstrating that elastin degradation can occur slowly and accumulate over a lifetime (Braverman and Fonferko, 1982). Repair of protease-damaged elastin can occur but, as with the inflexibility shown by scar tissue, does not appear to produce elastin of the same quality as when originally laid down during development. Elastic fibres are among the most difficult matrix structures to repair because of their size, molecular complexity and the requirement for numerous helper proteins. Two mechanisms of elastin repair have been described. A salvage method involves reutilisation of digested elastin peptides but the repaired elastin fibres are highly disorganised and not fully functional (Rucker and Dubick, 1984; Stone *et al.*, 1988). In contrast, another method involves *de novo* synthesis of new tropoelastin molecules which have been shown to be expressed in a rodent model of emphysema (Foster *et al.*, 1990). Soluble peptides produced by degradation of elastin with elastase have been demonstrated to increase tropoelastin mRNA levels in damaged cultures, thus acting as a feedback control mechanism serving to repair damaged tissues (Foster *et al.*, 1990). Soluble elastin peptides also cause vasodilation and are chemoattractants for monocytes, fibroblasts and neutrophils (Bisaccia *et al.*, 1994; Castiglione Morelli *et al.*, 1997; Grosso and Scott, 1993; Wachi *et al.*, 1995). Elastin fragments have been shown recently to drive disease progression in a murine model of emphysema (Houghton *et al.*, 2006). This suggests that protease degradation products derived from crosslinked material play a role in cell migration and perpetuating chronic inflammation.

Severe tissue destruction also occurs during bacterial infection. A combination of both bacterial and host components induce numerous signalling pathways resulting in inflammation and ultimate bacterial/host cell death. *S. aureus* interacts extensively with the ECM and it produces a range of extracellular proteases. During the course of an infection, both bacterial and host elastases are active. *S. aureus* is known to produce a cysteine protease, ScpB which degrades elastin tissue and a serine protease, SspA which inactivates α-1-proteinase inhibitor, a major factor which protects lungs from phagocytic proteases (Nowak and Miedzobrodzki, 1991). It has been shown recently that *S. aureus* induces multiple matrix metalloproteinases in elastin-synthesising cells such as dermal and synovial fibroblasts (Kanangat *et al.*, 2006). This would have implications in the pathogenesis of septic arthritis and soft tissue infections. The

activity of bacterial and host enzymes around the site of infection would lead to the presence of varying states of elastin tissue, in the process of being degraded or subsequently repaired. It is proposed that *S. aureus* has evolved to adapt to the conditions of its extracellular environment within host tissue and can specifically adhere to the various forms of elastin and other matrix proteins present. The fact that *S. aureus* extracellular adherence protein, Eap binds to collagen fibrils after their partial disintegration by matrix-degrading proteinases (Hansen *et al.*, 2006) (Section 1.2.4.2), shows that adherence to matrix structures by *S. aureus* can be supported by inflammatory reactions.

1.6 Rationale for this study

Elastin fibres are a major component of the extracellular matrix and play a crucial role in maintaining the structural integrity and function of many tissues. They are present in abundance in tissues that require elasticity such as the lung, skin, synovial lining of joints, heart valves and blood vessel walls, all of which are common sites for *S. aureus* infection causing pneumonia, impetigo, septic arthritis, infective endocarditis and sepsis, respectively. The invasive nature of *S. aureus* infections suggests that bacteria are likely to interact with the elastin matrix at sites of infection. Elastin is difficult to purify and is generally isolated from elastic tissue by removing all other connective tissue components by denaturing and degradation techniques to which elastin is relatively resistant. Oxalic acid is used in repeated cycles to produce soluble elastin peptides termed α-elastin. Park *et al.* (1996) demonstrated a specific interaction between the EbpS protein of *S. aureus* and soluble elastin. EbpS lacks an LPXTG sorting motif for cell wall anchoring and was shown to be an integral membrane protein with its N-terminus exposed on the cell surface, mediating binding to soluble elastin (Downer *et al.*, 2002). Adherence assays to immobilised elastin indicated that EbpS is not an MSCRAMM for elastin because an *ebpS* mutant of *S. aureus* adhered in a dose-dependent and similar manner to that of its isogenic parent (Roche *et al.*, 2004). However many clinical strains of *S. aureus* in exponential phase of growth adhere strongly to immobilised elastin. This was shown to be mediated by the fibronectin-binding proteins, FnBPA and FnBPB. An *S. aureus fnbAfnbB* mutant strain was unable to bind to immobilised elastin and this defect was complemented by overexpression of FnBPA or FnBPB from a multicopy plasmid. Subsequent molecular analysis showed that elastin bound to the A domain of FnBPA (Roche *et al.*, 2004) and further characterization of this interaction was required.

The aim of this study was to investigate the binding site(s) within the A domain of FnBPA for elastin and compare it to that for fibrinogen. This thesis examines the molecular interaction of FnBPA with both elastin and fibrinogen. Evidence for the binding of both ligands to the same site in region A of FnBPA is presented. Chapter 3 describes the specificity of the FnBPA-elastin interaction whereby inhibition of binding is achieved with soluble elastin peptides and anti-FnBPA antibodies. A minimum ligand-binding truncate of the A domain was produced which binds strongly to elastin and fibrinogen. A molecular model of the N2N3 subdomains of FnBPA was created based on the crystal structure of the equivalent domains of ClfA. C-terminal truncates of a recombinant protein spanning subdomains N2N3 shed light on the function of the latching peptide and its role in ligand binding. Finally, inhibition of bacteria expressing FnBPA binding to immobilised elastin and fibrinogen was achieved using (a) a peptide corresponding to the C-terminus of the γ chain of fibrinogen and (b) a monoclonal anti-FnBPA antibody. Chapter 4 describes the production of amino acid substituted FnBPA A domain proteins and their ability to bind antibodies and immobilised elastin and fibrinogen. Chapter 5 examines the properties of the A domain of FnBPA produced by *S. aureus* strain P1 which differs in amino acid sequence from strain 8325-4 and Chapter 6 tests the binding of region A of FnBPA and selected alanine-substituted proteins to the elastin monomer, tropoelastin.

2.1 Bacterial strains and growth conditions

Escherichia coli, *Staphylococcus aureus* and *Lactococcus lactis* strains used in this study are listed in Table 2.1. *E. coli* strains harbouring plasmids were routinely grown in L broth or L agar at 37°C supplemented with ampicillin (Amp) (100 μg/ml). *S. aureus* strains were grown in trypticase soy broth (TSB) or agar (TSA) incorporating antibiotics chloramphenicol (Cm) (10 μg/ml), erythromycin (Em) (10 μg/ml), kanamycin (Kan) (50 μg/ml) or tetracycline (Tet) (3 μg/ml) where appropriate. *E. coli* and *S. aureus* strains were routinely grown overnight in an orbital shaker at 37°C and 200 rpm. *L. lactis* strain NZ9800 was statically grown at 28°C in M17 broth or agar supplemented with 0.5% (w/v) glucose and chloramphenicol (10 μg/ml). *L. lactis* transformants were selected on M17 agar with 0.5% (w/v) glucose and chloramphenicol 5 μg/ml. Stocks of bacterial strains were made by supplementing broth cultures with 20% (v/v) glycerol and snap-freezing in liquid nitrogen.

2.2 Plasmids

All plasmids and derivatives used or constructed are listed in Table 2.2.

2.3 DNA manipulation

Standard methods were used for DNA manipulation techniques in constructing plasmids (Sambrook, 1989). Enzymes for DNA manipulation were purchased from New England Biolabs and Promega and were used according to the manufacturers' instructions. *E. coli* strains were transformed by the calcium chloride method of Sambrook (1989). All confirmatory DNA sequencing was performed by Lark Technologies.

2.3.1 Polymerase Chain Reaction (PCR)

PCR reactions were performed in 100 µl final volumes with 100 pM forward and reverse primers (Sigma Genosys), 10 ng plasmid DNA or 20 ng genomic DNA as template, 2.5 mM deoxynucleoside triphosphate (dNTPs) and 2 U *Pfu* polymerase (Promega) in a standard *Pfu* reaction buffer (Promega). Primer sequences are given in Table 2.3. Reactions typically consisted of 30 cycles with 1 min denaturation (at 95°C), 1 min annealing (temperature dependent on the primers used), and an extension step (at 72°C). 2 min were allowed per 1 kb of DNA to be amplified in the extension cycle. PCR products were purified using the High Pure PCR product purification kit (Roche) according to the manufacturers' instructions.

2.3.2 Isolation of plasmid DNA

Plasmids used in this study are listed in Table 2.2. Plasmid DNA was isolated using Promega Wizard SV Plus MiniPrep Plasmid purification kits, according to manufacturers' instructions, with the following modifications for gram-positive hosts: for *S. aureus* plasmid isolations 2 µg/ml lysostaphin (AMBI, New York) was added to the resuspension buffer, and for *L. lactis* plasmid isolations 400 µg/ml mutanolysin (Sigma) and 500 µg/ml lysozyme (Sigma) was added to the resuspension buffer, and incubated at 37 °C for 10 min to facilitate cell lysis.

Plasmids to be used for electroporation were ethanol precipitated to concentrate DNA and remove salts. Briefly, one third volume of 3 M sodium acetate (pH 5.2) and an equal volume of absolute ethanol were added to plasmid preparations, mixed thoroughly, and incubated at –70°C for at least 30 min. Precipitated DNA was pelleted at 4°C, washed with 70% (v/v) ethanol, air-dried and dissolved in water.

Table 2.1 Bacterial strains

Strain	Relevant properties	Source/Reference
E. coli		
XL-1 Blue	Highly transformable strain *recA1 endA1 gyrA96 thi-1 hsdR17 supE44 relA1 lac*(F' proAB *lacI*^{q} *ZΔM15* Tn*10* [Tet^{R}])	Stratagene
Topp 3	Protease-deficient strain. Used for recombinant protein expression Rif^{R}(F'*proAB lacI*^{q} *ZΔM15* Tn*10* [Tet^{R}]/[Kan^{R}])	Stratagene
S. aureus		
8325-4	NCTC 8325 cured of prophages	Novick, 1967
8325-4 *fnbA fnbB*	8325-4 derivative deficient in FnBPA and FnBPB. *fnbA*::Tc^{R} *fnbB*::Em^{R}	Greene *et al.*, 1995
MSSA476	Community-acquired strain from UK	Enright *et al.*, 2000
P1	Rabbit virulent strain. Strong adhesion to extracellular matrix proteins	Sherertz *et al.*, 1993
P1 *fnbA fnbB*	P1 derivative deficient in FnBPA and FnBPB. *fnbA*::Tc^{R} *fnbB*::Em^{R}	Roche *et al.*, 2004
P1 *fnbA fnbB* (pFnBA4)	P1 derivative deficient in FnBPA and FnBPB, overexpressing FnBPA from plasmid	Roche *et al.*, 2004
P1 *fnbA fnbB* (pFnBB4)	P1 derivative deficient in FnBPA and FnBPB, overexpressing FnBPB from plasmid	Roche *et al.*, 2004

Table 2.1 Bacterial strains, continued

Strain	Relevant properties	Source/Reference
L. lactis		
NZ9800	MG1363 derivative containing the nisin-sucrose conjugative transposon *Tn5276*, *ΔnisA*	Kuipers *et al.*, 1993

Table 2.2 Plasmids

Plasmid	Features	Marker(s)	Source/ Reference
pFnBA4	pSK265 derived multicopy plasmid containing entire *fnbA* gene from *S. aureus* 8325-4. Expression of FnBPA from *S. aureus*.	Cm^R	Greene *et al.*, 1995
pFnBB4	pSK265 derived multicopy plasmid containing entire *fnbB* gene from *S. aureus* 8325-4. Expression of FnBPB from *S. aureus*.	Cm^R	Greene *et al.*, 1995
pQE30	*E. coli* vector for the expression of hexa-histidine tagged recombinant proteins	Amp^R	Qiagen
pQE30 $FnBPA_{37-544}$	pQE30 derivative encoding residues 37-544 of FnBPA from strain 8325-4	Amp^R	Roche *et al.* 2004
pQE30 $FnBPB_{37-540}$	pQE30 derivative encoding residues 37-540 of FnBPB from strain 8325-4	Amp^R	Roche *et al.* 2004
pQE30 $FnBPA_{37-511}$	pQE30 derivative encoding residues 37-511 of FnBPA from strain 8325-4	Amp^R	This Work
pQE30 $FnBPA_{37-511}$ G222A	pQE30 derivative encoding residues 37-511 of FnBPA with mutations encoding the change G222A	Amp^R	This Work

Table 2.2 Plasmids, continued

Plasmid	Features	Marker(s)	Source/ Reference
pQE30 $FnBPA_{37\text{-}511}$ R224A	pQE30 derivative encoding residues 37-511 of FnBPA with mutations encoding the change R224A	Amp^R	This Work
pQE30 $FnBPA_{37\text{-}511}$ N304A	pQE30 derivative encoding residues 37-511 of FnBPA with mutations encoding the change N304A	Amp^R	This Work
pQE30 $FnBPA_{37\text{-}511}$ F306A	pQE30 derivative encoding residues 37-511 of FnBPA with mutations encoding the change F306A	Amp^R	This Work
pQE30 $FnBPA_{37\text{-}511}$ F355A	pQE30 derivative encoding residues 37-511 of FnBPA with mutations encoding the change F355A	Amp^R	This Work
pQE30 $FnBPA_{37\text{-}511}$ K357A	pQE30 derivative encoding residues 37-511 of FnBPA with mutations encoding the change K357A	Amp^R	This Work
pQE30 $FnBPA_{37\text{-}511}$ G497A	pQE30 derivative encoding residues 37-511 of FnBPA with mutations encoding the change G497A	Amp^R	This Work
pQE30 $FnBPA_{37\text{-}511}$ L498A	pQE30 derivative encoding residues 37-511 of FnBPA with mutations encoding the change L498A	Amp^R	This Work

Table 2.2 Plasmids, continued

Plasmid	Features	Marker(s)	Source/ Reference
pQE30 $FnBPA_{37\text{-}511}$ N304A/F306A	pQE30 derivative encoding residues 37-511 of FnBPA with mutations encoding the changes N304A and F306A	Amp^R	This Work
pQE30 $FnBPA_{37\text{-}511}$ T354A/N356G	pQE30 derivative encoding residues 37-511 of FnBPA with mutations encoding the changes T354A and N356G	Amp^R	This Work
pQE30 $FnBPA_{37\text{-}511}$ A415G/T417A	pQE30 derivative encoding residues 37-511 of FnBPA with mutations encoding the changes A415G and T417A	Amp^R	This Work
pQE30 $FnBPA_{194\text{-}511}$	pQE30 derivative encoding residues 194-511 of FnBPA from strain 8325-4	Amp^R	This Work
pQE30 $FnBPA_{194\text{-}509}$	pQE30 derivative encoding residues 194-509 of FnBPA from strain 8325-4	Amp^R	This Work
pQE30 $FnBPA_{194\text{-}498}$	pQE30 derivative encoding residues 194-498 of FnBPA from strain 8325-4	Amp^R	This Work
pQE30 $FnBPA_{194\text{-}483}$	pQE30 derivative encoding residues 194-483 of FnBPA from strain 8325-4	Amp^R	This Work
pQE30 $FnBPA_{194\text{-}336}$	pQE30 derivative encoding residues 194-336 of FnBPA from strain 8325-4	Amp^R	This Work

Table 2.2 Plasmids, continued

Plasmid	Features	Marker(s)	Source/ Reference
pQE30 $FnBPA_{337-511}$	pQE30 derivative encoding residues 337-511 of FnBPA from strain 8325-4	Amp^R	This Work
pBluescript::*fnbA* P1	pBluescript plasmid containing a 2.2 kb *Bam*HI-*Hin*dIII PCR-generated fragment of the *fnbA* gene from strain P1	Amp^R	Loughman, 2005
pQE30 $FnBPA_{194-511}$ (P1)	pQE30 derivative encoding residues 194-511 of FnBPA from strain P1	Amp^R	This Work
pNZ8037	Plasmid for controlled expression of heterologous proteins in *L. lactis*. *Nco*I site translationally fused to *nisA* nisin-inducible promoter	Cm^R	de Ruyter *et al.*, 1996
pNZ8037*fnbA*	pNZ8037 containing the full length *fnbA* gene, cloned from *S. aureus* 8325-4 in frame with the ATG start codon within the *Nco*I site	Cm^R	Fitzgerald *et al.*, 2006
pNZ8037*fnbB*	pNZ8037 containing the full length *fnbB* gene, cloned from *S. aureus* 8325-4 in frame with the ATG start codon within the *Nco*I site	Cm^R	Fitzgerald *et al.*, 2006

Table 2.2 Plasmids, continued

Plasmid	Features	Marker(s)	Source/ Reference
pNZ8037*fnbA*-A	pNZ8037 containing a truncated *fnbA* gene encoding an FnBPA protein lacking the BCD domains	Cm^R	Fitzgerald *et al.*, 2006
pNZ8037*fnbA*-BCD	pNZ8037 containing a truncated *fnbA* gene encoding an FnBPA protein lacking the A domain	Cm^R	Fitzgerald *et al.*, 2006
pNZ8037*fnbA* NF	pNZ8037 containing the full length *fnbA* gene incorporating the mutations encoding the changes N304A and F306A	Cm^R	This Work

Table 2.3 Primers

Primer	Sequence (5'-3')[a,b]	5' Restriction site
$FnBPA_{37}F$	CGC*GGATCC*GCATCAGAACAAAAGACAAC	*Bam*HI
$FnBPA_{194}F$	CGC*GGATCC*GGTACAGATGTAACAAGTAAAG	*Bam*HI
$FnBPA_{337}F$	CGC*GGATCC*TATAAAGATGGTATTGGG	*Bam*HI
$FnBPA_{511}R$	GACGC*GTCGAC*TTAATTTTTCTCATTTCCGTTCGC	*Sal*I
$FnBPA_{509}R$	GACGC*GTCGAC*TTACTCATTTCCGTTCGCTTTATTAC	*Sal*I
$FnBPA_{498}R$	GACGC*GTCGAC*TTATAAACCATTATCCCAAGTTAAGG	*Sal*I
$FnBPA_{483}R$	GACGC*GTCGAC*CTTATAAAGTTGCTCTGGATGTCC	*Sal*I
$FnBPA_{336}R$	GACGC*GTCGAC*TTATTTAACATCTAATTCCTTTG	*Sal*I
$FnBPA_{194}P1F$	CGC*GGATCC*GGCACAGATGTGACGAGTAAAG	*Bam*HI
$FnBPA_{511}P1R$	GACGC*AAGCTT*TAAATTCGTTCCATCACCTTTTGC	*Hin*dIII
$FnBPA_{G222A}F$	GAACCTCATGCAGCACAACGAGCGGTAC	
$FnBPA_{G222A}R$	GTACCGCTCGTTGTGCTGCATGAGGTTC	
$FnBPA_{R224A}F$	CCTCATGCAGGACAAGCAGCGGTAC	
$FnBPA_{R224A}R$	GTACCGCTGCTTGTCCTGCATGAGG	
$FnBPA_{N304A}F$	CGGCTGAACTAGAAATTGCTTTATTTATTGATCC	
$FnBPA_{N304A}R$	GGATCAATAAATAAAGCAATTTCTAGTTCAGCCG	
$FnBPA_{F306A}F$	CTAGAAATTAATTTAGCTATTGATCCTAAAAC	
$FnBPA_{F306A}R$	GTTTTAGGATCAATAGCTAAATTAATTTCTAG	
$FnBPA_{F355A}F$	GGATCGATTGAGACAGCTAATAAAGCGAATAATAG	
$FnBPA_{F355A}R$	CTATTATTCGCTTTATTAGCTGTCTCAATCGATCC	
$FnBPA_{K357A}F$	TCGATTGAGACATTTAATGCAGCGAATAATAGATTTTCGC	
$FnBPA_{K357A}R$	GCGAAAATCTATTATTCGCTGCATTAAATGTCTCAATCGA	
$FnBPA_{G497A}F$	CCTTAACTTGGGATAATGCTTTAGTTTTATACAG	
$FnBPA_{G497A}R$	CTGTATAAAACTAAAGCATTATCCCAAGTTAAGG	
$FnBPA_{L498A}F$	CTTGGGATAATGGTGCAGTTTTATACAG	
$FnBPA_{L498A}R$	CTGTATAAAACTGCACCATTATCCCAAG	
$FnBPA_{N304A/F306A}F$	CGGCTGAACTAGAAATTGCTTTAGCTATTGATCCTAAAAC	

Table 2.3 Primers, continued

Primer	Sequence (5'-3')[a,b]
$FnBPA_{N304A/F306A}R$	GTTTTAGGATCAATAGCTAAAGCAATTTCTAGTTCAGCCG
$FnBPA_{T354A/N356G}F$	AATGGATCGATTGAGGCATTTGGTAAAGCGAATAATAG
$FnBPA_{T354A/N356G}R$	CTATTATTCGCTTTACCAAATGCCTCAATCGATCCATT
$FnBPA_{A415G/T417A}F$	CGAAGAGTGTATATGGAAATGCGACAGATACTTCTA
$FnBPA_{A415G/T417A}R$	TAGAAGTATCTGTCGCATTTCCATATACACTCTTCG

[a] Restriction sites used for cloning are in italics [b] Nucleotides changed for site-directed mutagenesis are underlined

2.4 Cloning of FnBPA truncates and alanine substitutions

Gene fragments encoding FnBPA protein truncates were amplified by PCR using *Pfu* polymerase, using specific primer pairs (Table 2.3) designed to amplify the required segment of the gene from plasmid pQE30rAFnBPA$_{37\text{-}544}$ as a DNA template. Forward primers incorporated a *Bam*HI restriction site while reverse primers contained a *Sal*I restriction site.

2.4.1 rAFnBPA$_{37\text{-}511}$

The gene fragment encoding FnBPA residues 37-511 was amplified using primer pair FnBPA$_{37}$F and FnBPA$_{511}$R and plasmid pQE30rAFnBPA$_{37\text{-}544}$ as the template. *Bam*HI/*Sal*I cleaved DNA was ligated with pQE30 DNA cleaved with the same enzymes to generate plasmid pQE30rAFnBPA$_{37\text{-}511}$.

2.4.2 rAFnBPA$_{194\text{-}511}$

The gene fragment encoding FnBPA residues 194-511 was amplified using primer pair FnBPA$_{194}$F and FnBPA$_{511}$R and plasmid pQE30rAFnBPA$_{37\text{-}544}$ as the template. *Bam*HI/*Sal*I cleaved DNA was ligated with pQE30 DNA cleaved with the same enzymes to generate plasmid pQE30rAFnBPA$_{194\text{-}511}$.

2.4.3 rAFnBPA$_{194\text{-}509}$

The gene fragment encoding FnBPA residues 194-509 was amplified using primer pair FnBPA$_{194}$F and FnBPA$_{509}$R and plasmid pQE30rAFnBPA$_{37\text{-}544}$ as the template. *Bam*HI/*Sal*I cleaved DNA was ligated with pQE30 DNA cleaved with the same enzymes to generate plasmid pQE30rAFnBPA$_{194\text{-}509}$.

2.4.4 rAFnBPA$_{194\text{-}498}$

The gene fragment encoding FnBPA residues 194-498 was amplified using primer pair FnBPA$_{194}$F and FnBPA$_{498}$R and plasmid pQE30rAFnBPA$_{37\text{-}544}$ as the template. *Bam*HI/*Sal*I cleaved DNA was ligated with pQE30 DNA cleaved with the same enzymes to generate plasmid pQE30rAFnBPA$_{194\text{-}498}$.

2.4.5 rAFnBPA$_{194-483}$

The gene fragment encoding FnBPA residues 194-483 was amplified using primer pair FnBPA$_{194}$F and FnBPA$_{483}$R and plasmid pQE30rAFnBPA$_{37-544}$ as the template. *Bam*HI/*Sal*I cleaved DNA was ligated with pQE30 DNA cleaved with the same enzymes to generate plasmid pQE30rAFnBPA$_{194-483}$.

2.4.6 rAFnBPA$_{194-336}$

The gene fragment encoding FnBPA residues 194-336 was amplified using primer pair FnBPA$_{194}$F and FnBPA$_{336}$R and plasmid pQE30rAFnBPA$_{37-544}$ as the template. *Bam*HI/*Sal*I cleaved DNA was ligated with pQE30 DNA cleaved with the same enzymes to generate plasmid pQE30rAFnBPA$_{194-336}$.

2.4.7 rAFnBPA$_{337-511}$

The gene fragment encoding FnBPA residues 337-511 was amplified using primer pair FnBPA$_{337}$F and FnBPA$_{511}$R and plasmid pQE30rAFnBPA$_{37-544}$ as the template. *Bam*HI/*Sal*I cleaved DNA was ligated with pQE30 DNA cleaved with the same enzymes to generate plasmid pQE30rAFnBPA$_{337-511}$.

2.4.8 Site-directed mutagenesis of pQE30 and pNZ8037

The pQE30 expression plasmid containing the DNA sequence encoding rAFnBPA$_{37-511}$ was subjected to site-directed mutagenesis by the Quikchange method (Stratagene). Two complementary primers, each containing the desired nucleotide changes, were extended during thermal cycling, creating a mutated plasmid with staggered DNA nicks. The resulting PCR products were digested with *Dpn*I at 37°C for 1 h to remove parental methylated wild-type plasmid and then transformed into competent cells of *E. coli* strain XL-1 Blue. Transformants were screened by restriction analysis and verified by DNA sequencing. Plasmids containing the correct codon changes were further transformed into the restriction host, *E. coli* strain Topp 3 and recombinant proteins purified as described in Section 2.5.

The nisin-inducible pNZ8037*fnbA* plasmid encoding the entire FnBPA protein was also subjected to site-directed mutagenesis with primers FnBPA$_{N304A/F306A}$F and FnBPA$_{N304A/F306A}$R. Following PCR, the products were digested with *Dpn*I at 37°C for 1 h and subsequently transformed into electrocompetent *L. lactis* NZ9800 cells to yield strain NZ9800

expressing full-length FnBPA with the substitutions N304A and F306A which was used in bacterial adherence assays.

2.4.9 rAFnBPA$_{194\text{-}511}$ (P1)

The gene fragment encoding FnBPA residues 194-511 from *S. aureus* strain P1 was amplified using primer pair FnBPA$_{194}$P1F and FnBPA$_{511}$P1R and plasmid pBluescript::*fnbA* P1 as the template. *Bam*HI/*Hin*dIII cleaved DNA was ligated with pQE30 DNA cleaved with the same enzymes to generate plasmid pQE30rAFnBPA$_{194\text{-}511}$ P1.

2.5 Purification of recombinant proteins by metal chelate affinity chromatography

Recombinant domains of *S. aureus* surface associated proteins were expressed with an N-terminal hexa-histidine (His_6) affinity tag to allow high degree purification by nickel affinity chromatography. DNA encoding the region of interest was amplified by PCR and cloned into the pQE30 expression vector. pQE30 contains an isopropyl-β-D thiogalacto pyranoside (IPTG) inducible promoter to allow controlled expression of the recombinant protein and also contains sequences located 5' to the multiple cloning site that encode the 6 histidine residues. A pQE30 construct encoding residues 37-544 of FnBPA and 37-540 of FnBPB have been previously described (Roche *et al.*, 2004). Using these plasmids as templates, pQE30 derivatives containing truncated and mutated versions of the FnBP sequence were constructed using primers listed in Table 2.3. The products were cleaved with relevant restriction enzymes, ligated with pQE30 cleaved with the same enzymes and cloned into *E. coli* XL-1 Blue. All pQE30 constructs were transformed into the protease-deficient *E. coli* strain Topp 3 for large-scale protein production and purification. Cultures were grown in 6 litres L broth supplemented with ampicillin (100 μg/ml) to $OD_{600\ nm}$ of 0.5 and then induced with 1 mM IPTG for a further 4 h at 37°C. Cells were harvested by centrifugation and resuspended in 1/20 original culture volume of column binding buffer (5 mM imadazole, 0.5 M NaCl, 20 mM Tris-HCl, pH 7.9) before lysis in a French pressure cell at 1,500 psi. The lysate was centrifuged at 15000 *g* for 30 min to remove cellular debris and then filtered through a 0.45 μm Sartorius filter. A Hi-Trap ^{TM} Chelating HP column (5 ml; Amersham Pharacia) was equilibrated in binding buffer and then charged with 150 mM Ni^{2+}. The filtered cleared cell lysate was applied to the column at a flow rate of 0.5 ml/min. The column was

then washed with binding buffer at a flow rate of 1.5 ml/min until the $A_{280\ nm}$ of the eluate was <0.001. Bound protein was eluted from the column with a continuous linear gradient of imadazole (1-200 mM; total volume of 100 ml) in 0.5 M NaCl and 4 mM Tris-HCl (pH 7.9). Elution was monitored by measuring the $A_{280\ nm}$ of the eluate. Peak fractions were analysed by SDS-PAGE as described in Section 2.8.1. Ten µl of each fraction was separated through 10% acrylamide gels and visualised by Coomassie blue staining. Fractions containing the purified recombinant protein were dialysed against PBS for 16 h at 4°C.

Protein concentrations were determined either by measuring the abosrbance at 280 nm according to the Beer-Lambert law (A=E.c.l) or by using the BCA assay kit (Pierce) in accordance with the manufacturers' instructions.

2.6 Antibodies to *S. aureus* surface proteins

Polyclonal antibodies to *S. aureus* surface proteins FnBPA and FnBPB were generated by immunising rabbits with purified recombinant proteins. Preimmune sera were collected and specific pathogen free New England white rabbits were injected with 75 µg of purified $rAFnBPA_{37\text{-}544}$ and $rAFnBPB_{37\text{-}540}$ mixed 1:1 with complete Freunds adjuvant to a final volume of 1 ml. Booster injections (75 µg) mixed 1:1 with incomplete Freunds adjuvant were given at day 14 and 28. Sera were tested by Western blotting using purified recombinant rAFnBP antigen and cell surface expressed FnBPs. The immunoglobulin fraction was purified as previously described (Owen, 1985). Antibodies against ClfA were generated by immunisation with the A domain protein of ClfA ($rAClfA_{40\text{-}559}$) and were kindly provided by Dr. Judy Higgins, Trinity College. For Western blotting and dot-immunoblotting experiments, antibodies were generally diluted between 1/1000 and 1/5000 in PBS or 5% milk in TS buffer. All antibodies used in this study are described in Table 2.4.

2.7 Isolation of *S. aureus* surface proteins

Cell wall-associated proteins of *S. aureus* were isolated as previously described (Hartford *et al.*, 2001). In brief, cells from cultures of *S. aureus* were harvested by centrifugation, washed twice in PBS and adjusted to an $OD_{600\ nm}$ of 40 in 250 µl PBS. The cells were pelleted by centrifugation and resuspended in 250 µl of 20 mM Tris (pH 8.0), 10 mM $MgCl_2$ containing 30% raffinose (Sigma) in a microfuge tube. Complete ® Mini Protease Inhibitor Cocktail (Roche, 40 µl of a 10x stock) and 5 mM EDTA were added, along with 200

Table 2.4 Antibodies

Antibody	Antigen to which raised	Source
Anti-rAFnBPA	$rAFnBPA_{37-544}$	This work
1E6	$rAFnBPA_{37-544}$	Gift, Prof. P. Speziale, University of Pavia, Italy
1F9	$rAFnBPA_{37-544}$	Gift, Prof. P. Speziale, University of Pavia, Italy
1G8	$rAFnBPA_{37-544}$	Gift, Prof. P. Speziale, University of Pavia, Italy
7B7	$rAFnBPA_{37-544}$	Gift, Prof. P. Speziale, University of Pavia, Italy
7C5	$rAFnBPA_{37-544}$	Gift, Prof. P. Speziale, University of Pavia, Italy
8G8	$rAFnBPA_{37-544}$	Gift, Prof. P. Speziale, University of Pavia, Italy
11F6	$rAFnBPA_{37-544}$	Gift, Prof. P. Speziale, University of Pavia, Italy
Anti-rAFnBPB	$rAFnBPB_{37-540}$	This work
Anti-rAClfA	$rAClfA_{40-559}$	Gift, Dr. J. Higgins Trinity College, Dublin
Anti-EbpS	$rEbpS_{1-267}$	Gift, Dr. R. Downer Trinity College, Dublin
Anti-fibronectin	Human fibronectin	Gallus Immunotech
Anti-elastin	Human aortic α-elastin peptides	Elastin Products Company
Anti-fibrinogen	Human fibrinogen	Dako
Anti-histidine	Hexa-histidine	Gift, Prof. P. Speziale, University of Pavia, Italy

μg lysostaphin and the reaction was incubated at 37°C for 15 min with gentle mixing by inversion every 5 min. During this step, the cell wall-associated proteins are released due to the breakdown of the cell wall peptidoglycan by the murolytic enzymes and the formation of protoplasts occurs. The cell wall proteins were then harvested by pelleting of the protoplasts by centrifugation (10,000 x *g* for 10 min) and removal of the supernatant containing the solubilised cell wall-associated proteins, which were stored at -20°C.

2.8 Protein electrophoresis and immunoblotting

2.8.1 SDS-PAGE

Protein samples for electrophoresis by SDS-PAGE were adjusted to specific final concentrations in PBS and diluted 2-fold in final sample buffer (10% (v/v) glycerol, 5% (v/v) β-mercaptoethanol, 3% (w/v) SDS, 0.01% bromophenol blue in 62.5 mM Tris-HCl, pH 6.8). 20 μl volumes were separated by SDS-PAGE (Laemmli, 1970) using 4.5% (v/v) stacking and 10% (v/v) separating acrylamide gels. An aliquot of pre-stained protein molecular weight marker (New England Biolabs) was run on each gel. Protein samples were electrophoresed at 130 V. After separation, proteins were either visualised using Coomassie Blue stain or electroblotted onto PVDF membranes (Roche) for 1 h at 100 V using the wet transfer cell (BioRad) for detection.

2.8.2 Western immunoblotting

PVDF membranes containing electroblotted proteins were incubated in TS Tween buffer (10 mM Tris-HCl pH 7.4, 150 mM NaCl, 0.05% (v/v) Tween (Sigma)) containing 10% (w/v) skimmed milk for 16 h at 4°C to block any non-specific interactions. Primary antibodies were diluted to the required working concentration in TS Tween / 5% (w/v) skimmed milk and incubated with the membrane for 1.5 h at room temperature with shaking. Polyclonal antibodies against FnBPA and FnBPB A domains were used at a dilutions ranging from 1:1000 to 1:10000. Unbound antibody was removed by washing the membrane three times in TS buffer containing 0.05% Tween 20. The appropriate secondary antibody was diluted in TS Tween / 5% (w/v) skimmed milk and incubated with the membrane for 1.5 h with shaking. Excess secondary antibody was removed by washing three times in TS Tween buffer. The membrane was developed in the dark using the chemiluminescent substrate LumiGlo (New England BioLabs) as recommended by the manufacturer and exposed to X-Omat

autoradiographic film (Kodak). To strip antibodies from a blot that was already developed, the membrane was baked at 60°C for 30 min in 100 ml of 62.5 mM Tris HCl pH 6.8, 2% SDS, 100 mM β-mercaptoethanol. The membrane was then washed three times in TS Tween buffer and blocked again overnight in TS buffer containing 10% (w/v) skimmed milk.

2.8.3 Whole cell and recombinant protein dot immunoblotting

For whole cell dot immunoblotting, *L. lactis* cells were washed twice in PBS and adjusted to an $OD_{600\ nm}$ of 1.0 in PBS. For recombinant protein dot immunoblotting, $rAFnBPA_{37\text{-}544}$ and $rAFnBPB_{37\text{-}540}$ were diluted from 500-3.9 ng in PBS. 5 µl of each cell suspension or protein dilution to be analysed was applied to a nitrocellulose membrane (Protran, Schleicher & Schull) and allowed to dry. Membranes were blocked for 2 h in TS buffer (10 mM Tris-HCl, 0.9 % NaCl, pH 7.4) containing 10 % (w/v) skimmed milk powder (Marvel). Rabbit polyclonal anti-FnBP antibodies were diluted to a suitable concentration in 10% skimmed milk in TS buffer and incubated with the membrane for 1.5 h with shaking. Membranes were washed three times in TS buffer to remove unbound antibody. Membranes were then incubated with goat anti-rabbit antibodies conjugated to horseradish peroxidase (Dako) diluted 1:2000 in 10 % milk in TS buffer for 1.5 h. Membranes were then washed three times in TS buffer to remove unbound antibody. The membrane was developed in the dark using the chemiluminescent substrate LumiGlo (New England BioLabs) as recommended by the manufacturer and finally exposed to X-Omat autoradiographic film (Kodak).

2.9 Protease treatment of recombinant FnBP proteins

$rAFnBPA_{37\text{-}544}$ and $rAFnBPB_{37\text{-}540}$ were incubated in PBS with purified aureolysin (25 – 0.2 µg/ml) or V8 protease (100 – 0.8 µg/ml) for various times at 37°C. Reactions were stopped by addition of equal volumes of 2 x final sample buffer and placing on ice. Samples were boiled for 5 min and electrophoresed through 10% (w/v) acrylamide gels, which were subsequently stained with Coomassie blue.

2.10 Analysis of FnBPA and FnBPB expressed on the surface of *L. lactis*

2.10.1 Preparation and transformation of electrocompetent *L. lactis* NZ9800

L. lactis NZ9800 cells were made competent for DNA transformation (Wells *et al.*, 1993) by growth in 100 ml GM17 broth containing 2.5% (w/v) glycine. Cells were harvested

by centrifugation (8,300 x *g* for 10 min) and washed twice in 10 ml ice-cold 0.5 % sucrose/ 10 % (v/v) glycerol. Cells were finally resuspended in 1 ml of the same solution and kept chilled on ice. Electrocompetent cells (45 µl) were mixed with pNZ8037 DNA in a microfuge tube. DNA ligations were concentrated by ethanol precipitation and the DNA pellets resuspended in 5 µl nuclease-free H_2O before mixing with competent cells. Cell / DNA mixtures were transferred to pre-chilled 1 mm gap electroporation cuvettes (Flowgen) and electroporated using a Gene Pulsar apparatus (BioRad) with the following parameters: 2.0 kV, 200 Ω and 25 µF. Cells were immediately mixed with 950 µl recovery broth (GM17, 0.5 M sucrose, 20 mM $MgCl_2$, 2 mM $CaCl_2$), transferred to a microfuge tube, incubated on ice for 10 min and finally incubated at 30°C for 2 h. The cells were harvested by centrifugation, resuspended in 10 µl recovery broth and plated on GM17 agar incorporating 5 µg/ml Cm. Plates were incubated for 48 h at 30°C. Transformant colonies were inoculated into 3 ml GM17 containing 10 µg/ml Cm and 1.6 ng/ml nisin and grown for 16 h. Clones expressing the FnBPA-NF protein were identified by whole-cell dot immunoblotting (Section 2.8.3) or by ligand adherence assays (Section 2.11.1).

2.10.2 Induction of *L. lactis* strains carrying pNZ8037 derivatives with nisin

L. lactis NZ9800 cells carrying pNZ8037 plasmids (de Ruyter *et al.*, 1996; Kuipers *et al.*, 1993) were grown in 2 ml GM17 medium, incorporating 10 µg/ml Cm, for 16 h at 30°C. Cultures were diluted 1/100 into 5 ml fresh GM17 medium with 10 µg/ml Cm and grown to $OD_{600\ nm}$ of 0.5. Nisin (Sigma) was prepared at a stock concentration of 500 µg/ml in PBS and diluted into exponential phase cultures to the desired final concentration, typically in the range from 6.4 to 0.025 ng/ml. Induced cultures were grown at 30°C for 16 h. Cells were harvested by centrifugation, were washed twice in PBS and resuspended in 1 ml PBS. The optical density of cell suspensions ($OD_{600\ nm}$) was determined in a spectrophotometer.

2.11 Bacterial adherence assays

2.11.1 Bacterial adherence to immobilised elastin

The procedure to coat the wells of microtitre plates with elastin peptides is derived from the methods used previously (Hinek *et al.*, 1999) and has been previously described by (Roche *et al.*, 2004). Human aortic elastin was diluted in PBS and 50 µl volumes were added to the wells of microtitre plates (Povair). The elastin peptides were air dried under UV light

(366 nm) at room temperature for 18 h. Control wells contained PBS only. Plates were washed three times with PBS and remaining protein sites were blocked with TS buffer containing 5% (w/v) skimmed milk for 2 h at 37°C. *S. aureus* and *L. lactis* cultures were washed in PBS and resuspended to an $OD_{600\ nm}$ of 1 ($1x10^8$ cfu/ml). Bacterial cell adherence was measured using a nucleic acid binding probe, SYTO-13 (Molecular Probes), supplied as a 5 mM stock solution which was diluted 1:10 in 10 mM Tris-HCl (pH 7.5) to give a working solution of 0.5 mM. Washed bacterial cultures were incubated with SYTO-13 at a final concentration of 2.5 µM at room temperature for 15 min in the dark. Elastin-coated wells were washed three times with PBS and 100 µl of stained bacterial cells were added to each well and incubated in the dark at room temperature for 1.5 h. After incubation, wells were washed three times with PBS and the amount of cells bound was determined using a LS-50B fluorescent spectrophotometer with excitation at 488 nm and emission at 509 nm.

2.11.2 Bacterial adherence to immobilised fibrinogen and fibronectin

Bacterial adherence to immobilized fibrinogen and fibronectin was measured using a previously described assay (Wolz *et al.*, 1996) with a modified protocol. In brief, human fibrinogen (Enzyme Research Labs) or human fibronectin (Calbiochem or purified fibronectin, gift from Prof. P. Speziale, University of Pavia, Italy) were diluted to a specific concentration in PBS and 100 µl per well used to coat a 96-well flat bottomed plate (Sarstedt) for 16 h at 4°C. Control wells were included that only contained PBS. Wells were washed three times with 200 µl PBS and blocked with 200 µl 5% skimmed milk in TS buffer for 2 h at 37°C. The wells were washed three times with PBS and 100 µl washed bacterial cells in PBS ($OD_{600\ nm}$ of 1.0) were added. The plates were incubated at 30°C for 2 h. Non-adherent cells were removed by washing the wells three times with PBS and adherent cells were fixed using 100 µl 25% (v/v) formaldehyde per well for 15 min. The wells were washed three times in PBS and the adherent cells stained with 100 µl 0.5% (w/v) crystal violet per well for 1 min. The wells were extensively washed in PBS to remove excess stain. Cell-bound crystal violet was solubilised using 100 µl 5% (v/v) acetic acid per well and the plates gently shaken. Plates were then read after 5 min in an ELISA plate reader (Multiskan EX, Labsystems) at 570 nm.

Adherence graphs shown throughout this thesis are graphs of individual experiments that are representative of three independent experiments. Error bars shown in such graphs represent the average of triplicate wells, unless otherwise stated.

2.12 ELISA assays

2.12.1 Antibody ELISA

rAFnBPA, diluted to various concentrations in PBS, was coated onto microtitre plates (Sarstedt) in 100 µl volumes and kept at 4°C overnight. All wells were subsequently blocked with 5% skimmed milk in TS buffer for 2 h at 37°C. After washing three times with PBS supplemented with 0.05% Tween 20, various dilutions of polyclonal or monoclonal anti-rAFnBP antibodies were incubated in the wells for 1 h at room temperature. After three washes with PBS / Tween 20, a 1:2000 dilution of goat anti-rabbit HRP conjugated antibodies was added to the wells and the plate was incubated for 1 h at room temperature. After three further washes with PBS / Tween 20, bound HRP-conjugated antibodies were detected by the addition of 100 µl of 3,3',5,5'-tetramethylbenzidine (TMB) (0.1 mg/ml) (Sigma) prepared in 0.05 M phosphate citrate buffer containing 0.006% (v/v) hydrogen peroxide. Plates were then incubated at room temperature for 10 min. The reaction was stopped by the addition of 50 µl of 2 M H_2SO_4 to each well. Plates were read at 450 nm using an ELISA plate reader.

2.12.2 Ligand ELISA

Fibrinogen and fibronectin (10 µg/ml in PBS) were coated onto microtitre plates (Sarstedt) in 100 µl volumes and kept at 4°C overnight. Elastin (10 µg/ml in PBS) was immobilised onto microtitre plates (Nunc-Immuno^{TM} MaxiSorb^{TM}) in 50 µl volumes. The elastin peptides were air dried under UV light (366nm) at room temperature for 18 h. All wells were subsequently were blocked with 5% skimmed milk in TS buffer for 2 h at 37°C. After washing three times with PBS supplemented with 0.05% Tween 20, purified recombinant protein diluted to various concentrations in PBS was added and plates were incubated for 1 h at room temperature. The plate was again washed in PBS / Tween 20 and bound protein was detected by incubation with a 1:2000 dilution of polyclonal anti-rAFnBP antibodies for 1 h at room temperature. After three washes with PBS / Tween 20, a 1:2000 dilution of goat anti-rabbit HRP conjugated antibodies was added to the wells and the plate was incubated for 1 h at room temperature. After three further washes with PBS / Tween 20, bound HRP-conjugated antibodies were detected by the addition of 100 µl of 3,3',5,5'-tetramethylbenzidine (TMB) (0.1 mg/ml) (Sigma) prepared in 0.05 M phosphate citrate buffer containing 0.006% (v/v) hydrogen peroxide. Plates were then incubated at room temperature

for 10 min. The reaction was stopped by the addition of 50 µl of 2 M H_2SO_4 to each well. Plates were read at 450 nm using an ELISA plate reader.

ELISA-type binding graphs shown throughout this thesis are graphs of individual experiments that are representative of three independent experiments. Error bars shown in such graphs represent the average of triplicate wells, unless otherwise stated.

2.13 Inhibition assays

2.13.1 Inhibition of bacterial adherence to immobilised ligands with soluble inhibitor

Elastin- and fibrinogen/fibronectin-coated wells of microtitre plates were prepared as described in Section 2.11.1 and 2.11.2, respectively. Plates were washed three times with PBS and remaining protein sites were blocked with 5% (w/v) skimmed milk in TS buffer for 2 h at 37°C. Meanwhile, doubling dilutions of inhibitor (anti-fibronectin antibodies, anti-rAFnBP antibodies, fibrinogen γ chain peptides or monoclonal anti-FnBPA antibodies) were prepared in PBS and aliquoted into microfuge tubes. Bacterial cultures were washed in PBS and resuspended to an $OD_{600\ nm}$ of 2 ($2x10^8$ cfu/ml). Equal volumes of bacterial suspension were added to the various dilutions of inhibitor and the resulting mixtures were preincubated for 1h at room temperature. These solutions were added to the washed ligand-coated wells in 100 µl volumes and incubated for 1h at room temperature. The plate was again washed in PBS and adherent bacteria were detected by crystal violet (fibrinogen/fibronectin) or SYTO-13 (elastin) staining as described earlier. Fibrinogen- and fibronectin-coated plates were read at 570 nm using an ELISA plate reader and elastin-coated plates were measured using an LS-50B fluorescent spectrophotometer with excitation at 488 nm and emission at 509 nm.

2.13.2 Inhibition of recombinant protein binding to immobilised ligands with soluble inhibitor

Elastin- and fibrinogen-coated wells of microtitre plates were prepared as described in Section 2.11.1 and 2.11.2, respectively. Plates were washed three times with PBS and remaining protein sites were blocked with 5% (w/v) skimmed milk in TS buffer for 2 h at 37°C. Meanwhile, doubling dilutions of inhibitor (soluble elastin peptides, soluble fibrinogen, fibrinogen γ chain peptides and soluble desmosine/isodesmosine) were prepared in PBS and aliquoted into microfuge tubes. rAFnBPA and rAFnBPB proteins were diluted to a final concentration and equal volumes were added to the inhibitor dilutions. The resulting mixtures

were preincubated for 1h at room temperature. These solutions were added to the washed ligand-coated wells in 100 µl volumes and incubated for 1 h at room temperature. The plate was again washed in PBS and bound protein was detected by incubation with a 1:2000 dilution of polyclonal anti-rAFnBP antibodies for 1 h at room temperature. After three washes with PBS, a 1:2000 dilution of goat anti-rabbit HRP conjugated antibodies (Dako) was added to the wells and the plate was incubated for 1 h at room temperature. After three further washes with PBS, bound HRP-conjugated antibodies were detected by the addition of 100 µl of 3,3',5,5'-tetramethylbenzidine (TMB) (0.1 mg/ml) (Sigma) prepared in 0.05 M phosphate citrate buffer containing 0.006% hydrogen peroxide. Plates were then incubated at room temperature for 10 min. The reaction was stopped by the addition of 50 µl of 2 M H_2SO_4 to each well. Plates were read at 450 nm using an ELISA plate reader (Multiskan EX, Labsystems).

2.14 *In silico* analysis of ligand binding by *S. aureus* surface proteins

2.14.1 Generation of a 3D structural model for the N2N3 domains of FnBPA

A theoretical model of the structure of subdomains N2 and N3 of region A of FnBPA was obtained by submitting the amino acid sequence for this segment of the protein to the Protein homology recognition engine (Phyre) service of the 3D-PSSM website (http://www.sbg.bio.ic.ac.uk/phyre/) which models the structure of this sequence based on the known crystal structures of similar proteins. The resulting hits are scored based on the estimated precision of the prediction. The highest score for the N2N3 domains of FnBPA is a structure based on the equivalent domains of the apo form of *S. aureus* clumping factor ClfA. The accuracy of the structural prediction was estimated by the Phyre programme to be very high (e 1.2^{-33}). The second highest hit for the submitted sequence was a model of N2N3 of FnBPA based on the ligand-bound complex of an *S. epidermidis* fibrinogen-binding protein called SdrG. The pdb files supplied by the Phyre service were downloaded and viewed using the Chimera molecular modeling software package freely available from the University of California, San Francisco, UCSF (http://www.cgl.ucsf.edu/chimera/).

2.14.2 Docking of a fibrinogen ligand into the structural model of FnBPA

A fibrinogen ligand (C-terminal 8 amino acid peptide of the γ chain of fibrinogen, $G_{404}AKQAGDV_{411}$) was synthesized *in silico* using Sybyl 6.91 and docked into the predicted

3D structure of FnBPA using Autodock. The Autodock programme (http://autodock.scripps.edu/) is designed to predict how small molecules such as drug candidates or peptide ligands bind to a given receptor. This programme has been widely used, is fast and provides high quality predictions. A study on the reliability of the results obtained with Autodock concluded that the programme is successful in predicting protein-ligand complexes (Hetenyi and van der Spoel, 2002). The most energetically favourable docking solution for the peptide binding into the hydrophobic trench was chosen to study the interaction of FnBPA residues likely to be in contact with fibrinogen.

2.14.3 Viewing ClfA and SdrG crystal structures

The published crystal structures of the apo form of ClfA and the apo and ligand-bound form of SdrG were downloaded from the National Centre for Biotechnology Information (NCBI) website and viewed using the Chimera molecular modelling software package. The Protein Data Bank accession numbers for the ClfA, apo SdrG and ligand-bound SdrG are 1N67, 1R19 and 1R17, respectively. Files for downloading the Chimera software package and viewing the FnBPA N2N3 molecular model are available as supplementary material on a CD accompanying this thesis.

2.15 Circular Dichroism (CD) Spectroscopy

Circular dichroism spectroscopy was performed as previously described (Hartford *et al.*, 2001). Briefly, rAFnBPA$_{37\text{-}511}$ wild-type, N304A, F306A and N304A/F306A protein samples were dialysed overnight into 1 mM Tris-HCl pH 7.4. Far UV CD data were collected using a Jasco J-810 spectropolarimeter in a 0.5 mm path length cuvette at room temperature. Five scans were averaged for each spectrum and the contribution from buffer subtracted in each case. The mean residue elipticity (θ_{MWR}) was expressed in degrees·cm^2/dmol and all CD data were plotted against wavelength in the range 200-300 nm.

2.16 Surface Plasmon Resonance (SPR)

2.16.1 Surface Plasmon Resonance Analysis of Molecular Interactions

Kinetic analysis of the binding between tropoelastin and rAFnBPA proteins was examined using surface plasmon resonance (SPR). The Biacore 3000 system was used for this study (Biacore AB, Sweden). Full-length human tropoelastin was immobilized onto the

surface of a CM5 research-grade sensor chip using amine coupling. This was performed using 1-ethyl-3-(3-dimethylaminopropyl) carbodiimide hydrochloride (EDC), followed by N-hydroxysuccinimide (NHS) and ethanolamine-HCl, as described by the manufacturer. Tropoelastin protein was dissolved in 10 mM sodium acetate at pH 5.0 and then immobilized on the chip at a flow rate of 30 µl/min in HBS-Ca buffer (10 mM HEPES pH 7.2, 0.2 M NaCl, 1 mM $CaCl_2$, 0.005% Tween 20). This gave a response level of 4500 response units (RU). On a single flow cell, the dextran matrix was treated as described above but without tropoelastin present to provide a blank flow cell for these studies. All sensorgram data presented were subtracted from the corresponding data from the blank cell. The response generated from injection of buffer over the chip was also subtracted from all sensograms.

2.16.2 Surface plasmon resonance analysis of rAFnBPA$_{194-511}$, rAFnBPA$_{37-511}$ wt and rAFnBPA$_{37-511}$ site-directed mutants binding to tropoelastin

Sensograms were obtained for rAFnBPA proteins binding to immobilized tropoelastin using HBS-Ca buffer. rAFnBPA$_{194-511}$, rAFnBPA$_{37-511}$ wt and rAFnBPA$_{37-511}$ site-directed mutants were prepared by doubling dilutions in HBS-Ca to concentrations starting at 800 nM. These concentrations were injected for 8.33 min at a flow rate of 30 µl /min. Regeneration was performed after 30 min of dissociation using 1 M NaCl, 0.05 M NaOH and 10 mM glycine for 2 min. A typical experiment used 10 rAFnBPA protein concentrations and a control containing no rAFnBPA, followed by a regeneration step that was measured successful when the baseline returned to zero.

Rate constants for association (k_a) and dissociation (k_d) and the equilibrium dissociation constant (K_D) were obtained by globally fitting the data using the BIAevaluation software version 3.0 using the simple 1:1 Langmuir binding model. This method was preferred as the equilibrium binding state was not reached. All experiments were performed in triplicate. Statistical analysis of the curve fitting at both dissociation and association phases of the sensograms showed χ^2 values of less than 3.5 for k_d and less than 10 for k_a.

2.17 Statistical analysis

The statistical significance of differences between repeated experiments was determined by the Student t-test, using the online GraphPad software. Differences were considered significant if p-values were less than 0.05.

3.1 Introduction

S. aureus is a very important and versatile human pathogen. Much research has been focused on the virulence factors that are important in the initiation of staphylococcal infections which depend on the ability of the bacterium to adhere to the host's extracellular matrix (ECM) via surface-expressed ligand-binding proteins termed Microbial Surface Components Recognising Adhesive Matrix Molecules (MSCRAMMs). The interaction between *S. aureus* and elastin has been studied in some detail. It was reported previously that soluble ^{125}I-labelled α-elastin peptides from bovine ligament and ^{125}I-labelled recombinant tropoelastin, the monomeric precursor of elastin, bound specifically to *S. aureus* cells (Park *et al.*, 1991) and that this was mediated by the elastin-binding protein EbpS (Downer *et al.*, 2002; Park *et al.*, 1996). Binding experiments with an *ebpS* mutant of *S. aureus* strain Newman indicated that EbpS is the dominant factor for binding soluble elastin but bacteria possess a second elastin-binding moiety (Downer *et al.*, 2002). Subsequently, *S. aureus* strain P1 wild-type (Sherertz *et al.*, 1993) and an isogenic *ebpS* mutant were both shown to adhere in a dose-dependent manner to immobilised elastin peptides (Roche *et al.*, 2004). There was no significant difference in immobilised elastin-binding activity of the two strains, indicating that EbpS has no function in the adherence of *S. aureus* strain P1 to immobilised elastin and is thus not a true MSCRAMM.

In order to identify the protein responsible for bacterial adherence to immobilised elastin, cells from *S. aureus* strains Newman, P1, 8325-4, COL, MSSA476, EMRSA252, Cowan and RN4220 in both exponential and stationary phase of growth were tested previously for adherence to immobilised bovine elastin (Roche *et al.*, 2004). Strains Newman, 8325-4, COL, EMRSA252 and RN4220 all bound poorly to immobilised elastin peptides in both exponential and stationary phase. Of the laboratory strains tested, strains P1 and Cowan promoted strong adherence to immobilised elastin peptides in exponential phase only with no adherence detected with cells from the stationary phase of growth. Of the clinical strains tested only exponential phase cultures of strain MSSA476, a virulent strain isolated from community-acquired infections in the UK (Enright *et al.*, 2000), adhered strongly. Adherence to immobilised elastin was thus a feature of cells from the exponential phase of growth.

While an *ebpS* mutant of strain P1 had no adverse effect on adherence to immobilised elastin, a P1*fnbAfnbB* mutant was shown to be completely defective when compared to the parental P1 wild-type strain (Roche *et al.*, 2004). Thus the factors responsible for *S. aureus*

adherence to immobilised elastin are the fibronectin-binding proteins FnBPA and FnBPB. Expression of the *fnbA* and *fnbB* genes of *S. aureus* occurs in early exponential phase of growth with little or no FnBP protein detectable on the surface of cells from stationary phase cultures. This corresponds with the binding profile mentioned above whereby elastin-binding ability is lost as cultures of strain P1, Cowan and MSSA enter stationary phase.

In a previous study to investigate the site of the elastin-binding moiety within FnBPA, cells from an exponential phase culture of strain P1*fnbAfnbB* (pFnBA4), expressing the FnBPA protein from a multicopy plasmid, were preincubated with soluble human fibronectin (100 μg/ml). The ability of these cells to bind to immobilised human fibronectin and elastin peptides was tested. Preincubation of cells with soluble fibronectin resulted in a 76% inhibition of binding to immobilised fibronectin. Conversely, preincubation with soluble fibronectin did not inhibit binding to human aortic elastin (Roche *et al.*, 2004). This led to the conclusion that the elastin-binding site of FnBPA is not contained within the fibronectin-binding domains at the C-terminus of the molecule. In accordance with this, a recombinant protein encompassing region A plus the B repeats of FnBPA was shown to inhibit the adherence of strain P1*fnbAfnbB* (pFnBA4) to immobilised elastin. This gave strong indications that region A of the fibronectin-binding proteins supported adherence of *S. aureus* to immobilised elastin but further confirmation was needed using recombinant region A alone and specific anti-region A antibodies.

Studies of staphylococcal MSCRAMMs and their ligands are complicated by functional redundancy caused by the presence of several multi-functional ligand-binding proteins present on the surface of the cell. For this reason, a simpler system was needed without the complicating factors of competing ligand-binding surface proteins. Previous studies (Fitzgerald *et al.*, 2006; Loughman *et al.*, 2005) showed the benefits of expressing staphylococcal surface proteins such as ClfA and FnBPA on the surface of *Lactococcus lactis* strain NZ9800. *L. lactis* acts as a surrogate host, expressing the desired staphylococcal ligand-binding protein in isolation on the surface of the cell. In the nisin-inducible expression vector pNZ8037 the *nisA* promoter drives expression of the protein under investigation which has been translationally fused to the ATG codon and ribosome binding site provided by the vector. The levels of protein present on the cell surface can be thus be controlled by supplementing the growth medium with increasing amounts of exogenous nisin. This provides a tightly controlled, clean system for studying the role of individual staphylococcal surface proteins in binding to host ligands.

S. aureus produces four major extracellular proteases (Section 1.2.4.4), staphylococcal serine protease (V8 protease) (SspA), a metalloprotease named aureolysin (Aur) and two cysteine proteases ScpA and SspB. Proteases are generally negatively regulated by SarA and positively regulated by RNAIII as cells progress from exponential to post-exponential phase. This co-ordinated protease expression coincides with the decreased production of surface proteins and aids in the transition between the colonisation and invasive stages of *S. aureus* infections. It is also known that proteases directly cause the degradation and subsequent loss of ligand-binding cell wall proteins such as FnBPA (McGavin *et al.*, 1997). Previous studies have noted that the V8 serine protease is the most significant protease for degrading the FnBPs (Karlsson *et al.*, 2001).

ClfA is a well characterised fibrinogen-binding protein of *S. aureus*. The crystal structure of N2N3 of ClfA has been solved (Deivanayagam *et al.*, 2002) and has revealed that each subdomain is similarly folded into a variant of the immunoglobulin motif, termed a DE-variant or DEv-IgG fold (Section 1.3.1). The primary sequence alignment of the N2 and N3 subdomains shows 13% amino acid identity and 36% amino acid similarity, respectively, over their entire lengths. However, their secondary structure shows near identity in the topology of the β-strands comprising each domain. A fibrinogen γ chain peptide was docked *in silico* into the crystal structure of ClfA to aid in the understanding of the mechanism of ligand binding. This hypothesised that the fibrinogen ligand docked into the hydrophobic trench situated between N2 and N3. Residues of ClfA situated around this trench that were vital to fibrinogen binding were thus identified.

Subsequently, the crystal structure of another staphylococcal fibrinogen-binding surface protein (SdrG) was solved both in isolation and in complex with its fibrinogen ligand, the N-terminus of the β chain. The fibrinogen ligand was situated in the hydrophobic trench between N2 and N3. The open and closed complex showed differing structures with regard to the C-terminal β-strand. This led to a hypothesis of ligand binding which has been coined the "dock, lock and latch" model (Ponnuraj *et al.*, 2003). In this model, the fibrinogen peptide docks into the binding pocket between N2 and N3. In response to this, the G'' β-strand (latching peptide) of N3, folds over the ligand-occupied trench, securing fibrinogen in place and latches into a groove situated in N2 whereby β-strand complementation can occur between the G'' and E β-strands (Section 1.3.2). The position of the latching peptide observed in the crystal structure of ClfA is now thought to be an artefact of crystallisation as the latching peptide of the open complex of SdrG is shown to be extending away from the molecule

(Figure 3.1). The crystal structure of the apoprotein of ClfB N2N3 has also been studied (Deivanayagam and Narayara, S., unpublished data). In this case, the cleft between the D and E β-strands of N2 is occupied by the C-terminal latching peptide of a crystallographically neighbouring molecule. This shows how the sequence of the latching peptide is capable of forming β-strand complementation with residues situated in the E strand of N2. Sequence alignment of the N2N3 regions of four fibrinogen-binding MSCRAMMs of *S. aureus* (ClfA, ClfB, FnBPA and FnBPB) has indicated a similar domain arrangement. The fact that FnBPA binds to the same region of fibrinogen (C-terminus of the γ chain) as ClfA indicates that the two proteins may have a similar mechanism of binding. The aim of this project was to understand the mechanism of FnBP-fibrinogen binding based on previous work carried out with other staphylococcal fibrinogen-binding proteins. In doing so, the mechanism of elastin binding could be investigated to understand if these two diverse human matrix proteins could bind in a similar manner to FnBPA.

In this chapter, ligand binding by FnBPA and FnBPB expressed on the bacterial cell wall surface, as well as truncates of recombinant FnBPA and FnBPB is assessed. Recombinant derivatives of region A of FnBPA and FnBPB were produced and tested for their stability to heat, V8 serine protease and aureolysin as well as for their ability to bind immobilised elastin and fibrinogen in ELISA type assays. The proteins were also used to raise polyclonal anti-FnBP specific antibodies which were tested in inhibition studies with FnBPA-expressing bacteria. A 3D structural model of the N2N3 domains of FnBPA was created based on the known crystal structure of the corresponding domains of ClfA. This model gave an insight into the possible mechanism of fibrinogen/elastin binding and was used to design truncates of FnBPA lacking C-terminal residues. In this way, the role of amino acids putatively involved in the latching peptide of FnBPA was investigated. Finally, in order to ascertain if fibrinogen and elastin bound to FnBPA at similar or overlapping sites, inhibitors of the FnBPA-fibrinogen interaction were tested for their effects on elastin binding.

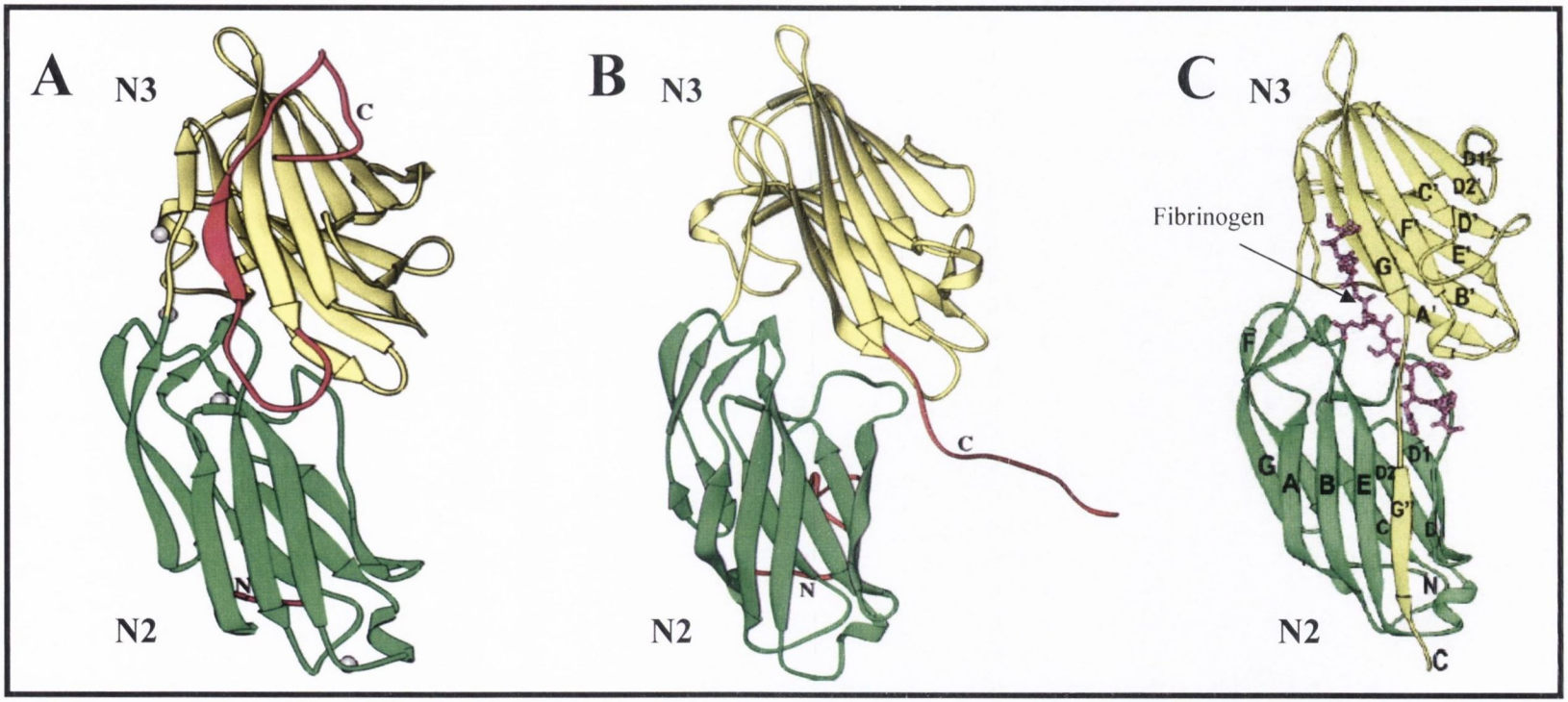

Figure 3.1 Ribbon diagram representation of the structure of ClfA, ClfB and SdrG N2N3 proteins

(A) The apo structure of N2N3 of ClfA. The C-terminal latching peptide (red) loops back and folds onto the N3 subdomain. (B) The apo structure of N2N3 of ClfB showing the extended conformation of the latching peptide (red) in the absence of fibrinogen. (C) The ligand bound complex of N2N3 of SdrG showing the position of the fibrinogen chain (purple) and the β-strand complementation occurring between the latching peptide and the E strand of N2. Taken from Ponnuraj *et al.*, 2003.

3.2 Results

3.2.1 *S. aureus* adheres to immobilised elastin peptides

Strain P1 was previously shown to bind immobilised elastin from three separate sources (Roche *et al.*, 2004). Human aortic elastin is prepared by repeated boiling of elastic tissue in hot oxalic acid (Partridge and Davis, 1955; Partridge *et al.*, 1955), human lung elastin is prepared by digestion with human sputum elastase (Starcher and Galione, 1976) while bovine ligament elastin is a sodium hydroxide solubilised form of insoluble elastin. To assess the ability of a clinical strain of *S. aureus* to bind to these three different types of elastin, exponential cultures of strain MSSA476 were washed, resuspended to $OD_{600\ nm} = 1$ and added to microtitre plates coated with human aortic elastin, human lung elastin and bovine ligament elastin. The cells from strain MSSA476 adhered in a dose-dependent manner to both human and bovine elastins with greater adherence observed to the human elastins (Figure 3.2). Due to the strong adherence of *S. aureus* strains to immobilised human aortic elastin, this form of elastin was used in all subsequent analysis of the interactions of FnBPs with elastin.

Due to regulatory defects, *S. aureus* strain 8325-4 expresses relatively low levels of surface proteins such as FnBPA and FnBPB compared to many clinical isolates (Peacock *et al.*, 1999). To study elastin binding by two different strains, cultures of strains 8325-4 wt (Novick, 1967), 8325-4 *fnbAfnbB*, P1 wt and P1 *fnbAfnbB* were grown to exponential and stationary phase before being washed and resuspended to $OD_{600\ nm} = 1$. Equal volumes of cells were added to elastin-coated wells for 1 hr and subsequently stained with crystal violet. Exponential phase cultures of 8325-4 wild-type did not adhere to immobilised elastin peptides (Figure 3.3). Only exponential phase cultures of strain P1 wt adhered to immobilised elastin with stationary phase cultures of the same strain unable to bind. This demonstrates the growth-phase dependence of elastin adherence which has been previously reported (Roche *et al.*, 2004). These data also confirm that *S. aureus* adherence to elastin is FnBP-dependent as binding did not occur with strain P1*fnbAfnbB*.

To study the effects of individual FnBPA and FnBPB proteins strain P1*fnbAfnbB* was previously complemented with a multicopy plasmid harbouring the *fnbA* or *fnbB* gene from strain 8325-4. Strain P1*fnbAfnbB* complemented with FnBPA or FnBPB both bound strongly to immobilised human aortic elastin in a dose-dependent manner (Figure 3.4) which confirms previously published data (Roche *et al.*, 2004). This figure highlights the fact that both 8325-4 proteins are fully functional in ligand binding. It also demonstrates that FnBPA and FnBPB

are each capable of contributing independently to the adherence of *S. aureus* to immobilised elastin.

3.2.2 Anti-human fibronectin antibodies inhibit FnBP-mediated adhesion to immobilised fibronectin but not to immobilised elastin

The fibronectin-binding proteins FnBPA and FnBPB are both responsible for the adherence of *S. aureus* cells to immobilised elastin peptides. Previous studies indicated that the C-terminal fibronectin-binding regions of FnBPA and FnBPB did not support bacterial attachment to elastin-coated surfaces (Roche *et al.*, 2004). In this experiment, anti-fibronectin antibodies were shown here to inhibit the adherence of bacterial cells to immobilised fibronectin but not to immobilised elastin (Figure 3.5). Preincubation of fibronectin- or elastin-coated wells with increasing concentrations of chicken anti-human fibronectin IgY antibodies resulted in the dose-dependent inhibition of *S. aureus* expressing FnBPA adhering to immobilised fibronectin but not to immobilised elastin. Pre-immune serum had no effect on adherence to either ligand indicating the specificity of the anti-fibronectin antibodies (data not shown).

As FnBPA can adhere to both fibronectin (Flock *et al.*, 1987) and fibrinogen (Wann *et al.*, 2000), it was important to determine whether the commercially available elastin peptides used in adherence assays were contaminated with either of these host proteins. Previously, it was shown that no immunoreactive proteins were detectable in the preparations of human lung elastin or human aortic elastin by Western immunoblotting with polyclonal chicken, goat or rabbit anti-human fibronectin antibodies or polyclonal anti-human fibrinogen antibodies (Roche *et al.*, 2004). In the case of chicken antibodies, the limit of detection of immobilised fibronectin by ELISA was 0.03 μg/ml, a concentration too low to support bacterial attachment. A high concentration (3 mg/ml) of chicken anti-human fibronectin antibodies caused a 60% reduction in adherence of P1 expressing FnBPA to immobilised fibronectin but had no effect on adherence to immobilised elastin, showing again that there is no contaminating fibronectin in the elastin preparations used in adherence assays.

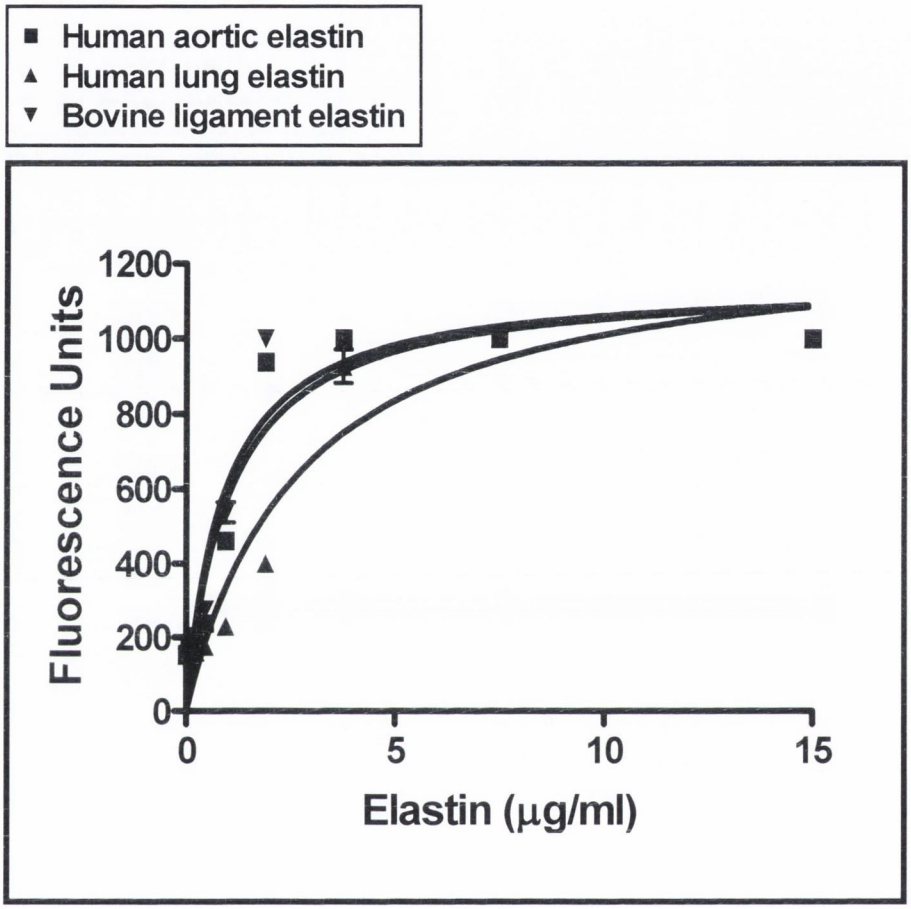

Figure 3.2 Adherence of *S. aureus* strain MSSA476 to human and bovine elastin

Adherence of cells from exponential phase cultures of *S. aureus* strain MSSA476 to immobilised human aortic elastin, human lung elastin and bovine ligament elastin. This figure is representative of two independent experiments.

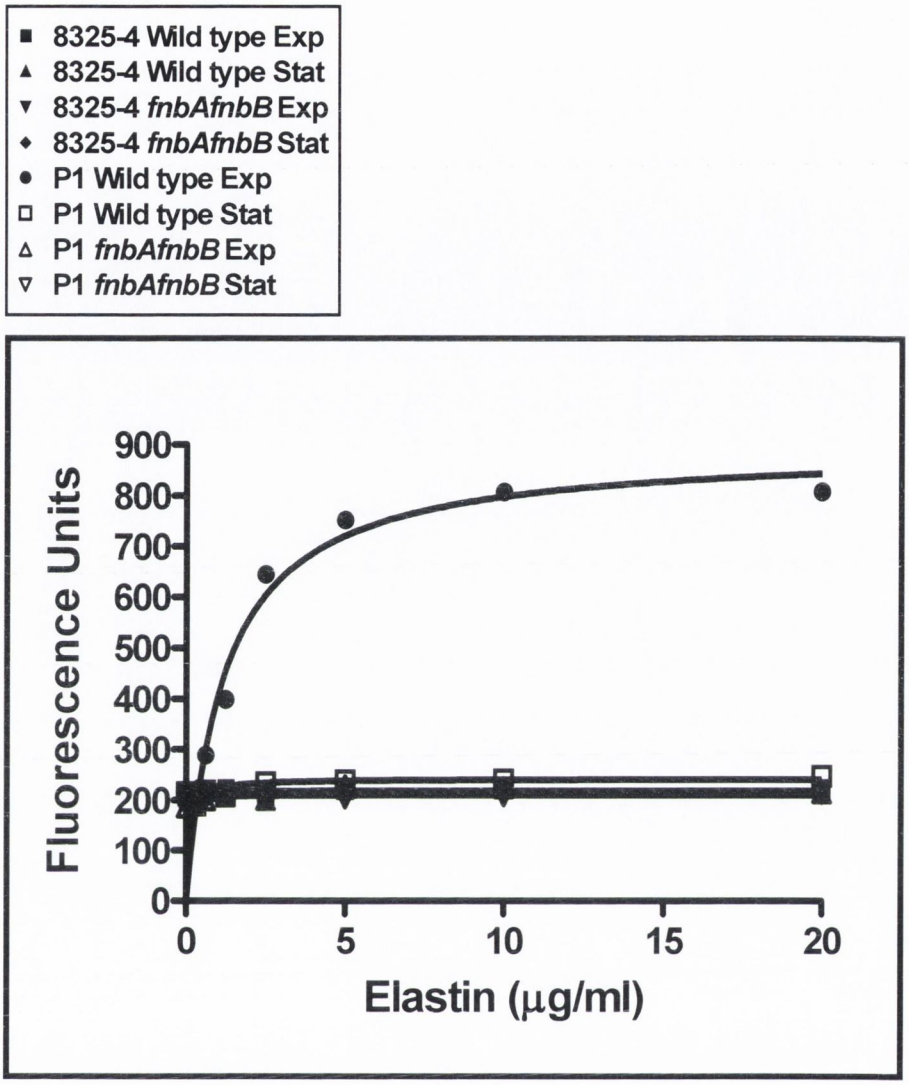

Figure 3.3 Adherence of *S. aureus* 8325-4 and P1 strains to human elastin

Adherence of cells from exponential and stationary phase cultures of *S. aureus* 8325-4, 8325-4 *fnbAfnbB*, P1 and P1 *fnbAfnbB* to immobilised human aortic elastin peptides. This figure is representative of two independent experiments.

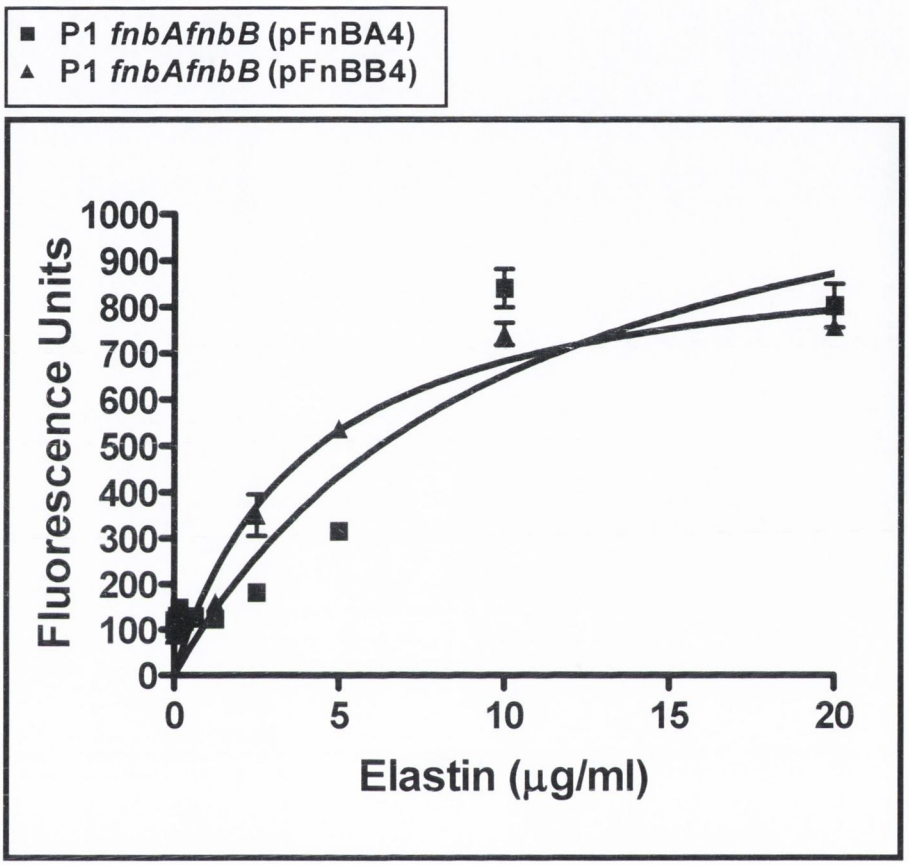

Figure 3.4 Adherence of *S. aureus* P1 strains to human elastin

Adherence of cells from exponential phase cultures of *S. aureus* P1 *fnbAfnbB* (pFnBA4) and P1 *fnbAfnbB* (pFnBB4) to immobilised human aortic elastin peptides. This figure is representative of three independent experiments.

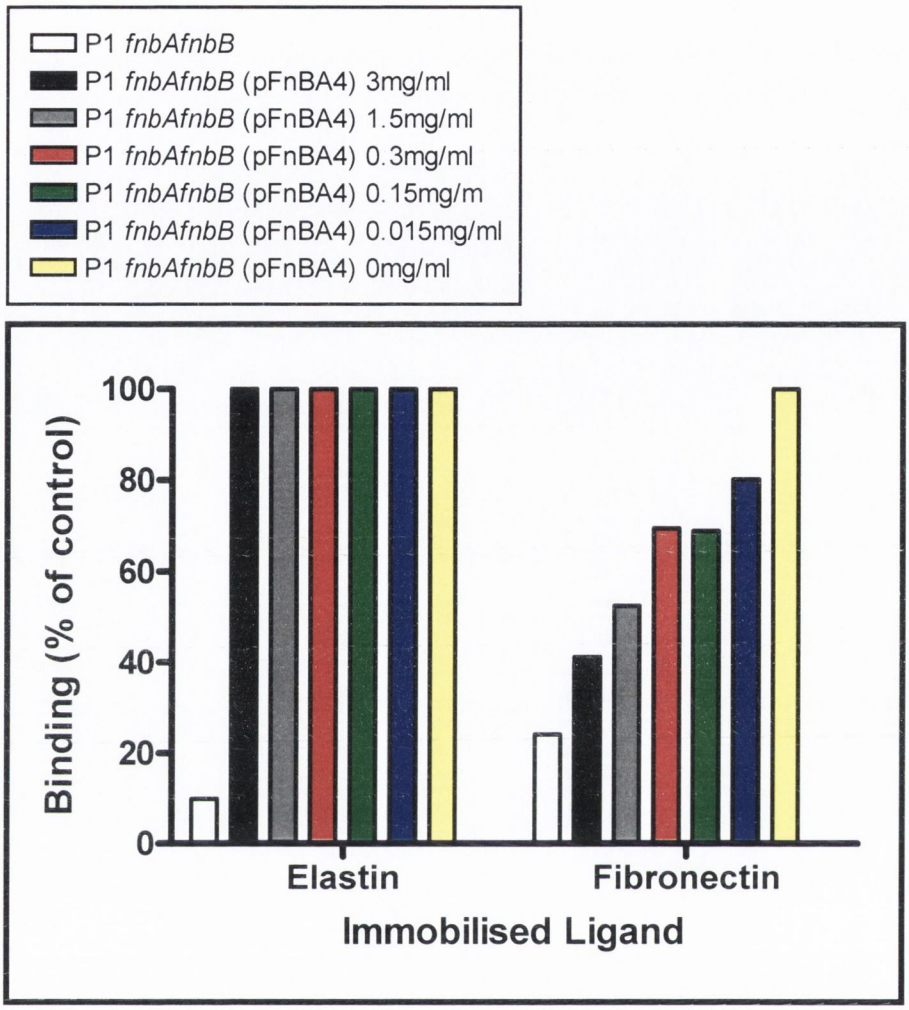

Figure 3.5 Inhibition of *S. aureus* P1 strains adhering to immobilised elastin and fibronectin by preincubation with anti-fibronectin antibodies

Inhibition of *S. aureus* strain P1 *fnbAfnbB* (pFnBA4) adherence to immobilised elastin and fibronectin (10 μg/ml) by preincubation with anti-fibronectin IgY antibodies. Bars represent the mean of duplicate wells and are expressed as a percentage of a control lacking inhibitor. This figure is representative of two independent experiments.

3.2.3 Adherence of *L. lactis* expressing full-length FnBPA, FnBPB and truncates of FnBPA to immobilised elastin

The above experiments, in conjunction with previous results (Roche *et al.*, 2004) indicate that the A domains of FnBPA and FnBPB promote bacterial adherence to immobilised elastin peptides. To analyse this further, *L. lactis* strains with genes encoding FnBPA and FnBPB cloned into the nisin-inducible expression vector pNZ8037 for expression on the surface of *L. lactis* (Fitzgerald *et al.*, 2006) were tested for their ability to bind immobilised elastin. The functional domains of FnBPA have been well defined and truncates of FnBPA corresponding to the separate ligand-binding regions were also cloned into the pNZ8037 vector (Fitzgerald *et al.*, 2006). Truncates comprising the fibrinogen-binding A domain but lacking the fibronectin-binding BCD domains (FnBPA-A) or the BCD domains but lacking the A domain (FnBPA-BCD) were expressed on the surface of *L. lactis*. *L. lactis* expressing full-length FnBPA and FnBPB along with FnBPA-A and FnBPA-BCD were tested for adhesion to both elastin and fibrinogen. Exponential phase cultures of *L. lactis* were induced with 3.2 ng/ml of nisin, grown overnight, washed and resuspended to equal optical densities before being added to ligand-coated wells in a microtitre plate. Strains expressing full-length FnBPA and FnBPB adhered strongly to immobilised elastin while the strain expressing the A domain alone adhered moderately well (Figure 3.6). The slightly impaired adhesion of cells expressing the A domain alone in comparison to the full-length FnBPA protein may reflect the closer proximity of the A domain to the bacterial cell wall as this strain lacks the BCD domains which likely serve as a stalk to project the A domain away from the bacterial cell surface. This demonstrates again that FnBPA and FnBPB are each capable of contributing to the elastin-binding phenotype of *S. aureus*. It also shows that *L. lactis* expressing the BCD domains of FnBPA do not adhere to immobilised elastin, giving fluorescence units comparable to wild-type *L. lactis* which expresses no elastin-binding protein. This experiment clearly indicates that the BCD domains of FnBPA have no role in elastin binding, whereas the N-terminal A domain is required.

In comparison, the *L. lactis* strains were tested for binding to immobilised fibrinogen. Both FnBPA and FnBPB expressed on the surface of *L. lactis* promoted strong adherence to immobilised fibrinogen as did expression of the A domain alone (Figure 3.7). It is possible that the affinity of the A domain of FnBPA for fibrinogen is significantly higher than that for elastin and this may explain how the proximity of the A domain to the cell surface affects elastin adherence to a greater extent than fibrinogen adherence. As expected, *L. lactis* strains

expressing the BCD domains alone did not adhere to immobilised fibrinogen, with background levels seen similar to that of wild-type *L. lactis*. The relative adherence of *L. lactis* strains expressing full-length FnBPA and FnBPA-A can be seen in Figure 3.8. With increasing concentrations of nisin, *L. lactis* expressing the A domain alone adhered as strongly as the full-length FnPBA to fibrinogen but not to elastin. Expression of the A domain alone has previously been shown to be as efficient as the expression of the full-length FnBPA protein by dot blot analysis of both strains using polyclonal anti-rAFnBPA antibodies (Loughman, 2005). *L. lactis* expressing the BCD domains of FnBPA did not adhere to either ligand (Figure 3.8).

The controlled expression of FnBPA on the surface of *L. lactis* is a valuable tool in assessing the role of FnBPA on the surface of the cell. *L. lactis* FnBPA was grown in the presence of increasing concentrations of nisin (6.4 – 0.006 ng/ml) and tested for adhesion to immobilised elastin (Figure 3.9) and fibrinogen (Figure 3.10). The increasing concentrations of nisin in the growth medium causes increased transcription of the *fnbA* gene cloned into the pNZ8037 vector and a resulting increase in the level of FnBPA protein present on the surface of the cell. This process shows that *L. lactis* adherence to fibrinogen and elastin occurs in a nisin concentration-dependent manner. The adherence of maximally induced empty pNZ8037 vector showed only background adherence to elastin and fibrinogen, which demonstrates the lack of ligand-binding proteins present of the surface of wild-type *L. lactis* cells (data not shown). In addition, *L. lactis* FnBPA cells, induced with high concentrations of nisin did not adhere to uncoated wells (data not shown) demonstrating the specificity of the FnBP-elastin interaction.

3.2.4 Expression of recombinant region A of FnBPA and FnBPB

Experiments with both *S. aureus* and *L. lactis* strains resulted in the hypothesis that the A domains of FnBPA and FnBPB promote attachment to immobilised elastin as well as to immobilised fibrinogen. To further study the binding of this region of the fibronectin-binding proteins to elastin, recombinant truncated derivatives of FnBPA and FnBPB were expressed in *E. coli* as N-terminal 6xHis fusion proteins. The gene regions encoding amino acid residues 37-544 of FnBPA and 37-540 of FnBPB were amplified by PCR from plasmid pFnBPA4 and pFnBPB4, respectively, cloned into the *E. coli* expression vector pQE30 and expressed in the protease-deficient *E. coli* strain Topp 3 (Figure 3.11). The recombinant proteins, $rAFnBPA_{37-544}$ and $rAFnBPB_{37-540}$, were purified from *E. coli* lysates by nickel-chelate affinity

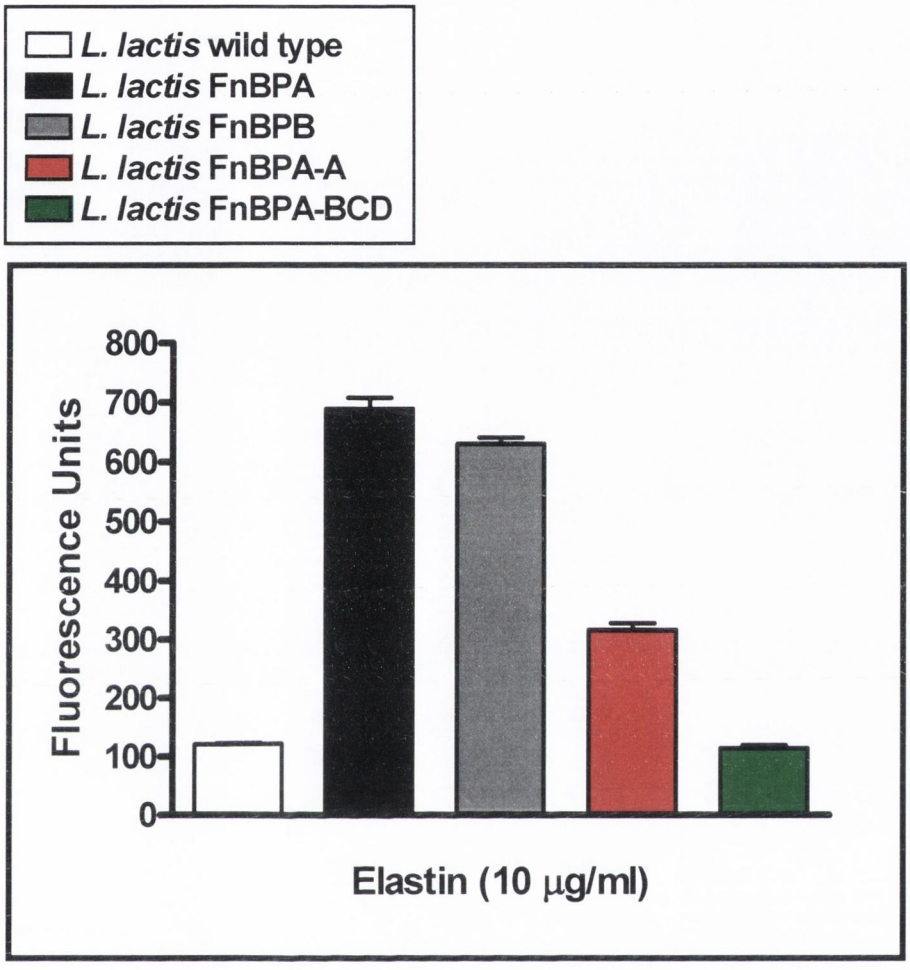

Figure 3.6 Adherence of *L. lactis* strains to human elastin

Adherence of *L. lactis* NZ9800 (pNZ8037), NZ9800 (pNZ8037*fnbA*), NZ9800 (pNZ8037*fnbB*), NZ9800 (pNZ8037*fnbA*-A) and NZ9800 (pNZ8037*fnbA*-BCD), induced at 3.2 ng/ml nisin, to immobilised human aortic elastin (10 μg/ml). This figure is representative of three independent experiments.

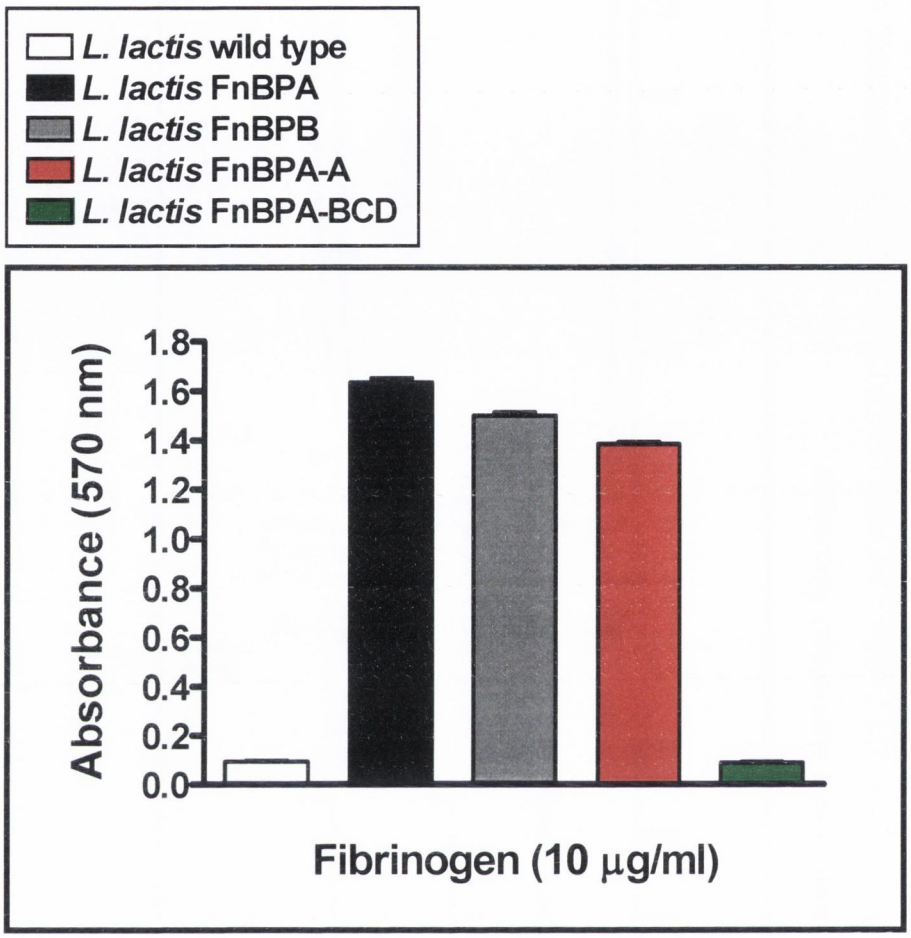

Figure 3.7 Adherence of *L. lactis* strains to human fibrinogen

Adherence of *L. lactis* NZ9800 (pNZ8037), NZ9800 (pNZ8037*fnbA*), NZ9800 (pNZ8037*fnbB*), NZ9800 (pNZ8037*fnbA*-A) and NZ9800 (pNZ8037*fnbA*-BCD), induced at 3.2 ng/ml nisin, to immobilised human fibrinogen (10 μg/ml). This figure is representative of three independent experiments.

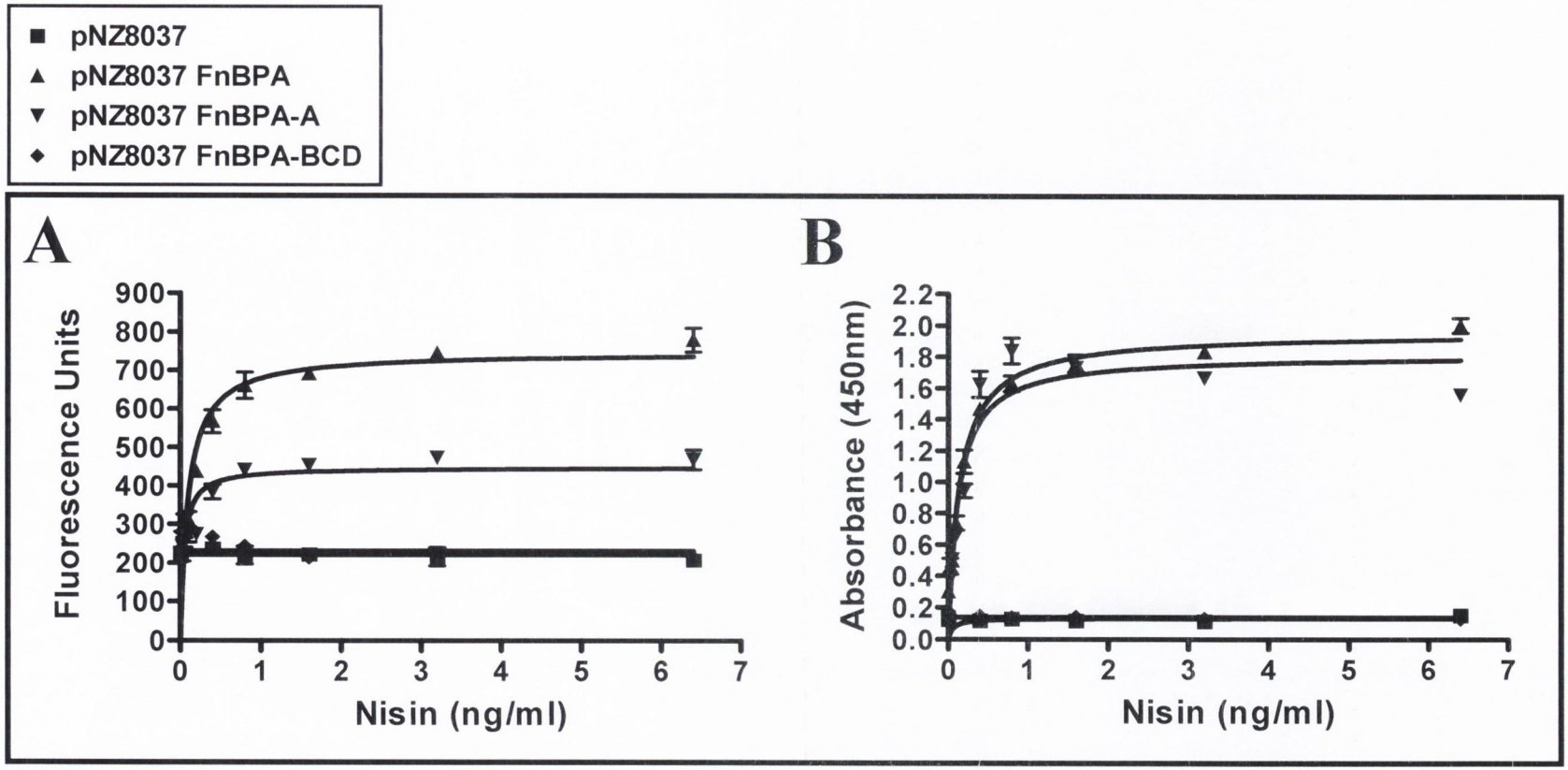

Figure 3.8 Adherence of *L. lactis* strains to immobilised elastin and fibrinogen

Adherence of *L. lactis* NZ9800 (pNZ8037), NZ9800 (pNZ8037 FnBPA), NZ9800 (pNZ8037 FnBPA-A) and NZ9800 (pNZ8037 FnBPA-BCD), induced at various nisin concentrations (6.4 – 0 ng/ml), to 10 μg/ml of immobilised elastin (A) and fibrinogen (B). This figure is representative of three independent experiments.

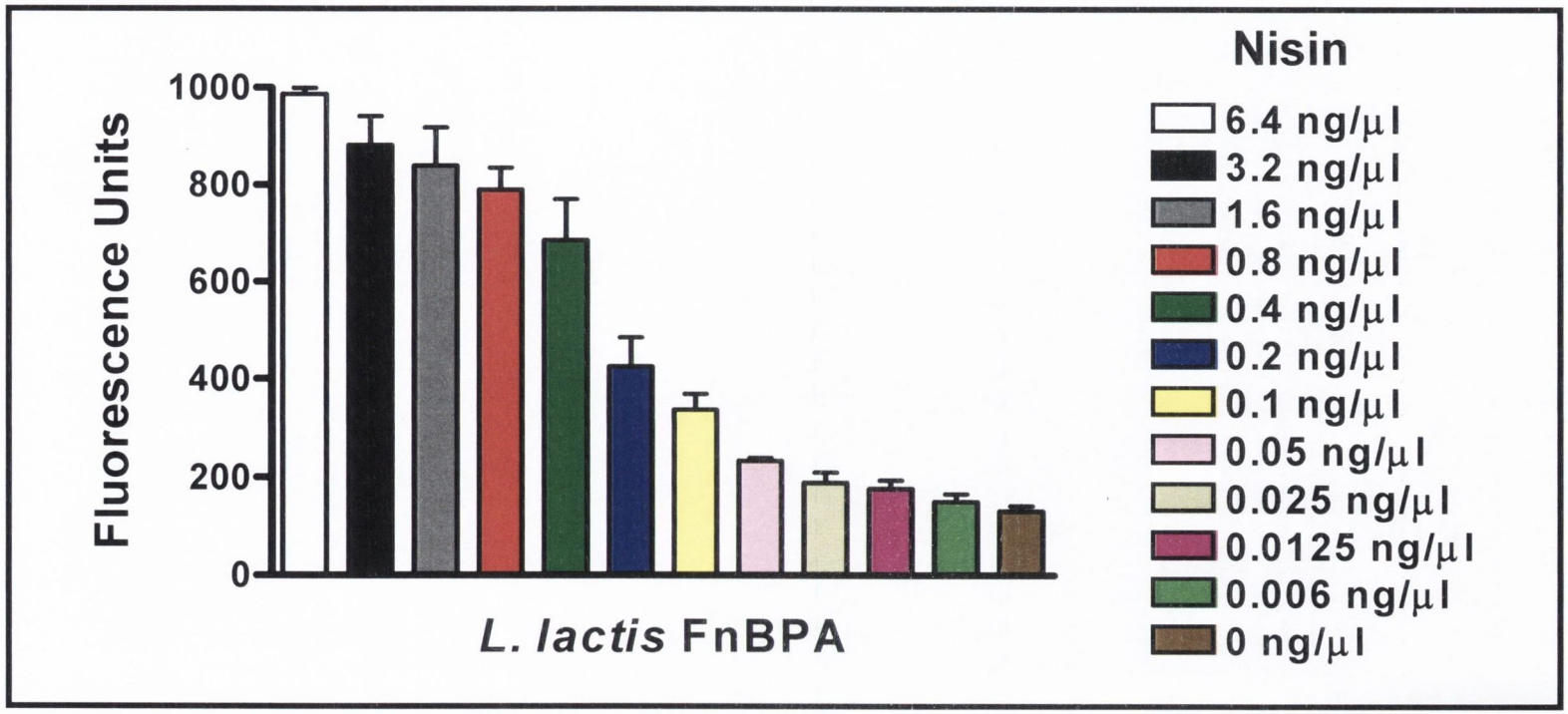

Figure 3.9 Adherence of *L. lactis* FnBPA to human elastin

Adherence of *L. lactis* NZ9800 (pNZ8037*fnbA*) to immobilised human elastin (10 µg/ml). *L. lactis* FnBPA was induced with increasing concentrations of nisin (6.4 ng/ml - 0 ng/ml) before being added to elastin-coated wells. Adherent bacteria were stained using SYTO-13 fluorescent dye.

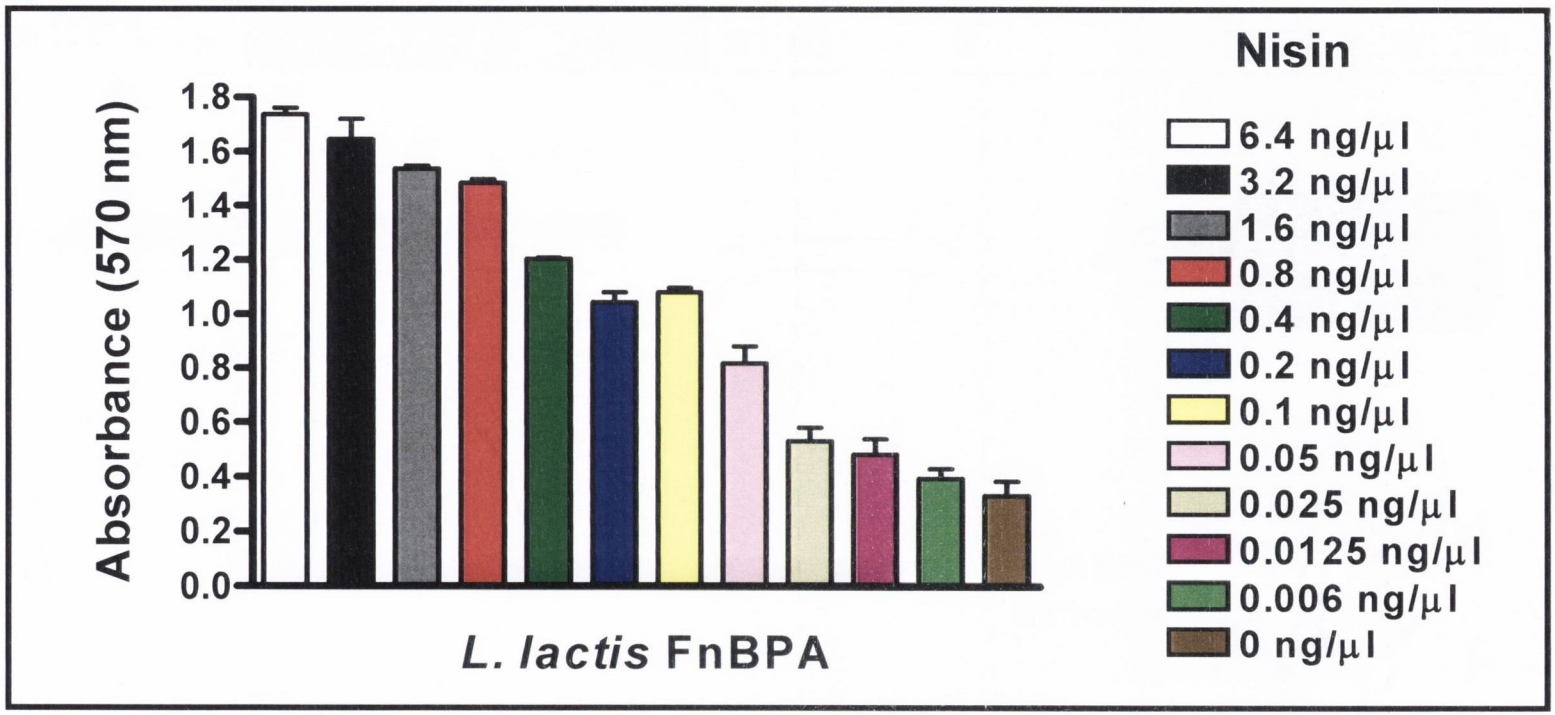

Figure 3.10 Adherence of *L. lactis* FnBPA to human fibrinogen

Adherence of *L. lactis* NZ9800 (pNZ8037*fnbA*) to immobilised human fibrinogen (10 µg/ml). *L. lactis* FnBPA was induced with increasing concentrations of nisin (6.4 ng/ml - 0 ng/ml) before being added to fibrinogen-coated wells. Adherent bacteria were stained using crystal violet.

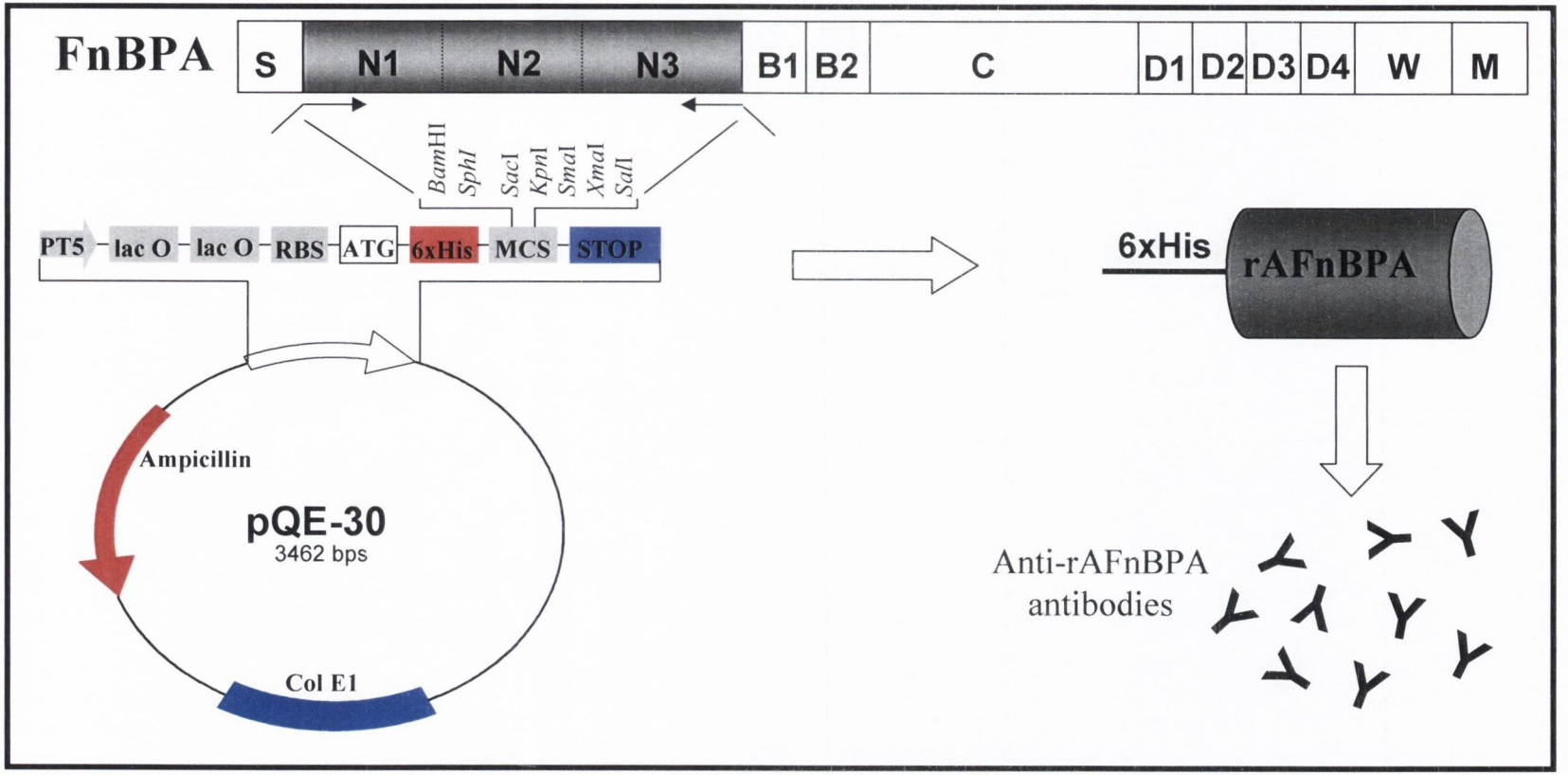

Figure 3.11 Production of recombinant FnBPA$_{37\text{-}544}$

DNA encoding the A region of FnBPA was cloned into the *E. coli* pQE-30 expression vector using *Bam*HI and *Sal*I restriction sites. Recombinant protein was purified from *E. coli* lysates using nickel affinity and anion exchange chromatography. A similar method was used for recombinant rAFnBPB and all subsequent rAFnBPA truncates. Recombinant rAFnBPA$_{37\text{-}544}$ and rAFnBPB$_{37\text{-}540}$ were used to raise polyclonal rabbit antibodies.

chromatography and analysed by SDS-PAGE and stained with Coomassie blue. Aliquots of the recombinant proteins were emulsified with Freunds Adjuvant and used to raise polyclonal anti-FnBP antibodies in rabbits.

The stability of recombinant FnBP proteins was tested by incubation at 37°C. Aliquots of 1 mg/ml of each protein were incubated at 37°C for 0.5 – 18 h and compared by SDS-PAGE analysis with protein that had not been incubated (Figure 3.12). rAFnBPA$_{37\text{-}544}$ and rAFnBPB$_{37\text{-}540}$ both migrate with an apparent molecular weight of 83 kDa, which is slightly higher than their molecular masses of 57.6 kDa and 57.4 kDa, respectively. It is shown here that both proteins are resistant to breakdown even after 18 h incubation, with no increase in breakdown products. This implies that recombinant rAFnBPA$_{37\text{-}544}$ and rAFnBPB$_{37\text{-}540}$ proteins are intrinsically stable, can withstand treatment at 37°C for a sustained period of time and that no proteases have been co-purified with either protein.

The susceptibility of rAFnBPA$_{37\text{-}544}$ and rAFnBPB$_{37\text{-}540}$ to V8 serine protease and aureolysin metalloprotease, was also determined. It was reported previously that culture supernatants enriched for V8 serine protease caused a reduction in adhesion of *S. aureus* strain L170 to fibronectin-coated surfaces (McGavin *et al.*, 1997). Here, recombinantly produced FnBP proteins were tested for their susceptibility to V8 protease. Protein samples (10μg) were incubated with increasing amounts of V8 protease (100 – 0.8 μg/ml) for 5 min before being analysed by SDS-PAGE (Figure 3.13). A stepwise pattern of breakdown was seen in response to the increased levels of protease. The sensitivity of FnBPA and FnBPB to V8 protease can be explained by the substrate specificity of the enzyme and the amino acid composition of the FnBPs. V8 protease cleaves on the carboxyl side of glutamic acid (Houmard and Drapeau, 1972) which is an abundant residue found throughout FnBPA and FnBPB. Glutamic acid comprises 8.5% and 10.5% of the amino acid content of the A domain of FnBPA and FnBPB, respectively. Glutamic acid is also abundant in the fibronectin-binding motifs at the C-terminus of the molecule and may aid in the detachment of cells from fibronectin-coated surfaces to promote in dissemination of bacteria.

rAFnBPA$_{37\text{-}544}$ and rAFnBPB$_{37\text{-}540}$ were also tested for their susceptibility to aureolysin. Protein samples were largely unaffected after incubation for 5 mins with the range of aureolysin metalloprotease concentrations tested (Figure 3.14). A decrease in the intensity of the full-length protein band and an increased level of breakdown products is evident in rAFnBPA$_{37\text{-}544}$ and rAFnBPB$_{37\text{-}540}$ samples incubated with the highest concentration of aureolysin (25 μg/ml). A further investigation into the susceptibility of these proteins to

aureolysin showed that rAFnBPA$_{37-544}$ is more stable than FnBPB. Protein aliquots were incubated with 25 μg/ml of aureolysin for longer time periods demonstrating that rAFnBPB$_{37-540}$ is significantly more susceptible to breakdown than rAFnBPA$_{37-544}$ which was degraded more slowly (Figure 3.15). The relative stability of rAFnBPA$_{37-544}$ to aureolysin is in contrast to the A domains of ClfA and ClfB, two other staphylococcal fibrinogen-binding proteins, which are susceptible to cleavage by aureolysin at a SLAVA / SLAAVA motif located between subdomains N1 and N2 and are relatively resistant to cleavage by V8 protease. In contrast to ClfA, the cleavage of ClfB at SLAVA results in the loss of the protein's fibrinogen-binding ability (McAleese *et al.*, 2001). A SLAVA-like motif occurs in both FnBP proteins with S$_{177}$ADVA$_{181}$ and S$_{144}$TDVTA$_{149}$ present in FnBPA and FnBPB, respectively but these motifs may not be optimal for aureolysin recognition.

3.2.5 Titration of anti-rAFnBPA and anti-rAFnBPB antibodies

Polyclonal rabbit antibodies raised against rAFnBPA$_{37-544}$ and rAFnBPB$_{37-540}$ were tested for their affinities to their respective antigens. Samples of each protein (500 – 3.9 ng) were applied to nitrocellulose membrane strips and probed with dilutions of antibodies (1:5,000 – 1:160,000) (Figure 3.16). An equally sensitive reaction was observed for both antibodies to their antigens with nanogram amounts of protein detected by both antibodies at high dilutions. The antibodies were also used to detect FnBP proteins released from cell wall extracts of *S. aureus* strain P1. A high concentration of anti-rAFnBP antibodies were needed to detect full-length FnBP released from the surface of P1 (Figure 3.17). The antibodies were raised against the 8325-4 proteins and it is now known that substantial antigenic variation exists between FnBPs produced by strain P1 and strain 8325-4. This will be discussed further in Chapter 5. The large immunoreactive band between 47 and 62 kDa is the IgG binding protein A (Spa) of *S. aureus*. The equal intensity of this band in each lane pair, demonstrates the equal loading of all samples. The absence of high molecular weight immunoreactive bands in strain P1*fnbAfnbB* is indicative of the FnBP-specificity of both antibodies. Also, each antibody reacted with only one high molecular weight band in wild-type P1 samples. This shows the lack of cross reactivity of these antibodies to other staphylococcal surface proteins.

The cross-reactivity of the anti-rAFnBPA and anti-rAFnBPB antibodies was determined by Western blotting with recombinant proteins. 0.25 μM of each recombinant 8325-4 protein was subjected to SDS-PAGE followed by Coomassie staining or transfer onto

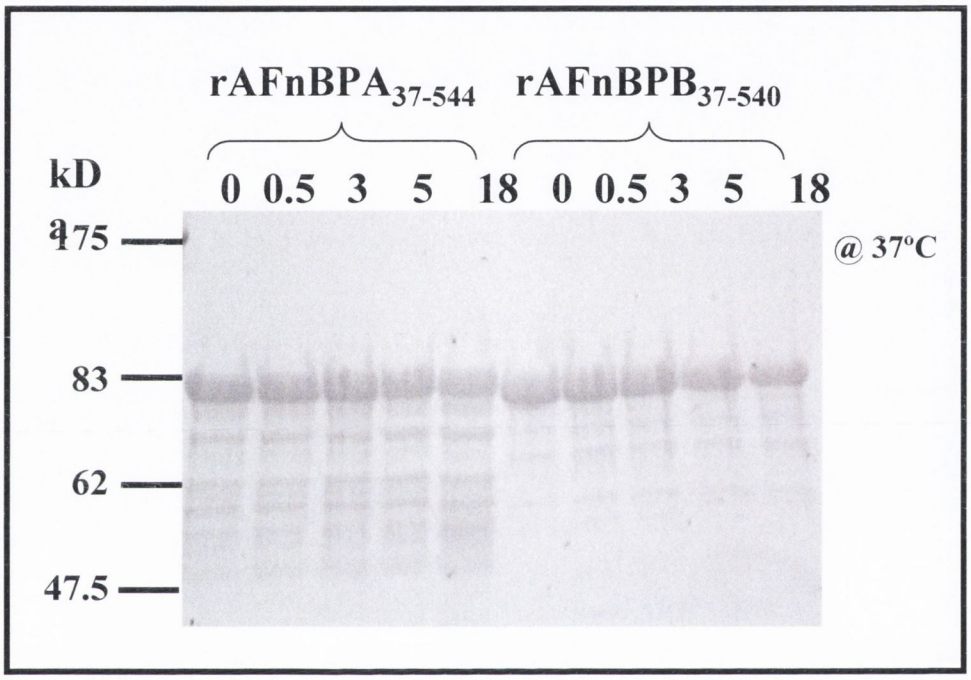

Figure 3.12 Stability of $rAFnBPA_{37-544}$ and $rAFnBPB_{37-540}$

1 mg/ml of $rAFnBPA_{37-544}$ or $rAFnBPB_{37-540}$ in PBS was incubated for 0, 0.5, 3, 5, and 18 h at 37°C before being analyzed by SDS-PAGE and stained with Coomassie Blue.

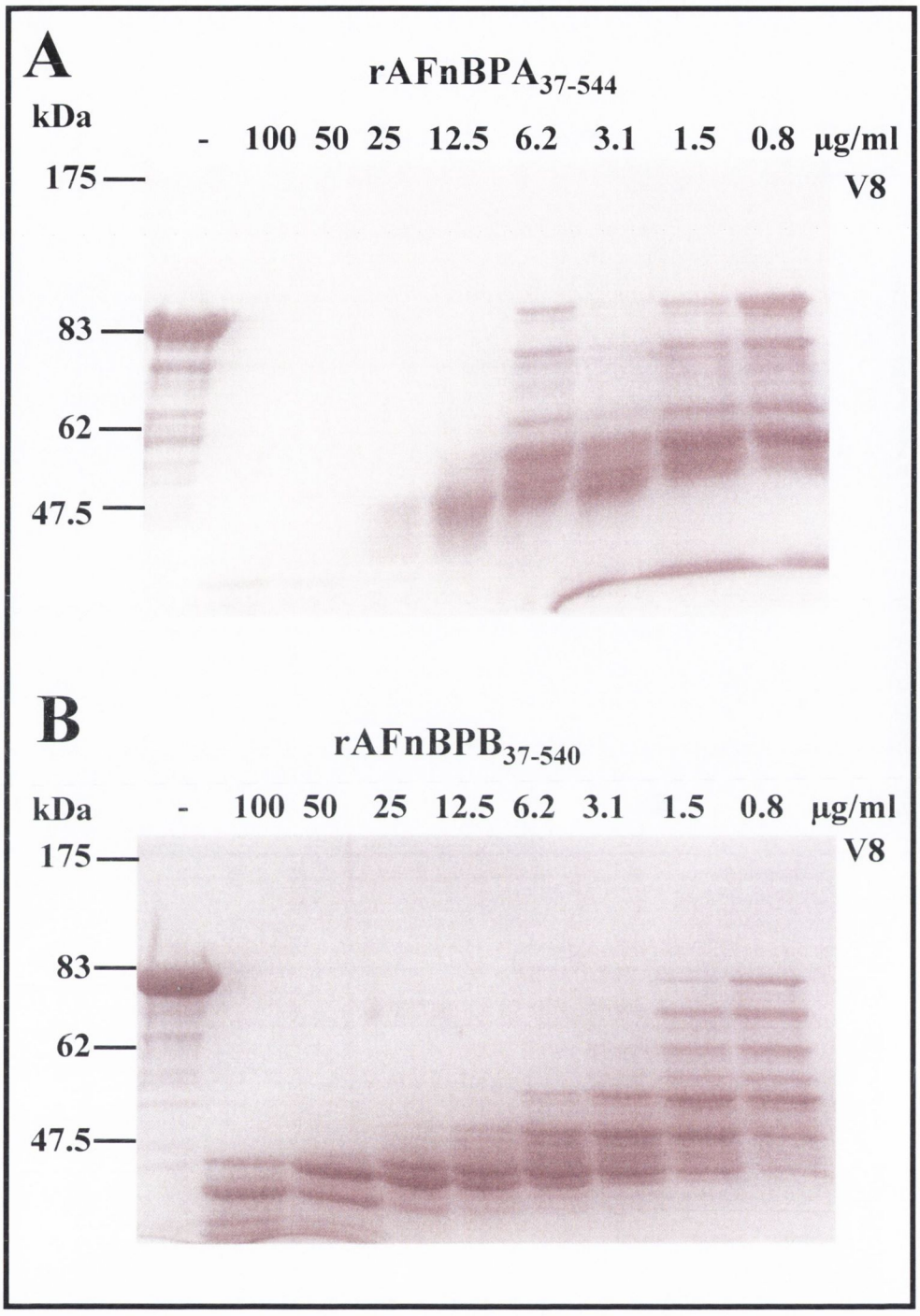

Figure 3.13 Susceptibility of rAFnBPA$_{37-544}$ and rAFnBPB$_{37-540}$ to V8 serine protease

10 µg of rAFnBPA$_{37-544}$ (A) and rAFnBPB$_{37-540}$ (B) was incubated with various concentrations of V8 serine protease for 5 min at 37°C before being analysed by SDS-PAGE and stained with Coomassie Blue.

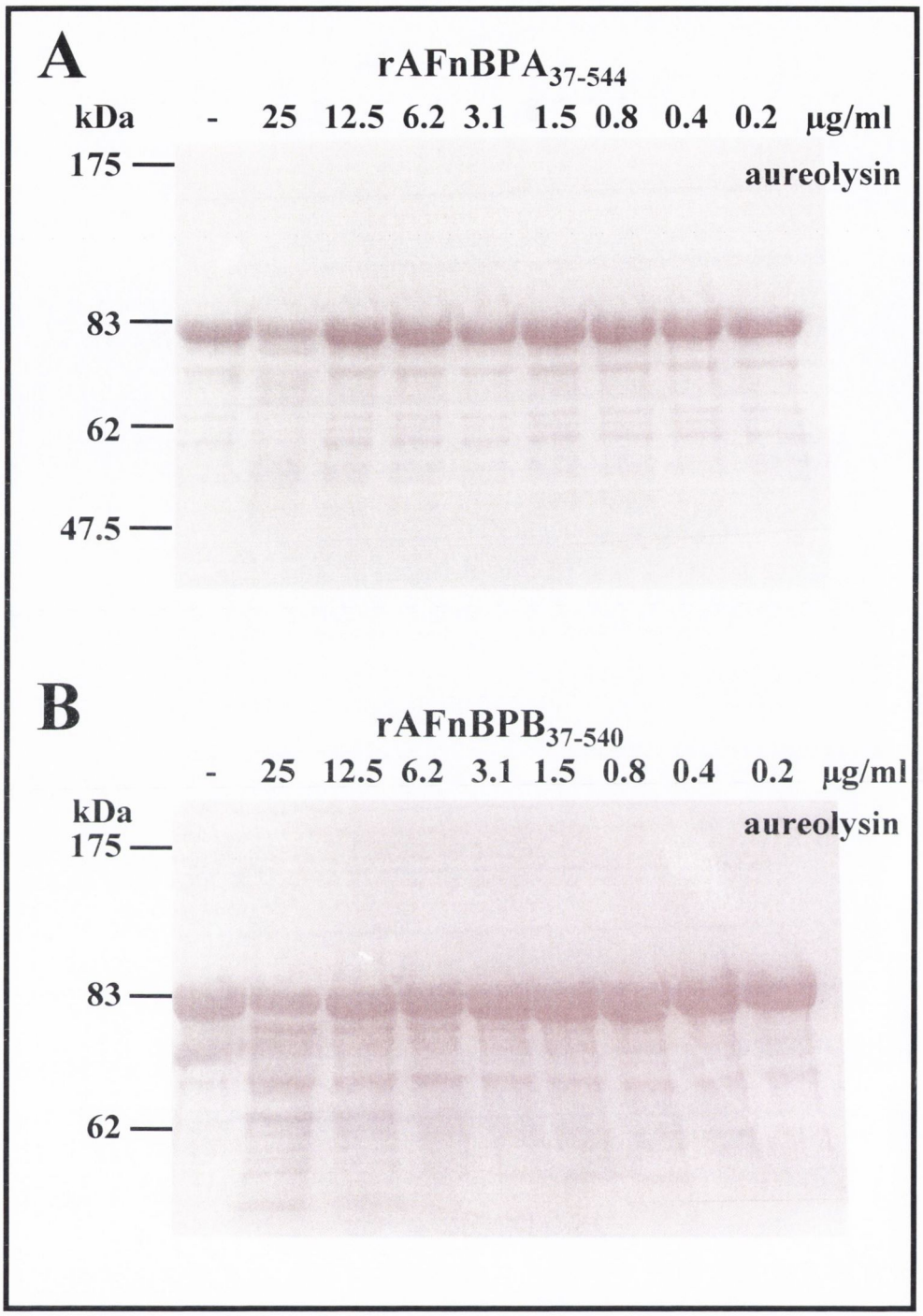

Figure 3.14 Susceptibility of rAFnBPA$_{37-544}$ and rAFnBPB$_{37-540}$ to aureolysin

10 µg of rAFnBPA$_{37-544}$ (A) or rAFnBPB$_{37-540}$ (B) was incubated with various concentrations of aureolysin for 5 min at 37°C before being analysed by SDS-PAGE and stained with Coomassie Blue.

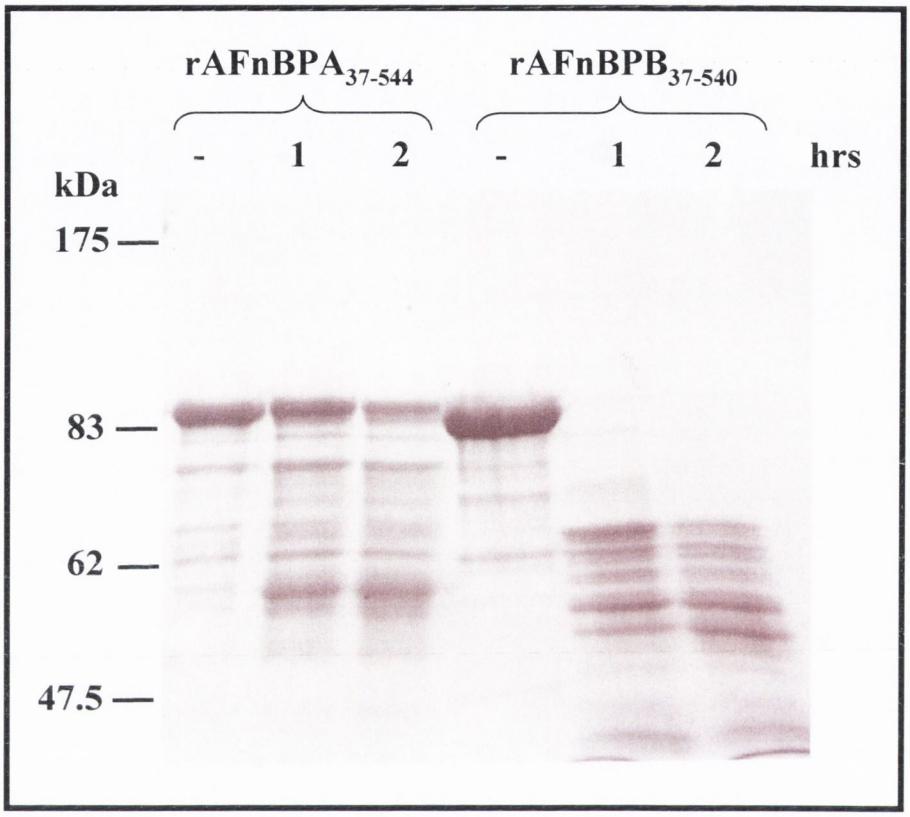

Figure 3.15 Susceptibility of $rAFnBPA_{37-544}$ and $rAFnBPB_{37-540}$ to aureolysin over time

10 μg/ml of $rAFnBPA_{37-544}$ or $rAFnBPB_{37-540}$ was incubated with 25 μg/ml of aureolysin for 0, 1 or 2 h at 37°C before being analysed by SDS-PAGE and stained with Coomassie Blue.

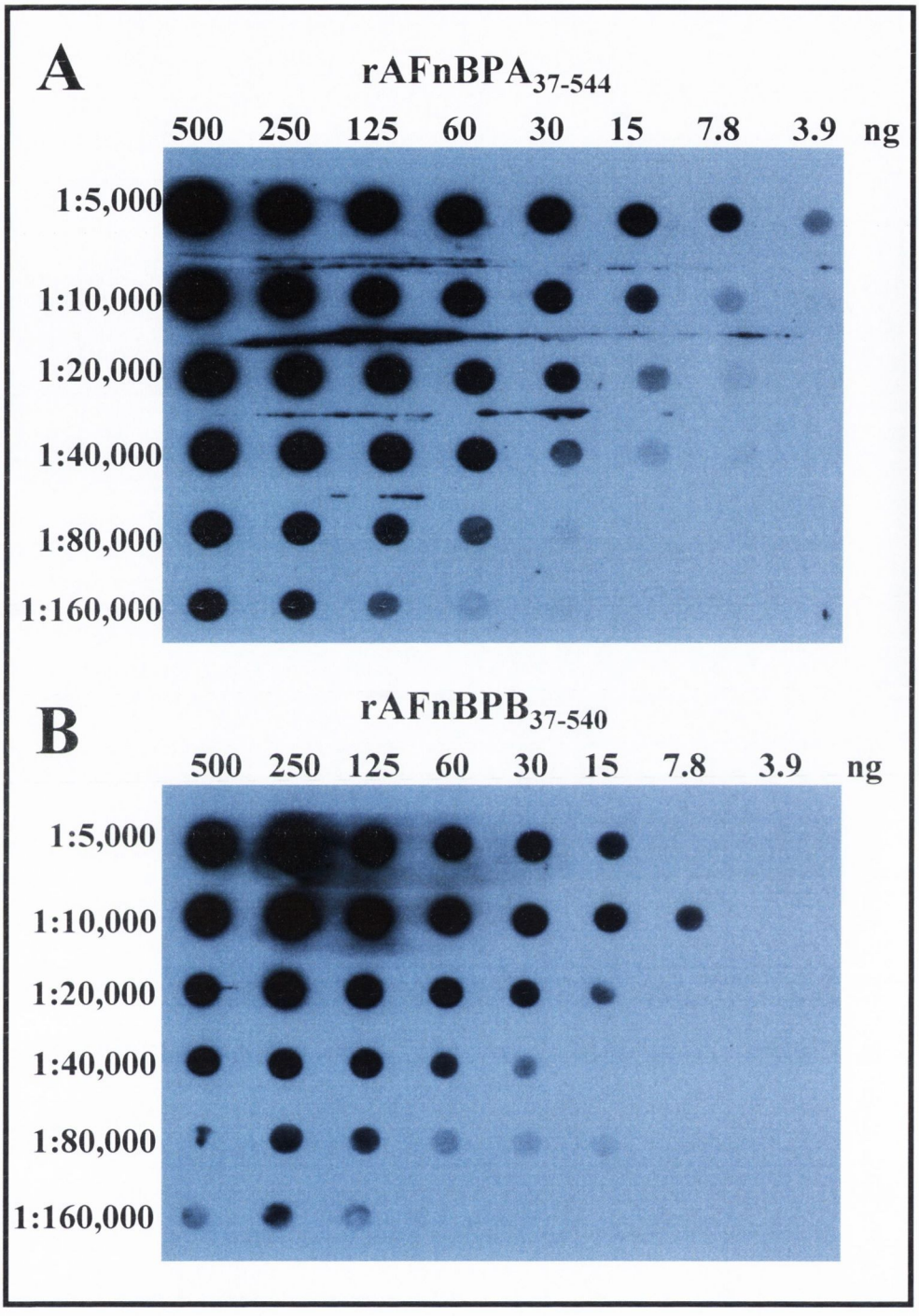

Figure 3.16 Titre of anti-rAFnBPA and anti-rAFnBPB antibodies for recombinant proteins

Titre of polyclonal rabbit anti-rAFnBPA (A) and anti-rAFnBPB (B) antibodies for their respective antigens in recombinant form. Doubling dilutions of recombinant proteins were dotted onto nitrocellulose membranes and probed with various dilutions of anti-rA antibodies followed by detection with goat anti-rabbit HRP.

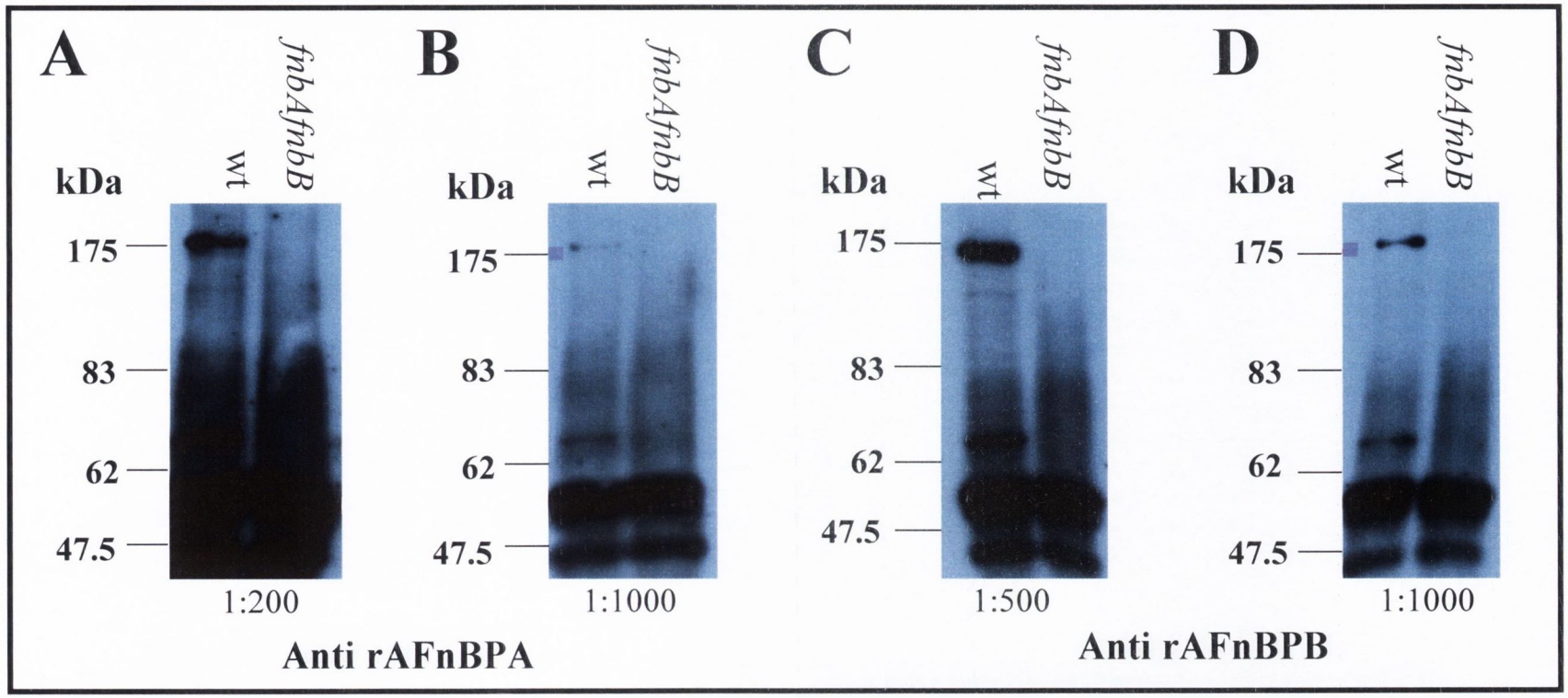

Figure 3.17 Affinity of anti-rAFnBPA and anti-rAFnBPB antibodies for full-length FnBP proteins released from *S. aureus* cell wall extracts

Affinity of polyclonal rabbit anti-rAFnBPA (A & B) and anti-rAFnBPB (C & D) antibodies for their respective proteins released from cell wall digests of *S. aureus* strain P1 wt and an isogenic *fnbAfnbB* mutant. Cell wall extracts were analysed by SDS-PAGE, transferred to PVDF membranes and probed with anti-rAFnBP antibodies followed by detection with goat anti-rabbit HRP.

PVDF membranes. Each membrane was probed with 1:10,000 dilution of anti-rAFnBPA or anti-rAFnBPB antibody followed by goat anti-rabbit-HRP conjugated antibodies (Figure 3.18). Each antibody shows potent activity against the full-length A domain as well as some breakdown products. The affinity of each antibody is greater for its cognate antigen. However, some cross-reactivity is evident, likely due to the A domains of FnBPA and FnBPB sharing 43% residue identity.

The ability of antibodies raised against rAFnBPA$_{37\text{-}544}$ to block adhesion of bacterial cells to immobilised elastin was tested. P1*fnbAfnbB* (pFnBA4) cells were preincubated with increasing amounts of anti-rAFnBPA antibodies or anti-EpbS antibodies, which recognise the N-terminus of EbpS (Downer *et al.*, 2002) and adherence to immobilised human aortic elastin was measured. The anti-rAFnBPA antibodies inhibited FnBPA-mediated adherence to elastin in a dose-dependent manner with the highest concentration of inhibiting antibody (100 μg/ml) resulting in 87% inhibition (Figure 3.19). The same range of concentrations of the control anti-EbpS antibodies did not inhibit elastin binding. This is further evidence that the elastin-binding domain of FnBPA is located within region A. A similar experiment was carried out with an *L. lactis* strain expressing FnBPA, whereby cells were preincubated with anti-rAFnBPA antibodies. A lower concentration of antibody was required to inhibit *L. lactis* adherence to immobilised elastin (Figure 3.20) compared to adherence of strain P1*fnbAfnbB* (pFnBA4), which demonstrates the simplicity of the *L. lactis* system as a surrogate host for surface proteins.

3.2.6 Binding of rAFnBPA$_{37\text{-}544}$ and rAFnBPB$_{37\text{-}540}$ to immobilised elastin and fibrinogen

Recombinant rAFnBPA$_{37\text{-}544}$ and rAFnBPB$_{37\text{-}540}$ proteins were tested for their ability to bind immobilised elastin and fibrinogen by ELISA type assays. Human aortic elastin peptides (20 μg/ml) or human fibrinogen (10 μg/ml) was coated onto the wells of microtitre plates. Increasing concentrations of rAFnBPA$_{37\text{-}544}$ and rAFnBPB$_{37\text{-}540}$ were incubated in the wells. rAClfA$_{40\text{-}559}$ (gift, Dr. J. Higgins, Trinity College, Dublin) was included as a positive control for fibrinogen binding. Bound protein was detected with polyclonal antibodies recognising the A domains of FnBPA, FnBPB or ClfA as appropriate. This experiment demonstrated dose-dependent and saturable binding of FnBP recombinant proteins to immobilised elastin and fibrinogen (Figure 3.21). rAFnBPB$_{37\text{-}540}$ appears to have a greater affinity for elastin than rAFnBPA$_{37\text{-}544}$ as reflected in the half maximum binding values of 21.39 ± 9.53 nM and 38.9 ± 20.9 nM, respectively. rAFnBPB$_{37\text{-}540}$ is also shown to have a higher binding specificity for

fibrinogen compared with rAFnBPA$_{37-544}$, with half maximum binding values of 0.214 ± 0.096 nM and 6.78 ± 3.41 nM, respectively. Moreover, the affinity of rAFnBPB$_{37-540}$ for fibrinogen is demonstrated to be higher than that of rAClfA$_{40-559}$, one of the major *S. aureus* fibrinogen-binding proteins. The reason for the putative increased affinity of rAFnBPB over rAFnBPA for fibrinogen and elastin has not been further investigated and needs to be tested by other methods. rAFnBPA$_{37-605}$ (A domain plus two B repeats) was previously shown to bind fibrinogen with a higher affinity than rAClfA$_{40-559}$ by ELISA methods (Wann *et al.*, 2000). This, however, is the first demonstration that rAFnBPB could bind fibrinogen and that rAFnBPA and rAFnBPB could bind specifically to immobilised elastin.

It was important to investigate if the increased affinity for rAFnBPB$_{37-540}$ over rAFnBPA$_{37-544}$ for immobilised elastin was due to a discrepancy in antibody sensitivity. Both anti-rAFnBPA and anti-rAFnBPB antibodies, however, proved to be equally sensitive in detecting their cognate recombinant FnBP proteins in an ELISA assay. Equal concentrations of rAFnBPA$_{37-544}$ and rAFnBPB$_{37-540}$ were coated onto microtitre plates and probed with a 1:2000 dilution of anti-rAFnBPA or anti-rAFnBPB antibodies (Figure 3.22). Both antibodies showed an equal sensitivity for their respective antigens, demonstrating that the relative affinities observed for rAFnBPA$_{37-544}$ and rAFnBPB$_{37-540}$ for fibrinogen and elastin are likely to be true.

As a further control for elastin-binding experiments, it was important to determine whether human aortic elastin dried under UV light onto the wells of a microtitre plate behaves similarly to the native protein. Polyclonal antibodies raised against the α-elastin fraction of human aortic elastin were tested for their ability to bind human aortic elastin dried onto the surface of microtitre plates by UV light. Microtitre plates were coated with increasing concentrations of human elastin (20 – 0 μg/ml) and probed with a 1:2000 dilution of anti-elastin antibodies (Figure 3.23 A). Conversely, a constant concentration of human elastin (20 μg/ml) was coated onto microtitre plates and doubling dilutions of anti-elastin antibodies were added (Figure 3.23 B). In both cases, the antibodies bound in a dose-dependent manner, indicating that many epitopes from native elastin are present in the UV-immobilised peptides.

3.2.7 Inhibition of rAFnBPA$_{37-544}$ and rAFnBPB$_{37-540}$ binding to immobilised elastin using soluble elastin peptides

In order to demonstrate that the FnBP-elastin interaction was specific, inhibition studies were carried out using soluble elastin peptides. Recombinant rAFnBPA$_{37-540}$ and

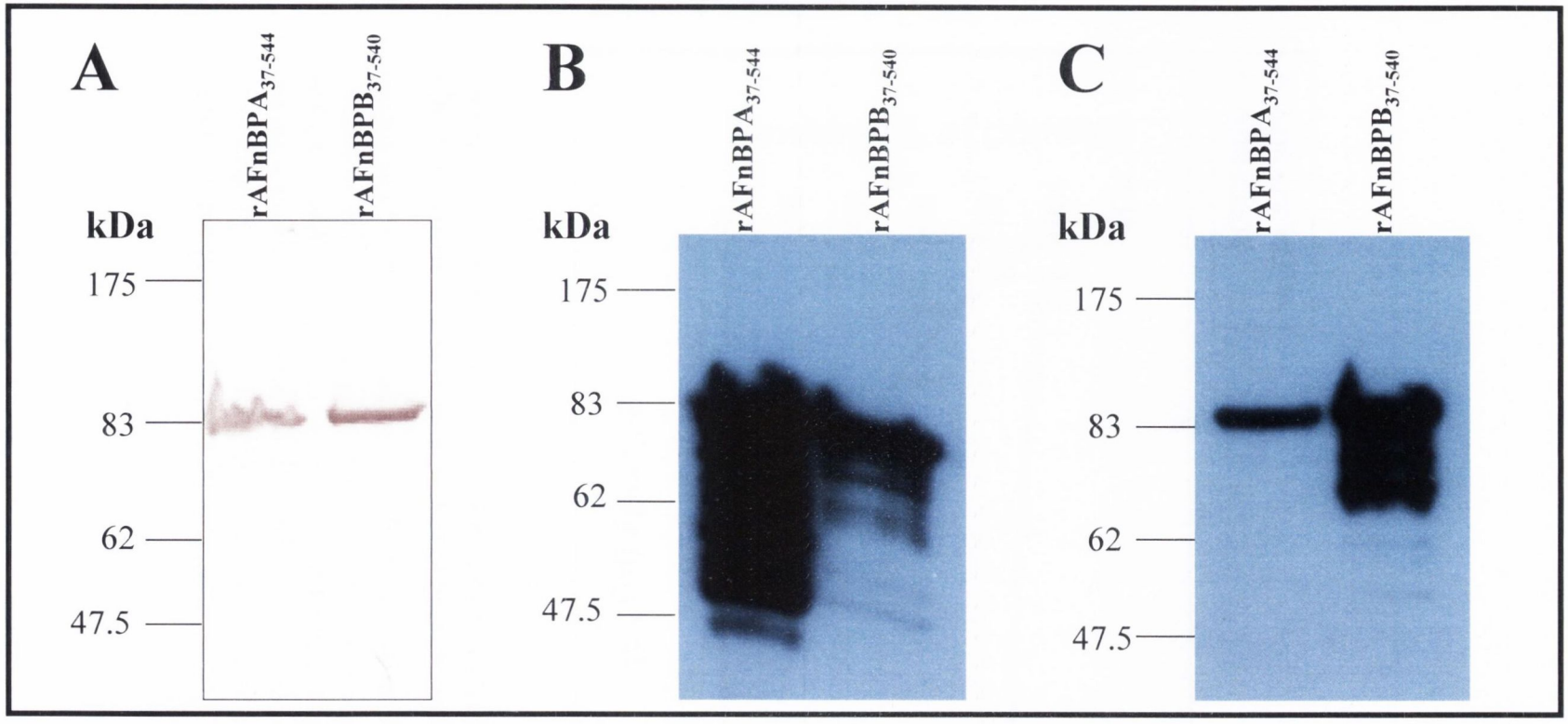

Figure 3.18 Cross-reactivity of anti-rAFnBPA and anti-rAFnBPB antibodies for recombinant FnBP proteins

0.25 μM each of $rAFnBPA_{37\text{-}544}$ and $rAFnBPB_{37\text{-}540}$ were analysed by SDS-PAGE, stained with Coomassie Blue (A) or transferred to PVDF membranes and probed with 1:10,000 dilution of anti-rAFnBPA (B) and 1:10,000 dilution of anti-rAFnBPB (C) antibodies followed by detection with goat anti-rabbit-HRP.

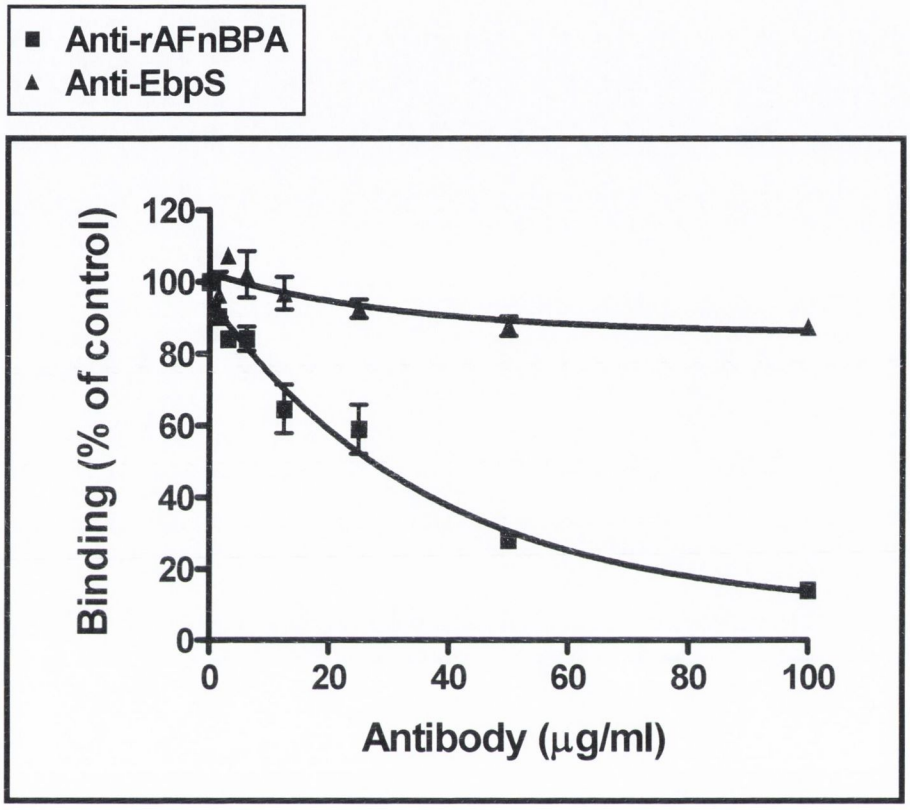

Figure 3.19 Inhibition of *S. aureus* P1 *fnbAfnbB* (pFnBA4) adherence to elastin by preincubation with antibodies

Inhibition of cells of *S. aureus* strain P1 *fnbAfnbB* (pFnBA4) binding to immobilised elastin (10 μg/ml) by preincubation with anti-rAFnBPA$_{37\text{-}544}$ and anti-rEbpS$_{1\text{-}267}$ antibodies. Data points represent the mean of triplicate wells and are expressed as a percentage of a control lacking inhibitor. This figure is representative of three independent experiments.

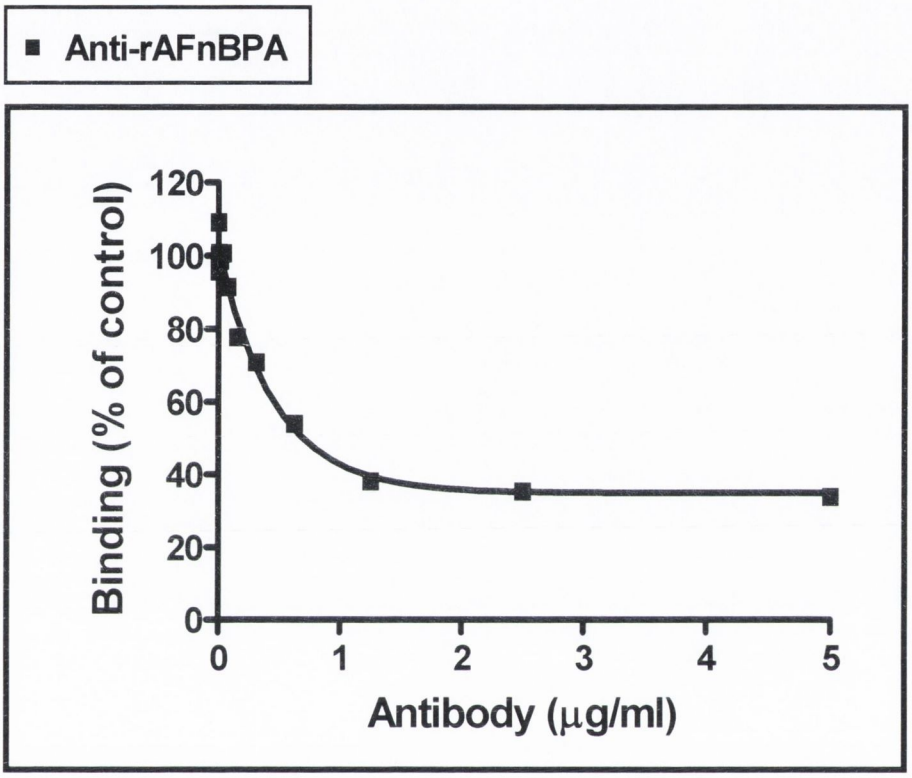

Figure 3.20 Inhibition of *L. lactis* pNZ8037*fnbA* adherence to elastin by preincubation with anti-rAFnBPA antibodies

Inhibition of cells of *L. lactis* strain NZ9800 pNZ8037*fnbA*, induced at 0.8 ng/ml nisin, binding to immobilised elastin (10 μg/ml) by preincubation with anti-rAFnBPA$_{37\text{-}544}$ antibodies. Data points are expressed as a percentage of a control lacking inhibitor. This figure is representative of two independent experiments.

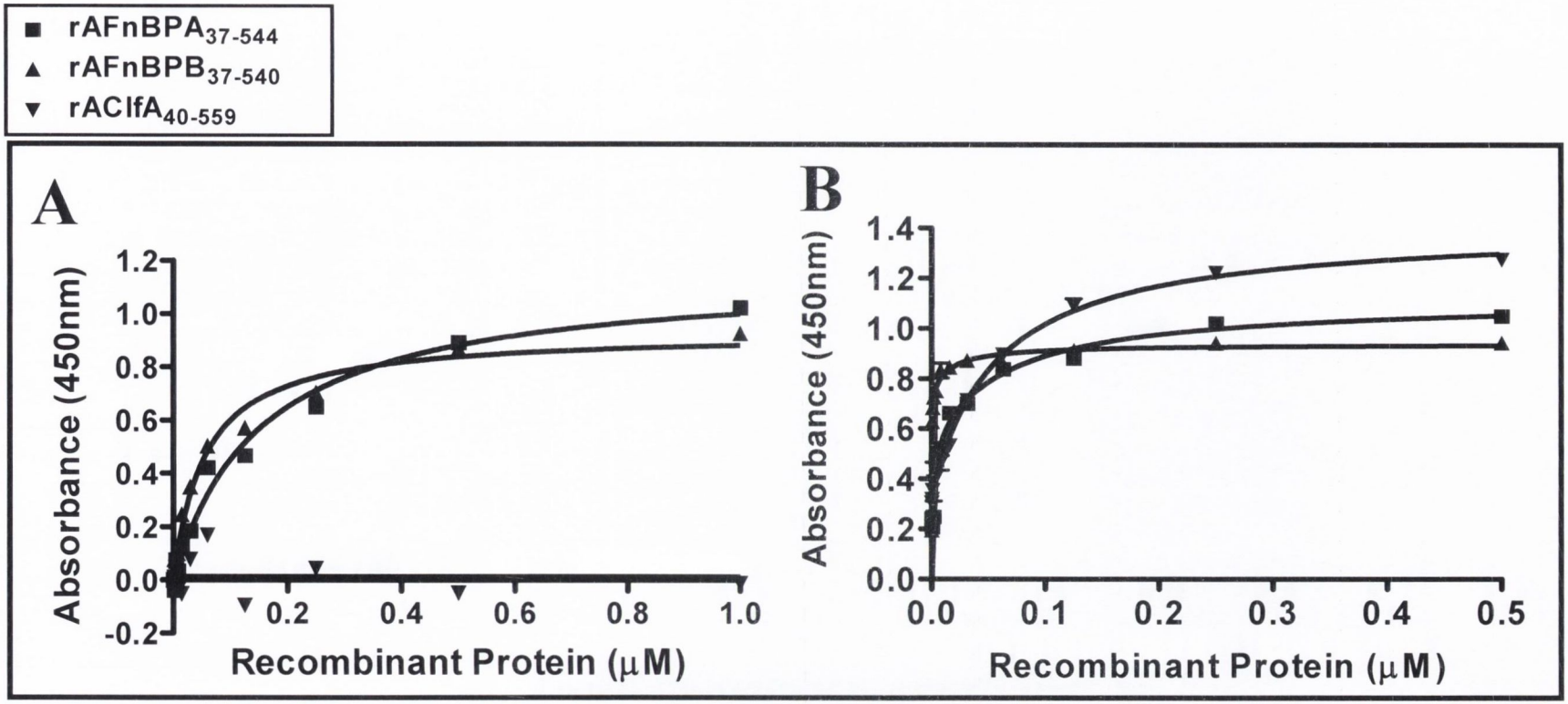

Figure 3.21 Binding of $rAFnBPA_{37-544}$, $rAFnBPB_{37-540}$ and $rAClfA_{40-559}$ to immobilised elastin and fibrinogen

Microtitre plates were coated with 20 μg/ml human aortic elastin (A) or 10 μg/ml human fibrinogen (B) and increasing concentrations of $rAFnBPA_{37-544}$, $rAFnBPB_{37-540}$ and $rAClfA_{40-559}$ were added for 1h at room temperature. Bound protein was detected with polyclonal anti-rAFnBP or anti-rAClfA antibodies and goat anti-rabbit HRP-conjugated antibodies followed by development with TMB substrate. Data points represent the mean of triplicate wells and this figure is representative of three independent experiments.

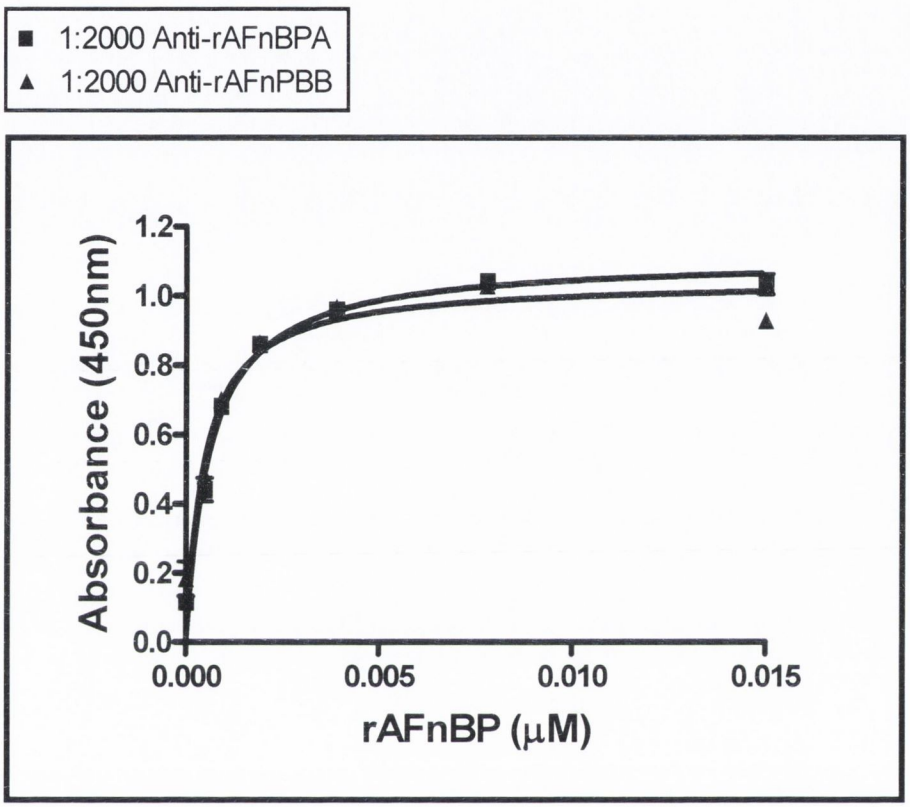

Figure 3.22 Binding of anti-rAFnBP antibodies to immobilised rAFnBP proteins

Microtitre plates were coated with various amounts of $rAFnBPA_{37-544}$ or $rAFnBPB_{37-540}$ and a 1:2,000 dilution of polyclonal anti-rAFnBPA or anti-rAFnBPB antibodies were added for 1h at room temperature. Bound antibody was detected with polyclonal goat anti-rabbit HRP-conjugated antibodies followed by development with TMB substrate. Data points represent the mean of triplicate wells and this figure is representative of three independent experiments.

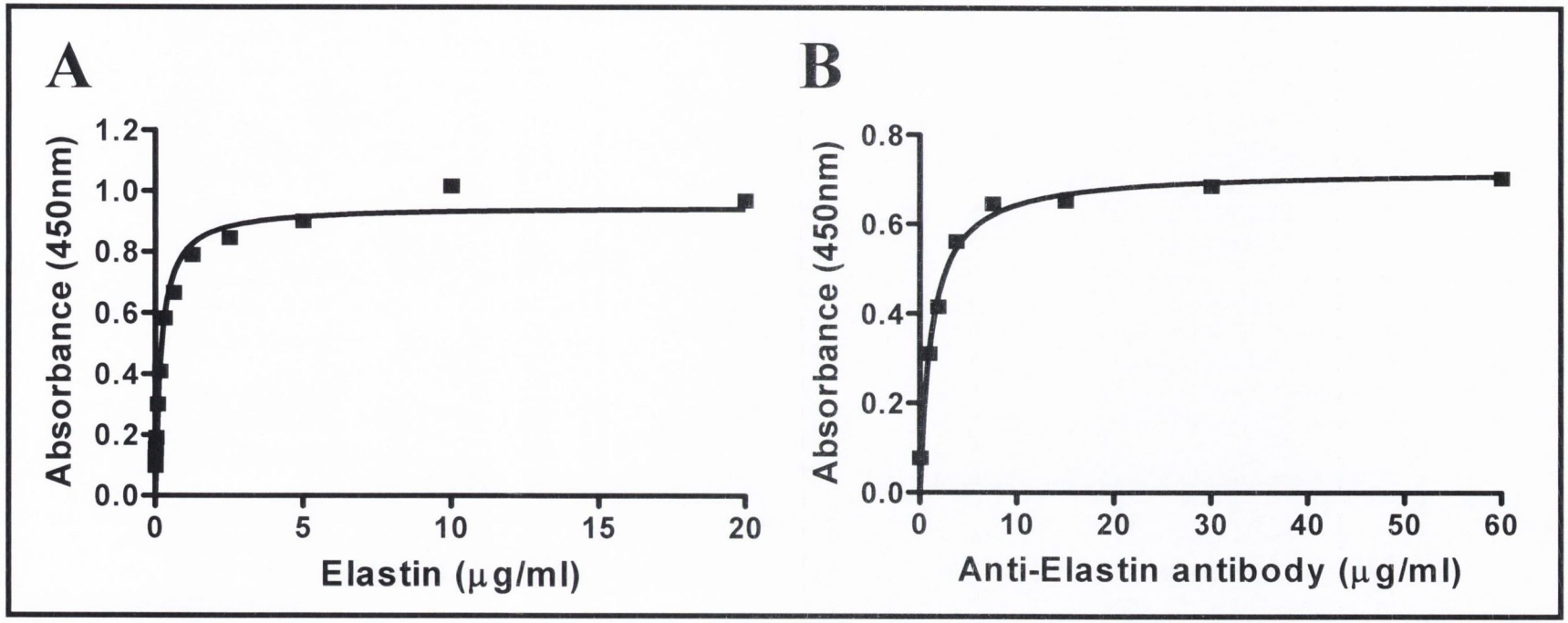

Figure 3.23 Binding of anti-elastin antibodies to immobilised elastin

(A) Microtitre plates were coated with various amounts of human aortic elastin and a 1:2,000 dilution (30 µg/ml) of polyclonal anti-elastin antibodies was added for 1h at room temperature. (B) Microtitre plates were coated with 20 µg/ml human aortic elastin and doubling dilutions of anti-elastin antibodies were added for 1 h at room temperature. Bound anti-elastin antibody was detected with polyclonal goat anti-rabbit HRP-conjugated antibodies followed by development with TMB substrate. Data points represent the mean of triplicate wells.

rAFnBPB$_{37\text{-}540}$ were preincubated with soluble elastin peptides before being added to elastin-coated wells. Soluble elastin peptides inhibited both recombinant FnBP proteins from binding to immobilised elastin in a dose-dependent manner. The highest concentration of soluble elastin (250μg/ml) resulted in ~80% inhibition of rAFnBPA$_{37\text{-}544}$ binding to immobilised elastin while ~62% inhibition was observed for rAFnBPB$_{37\text{-}540}$ (Figure 3.24). These data indicate the FnBP binding to immobilised elastin peptides is a specific receptor-ligand interaction.

3.2.8 Re-defining the A domain of FnBPA

The interaction of bacterial fibronectin-binding proteins with fibronectin has been studied in detail (Pilka *et al.*, 2006; Schwarz-Linek *et al.*, 2003). The structure of the B3 peptide from a fibronectin-binding protein of *S. dysgalactiae* in complex with the ^{1}F1^{2}F1 pair of type 1 modules at the N-terminus of fibronectin was studied by NMR spectroscopy. It was shown that a tandem β-zipper mechanism of binding occurred whereby the bacterial fibronectin-binding peptide contributes a fourth antiparallel strand to the triple-stranded β-sheet present in the F1 modules. Bioinformatic analysis resulted in the assignment of residues located between the C-terminus of the A domain and the cell wall spanning region of FnBPA from *S. aureus* into 11 putative F1 binding motifs. The first domain was shown to be almost entirely contained within the previously defined A domain of FnBPA (Figure 3.25). Recombinant protein rAFnBPA$_{37\text{-}544}$ therefore contains, at its C-terminus, 33 amino acid residues that were predicted to be involved in fibronectin binding. It was therefore important to ascertain if this recombinant protein could support binding to immobilised human fibronectin. An ELISA-type binding assay demonstrated that rAFnBPA$_{37\text{-}544}$ could bind to fibronectin in a dose-dependent and saturable manner. Doubts were cast over the purity of the commercial fibronectin with the possibility that contaminating fibrinogen was present. This could account for the dose-dependent binding of rAFnBPA$_{37\text{-}544}$. In order to test the purity of Calbiochem fibronectin used in these assays, anti-fibrinogen antibodies were tested for their affinity to immobilised fibronectin (Figure 3.26). Anti-fibrinogen antibodies bound in a dose-dependent manner to immobilised fibronectin indicating the presence of contaminating fibrinogen within the commercially available fibronectin samples. In response to this, purified human fibronectin was obtained from collaborators in Italy, to which anti-fibrinogen antibodies no longer bound (data not shown). This fibronectin supported binding of rAFnBPA$_{37\text{-}544}$ (Figure 3.27 A), demonstrating the presence of a fibronectin-binding motif at

the C-terminus of the previously defined A domain of FnBPA. These data indicate that the N-terminal 33 amino acid residues of the first fibronectin-binding segment of FnBPA are sufficient to promote strong and saturable binding to immobilised fibronectin and that the presence of the A domain does not interfere with fibronectin binding. The recombinant protein $rAFnBPA_{37-544}$ is thus capable of binding immobilised elastin, fibrinogen and fibronectin. As a negative control this protein was tested for binding to immobilised human collagen. No binding was detected over the range of protein concentrations used (Figure 3.27 B).

3.2.9 The N2N3 subdomains of FnBPA contain the ligand-binding function

Following the mapping of the 11 fibronectin-binding motifs of FnBPA, the co-ordinates of the A domain were redefined to span residues 37-511. A recombinant protein was produced encompassing these residues and was shown to be unable to bind fibronectin and collagen (Figure 3.27). This protein did promote binding to immobilised elastin and fibrinogen (Figure 3.28) supporting the redefinition of the A domain. The half maximum binding for this protein to immobilised elastin and fibrinogen was 45.6 ± 10.3 nM and 4.7 ± 1.8 nM, respectively. This shows that the affinity of the A domain of FnBPA for elastin is approximately 10-fold less than that for fibrinogen. A sequence alignment of the four fibrinogen-binding surface proteins of *S. aureus* (ClfA, ClfB, FnBPA and FnBPB) proposed that the N2 subdomain of FnBPA begins with residues $G_{194}TD_{196}$ (Deivanayagam *et al.*, 2002). The GTD motif is present at the equivalent position in ClfA and a similar GTN motif is present in ClfB. The N2N3 subdomains of ClfA and ClfB have been shown previously to be able to bind fibrinogen (McDevitt *et al.*, 1995; Perkins *et al.*, 2001). It was of interest therefore to ascertain if an N2N3 truncate of FnBPA could bind fibrinogen and elastin. A recombinant protein spanning residues 194-511 of FnBPA was expressed. This protein bound to immobilised fibrinogen and elastin in a dose-dependent and saturable manner (Figure 3.28). $rAFnBPA_{194-511}$ bound to elastin and fibrinogen in the low nanomolar range with a similar half maximum binding value to that of $rAFnBPA_{37-511}$. The half maximum binding for $rAFnBPA_{194-511}$ to immobilised elastin and fibrinogen was 51.77 ± 12.2 nM and 4.02 ± 0.23 nM, respectively. Neither $rAFnBPA_{37-511}$ nor $rAFnBPA_{194-511}$ bound to uncoated wells (Figure 3.28) indicating that the binding to both ligands is specific. These data indicate that, similar to ClfA and ClfB, the N1 domain of FnBPA is not required for ligand binding. The binding site for fibrinogen and elastin within FnBPA has thus been narrowed down to residues 194-511.

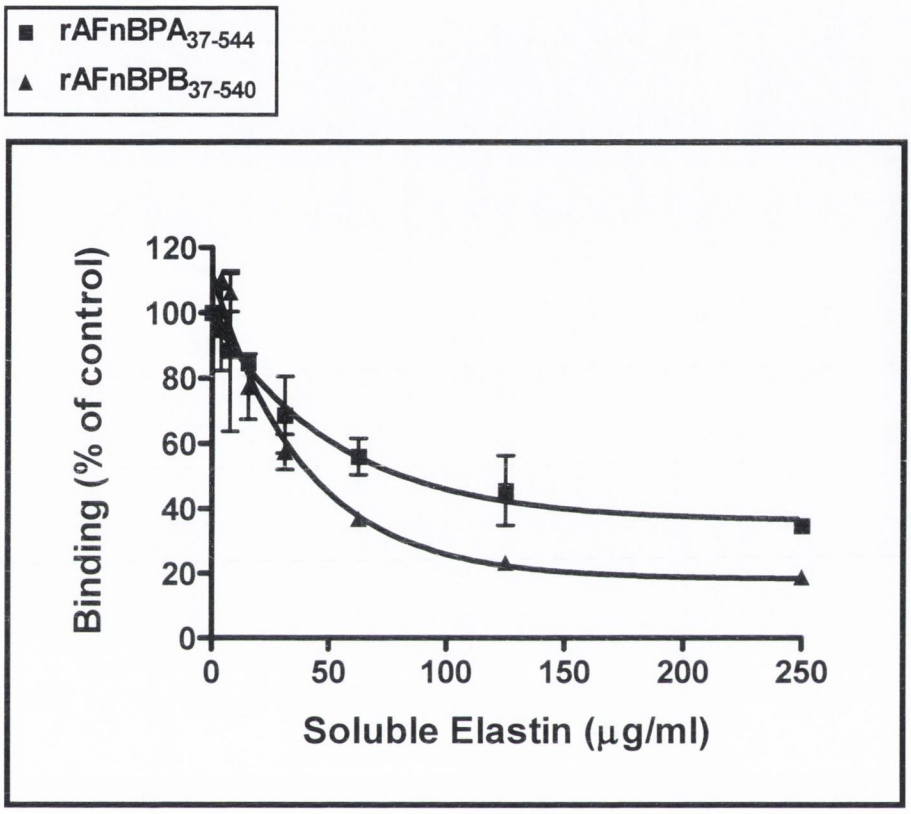

Figure 3.24 Inhibition of rAFnBPA$_{37-544}$ and rAFnBPB$_{37-540}$ binding to immobilised elastin using soluble elastin peptides

Microtitre plates were coated with 50 μg/ml human elastin. rAFnBPA$_{37-544}$ (0.1 μM) and rAFnBPB$_{37-540}$ (0.07 μM) were preincubated with increasing concentrations of soluble elastin peptides for 1 h before being added to elastin-coated wells. Bound protein was detected with polyclonal anti-rAFnBP antibodies, goat anti-rabbit HRP-conjugated antibodies followed by development with TMB substrate. Data points represent the mean of triplicate wells and are expressed as percentages of control lacking an inhibitor. This figure is representative of three independent experiments.

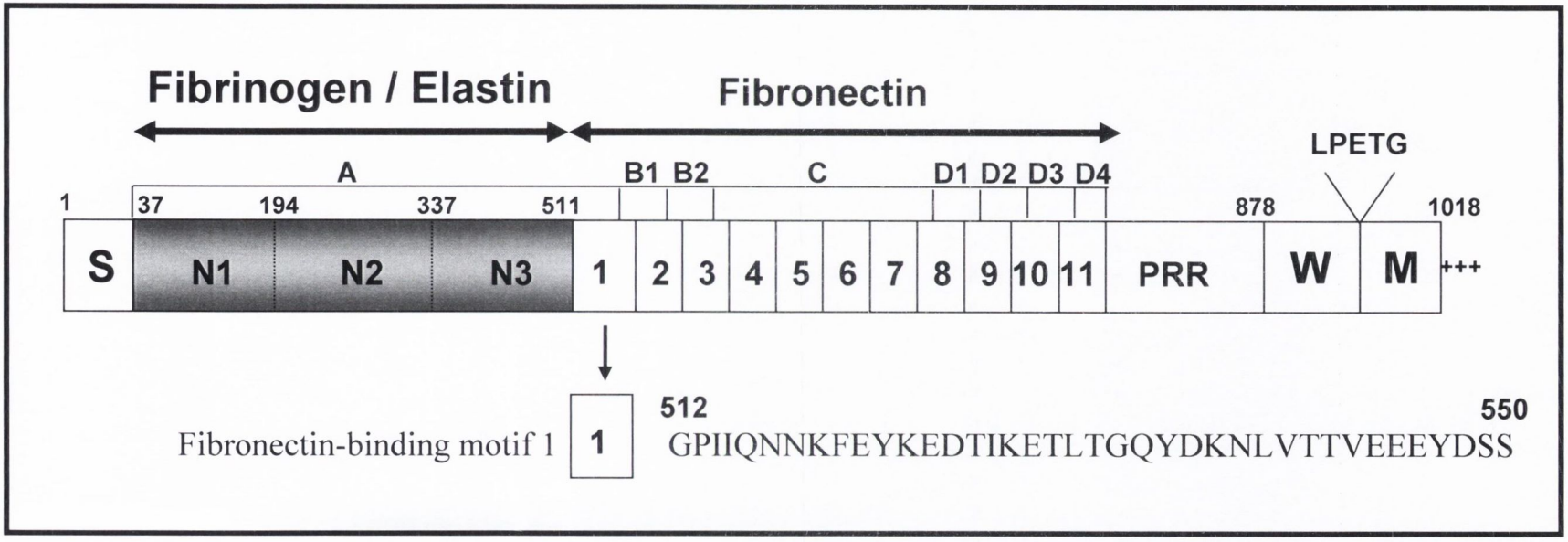

Figure 3.25 Re-defining the A domain of FnBPA

Mapping of the 11 fibronectin-binding tandem motifs at the C-terminus of FnBPA resulted in the redefining of the A domain of the protein. C-terminal residues 512-544 of the A domain are actually contained within the first fibronectin-binding motif (sequence given) which spans residues 512-550. The true A domain of FnBPA thus ends at residue 511.

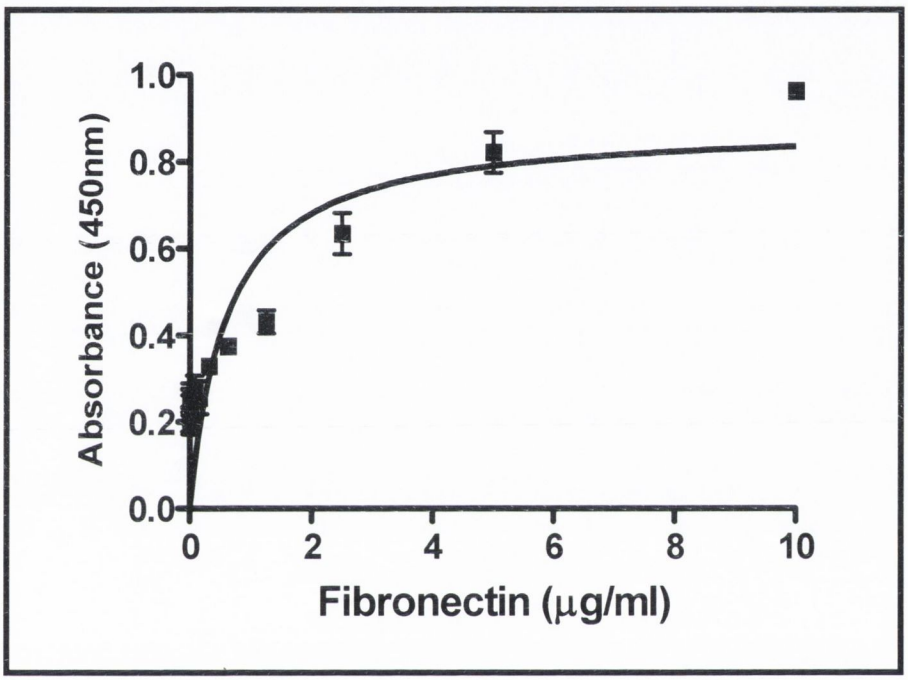

Figure 3.26 Binding of anti-fibrinogen antibodies to immobilised human fibronectin

Microtiter plates were coated with Calbiochem human fibronectin and probed with 1:2000 anti-fibrinogen-HRP conjugated antibodies. Plates were developed with TMB substrate. Data points represent the mean of triplicate wells.

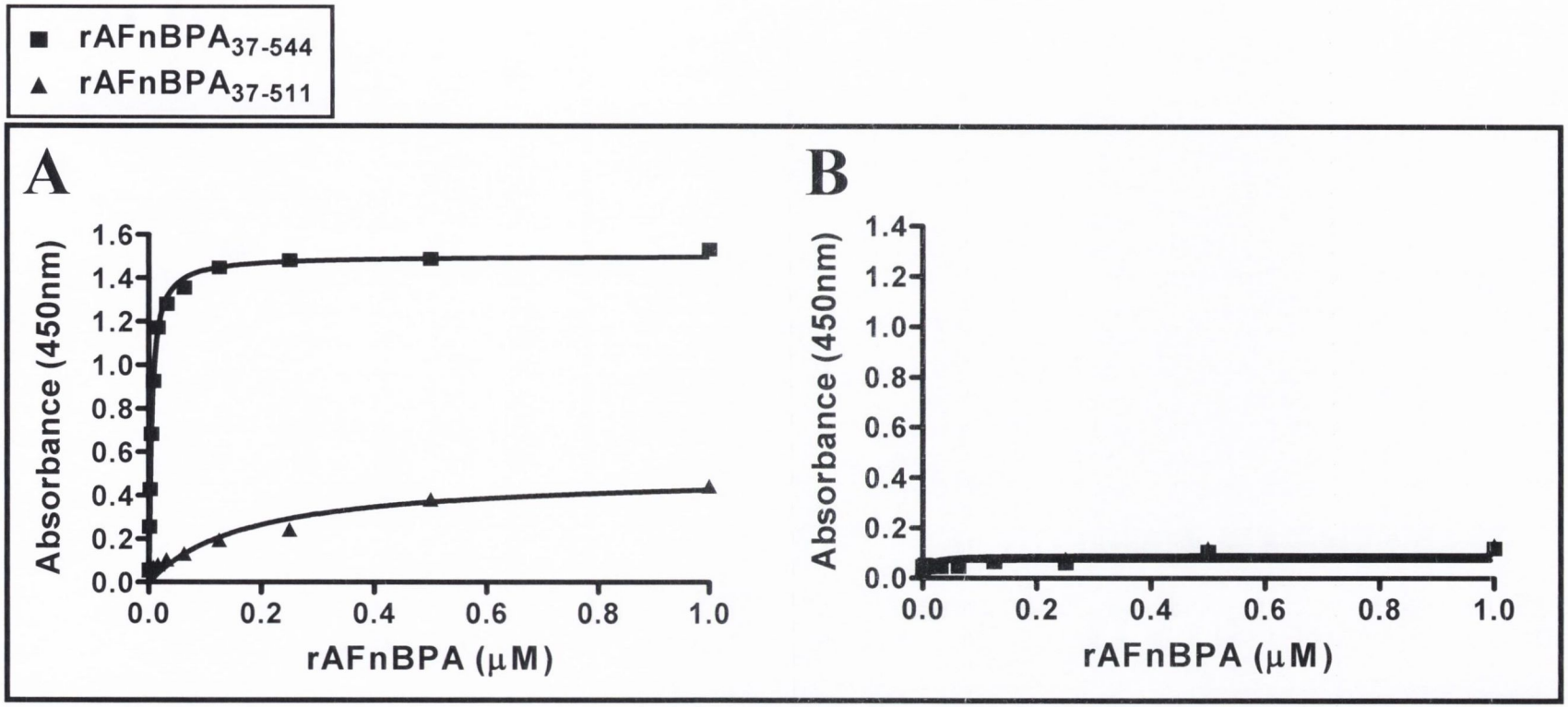

Figure 3.27 Binding of rAFnBPA$_{37-544}$ and rAFnBPA$_{37-511}$ to immobilised human fibronectin and collagen

Microtiter plates were coated with 10 μg/ml of human fibronectin (A) or human collagen (B) and increasing concentrations of rAFnBPA$_{37-544}$ or rAFnBPA$_{37-511}$ were incubated in ligand-coated wells for 1h. Bound protein was detected with polyclonal anti-rAFnBPA antibodies, followed by goat anti-rabbit-HRP conjugated antibodies. Plates were developed with TMB substrate. Data points represent the mean of triplicate wells and this figure is representative of three independent experiments.

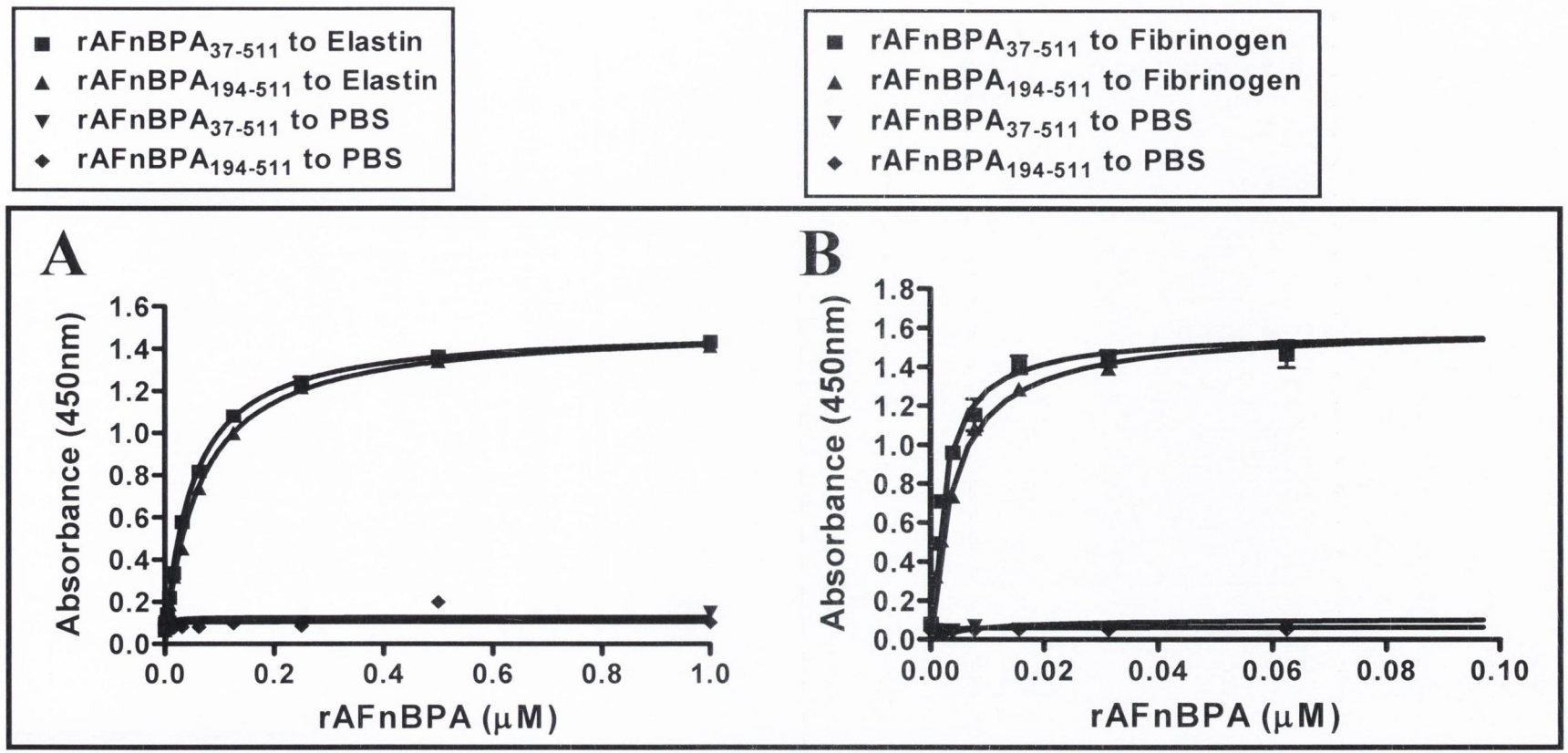

Figure 3.28 Binding of rAFnBPA$_{37-511}$ and rAFnBPA$_{194-511}$ to immobilised elastin and fibrinogen

Microtitre plates were coated with 10 μg/ml human aortic elastin (A) or fibrinogen (B) and increasing concentrations of rAFnBPA$_{37-511}$ and rAFnBPA$_{194-511}$ were added for 1h at room temperature. Bound protein was detected with polyclonal anti-rAFnBPA antibodies and goat anti-rabbit HRP-conjugated antibodies followed by development with TMB substrate. Data points represent the mean of triplicate wells and this figure is representative of three independent experiments.

3.2.10 Modelling the 3D structure of rAFnBPA$_{194-511}$

The ligand-binding N2N3 domains of ClfA and SdrG have been crystallised and studied in detail (Deivanayagam *et al.*, 2002; Ponnuraj *et al.*, 2003). It was hypothesised that the DEv-IgG fold, revealed in the crystal structure of ClfA, was also present in the corresponding regions of the A domains of ClfB, FnBPA and FnBPB. Further insight into the mechanism of fibrinogen binding by staphylococcal surface proteins came with the co-crystallisation of SdrG with its fibrinogen ligand, the N-terminus of the β chain. In this structure, it was clear that the orientation of the C-terminal β strand (latching peptide) could vary in response to the presence of fibrinogen. This mechanism of ligand binding was termed "dock, lock and latch".

The A domain of FnBPA has ~20% amino acid identity to the A domain of ClfA. In contrast to ClfB, FnBPA binds to the same region of fibrinogen as ClfA, the extreme C-terminus of the γ chain. To compare the mechanism of fibrinogen binding of FnBPA with that of ClfA and to understand the process of elastin binding, a molecular model of N2N3 of FnBPA was needed. The primary sequence of N2N3 (residues 194-544) of FnBPA was submitted to the Protein homology/analogy recognition engine (Phyre) from the Imperial College, London (http://www.sbg.bio.ic.ac.uk/~phyre/). This service predicts the 3D folding of the submitted sequence based on the crystal structures of similar proteins. The predictions are graded on the percent precision of the predicted structure compared to that on which it is modelled. The first two recommendations for the structure of FnBPA are based on ClfA and SdrG, respectively. It was decided to study the ClfA-based structure of FnBPA due to the greater similarity of the two proteins and the fact that they bind to the same region of fibrinogen. Following this, a computer-generated fibrinogen ligand (C-terminal 8 amino acid peptide of the γ chain of fibrinogen, $G_{404}AKQAGDV_{411}$) was docked *in silico* into the predicted structural model of FnBPA using Autodock (http://autodock.scripps.edu/). Autodock is a software package that is designed to predict how small molecules such as a ligand peptide or drug candidate, can bind to a receptor of known 3D structure (Hetenyi and van der Spoel, 2002). A histogram was provided of all the docking solutions and the most energetically favourable docking solution for the fibrinogen peptide binding into the hydrophobic trench was analysed. The resulting figure was viewed using the Chimera molecular viewer from the University of California, San Francisco (http://www.cgl.ucsf.edu/chimera/) and can be seen in Figure 3.29. This shows the

independently folded subdomains N2 and N3 composed largely of anti-parallel β-strands. The fibrinogen ligand is predicted to dock into the hydrophobic trench situated between N2 and N3 and is shown in ball and stick format (see supplementary material on accompanying CD). Interestingly, the orientation of the fibrinogen ligand is the same as that seen in the co-crystallisation of SdrG with its fibrinogen ligand. The fibrinogen residues, G_{404}AKQAGDV_{411}, are situated running along the trench from top left to bottom right. To clarify this, the C-terminal valine residue is labelled with the suffix f (V411f) to indicate fibrinogen. The position of the latching peptide is shown to be wound around domain N3 in a similar position to the same strand in the crystal structure of ClfA, on which this model was based. This is most likely an artefact and the exact position of the latching peptide of ClfA or FnBPA in the presence or absence of fibrinogen, is unknown. The fibronectin-binding motif situated at the C-terminus of the A domain of FnBPA that is not involved in fibrinogen or elastin binding is shown in green. This is predicted to span half of the final latching β-strand plus the remaining loop region. It is possible therefore that the rAFnBPA$_{37\text{-}511}$ and rAFnBPA$_{194\text{-}511}$ proteins tested above, do not have a complete latching peptide. Despite this, they both bind strongly to fibrinogen and elastin indicating that the remaining residues present in the latching peptide are sufficient to form any β-strand complementation needed in N2.

3.2.11 Construction of A domain truncates of FnBPA lacking C-terminal residues

The structure of the N2N3 subdomains of FnBPA is likely to be critical for binding to fibrinogen and elastin. Further truncation of rAFnBPA$_{194\text{-}511}$ would most likely impinge on the DEv-IgG fold of the protein and thus affect binding. The molecular model described above served to give a more detailed insight into the possible mechanism of ligand binding of FnBPA and allowed a more specific truncation approach to be adopted. One of the objectives of this project was to construct truncates of FnBPA that would help determine if elastin and fibrinogen bind to similar or distinct regions of the A domain. To further narrow down the binding site for fibrinogen and elastin within FnBPA, truncates of the A domain were constructed lacking C-terminal residues. In this way, the role of residues contained in the putative latching peptide could be investigated. The role of residues N-terminal to this β-strand could also be explored. Three C-terminally truncated derivatives were constructed and purified. The first truncate lacked two C-terminal amino acid residues in comparison to rAFnBPA$_{194\text{-}511}$ (Figure 3.29). These two residues were predicted to form the remainder of the putative latching peptide. The second truncate spans residues 194-498 which is devoid of the

Figure 3.29 Predicted 3D structure of rAFnBPA$_{194-544}$

Predicted 3D structural model of subdomains N2N3 of FnBPA (rAFnBPA$_{194-544}$) based on homology modelling with the equivalent domains of ClfA. The C-terminal 8 amino acids of the γ chain of fibrinogen (G_{404}AKQAGDV_{411}) have been docked into the hydrophobic trench of this structure and are shown in ball and stick format with the C-terminal valine residue labelled with the suffix f (V411f). Green shows the fibronectin-binding domain at the end of N3, while successive C-terminal deletion constructs are indicated in yellow (194-509, 194-498 and 194-483). The boundary between N2 and N3 (Y337) is also indicated in yellow.

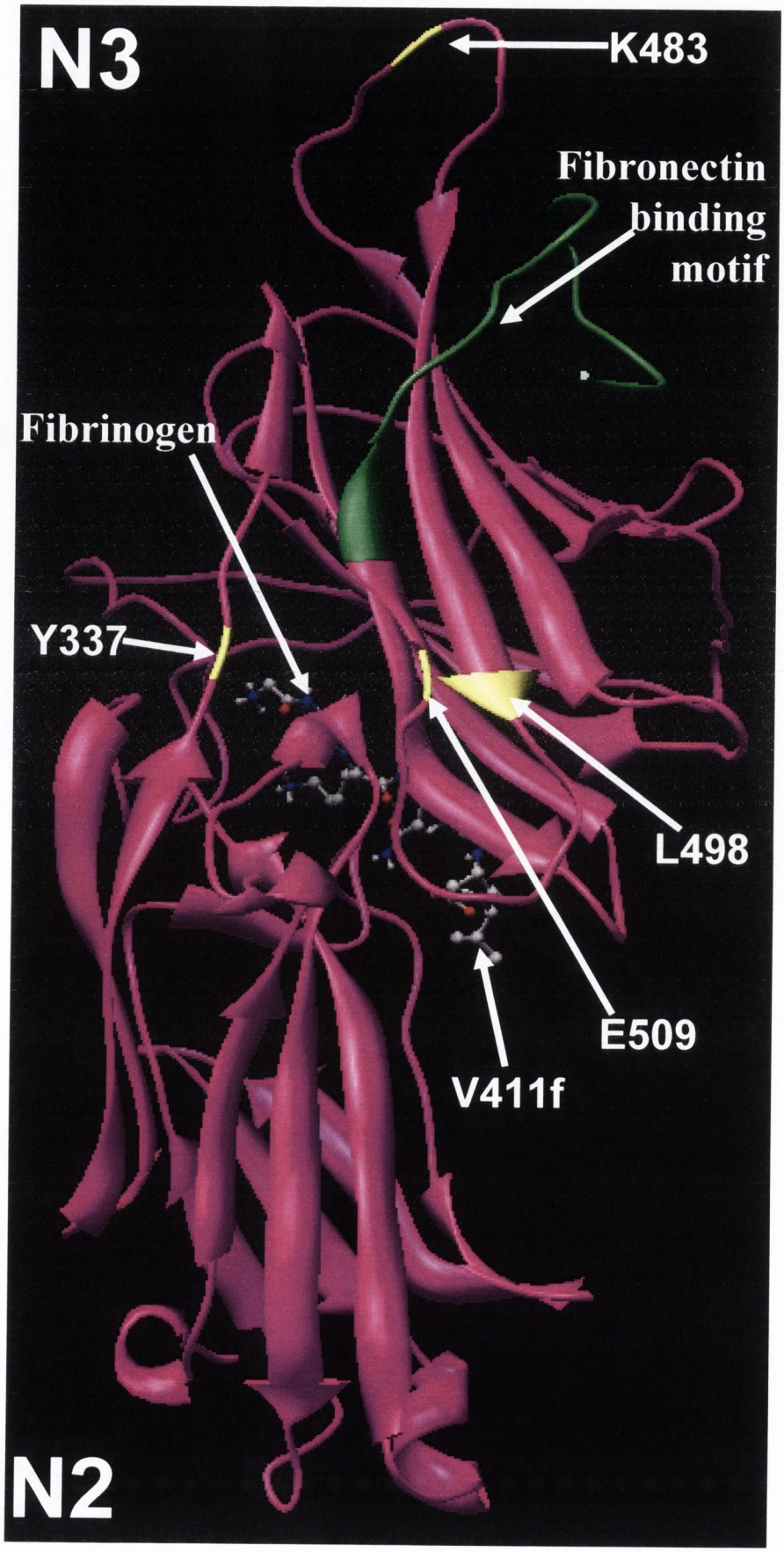
N3
K483
Fibronectin
binding
motif
Fibrinogen
Y337
L498
E509
V411f
N2

entire loop region between the two β-strands in the model. This loop region is likely to form the hinge segment that folds across the fibrinogen ligand in the hydrophobic trench. The final truncate lacks the latching peptide, hinge region and all of the preceding β-strand plus half of the loop segment N-terminal to this. This protein was designed as a negative control for fibrinogen and elastin binding to show the importance of the structural fold of N3. All proteins were analysed by SDS-PAGE (Figure 3.30) and were compared directly with $rAFnBPA_{194\text{-}511}$ in ELISA type assays for binding to immobilised elastin and fibrinogen. $rAFnBPA_{194\text{-}509}$ bound to fibrinogen with a statistically significant difference in half maximum binding compared to that of $rFnBPA_{194\text{-}511}$ (half maximum binding of $rAFnBPA_{194\text{-}511}$ = 4.02 ± 0.23 nM, half maximum binding of $rAFnBPA_{194\text{-}509}$ = 20.94 ± 7.5 nM: p-value = 0.0175) whereas there was no significant difference in the half maximum binding for elastin (half maximum binding of $rAFnBPA_{194\text{-}511}$ = 51.77 ± 12.2 nM, half maximum binding of $rAFnBPA_{194\text{-}509}$ = 47.6 ± 14.8 nM: p-value = 0.7256) (Figure 3.31). In contrast, a further deletion, $rFnBPA_{194\text{-}498}$, which lacks the entire hinge region, did not bind detectably to either ligand (Figure 3.32). These results are consistent with FnBPA binding both ligands by a dock, lock and latch mechanism because $rAFnBPA_{194\text{-}498}$ lacks residues that would comprise the latching peptide and the hinge region covering the ligand-occupied trench. The third construct, $rAFnBPA_{194\text{-}483}$ was also unable to bind fibrinogen or elastin (Figure 3.33). This indicates the importance of the structural fold of the N3 domain on ligand binding. These data also show that an alteration of the structure of N2N3 of FnBPA that affects the binding to fibrinogen, also affects the binding to elastin, suggesting that the two ligands bind to FnBPA in a similar manner.

3.2.12 Individual N2 and N3 subdomains of FnBPA cannot bind elastin or fibrinogen

To complete the truncation studies of the A domain of FnBPA, the individual subdomains N2 and N3 were expressed and purified. Each recombinant protein was tested for binding to immobilised ligands by ELISA type methods. Neither subdomain alone could support binding to elastin or fibrinogen (Figure 3.34 and Figure 3.35). These data are in agreement with previous results whereby the individual subdomains of ClfB (Perkins 2001) and ClfA are unable to bind to immobilised fibrinogen (Deivanayagam *et al.*, 2002). A summary of the half maximum binding values obtained for rAFnBPA truncates binding to immobilised elastin and fibrinogen is presented in Table 3.1.

3.2.13 Inhibition of FnBPA binding to immobilised elastin and fibrinogen

In order to investigate further if elastin binds to rAFnPBA in a similar manner to that of fibrinogen, inhibition assays were carried out. Exogenous soluble fibrinogen was tested for its ability to inhibit the binding of $rAFnBPA_{37\text{-}511}$ to immobilised elastin. As recorded previously (Wann *et al.*, 2000), soluble fibrinogen inhibited the binding of $rAFnBPA_{37\text{-}511}$ to immobilised fibrinogen. A concentration of 500 μg/ml of soluble fibrinogen resulted in ~80% inhibition of binding of $rAFnBPA_{37\text{-}511}$ to immobilised fibrinogen. The same concentration of fibrinogen resulted in ~90% inhibition of binding to immobilised elastin (Figure 3.36). Preincubation of $rAFnBPA_{37\text{-}511}$ with soluble fibrinogen, saturates the binding sites and renders the protein unable to bind to immobilised elastin. This indicates that the binding sites within rAFnBPA for fibrinogen and elastin are similar or overlapping.

The fibrinogen used in the above assays, however is a large protein and the possibility of inhibition by steric hindrance cannot be ruled out. Thus, a synthetic fibrinogen γ chain peptide (G_{395}EGQQHHLGGAKQAGDV_{411}) containing the precise binding site for FnBPA was shown to inhibit the binding of $rAFnBPA_{37\text{-}511}$ to immobilised elastin as well as fibrinogen in a dose-dependent and saturable manner. Binding was reduced to ~20% and ~10% for fibrinogen and elastin, respectively, in comparison to $rAFnBPA_{37\text{-}511}$ alone (Figure 3.37). A control peptide, representing a scrambled version of the same C-terminal γ chain peptide (GHEHGLQGQGAVKDGAQ: gift, Prof. M. Hook, Texas A&M University) caused no inhibition to either ligand confirming the specificity of the γ chain-FnBPA interaction.

L. lactis expressing the full-length FnBPA protein on the bacterial cell surface was also tested to analyse the effect of the fibrinogen γ chain peptide on bacterial adherence to immobilised elastin. Dose-dependent and saturable inhibition of adherence of *L. lactis* FnBPA to both fibrinogen and elastin was observed. Maximum inhibition of adherence to fibrinogen (~70%) was achieved only at the highest concentration of peptide (400 μM) whereas ~85% inhibition of adherence to elastin was achieved with 100 μM peptide. In both cases the scrambled peptide had no effect (Figure 3.38). The more potent inhibition of binding to elastin by the fibrinogen peptide possibly reflects the higher affinity of FnBPA for fibrinogen compared to elastin. These data show that excess fibrinogen γ chain peptide can inhibit the adherence of bacterial cells to immobilised fibrinogen and elastin. This is further evidence that fibrinogen and elastin bind to a similar or overlapping site within region A of FnBPA.

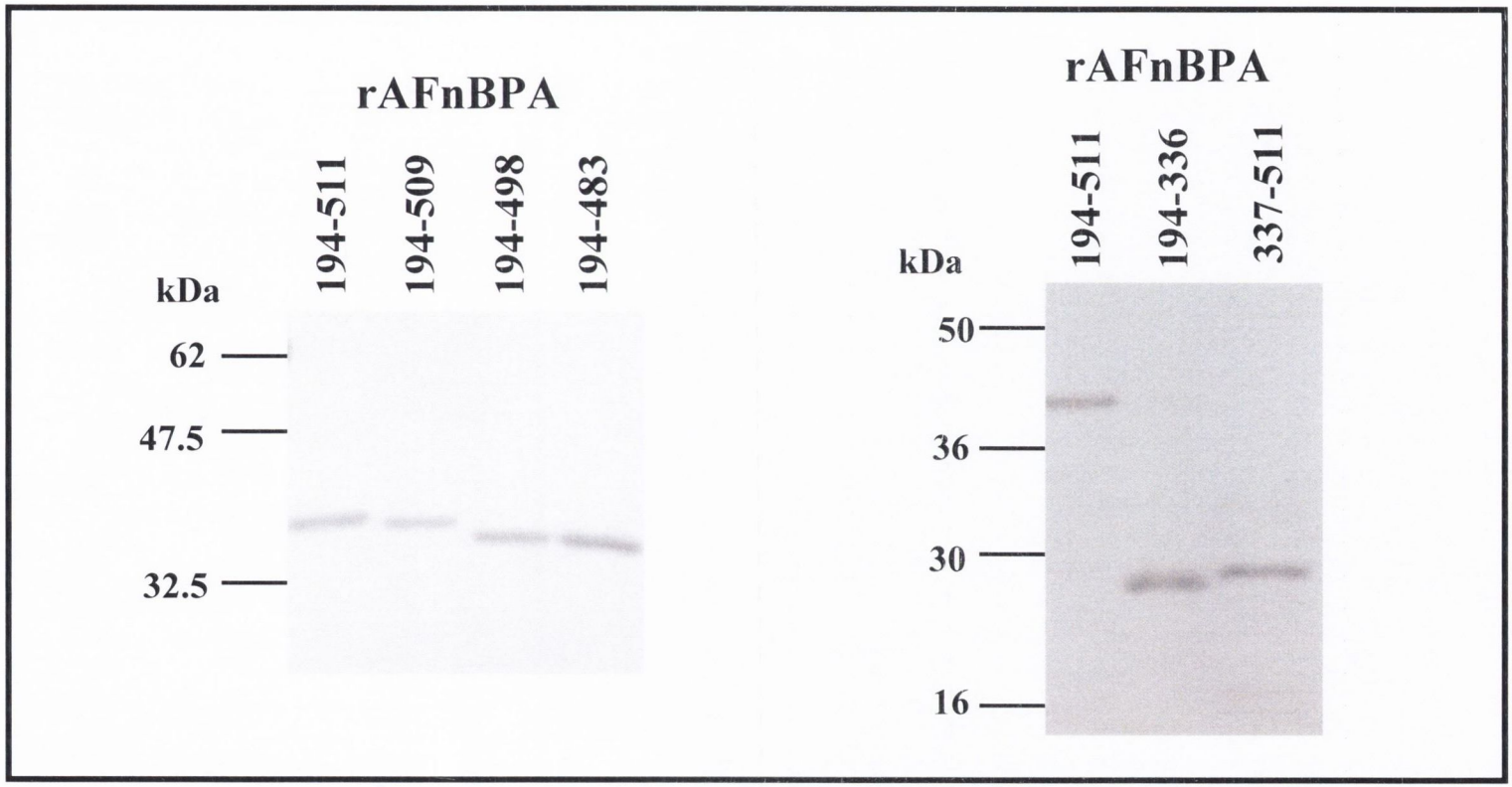

Figure 3.30 Truncates of the A domain of FnBPA

Equal amounts (1 μg) of $rAFnBPA_{194-511}$, $rAFnBPA_{194-509}$, $rAFnBPA_{194-498}$ and $rAFnBPA_{194-483}$ (A) and $rAFnBPA_{194-511}$, $rAFnBPA_{194-366}$ and $rAFnBPA_{337-511}$ (B) were analysed by SDS-PAGE and stained with Coomassie Blue.

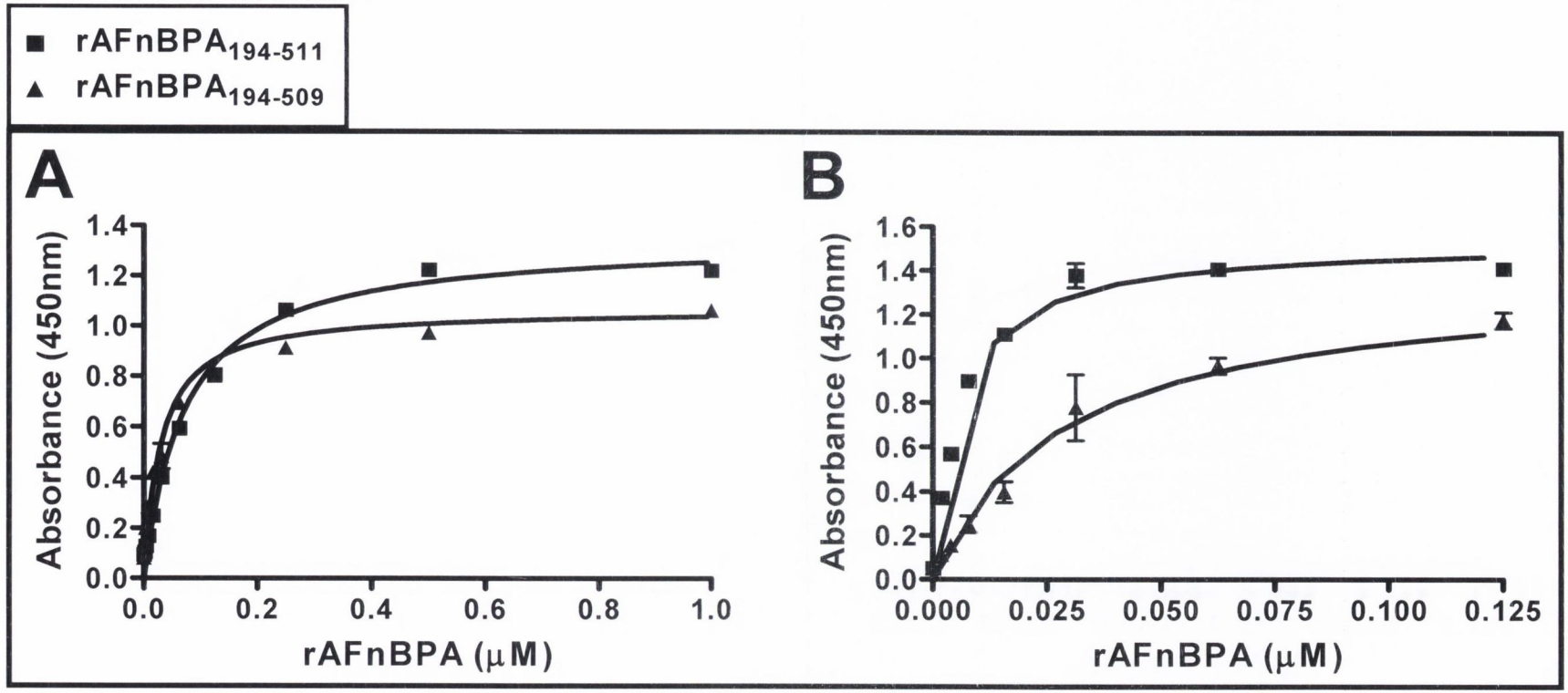

Figure 3.31 Binding of rAFnBPA$_{194-511}$ and rAFnBPA$_{194-509}$ to immobilised elastin and fibrinogen

Microtitre plates were coated with 10 μg/ml human aortic elastin (A) or fibrinogen (B) and increasing concentrations of rAFnBPA$_{194-511}$ and rAFnBPA$_{194-509}$ were added for 1h at room temperature. Bound protein was detected with polyclonal anti-rAFnBPA antibodies and goat anti-rabbit HRP-conjugated antibodies followed by development with TMB substrate. Data points represent the mean of triplicate wells and this figure is representative of three independent experiments.

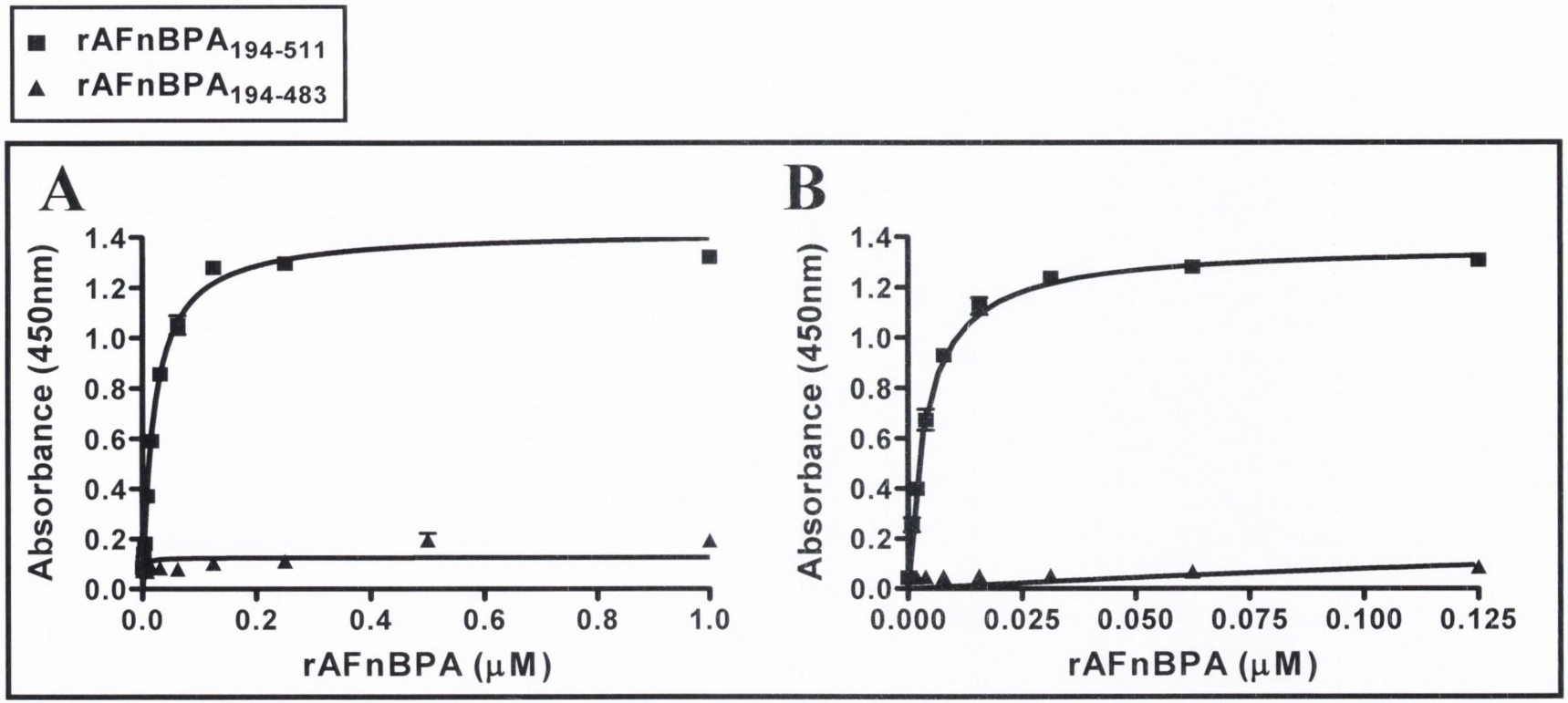

Figure 3.33 Binding of $rAFnBPA_{194-511}$ and $rAFnBPA_{194-483}$ to immobilised elastin and fibrinogen

Microtitre plates were coated with 10 μg/ml human aortic elastin (A) or fibrinogen (B) and increasing concentrations of $rAFnBPA_{194-511}$ and $rAFnBPA_{194-483}$ were added for 1h at room temperature. Bound protein was detected with polyclonal anti-rAFnBPA antibodies and goat anti-rabbit HRP-conjugated antibodies followed by development with TMB substrate. Data points represent the mean of triplicate wells and this figure is representative of three independent experiments.

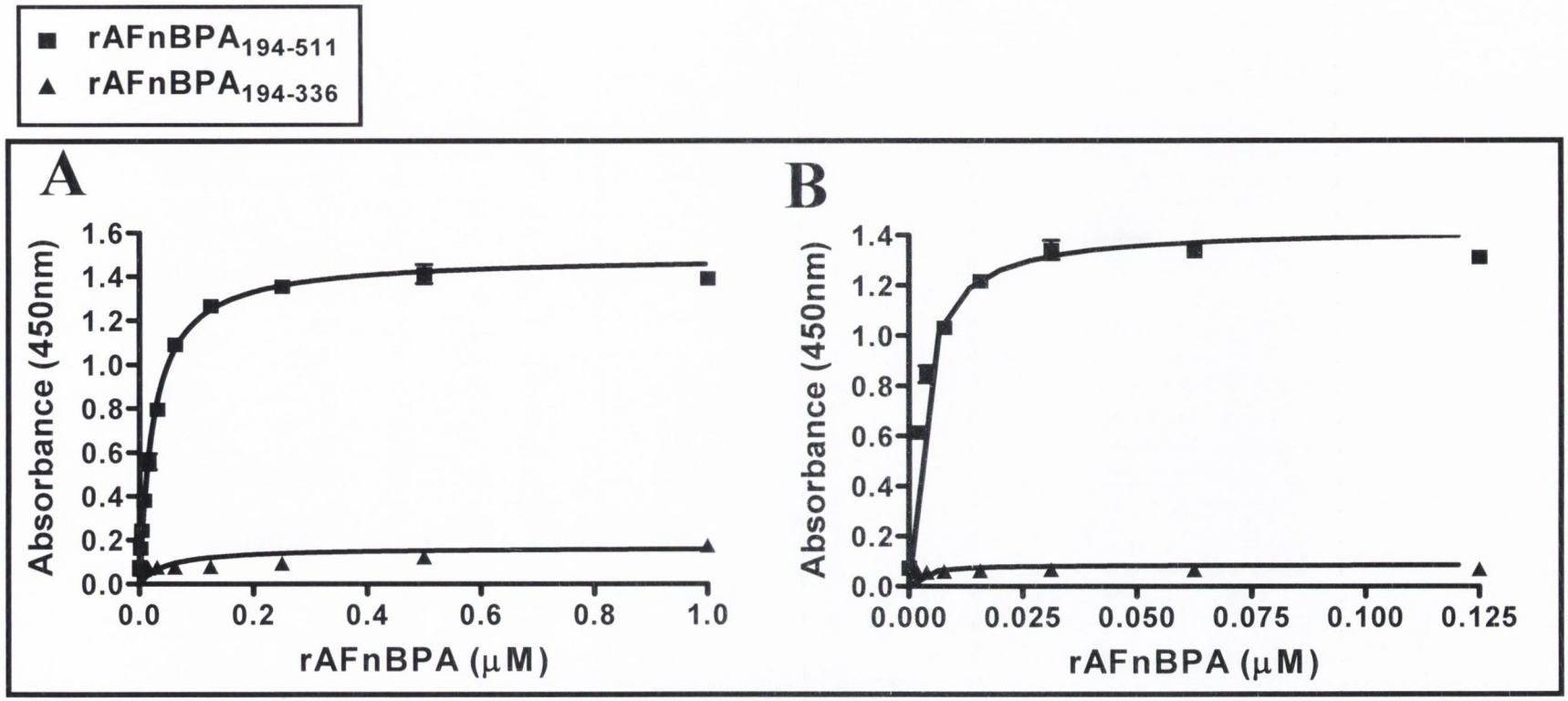

Figure 3.34 Binding of rAFnBPA$_{194-511}$ and rAFnBPA$_{194-336}$ to immobilised elastin and fibrinogen

Microtitre plates were coated with 10 μg/ml human aortic elastin (A) or fibrinogen (B) and increasing concentrations of rAFnBPA$_{194-511}$ and rAFnBPA$_{194-336}$ were added for 1h at room temperature. Bound protein was detected with polyclonal anti-rAFnBPA antibodies and goat anti-rabbit HRP-conjugated antibodies followed by development with TMB substrate. Data points represent the mean of triplicate wells and this figure is representative of three independent experiments.

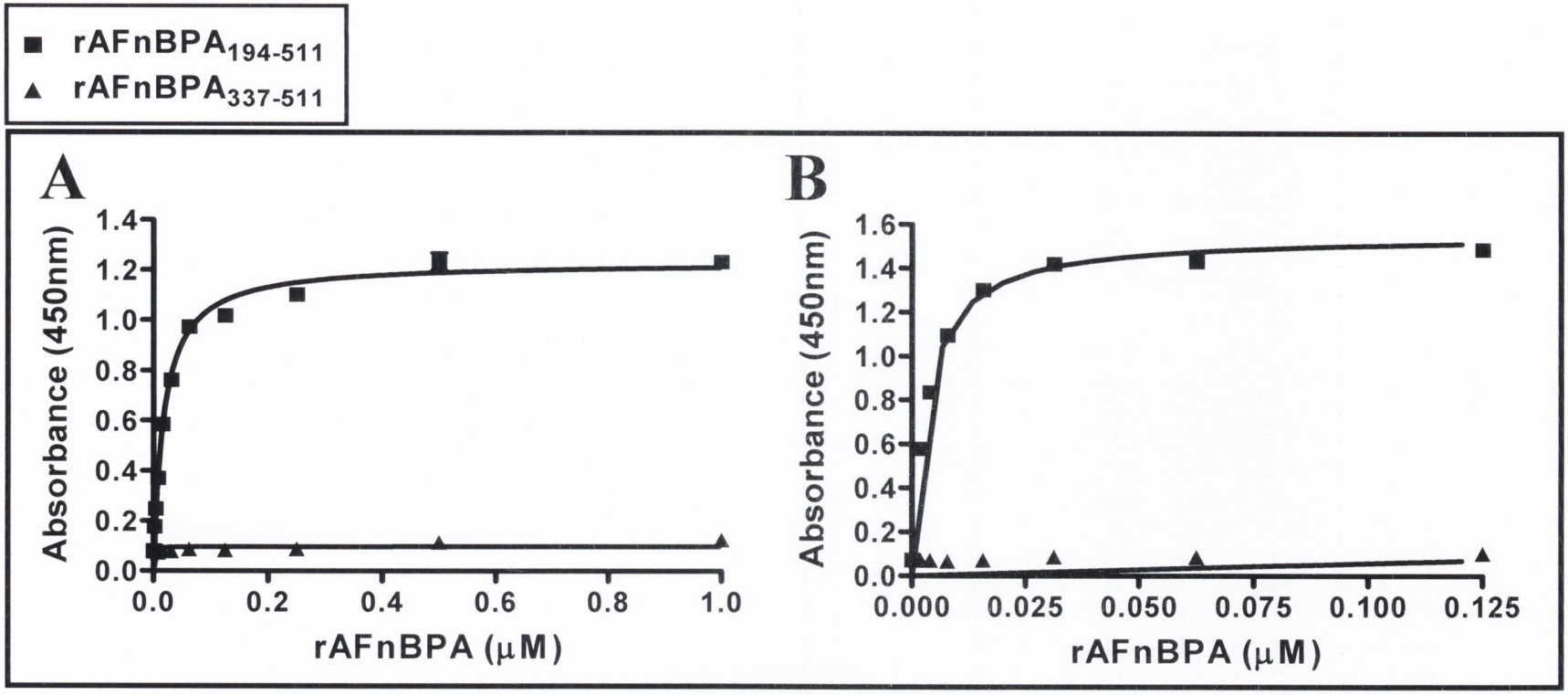

Figure 3.35 Binding of rAFnBPA$_{194-511}$ and rAFnBPA$_{337-511}$ to immobilised elastin and fibrinogen

Microtitre plates were coated with 10 μg/ml human aortic elastin (A) or fibrinogen (B) and increasing concentrations of rAFnBPA$_{194-511}$ and rAFnBPA$_{337-511}$ were added for 1h at room temperature. Bound protein was detected with polyclonal anti-rAFnBPA antibodies and goat anti-rabbit HRP-conjugated antibodies followed by development with TMB substrate. Data points represent the mean of triplicate wells and this figure is representative of three independent experiments.

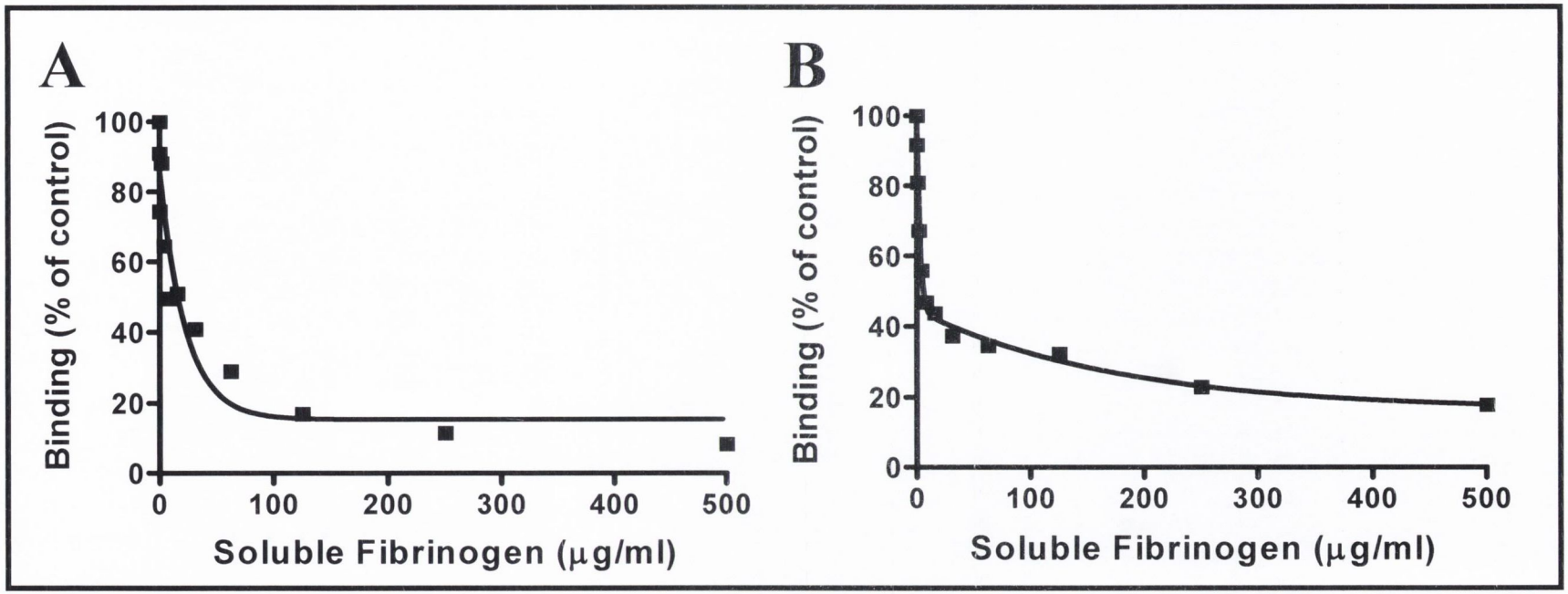

Figure 3.36 Inhibition of rAFnBPA$_{37\text{-}511}$ binding to immobilised elastin and fibrinogen using soluble fibrinogen

Microtitre plates were coated with 10 µg/ml human aortic elastin (A) or fibrinogen (B). (A) rAFnBPA$_{37\text{-}511}$ (0.1 µM) was preincubated with increasing amounts of soluble fibrinogen (0 µg/ml – 500 µg/ml) before being added to elastin-coated wells. (B) rAFnBPA$_{37\text{-}511}$ (0.05µM) was preincubated with increasing amounts of soluble fibrinogen (0 µg/ml – 500 µg/ml) before being added to fibrinogen-coated wells. Bound protein was detected with polyclonal anti-rAFnBPA antibodies and goat anti-rabbit HRP-conjugated antibodies followed by development with TMB substrate. Data points represent the mean of triplicate wells and are expressed as a percentage of control wells lacking inhibitor. This figure is representative of three independent experiments.

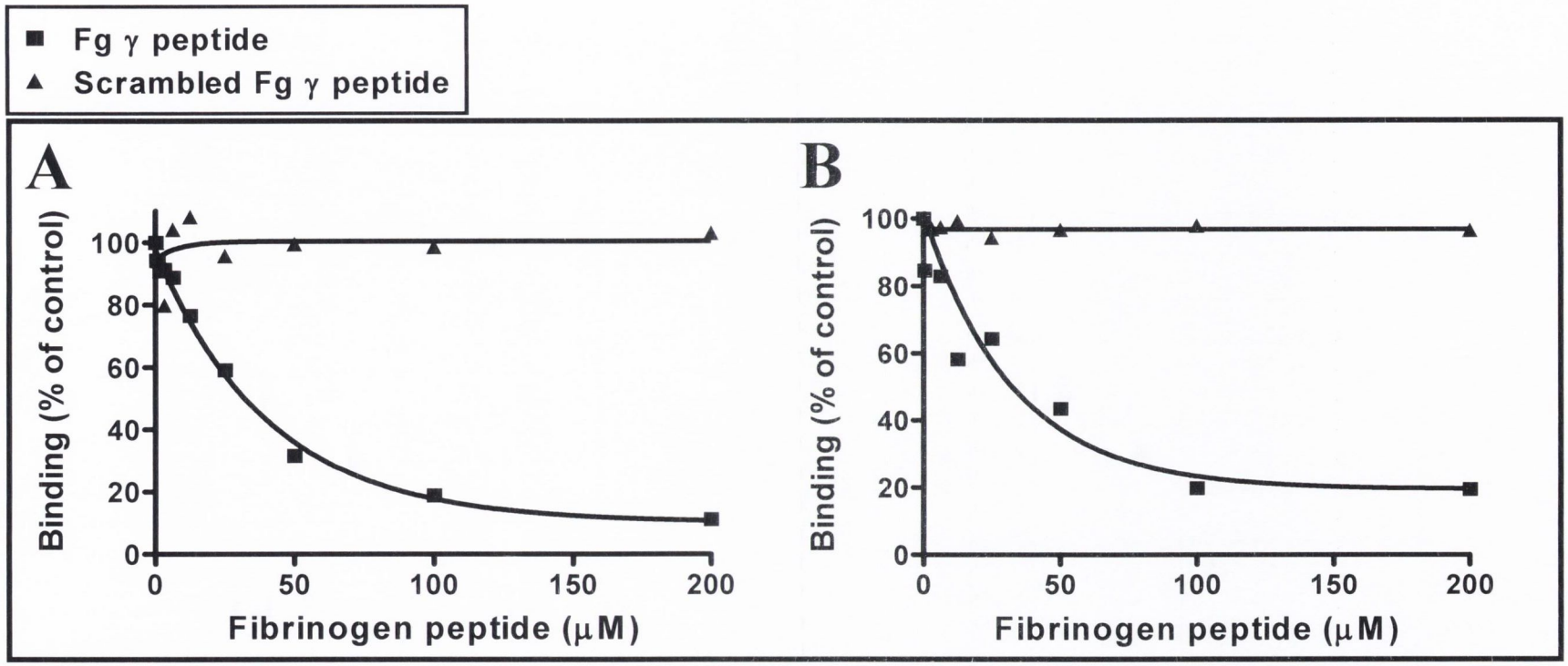

Figure 3.37 Inhibition of rAFnBPA$_{37\text{-}511}$ binding to immobilised elastin and fibrinogen using fibrinogen γ chain peptides

Microtitre plates were coated with 10 μg/ml human aortic elastin (A) or fibrinogen (B). 0.1 μM (A) or 0.025 μM (B) of rAFnBPA$_{37\text{-}511}$ was preincubated with increasing amounts of fibrinogen γ chain peptides (200 μM – 0 μM) before being added to ligand-coated wells. Bound protein was detected with polyclonal anti-rAFnBPA antibodies and goat anti-rabbit HRP-conjugated antibodies followed by development with TMB substrate. Data points represent the mean of triplicate wells and are expressed as a percentage of control wells lacking inhibitor. This figure is representative of three independent experiments.

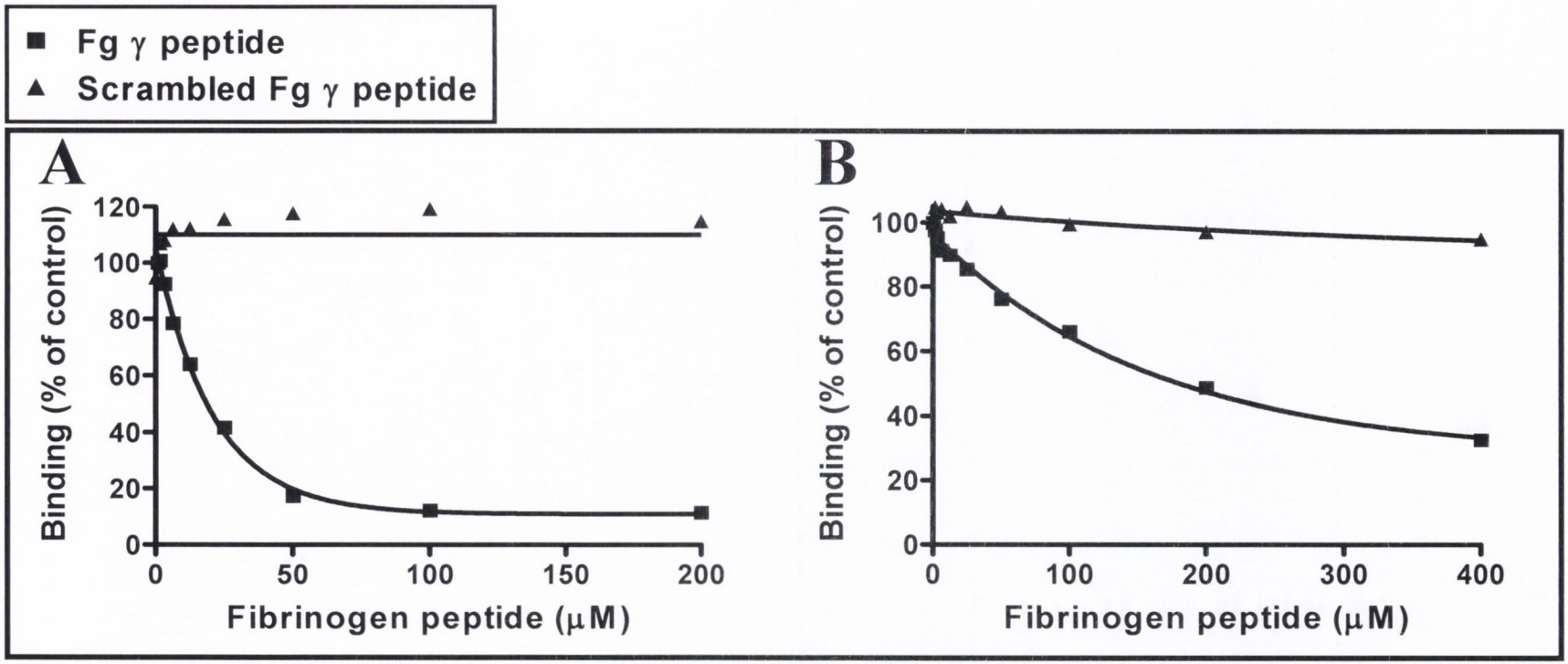

Figure 3.38 Inhibition of *L. lactis* expressing FnBPA binding to immobilised elastin and fibrinogen using fibrinogen γ chain peptides

Microtitre plates were coated with 10 μg/ml human aortic elastin (A) or fibrinogen (B). *L. lactis* cultures were induced with 0.8 ng/ml (A) or 0.1 ng/ml (B) nisin and preincubated with increasing amounts of fibrinogen γ chain peptides (400 μM – 0 μM) before being added to ligand-coated wells. Adherence of bacteria to elastin and fibrinogen was measured using SYTO-13 fluorescent dye and crystal violet, respectively. Data points represent the mean of triplicate wells and are expressed as a percentage of control wells lacking inhibitor. This figure is representative of three independent experiments.

	Elastin			Fibrinogen		
rAFnBPA	Half max binding ± SD (nM)	2-tailed p-value	Significant difference	Half max binding ± SD (nM)	2-tailed p-value	Significant difference
37-511	45.6 ± 10.3			4.7 ± 1.8		
			To 37-511			To 37-511
37-544	38.9 ± 20.9	0.6446	No	6.78 ± 3.41	0.403	No
194-511	51.77 ± 12.2	0.5399	No	4.02 ± 0.23	0.5517	No
			To 194-511			To 194-511
194-509	47.6 ± 14.8	0.7256	No	20.94 ± 7.5	0.0175	Yes
194-498	ND	ND	ND	488.7 ± 74.2	0.0003	Yes
194-483	ND	ND	ND	723.56 ± 345.6	0.0226	Yes
194-336	ND	ND	ND	ND	ND	ND
337-511	ND	ND	ND	ND	ND	ND

Table 3.1 Half maximum binding values for rAFnBPA proteins binding to immobilised elastin and fibrinogen

The relative affinities of $rAFnBPA_{37\text{-}511}$ and truncates thereof were assessed by ELISA-type binding assays to immobilised elastin and fibrinogen. Half maximum binding values given are approximated by the GraphPad Prism software package and are averaged over at least three experiments. The p-value given represents the statistical significant difference between the binding for each variant compared to that of $rAFnBPA_{37\text{-}511}$ or $rAFnBPA_{194\text{-}511}$ as indicated. *ND = no detectable binding observed.

To investigate the similarities of fibrinogen and elastin binding in more detail, another known inhibitor of fibrinogen binding was tested for its effect on FnPBA binding to immobilised elastin. Monoclonal antibody 7C5 was previously shown to inhibit FnBPA-expressing bacteria from adherence to fibrinogen (Fitzgerald *et al.*, 2006). Here the ability of the antibody to inhibit bacterial attachment to immobilised fibrinogen and elastin was tested. 7C5 was shown to inhibit adherence of *L. lactis* expressing FnBPA to immobilised fibrinogen to a maximum of 60%. It also strongly inhibited adherence of *L. lactis* to immobilised elastin with ~80% inhibition being achieved at 50 μg/ml of antibody. An isotype-matched control monoclonal antibody, 1F9 was known not to inhibit fibrinogen binding. This antibody failed to inhibit elastin binding (Figure 3.39). These experiments are consistent with the interpretation that fibrinogen and elastin bind to FnBPA at sites that overlap.

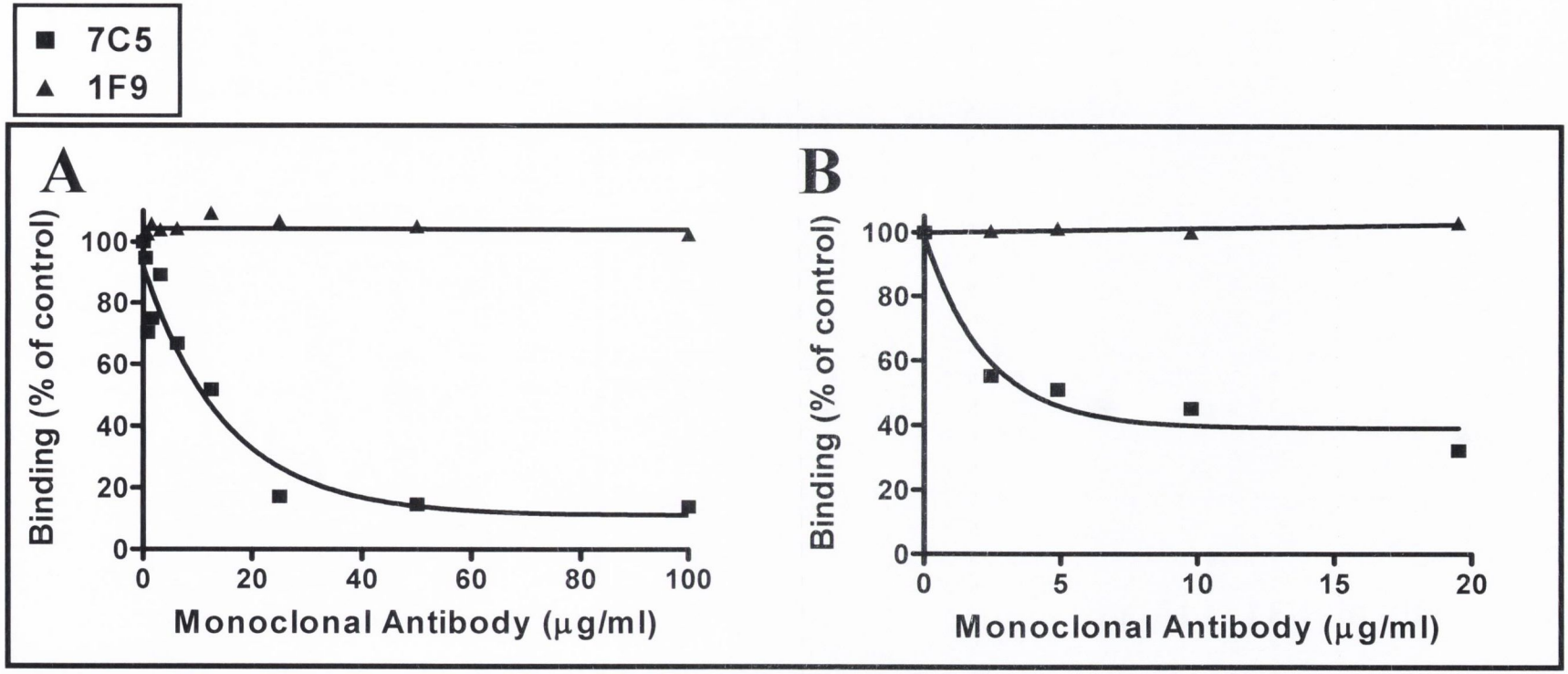

Figure 3.39 Inhibition of *L. lactis* expressing FnBPA binding to immobilised elastin and fibrinogen using monoclonal antibodies

Microtitre plates were coated with 10 µg/ml human aortic elastin (A) or fibrinogen (B). *L. lactis* cultures were induced with 0.8 ng/ml (A) or 0.1 ng/ml (B) of nisin and preincubated with increasing amounts of monoclonal antibodies 7C5 and 1F9 (100 µg/ml – 0 µg/ml) before being added to ligand-coated wells. Adherence of bacteria to elastin and fibrinogen was measured using SYTO-13 fluorescent dye and crystal violet, respectively. Values represent the mean of triplicate wells and are expressed as a percentage of control wells lacking inhibitor. This figure is representative of three independent experiments.

3.3 Discussion

An important factor in bacterial pathogenesis is the ability of the invading organism to colonise host tissue. *S. aureus* possesses, on its cell surface, a number of proteins, collectively called MSCRAMMs, which promote the binding of the organism to components of the host extracellular matrix and play an important role in bacterial virulence. *S. aureus* causes a number of diseases of elastin-rich tissue such as lung and heart valves, and for this reason, the interaction of the organism with elastin was examined. Recent studies have found that the elastin-binding protein, EbpS, was responsible for the binding of *S. aureus* to soluble elastin but had no role in adherence to immobilised elastin (Roche *et al.*, 2004). The fibronectin-binding proteins of *S. aureus* have been shown here to bind specifically to immobilised elastin as well as to fibrinogen. Strains of *S. aureus* bind to three sources of immobilised elastin in exponential phase of growth only, when FnBPA and FnBPB are maximally expressed. Inhibition studies with anti-rAFnBPA antibodies have shown that the elastin-binding phenotype of FnBPA is contained within the A domain of the protein. This was confirmed using *L. lactis* strains expressing the A domain alone of FnBPA which bound to fibrinogen and elastin. The lower affinity of FnBPA for elastin is consistent with the observation that the A domain expressed alone on the surface of *L. lactis* does not bind as well to elastin as to fibrinogen. Lacking the BCD regions that could act as a stalk to project the A domain away from the cell surface could mean that some molecules may be partially buried in the peptidoglycan and are not fully functional. This would impact greater on the lower affinity elastin-binding interaction. It has been observed for ClfA that truncation of the SD repeats, that project the A domain away from the cell surface, impairs ligand binding (Hartford *et al.*, 1997). The nisin-inducible system of *L. lactis* strain NZ9800 (pNZ8037) is tightly controlled and allows high level expression of FnBPA on the surface of the cell. This will be invaluable in all further investigation in the properties of FnBPA. Indeed this system has already been used to study the roles of fibrinogen, fibronectin, domain-specific antibodies and complement in the activation of human platelets by FnBPA (Fitzgerald *et al.*, 2006).

To show unequivocally that region A of FnBPA and FnBPB support the binding to immobilised elastin peptides, recombinant rAFnBPA$_{37\text{-}544}$ and rAFnBPB$_{37\text{-}540}$ were expressed and purified from the *E. coli* pQE30 vector. These proteins were found to be relatively stable to heating at 37°C. They were also tested for their susceptibility to two major staphylococcal proteases. Both rAFnBPA$_{37\text{-}544}$ and rAFnBPB$_{37\text{-}540}$ were extremely susceptible to V8 serine

protease with cleavage occurring along the length of the protein. It has been noted before that the FnBPs are prone to rapid degradation by V8 (Karlsson *et al.*, 2001; McGavin *et al.*, 1997). In contrast to FnBPA and FnBPB which appear to be undergo complete breakdown, ClfA has been shown to be cleaved by V8 at distinct sites in N1, leaving the N2N3 subdomains intact (Higgins, 2006). The relative resistance of the fibrinogen-binding N2N3 domains of ClfA to V8 is important, given that ClfA is preferentially expressed in stationary phase of growth, when V8 is abundant. In contrast to V8, both recombinant FnBP proteins are quite stable in the presence of aureolysin metalloprotease. This protease cleaves the clumping factors, ClfA and ClfB removing domain N1 and leaving domains N2N3 intact on the cell surface. In contrast to ClfA, the cleaving of ClfB by aureolysin results in the loss of fibrinogen-binding ability (McAleese *et al.*, 2001). The production of extracellular proteases such as V8 and aureolysin occurs in post-exponential phase and is regulated by the *agr* mechanism. As cell density increases during exponential phase, RNAIII is produced by the *agr* system and downregulates the expression of surface proteins while upregulating the synthesis of extracellular proteins such as toxins and proteases. The *sar* locus also regulates the production of FnBPs by a direct mechanism and an indirect mechanism via its control over *agr*. The proteases produced by the coordinated control of *agr* and *sar* appear to function in the degradation of both host and bacterial proteins. The degradation of surface-expressed ligand-binding proteins serves to aid in the transition of the bacterium from colonisation to invasive stages of infection.

Antibodies raised against the recombinant A domains of FnBPA and FnBPB show high levels of sensitivity against their respective antigen and also some cross-reactivity. This is likely due to the 43% amino acid identity that occurs between the A domains of these two proteins. In addition to this, the secondary structure of both proteins is now thought to be highly homologous, possibly leading to common epitopes occurring on both proteins. The antibodies were also tested for their affinity to full-length FnBP proteins released from cell wall extracts of *S. aureus* strain P1. Strain P1 has been shown to possess both *fnbA* and *fnbB* genes although there is no conclusive evidence that it expresses high levels of both proteins on the cell surface. The presence of a single high molecular weight band on Western blots probed with anti-FnPBA and anti-FnBPB antibodies indicates that P1 may only express one FnBP on its surface. The more intense reaction of anti-rAFnBPB antibodies with this band may suggest that FnBPA is not expressed by this strain. It is possible however, that both proteins are so similar in size that they cannot be separated by SDS-PAGE, unlike the FnBPA

and FnBPB produced by strain 8325-4 which are sufficiently different in size to be separated by SDS-PAGE. Construction of single *fnb* mutants of strain P1 would give some information on the relative expression of both proteins and research into this area is ongoing in the laboratory. The low affinity of antibodies raised against the A domains of FnPBs from stain 8325-4 for their corresponding antigens produced by strain P1 will be discussed further in Chapter 5. The antibodies have been shown to inhibit both *L. lactis* and *S. aureus* P1 cells expressing FnBPA (8325-4 sequence) from binding to immobilised elastin, thus indicating the specificity of the FnPB-elastin interaction.

Recombinant rAFnBPA$_{37\text{-}544}$ and rAFnBPB$_{37\text{-}540}$ both bound to immobilised elastin and fibrinogen in a dose-dependent and saturable manner. Binding was inhibited by preincubation with soluble elastin peptides, which is indicative of a specific receptor-ligand interaction. FnBPB appears to have a higher specificity for elastin and fibrinogen than the FnBPA protein as detected by direct ELISA assays although this needs to be treated with caution until verified by another method. Most investigations of the fibronectin- and fibrinogen-binding abilities of the FnBPs have focused on FnBPA. It would be of interest, therefore to carry out a detailed study on the affinity of FnBPB and some specific truncates to its ligands. To coat the wells of microtitre plates, elastin peptides were dried onto the plastic surface under a UV lamp. This method has been used to study the effects of immobilised elastin peptides on the elastin receptors of mammalian cells (Hinek *et al.*, 1999). To ensure that peptides retained epitopes specific to elastin, the ability of anti-human aortic elastin antibodies to recognise immobilised human aortic elastin was assessed by ELISA. These antibodies bound in a dose-dependent manner to the immobilised antigen. This finding suggests that the overall structure of immobilised elastin peptides was not grossly affected by drying under UV light and that the protein retained many of the epitopes in the soluble form of the antigen. Therefore, the adherence assays used in these studies is an effective and reliable method of studying the interactions of *S. aureus* surface proteins with mammalian elastin.

Subsequent to the work described above, a detailed examination of the fibronectin-binding domains of FnBP from *Streptococcus dysgalactiae* was carried out (Schwarz-Linek *et al.*, 2003). The crystal structure of the B3 peptide from FnBP and the ^{1}F1^{2}F1 module pair of fibronectin demonstrated a unique mechanism of ligand binding termed a tandem β-zipper. In this mechanism, the β-strand of the B3 bacterial peptide contributes a fourth antiparallel strand to the triple stranded β-sheet of sequential F1 modules. Sequence analysis indicated that the C-terminal regions of the *S. aureus* FnBPA could be arranged into 11 segments such that each

(except segment 7) contains a similar series of putative F1 binding motifs (Schwarz-Linek *et al.*, 2003). The first motif lay inside the previously defined boundary of the A domain of FnBPA. This domain was previously thought to span residues 37-544. However, fibronectin-binding motif 1 was shown to be located from residues 512-550. This had implications on the experimentation carried out above and rAFnBPA$_{37-544}$ was shown to be capable of binding purified immobilised fibronectin, demonstrating the presence of a functional fibronectin-binding motif at the C-terminus of this protein. A new recombinant A domain protein was then constructed lacking the fibronectin-binding phenotype but retaining the ability to bind to immobilised elastin and fibrinogen. This shows that there is no adverse effect on fibrinogen or elastin binding by removing the C-terminal 33 amino acids from the originally defined A domain. The minimum A domain of FnBPA thus spans residues 37-511.

To narrow down the binding site within region A of FnBPA for elastin and fibrinogen, an N2N3 truncate was constructed to assess the function of N1 in ligand binding. A previous alignment of the fibrinogen-binding regions of ClfA, ClfB, FnBPA, FnBPB proposed that the N2 subdomain of FnBPA begins at residue 194 (Deivanayagam *et al.*, 2002). A construct spanning residues 194-511, retained the ability to bind both immobilised fibrinogen and elastin. This indicates that N1 does not have any role in ligand binding. This is in accordance with the A domains of ClfA and ClfB which are both capable of binding fibrinogen in their N2N3 states (Deivanayagam *et al.*, 2002; Perkins *et al.*, 2001). The binding site for both fibrinogen and elastin in FnBPA has thus been further localized to residues 194-511 of FnBPA.

The precise structure of region A of FnBPA is unknown. Studies have predicted that this protein is likely to have a similar fold to the corresponding domains of ClfA (Deivanayagam *et al.*, 2002). The Phyre website is a valuable tool in predicting the 3D structure of a submitted amino acid sequence based on the known crystal structure of similar proteins. The resulting model of FnBPA shows a structure dominated by β-strands, forming an IgG-like fold. The last 8 amino acids of the γ chain of fibrinogen were docked *in silico* into this structure and are located in the hydrophobic trench situated between N2 and N3. This trench was predicted to bind the same fibrinogen γ chain ligand in studies with ClfA and has been shown to contain the β chain of fibrinogen in co-crystallisation studies with SdrG. The orientation of the docked fibrinogen ligand in this model of FnBPA is in accordance with that of the β chain of fibrinogen in SdrG. It is possible that fibrinogen approaches the A domain of FnBPA from the top right position in Figure 3.29 with the C-terminus of the γ chain exposed

and available for binding down along into the hydrophobic trench. The structure and position of the N1 subdomain has never been investigated but it does not to interfere with fibrinogen binding. The C-terminal latching peptide in the model of FnBPA is folded over the N3 subdomain. This is due to the model being based on the crystal structure of ClfA. The precise location of this strand in FnBPA in the presence and absence of fibrinogen is not known. Attempts at crystallising the A domain of FnBPA in complex with its fibrinogen ligand are ongoing in the laboratory of Prof. M. Hook, Texas A&M University, Houston, Texas, USA. Defined crystals would inform greatly on the true nature of the mechanism of fibrinogen binding and may shed some light on a putative mechanism of elastin binding. Until a reliable structure is obtained and analysed, this model of N2N3 of FnBPA based on its nearest homologue, ClfA, was used to give an insight into role of residues located within the ligand-binding trench and those comprising the latching peptide.

The true A domain was thought to be contained within residues 37-511. The asparagine at position 511 is predicted to be situated mid way along the latching peptide on the 3D model of FnBPA. Residues GPI comprising the first 3 amino acids of the first fibronectin-binding domain, are predicted to form the remainder of the latching peptide. The absence of these three residues in recombinant proteins rAFnBPA$_{37\text{-}511}$ and rAFnBPA$_{194\text{-}511}$, does not influence ligand binding. It can be deduced, therefore that if the dock, lock and latch model is accurate, the remaining residues of the latching peptide are sufficient to undergo β-strand complementation in N3. If the dock, lock and latch mechanism was critical in the binding of fibrinogen and/or elastin, then the residues located in the latching peptide would have a vital role to play in ligand binding. This hypothesis was tested by constructing truncates of the N2N3 protein (rAFnBPA$_{194\text{-}511}$) that lacked successive C-terminal residues. The first truncate rAFnBPA$_{194\text{-}509}$ lacked the remaining two residues of the latching peptide and this was shown to cause a significant decrease in fibrinogen binding but not in elastin binding. This indicates that there are subtle differences in the binding of elastin and fibrinogen. A second truncate, rAFnBPA$_{194\text{-}498}$, lacking the latching peptide and the preceding loop region that may act as a hinge, did not bind to either ligand. This indicates the importance of this region on the binding of both fibrinogen and elastin. A third truncate, rAFnBPA$_{194\text{-}483}$, that would likely alter the conformation of the N3 subdomain, also did not bind to either ligand. These data, in conjunction with the fact that neither the N2 nor N3 subdomain alone can bind to fibrinogen or elastin, demonstrates the importance of the overall IgG fold of the A domain.

In conclusion, the C-terminal residues of the N2N3 protein of FnBPA have an important role in ligand binding and truncates lacking these residues are defective in both fibrinogen and elastin binding. As mentioned, the precise location of the latching peptide of FnBPA is unknown. The N2N3 subdomains of FnBPA have also been modelled based on the known crystal structure of the ligand bound complex of SdrG. This model (Figure 3.40) predicts the latching peptide to be N-terminal to that predicted by the ClfA-based model. The binding of the C-terminal truncates of FnBPA could be in agreement with this model. rAFnBPA$_{194\text{-}511}$ binds tightly to fibrinogen and elastin as the latching peptide is intact. rAFnPBA$_{194\text{-}509}$ also contains the full latching peptide and has only a slightly lower affinity for fibrinogen than rAFnBPA$_{194\text{-}511}$ and no defect in elastin binding. Deletion of residues to position 498, however, removes the entire latching peptide and most of the hinge region and the rAFnBPA$_{194\text{-}498}$ protein is thus devoid of fibrinogen- and elastin-binding ability. The ClfA-based model of FnBPA was researched in more detail throughout this project as FnBPA and ClfA share a higher percentage similarity and bind to the same region of the γ chain of fibrinogen. The value of the SdrG-based model of FnBPA, however, lies in the fact that a ligand bound crystal complex was obtained and the position of the latching peptide informs on the mechanism of dock, lock and latch binding. This latter model can therefore not be ruled out. The proximity of the fibrinogen/elastin- and fibronectin-binding regions at the junction of the latching peptide raises some interesting questions. It is not yet known how the binding of fibronectin to the first fibronectin-binding motif (512-550) would affect the subsequent binding of fibrinogen or elastin to the A domain. Competition studies involving fibronectin and the γ chain peptide of fibrinogen would be valuable in elucidating the dock, lock and latch model of FnPBA.

To further examine the hypothesis that fibrinogen and elastin bind to FnBPA in a similar manner, known inhibitors of the FnBPA-fibrinogen interaction were tested for their effect on elastin binding. Preincubation of FnBPA with both soluble whole fibrinogen and the C-terminal γ chain peptide inhibited binding to elastin as well as to fibrinogen. This indicates that the presence of fibrinogen in the hydrophobic trench hinders the binding of elastin. It is likely therefore that elastin binds to FnBPA in a similar manner, possibly in the same trench. A monoclonal antibody that has been shown to inhibit the binding of FnBPA to fibrinogen also inhibited elastin binding. The binding of this monoclonal antibody to FnBPA is thought to alter the overall conformation of the molecule, thus rendering the protein unable to bind to

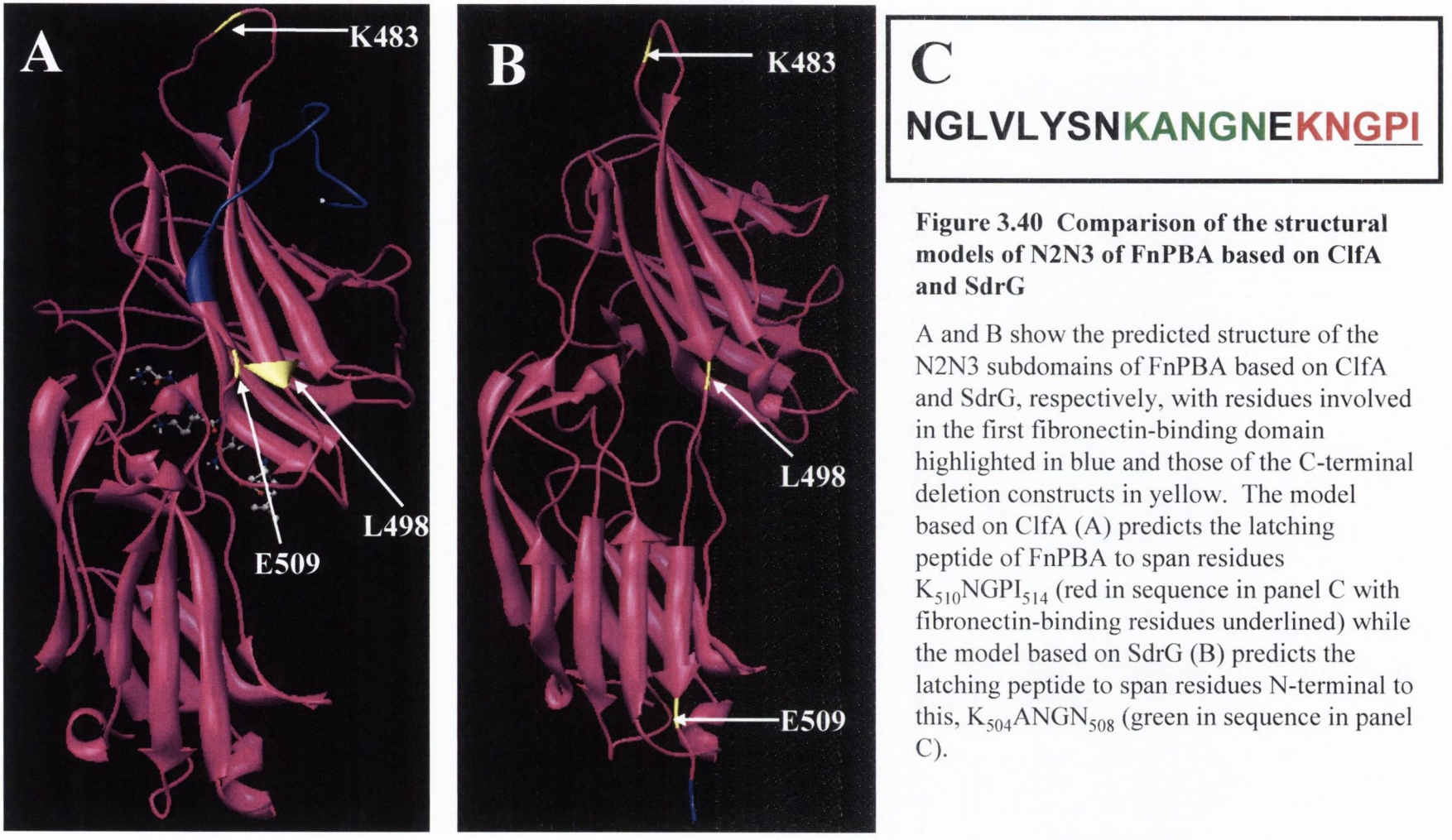

Figure 3.40 Comparison of the structural models of N2N3 of FnPBA based on ClfA and SdrG

A and B show the predicted structure of the N2N3 subdomains of FnPBA based on ClfA and SdrG, respectively, with residues involved in the first fibronectin-binding domain highlighted in blue and those of the C-terminal deletion constructs in yellow. The model based on ClfA (A) predicts the latching peptide of FnPBA to span residues $K_{510}NGPI_{514}$ (red in sequence in panel C with fibronectin-binding residues underlined) while the model based on SdrG (B) predicts the latching peptide to span residues N-terminal to this, $K_{504}ANGN_{508}$ (green in sequence in panel C).

both fibrinogen and elastin. The exact epitope to which this monoclonal antibody binds is yet unknown. Further work carried out with 7C5 will be discussed further in Chapter 5.

In this chapter, work with *S. aureus* and *L. lactis* bacterial cells demonstrated that the A domain of the fibronectin-binding proteins supports binding to immobilised elastin as well as to fibrinogen. Recombinant A domains of FnBPA and FnBPB were expressed and purified and both proteins were shown to bind to immobilised elastin and fibrinogen in a dose-dependent and saturable manner indicating the specificity of the interactions. A truncated N2N3 protein of FnBPA was shown to bind to elastin and fibrinogen with a similar affinity to that of N1N2N3, demonstrating that subdomain N1 has no function in ligand binding. A 3D structural model of the N2N3 subdomains of FnBPA was created based on the crystal structure of the same region of ClfA. This model identified the residues involved in the latching peptide of FnBPA and allowed truncates to be constructed which determine the minimum ligand-binding region. Finally, two known inhibitors of fibrinogen binding by FnBPA were also shown to inhibit elastin binding. This indicates that elastin and fibrinogen bind to FnBPA in a similar manner.

Chapter 4

Site-directed mutagenesis of DNA encoding region A of FnBPA

4.1 Introduction

S. aureus surface proteins are known to be multi-functional and can possess functional redundancy with other ligand-binding surface proteins. This is typified by the fibronectin-binding proteins, FnBPA and FnBPB which have been shown to bind fibronectin (Jonsson *et al.*, 1991; Signas *et al.*, 1989) as well as fibrinogen (Roche *et al.*, 2004; Wann *et al.*, 2000) and elastin (Roche *et al.*, 2004). As the fibrinogen- and elastin-binding phenotypes of FnBPA are both conveyed by the N2N3 subdomains of region A of the protein, further investigation of this segment was required. The truncation approach adopted in Chapter 3 was shown to be inadequate as deletion of the C-terminal residues involved in the latching peptide rendered the protein unable to bind to either ligand. Thus further analysis of the 3D structural model generated for region A of FnBPA allowed a closer inspection of the potential mechanisms involved in binding to both elastin and fibrinogen. To do this, comparisons were drawn with the binding mechanisms postulated for similar ligand-binding proteins, ClfA and SdrG.

ClfA is a well characterised fibrinogen-binding protein of *S. aureus*. The crystal structure of N2N3 of ClfA ($rAClfA_{221-559}$) has been solved (Deivanayagam *et al.*, 2002). This structure has been discussed previously in Sections 1.3 and 3.1 and was shown to consist of two similarly folded subdomains which mimic the recognised immunoglobulin (IgG) fold. The focus on this structure up to now has been on the C-terminal regions that are likely to be involved in the latching mechanism of ligand binding. In this chapter, the central residues situated around the hydrophobic trench located between subdomain N2 and N3 will be investigated. In the structural analysis of ClfA a fibrinogen γ chain peptide was docked *in silico* into the crystal structure to aid in the understanding of ligand binding. A brute force docking procedure (Softdock) was employed which yielded several solutions. The top 20 docking solutions were examined and further scored on the basis of interactions between the fibrinogen ligand and $rAClfA_{221-559}$. In seven of the top 20 solutions, the C-terminal fibrinogen residues ($A_{408}GDV_{411}$) were found to be extensively in contact with $rAClfA_{221-559}$ residues. In all of these solutions, the fibrinogen peptide docked into the hydrophobic pocket formed at the interface between the N2 and N3 subdomains. It was noted that this trench contained the V527 residue that was found in a previous study to be important for fibrinogen binding by ClfA (Hartford *et al.*, 2001). In the ClfA crystal structure containing the docked fibrinogen ligand, this V527 residue was in contact with the C-terminal valine of the fibrinogen γ chain (V411). Glutamate 526 and valine 527 of ClfA were found to be important

in ClfA binding in an empirical study carried out before the 3D structure of ClfA was understood (Hartford *et al.*, 2001). It was noted that antibodies raised against the C-terminus of ClfA, rAClfA$_{500-559}$, inhibited binding to immobilised fibrinogen by bacteria expressing ClfA and by recombinant ClfA protein. This indicated that the C-terminus of the molecule is very important in ligand binding, a concept that is understood in greater detail today. It was also noticed that substitution of K406 of the fibrinogen γ chain resulted in loss of affinity of this peptide to rAClfA (Hartford *et al.*, 2001). It was concluded therefore that this lysine may be involved in important interactions with a negatively-charged residue in ClfA. In response to this, negatively-charged residues at the C-terminus of ClfA were targeted by site-directed mutagenesis. Thus, E526, D537, E546 and E559 of ClfA were all tested for their role in fibrinogen binding. Of these substitutions, E526A was the only one that caused an effect, with a 16-fold reduction in affinity for fibrinogen. Residues adjacent to this amino acid were also targeted and the substitution of the residue C-terminal to E526 (V527S) was shown to have an 8-16 fold lower titre for fibrinogen. The double mutant containing both these substitutions however, exhibited a 512-fold lower titre for immobilised fibrinogen compared to that of wild-type region A of ClfA (Hartford *et al.*, 2001).

The other residues of ClfA that were predicted in the docking studies of the crystallised structure to be in contact with the fibrinogen ligand were Tyr256, Pro336 and Tyr338 in the N2 subdomain and Ile387 and Lys389 in the N3 subdomain (Deivanayagam *et al.*, 2002). These residues of ClfA are situated around the hydrophobic trench and were targeted by site-directed mutagenesis, for substitution by an alanine or serine residue. The variant rAClfA$_{221-559}$ proteins were tested for their ability to bind immobilised fibrinogen in a direct ELISA-type assay as well as by inhibition ELISA assays where the ability of the mutant protein to inhibit the binding of biotin-labelled wild-type rAClfA$_{221-559}$ to immobilised fibrinogen was determined. The results of these assays showed that the Y338A protein was unable to bind to immobilised fibrinogen, whereas the Y256A, K389A and P336S proteins exhibited markedly reduced affinities for fibrinogen. In contrast, the A254S and I387S proteins had somewhat reduced affinities. Fluorescent polarization was used to quantify the binding of rAClfA$_{221-559}$ wild-type and mutant proteins to a fluorescein-labelled 17 amino acid synthetic peptide corresponding to the C-terminus of the γ chain of fibrinogen. The K_D values obtained from these experiments showed that Tyr338, Pro336, Tyr256 and Lys389 had important roles to play in fibrinogen binding by ClfA. A254 and I387 were less crucial to the ligand-binding

function. It was concluded from this study that Tyr338, Tyr256 and Lys389 were likely to have charge-charge interactions with the $A_{408}GDV_{411}$ residues of the fibrinogen γ chain.

Following the study on ClfA, the crystal structure of another staphylococcal fibrinogen-binding surface protein (SdrG) was solved both in its apo and ligand-bound forms (Ponnuraj *et al.*, 2003). In contrast to ClfA, SdrG binds to the N-terminus of the β chain of fibrinogen. The co-crystallised fibrinogen ligand was found to be situated in the hydrophobic trench between N2 and N3, confirming the docking procedure carried out for ClfA. The open and closed complex showed differing structures with regard to the C-terminal β-strand, which led to conclusions about the dock, lock and latch mechanism of ligand binding. As discussed in the last chapter, the co-crystallised complex gave an important insight into the role of residues located at the C-terminus of the molecule which are important in the latching peptide. The aim of the studies carried out in this chapter however, was to investigate the role of residues located around the hydrophobic trench that are crucial in ligand binding. In studying the crystal structure of SdrG, two residues were targeted by site-directed mutagenesis and both were found to be crucial for fibrinogen binding. Ser338 and Asp339 are adjacent amino acids located on a loop region between β-strands C and D of subdomain N2. They are situated within 3 Angstroms (Å) of the fibrinogen ligand and were changed to histidine and alanine, respectively. Both changes independently resulted in the variant $rSdrG_{273-596}$ protein being unable to bind immobilised fibrinogen β chain peptide in Biacore and ELISA assays. It was hypothesised that the S338H substitution would introduce a larger side chain within the binding region, occupying the space where the peptide docks, thus preventing ligand binding. Attention was also focused on the residues of the fibrinogen ligand that were crucial in binding SdrG. A panel of mutant fibrinogen peptides were synthesised where each residue in the native fibrinogen sequence was replaced with an alanine (or serine if alanine is present in the native sequence) and subsequently tested for SdrG protein binding. It was deduced that residues $F_{10}FSARG_{15}$ of fibrinogen were the most significant in contributing to the binding to SdrG. An extra Phe residue at the N-terminus of the fibrinogen peptide and a G15S substitution of this peptide resulted in tighter binding to $rSdrG_{276-596}$. Due to SdrG binding to a distinct region of fibrinogen compared to FnBPA, the above information on optimal peptide binding is of limited value. However, it has been noted that a similar situation occurs in ClfA, whereby synthetic peptide analogues representing amino acid variants of the fibrinogen γ chain show higher affinity for the recombinant $rAClfA_{221-559}$ than the native fibrinogen

sequence (M. Hook, unpublished data). In this way, staphylococcal surface proteins can accommodate linear peptides with a certain degree of sequence variability.

The A domain of FnBPA has long been known to exhibit substantial amino acid sequence similarity with the A domain of ClfA (McDevitt *et al.*, 1994). This led to the investigation into a biological role for the A domain and it was subsequently determined that, similar to ClfA, the A domain of FnBPA bound to fibrinogen (Wann *et al.*, 2000). In contrast to ClfA, the A domain of FnBPA also bound elastin (Roche *et al.*, 2004). Until this study began, the structural elements (β-strands and adjoining loops) of region A of FnBPA were predicted based on alignments of the primary amino acid sequence of this region with the equivalent domains of ClfA. Upon the crystallisation of the A domain of ClfA, a closer inspection of the sequence similarity allowed prediction of the secondary structural elements of FnPBA (Deivanayagam *et al.*, 2002) which is evident in the alignment diagram of Figure 4.1. Attempts are ongoing in the laboratory of Prof M. Hook, Texas A&M University, Houston, Texas to crystallise the N2N3 domains of FnBPA, preferably in complex with its fibrinogen ligand. Until this is available, a computer modelled structural prediction gives the best insight into the mechanism of ligand binding by region A of FnBPA.

In this chapter, the 3D structural model of FnBPA was studied in detail, with and without the fibrinogen γ chain peptide docked *in silico* into the putative ligand-binding trench. Amino acid residues were chosen at various locations around the hydrophobic trench and substituted to alanine or glycine. The effects of these substitutions on the ability of recombinant $rAFnBPA_{37\text{-}511}$ proteins to bind to immobilised elastin and fibrinogen was determined by ELISA-type binding assays. The reductions in binding were correlated with the position of the substituted amino acid and the likely contact points between the atoms of these residues and the nearest residue of the fibrinogen γ chain. In this way, residues likely to be involved in the binding to fibrinogen and/or elastin as well as those potentially involved in the latching mechanism of ligand binding were identified.

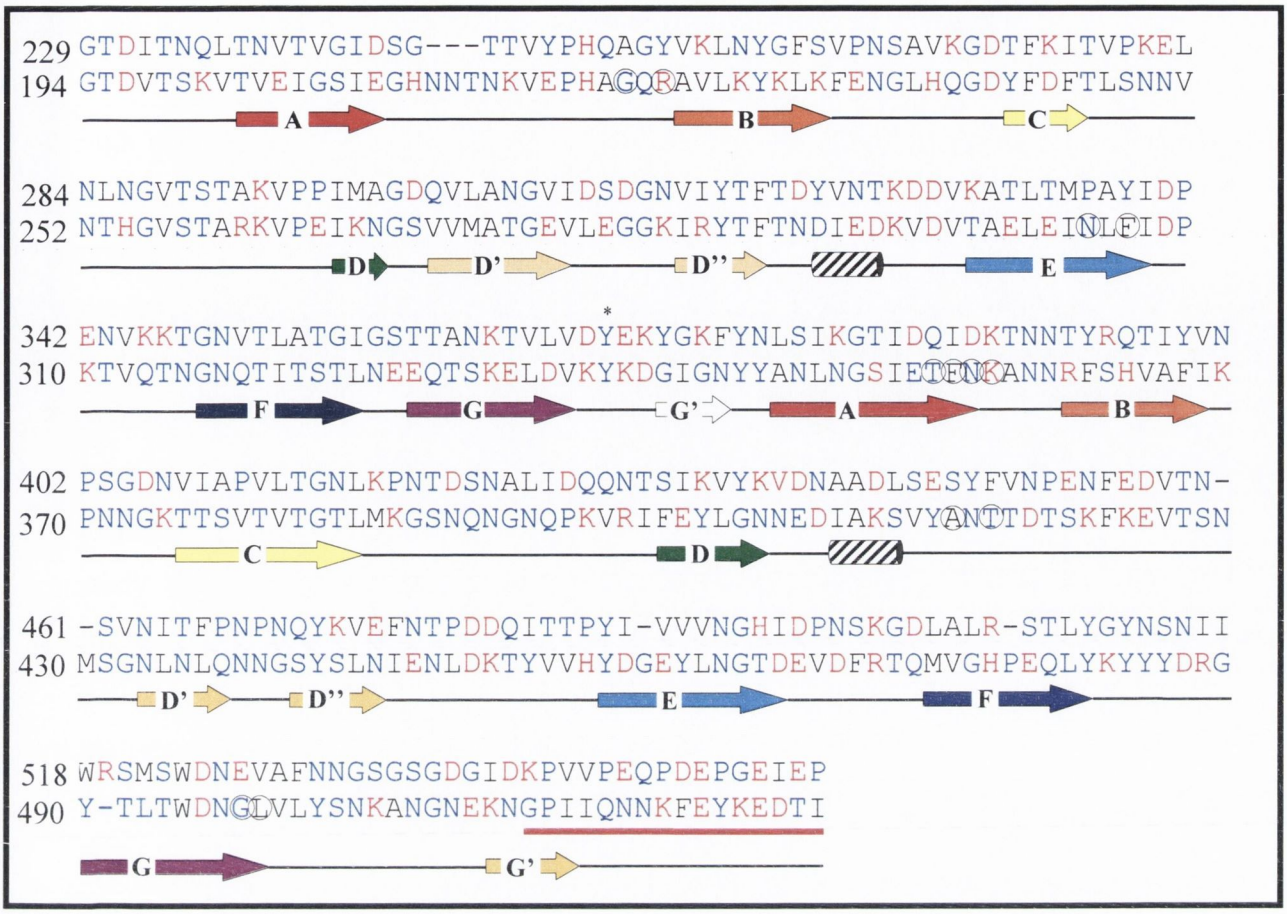

Figure 4.1 Sequence alignment of the N2N3 subdomains of ClfA (top) and FnBPA (bottom)

Red, blue and black letters represent charged, polar and hydrophobic residues, respectively. The conserved Tyr residue in the connector between the N2 and N3 subdomains is marked with an asterisk. The secondary structural elements are represented as arrows below the text. The red line under the text represents the first fibronectin-binding motif of FnBPA. Residues of FnBPA targeted for site-directed mutagenesis are circled. Adapted from Deivanayagam *et al.*, 2002.

4.2 Results

4.2.1 Modelling the 3D structure of rAFnBPA$_{194-511}$

It has been shown in Chapter 3 that rAFnBPA$_{194-511}$ binds elastin and fibrinogen with high affinity. Further truncation of this protein would likely disrupt the overall secondary structure of the subdomains of region A and thus indirectly affect ligand binding. A more precise approach was required. It was suggested previously that the DEv-IgG fold, revealed in the crystal structure of the apo form of ClfA is also present in the corresponding regions of the A domains of ClfB, FnBPA and FnBPB. In accordance with this, the structure of the ligand-binding N2N3 domains of FnBPA was predicted based on the crystal structure of the equivalent domains of ClfA (Deivanayagam *et al.*, 2002). As described in Section 3.2.10, the Phyre molecular modelling engine was used to create a 3D structure of FnBPA in order to study the possible mechanisms of ligand binding. Further insight into the mechanism of fibrinogen binding by staphylococcal surface proteins came with the co-crystallisation of SdrG with its ligand, the N-terminus of the β chain of fibrinogen. In this structure, it was clear that the orientation of the latching peptide could vary in response to the presence of fibrinogen. This mechanism of ligand binding was termed dock, lock and latch (Ponnuraj *et al.*, 2003). In order to investigate the role of residues around the hydrophobic trench of FnBPA that may be involved in ligand binding, it was necessary to dock the fibrinogen ligand into this structure using computer software. To do this a computer-generated fibrinogen ligand (C-terminal 8 amino acid peptide of the γ chain of fibrinogen, G_{404}AKQAGDV_{411}) was docked *in silico* into the predicted structural model of FnBPA using Autodock. This structure has been described in Section 3.2.10. Interestingly, the orientation of the fibrinogen ligand is the same as that seen in the co-crystallisation of SdrG with its fibrinogen ligand. The fibrinogen residues, G_{404}AKQAGDV_{411}, are situated running along the trench from top left to bottom right. The docking of the fibrinogen peptide into N2N3 of FnBPA provided a rationale for identifying residues lining the hydrophobic trench of FnBPA to be investigated for a role in ligand binding.

4.2.2 Rationale for choosing residues of rAFnBPA$_{37-511}$ to be altered by site-directed mutagenesis

With the docking of the fibrinogen γ chain into the modelled structure of FnBPA, it was possible to identify those residues with side chains pointing into the trench which were in

close proximity to the ligand. The Chimera molecular modelling software package allowed identification of the residues of FnBPA that are within a defined distance from the fibrinogen ligand. In this way Chimera was used to highlight residues within 3 Å from the fibrinogen γ chain peptide. Among those residues highlighted by this method were T354 and N356 as well as A415 and T417. These residues were the first to be targeted for site-directed mutagenesis by the Quikchange method. It was first decided to make the minimum nucleotide changes necessary to produce a codon for amino acids such as alanine or glycine. Thus ACA was altered to GCA to change T354 to alanine and AAT was altered to GGT to change N356 to glycine. This gave a total of 3 nucleotide mismatches in both the forward and reverse primer to create the double mutant T354A/N356G. A similar method was used to construct A415G/T417A. Subsequent to this, it was discovered that the Quikchange method was successful even if all three nucleotides of a codon were changed so all further site-directed mutants were constructed changing the relevant residue to alanine.

Seven other site-directed mutants were made based on analysis of region A of ClfA (Deivanayagam *et al.*, 2002). In that study A254, Y256, P336, Y338, I387 and K389 of region A of ClfA were changed to alanine or serine. Thus the residues in equivalent positions in FnBPA were targeted, yielding rAFnBPA$_{37\text{-}511}$ G222A, R224A, N304A, F306A, F355A, K357A and the double mutant N304A/F306A. The final two residues chosen for alteration were in the equivalent position to two residues found to be important in an empirical study of fibrinogen binding by ClfA (Hartford *et al.*, 2001). In that study E526 and V527 were identified as being important for fibrinogen binding. The residues of FnBPA in the equivalent positions were also changed. This led to the construction of rAFnBPA$_{37\text{-}511}$ G497A and L498A. All residues chosen for site-directed mutagenesis are circled in the primary sequence alignment of ClfA and FnBPA in Figure 4.1. These residues are also shown in yellow in the 3D structural model (Figure 4.2) with individual residues labelled in the enlarged version in Figure 4.3.

4.2.3 Expression of alanine-substituted variant proteins of rAFnBPA$_{37\text{-}511}$

Relevant mutagenic primers and pQE30 rAFnBPA$_{37\text{-}511}$ template DNA were used in the Quikchange method of site-directed mutagenesis as described in Section 2.4.8 and illustrated in Figure 4.4. The resulting PCR products were digested with *Dpn*1 to remove any wild-type methylated DNA and the remaining DNA transformed into *E. coli* XL-1 Blue cells. Resulting clones were purified, plasmid DNA isolated and verified by sequencing. Positive

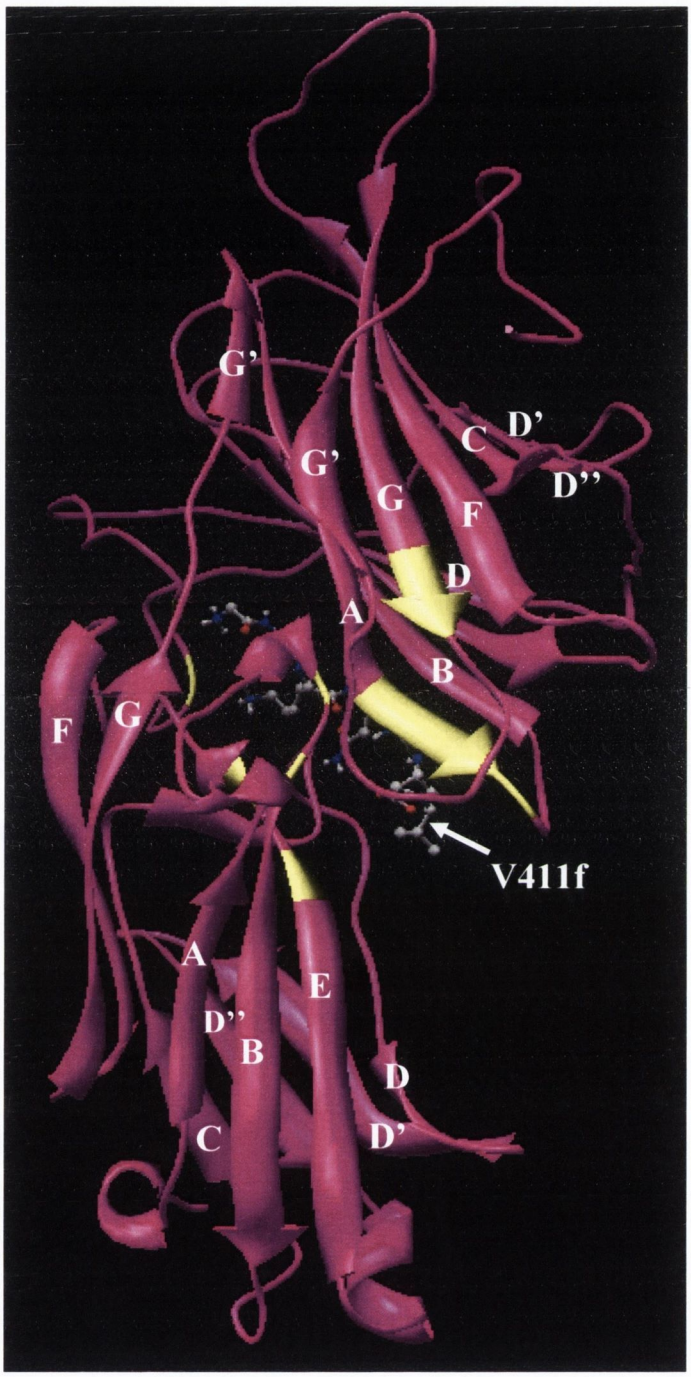

Figure 4.2 3D structural model of N2N3 of FnBPA

Structural model of the N2N3 subdomains of FnBPA with the fibrinogen peptide docked into the hydrophobic trench (C-terminal valine residue is labelled with a suffix "f" to indicate fibrinogen). β-strands are labelled according to the crystal structure of ClfA (Deivanayagam *et al.*, 2002). Residues altered by site-directed mutagenesis are highlighted in yellow.

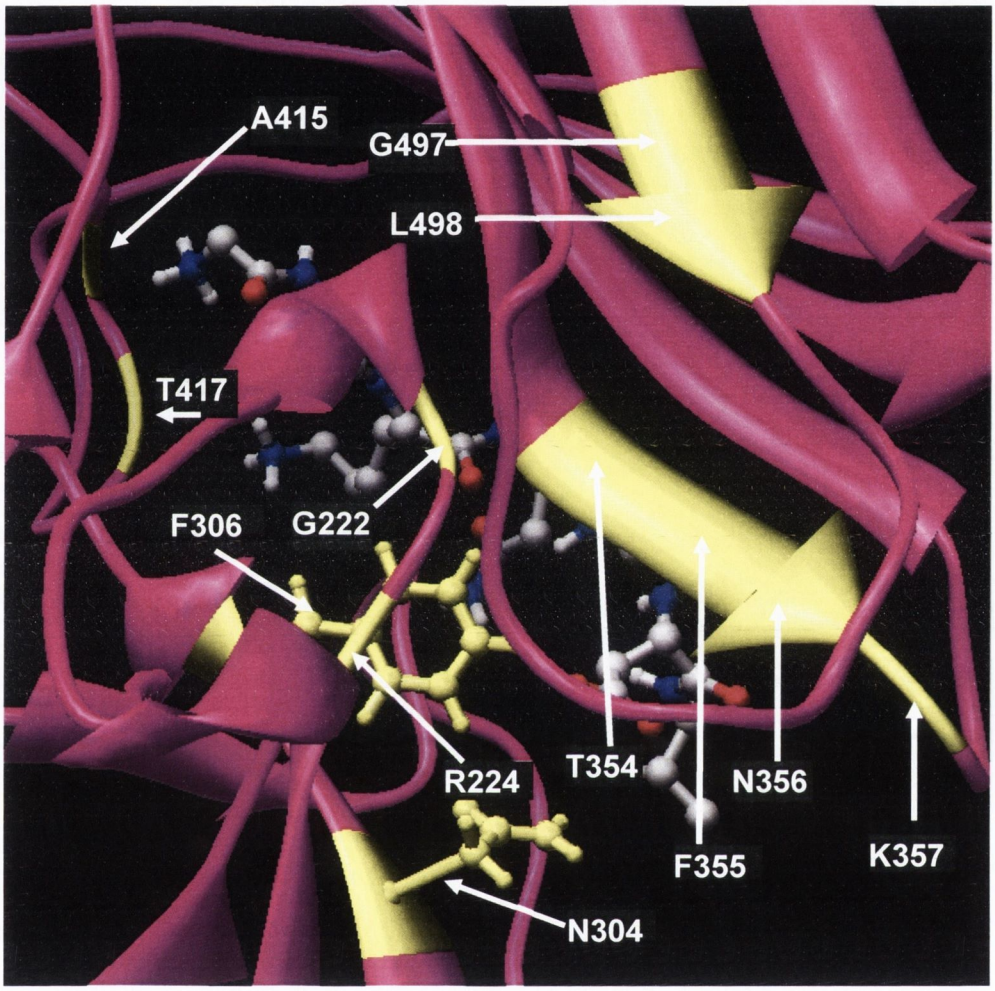

Figure 4.3 Hydrophobic trench of 3D structural model of N2N3 of FnBPA

Enlarged section of the structural model of the N2N3 subdomains of FnBPA with the fibrinogen peptide (ball and stick format) docked into the hydrophobic trench. Residues altered by site-directed mutagenesis are labelled and highlighted in yellow. The side chain of the N304 and F306 residues are shown in yellow ball and stick format.

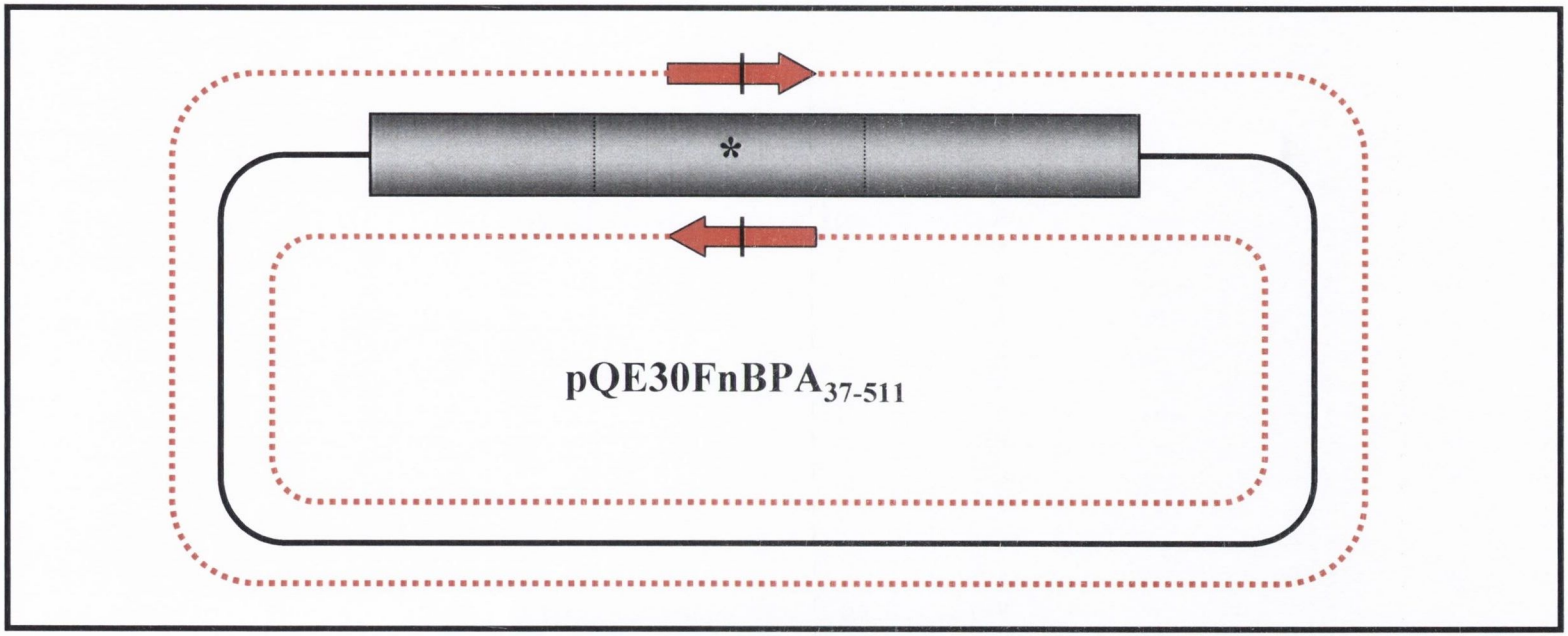

Figure 4.4 Site-directed mutagenesis of region A of FnBPA

A plasmid containing the coding sequence for rAFnBPA$_{37\text{-}511}$ was used as a template in PCR with mutagenic primers containing the desired codon change(s). These primers anneal to both DNA strands surrounding the target site for mutation (*) and are extended by *Pfu* polymerase to generate daughter plasmids that are circular but nicked. The resulting PCR mixture is treated with *Dpn*I to digest the original wild-type parental plasmid DNA which is methylated. The remaining plasmids are transformed into *E. coli* where nicked strands are repaired and plasmid replication can take place.

transformants were subcloned into the protease-deficient *E. coli* host, TOPP3 for recombinant protein production. Purified proteins were dialysed against PBS, quantified by A_{280} readings or BCA kit (Pierce) and stored at -80°C. Equal amounts of rAFnBPA$_{37\text{-}511}$ wild-type and site-directed mutants were analysed by SDS PAGE and stained with Coomassie Blue (Figure 4.5). This gel shows bands of similar sizes with some breakdown products visible for R224A and K357A.

4.2.4 Circular dichroism (CD) spectroscopy of rAFnBPA$_{37\text{-}511}$ wild-type, rAFnBPA$_{37\text{-}511}$ N304A, rAFnBPA$_{37\text{-}511}$ F306A and rAFnBPA$_{37\text{-}511}$ N304A/F306A

Circular dichroism (CD) spectroscopy is a form of light absorption spectroscopy that can be used to determine the secondary structure of protein molecules. The ultraviolet (UV) CD spectrum of proteins can predict important characteristics of their secondary structure. It can be used to estimate the extent of α-helix, β-sheet and other (random coil) conformations. In this study, CD spectroscopy is a valuable tool to estimate the potential structural alterations due to substitution of amino acid residues. This technique can be used to compare the overall structure of altered proteins with that of the wild-type recombinant protein. Due to limited resources, only those proteins that exhibited the most dramatic effect on fibrinogen and elastin binding were analysed by CD spectroscopy in this study. Thus proteins rAFnBPA$_{37\text{-}511}$ N304A, rAFnBPA$_{37\text{-}511}$ F306A and the double mutant rAFnBPA$_{37\text{-}511}$ N304A/F306A were dialysed against a solution of 1 mM Tris-HCl pH 7.4 and scanned between wavelengths 300-200 nm. Each protein was scanned five times and the average of each was plotted on the same axes (Figure 4.6). Proteins rAFnBPA$_{37\text{-}511}$ N304A and rAFnBPA$_{37\text{-}511}$ N304A/F306A each had a very similar spectrum to that of rAFnBPA$_{37\text{-}511}$ wild-type with slight deviations in the 230-210 nm range. CD spectroscopy is extremely sensitive to sample concentration and the slightest variation in protein concentration can result in altered spectra. This is evident with the rAFnBPA$_{37\text{-}511}$ F306A sample. This protein gives a slightly different spectrum to rAFnBPA$_{37\text{-}511}$ wild-type in the 210-200 nm range as it is missing the small peak in this range. A 1.33-fold dilution of the same protein gave an altered spectrum of similar shape demonstrating the concentration sensitivity of this technique. The overall conclusion to this experiment was that rAFnBPA$_{37\text{-}511}$ N304A and N304A/F306A were sufficiently similar to that of rAFnBPA$_{37\text{-}511}$ wild-type to indicate that no gross conformational changes had occurred. It is possible that rAFnBPA$_{37\text{-}511}$ F306A had some conformational changes in the particular batch of protein tested. However, it is notable that rAFnBPA$_{37\text{-}511}$ F306A behaved

in a similar manner to other rAFnBPA$_{37-511}$ proteins in surface plasmon resonance experiments (Chapter 6) and it is reassuring to note that rAFnBPA$_{37-511}$ N304A/F306A, containing the F306A substitution, did not differ considerably from rAFnBPA$_{37-511}$ wild-type.

4.2.5 Binding of polyclonal anti-rAFnBPA antibodies to rAFnBPA$_{37-511}$ wild-type and variant proteins

To assess the ability of polyclonal anti-rAFnBPA antibodies to bind to rAFnBPA$_{37-511}$ wild-type and all variant proteins, doubling dilutions of recombinant proteins were immobilised onto microtitre plates. After blocking the plates with skimmed milk, a 1:2000 dilution of anti-rAFnBPA antibodies was added, followed by goat anti-rabbit antibodies conjugated to HRP. Development of the ELISAs showed that each recombinant protein reacted equally potently with the antibodies (Figure 4.7). This validates the use of the polyclonal antibodies to detect variant recombinant proteins in solid phase ligand-binding assays.

4.2.6 Binding of monoclonal anti-rAFnBPA antibodies to rAFnBPA$_{37-511}$ wild-type and variant proteins

A panel of monoclonal antibodies raised in mice against rAFnBPA$_{37-544}$ was obtained from collaborators in Italy. These antibodies were tested by ELISA for reactivity against rAFnBPA$_{37-511}$ wild-type and variant proteins. Each monoclonal antibody was added to a microtitre plate containing equal amounts (50 nM) of immobilised recombinant rAFnBPA$_{37-511}$ protein. Precise protein concentration is often difficult to estimate accurately and slight variances in reactivity of antibodies to individual recombinant proteins are to be expected. Due to limited amounts of each monoclonal antibody, these ELISA assays were performed just once. Monoclonal antibody 1E6 and 1F9 show equal reactivity with all rAFnBPA proteins with the reactivity of 1F9 to rAFnBPA$_{37-511}$ F306A being slightly weaker than to all other recombinant proteins (Figure 4.8). The starting concentration of 1F9 (5 μg/ml) has a far more sensitive reaction with all proteins compared to the equivalent concentration of 1E6. Monoclonal antibody 1G8 also gave a strong reaction to all rAFnBPA proteins with rAFnBPA$_{37-511}$ G222A and N304A/F306A giving slightly higher absorbance values (Figure 4.9 A). Monoclonal antibody 7B7 gave a weaker reaction but reacted similarly with all recombinant proteins (Figure 4.9 B). Monoclonal antibody 8G3 gave a strong reaction with most rAFnBPA proteins. It did not however, react well with rAFnBPA$_{37-511}$ F355A, K357A

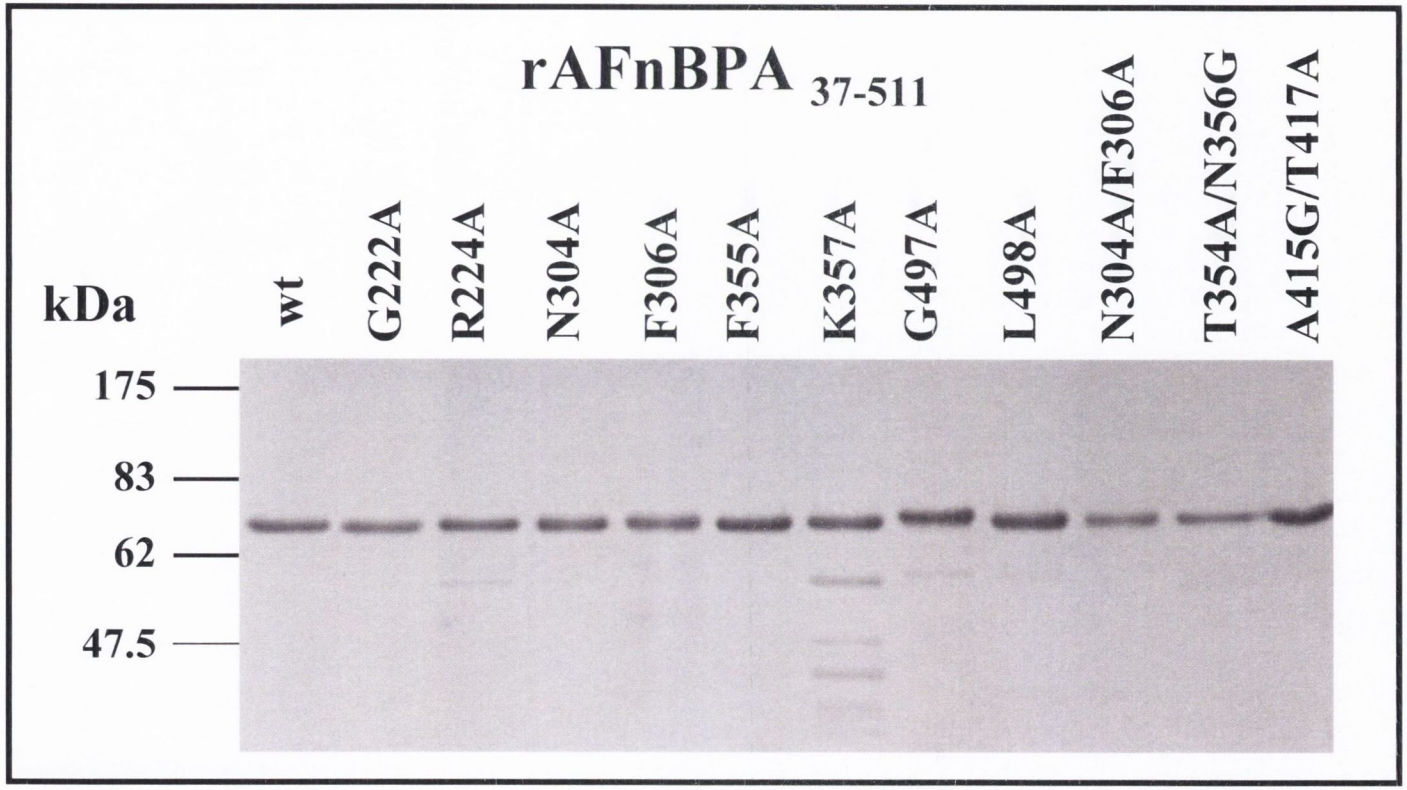

Figure 4.5 Alanine-substituted variants of rAFnBPA$_{37\text{-}511}$

Equal amounts (2 μM) of rAFnBPA$_{37\text{-}511}$ wild-type and variant proteins were analysed by SDS-PAGE and stained with Coomassie Blue.

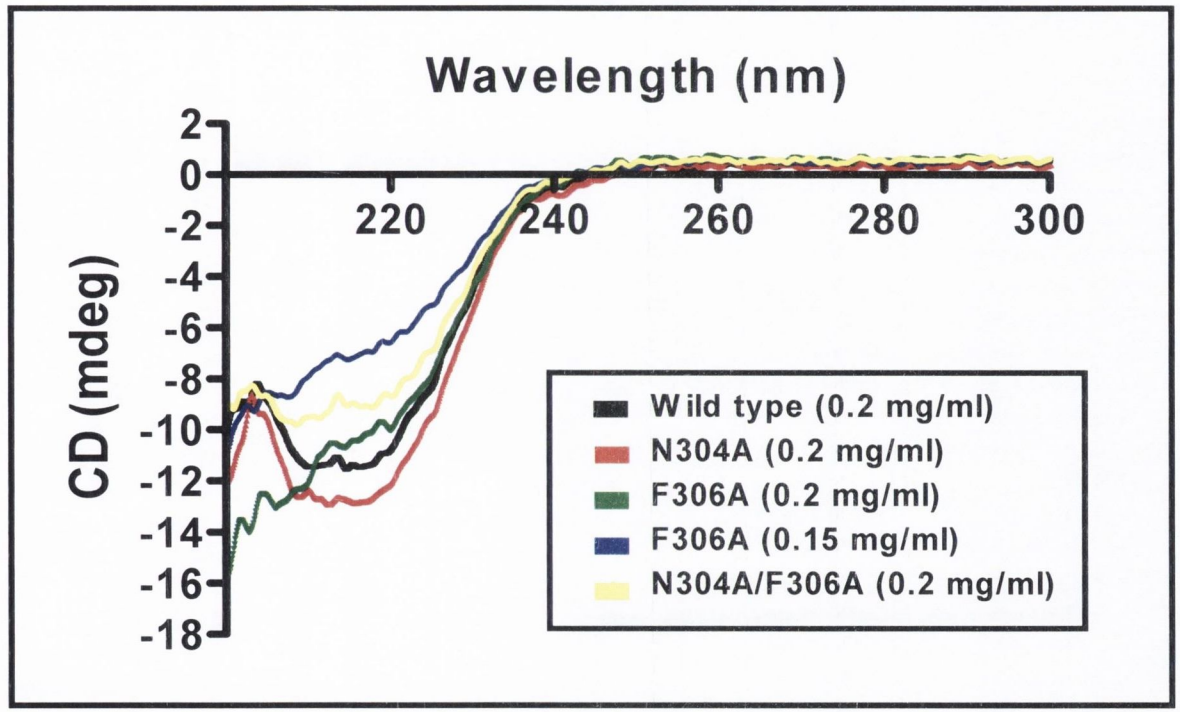

Figure 4.6 Circular dichroic scan of recombinant proteins rAFnBPA$_{37\text{-}511}$ wt, N304A, F306A and N304A/F306A

Equal amounts of rAFnBPA$_{37\text{-}511}$ proteins were analysed by circular dichroism (CD) spectroscopy. F306A is shown at two different concentrations to indicate the concentration sensitivity of the technique.

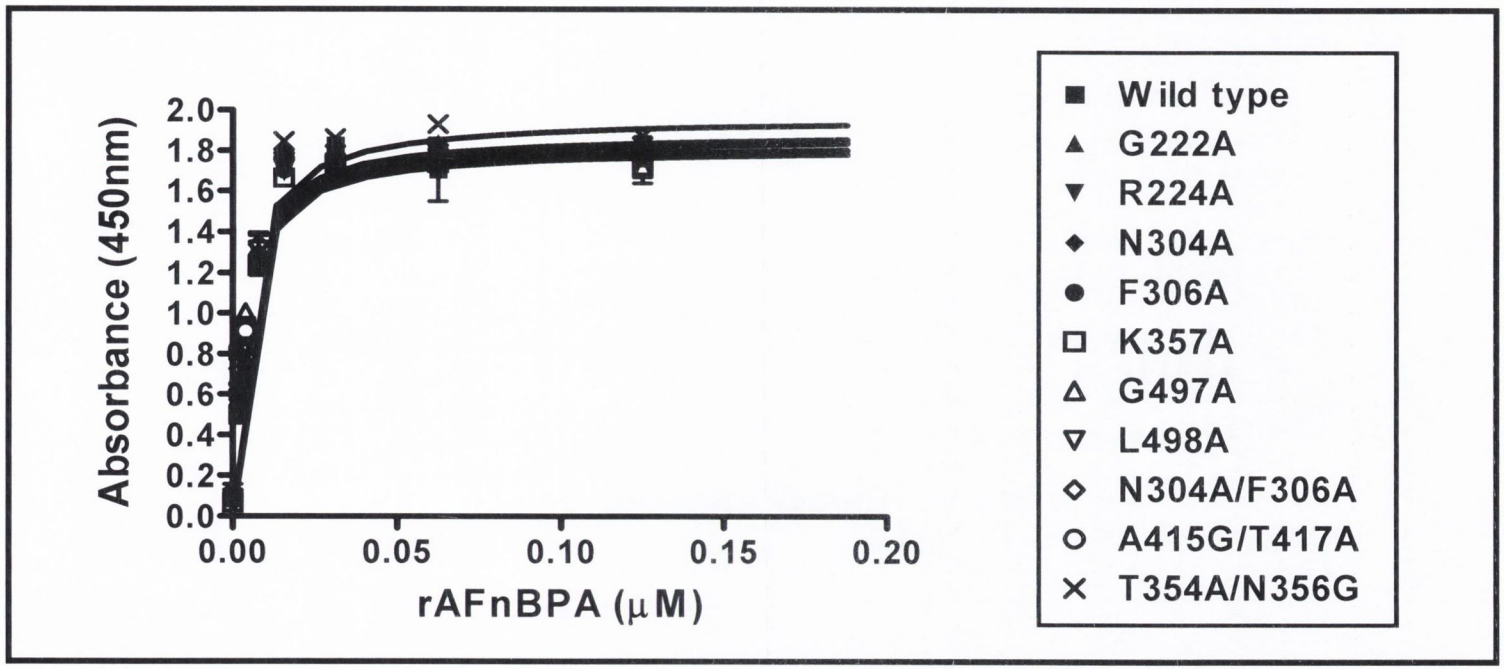

Figure 4.7 Affinity of polyclonal anti-rAFnBPA antibodies for immobilised $rAFnBPA_{37-511}$ wt and site-directed mutants (SDMs)

Equal amounts of $rAFnBPA_{37-511}$ wt and SDMs were coated onto the wells of a microtiter plate. A 1:2000 dilution of anti-rAFnBPA antibodies was added to each well followed by goat anti-rabbit-HRP antibodies and development with TMB substrate. Data points represent the mean of triplicate wells and this figure is representative of two independent experiments.

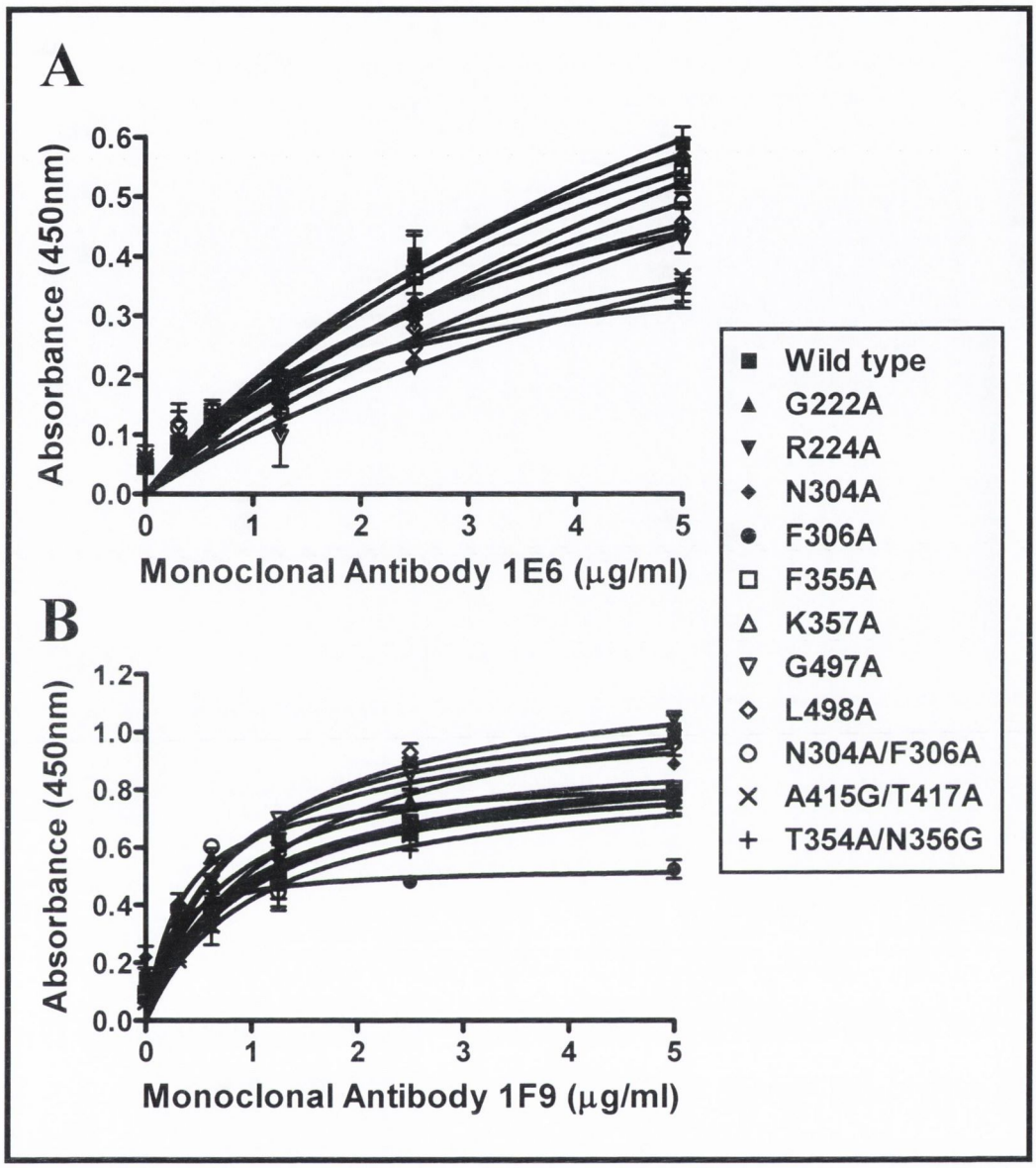

Figure 4.8 Binding of monoclonal antibodies 1E6 and 1F9 to immobilised rAFnBPA$_{37\text{-}511}$ wt and site-directed mutants

Equal amounts of rAFnBPA$_{37\text{-}511}$ wt and site-directed mutants (50 nM) were immobilised onto mircrotitre wells. Increasing concentrations of monoclonal antibodies 1E6 (A) and 1F9 (B) were added and bound antibody detected with rabbit anti-mouse HRP antibodies followed by development with TMB substrate. Data points represent the mean of triplicate wells. Due to shortage of monoclonal antibodies, this experiment was performed once.

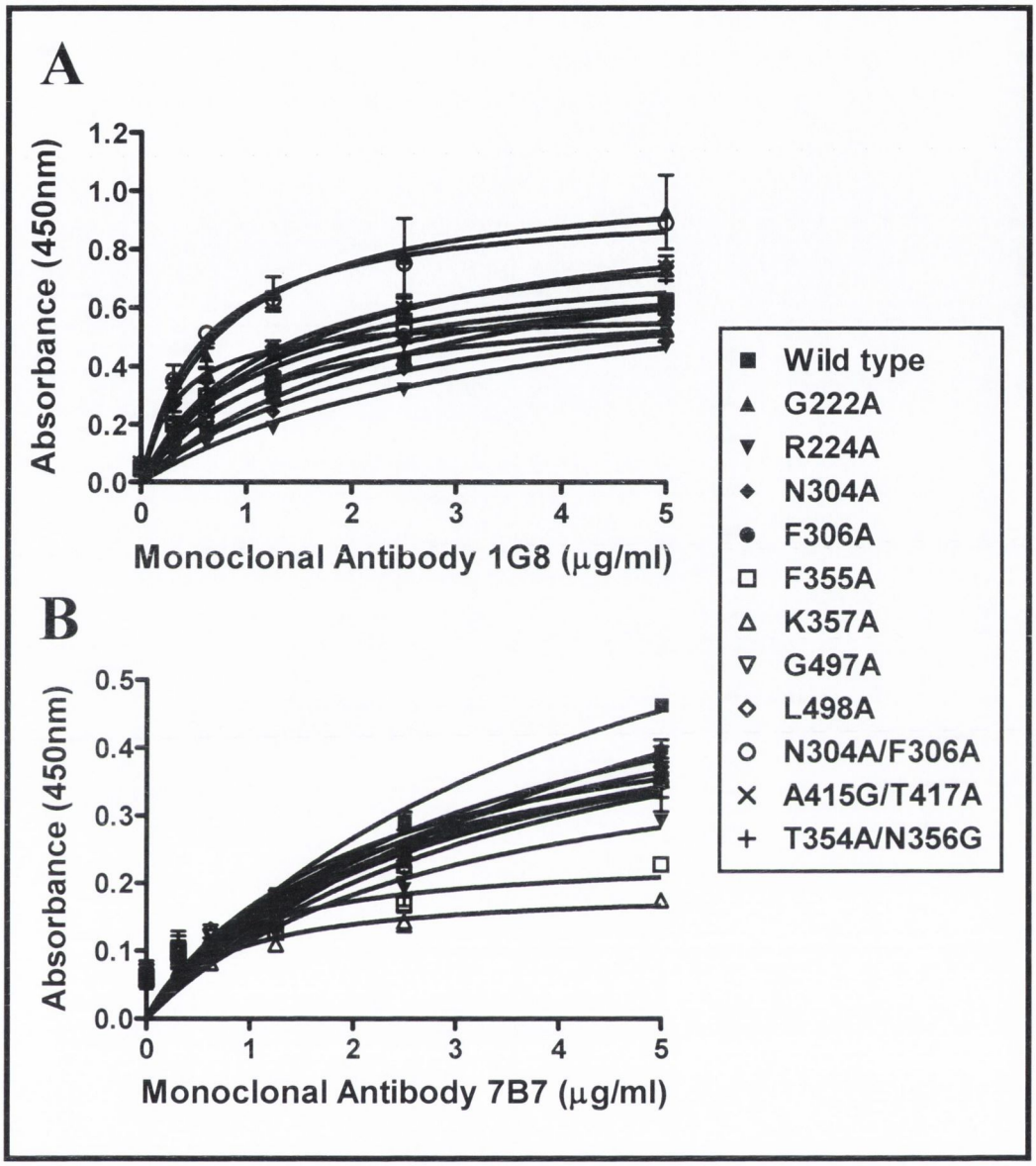

Figure 4.9 Binding of monoclonal antibodies 1G8 and 7B7 to immobilised rAFnBPA$_{37\text{-}511}$ wt and site-directed mutants

Equal amounts of rAFnBPA$_{37\text{-}511}$ wt and site-directed mutants (50 nM) were immobilised onto mircrotitre wells. Increasing concentrations of monoclonal antibodies 1G8 (A) and 7B7 (B) were added and bound antibody detected with rabbit anti-mouse HRP antibodies followed by development with TMB substrate. Data points represent the mean of triplicate wells. Due to shortage of monoclonal antibodies, this experiment was performed once.

and T354A/N356G (Figure 4.10 A). These amino acids (T, F, N and K) are all adjacent amino acids along the upper β-strand of the hydrophobic trench situated between subdomains N2 and N3 of region A (Figure 4.11). It is possible therefore that this area constitutes some or all of the epitope to which monoclonal antibody 8G3 binds. Monoclonal antibody 11F6 reacted similarly with most recombinant proteins with rAFnBPA$_{37\text{-}511}$ K357A exhibiting the weakest interaction compared to the wild-type recombinant protein (Figure 4.10 B).

4.2.7 Binding of rAFnBPA$_{37\text{-}511}$ wild-type and variant proteins to immobilised elastin and fibrinogen

The binding of substituted rAFnBPA$_{37\text{-}511}$ proteins to immobilised elastin and fibrinogen was tested in ELISA-based assays and compared directly with the binding of rAFnBPA$_{37\text{-}511}$ wild-type protein. Elastin and fibrinogen (10 μg/ml) were immobilised onto the wells of microtitre plates with control wells containing PBS only. The plates were blocked with skimmed milk to cover remaining binding sites on the plastic surface and doubling dilutions of rAFnBPA$_{37\text{-}511}$ proteins were added and incubated for 1 hr. Bound protein was detected with polyclonal anti-rAFnBPA antibodies followed by goat anti-rabbit-HRP conjugated antibodies. Plates were developed using the TMB substrate and measured by absorbance at 450 nm. All variant recombinant proteins are discussed individually below followed by a table summarising the affinities of all rAFnBPA proteins to immobilised elastin and fibrinogen.

4.2.7.1 Binding of rAFnBPA$_{37\text{-}511}$ G222A to immobilised elastin and fibrinogen

rAFnBPA$_{37\text{-}511}$ G222A contains a substitution that replaces the side chain of glycine (a single hydrogen atom) with that of alanine (a methyl group). This residue was chosen as it is in the equivalent position as A254 of ClfA which was substituted with serine in the study on ligand binding by ClfA (Deivanayagam *et al.*, 2002). The position of the glycine in question is just before the beginning of β-strand B of subdomain N2 of FnBPA (Figure 4.2). It is not predicted by the structural model to be in close contact with the docked fibrinogen ligand (Figure 4.12). In agreement with the above prediction, the substituted recombinant protein was shown to bind well to both elastin and fibrinogen (Figure 4.13). There was a slight defect in elastin binding with a barely significant p-value of 0.05. The binding to immobilised fibrinogen was shown to be almost identical to that of rAFnBPA$_{37\text{-}511}$ wild-type indicating

that, despite its position along the hydrophobic trench, Gly222 does not have a significant role to play in fibrinogen binding. This area however may be involved in binding to elastin.

4.2.7.2 Binding of rAFnBPA$_{37-511}$ R224A to immobilised elastin and fibrinogen

Arginine 224 is also at the beginning of β-strand B of N2 and is in an equivalent position to Y256 of ClfA that was shown to have a significant role in fibrinogen binding (Deivanayagam *et al.*, 2002). The long basic side chain of R224 stretches into the ligand-occupied space of region A of FnBPA and, in contrast to G222, is predicted by the molecular model to be in close proximity to the carboxyl side chain of the D410 residue of the fibrinogen γ chain (Figure 4.14). If a potential charge interaction is important, substitution of the arginine side chain with the methyl group of alanine would likely cause a defect in ligand binding. This was tested by ELISA assays and rAFnBPA$_{37-511}$ R224A showed reduced binding to elastin and to fibrinogen (Figure 4.15). The differences in half maximum binding values between substituted and wild-type protein for both ligands was significant with p-values of 0.0022 for elastin and 0.0083 for fibrinogen. This single amino acid substitution caused a similar effect on the binding of elastin and fibrinogen, strengthening the hypothesis that both ligands bind to a similar or overlapping region of the hydrophobic trench of rAFnBPA.

4.2.7.3 Binding of rAFnBPA$_{37-511}$ N304A to immobilised elastin and fibrinogen

The asparagine residue at position 304 is towards the end of β-strand E of subdomain N2 and is in the equivalent position as a crucial fibrinogen-binding residue in ClfA (P336) (Deivanayagam *et al.*, 2002). Based on analysis of the 3D structural model of rAFnBPA, the side chain of N304 could be in contact with the penultimate D410 residue of the fibrinogen γ chain (Figure 4.16). Upon conversion of this residue to alanine, the resulting recombinant protein was severely defective in binding to elastin and fibrinogen (Figure 4.17). The half maximum binding value for this protein was in the μM range compared to the low nanomolar range of the corresponding wild-type protein. The dramatic decrease in affinity of rAFnBPA$_{37-511}$ N304A protein for elastin and fibrinogen was reproducible and significant.

4.2.7.4 Binding of rAFnBPA$_{37-511}$ F306A to immobilised elastin and fibrinogen

Phenylalanine 306 is the second last residue of β-strand E of subdomain N2 of FnBPA and is in the equivalent position as tyrosine 338 of ClfA that has been shown to be crucial for fibrinogen binding (Deivanayagam *et al.*, 2002; Loughman *et al.*, 2005). The aromatic side

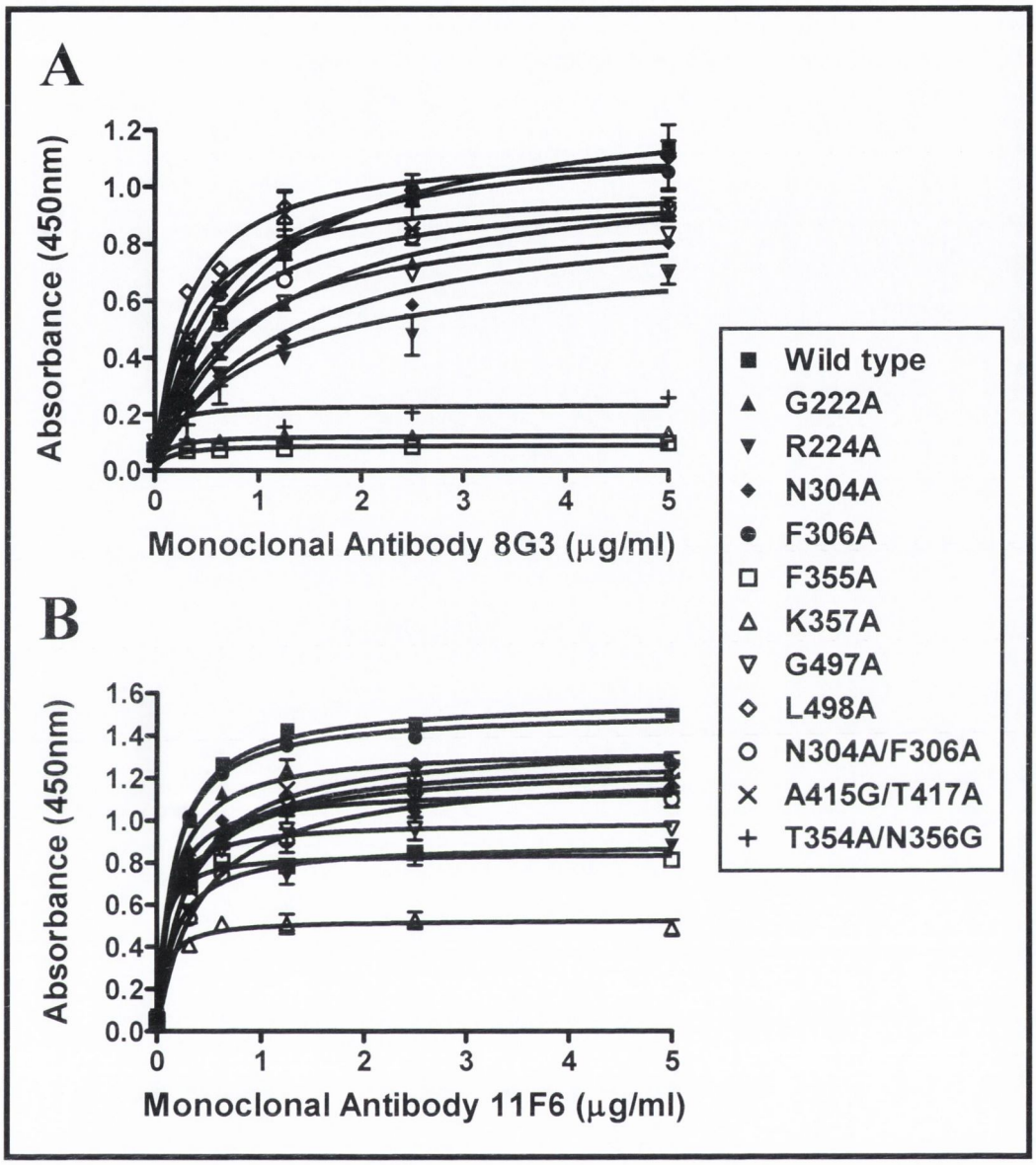

Figure 4.10 Binding of monoclonal antibodies 8G3 and 11F6 to immobilised rAFnBPA$_{37\text{-}511}$ wt and site-directed mutants

Equal amounts of rAFnBPA$_{37\text{-}511}$ wt and site-directed mutants (50 nM) were immobilised onto mircrotitre wells. Increasing concentrations of monoclonal antibodies 8G3 (A) and 11F6 (B) were added and bound antibody detected with rabbit anti-mouse HRP antibodies followed by development with TMB substrate. Data points represent the mean of triplicate wells. Due to shortage of monoclonal antibodies, this experiment was performed once.

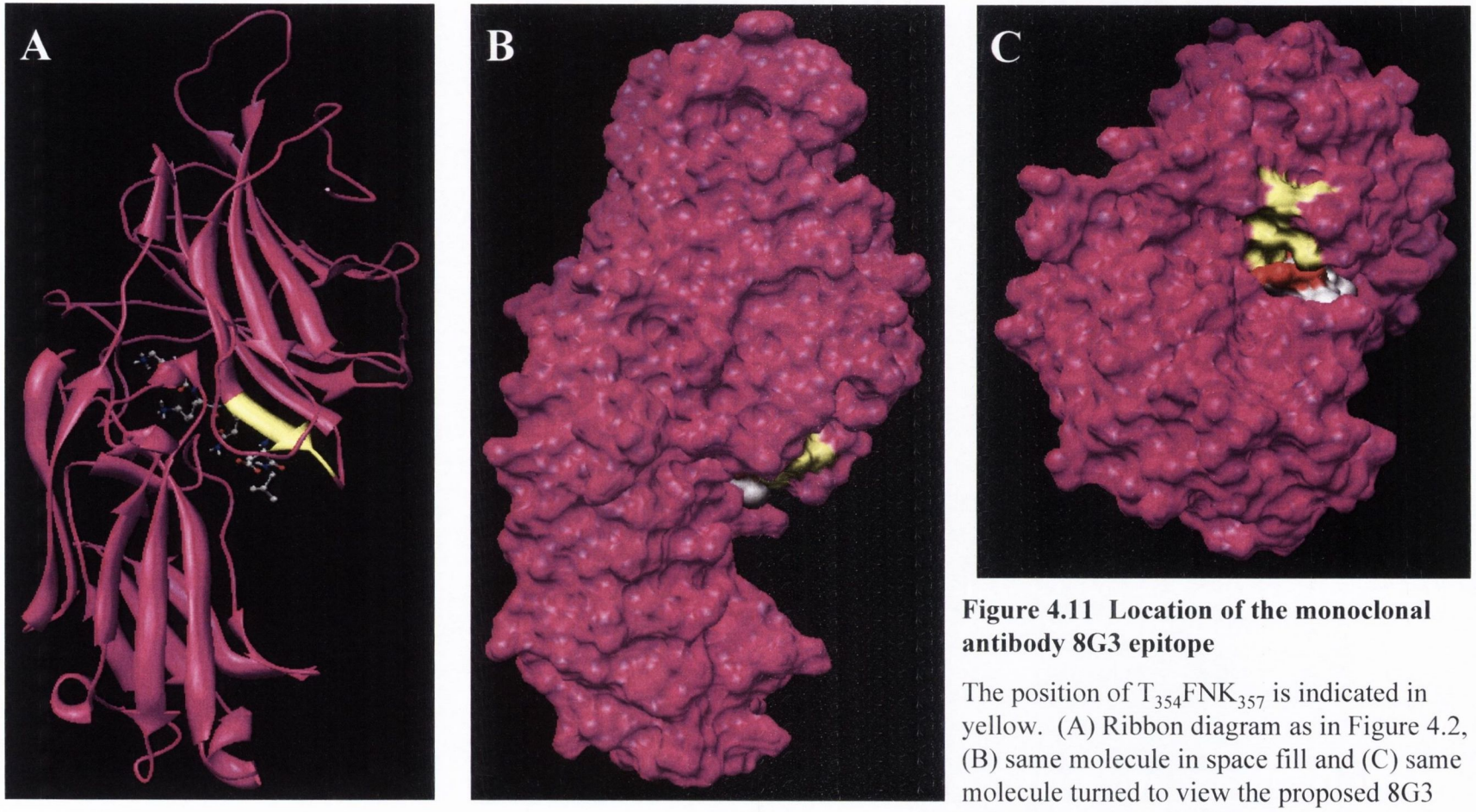

Figure 4.11 Location of the monoclonal antibody 8G3 epitope

The position of $T_{354}FNK_{357}$ is indicated in yellow. (A) Ribbon diagram as in Figure 4.2, (B) same molecule in space fill and (C) same molecule turned to view the proposed 8G3 epitope more clearly.

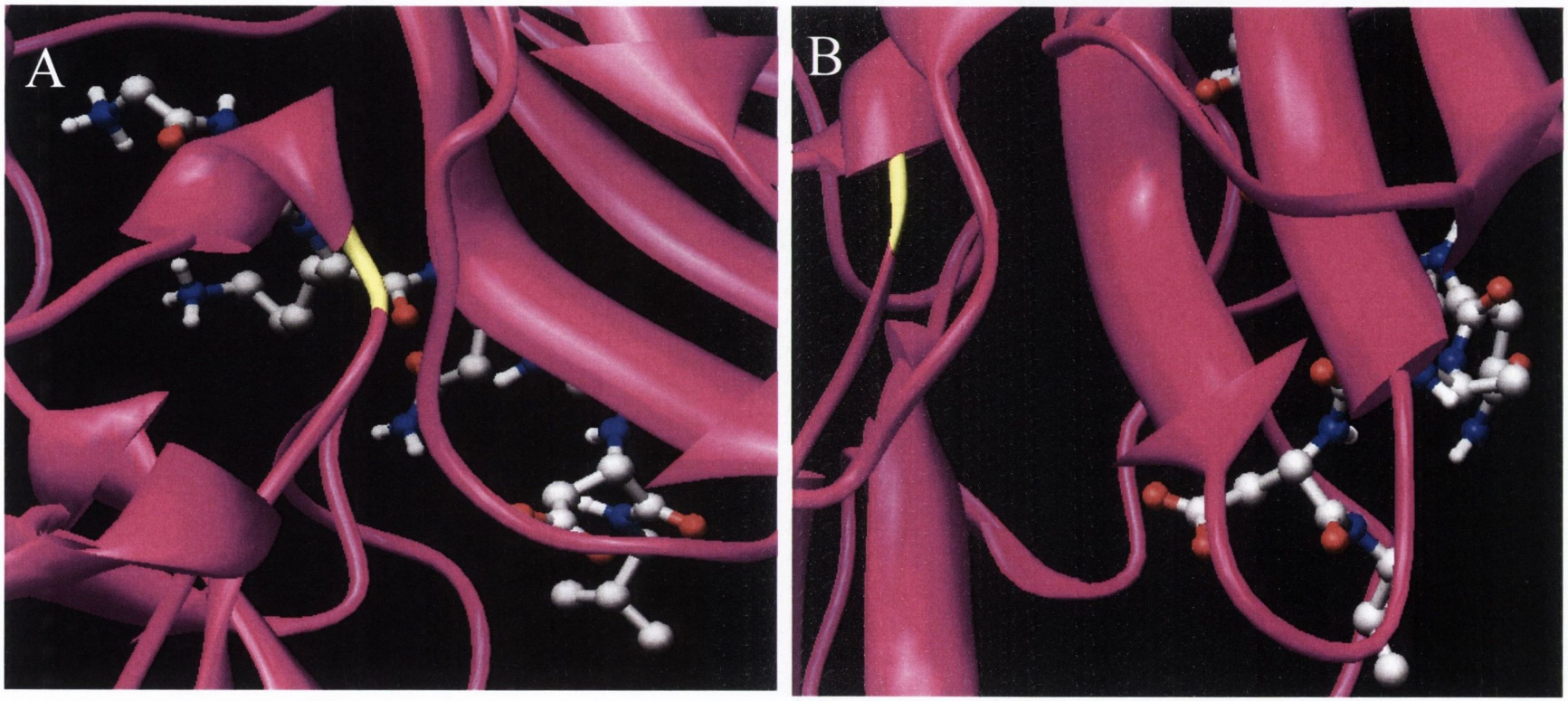

Figure 4.12 Position of the G222A substitution in rAFnBPA

Enlarged section of the structural model of the N2N3 subdomains of FnBPA with the fibrinogen peptide (ball and stick format) docked into the hydrophobic trench. Residue G222 is highlighted in yellow. The side chain (hydrogen) of this residue is not visible. A shows the hydrophobic trench from the viewing position of Figure 4.2 while B is a tilted view of the model to show the proximity of G222 to the fibrinogen ligand.

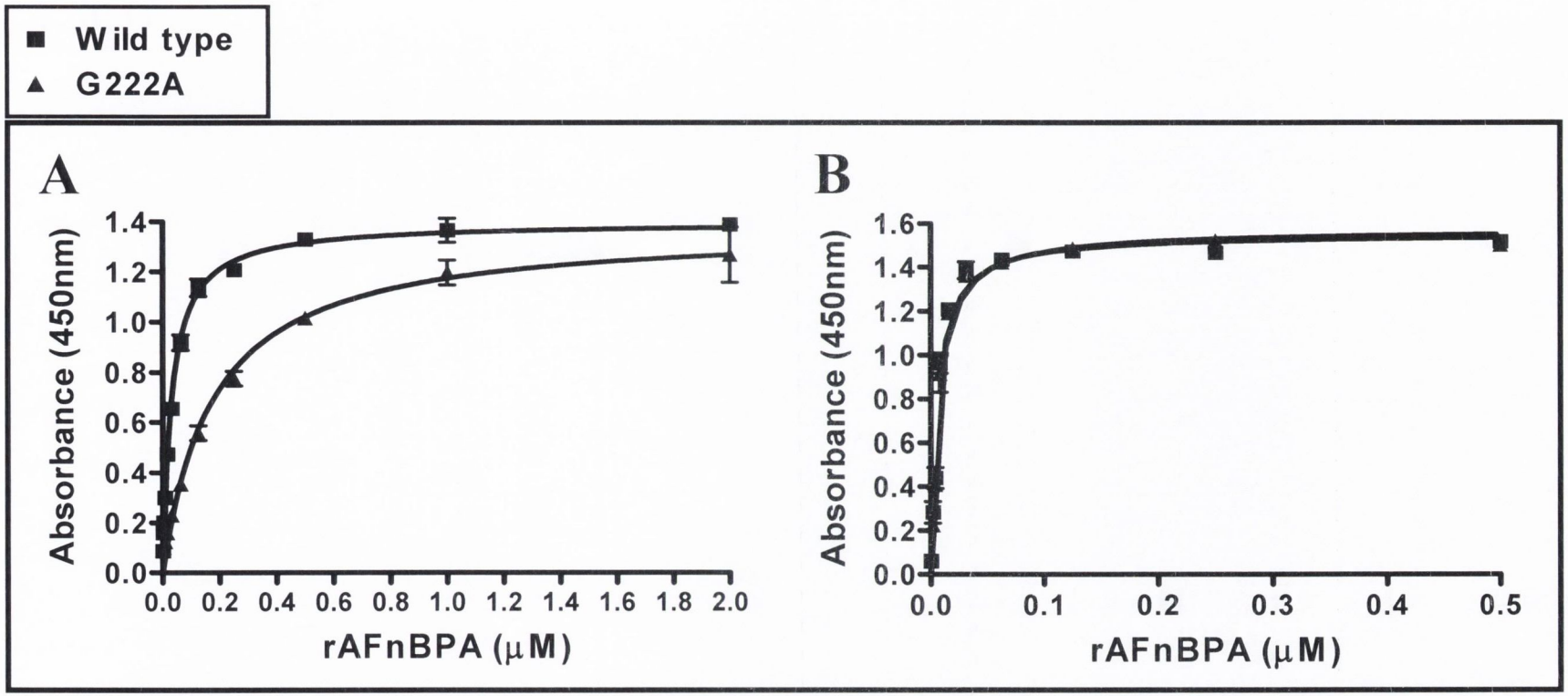

Figure 4.13 Binding of recombinant proteins rAFnBPA$_{37\text{-}511}$ wt and rAFnBPA$_{37\text{-}511}$ G222A to immobilised human elastin and fibrinogen

Microtiter wells were coated with 10 μg/ml human elastin (A) or fibrinogen (B) and increasing concentrations of rAFnBPA proteins were added for 1 h. Bound protein was detected with polyclonal anti-rAFnBPA antibodies, HRP-conjugated goat anti-rabbit antibodies followed by TMB substrate. Data points represent the mean of triplicate wells and this figure is representative of three independent experiments.

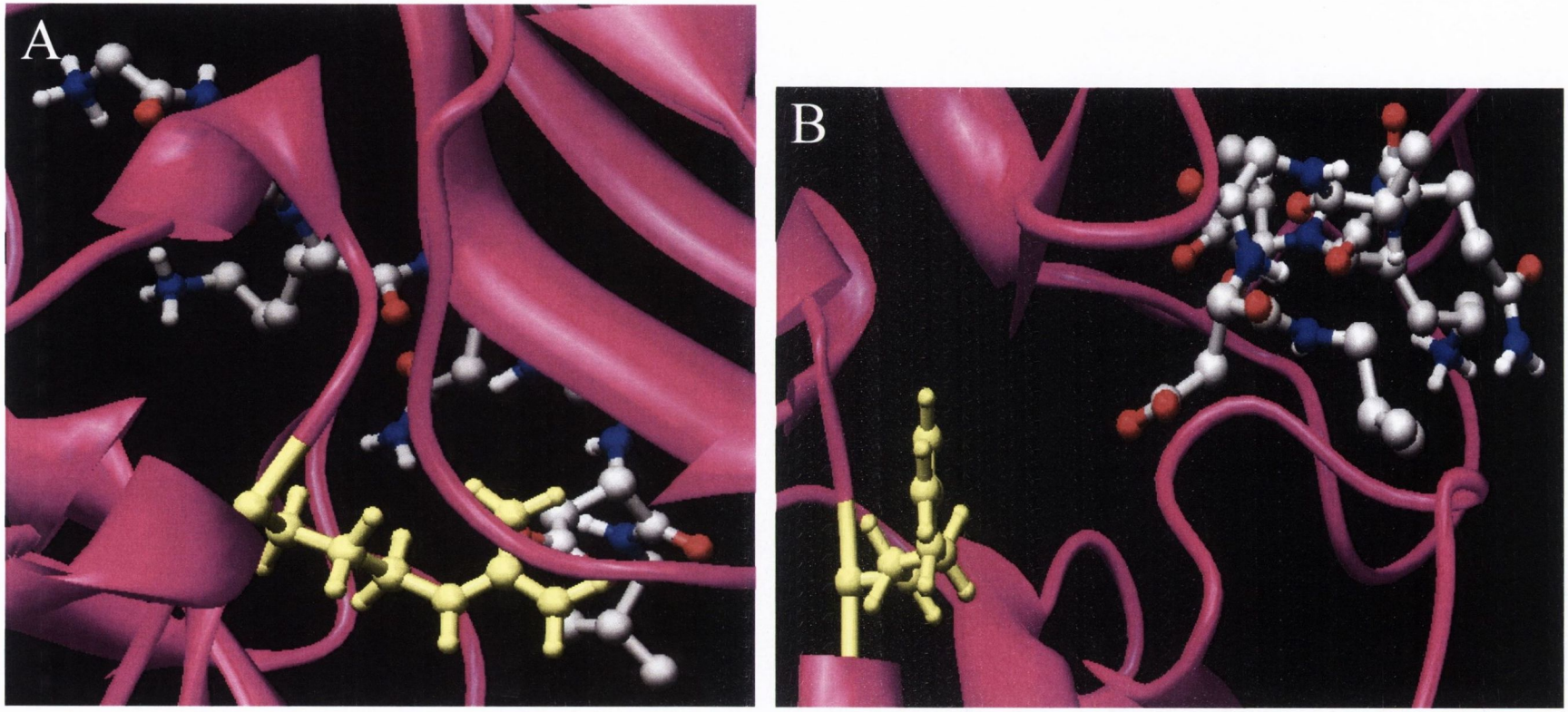

Figure 4.14 Position of the R224A substitution in rAFnBPA

Enlarged section of the structural model of the N2N3 subdomains of FnBPA with the fibrinogen peptide (ball and stick format) docked into the hydrophobic trench. Residue R224 is highlighted in yellow with the side chain visible in ball and stick format. A shows the hydrophobic trench from the viewing position of Figure 4.2 while B is a tilted view of the model to show the proximity of R224 to the fibrinogen ligand.

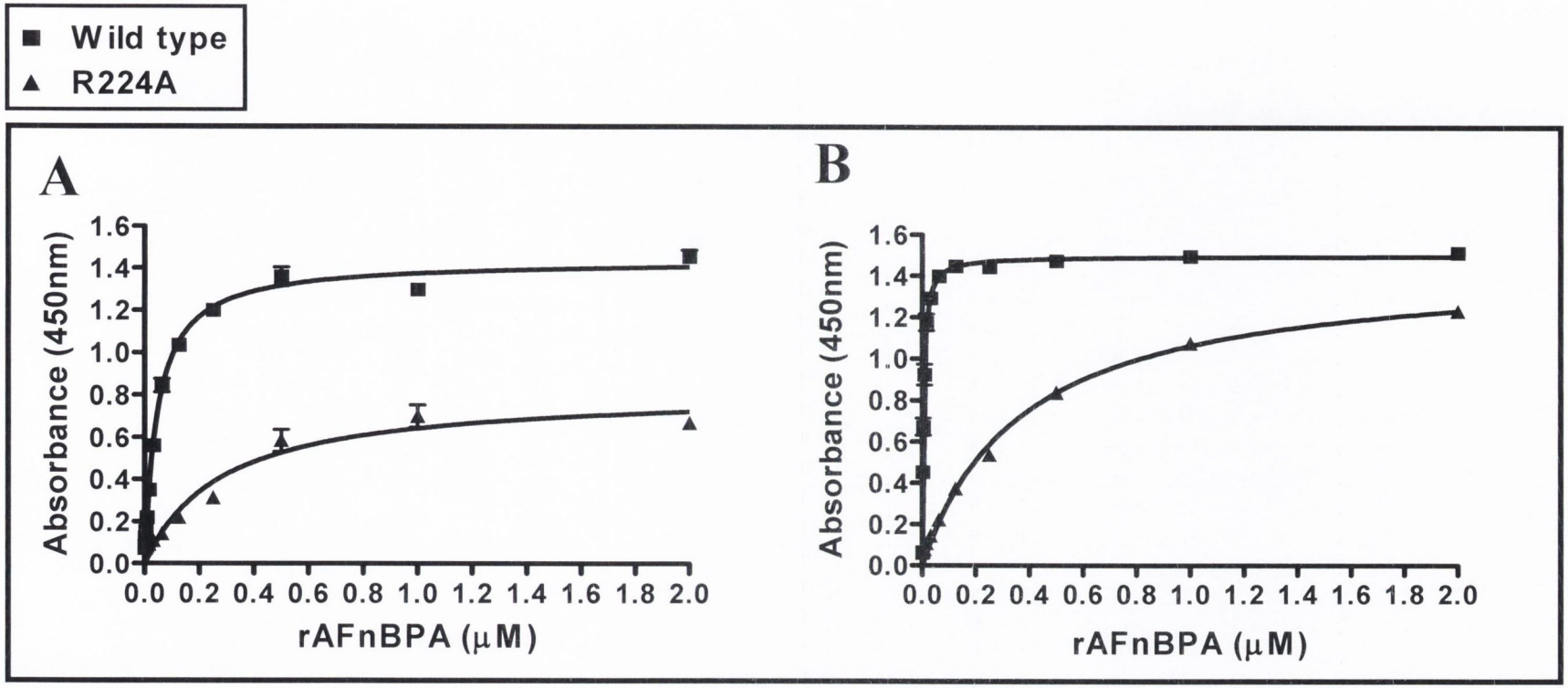

Figure 4.15 Binding of recombinant proteins rAFnBPA$_{37\text{-}511}$ wt and rAFnBPA$_{37\text{-}511}$ R224A to immobilised human elastin and fibrinogen

Microtiter wells were coated with 10 μg/ml human elastin (A) or fibrinogen (B) and increasing concentrations of rAFnBPA proteins were added for 1 h. Bound protein was detected with polyclonal anti-rAFnBPA antibodies, HRP-conjugated goat anti-rabbit antibodies followed by TMB substrate. Data points represent the mean of triplicate wells and this figure is representative of three independent experiments.

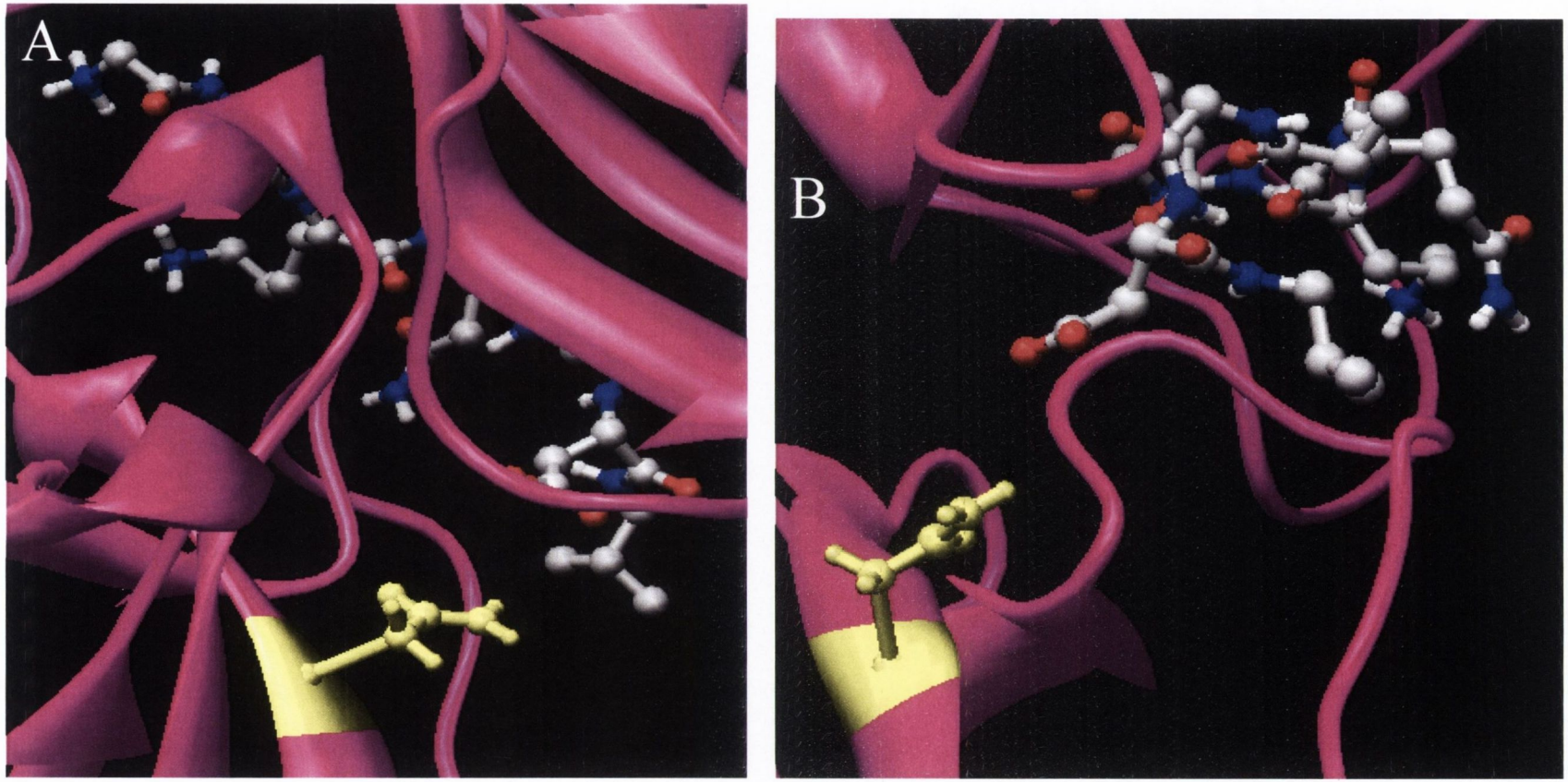

Figure 4.16 Position of the N304A substitution in rAFnBPA

Enlarged section of the structural model of the N2N3 subdomains of FnBPA with the fibrinogen peptide (ball and stick format) docked into the hydrophobic trench. Residue N304 is highlighted in yellow with the side chain visible in ball and stick format. A shows the hydrophobic trench from the viewing position of Figure 4.2 while B is a tilted view of the model to show the proximity of N304 to the fibrinogen ligand.

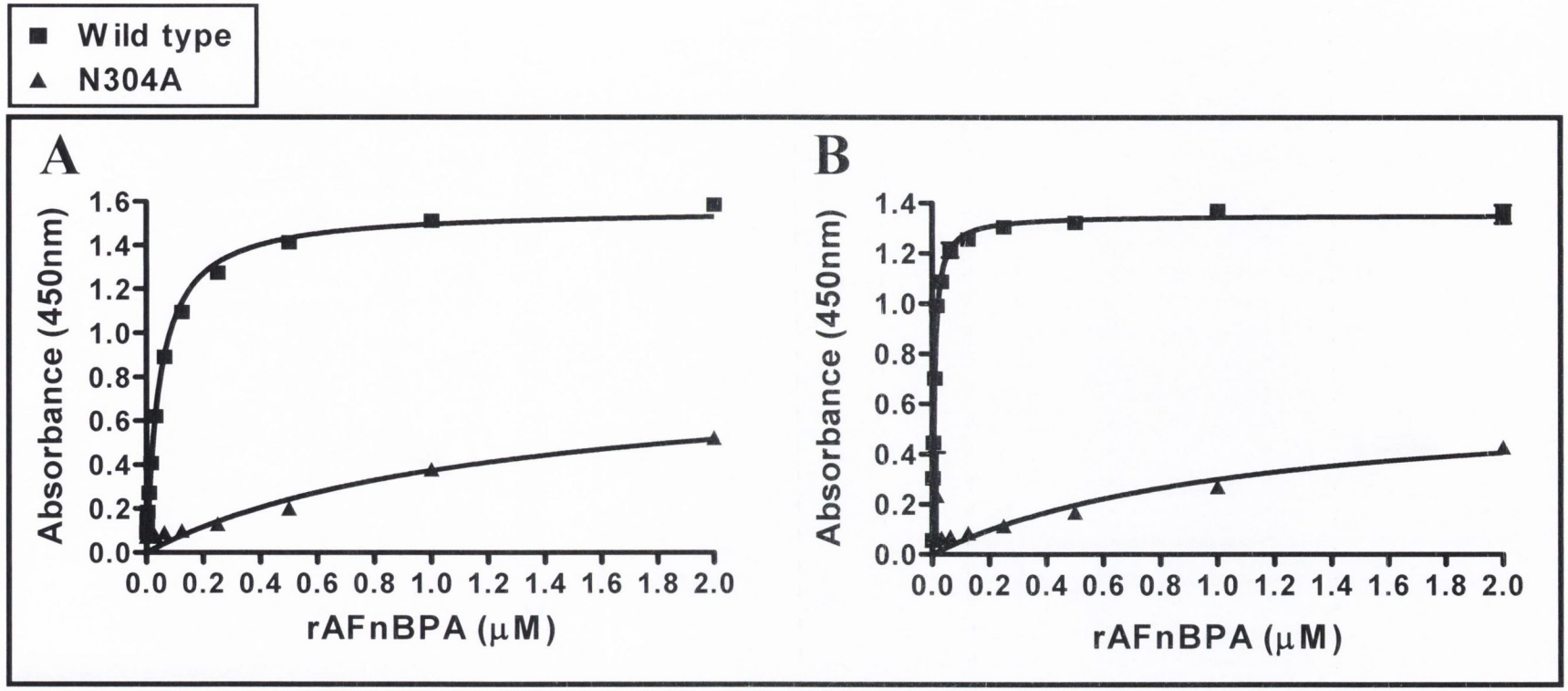

Figure 4.17 Binding of recombinant proteins rAFnBPA$_{37\text{-}511}$ wt and rAFnBPA$_{37\text{-}511}$ N304A to immobilised human elastin and fibrinogen

Microtiter wells were coated with 10 μg/ml human elastin (A) or fibrinogen (B) and increasing concentrations of rAFnBPA proteins were added for 1 h. Bound protein was detected with polyclonal anti-rAFnBPA antibodies, HRP-conjugated goat anti-rabbit antibodies followed by TMB substrate. Data points represent the mean of triplicate wells and this figure is representative of three independent experiments.

chain of this residue is predicted by the 3D structural model to point in to the fibrinogen ligand, possibly contacting the D410 residue of the fibrinogen γ chain (Figure 4.18). In this way, it was expected that the substitution of F306 to alanine would affect ligand binding. When this aromatic side chain was removed and replaced by a methyl group, the binding to elastin and fibrinogen was severely affected. It was not possible to estimate a half maximum binding value for the rAFnBPA$_{37\text{-}511}$ F306A recombinant protein (Figure 4.19). The equivalent substitution in ClfA (Y338A) did not bind detectably to fibrinogen in fluorescence polarization studies using a labelled fibrinogen peptide (Deivanayagam *et al.*, 2002). The defect of F306A binding to fibrinogen and elastin is also reproducible and significant. It is also interesting that substitutions R224A, N304A and F306A caused reductions in the binding of both ligands, indicating that fibrinogen and elastin have a similar binding site and may bind in a similar manner.

4.2.7.5 Binding of rAFnBPA$_{37\text{-}511}$ F355A to immobilised elastin and fibrinogen

The substitution of phenylalanine 335 did not cause a large defect in ligand binding. F355 is situated along the upper part of the hydrophobic trench, on β-strand A of subdomain N3. It is in the same position as I387 of ClfA, the substitution of which did not cause a significant defect in fibrinogen binding (Deivanayagam *et al.*, 2002). The side chain of F355 points in the opposite direction to that of the docked fibrinogen ligand in the proposed structural model of rAFnBPA (Figure 4.20). rAFnBPA$_{37\text{-}511}$ F355A is somewhat defective in binding to fibrinogen (Figure 4.21 B) but the large variation in half maximum binding values from repeated experiments caused only a slightly significant p-value of 0.026. The slight decrease in elastin binding (Figure 4.21 A) was also accompanied with a large variation around the average half maximum binding constant and was deemed not to be significant. Based on the structural model of N2N3 of FnBPA, it is possible that the changes seen in ligand binding with this protein are due to small localized conformational changes of the β-sheet structure and not due to changes in the contact points of FnBPA with elastin or fibrinogen.

4.2.7.6 Binding of rAFnBPA$_{37\text{-}511}$ K357A to immobilised elastin and fibrinogen

The lysine residue K357 is located close to F355 and the substitution K357A behaves in similar manner to F355A. Residue K357 is situated at the end of β-strand A of subdomain N3 and is in the equivalent position to K389 of ClfA (Deivanayagam *et al.*, 2002). The side

chain of K357 of FnPBA also points in the opposite direction to the hydrophobic trench occupied by the fibrinogen ligand in the predicted structural model (Figure 4.22). When the recombinant protein rAFnBPA$_{37\text{-}511}$ K357A was tested in ELISA assays for binding to immobilised ligands, it was found that there was no statistical significance in the difference to elastin and a slightly significant difference in binding to fibrinogen compared to the wild-type protein (Figure 4.23). As with F355, the changes in ligand binding occur with the higher affinity fibrinogen interaction and are likely to be caused by localized conformational changes in the surrounding β-sheet structure.

4.2.7.7 Binding of rAFnBPA$_{37\text{-}511}$ G497A to immobilised elastin and fibrinogen

Glycine 497 of FnBPA was chosen for site-directed mutagenesis as it is in the equivalent position to E526 of ClfA which was shown previously to be important in fibrinogen binding (Hartford *et al.*, 2001). The position of G497 in the structural model of FnBPA is at the end of the G strand of subdomain N3. The side chain of this residue is a single hydrogen atom and is not situated near the docked fibrinogen ligand (Figure 4.24). The substitution of this residue with alanine introduces a methyl group which caused a significant decrease in the affinity for both elastin and fibrinogen (Figure 4.25). The binding profile of rAFnBPA$_{37\text{-}511}$ G497A to fibrinogen reached high levels at high concentrations but the decreased affinity at lower concentrations was reproducible and represents a significant difference compared to the binding of wild-type rAFnPBA. The position of the glycine at the junction of β-strand G and the hinge region is likely to be important in the latching mechanism of ligand binding. Glycine is known for its ability to induce bends into the secondary structure of proteins and its substitution to alanine might affect its role in bending the hinge region across the hydrophobic trench to allow latching of β-strand G'' into position in N2.

4.2.7.8 Binding of rAFnBPA$_{37\text{-}511}$ L498A to immobilised elastin and fibrinogen

Leucine 498 is adjacent to the glycine discussed above and was chosen as it is in the equivalent position as V527 of ClfA that has been shown in a previous study to be important in fibrinogen binding (Hartford *et al.*, 2001). Upon crystallisation of ClfA, it was noted that V527 was at the opening to the hydrophobic trench and may interact with the C-terminal V411 of the fibrinogen γ chain peptide (Deivanayagam *et al.*, 2002). It was also noted that valine was also present at this position in FnBPB and occurred as a conserved substitution (Leu) in FnBPA. It was of interest to investigate the role of this residue (L498) in fibrinogen binding

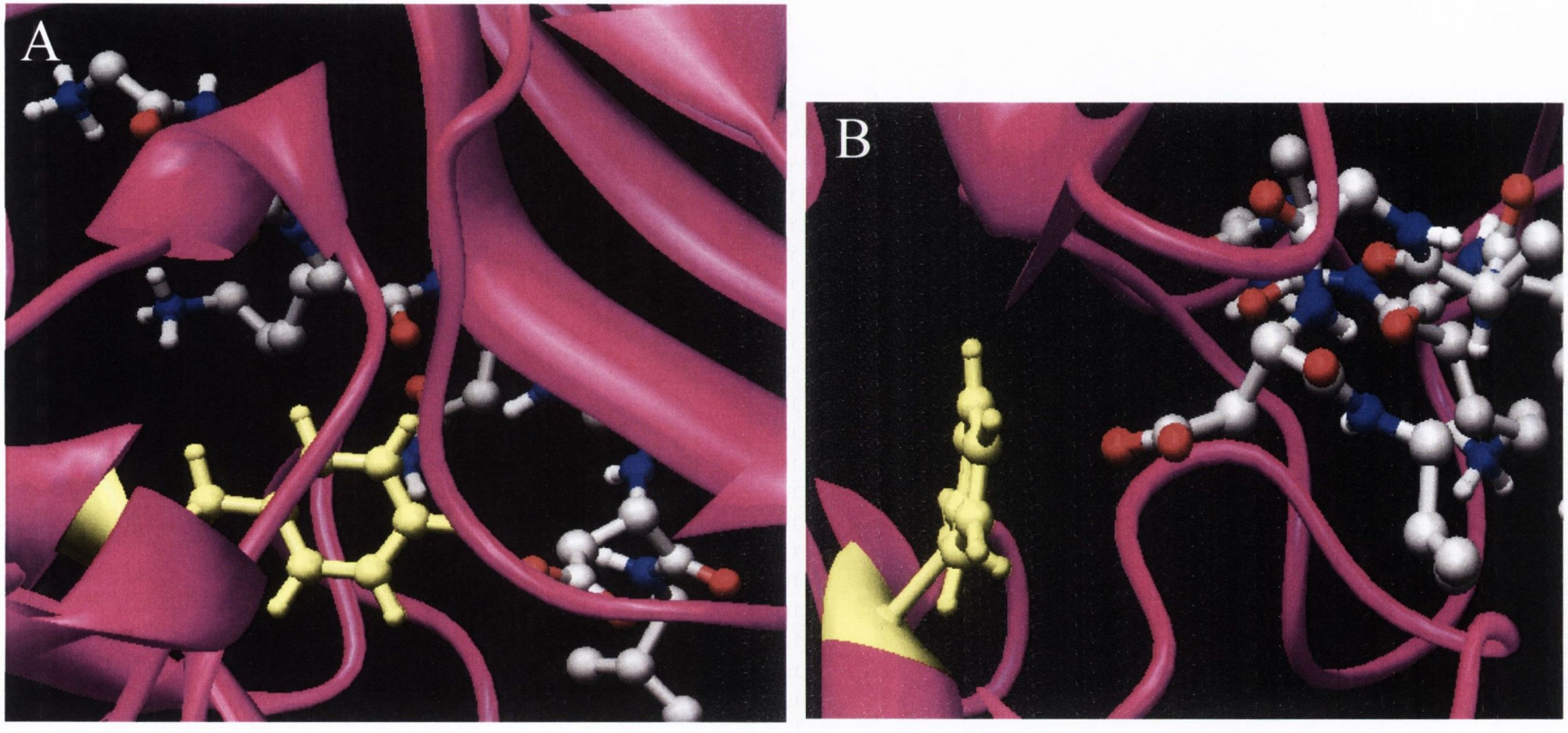

Figure 4. 18 Position of the F306A substitution in rAFnBPA

Enlarged section of the structural model of the N2N3 subdomains of FnBPA with the fibrinogen peptide (ball and stick format) docked into the hydrophobic trench. Residue F306 is highlighted in yellow with the side chain visible in ball and stick format. A shows the hydrophobic trench from the viewing position of Figure 4.2 while B is a tilted view of the model to show the proximity of F306 to the fibrinogen ligand.

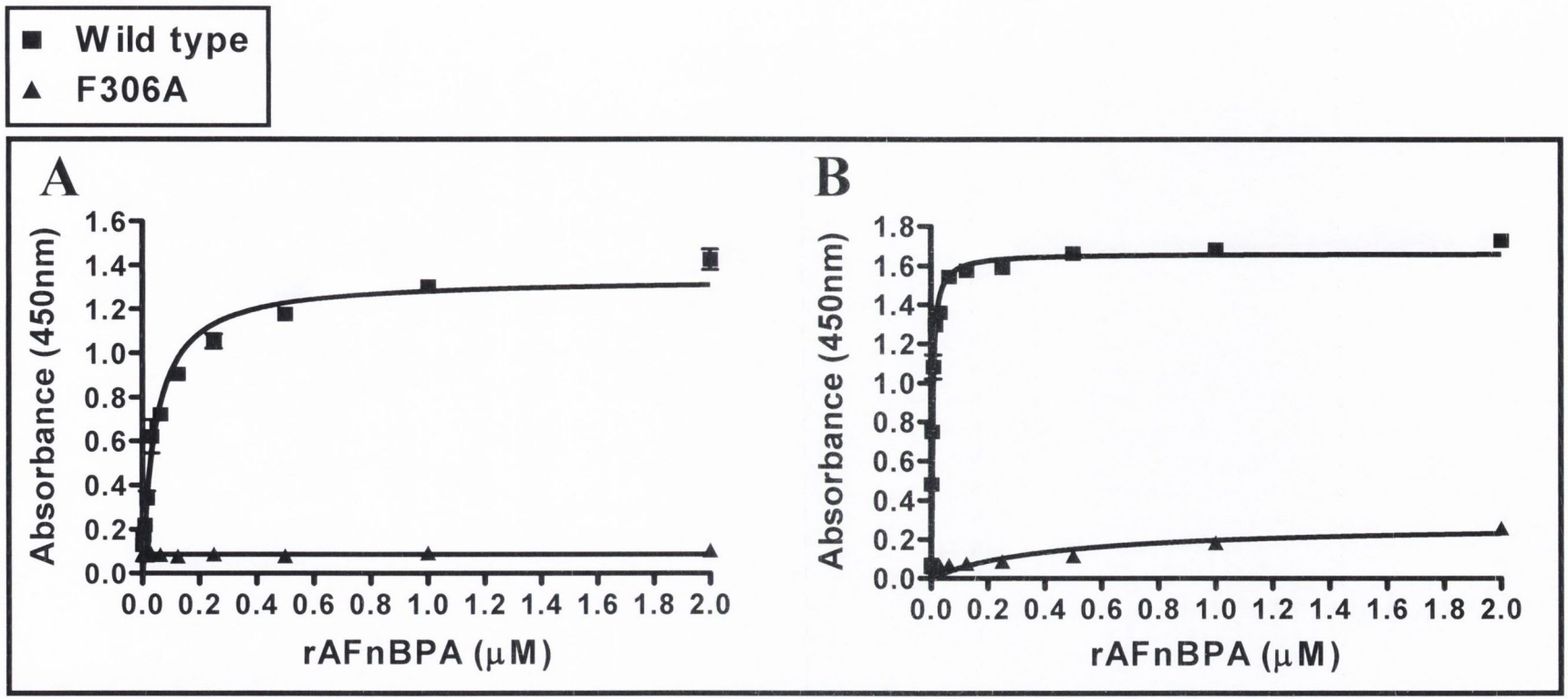

Figure 4.19 Binding of recombinant proteins rAFnBPA$_{37\text{-}511}$ wt and rAFnBPA$_{37\text{-}511}$ F306A to immobilised human elastin and fibrinogen

Microtiter wells were coated with 10 μg/ml human elastin (A) or fibrinogen (B) and increasing concentrations of rAFnBPA proteins were added for 1 h. Bound protein was detected with polyclonal anti-rAFnBPA antibodies, HRP-conjugated goat anti-rabbit antibodies followed by TMB substrate. Data points represent the mean of triplicate wells and this figure is representative of three independent experiments.

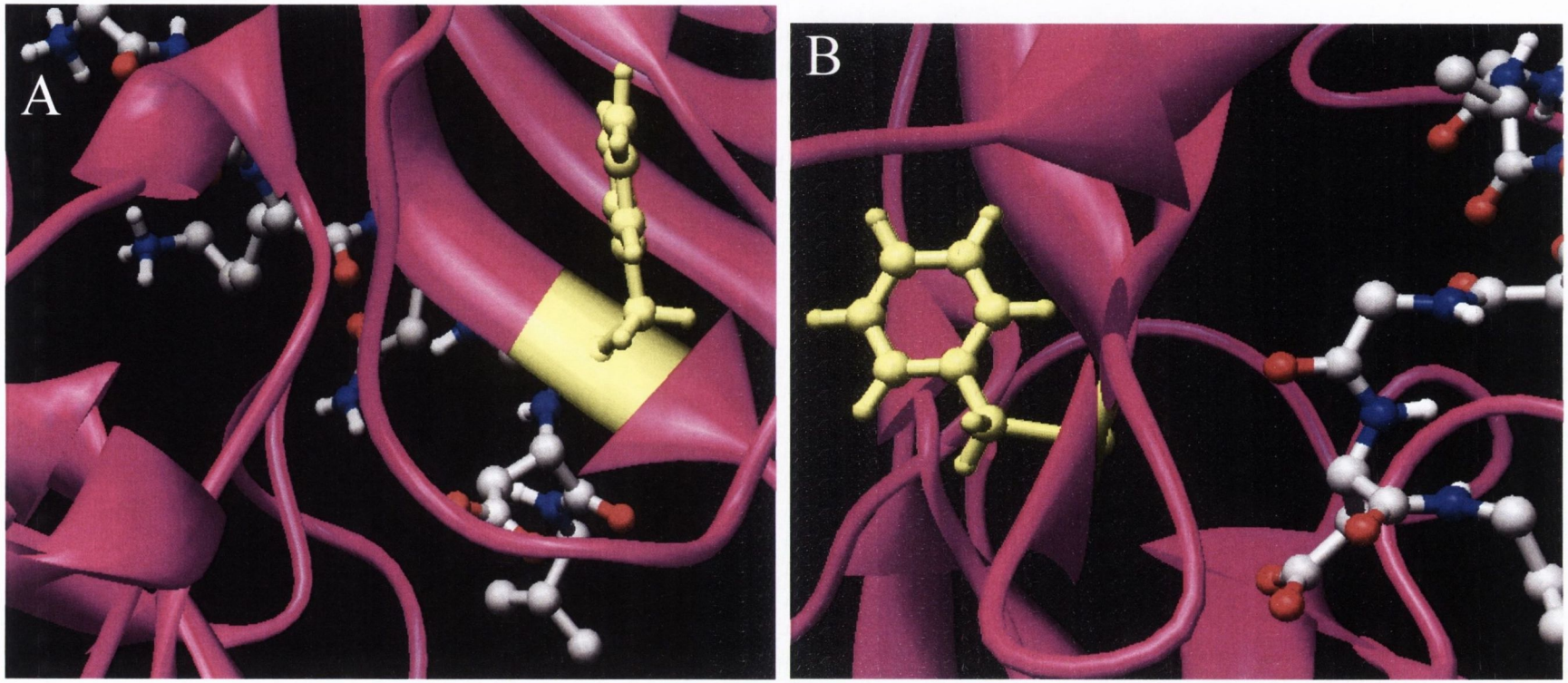

Figure 4.20 Position of the F355A substitution in rAFnBPA

Enlarged section of the structural model of the N2N3 subdomains of FnBPA with the fibrinogen peptide (ball and stick format) docked into the hydrophobic trench. Residue F355 is highlighted in yellow with the side chain visible in ball and stick format. A shows the hydrophobic trench from the viewing position of Figure 4.2 while B is a tilted view of the model to show the proximity of F355 to the fibrinogen ligand.

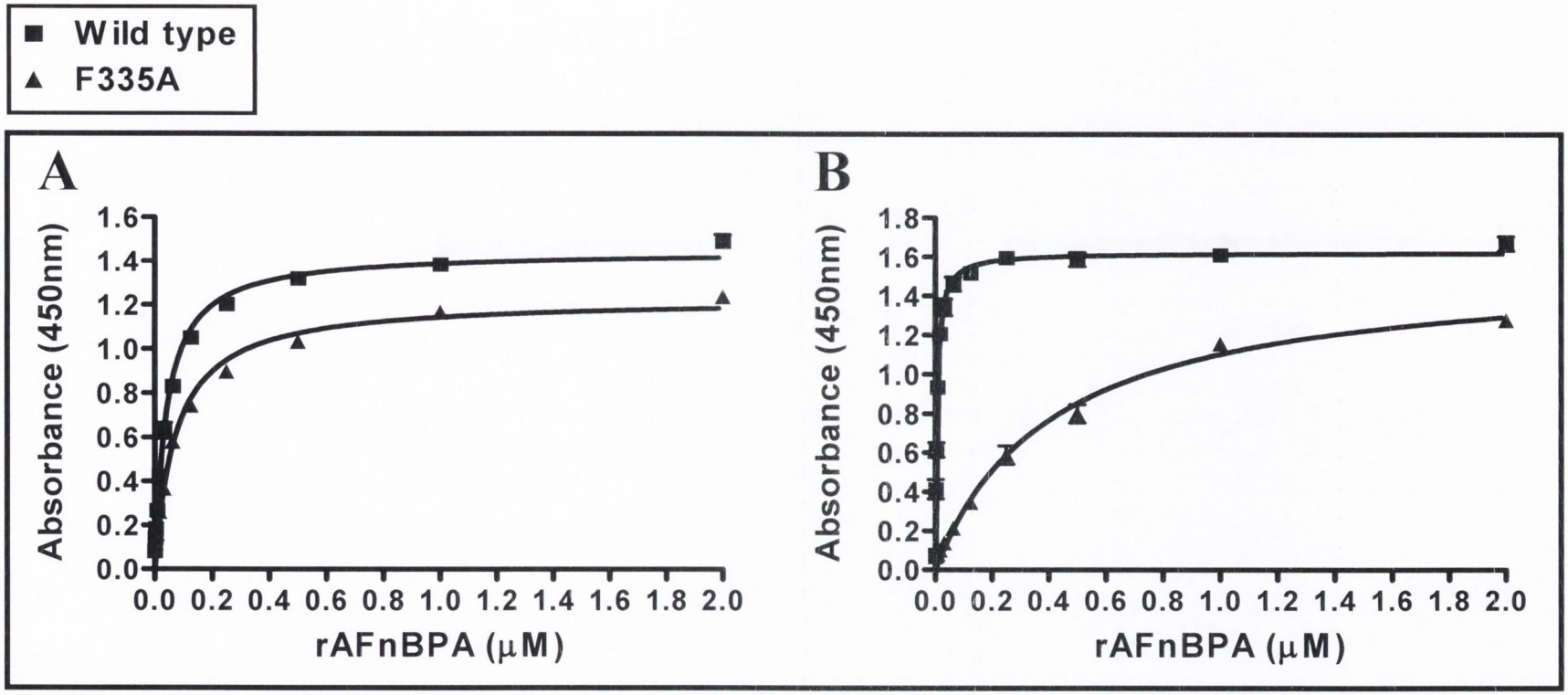

Figure 4.21 Binding of recombinant proteins rAFnBPA$_{37\text{-}511}$ wt and rAFnBPA$_{37\text{-}511}$ F355A to immobilised human elastin and fibrinogen

Microtiter wells were coated with 10 μg/ml human elastin (A) or fibrinogen (B) and increasing concentrations of rAFnBPA proteins were added for 1 h. Bound protein was detected with polyclonal anti-rAFnBPA antibodies, HRP-conjugated goat anti-rabbit antibodies followed by TMB substrate. Data points represent the mean of triplicate wells and this figure is representative of three independent experiments.

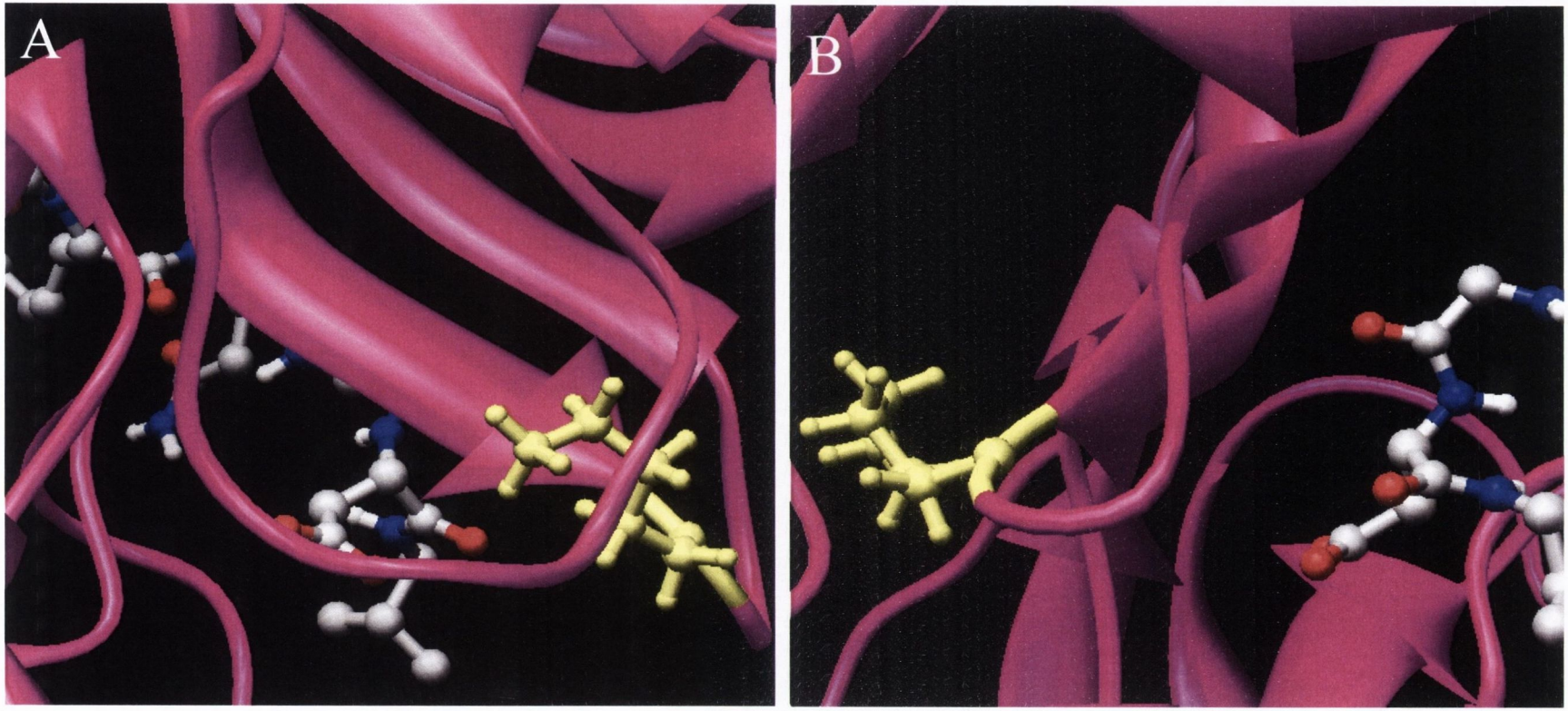

Figure 4.22 Position of the K357A substitution in rAFnBPA

Enlarged section of the structural model of the N2N3 subdomains of FnBPA with the fibrinogen peptide (ball and stick format) docked into the hydrophobic trench. Residue K357 is highlighted in yellow with the side chain visible in ball and stick format. A shows the hydrophobic trench from the viewing position of Figure 4.2 while B is a tilted view of the model to show the proximity of G222A to the fibrinogen ligand.

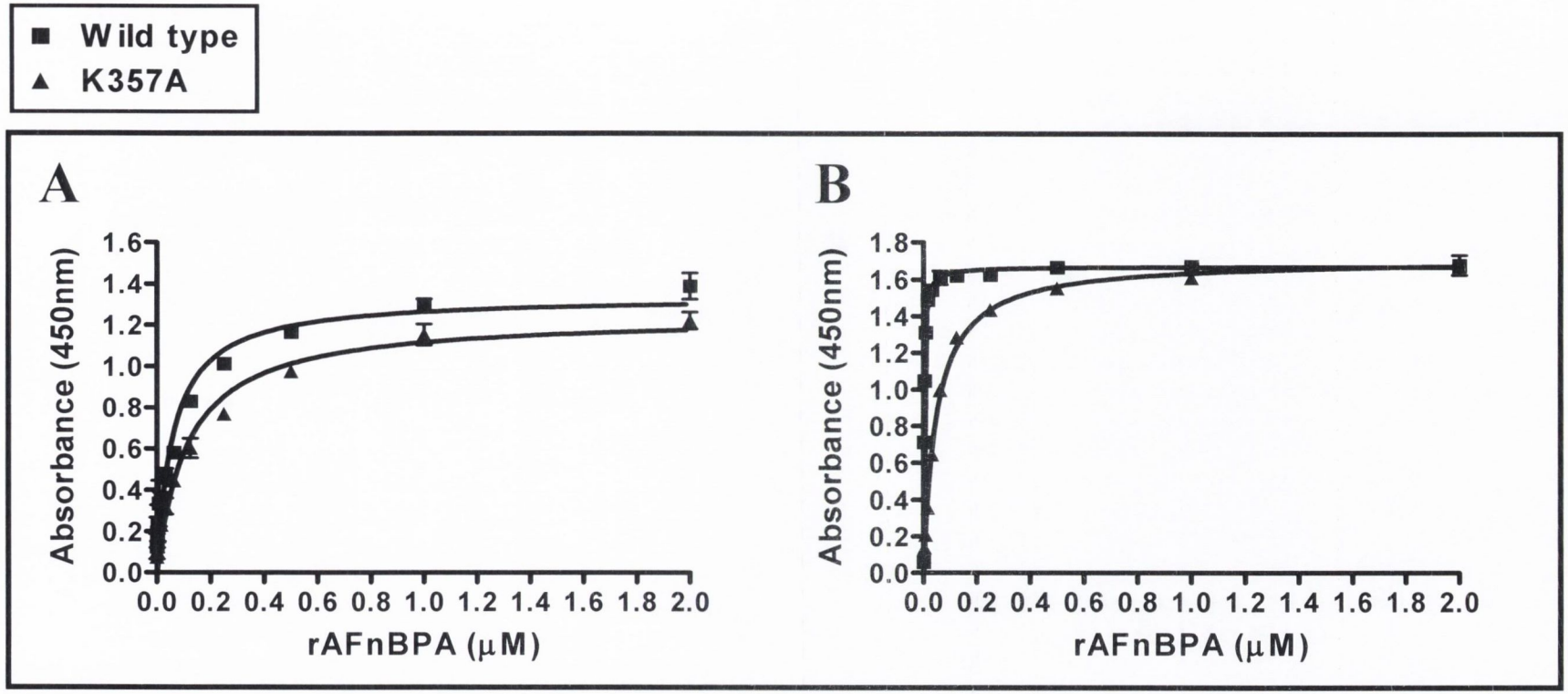

Figure 4.23 Binding of recombinant proteins rAFnBPA$_{37\text{-}511}$ wt and rAFnBPA$_{37\text{-}511}$ K357A to immobilised human elastin and fibrinogen

Microtiter wells were coated with 10 μg/ml human elastin (A) or fibrinogen (B) and increasing concentrations of rAFnBPA proteins were added for 1 h. Bound protein was detected with polyclonal anti-rAFnBPA antibodies, HRP-conjugated goat anti-rabbit antibodies followed by TMB substrate. Data points represent the mean of triplicate wells and this figure is representative of three independent experiments.

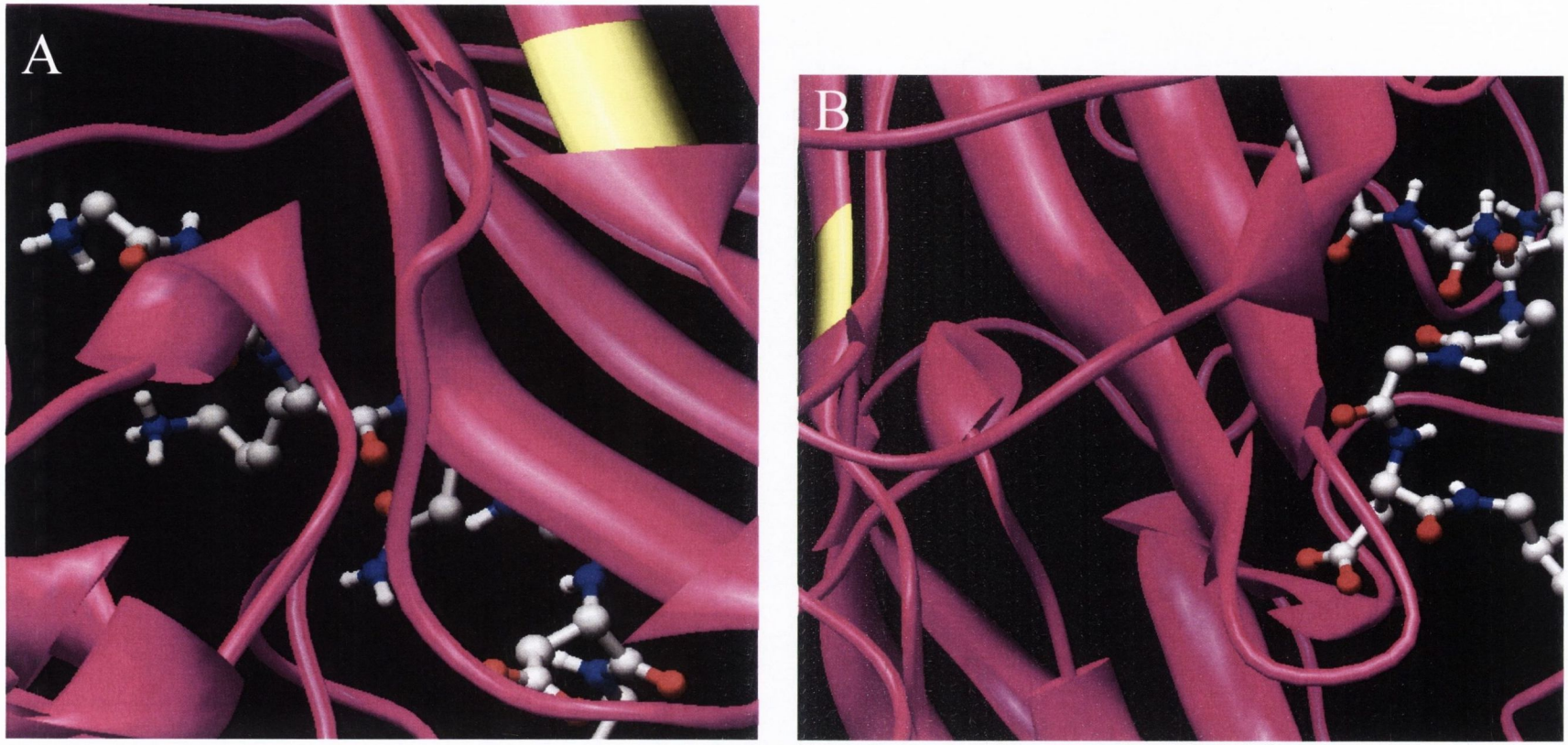

Figure 4.24 Position of the G497A substitution in rAFnBPA

Enlarged section of the structural model of the N2N3 subdomains of FnBPA with the fibrinogen peptide (ball and stick format) docked into the hydrophobic trench. Residue G497 is highlighted in yellow. The side chain (H) of this residue is not visible. A shows the hydrophobic trench from the viewing position of Figure 4.2 while B is a tilted view of the model to show the proximity of G497 to the fibrinogen ligand.

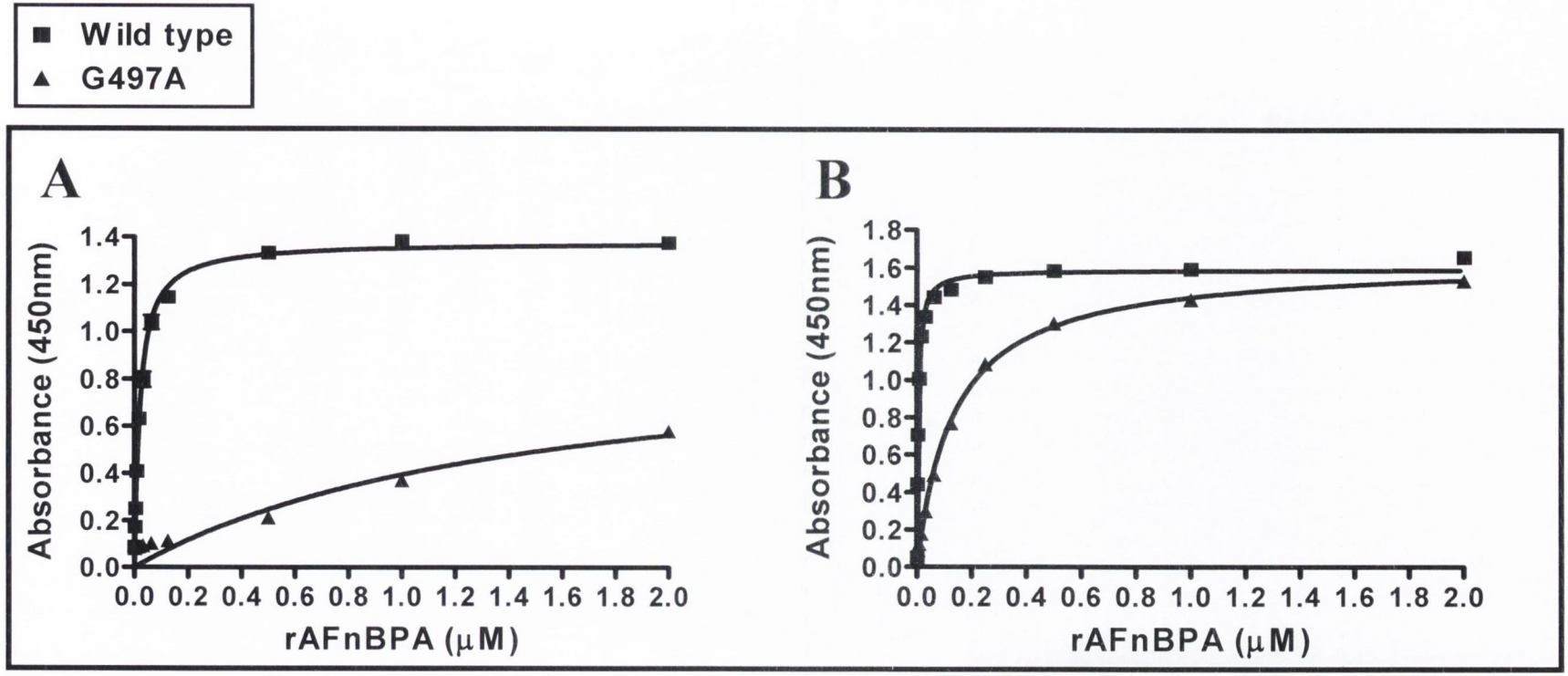

Figure 4.25 Binding of recombinant proteins rAFnBPA$_{37\text{-}511}$ wt and rAFnBPA$_{37\text{-}511}$ G497A to immobilised human elastin and fibrinogen

Microtiter wells were coated with 10 μg/ml human elastin (A) or fibrinogen (B) and increasing concentrations of rAFnBPA proteins were added for 1 hr. Bound protein was detected with polyclonal anti-rAFnBPA antibodies, HRP-conjugated goat anti-rabbit antibodies followed by TMB substrate. Data points represent the mean of triplicate wells and this figure is representative of three independent experiments.

of FnBPA and determine if it also affected elastin binding. From the structural model created with FnBPA and fibrinogen, L498 is some distance from the fibrinogen ligand (Figure 4.26) and potential contact points between the two are difficult to see. Conversion of this leucine to alanine causes a significant decrease in affinity for both elastin and fibrinogen (Figure 4.27). It must be remembered that the structural model of FnBPA created in this study is in the apo form and conformational changes are likely to occur upon binding of fibrinogen. The importance of this residue may lie in its potential contact with the C-terminal valine residue of the fibrinogen γ chain or in its potential role in covering the ligand bound hydrophobic trench during the latching mechanism.

4.2.7.9 Binding of rAFnBPA$_{37\text{-}511}$ N304A/F306A to immobilised elastin and fibrinogen

The residues that caused the most severe loss in ligand binding (N304 and F306) were combined in a double amino acid substitution to yield rAFnBPA$_{37\text{-}511}$ N304A/F306A. These residues are in the equivalent position to Pro336 and Tyr338 of ClfA, respectively, which were shown to have an important role in fibrinogen binding (Deivanayagam *et al.*, 2002). The double mutant created in FnBPA mimics the ClfA PY protein that was shown to be defective in binding fibrinogen when expressed on the surface of *S. aureus* and *L. lactis* (Loughman *et al.*, 2005). Due to the location of the side chains of N304 and F306 as described in Sections 4.2.6.3 and 4.2.6.4 above (Figure 4.28), it was expected that this recombinant protein would be defective in ligand binding. The protein was tested in ELISA assays and was unable to bind to immobilised elastin and fibrinogen (Figure 4.29). No detectable binding to either ligand was observed. This demonstrates the crucial role that these residues have in binding both ligands and further emphasizes the possibility that elastin binds to FnBPA in a similar manner to fibrinogen.

4.2.7.10 Binding of rAFnBPA$_{37\text{-}511}$ T354A/N356G to immobilised elastin and fibrinogen

With the Chimera molecular modelling software package it was possible to identify residues of FnBPA that are located within 3 Å of the fibrinogen ligand. Amino acids highlighted by this method were H254, S257*, T258, A259, R260*, K261, F306, T354*, N356, S363, V365, Y402, A415*, T417, F423, V454 and H456 (those residues marked with an asterisk are deemed to be within 2 Å of fibrinogen). Some of these residues were altered to alanine by Quikchange. Two double mutants, rAFnBPA$_{37\text{-}511}$ T354A/N456G and rAFnBPA$_{37\text{-}511}$ A415G/T417A were constructed. The first of these proteins contains alterations to residues

adjacent to F355 and K357 investigated above. As the side chains of alternate residues of a β-strand point in opposite directions, the side chains of T354 and N356 point in towards the ligand-occupied space and could potentially be involved in contacting the penultimate D410 residue of the fibrinogen γ chain (Figure 4.30). The recombinant protein rAFnPBA$_{37\text{-}511}$ T354A/N356G was shown to have a significant reduction in binding to immobilised elastin but not to fibrinogen (Figure 4.31). This is the only variant protein that was defective in binding to fibrinogen but not to elastin.

4.2.7.11 Binding of rAFnBPA$_{37\text{-}511}$ A415G/T417A to immobilised elastin and fibrinogen

The other alteration proposed by Chimera was substitution of two residues located at the opposite end of the hydrophobic trench. According to the FnBPA molecular model, these residues are positioned in a random coil situated between β-strands D and D' of subdomain N3. The side chains of A415 and T417 point in towards the ligand-occupied space and may form contact points with G404 and K406, respectively, of the fibrinogen γ chain peptide (Figure 4.32). This protein was tested in ELISA assays for binding to immobilised elastin and fibrinogen and was found to show a significant reduction in the binding to both ligands (Figure 4.33).

In conclusion it can be noted that substitution of residues located along the hydrophobic trench of rAFnBPA caused various defects in ligand binding (Table 4.1). The effects of alterations to the affinity of recombinant FnBPA for fibrinogen and elastin fell into four categories (i) no significant reduction in fibrinogen or elastin binding (G222A), (ii) small reductions in fibrinogen binding and greater, more significant reductions in elastin binding (T354A/N356G), (iii) barely significant reductions in affinity for fibrinogen with no significance in the reduction to elastin binding (F355A, K357A) and (iv) significant reductions in binding to both ligands (R224A, N304A, F306A, G497A, L498A, N304A/F306A and A415G/T417A). The affinities of all proteins for immobilised elastin and fibrinogen is summarised in Table 4.1. It is noteworthy that the residues that line the base of the trench between N2 and N3 all fall into the last class which strongly supports the notion that both fibrinogen and elastin bind to the same region. Alterations in residues comprising the β-strand that lines the upper part of the trench have less severe effects (T354, F355, N356, K357) although T354A/N356G does significantly effect elastin binding. F355 and K357 are not predicted to be in close contact with fibrinogen so the reductions in binding might be indirect due to a localized alteration in conformation. The alanine-substitution experiments are

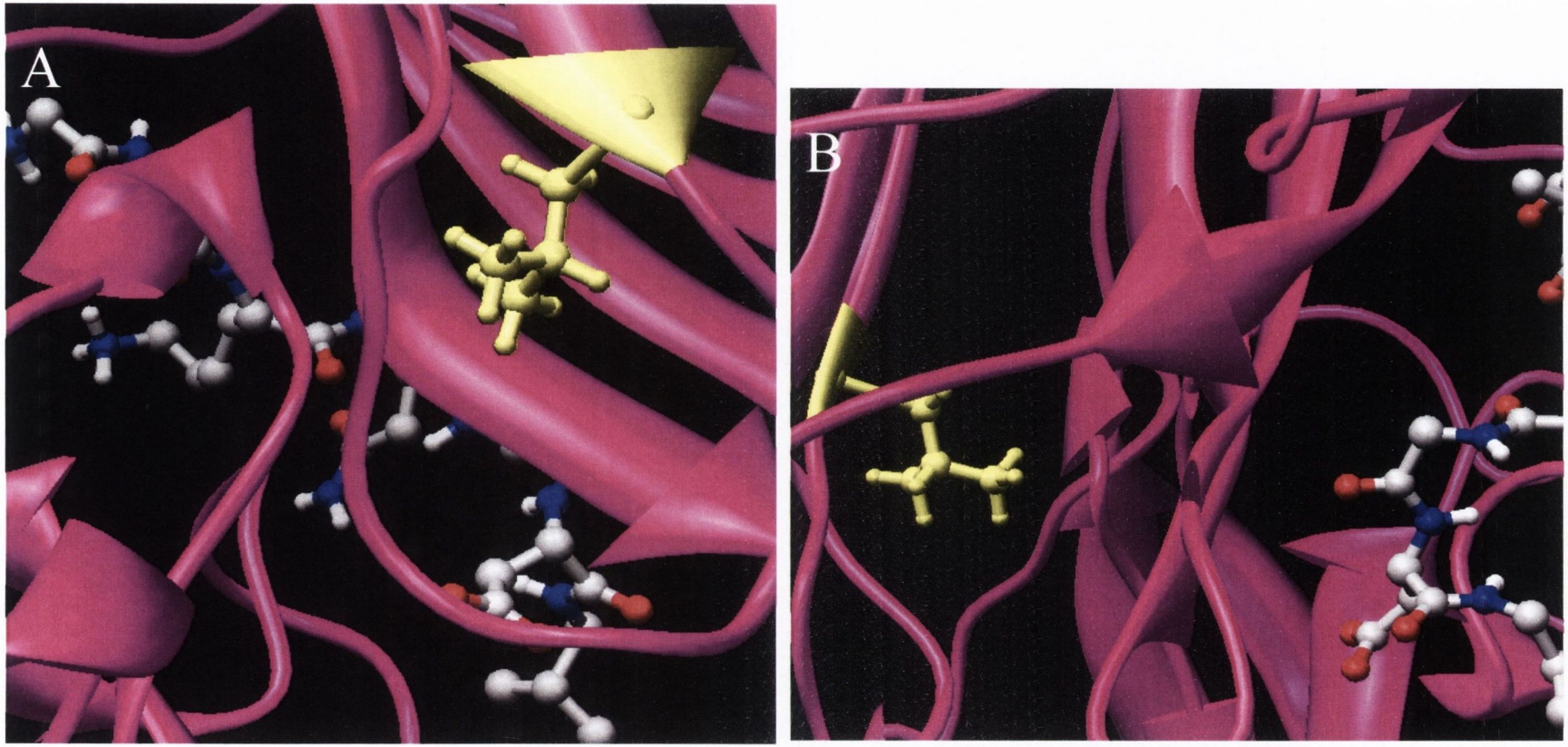

Figure 4.26 Position of the L498A substitution in rAFnBPA

Enlarged section of the structural model of the N2N3 subdomains of FnBPA with the fibrinogen peptide (ball and stick format) docked into the hydrophobic trench. Residue L498 is highlighted in yellow with the side chain visible in ball and stick format. A shows the hydrophobic trench from the viewing position of Figure 4.2 while B is a tilted view of the model to show the proximity of L498 to the fibrinogen ligand.

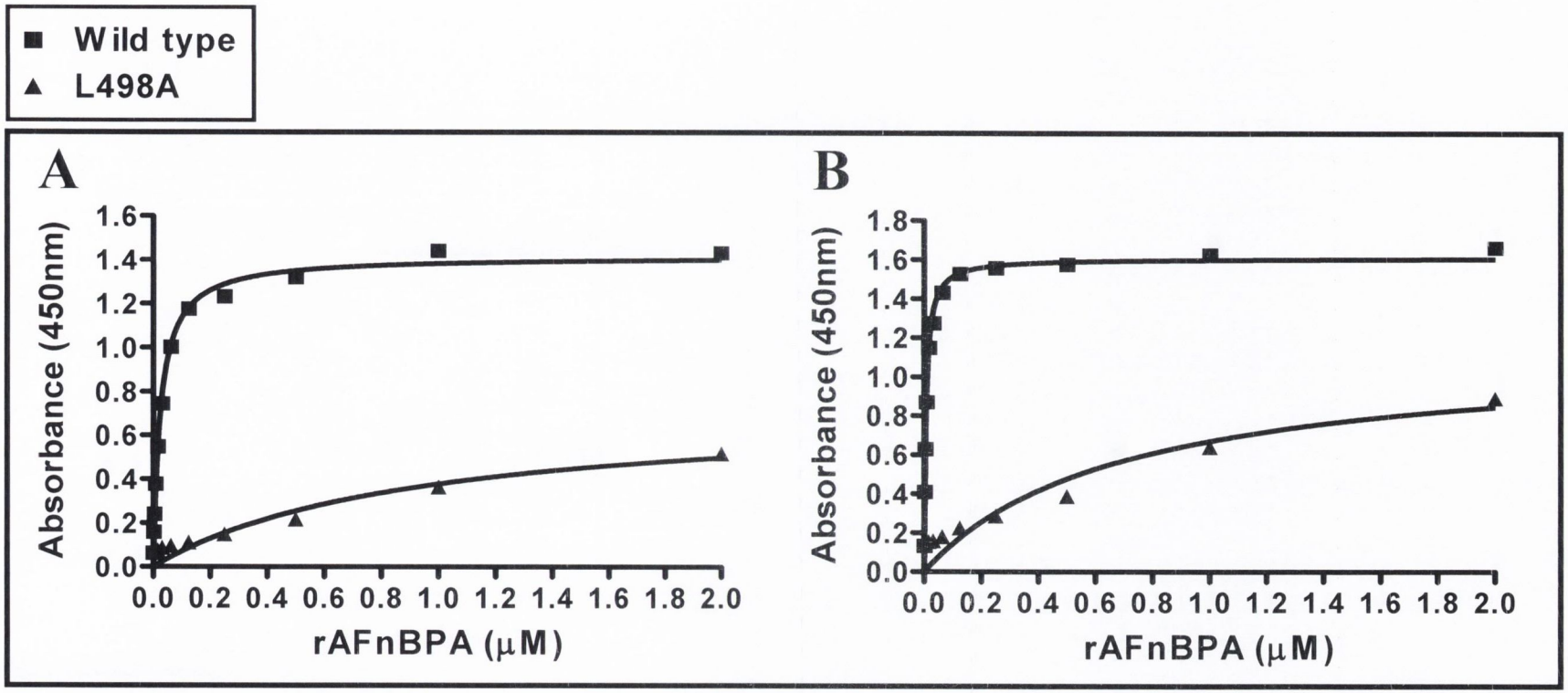

Figure 4.27 Binding of recombinant proteins rAFnBPA$_{37\text{-}511}$ wt and rAFnBPA$_{37\text{-}511}$ L498A to immobilised human elastin and fibrinogen

Microtiter wells were coated with 10 μg/ml human elastin (A) or fibrinogen (B) and increasing concentrations of rAFnBPA proteins were added for 1 h. Bound protein was detected with polyclonal anti-rAFnBPA antibodies, HRP-conjugated goat anti-rabbit antibodies followed by TMB substrate. Data points represent the mean of triplicate wells and this figure is representative of three independent experiments.

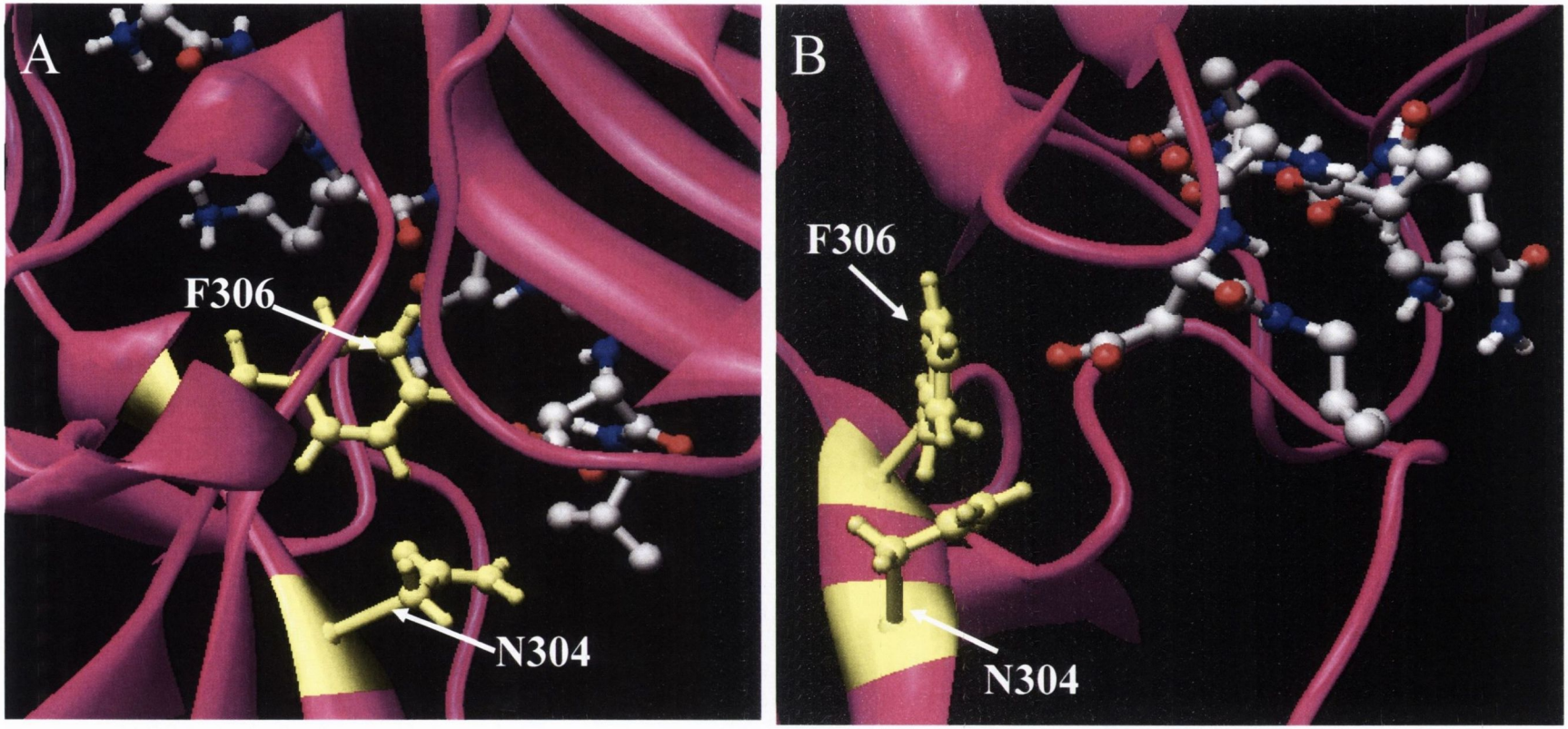

Figure 4.28 Position of the N304A/F306A substitutions in rAFnBPA

Enlarged section of the structural model of the N2N3 subdomains of FnBPA with the fibrinogen peptide (ball and stick format) docked into the hydrophobic trench. Residues N304 and F306 are highlighted in yellow with the side chains of both visible in ball and stick format. A shows the hydrophobic trench from the viewing position of Figure 4.2 while B is a tilted view of the model to show the proximity of N304/F306 to the fibrinogen ligand.

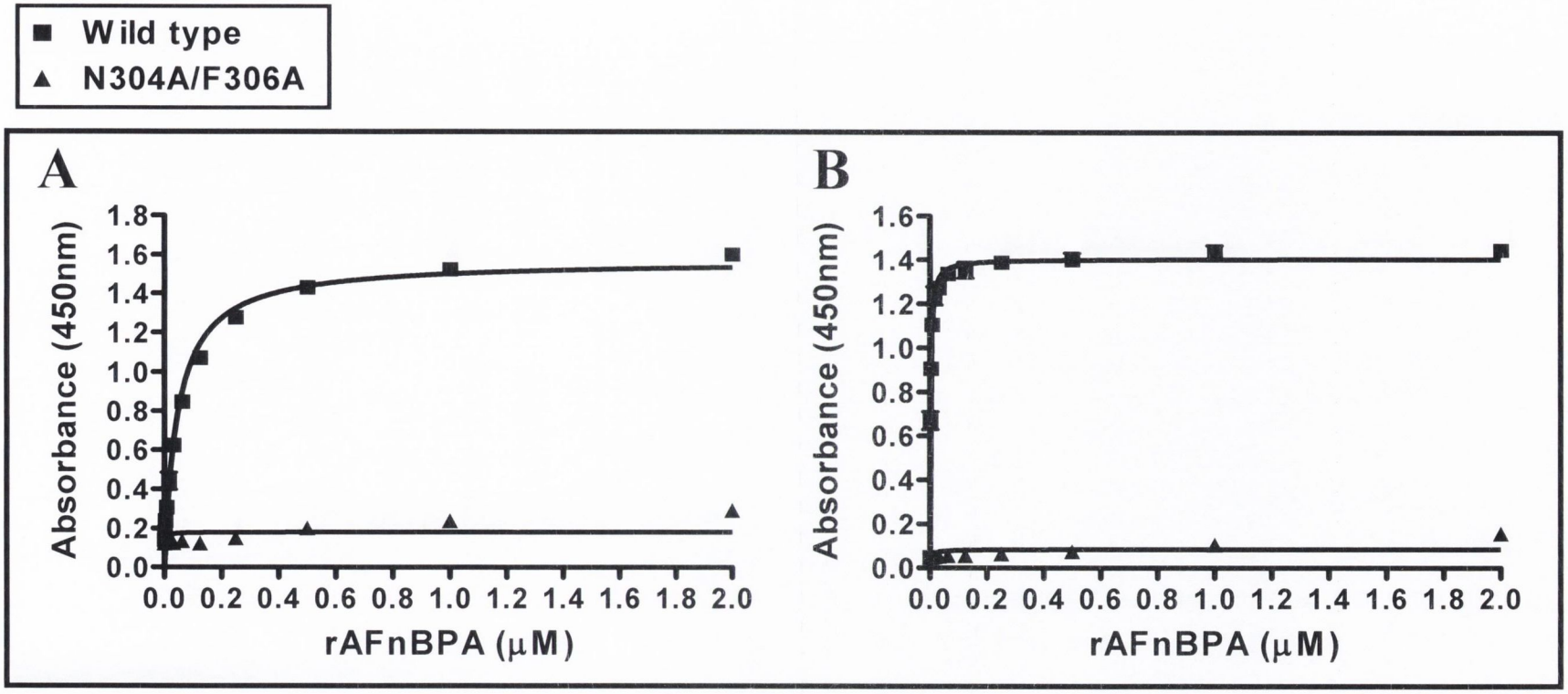

Figure 4.29 Binding of recombinant proteins rAFnBPA$_{37\text{-}511}$ wt and rAFnBPA$_{37\text{-}511}$ N304A/F306A to immobilised human elastin and fibrinogen

Microtiter wells were coated with 10 μg/ml human elastin (A) or fibrinogen (B) and increasing concentrations of rAFnBPA proteins were added for 1 h. Bound protein was detected with polyclonal anti-rAFnBPA antibodies, HRP-conjugated goat anti-rabbit antibodies followed by TMB substrate. Data points represent the mean of triplicate wells and this figure is representative of three independent experiments.

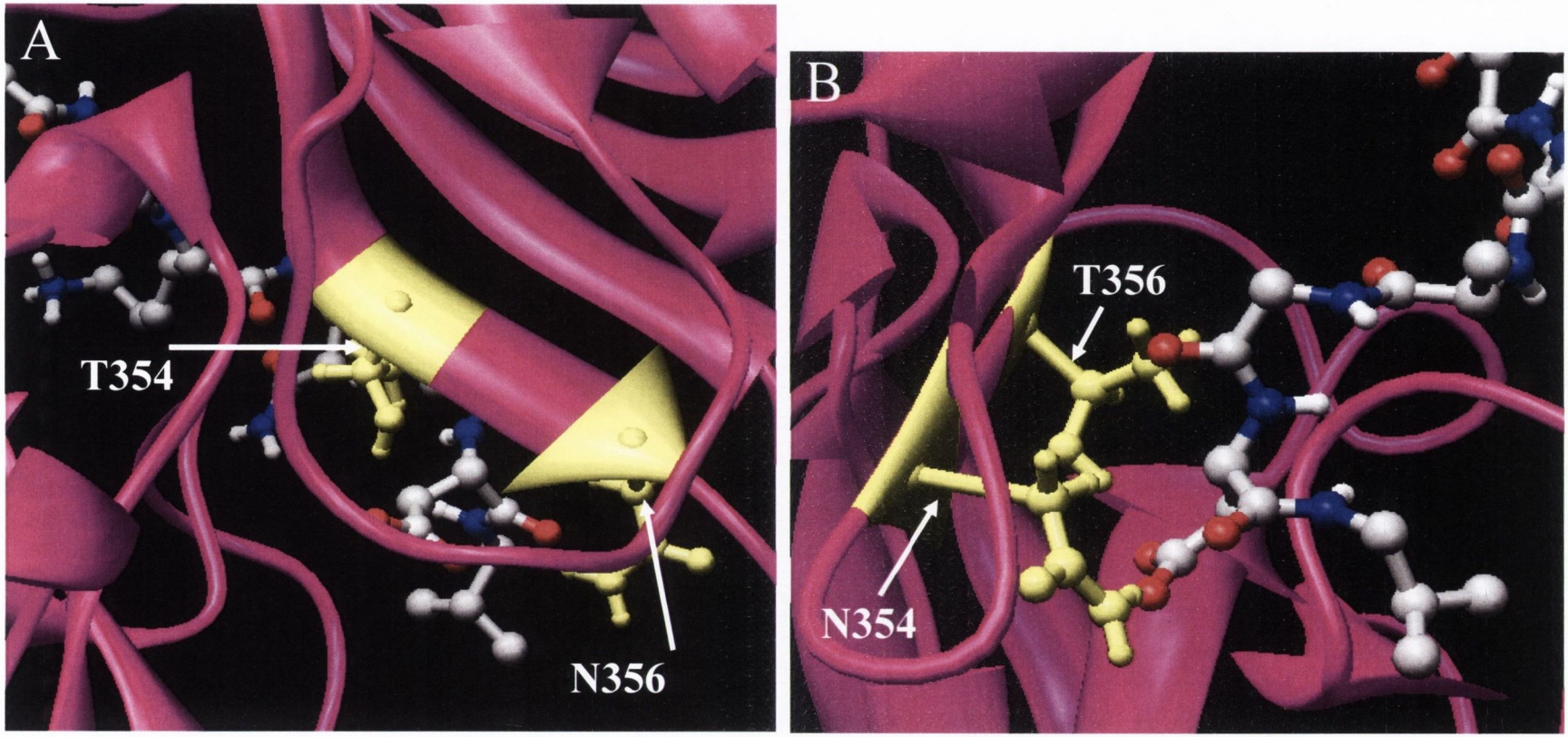

Figure 4.30 Position of the T354A/N356G substitutions in rAFnBPA

Enlarged section of the structural model of the N2N3 subdomains of FnBPA with the fibrinogen peptide (ball and stick format) docked into the hydrophobic trench. Residues T354 and N356 are highlighted in yellow with the side chains of both visible in ball and stick format. A shows the hydrophobic trench from the viewing position of Figure 4.2 while B is a tilted view of the model to show the proximity of T354/N356 to the fibrinogen ligand.

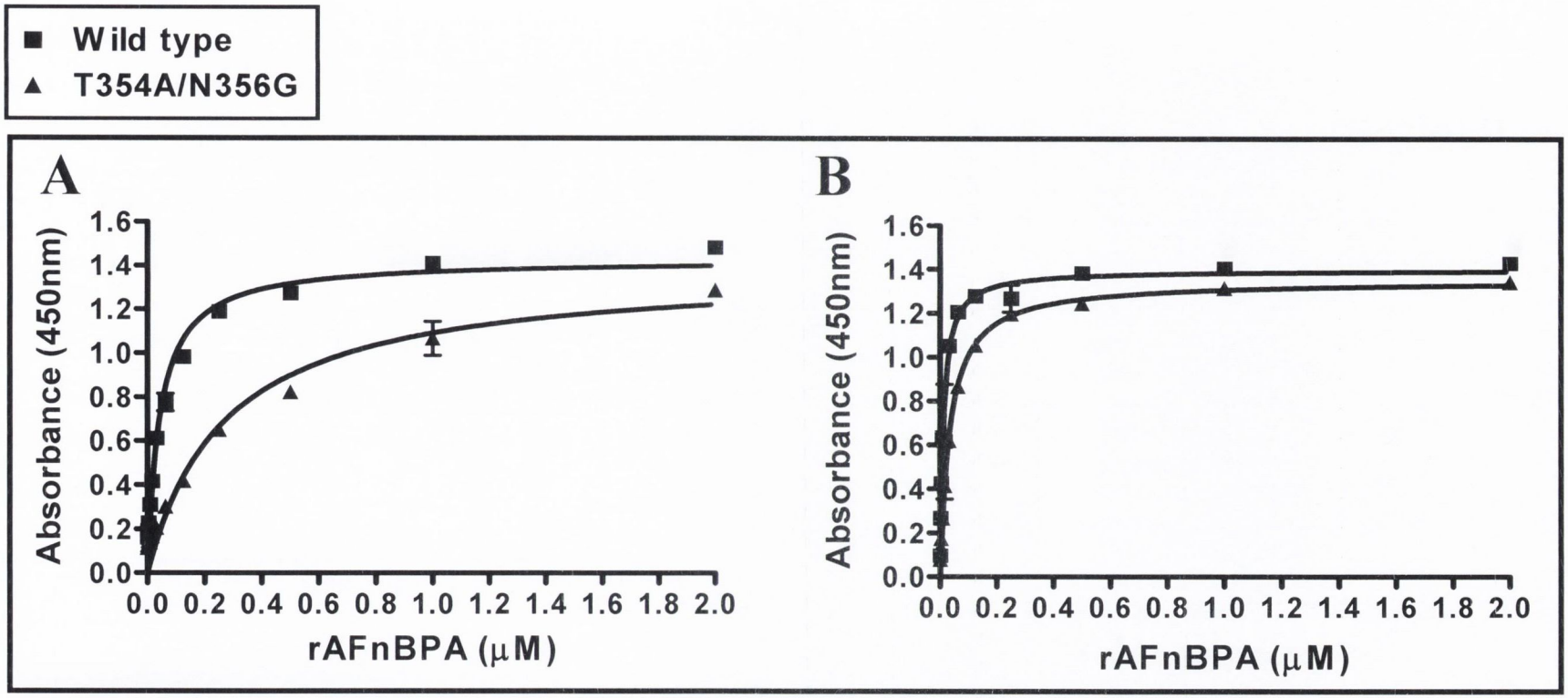

Figure 4.31 Binding of recombinant proteins rAFnBPA$_{37-511}$ wt and rAFnBPA$_{37-511}$ T354A/N356G to immobilised human elastin and fibrinogen

Microtiter wells were coated with 10 μg/ml human elastin (A) or fibrinogen (B) and increasing concentrations of rAFnBPA proteins were added for 1 h. Bound protein was detected with polyclonal anti-rAFnBPA antibodies, HRP-conjugated goat anti-rabbit antibodies followed by TMB substrate. Data points represent the mean of triplicate wells and this figure is representative of three independent experiments.

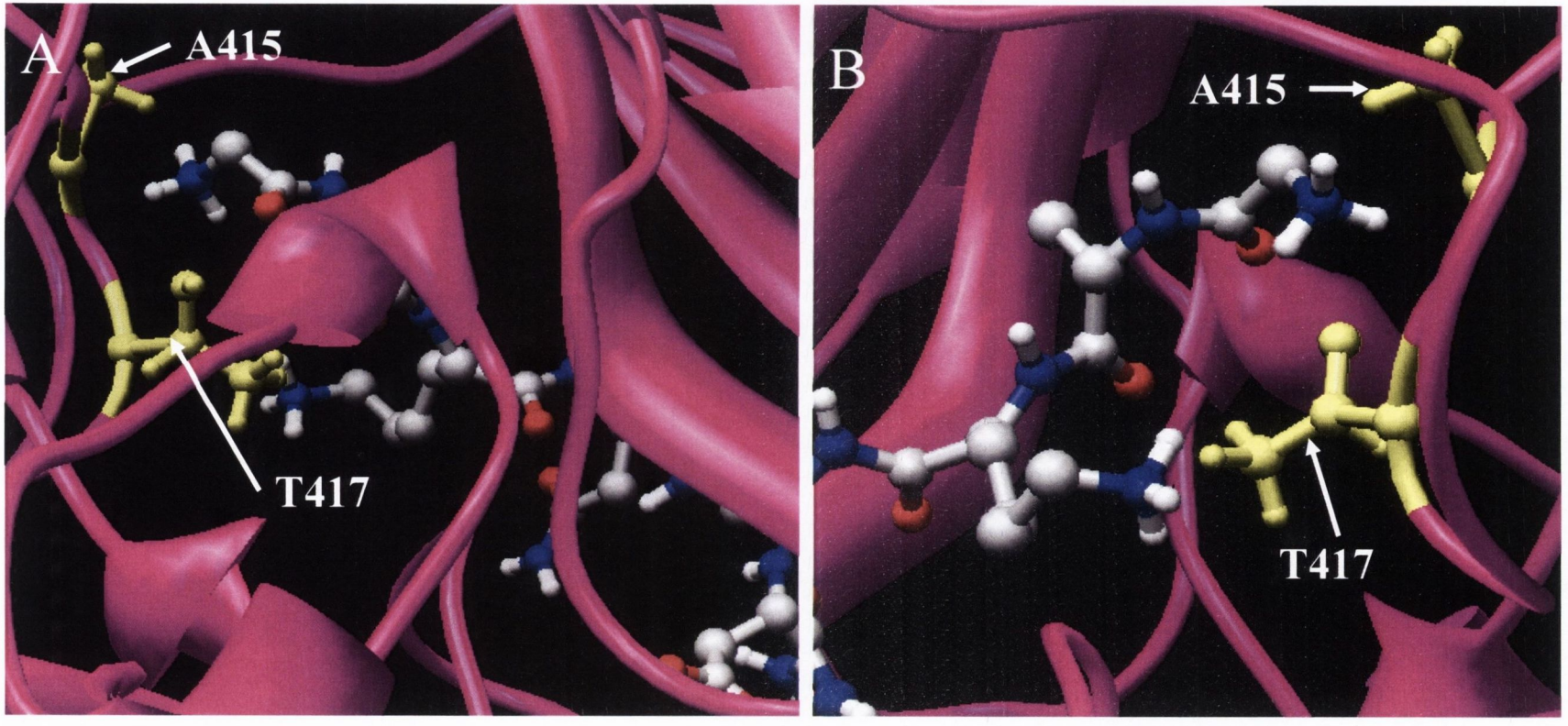

Figure 4.32 Position of the A415G/T417A substitutions in rAFnBPA

Enlarged section of the structural model of the N2N3 subdomains of FnBPA with the fibrinogen peptide (ball and stick format) docked into the hydrophobic trench. Residues A415 and T417 are highlighted in yellow with the side chains of both visible in ball and stick format. A shows the hydrophobic trench from the viewing position of Figure 4.2 while B is a tilted view of the model to show the proximity of G222A to the fibrinogen ligand.

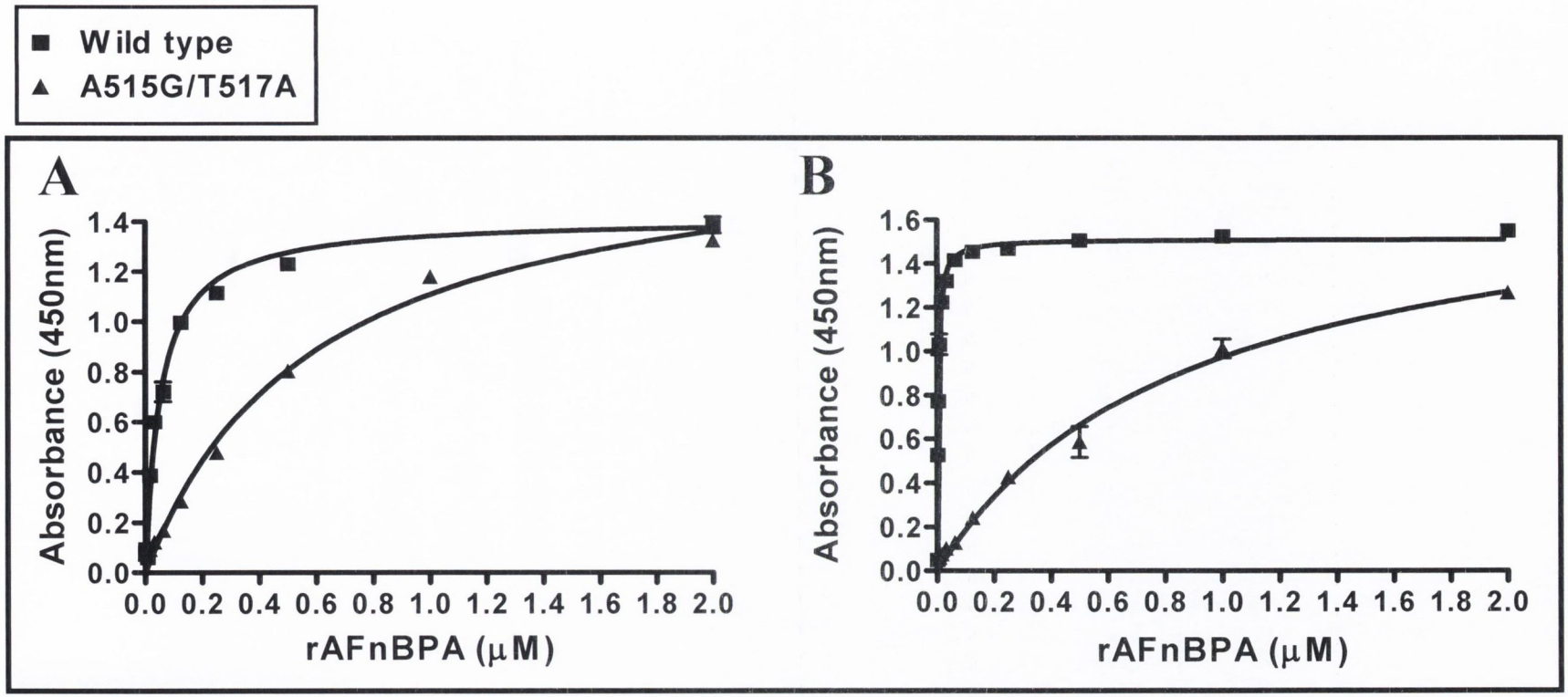

Figure 4.33 Binding of recombinant proteins rAFnBPA$_{37\text{-}511}$ wt and rAFnBPA$_{37\text{-}511}$ A415G/T417A to immobilised human elastin and fibrinogen

Microtiter wells were coated with 10 μg/ml human elastin (A) or fibrinogen (B) and increasing concentrations of rAFnBPA proteins were added for 1 h. Bound protein was detected with polyclonal anti-rAFnBPA antibodies, HRP-conjugated goat anti-rabbit antibodies followed by TMB substrate. Data points represent the mean of triplicate wells and this figure is representative of three independent experiments.

	Elastin			Fibrinogen		
Protein $rAFnBPA_{37-511}$	**Half maximum binding ± SD (nM)**	**p-value**	**Significant difference**	**Half maximum binding ± SD (nM)**	**p-value**	**Significant difference**
Wild type	45.6 ± 10.3	-	-	4.7 ± 1.8	-	-
G222A	288.4 ± 145.6	0.05	No	6.7 ± 1.5	0.2134	No
R224A	520.6 ± 169	0.0083	Yes	120.9 ± 28.8	0.0022	Yes
N304A	1227.3 ± 106	0.0001	Yes	1032.2 ± 112	0.0001	Yes
F306A	ND*	ND	Yes	ND*	ND	Yes
F355A	236.6 ± 182.5	0.145	No	412.5 ± 205	0.0033	Yes
K357A	68.1 ± 27.1	0.25	No	31.5 ± 14.2	0.0316	Yes
G497A	665.7 ± 156.4	0.0024	Yes	82.2 ± 14.9	0.0009	Yes
L498A	959 ± 368.5	0.0127	Yes	682.1 ± 96	0.0003	Yes
N304A/F306A	ND*	ND	Yes	ND*	ND	Yes
T354A/N356G	370.1 ± 97.6	0.0046	Yes	23.9 ± 14.9	0.091	No
A415G/T417A	630.2 ± 227.5	0.0113	Yes	697.7 ± 266.7	0.0108	Yes

Table 4.1. The relative affinities of $rAFnBPA_{37-511}$ wt and 11 amino acid-substituted proteins for immobilised elastin and fibrinogen

The affinities of proteins were assessed by ELISA-type binding assays to immobilised elastin and fibrinogen. Half maximum binding values given are approximated by the GraphPad Prism software package and are averaged over at least 3 experiments. The p-value given represents the statistical significant difference between the bindings for each variant compared to that of $rAFnBPA_{37-511}$ wild type to each ligand. *ND = no detectable binding observed.

consistent with elastin and fibrinogen binding to the same region of FnBPA with some differences in amino acids in FnBPA that are involved in contacts with the two ligands. It is particularly notable that residues N304 and F306 that are in equivalent positions to two crucial residues in ClfA (P336, Y338) show the greatest defects in ligand-binding when converted to alanine. In order to study the effects of these two residues in a more relevant setting, it was decided to construct a plasmid which would express FnBPA N304A/F306A on the surface of bacterial cells.

4.2.8 Construction and analysis of *L. lactis* NZ9800 (pNZ8037 FnBPA-NF)

To study the ligand-binding ability of bacteria expressing the N304A and F306A altered protein, plasmid pNZ8037 FnBPA (Section 3.2.3) was isolated from *L. lactis* cells and subjected to Quikchange site-directed mutagenesis using the same primers as those used to generate pQE30 rAFnBPA$_{37\text{-}511}$ N304A/F306A (Figure 4.34). The resulting PCR product was digested with *Dpn*1 to remove wild-type methylated DNA and the remaining plasmid was transformed into electrocompetent *L. lactis* NZ9800 cells. Subsequent clones were verified by sequencing of the pNZ8037 plasmid DNA as well as by whole cell dot immunoblotting with anti-rAFnBPA antibodies. Equal drops of doubling dilutions of cultures of *L. lactis* wild-type as well as *L. lactis* pNZ8037 FnBPA and *L. lactis* pNZ8037 FnBPA NF were spotted onto the surface of a nitrocellulose membrane and blocked with skimmed milk. Anti-rAFnBPA antibodies were added and detected with goat anti-rabbit HRP conjugated antibodies. This dot immunoblot shows strong expression of FnBPA from pNZ8037 FnBPA and only a slight (2-4 fold) decrease in FnBPA-NF production (Figure 4.35). No cross reactivity was observed with cells from *L. lactis* wild-type. *L. lactis* pNZ8037 FnBPA-NF was then tested for its ability to bind to immobilised elastin and fibrinogen. This strain was unable to adhere to either ligand. In contrast, *L. lactis* pNZ8037 FnBPA promoted strong adherence to elastin and fibrinogen (Figure 4.36). This is conclusive evidence that N304 and F306 are crucial amino acids for binding of cell surface FnBPA to both elastin and fibrinogen. As a further demonstration of the functional integrity of the surface-expressed FnBPA proteins, *L. lactis* pNZ8037 FnBPA and *L. lactis* pNZ8037 FnBPA-NF were both capable of binding immobilised fibronectin in a similar and dose-dependent manner (Figure 4.37). This confirms the ligand-binding results obtained with recombinant rAFnBPA$_{37\text{-}511}$ N304A/F306A protein.

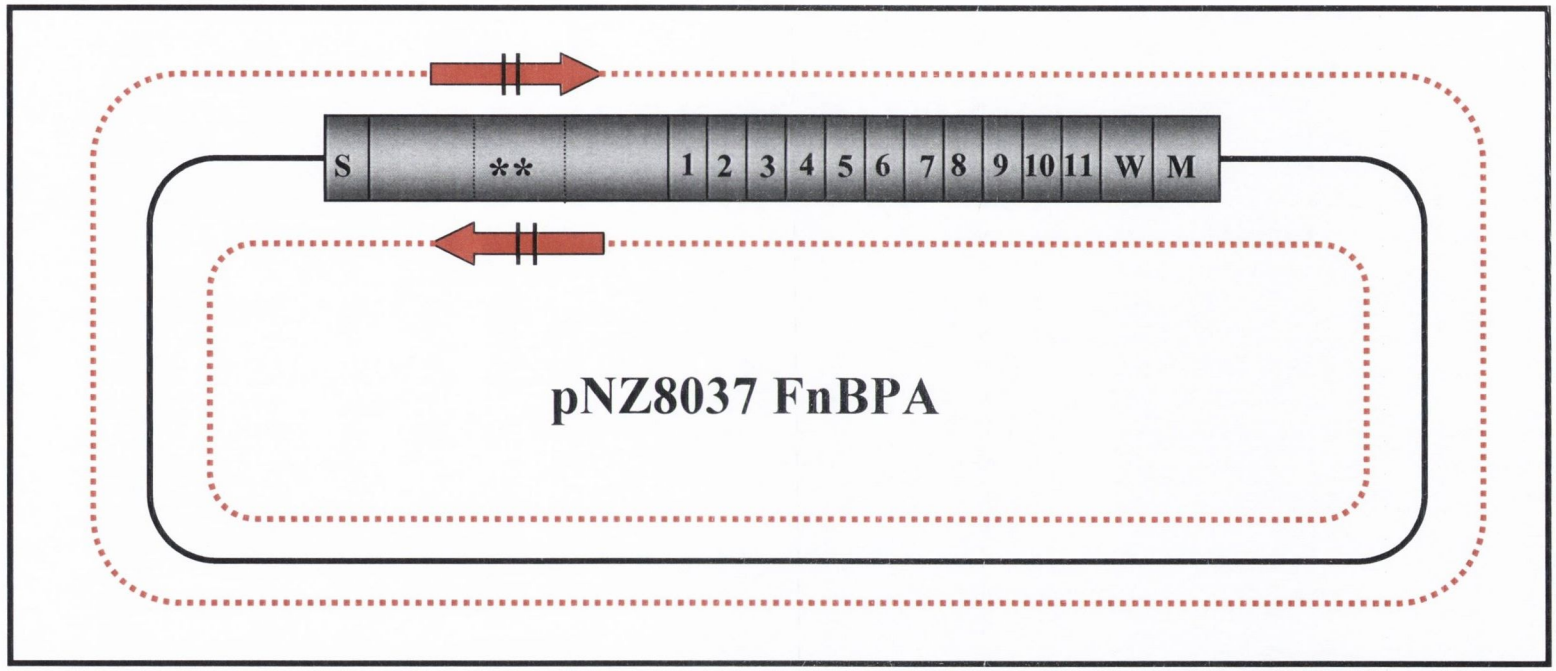

Figure 4.34 Site-directed mutangenesis of plasmid pNZ8037 FnBPA

Primers incorporating codon changes N304A and F306A were used in a PCR reaction to amplify pNZ8037FnBPA. Parental wild-type DNA was digested with *Dpn*I and the remaining mutated plasmid electroporated into *L. lactis*, yielding strain NZ9800 pNZ8037 FnBPA-NF.

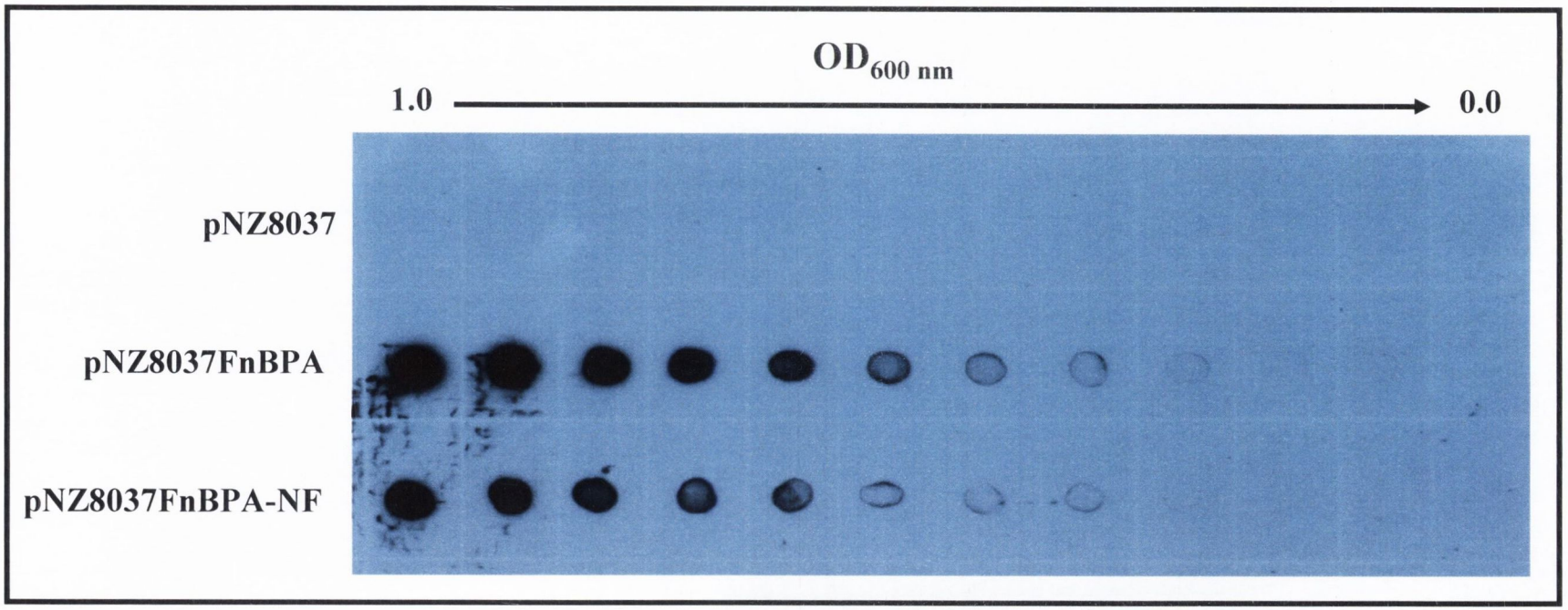

Figure 4.35 FnBPA and FnBPA-NF expression at the same concentration of nisin

L. lactis NZ9800 (pNZ8037) and *L. lactis* NZ9800 expressing FnBPA (pNZ8037FnBPA) and FnBPA-NF (pNZ8037FnBPA-NF) were grown for 16 h in the presence of 1.6 ng/ml nisin. Cells were washed twice in PBS and suspended to OD_{600nm} of 1.0 in PBS. Serial dilutions were made in PBS in 96-well microtitre dishes. 5 µl of each dilution was applied to nitrocellulose membranes and blocked in 10 % skimmed milk solution for 2 h. Membranes were then incubated with rabbit anti-FnBPA antibodies (1:1000) and goat anti-rabbit HRP-conjugated antibodies (1:2000). Membranes were developed by chemiluminescence and exposed to autoradiographic film.

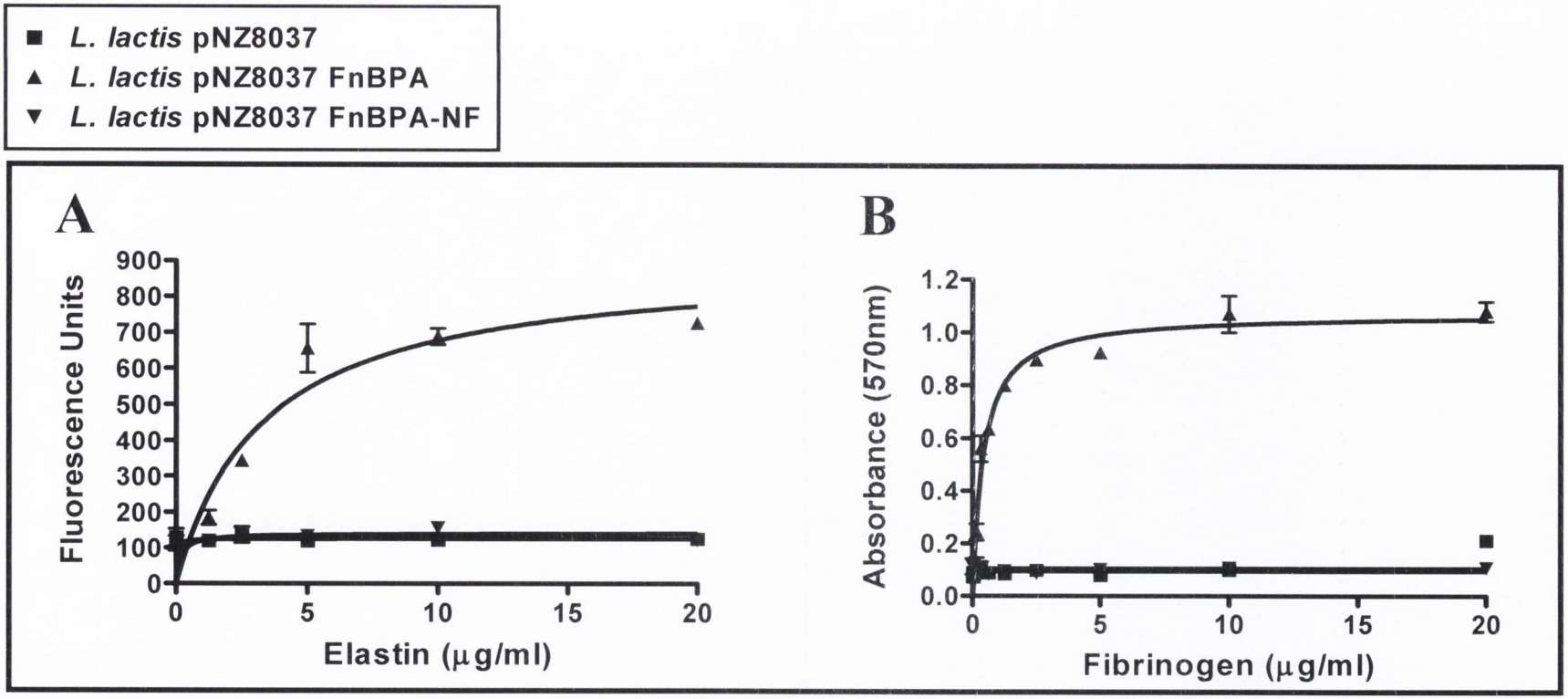

Figure 4.36 Adherence of *L. lactis* strains expressing full-length FnBPA or FnBPA-NF to immobilised elastin and fibrinogen

L. lactis NZ9800 (pNZ8037) and *L. lactis* NZ9800 expressing FnBPA and FnBPA-NF were grown for 16 h in the presence of 1.6 ng/ml nisin. Washed cells (OD_{600nm}=1.0) were added to ligand coated wells for 1.5 h. Bacterial adherence to elastin (A) was measured using SYTO-13 fluorescent dye while fibrinogen adherence (B) was measured by staining with crystal violet. This figure is representative of three independent experiments.

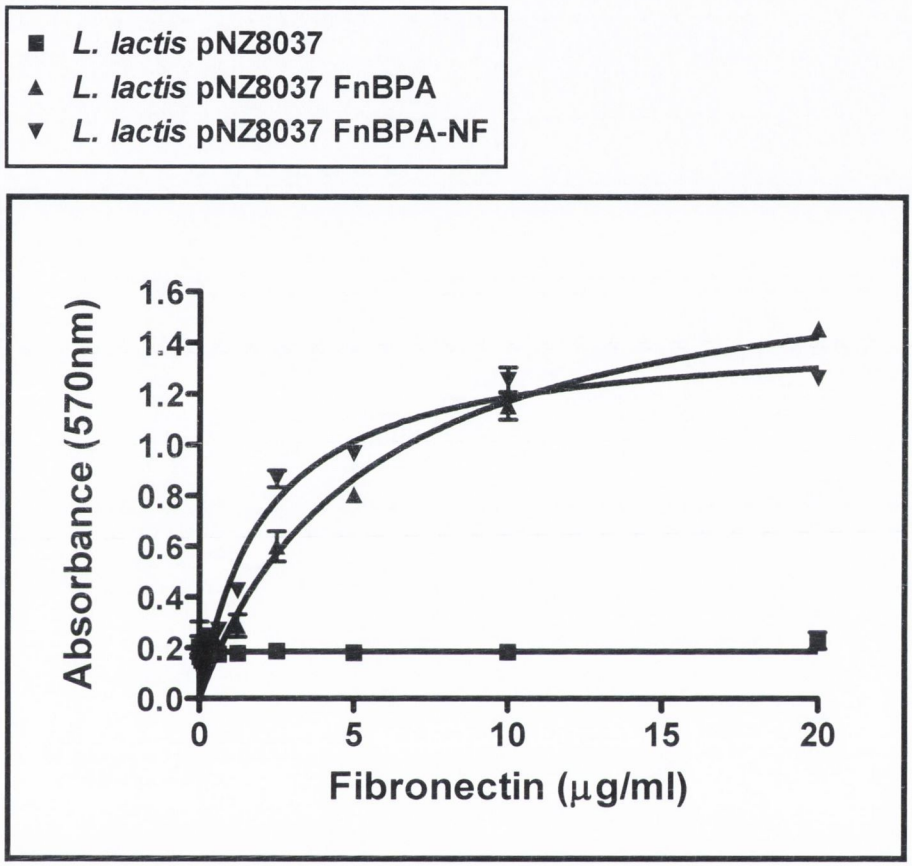

Figure 4.37 Adherence of *L. lactis* strains expressing full-length FnBPA or FnBPA-NF to immobilised fibronectin

L. lactis NZ9800 (pNZ8037) and *L. lactis* NZ9800 expressing FnBPA and FnBPA-NF were grown for 16 h in the presence of 1.6ng/ml nisin. Washed cells (OD_{600nm}=1.0) were added to fibronectin-coated wells for 1.5 h. Bacterial adherence was measured by staining with crystal violet. This figure is representative of three independent experiments.

4.3 Discussion

The structure of the N2N3 subdomains of staphylococcal surface proteins has greatly increased our understanding of the mechanism by which these proteins can bind to peptide ligands. A dynamic mechanism has been proposed called dock, lock and latch whereby the fibrinogen ligand docks into a hydrophobic trench situated between N2 and N3 of region A, the flexible linker region or hinge folds over the fibrinogen peptide making vital contact points to lock the ligand in place. Upon locking, the C-terminal β-strand of N3 slots into place between the D and E β-strands of N2, forming the latching mechanism. Sequence analysis has shown that structurally related ligand-binding regions from the A domains of staphylococcal MSCRAMMs share conserved motifs (Ponnuraj *et al.*, 2003). These motifs include a potential latching sequence along with a conserved TYTFTDYVD-like motif situated around the cleft of N2, into which the latching peptide binds. It has been proposed therefore, that the dock, lock and latch mechanism of ligand binding is a common theme among such proteins.

A 3D molecular model of the N2N3 domains of FnBPA, based on the known structure of ClfA, facilitated analysis of the binding sites for elastin and fibrinogen. C-terminal truncation techniques as well as expression of N2 and N3 alone suggested that the overall IgG fold of this region was crucial for the binding of both elastin and fibrinogen. In order to further define the precise ligand-binding sites in FnBPA, amino acid substitutions were created in the putative ligand-binding trench located between N2 and N3. Residues were chosen due to their proximity to the docked fibrinogen ligand (T354, N356, A415 and T417 are all within 3 Å of the ligand) or due to their being in the equivalent positions as residues previously tested for their importance in fibrinogen binding by ClfA (Deivanayagam *et al.*, 2002). Thus, G222, R224, N304, F306, F355 and K357 of FnBPA are all in the equivalent positions as A254, Y256, P336, Y338, I387 and K389 of ClfA, respectively. Residues G497 and L498 are in the equivalent positions as E526 and V527 of ClfA, found by another study to be important in fibrinogen binding by ClfA (Hartford *et al.*, 2001).

Mutations in pQE30 rAFnBPA$_{37\text{-}511}$ were constructed and variant recombinant proteins were expressed, purified and shown to be intact by Coomassie staining after SDS-PAGE analysis. Proteins had the same affinity for anti-rAFnBPA$_{37\text{-}511}$ antibodies. Monoclonal antibodies were also tested for their reactivity against the variant rAFnBPA$_{37\text{-}511}$ proteins. Variations in protein concentrations might be responsible for the observed variation of the affinity of monoclonal antibodies for some of the recombinant proteins. Monoclonal antibody

8G3 had very poor reactivity with rAFnBPA$_{37\text{-}511}$ F335A, K357A and T354A/N356G, all of which lie adjacent to each other along β-strand A of N3 of FnBPA. It is tempting to speculate that this area contains at least part of the epitope to which monoclonal antibody 8G3 binds. Circular dichroism spectroscopy of proteins that caused the most severe defects to ligand binding showed that rAFnBPA$_{37\text{-}511}$ N304A was similar in structure to that of rAFnBPA$_{37\text{-}511}$ wild-type. rAFnBPA$_{37\text{-}511}$ F306A showed a slight deviation from the wild-type spectrum in the 210-200 nm range. This protein however reacted strongly with several monoclonal antibodies and behaved in a similar manner to other variant rAFnBPA proteins in Biacore assays (Section 6.2.1.3). The CD spectrum of rAFnBPA$_{37\text{-}511}$ N304A/F306A (which contains the F306A substitution) was equivalent to that of the wild-type protein, indicating that the F306A substitution is unlikely to cause a major change in 3D structure.

The substitutions of rAFnBPA caused a variety of defects in ligand binding (Table 4.1). The reduction in ligand binding can be correlated with the position of residues in the hydrophobic trench and the predicted interactions of their side chains with residues of the fibrinogen peptide. In some cases, estimates of half maximum binding values were accompanied with large standard deviations indicating the variability of this technique. This has been found in previous studies however with the important P336 substitution of ClfA having an estimated K_D of 64.2 ± 55.6 μM (Deivanayagam *et al.*, 2002). The substitution of rAFnBPA that caused the least effect on ligand binding is G222A. This glycine residue likely does not have a role to play in ligand binding whereas the substitution of another glycine, G497 does have an effect on ligand binding. This can be explained by G222 being located within the hydrophobic trench but it is some distance from the fibrinogen ligand. In contrast, G497 is located at the junction of the penultimate β-strand of N3 and the loop segment that most likely acts as the hinge that traverses the hydrophobic trench when the ligand is bound. Glycine is known for its ability to induce bends into a protein structure and this residue could have a role in bending the hinge region over the fibrinogen ligand. In a similar vein, the adjacent leucine residue L498 could have the same role as that ascribed to isoleucine 581 of SdrG. L498 might be important in repositioning the latching peptide during its conformational change to stabilize fibrinogen binding as occurs with I581 that is in a similar position in the ligand bound complex of SdrG (Ponnuraj *et al.*, 2003). I581 of SdrG is at the beginning of the flexible linker region and after docking of fibrinogen, a structural rearrangement at the C-terminus of the N2N3 domains begins with a deviation in the strand direction at I581. The effects of the remaining residues that were substituted can be viewed in relation to the

potential interactions of their side chains with residues of the docked fibrinogen ligand. According to the structural model, residue R224 is within 5 Å and residues N304 and F355 are within 4 Å of the fibrinogen ligand. In addition, residues N356, T417 and F306 are within 3 Å with residues T354 and A415 within 2 Å of the fibrinogen γ chain peptide. Of these, amino acids N304 and F306 were shown to be particularly important for binding both ligands and are predicted to be in close proximity to the side chain of D410 of fibrinogen. They are located in equivalent positions to the crucial residues P336 and Y338 of ClfA (Deivanayagam *et al.*, 2002; Loughman *et al.*, 2005). The substitution of either of these residues has the most dramatic effect on ligand binding. It is interesting to note, as with the substitution of some other residues, that one amino acid change can dramatically affect the binding to both fibrinogen and elastin. Along with inhibition studies carried out in Section 3.2.13, this is strong evidence that fibrinogen and elastin bind to similar or overlapping regions of FnBPA. A model of the proposed mechanism of ligand binding by rAFnBPA is shown in Figure 4.38. In this model, fibrinogen enters the hydrophobic trench and causes a conformational change in the C-terminal region of N3. It is possible that residue G497 facilitates this change and it is hypothesized here that the adjacent L498 residue makes contact with the C-terminal valine residue of fibrinogen. In addition to this, residues lining the trench such as N304 and F306 are involved in vital interactions with the fibrinogen ligand. A substitution of these residues to alanine has drastic consequences on the binding of rAFnBPA to its ligands via the proposed dock-lock and latch mechanism.

Studies investigating the importance of amino acids in the fibrinogen γ chain peptide in binding to FnBPA are ongoing in the laboratory of Prof M. Hook, Texas A&M University. A panel of peptides in which each residue has been replaced by alanine is being tested for their affinities for recombinant rAFnBPA protein. In this way, it will be evident if the penultimate aspartate residue of the fibrinogen γ chain is crucial in binding FnBPA. As mentioned in Section 4.1, the native fibrinogen sequence is not the most optimal sequence for binding SdrG (Ponnuraj *et al.*, 2003). It is very interesting to note that the hydrophobic trench of ligand-binding surface proteins can accommodate peptides of different sequence. An example of such is the A domain of ClfB which binds to the α-chain of fibrinogen (Ni Eidhin *et al.*, 1998) and to the C-terminus of cytokeratin 10 (Walsh *et al.*, 2004). This is relevant to FnBPA, where both fibrinogen and elastin can bind to this region. This observation raises the question of sequence similarity between the two ligands. This is complicated by the nature of the elastin used in the ELISA assays which is a heterogeneous mixture of peptides (10 -50 kDa)

resulting from the digestion of human aortic elastin by hot oxalic acid which cleaves crosslinked elastin at hydrophilic sites. The digestion results in exposure of novel sites created by the fragmentation of the tropoelastin backbone whilst preserving the desmosine crosslinks. It is these free peptides that are likely to bind into the hydrophobic trench of FnBPA. The possibility of a range of different elastin peptides binding into the hydrophobic trench of rAFnBPA may explain cases whereby an alanine substitution of a single amino acid causes a defect in fibrinogen binding but less of an effect in elastin binding as is the case with F355A, K357A and L498A. It is not possible however to detect any sequence identity between the fibrinogen γ chain peptide and the primary tropoelastin sequence.

The work carried out above with alanine-substituted recombinant proteins was tested further by introducing N304A and F306A substitutions into the FnBPA protein expressed on the surface of *L. lactis*. Plasmid pNZ8037 FnBPA was subjected to site-directed mutagenesis using primers incorporating the N304A and F306A codon changes. Bacteria expressing the FnBPA-NF protein were unable to adhere to immobilised elastin or fibrinogen but retained the ability to bind to immobilised fibronectin in a manner similar to wild-type FnBPA-expressing bacteria. This supports the work undertaken with recombinant proteins and shows once again, the crucial role played by two amino acids in the binding of the full-length FnBPA protein to elastin and fibrinogen. This is further evidence that elastin and fibrinogen bind to FnBPA in a similar manner. The molecular model created in this study can be used to explain why N304 and F306 are involved in ligand binding and this lends support to the use of such molecular models in the understanding of the mechanisms by which staphylococcal MSCRAMMs bind to their ligands.

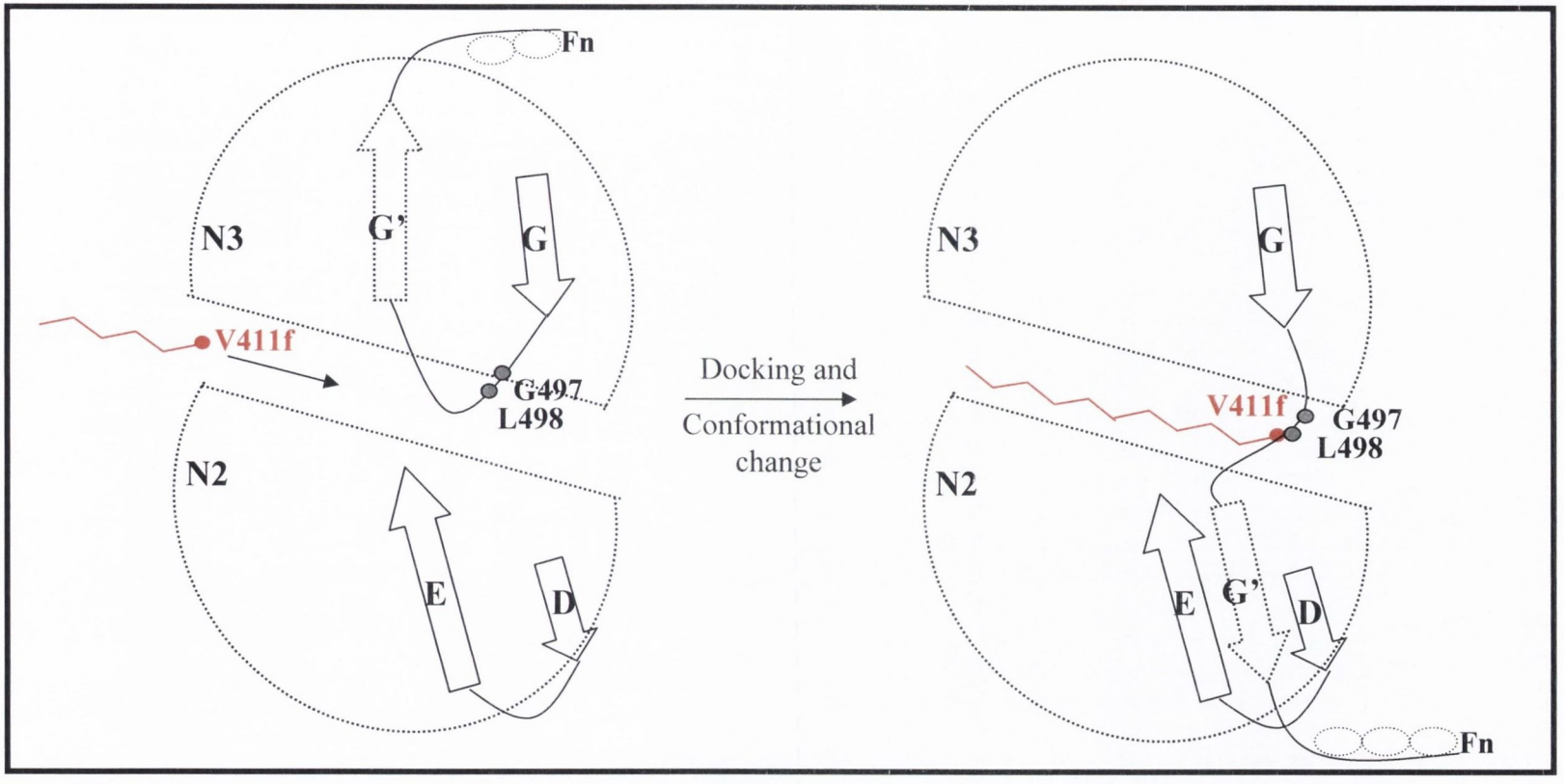

Figure 4.38 Proposed model of ligand binding for rAFnBPA

Upon docking of the fibrinogen γ chain peptide (red – with C-terminal valine residue labelled) into the hydrophobic trench situated between N2 and N3, a conformational change occurs at the C-terminus of N3 allowing the hinge region to traverse the ligand-occupied space. Residue G497 may aid in the bending of this loop region while L498 is predicted to contact the valine residue of fibrinogen in a similar manner to that of I581 of SdrG. The G' β-strand of N3 then locks the ligand in place by slotting in between β-strands D and E of N2.

Chapter 5

Sequence diversity of region A of FnPBA from *S. aureus* strains 8325-4 and P1

5.1 Introduction

An extensive and diverse array of ligand-binding proteins is displayed on the surface of *S. aureus* cells. These proteins have evolved to recognise distinct elements of the host extracellular matrix in an attempt to evade the host immune system and establish a focus of infection. Despite examples of functional redundancy, each protein targets specific ligands, the exact binding sites of which are still under investigation. The importance of ligand-binding surface proteins of *S. aureus* has been demonstrated in numerous studies. Their importance is highlighted by the fact that many of the genes encoding these proteins (e.g. *clfA* and *fnbA*) are present in almost all invasive isolates of *S. aureus* tested (Peacock *et al.*, 2002). A study on the diversity of *fnb* genes present in a large sample of clinical isolates showed that *fnbA* was present in all 163 strains with both *fnbA* and *fnbB* present in ~66% (Enright *et al.*, 2000), although the latter figure was as high as 91% in a study of MRSA isolates (Rice *et al.*, 2001a). However, the ability to adhere to immobilised fibronectin does not vary in relation to the number of *fnb* genes (Enright *et al.*, 2000) or the number of fibronectin-binding motifs within the FnBP molecule (Rice *et al.*, 2001a). This indicates that ligand binding is conserved despite sequence variation. The variation in fibronectin binding by different isolates of *S. aureus* was attributed to the transcriptional activity of the *agr* locus and to protease activity (Rice *et al.*, 2001a).

A more recent study investigated the divergence of 17 *S. aureus* genes in a collection of 60 *S. aureus* strains (Kuhn *et al.*, 2006). These genes included ten genes encoding surface proteins (*clfA*, *clfB*, *fnbA*, *fnbB*, *ebpS*, *map*, *sdrC*, *sdrD*, *sdrE* and *spa*) which were compared to seven housekeeping genes routinely used in multilocus sequencing typing (MLST) (*arcC*, *aroE*, *glpF*, *gmk*, *pta*, *tpi* and *yqiL*). The ten surface protein-encoding genes were divided into two groups, the core genes (*clfA*, *clfB*, *fnbA*, *map*, *sdrC* and *spa*) which were present in all strains and the accessory genes (*fnbB*, *ebpS*, *sdrD* and *sdrE*) which were not present in all strains. It had been noted previously that up to 22% of all genes in the *S. aureus* genome could be considered as accessory genes (Fitzgerald *et al.*, 2001). Thus there is a considerable portion of the *S. aureus* genome that is not to be essential and has contributed to genetic differences between strains. Both sets of surface protein-encoding genes were shown to have undergone a higher degree of nucleotide diversity compared to housekeeping genes. The amount of diversity varied, ranging from 2-fold for *spa* to greater than 10-fold for *fnbA* and *fnbB*. This study analysed a diverse collection of isolates, included the most variable class of

genes which were distributed over the whole chromosome and thus concluded that there is good evidence for predominantly clonal evolution of *S. aureus*.

An investigation into the A domains of FnBPA from the seven sequenced *S. aureus* genomes available in 2005 (8325-4, COL, MW2, MSSA476, N315, Mu50 and MRSA252) showed that significant diversity existed among strains from different multilocus sequence types (ST) (Loughman, 2005). As an example, the A domain of FnBPA from strain 8325-4 (ST 8) shares only 76.7% identity with the corresponding domain of strain MW2 (ST 1) and 75.3% identity with the FnBPA A domain of strain N315 (ST 5). There are two major clusters of *S. aureus* strains, group 1 (1a and 1b) and group 2 (Cooper and Feil, 2006). Of all the above sequenced strains, only strain MRSA252 belongs to group 1. This strain shared between 73-79% identity in the A domains of FnBPA with all the other sequenced strains. A similar diversity was also observed for the A domains of FnBPB from the sequenced *S. aureus* strains (Loughman, 2005). The 5' end of the *fnbA* gene from *S. aureus* strain P1 was previously cloned and sequenced. The deduced DNA and amino acid sequence was aligned with the sequences from 8325-4 and showed a similar diversity with an overall identity of 73.5% (Loughman, 2005). This indicates that the observed diversity between the A domains of FnBPA from *S. aureus* strains is common theme among different clonal lineages of *S. aureus*.

Observations in Chapter 3 that antibodies raised against the A domain of FnBPA from strain 8325-4 reacted poorly with *S. aureus* strain P1 (Figure 3.17) suggests that the sequence variation in the A domain of FnBPA has led to antigenic variation. Strain P1 has been used previously to study the fibrinogen- and elastin-binding activity of its surface-expressed FnBPs (Downer, 2002; Roche *et al.*, 2004). It has been shown that wild-type P1 cells adhere strongly to immobilised human elastin and that this was mediated by the FnBPs as a P1*fnbAfnbB* mutant was unable to adhere to elastin (Roche *et al.*, 2004). Strain P1 possesses both *fnbA* and *fnbB* genes but it is not known if both proteins are expressed in a functional manner on the cell surface. The defect in elastin binding by strain P1*fnbAfnbB* could be complemented by expression of FnBPA or FnBPB from a multicopy plasmid bearing the 8325-4 *fnbA* or *fnbB* gene sequences (Roche *et al.*, 2004). Following the Western blotting analysis discussed in Section 3.2.5, where a high concentration of anti-rAFnBPA (8325-4) antibodies were needed to detect full-length FnBPA present in the cell wall extracts of strain P1, tests were carried out with the complemented P1 strains expressing the 8325-4 FnBP proteins (Loughman, 2005). Human fibronectin was used in ligand affinity blotting to detect FnBPA and/or FnBPB (Figure

5.1). In addition, anti-rAFnBPA or anti-rAFnBPB antibodies showed a strong reaction with their cognate antigen present in either complemented strain but failed to react detectably with FnBPA expressed by wild-type P1.

The finding by Kuhn *et al.*, (2006) that *fnb* genes from diverse strains of *S. aureus* have undergone greater sequence divergence than other surface protein genes such as *clf*B and *clfA*, along with the FnBP sequence variation previously noted (Loughman, 2005) and the Western blotting studies described in Chapter 3, prompted the present investigation. It was hypothesised that the FnBPA protein can undergo a significant level of amino acid sequence diversification sufficient to achieve antigenic variation while still retaining ligand-binding functions. In this chapter, this hypothesis was tested for region A of FnBPA expressed by strain P1. Examination of the primary amino acid sequence showed a high level of sequence diversity, especially in subdomains N2 and N3. The recombinant protein was expressed and purified and shown to bind to elastin and fibrinogen. In addition, it reacted poorly with polyclonal antibodies raised against the A domain of FnBPA from strain 8325-4 and did not react with 5 monoclonal antibodies raised against the same protein including the important function blocking monoclonal, 7C5, the epitope of which is contained in the variant residues of the N2 subdomain of rAFnBPA from strain 8325-4.

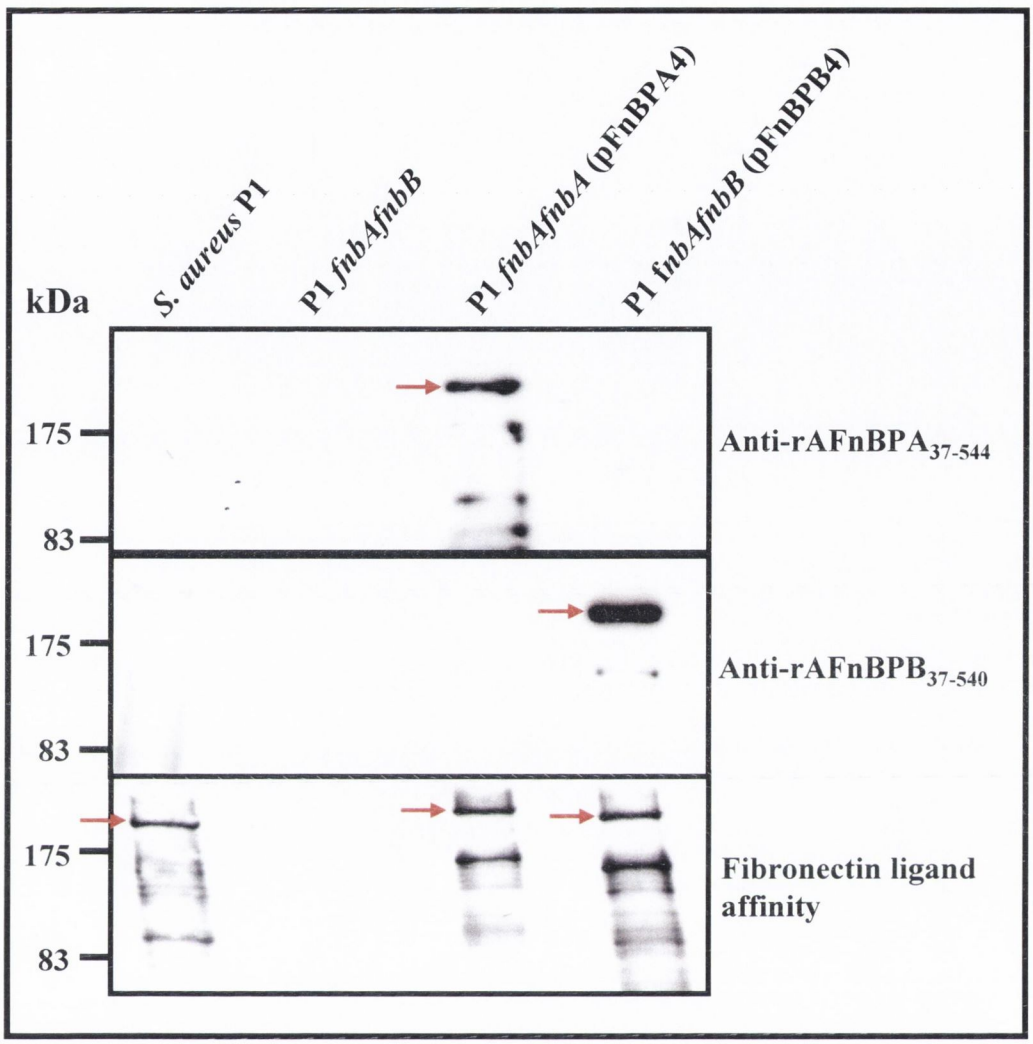

Figure 5.1 Detection of FnBPs in cell wall extracts of *S. aureus* P1 and its derivative strains

Cell wall proteins of *S. aureus* P1 wild-type, *S. aureus* P1 *fnbAfnbB*, *S. aureus* P1 *fnbAfnbB* (pFnBA4) and *S. aureus* P1 *fnbAfnbB* (pFnBB4) were separated on 7.5% acrylamide gels and electroblotted onto PVDF membranes. Membranes were probed with polyclonal antibodies recognising the A domains of FnBPA or FnBPB or a solution of biotinylated fibronectin (30 μg/ml). Bound probe was detected with the appropriate conjugated substrate and the membranes developed by chemiluminescence. Red arrows denote the position of full length FnBPs, with lower molecular weight bands reflecting breakdown products of the full-length protein. Taken from Loughman, 2005.

5.2 Results

5.2.1 Antibodies raised against FnBPA and FnBPB from *S. aureus* strain 8325-4 react poorly with strain P1

As described in Section 3.2.5, polyclonal antibodies were raised in rabbits against the region A recombinant proteins of FnBPA and FnBPB from strain 8325-4, rAFnBPA$_{37\text{-}544}$ and rAFnBPB$_{37\text{-}540}$, respectively. These antibodies were shown in dot immunoblotting analysis to exhibit an equally sensitive reaction to their cognate antigens with nanogram amounts of protein detected by both antibodies at high dilutions (Figure 3.16). These antibodies were also used to detect FnBP proteins released from cell wall extracts of *S. aureus* strain P1. A high concentration of anti-rAFnBP antibodies were needed to detect full-length FnBP released from the surface of P1 (Figure 3.17). Previous immunoblotting experiments with proteins released from whole cells showed that the FnBP proteins of P1 reacted weakly with polyclonal antibodies raised against rAFnBPA from strain 8325-4 (Loughman, 2005). However, P1 strains complemented with the pFnBPA4 or pFnBPB4 plasmids, expressing FnBPA or FnBPB of strain 8325-4, react well with the same antibodies (Figure 5.1). A report that *fnb* genes from diverse strains of *S. aureus* have undergone greater sequence divergence than other surface protein genes such as *clf*B and *clfA* (Kuhn *et al.*, 2006) prompted an examination of the A domain of FnBPA from strain P1. DNA coding for the entire A domain was amplified by PCR, sequenced and the amino acid sequence deduced and compared with that of strain 8325-4 (Figure 5.2). The overall amino acid sequence identity between the two proteins was ~73.5% but closer examination indicated that the greatest divergence occurred in domains N2 and N3. The N1 domains are 91.4% identical, the N2 domains are 78.3% identical while the N3 domains are only 59.2% identical (Figure 5.3). Taken together, these data indicate that *S. aureus* strain P1 produces a fibronectin-binding protein A domain that is antigenically distinct from that of strain 8325-4.

5.2.2 rAFnBPA$_{194\text{-}511}$ (P1) binding to immobilised elastin and fibrinogen

In order to assess the properties of region A of FnBPA encoded by strain P1, the DNA sequence encoding the precise ligand-binding domains of region A of FnBPA from strain P1 (rAFnBPA$_{194\text{-}511}$ (P1)) was cloned into the expression vector pQE30 using P1 genomic DNA and P1-specific primers designed using the deduced P1 *fnbA* DNA sequence. This plasmid

was transformed into *E. coli* cells and yielded recombinant protein which was purified by nickel affinity chromatography (Figure 5.4).

This protein was used in ELISA-type binding assays to determine its affinity for immobilised elastin and fibrinogen and to compare it to the equivalent protein from 8325-4. The P1 protein bound to both ligands. It had the same affinity for fibrinogen as the 8325-4 protein with a half maximum binding value of 4.43 ± 3.8 nM (Figure 5.5 B). Interestingly it had a significantly higher affinity for elastin (half maximum binding rAFnBPA$_{194\text{-}511}$ 8325-4 for elastin = 51.77 ± 12.2 nM; half maximum binding rAFnBPA$_{194\text{-}511}$ P1 for elastin = 4.12 ± 3.8 nM, p-value = 0.003) (Figure 5.5 A). This indicates that the recombinant protein is fully functional and that the residues spanning 194-511 are also sufficient for ligand binding in strain P1. The variant residues occurring in the N2N3 subdomains of FnBPA from strain P1 therefore does not hinder binding to either ligand and even increases the affinity of this protein for elastin.

5.2.3 Reactivity of rAFnBPA$_{194\text{-}511}$ (P1) to polyclonal anti-rAFnBPA antibodies

Region A of FnBPA from strain P1 bound to elastin and fibrinogen with the same or greater affinity than that of 8325-4. It was therefore hypothesized that the variant residues changed the surface epitopes of this protein rather than changing crucial ligand-binding residues in the hydrophobic trench region. The ability of rAFnBPA$_{194\text{-}511}$ (P1) to bind to polyclonal antibodies raised against the 8325-4 protein was tested. Firstly, increasing amounts of both recombinant proteins were immobilised on microtitre plates and probed with a 1:2000 dilution of polyclonal anti-rAFnBPA$_{37\text{-}544}$ (8325-4) antibodies. Paradoxically, it was suggested that the P1 protein had a higher affinity for the antibodies than the cognate 8325-4 antigen (Figure 5.6). This contradicted earlier Western blotting analysis with whole cell lysates of strain P1 (Section 5.2.1). The two methods differ however, with PVDF membrane-bound protein possibly behaving differently to plastic well-bound protein. The ability of the P1 protein to bind microtitre plates was compared to that of its 8325-4 counterpart. Equal amounts of the two proteins were coated onto the wells of the same plate and bound protein was detected using a monoclonal antibody directed against the 6xHis tag at the N-terminus of both proteins. rAFnBPA$_{194\text{-}511}$ (P1) coated the plastic with a far greater efficiency than that of the 8325-4 protein (Figure 5.7) thus explaining the apparent greater affinity of the polyclonal antibodies to the P1 protein and demonstrating that such comparisons cannot be made using ELISA assays.

Figure 5.2 Sequence alignment of region A of FnBPA from *S. aureus* strains 8325-4 and P1

Amino acid alignment of region A (37-514) of FnBPA from *S. aureus* strains 8325-4 and P1 showing the extent of residue diversity along subdomains N1 (black), N2 (red) and N3 (blue). * indicates an identical residue while : and . indicate conserved and semi-conserved mutations, respectively.

8325 37 ASEQKTTTVEENGNSATDNKTSETQTTATNVNHIEETQSYNATVTEQPSNATQVTTEEAP
P1 37 ASEQKTTTVEENGNSATDNKVSETQTTTTNVNTIDETQSYSATATEQPSNATQVTTEEAP
8325 97 KAVQAPQTAQPANIETVKEEVVKEEAKPQVKETTQSQDNSGDQRQVDLTPKKATQNQVAE
P1 97 KAVQAPQTAQPANVETVKEEVVKEEAKPQVKETTQSQDNSGDQRQVDLIPKKVTQNQVAE
8325 156 TQVEVAQPRTASESKPRVTRSADVAEAKEASNAKVETGTDVTSKVTVEIGSIEGHNNTNK
P1 156 TQVEVAQPRTVSESKPRVTRSADVVEAKDASDVTEVKGTDVTSKVTVESGSIEAPQG-NK
8325 217 VEPHAGQRAVLKYKLKFENGLHQGDYFDFTLSNNVNTHGVSTARKVPEIKNGSVVMATGE
P1 216 VEPHAGQRVVLKYKLKFEKGLHKGDYFDFTLSNNVNTYGVSTARKVPEIKNGSVVMATGQ
8325 276 VLEGGKIRYTFTNDIEDKVDVTAELEINLFIDPKTVQTNGNQTITSTLNEEQTSKELDVK
P1 275 LLGNGKIRYTFTDYIDYKVNVTADLEINLFIDPKTVQSNGQQTITSTLNDRETKNTLPIE
8325 336 YKDGIGNYYANLNGSIETFNKANNRFSHVAFIKPNNG-KTTSVTVTGTLMKGSNQNGNQP
P1 335 YNPGVSNSYANVNGSIETFDKGNNRFTHVAYIKPQNGHKSDSVSITGTLTQGSKANGNAP
8325 395 KVRIFEYLGNNEDIAKSVYANTTDTSKFKEVTSNMSGNLNLQNNGSYSLNIENLDKTYVV
P1 395 TVKVYEVLKDAKELPESVYANISDSTMFKDVTQEMKDKLKVENNGSYKLDIEKLEKSYVI
8325 455 HYDGEYLNGTDEVDFRTQMVGHPEQLYKYYYDR-GYTLTWDNGLVLYSNKANGNEKNGPI
P1 455 HYDGEYLSGSDQVNFRTHMFGYPEQQYKYYYTHLGYQLTWDNGLVLYSNKAKGDGTNGTI

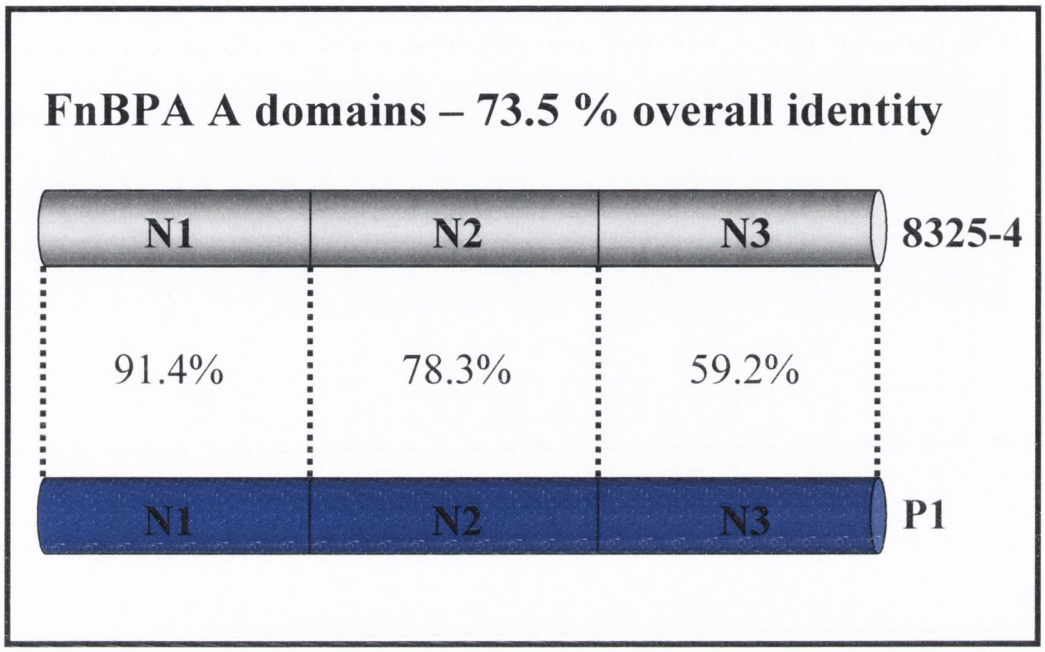

Figure 5.3 Diversity in the amino acid sequences of region A of FnBPA from *S. aureus* strains 8325-4 and P1

Genomic DNA of *S. aureus* P1 was used to clone the DNA sequence encoding region A of FnBPA. Sequenced DNA was translated into amino acid sequences and aligned with region A of FnBPA from strain 8325-4. The percentage amino acid indentities between the subdomains (N1, N2 and N3) are shown. Taken from Loughman, 2005.

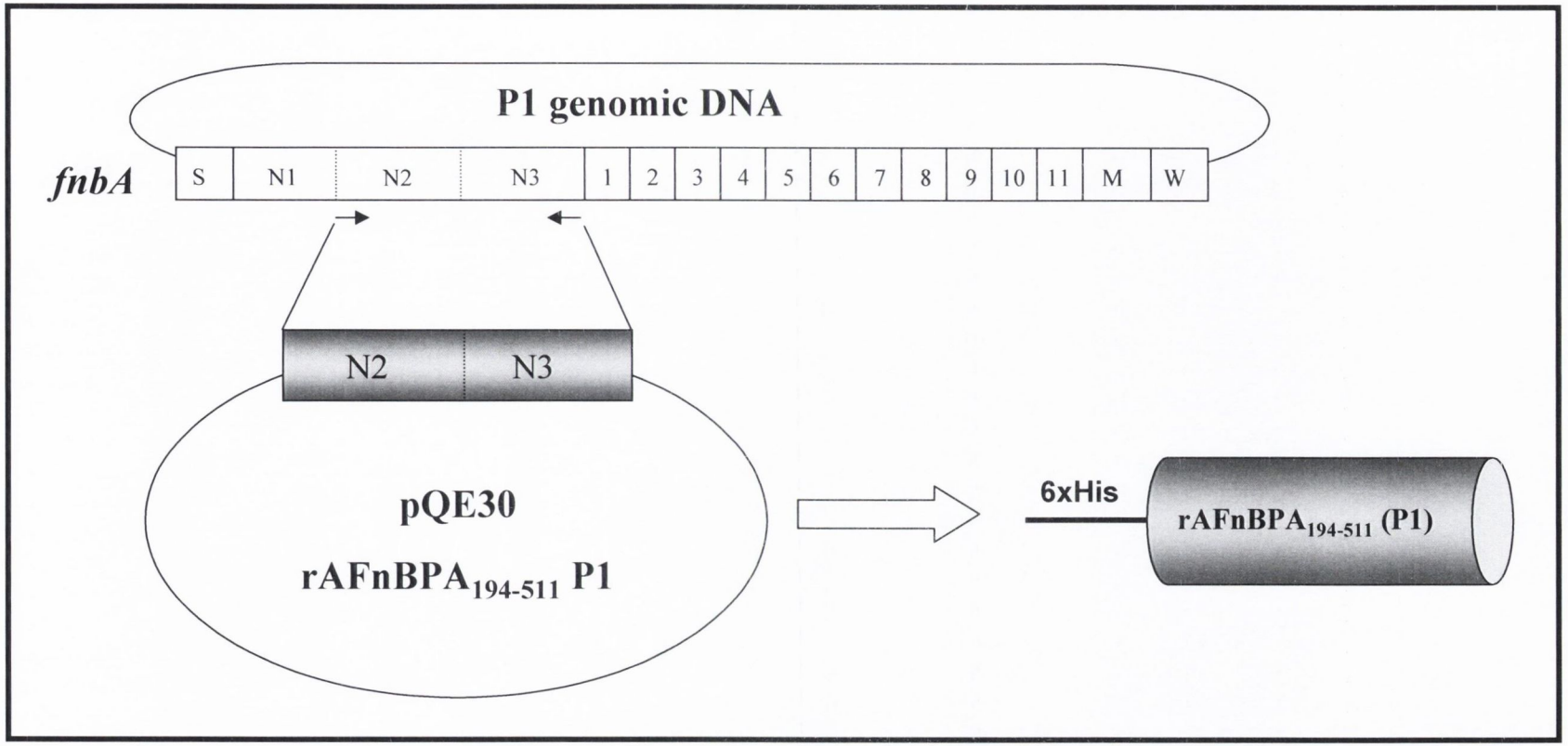

Figure 5.4 Cloning of rAFnBPA$_{194\text{-}511}$ (P1)

Genomic DNA from *S. aureus* strain P1 was used as template DNA in a PCR reaction to generate a fragment encoding the N2N3 subdomains of FnBPA which was cloned into pQE30. The resulting plasmid was transformed into *E. coli* and recombinant protein purified by nickel affinity and anion exchange chromatography, producing protein rAFnBPA$_{194\text{-}511}$ (P1).

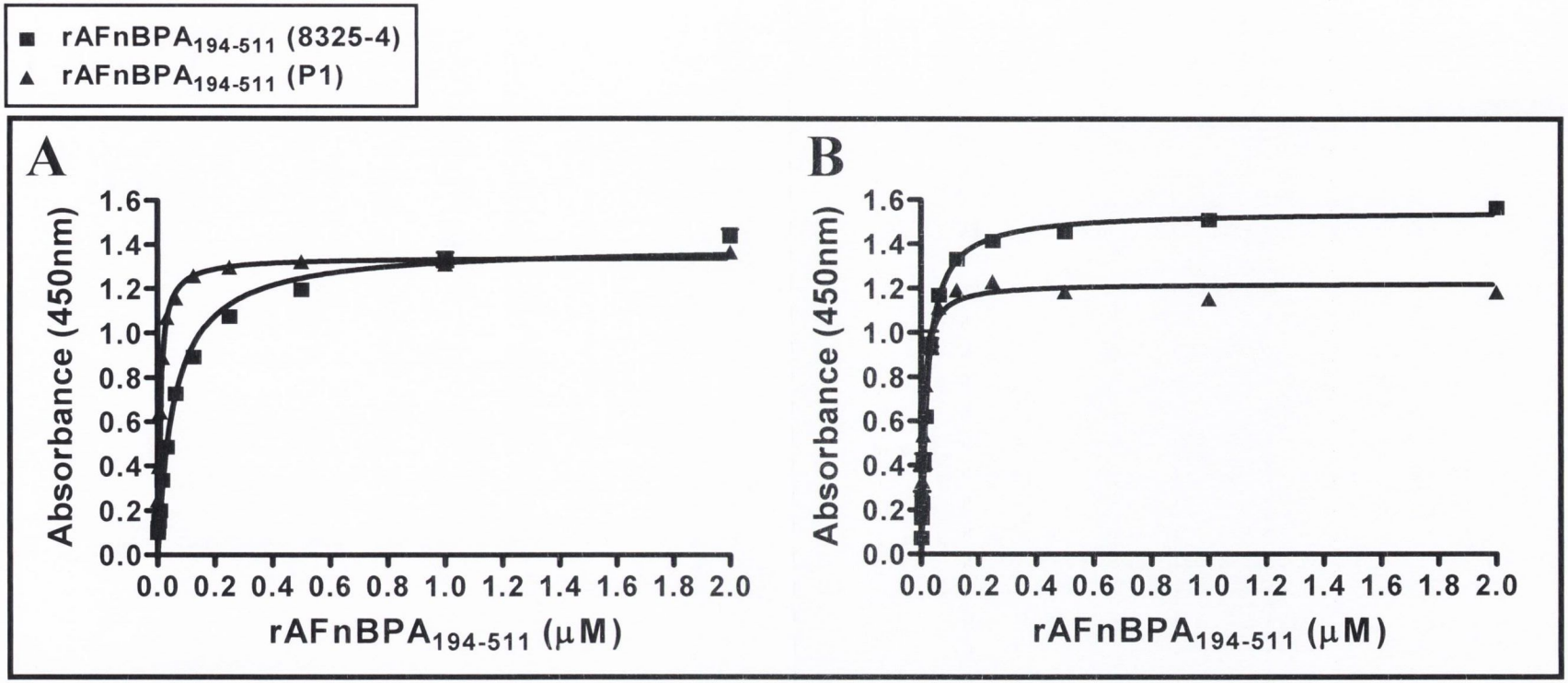

Figure 5.5 Binding of rAFnBPA$_{194-511}$ (8325-4) and rAFnBPA$_{194-511}$ (P1) to immobilised elastin and fibrinogen

Microtitre plates were coated with 10 μg/ml human aortic elastin (A) or fibrinogen (B) and increasing concentrations of rAFnBPA$_{194-511}$ (8325-4) and rAFnBPA$_{194-511}$ (P1) were added. Bound protein was detected with polyclonal anti-rAFnBPA antibodies and goat anti-rabbit HRP-conjugated antibodies. Data points represent the mean of triplicate wells and this figure is representative of three independent experiments.

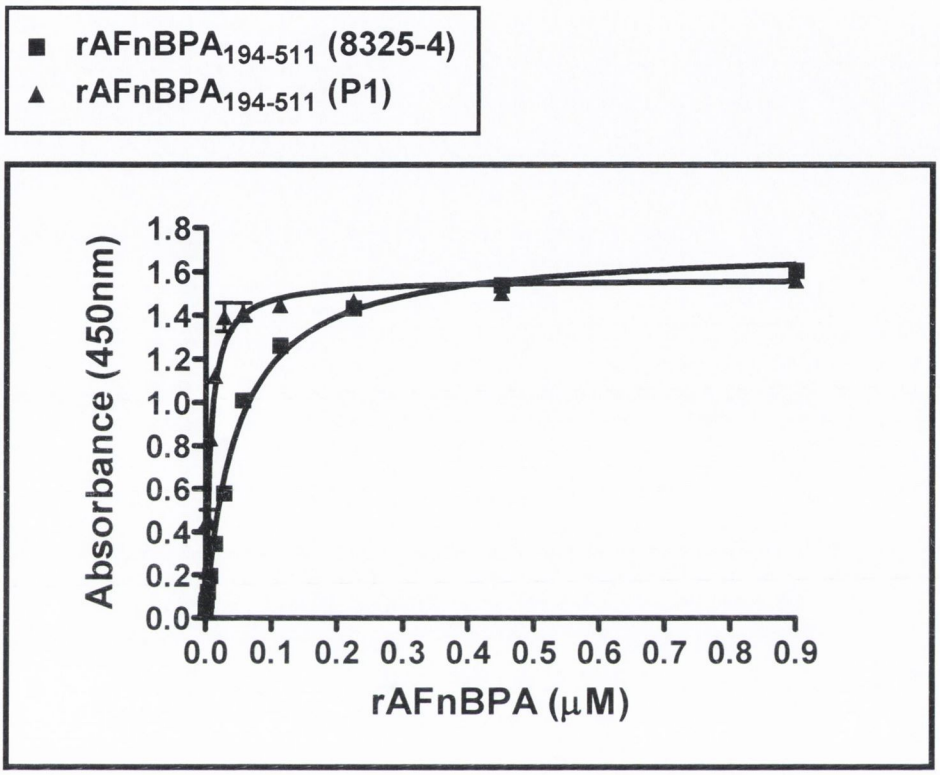

Figure 5.6 Binding of anti-rAFnBPA polyclonal antibodies to immobilised rAFnBPA$_{194-511}$ (8325-4) and rAFnBPA$_{194-511}$ (P1)

Microtitre plates were coated with various concentrations (0.9 μM – 0 μM) of rAFnBPA$_{194-511}$ (8325-4) or rAFnBPA$_{194-511}$ (P1). Bound protein was detected with polyclonal anti-rAFnBPA antibodies (1:2000) and goat anti-rabbit HRP-conjugated antibodies followed by development with TMB substrate. Data points represent the mean of triplicate wells and this figure is representative of three independent experiments.

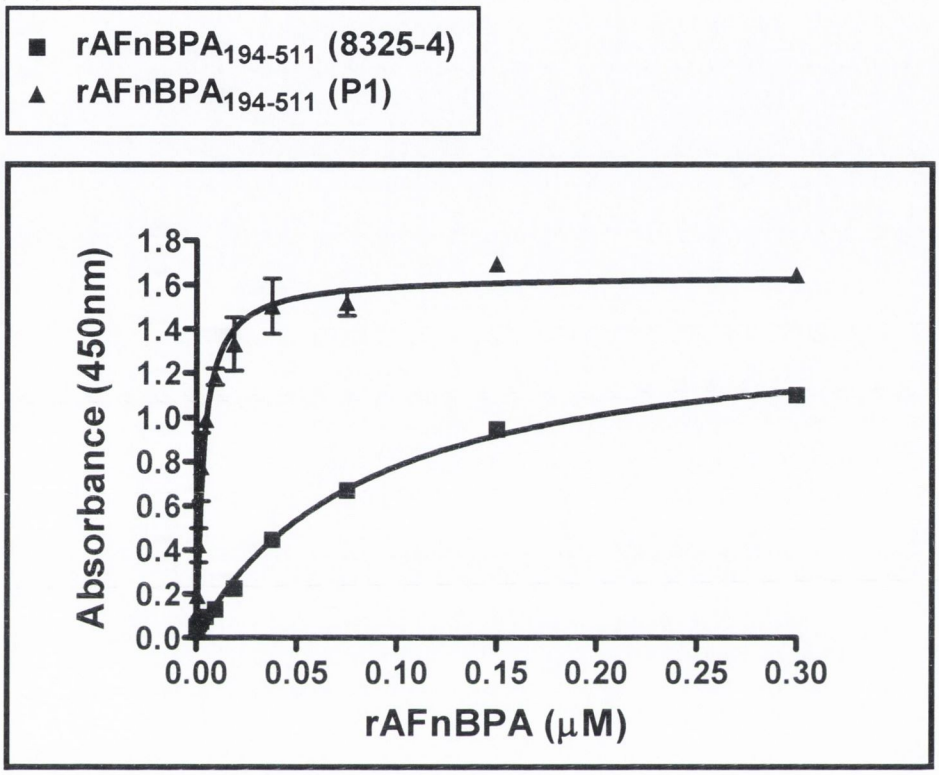

Figure 5.7 Binding of anti-histidine monoclonal antibodies to immobilised rAFnBPA$_{194-511}$ (8325-4) and rAFnBPA$_{194-511}$ (P1) Microtitre plates were coated with various concentrations (0.3 μM – 0 μM) of rAFnBPA$_{194-511}$ (8325-4) or rAFnBPA$_{194-511}$ (P1). Bound protein was detected with monoclonal anti-histidine antibodies conjugated to HRP. Data points represent the mean of triplicate wells and this figure is representative of two independent experiments.

To conclusively test the relative affinities of both proteins, increasing amounts of rAFnBPA from strains P1 and 8325-4, ranging from 0.125-1.0 μg, were subjected to SDS-PAGE and probed with polyclonal antibodies in Western immunoblotting (Figure 5.8). It is evident that the P1 protein has a significantly lower affinity for polyclonal antibodies (Figure 5.8). By densitometry, the lanes containing 1.0, 0.5, 0.25 and 0.125 μg of the P1 protein showed 1.5-, 2-, 3- and 12-fold lower affinities, respectively, for the polyclonal antibodies compared to the equivalent amounts of the 8325-4 protein. This indicates that the observed variant residues do indeed contribute to the reduced immune reactivity of FnBPA from strain P1.

5.2.4 Reactivity of rAFnBPA$_{194-511}$ (P1) to monoclonal anti-rAFnBPA (8325-4) antibodies

To further test the reactivity of antibodies raised against the A domain of FnBPA from strain 8325-4 to the P1 protein, a panel of monoclonal antibodies (Section 4.2.6) was studied. PVDF membranes containing doubling dilutions of rAFnBPA$_{194-511}$ from strain P1 and 8325-4 were probed. The four antibodies (including the function blocking antibody, 7C5) failed to react detectably with rAFnBPA$_{194-511}$ (P1) (Figure 5.9). This demonstrates that the monoclonal antibodies raised against rAFnBPA$_{37-544}$ (8325-4) are reactive to epitopes contained within the N2N3 domains of this protein. This indicates further that the variant residues of the P1 protein sequence are contained within important epitopes on the surface of the protein.

5.2.5 Examination of the locations of variant residues between rAFnBPA of strains 8325-4 and P1

The variant residues between rAFnBPA from strain P1 and 8325-4 were studied in the context of the 3D model of subdomains N2N3 of 8325-4. Those residues of 8325-4 that were different in strain P1 were highlighted and coloured green (N2) and blue (N3) (Figure 5.10). As can be seen in panel A, differences occur throughout the molecule with N3 exhibiting greater variance than N2 as reflected in the 78.3 % and 59.2 % amino acid identity between subdomains N2 and N3, respectively. Some changes occurred in the putative ligand-binding trench, the predicted latching peptide and the slot in N2 into which the latching peptide would insert during the dock, lock and latch mechanism of ligand binding. However these changes do not cause any adverse effect on ligand binding and indeed some caused a ~10-fold increase in the affinity of this protein for elastin. The residues of FnBPA altered by mutagenesis

(Chapter 4) were conserved between the two proteins with the exception of N356 and T417 of 8325-4 which were altered to D356 and I417, respectively, in P1. An alignment of the FnBPA amino acid sequences from *S. aureus* strains N315, 8325-4, MSSA476, COL, MRSA252, Mu50, MW2 showed G222, R224, N304, F306, F355, K357, G497, L498, T354, A415 and T417 to be entirely conserved. Only strain MRSA252 contains an aspartic acid residue at position 356 instead of asparagine.

The majority of variant residues were predicted to be exposed on the surface of the protein. When the 3D structure of the protein is viewed in space fill mode, the variant residues are visible. It is important to place this in the context of the entire protein. The structure of the N1 subdomain and the impact that this and the fibronectin-binding domains linked to the C-terminus of the latching peptide might have on the conformation and exposure of residues of subdomains N2 and N3 is not known. It is possible therefore that some residues that are surface-exposed on the 3D structural model of N2N3 of FnBPA, may not be surface-exposed on the full-length protein expressed on the surface of the bacterial cell. Here it has been shown that at least some of the variant residues are surface exposed and contribute to the antigenic variation observed by FnBPA from strain P1.

5.2.6 Binding of function-blocking monoclonal antibody 7C5 to rAFnBPA

It has been shown previously that monoclonal antibody 7C5 blocks binding of FnBPA from strain 8325-4 to immobilised fibrinogen or elastin (Figure 3.39). Attempts were made to understand the nature of the inhibition by examining the region of FnBPA to which 7C5 binds. It has been shown by Western blotting that 7C5 binds to rAFnBPA from strain 8325-4 and not to the equivalent protein of strain P1 (Figure 5.9). Equal amounts of recombinant FnBPA protein from strains 8325-4 and P1 were immobilised onto microtitre plates and probed with monoclonal antibody 7C5 (Figure 5.11). A previous experiment showed that the P1 protein is more efficient at coating the plastic surface of microtitre plates than the 8325-4 protein (Figure 5.7). Despite this, no reaction was seen with 7C5 binding to wells coated with rAFnBPA (P1). This confirms that the epitope recognized by monoclonal antibody 7C5 is not present on rAFnBPA from strain P1. The altered residues present in FnBPA from strain P1 are therefore involved in antigenic variation.

Monoclonal 7C5 was raised by immunising mice with the initial A domain construct of strain 8325-4, rAFnBPA$_{37\text{-}544}$. The minimum ligand-binding construct comprises subdomains N2 and N3 only. Therefore it was expected that 7C5 would bind to this N2N3 truncate.

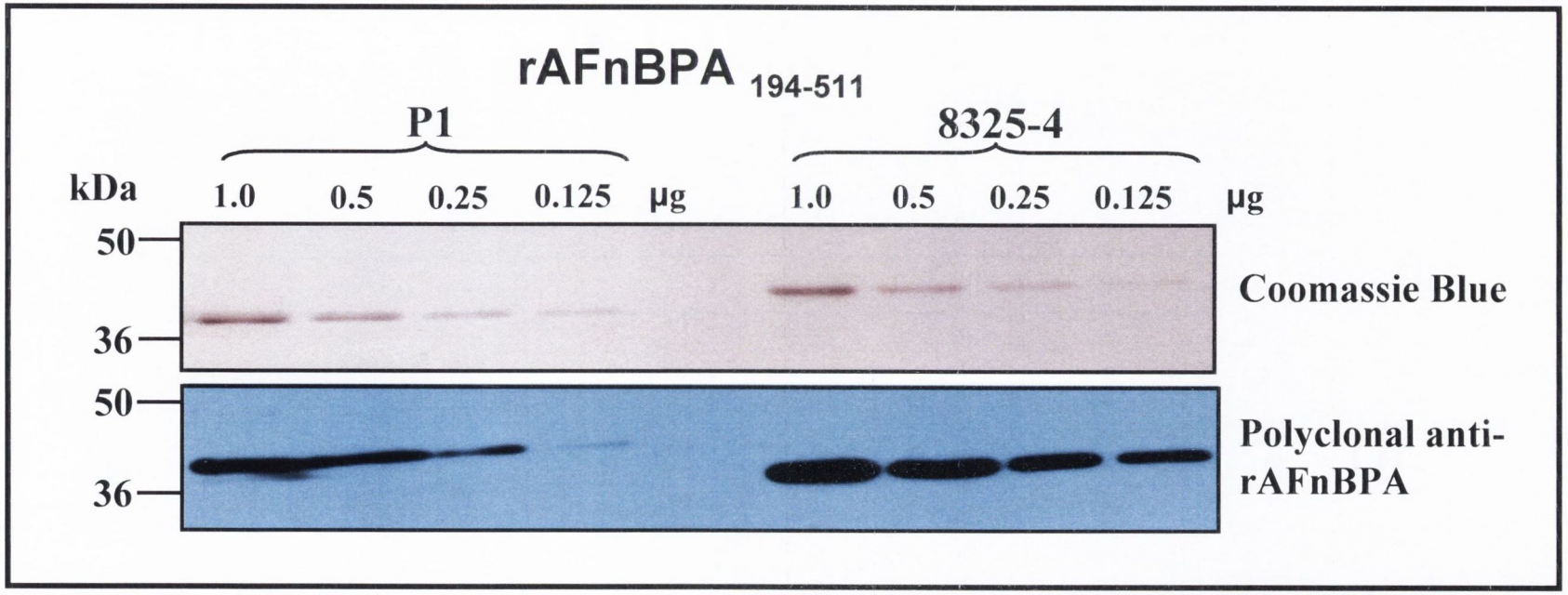

Figure 5.8 Coomassie and Western blot analysis of rAFnBPA$_{194-511}$ from *S. aureus* strains 8325-4 and P1

Doubling dilutions of rAFnBPA$_{194-511}$ (P1) and rAFnBPA$_{194-511}$ (8325-4) protein (1.0 µg – 0.125 µg) were analysed by SDS-PAGE and stained with Coomassie Blue or transferred to PVDF membrane and probed with polyclonal anti-rAFnBPA antibodies (1.6 µg/ml).

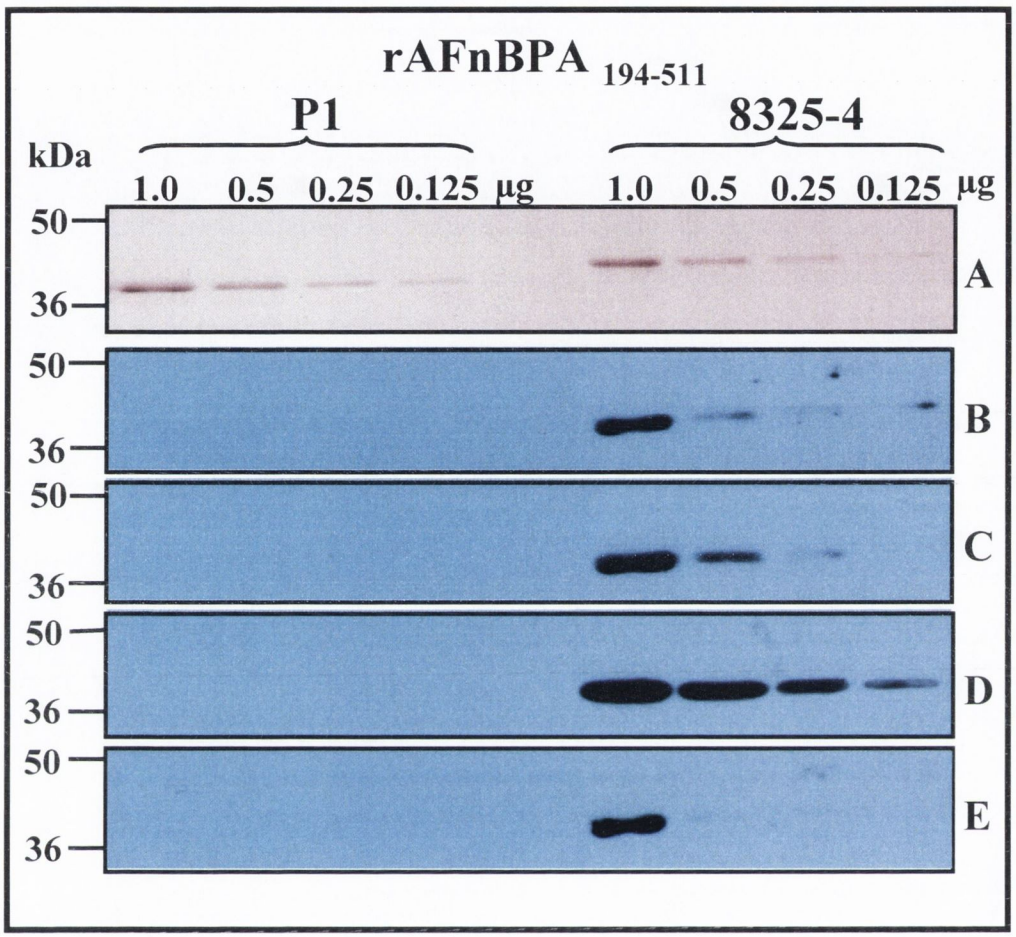

Figure 5.9 Coomassie and Western blot analysis of rAFnBPA$_{194-511}$ from *S. aureus* strains 8325-4 and P1

Doubling dilutions of rAFnBPA$_{194-511}$ (P1) and rAFnBPA$_{194-511}$ (8325-4) proteins (1.0 µg – 0.125 µg) were subjected to SDS-PAGE and stained with Coomassie Blue (A) or transferred to PVDF membrane and probed with monoclonal antibodies 7C5 (2.5 µg/ml) (B), 1E6 (C), 1F9 (D) and 1G8 (E) (1.25 µg/ml).

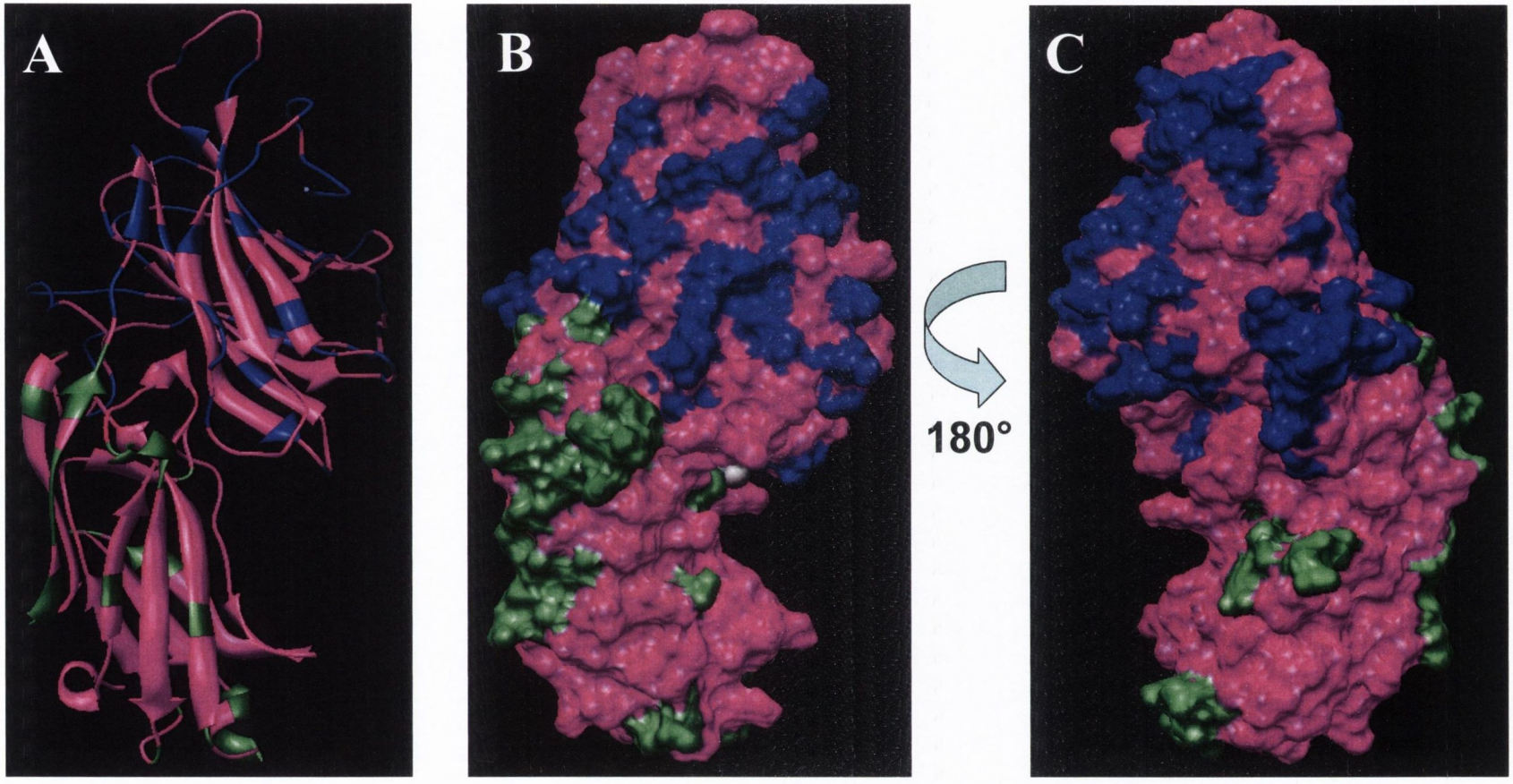

Figure 5.10 Position of variant residues between rAFnBPA from strains 8325-4 and P1

(A) Ribbon model of the predicted 3D structure of the N2N3 domains of region A of FnBPA from *S. aureus* strain 8325-4 with those residues that differ in FnBPA of strain P1 highlighted in green (N2) and blue (N3). (B) Space filled model in the orientation as per ribbon diagram in A. (C) Space filled model of same protein turned 180 degrees.

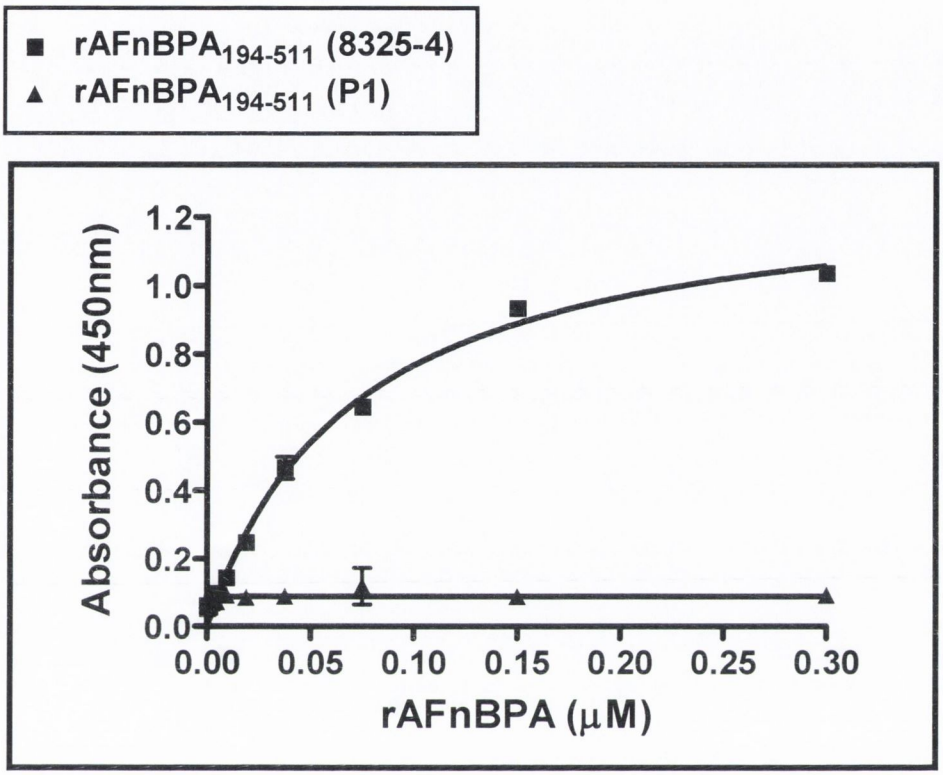

Figure 5.11 Binding of monoclonal antibody 7C5 to immobilised rAFnBPA$_{194-511}$ (8325-4) and rAFnBPA$_{194-511}$ (P1)

Increasing amounts of recombinant proteins rAFnBPA$_{194-511}$ (8325-4) and rAFnBPA$_{194-511}$ (P1) were immobilised onto a microtitre plate. Monoclonal antibody 7C5 (12.5 μg/ml) was added to each well followed by rabbit anti-mouse HRP conjugated antibody. Data points represent the mean of triplicate wells and this figure is representative of two independent experiments.

ELISA assays were used to test the binding of monoclonal antibody 7C5 to immobilised rAFnBPA$_{37\text{-}511}$ and rAFnBPA$_{194\text{-}511}$ from 8325-4. Three separate dilutions of 7C5 showed a dose-dependent and saturable binding response to both proteins (Figure 5.12). This confirms that the epitope to which 7C5 binds is contained within the N2N3 subdomains of rAFnBPA from strain 8325-4.

It has been hypothesized previously that some function-blocking monoclonal antibodies of ClfA might act by binding to the latching peptide, thereby preventing conformational change during the dock, lock and latch mechanism of ligand binding. Indeed several function-blocking monoclonal antibodies of ClfA bind to the N3 subdomain of ClfA. In order to further narrow down the binding site within rAFnBPA for 7C5, whole cell lysates of *E. coli* strains bearing plasmids encoding C-terminal truncates of rAFnBPA and individual N2 and N3 subdomains of FnBPA were subjected to SDS-PAGE and stained with Coomassie Blue or transferred to PVDF membrane. The membrane was then probed with monoclonal antibody 7C5 followed by detection with rabbit anti-mouse HRP conjugated antibody and development by chemiluminescence. 7C5 reacted with rAFnBPA$_{37\text{-}511}$ and all C-terminal truncates, rAFnBPA$_{194\text{-}509}$, rAFnBPA$_{194\text{-}498}$ and rAFnBPA$_{194\text{-}483}$ (Figure 5.13). The antibody reacted with rAFnBPA$_{194\text{-}336}$ (N2) but not with rAFnBPA$_{337\text{-}511}$ (N3). This suggested that 7C5 binds to the N2 subdomain of rAFnBPA.

To investigate this further, rAFnBPA$_{194\text{-}336}$ and rAFnBPA$_{337\text{-}511}$ were purified and immobilised onto the wells of a microtitre plate and probed with dilutions of 7C5. A dose-dependent and saturable response was seen for 7C5 binding to immobilised rAFnBPA$_{194\text{-}336}$ whereas no reaction was detected for 7C5 binding to rAFnBPA$_{337\text{-}511}$ (Figure 5.14). This is further evidence that the 7C5 monoclonal antibody binds to the N2 subdomain of region A of FnBPA. Taken together with the data showing that 7C5 binds to rAFnBPA from strain 8325-4 but not to P1, it is now known that residues of subdomain N2 of FnBPA from strain 8325-4 that are not conserved in FnBPA from strain P1 (see Figure 5.2) are involved in comprising the epitope to which this important monoclonal antibody binds.

5.2.7 Ability of monoclonal antibody 7C5 to bind to rAFnBPA$_{194\text{-}511}$ already bound to immobilised fibrinogen

It has been noted previously that function blocking monoclonal antibodies of ClfA can bind to ClfA after the fibrinogen molecule has docked into the hydrophobic trench (Mitchell, 2004). This confers a displacing function on some of these monoclonal antibodies whereby

the bound fibrinogen molecule is then released. 7C5 was tested for its ability to bind FnBPA already bound to immobilised fibrinogen (Figure 5.15). Microtitre plates were coated with 10 μg/ml of human fibrinogen and increasing amounts of $rAFnBPA_{194-511}$ were allowed to bind. Following this, either polyclonal anti-rAFnBPA antibodies or monoclonal antibody 7C5 was added. Detection was carried out with goat anti-rabbit and rabbit anti-mouse antibodies, respectively. As a positive control, polyclonal anti-rAFnBPA antibodies demonstrated dose-dependent and saturable binding. If monoclonal antibody 7C5 had a displacing function, binding of this antibody to $rAFnBPA_{194-511}$ would cause the recombinant FnBPA protein to disassociate with the immobilised fibrinogen and both it and the monoclonal antibody would wash off at this stage. This however was not the case as rabbit anti-mouse antibodies detected the monoclonal antibody, showing dose-dependent binding in response to the levels of increasing concentrations of $rAFnBPA_{194-511}$. This indicates that monoclonal antibody 7C5 can bind to $rAFnBPA_{194-511}$ after this protein has bound to its fibrinogen ligand and conformational changes involved in binding to fibrinogen do not alter the epitope to which 7C5 binds. Further experimentation with bacterial cells expressing FnBPA would give information regarding the potential displacing activity of this monoclonal antibody.

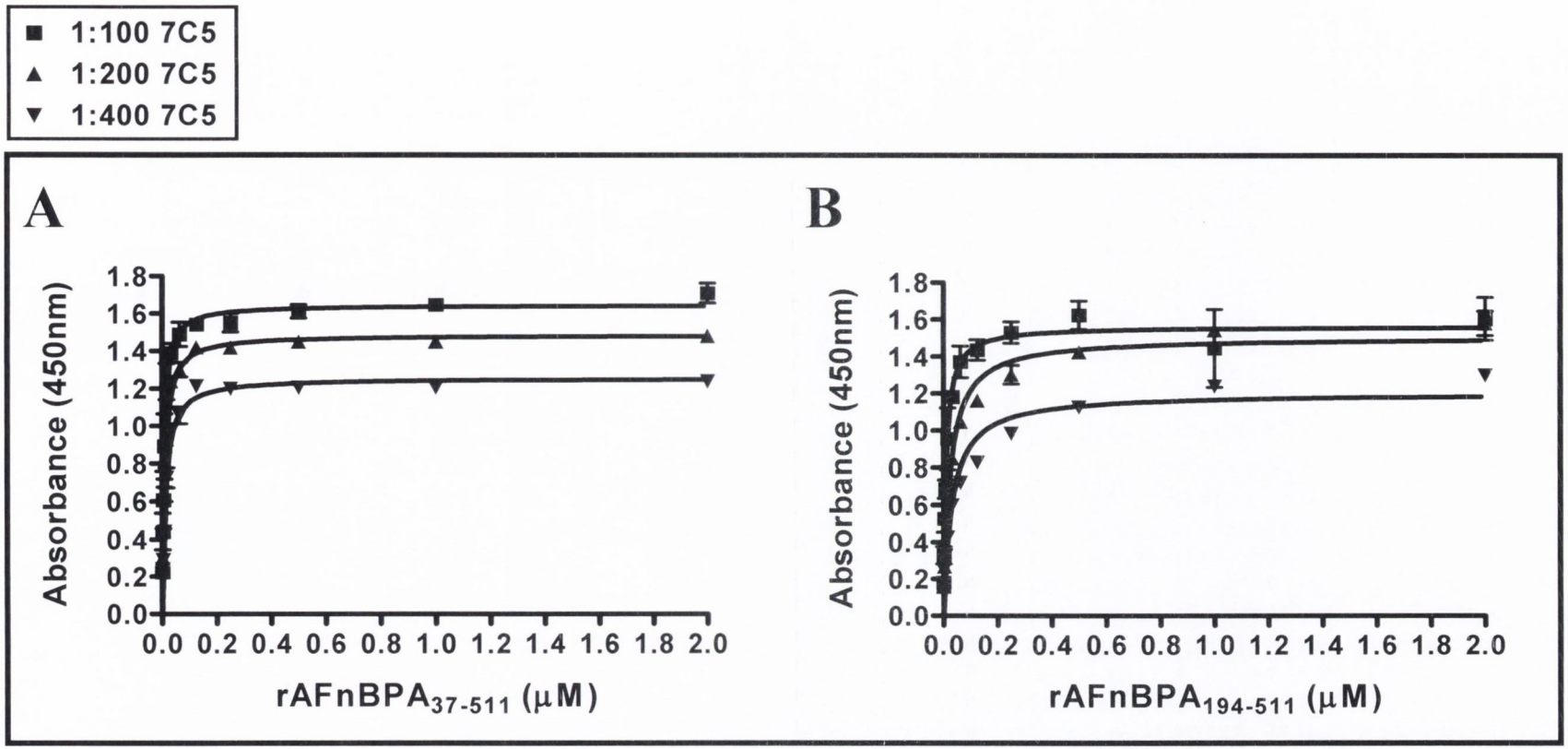

Figure 5.12 Binding of monoclonal antibody 7C5 to immobilised rAFnBPA$_{37\text{-}511}$ and rAFnBPA$_{194\text{-}511}$

Increasing amounts of rAFnBPA$_{37\text{-}511}$ and rAFnBPA$_{194\text{-}511}$ from *S. aureus* strain 8325-4 were immobilised onto microtitre plates. Three dilutions of monoclonal antibody 7C5 was added to wells followed by rabbit anti-mouse HRP conjugated antibody. Data points represent the mean of triplicate wells and this figure is representative of two independent experiments.

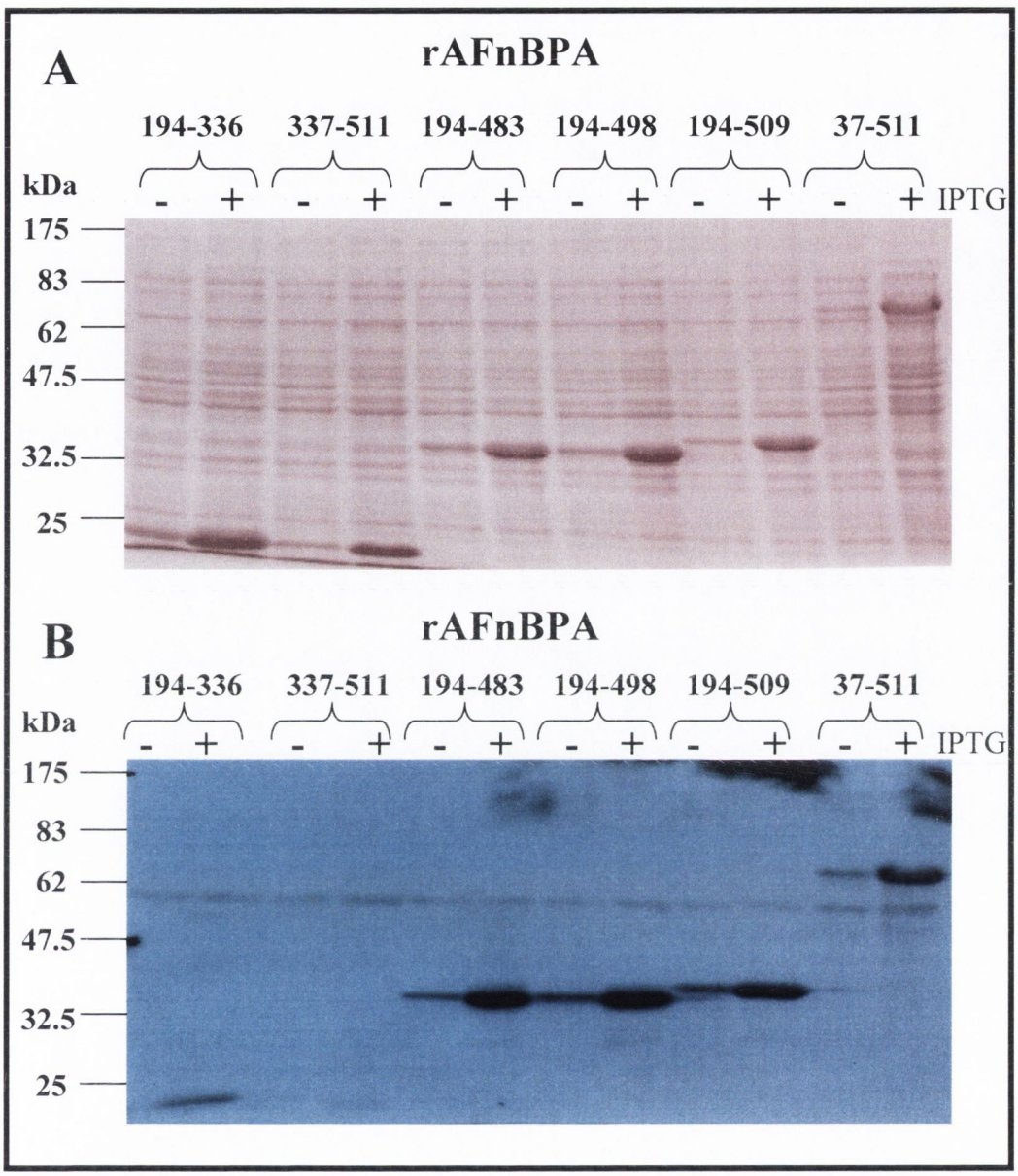

Figure 5.13 Analysis of *E. coli* strains expressing rAFnBPA truncates

E. coli cells harbouring plasmids encoding FnBPA truncates spanning residues 194-336, 337-511, 194-483, 194-498, 194-509 and 37-511 were incubated with (+) or without (-) IPTG after reaching $OD_{600\,nm}$ =0.5. Equal loading of lysed cells were analysed by SDS-PAGE, stained with Coomassie Blue (A) or electroblotted onto PVDF membrane and probed with monoclonal antibody 7C5 (1.8 μg/ml) followed by rabbit anti-mouse HRP conjugated antibody (B).

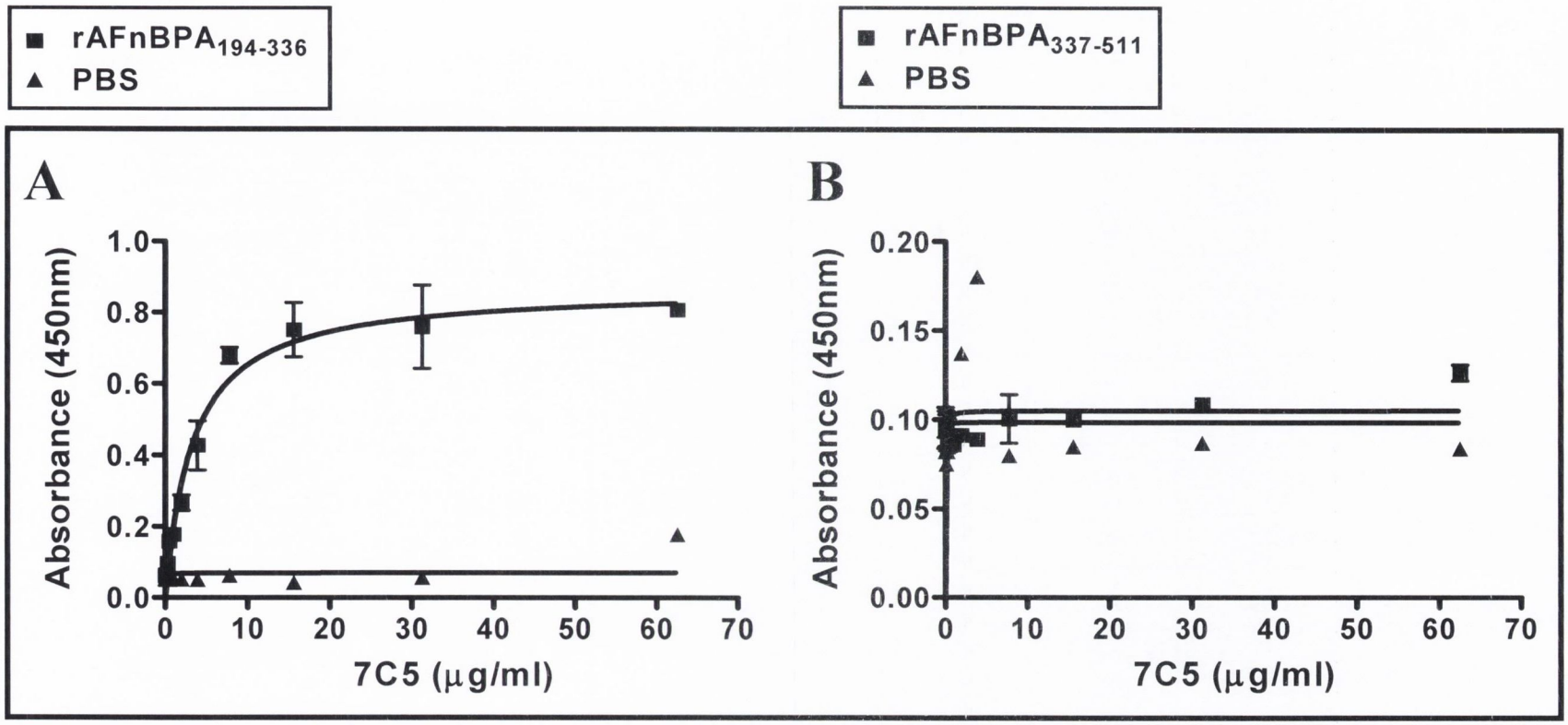

Figure 5.14 Binding of monoclonal antibody 7C5 to immobilised rAFnBPA$_{194-336}$ and rAFnBPA$_{337-511}$

rAFnBPA$_{194-336}$ (5 µM) and rAFnBPA$_{337-511}$ (2.5 µM) from *S. aureus* strain 8325-4 were immobilised onto microtitre plates. Monoclonal antibody 7C5 was added to each well followed by rabbit anti-mouse HRP conjugated antibody. Data points represent the mean of triplicate wells and this figure is representative of two independent experiments.

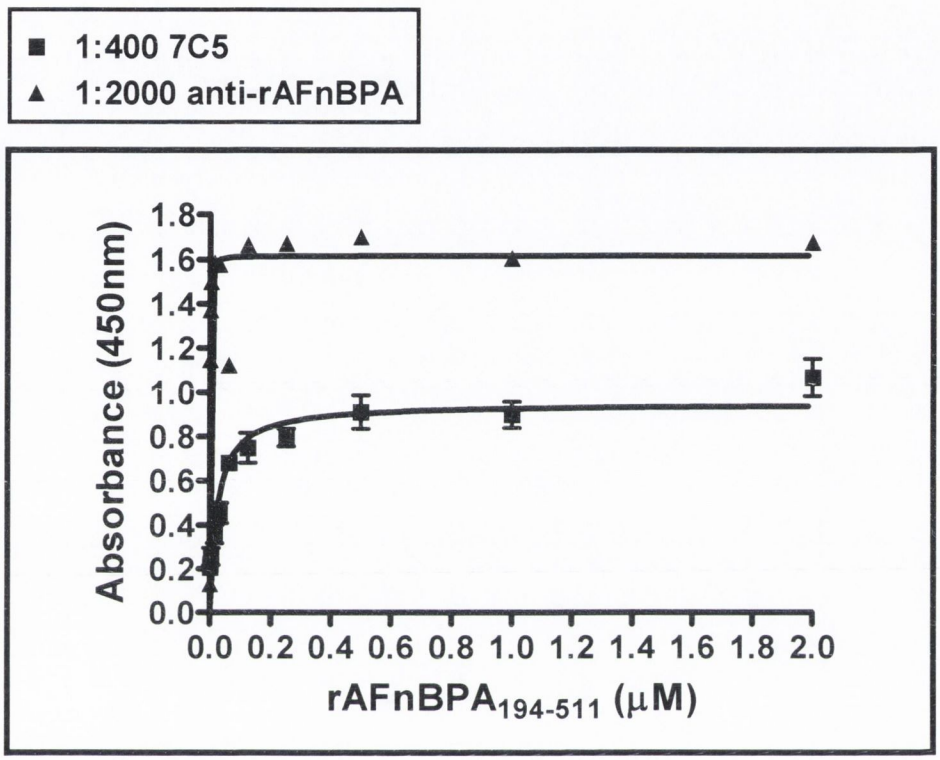

Figure 5.15 Binding of monoclonal antibody 7C5 to rAFnBPA$_{194-511}$ (8325-4) bound to immobilised fibrinogen

Microtitre plates were coated with 10 μg/ml human fibrinogen and increasing amounts of rAFnBPA$_{194-511}$ (8325-4) were added. Bound protein was detected with monoclonal antibody 7C5 (3 μg/ml) or polyclonal anti-rAFnBPA antibodies followed by rabbit anti-mouse HRP conjugated antibody or goat anti-rabbit HRP conjugated antibody, respectively. Data points represent the mean of triplicate wells.

5.3 Discussion

The fibronectin-binding repeat regions of FnBPA and FnBPB from *S. aureus* strain 8325-4 are highly homologous, sharing 94% identity (Jonsson *et al.*, 1991). In contrast, the A domains of FnBPA and FnBPB from strain 8325-4 share only 45% amino acid identity (Jonsson *et al.*, 1991). Analysis of the polyclonal antisera raised against the FnBPA A domain of strain 8325-4 (Section 3.2.5) showed partial reactivity with the FnBPB A domain of the same strain. Similarly, antibodies raised to the FnBPB A domain cross reacted with the A domain of FnBPA (Figure 3.18). It was also observed that these antibodies did not efficiently recognize the FnBPs expressed by *S. aureus* strain P1 (Figure 3.17 and Figure 5.1). This raised the possibility that antigenic variation has occurred between these two strains due to differences in FnBPA amino acid sequences. The amino acid sequence of the A domain of FnBPA from strain P1 was deduced and compared with that of strain 8325-4 and showed 73.5% overall identity. The extent of the identity differed throughout the length of the A domain with the N1 subdomains being 91.4% identical and the N2 and N3 subdomains showing only 78.3% and 59.2% identity, respectively. Similar levels of diversity were found in the FnBPA A domains deduced from the genome sequences of seven sequenced *S. aureus* strains. In contrast, the fibronectin-binding motifs at the C-terminus of FnBPA and the A domains of ClfA from these strains were highly conserved with 90-95% identity, in any pairwise alignment (Loughman, 2005).

DNA encoding the minimum N2N3 domains of FnBPA from strain P1 was cloned into the expression vector pQE30 which allowed purification of the recombinant protein rAFnBPA$_{194\text{-}511}$ (P1). This protein was shown in ELISA assays to adhere strongly to immobilised fibrinogen and elastin demonstrating the functional integrity of the recombinant protein and indicating that the N2N3 subdomains of the P1 protein also contain the ligand binding site. The P1 and 8325-4 proteins had similar affinities for fibrinogen but interestingly, the P1 protein had an increased affinity for immobilised elastin peptides compared to its 8325-4 counterpart. Thus the sequence variation between these two proteins has no adverse effect on ligand binding with those changes situated around the putative ligand-binding trench or latching peptide possibly involved in the increased binding to elastin. An alignment of the A domain of FnBPA from strains 8325-4 and P1 shows those amino acids that are important in ligand binding (Section 4.2.7) are conserved. In particular residues N304 and F306 are present in both strains. In fact, an alignment of FnBPA sequences from the seven strains listed

in Section 5.2.5 above, shows that G222, R224, N304, F306, T354, F355, K357, A415, G497 and L498 are entirely conserved. In two strains, P1 and MRSA252, N356 is changed to D356 and in strain P1 T417 is changed to I417. It is predicted therefore that the variant A domains of FnBPA from these strains can each bind to fibrinogen and elastin. It can thus be concluded that residues important in contacting ligands entering the hydrophobic trench between N2 and N3 are conserved in order to retain ligand-binding function.

The FnBPA A domains of strains 8325-4 and P1 were tested for their ability to bind polyclonal antibodies raised against the A domain of FnBPA from strain 8325-4. Paradoxically, it was initially suggested that rAFnBPA$_{194\text{-}511}$ (P1) had a stronger affinity for polyclonal antibodies than rAFnBPA$_{194\text{-}511}$ (8325-4). However this was due to the higher coating efficiency of the P1 protein onto the plastic wells of microtitre plates. Western blotting analysis showed that the monoclonal antibodies raised against rAFnBPA$_{37\text{-}544}$ (8325-4) reacted well with the N2N3 truncate of this protein demonstrating that important epitopes are likely to be contained within the ligand-binding region of the A domain of FnBPA. Western blotting also indicated that polyclonal anti-rAFnBPA (8325-4) antibodies had a 3-12 fold lower affinity for the N2N3 domains of FnBPA from strain P1 compared to that of strain 8325-4. Four monoclonal antibodies, raised against rAFnBPA$_{37\text{-}544}$ from strain 8325-4 were also unable to bind the P1 protein. The residues of rAFnBPA (8325-4) that are not conserved in strain P1 were shown on the 3D-structural model to be mostly surface exposed. This suggests a selective advantage in variation in FnBPA A domains, perhaps as a mechanism of evasion of host immune responses through antigenic variation, while still retaining ligand-binding activity. This might also reduce the efficiency of opsonisation during the early stages of infection. A similar mechanism of antigenic variation in the 11 fibronectin-binding motifs would not confer a similar advantage as antibodies against this region only recognize neo-epitopes formed upon binding of fibronectin (Casolini *et al.*, 1998) and are thus not protective.

Among the monoclonal antibodies that were unable to bind to rAFnBPA$_{194\text{-}511}$ (P1) was the functional blocking monoclonal antibody 7C5 which was unable to bind to this protein in Western blotting and ELISA assays. This indicated that the a subset of the residues of rAFnBPA (8325-4) that are substituted in strain P1 represent the epitope to which 7C5 binds. It was shown by Western blotting and ELISA that 7C5 binds to the N2N3 domain. Western blotting analysis indicated that 7C5 bound to all C-terminal truncates of rAFnBPA$_{194\text{-}511}$, eliminating residues 483-511 as part of the epitope. Furthermore the monoclonal antibody bound to subdomain N2 and not to N3. This is consistent with the observation that 7C5 does

not bind to the latching peptide. It is possible that 7C5 binds to the region of N2 into which the latching peptide slots during the dock-lock and latch mechanism. ELISA experiments show that 7C5 can bind to rAFnBPA already bound to immobilised fibrinogen which indicates that the epitope for 7C5 is not altered upon ligand binding. The epitope to which 7C5 binds could be further identified by studying the variant residues of subdomain N2 and focusing on the variations that exist between N2 of FnBPA from strains 8325-4 and P1. As Figure 5.2 illustrates, there are 30 amino acid differences between the N2 subdomains of these strains with 18 of these being conserved mutations. Taking into account their position and orientation on the 3D structural model, the remaining 12 residues could be altered by site-directed mutagenesis to a suitably different residue in an attempt to pinpoint some residues involved in the epitope for monoclonal antibody 7C5.

It has been reported that the *fnbA* and *fnbB* genes from 50 different strains representing the major MRSA clones found in Europe have undergone greater sequence divergence than genes encoding surface proteins such as *clfA* and *clfB* (Kuhn *et al.*, 2006). The amino acid sequence of the A domain of FnBPA of strain P1 was shown here to be 73.5% identical to that of 8325-4. Interestingly the differences were not spread evenly. Domain N1 was more highly conserved while domain N3 was the most divergent. Using the 3D model of the 8325-4 FnBPA A domain it is evident that the majority of variant residues are located on the surface of the protein. Residues identified by mutagenesis to be important in ligand binding were mostly conserved. It is not fully understood why the fibronectin-binding proteins of *S. aureus* are subject to a greater degree of sequence variation compared to the clumping factors, ClfA and ClfB. It may be due to the importance of these proteins in the early stages of infection. In contrast to FnBPA and FnBPB, ClfA is predominately expressed in the stationary phase of growth. While ClfB is produced in exponential phase and has been shown to bind fibrinogen (Ni Eidhin *et al.*, 1998) and keratin (Walsh *et al.*, 2004), the importance of this protein mainly lies in its role in nasal colonization (Schaffer *et al.*, 2006). Resisting opsonisation by undergoing sequence variation and antigenic variation would aid in the survival of the bacteria at the crucial initial stages of infection, thereby allowing them to be subsequently internalized into endothelial cells. This would serve to protect the bacterium from the host immune system and allow the spread of infection. A similar observation of antigenic variation with conserved function in the coagulase protein of *S. aureus* has also been proposed to evade the host immune response (Watanabe *et al.*, 2005). The observed gradient of antigenic variation from subdomains N1 to N2 to N3 of FnBPA is also quite interesting and hints at the increased

importance of the latter subdomains in ligand binding and conformational changes during dock, lock and latch. The consequences of this sequence divergence were reduced ability of antibodies raised against the 8325-4 protein to bind to the P1 protein while retaining the ability to bind to both fibrinogen and elastin. This suggests that the ability of FnBPA to bind these ligands during infection is important and further supports the contention that binding of fibrinogen and elastin occurs at the same site. Investigation of this phenomenon is ongoing to include FnBPs from a variety of clonal types in order to determine the extent of the sequence divergence and antigenic variation, and their relevance to evasion of immune responses during infection.

Chapter 6

Region A of FnBPA binds to the elastin monomer, tropoelastin

6.1 Introduction

The A domain of FnBPA is homologous to the ClfA surface protein of *S. aureus* and indeed binds to the same region of the γ chain of fibrinogen (Wann *et al.*, 2000). It was subsequently discovered that the A domain of this protein also bound to immobilised elastin peptides and promoted adhesion of bacterial cells to elastin-coated surfaces (Roche *et al.*, 2004). The binding site for elastin peptides within region A of FnBPA has been narrowed down from rAFnBPA$_{37-544}$ to rAFnBPA$_{194-511}$, encompassing subdomains N2 and N3. These two subdomains have been predicted to adopt a folded structure similar to ClfA (Deivanayagam *et al.*, 2002). Based on a model of the predicted structure of N23 of FnBPA, residues crucial for the binding of elastin peptides were identified by alanine substitution (Section 4.2.7). In particular, changes to residues N304 and F306 caused a significant decrease in the affinity for immobilised elastin peptides. The double N304A/F306A substitution was completely defective in elastin binding (Figure 4.31).

An important aspect in understanding the *S. aureus*- elastin interaction is to assess if the bacterium is capable of binding tropoelastin, the monomeric precursor of elastin. It might then be possible to identify the binding domain for FnBPA within this molecule. Tropoelastin is expressed and secreted by diverse cells such as fibroblasts, endothelial cells, chrondoblasts and vascular smooth muscle cells (Rosenbloom, 1982). Two major types of domains are found in tropoelastin, (a) hydrophobic domains which consist primarily of the four amino acids, glycine, alanine, valine and proline, which make up to 75% of the entire protein and which often occur in repeats of three to six peptides such as GVGVP, GGVP and GVGVAP; (b) hydrophilic domains, typically rich in lysine and alanine that are involved in crosslinking. These domains often consist of stretches of lysine separated by two or three alanine residues such as AAAKAAKAA. In general these hydrophobic and hydrophilic domains alternate (Figure 6.1 A). The C-terminus of tropoelastin is highly basic and is very strongly conserved among all species. It contains the only two cysteine residues in the protein, which are known to form a disulphide bridge, and terminates with a positively-charged RKRK sequence. Tropoelastin is synthesized with an N-terminal 26 amino acid signal peptide and is secreted as an approximately 72 kDa protein in the human although there is some variation due to different isoforms resulting from alternative splicing of introns. Tropoelastin undergoes very little post-translational modification and there is no evidence for glycosylation (Vrhovski and Weiss, 1998). Deposition of tropoelastin into the extracellular space occurs only at specific

regions on the cell surface and tropoelastin has been shown to interact specifically with the microfibril fibres that form a scaffold to enable the growing elastin fibre to polymerise. The process of elastic fibre formation involves a number of steps, beginning with coacervation.

Coacervation is a thermodynamically controlled process which has been proposed to concentrate and align tropoelastin monomers into an ordered fibrillar structure on the surface of the cell (Cox *et al.*, 1973). Tropoelastin is soluble in cold aqueous solutions of less than 20°C. However, on raising the temperature towards the physiological range the solution becomes cloudy as the tropoelastin molecules aggregate by interactions between hydrophobic domains. Coacervation is an important step in fibre formation as the correct alignment of monomers allows the intermolecular and intramolecular crosslinking of the lysine residues in the hydrophilic domains (Figure 6.1 B and C). This is carried out by the enzyme lysyl oxidase which oxidatively deaminates lysine residues to form a unique amino acid called allysine (Figure 6.2 A). Subsequent condensation reactions of two or more allysines produce crosslinks involving novel amino acids such as desmosine and isodesmosine (Figure 6.2 B).

The elastin used in ELISA assays described in Chapters 3, 4 and 5 is a commercially available preparation made by the digestion of elastic fibres purified from human aorta. In the purification procedure, powdered elastic fibres are treated with repeated cycles of hot oxalic acid and then cooled, precipitated and dialysed free of contaminants. This results in a heterogeneous mixture of elastin peptides (10 – 50 kDa) termed α-elastin. In this preparation no full-length tropoelastin molecules remain intact, however the unique desmosine crosslinks are present (Figure 6.1 C). The major differences between α-elastin and tropoelastin are (a) the presence of various but unknown exposed sites due to the cleavage of oxalic acid and (b) the presence of native elastic fibre crosslinks. It is possible that either of these elements is responsible for the binding of rAFnBPA. It was of interest therefore to determine if rAFnBPA could bind to the monomer of elastin, tropoelastin which would lack both novel exposed sites and desmosine crosslinks. The difficulty in purifying monomeric tropoelastin from human tissue has resulted in recombinantly expressed tropoelastin being used extensively to study the interactions of this monomer with host proteins including microfibril associated glycoprotein 1 (MAGP-1) (Clarke and Weiss, 2004) and integrin $\alpha_V\beta_3$ (Rodgers and Weiss, 2004). Recombinant tropoelastin was produced by collaborators in the University of Sydney, Australia by synthesizing the entire human elastin gene and expressing it in bacteria. Recombinant tropoelastin reacts with elastin antibodies, demonstrates coacervation ability and has the same circular dichroic spectrum as naturally-derived tropoelastin.

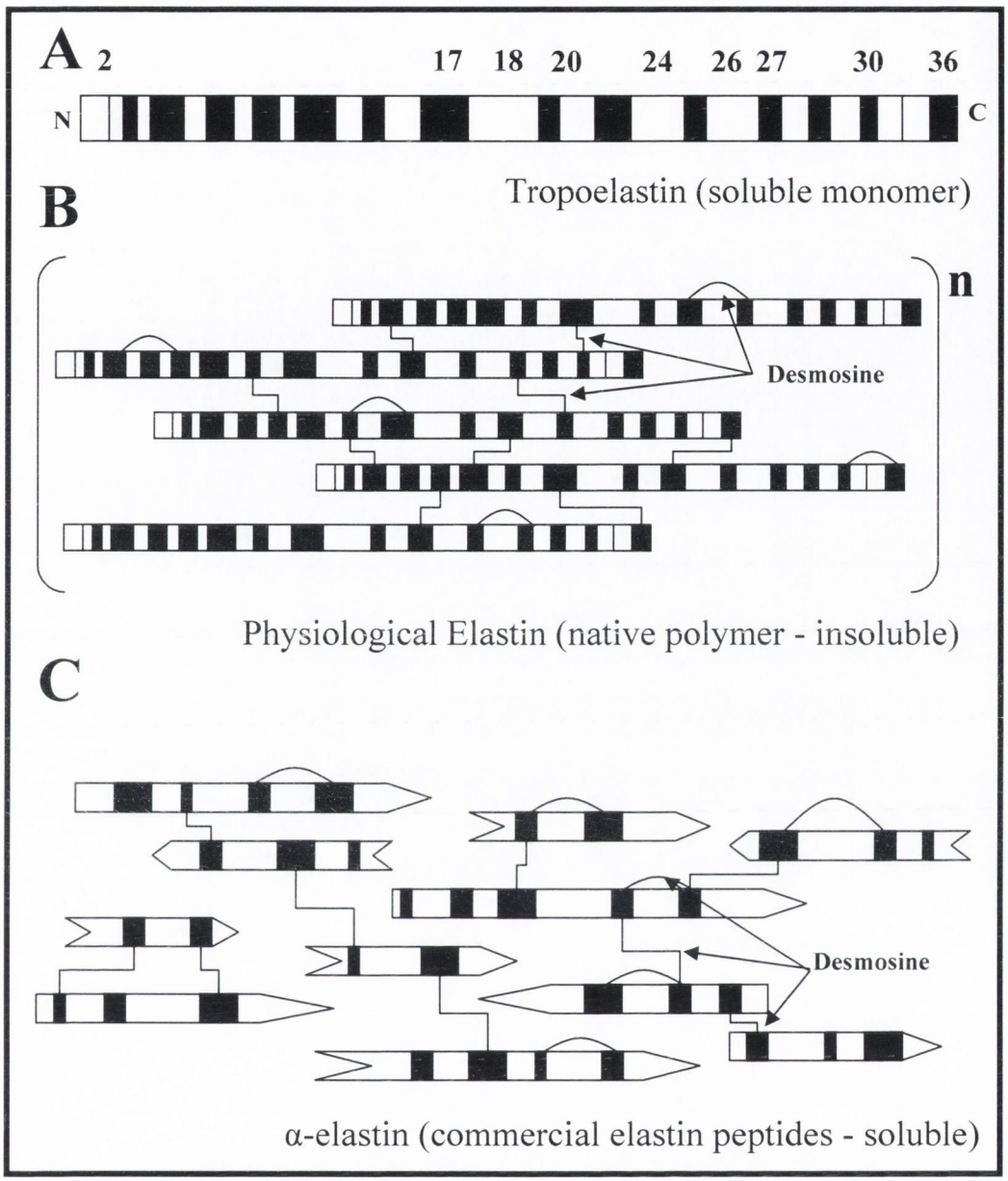

Figure 6.1 Elastin in various forms

(A) The tropoelastin monomer is composed of alternating hydrophobic (white) and hydrophilic (black) domains. (B) The process of coacervation aligns the tropoelastin monomers in such a way to allow lysyl oxidase to crosslink the lysine residues of hydrophilic domains to yield elastin, an amorphous, highly insoluble polymer found in tissues such as skin, lungs, blood vessels and ligaments. (C) The treatment of purified elastin from human tissue with hot oxalic acid results in cleavage at hydrophilic sites to yield a heterogeneous mixture of elastin peptides (α-elastin) which retain the unique crosslinks (desmosines).

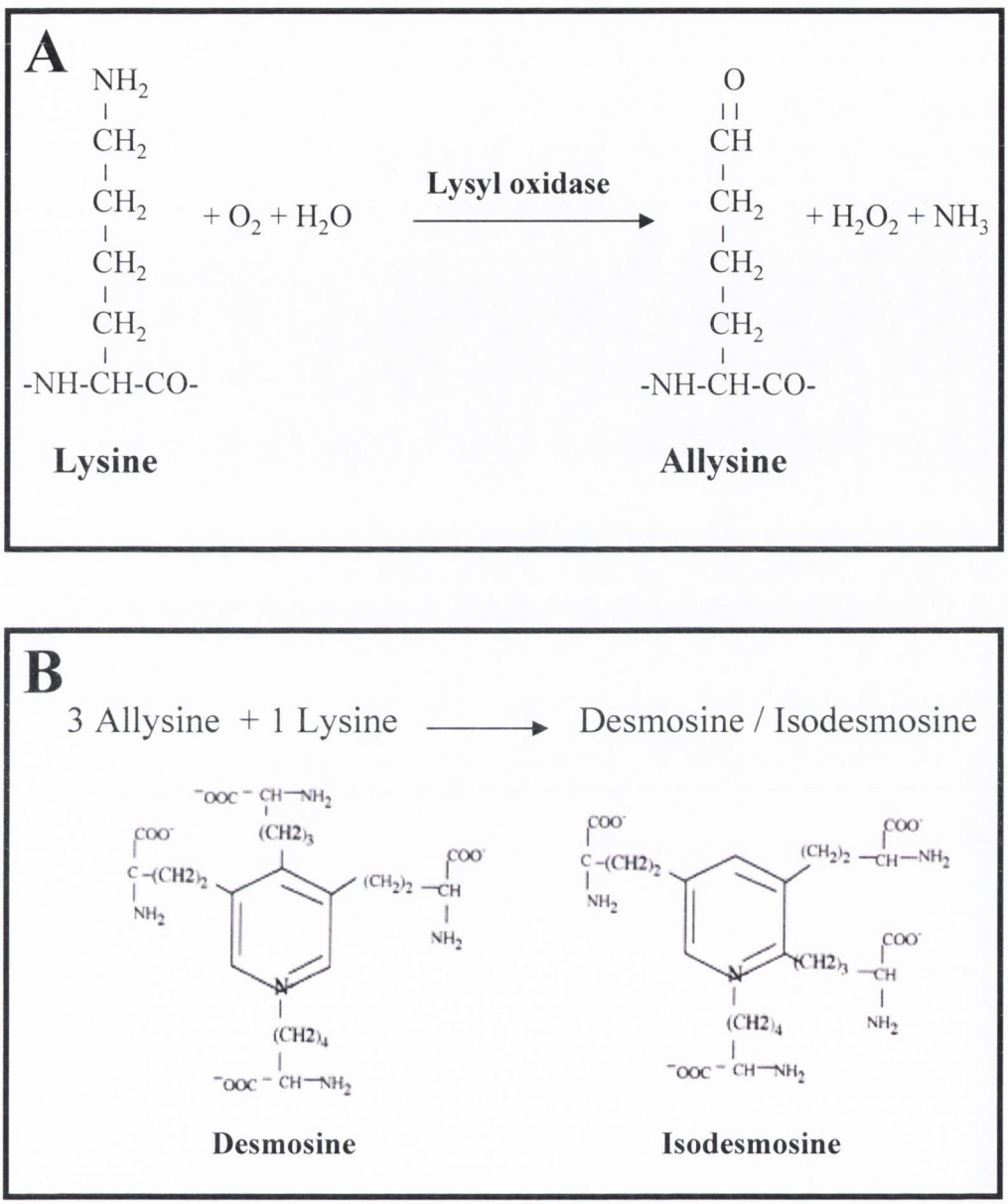

Figure 6.2 Formation of crosslinks in elastin

(A) Lysyl oxidase oxidatively deaminates a peptidyl lysine to generate a peptidyl α-aminoadipic-δ-semialdehyde (allysine). (B) Desmosine and isodesmosine are rare isomeric amino acids found only in elastin and are formed by condensation of one molecule of lysine with 3 molecules of a lysine derivative, allysine, into a pyridinium ring.

A sample of rAFnBPA$_{37-544}$, which was shown in Section 3.2.6 to bind to immobilised human aortic elastin peptides, was sent to the laboratory of Prof. Anthony Weiss at the University of Sydney to test for binding to immobilised recombinant human tropoelastin. Investigations were carried out there to measure binding of rAFnBPA$_{37-544}$ to immobilised human tropoelastin by surface plasmon resonance (SPR). A K_D of 29 ± 0.1 nM was obtained for rAFnBPA$_{37-544}$ binding to full-length tropoelastin (Clarke, 2006). This was the first evidence that a staphylococcal cell wall anchored surface protein can bind to monomeric human tropoelastin. To narrow down the binding site within tropoelastin for FnBPA, further tests were carried out by the Weiss laboratory to determine the binding of rAFnBPA$_{37-544}$ to three separate truncates of tropoelastin, encompassing the N-terminus of the protein (SHELN-18), exons 17-27 (SHEL17-27) and the C-terminus of the protein (SHEL27-C) (Figure 6.3 A). It was found that rAFnBPA$_{37-544}$ bound to all three segments of tropoelastin. rAFnBPA$_{37-544}$ interacted with SHELN-18 with a dissociation constant of 31 ± 0.1 nM. A slightly weaker interaction was observed between rAFnBPA$_{37-544}$ and SHEL17-27 with a K_D of 57 ± 0.4 nM. rAFnBPA$_{37-544}$ also interacted with SHEL27-C but no reliable kinetic data was obtained (Clarke, 2006) (Figure 6.3 B). From these data, it is clear that FnBPA is capable of binding all three segments of tropoelastin indicating that multiple binding sites for FnBPA occur within the tropoelastin molecule. This indicates a possibility that FnBPA binds to a repetitive sequence in tropoelastin that is present is all three truncates. Tropoelastin contains numerous short peptide repeat sequences (Figure 1.9) which could be involved in contact with FnBPA.

To investigate the FnBPA-tropoelastin interaction in more detail, further SPR experiments were carried out by the Weiss laboratory using varying pH. Analysing the amino acid sequences, titration curves of rAFnBPA$_{37-544}$ and tropoelastin were generated. Tropoelastin undergoes a sharp positive to negative charged state transition at its isoelectric point (pI) of 11. This is in stark contrast to rAFnBPA$_{37-544}$ which has an isoelectric point of 5. It remains only slightly negatively charged until pH above 10 (Figure 6.4 A). The effect of pH on the binding of these two proteins was investigated. When rAFnBPA$_{37-544}$ was injected over a tropoelastin-coated surface at various pH, the response differed. At low pH the interaction was strong with non-saturable binding. As the pH increased the interaction weakened and saturable binding was observed at pH 10.6. At pH 11 all interactions between the proteins ceased (Clarke, 2006) (Figure 6.4 B).

This work carried out by the laboratory of Prof. Weiss established that rAFnBPA can bind to immobilised tropoelastin in a dose-dependent and saturable manner and that binding

sites for rAFnBPA occurred throughout the tropoelastin molecule. A pH dependency for the interaction was also discovered. This interaction warranted further investigation and the aim of the studies carried out in this chapter was to examine the binding of rAFnBPA truncates and alanine-substituted variants to tropoelastin. SPR analysis was carried out in the University of Sydney with rAFnBPA proteins. Amine coupling was used to immobilise full-length tropoelastin onto the surface of a dextran chip (Figure 6.5 A). Dilutions of each rAFnBPA protein were passed over this chip to measure the binding kinetics of the two proteins (Figure 6.5 B). The Biacore sensograms generated have four main phases, establishment of baseline, association, dissociation and regeneration as outlined in Figure 6.6. Using these techniques to assess the binding of rAFnBPA truncates and alanine-substituted variants, the hypothesis that the tropoelastin monomer was binding to FnBPA by docking into the hydrophobic trench between N2 and N3 in a similar manner to that of elastin peptides, could be tested.

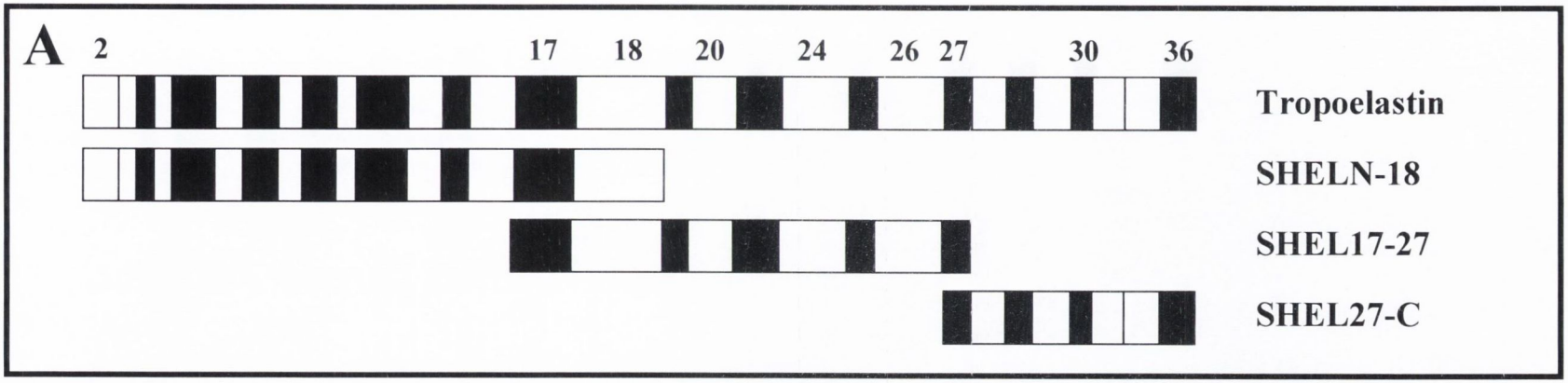

B

Construct	k_a (1/Ms)	k_d (1/s)	K_D (nM)	χ^2
Tropoelastin	$7.10 \pm 0.02 \times 10^{3}$	$2.00 \pm 0.002 \times 10^{-4}$	28 ± 0.1	4.7
SHELN-18	$8.80 \pm 0.02 \times 10^{3}$	$2.80 \pm 0.005 \times 10^{-4}$	31 ± 0.1	0.2
SHEL17-27	$7.95 \pm 0.05 \times 10^{3}$	$2.15 \pm 0.005 \times 10^{-3}$	270 ± 3	9.2

Figure 6.3 rAFnBPA binding to tropoelastin truncates

(A) The domain structure of full-length human tropoelastin is compared with that of constructs SHELN-18, SHEL 17-27 and SHEL27-C, spanning domains 2-18, 17-27 and 27-36, respectively. White segments represent hydrophobic domains while black segments represent hydrophilic crosslinking domains. (B) The rate association constant (k_a), the rate dissociation constant (k_d) and the equilibrium dissociation constant (K_D) of $rAFnBPA_{37-544}$ binding to tropoelastin, SHELN-18 and SHEL17-27 was calculated by curve fitting. The standard error (S.E.) and goodness of the fit (χ^2) is also given. Taken from Clarke, 2006.

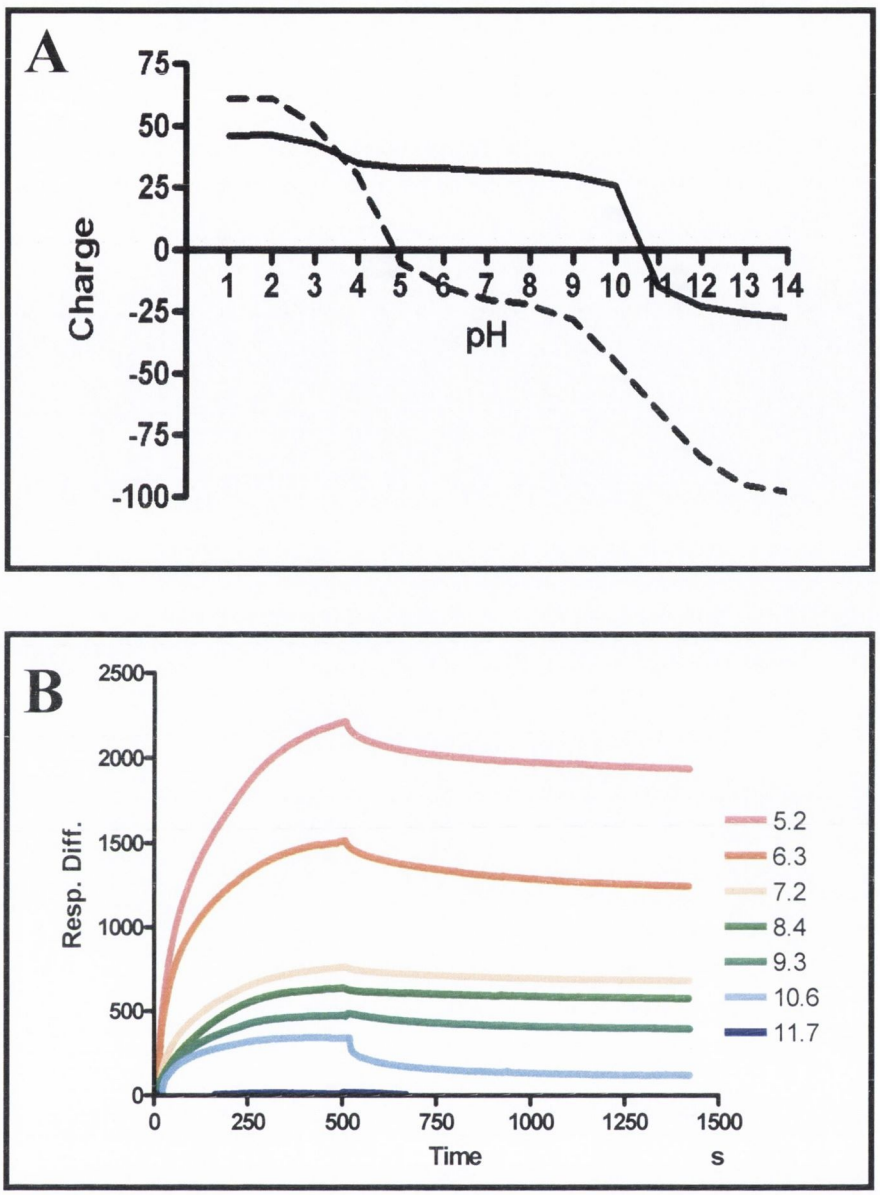

Figure 6.4 Effect of pH on interaction between rAFnBPA$_{37-544}$ and tropoelastin

(A) Titration curve for rAFnBPA$_{37-544}$ and tropoelastin. rAFnBPA$_{37-544}$ (broken line) undergoes a charge transition at is pI of 5 and becomes further negatively charged at pH > 10. Tropoelastin (solid line) undergoes a charge transition at its basic pI of 11. (B) rAFnBPA$_{37-544}$ binding to tropoelastin over a pH range of 5.2 to 11.7. rAFnBPA$_{37-544}$ bound strongly to tropoelastin at low pH with the interaction weakening at higher pH until no interaction was observed at pH=11.7. Taken from Clarke, 2006.

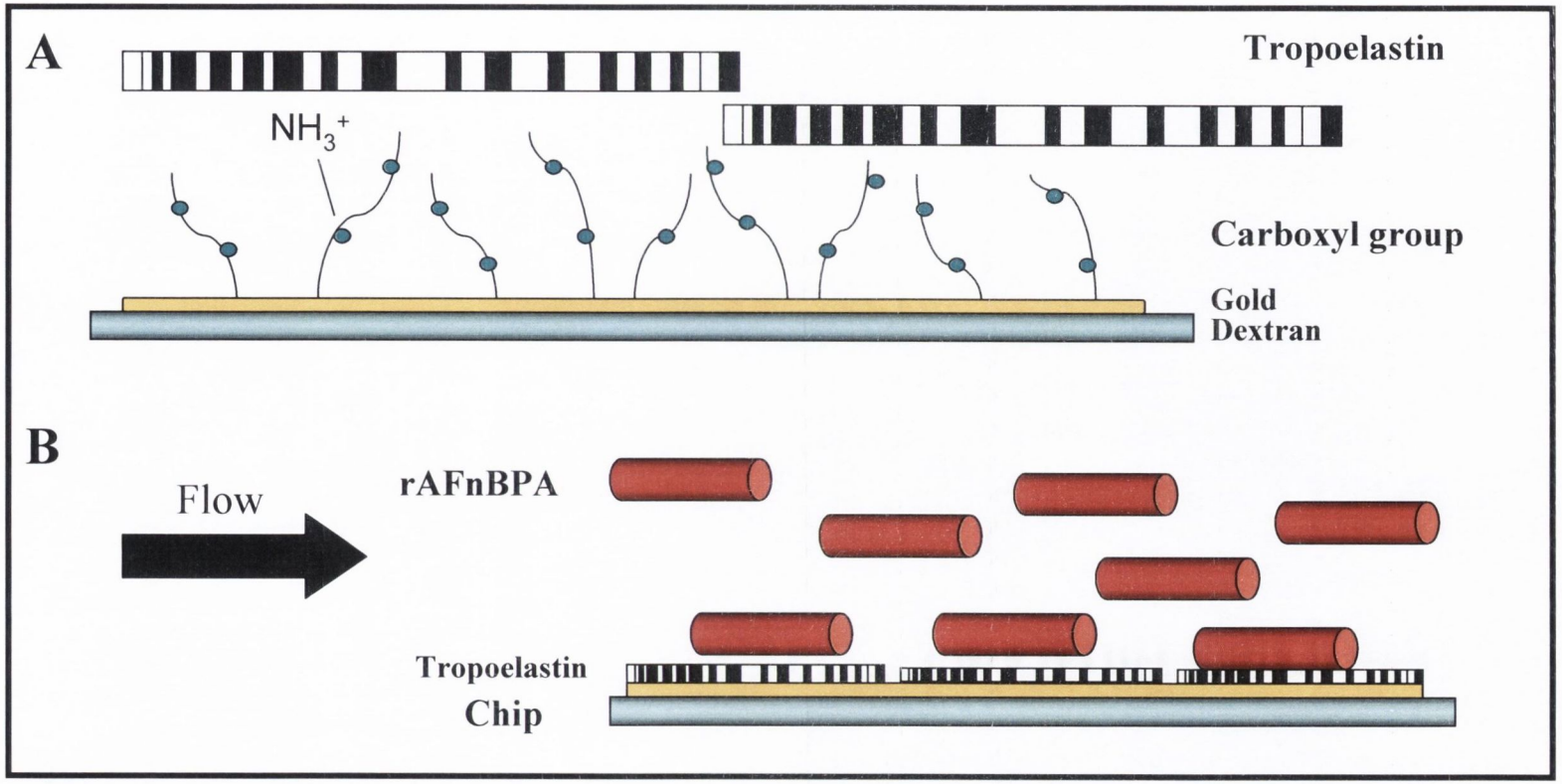

Figure 6.5 Biacore procedure

(A) Full-length recombinant human tropoelastin is immobilised onto a CM5 sensor chip using amine coupling of the lysine residues of tropoelastin to the carboxyl moieties on the dextran chip. (B) Recombinant rAFnBPA proteins are passed over this chip to investigate the kinetics of binding of this protein to immobilised tropoelastin.

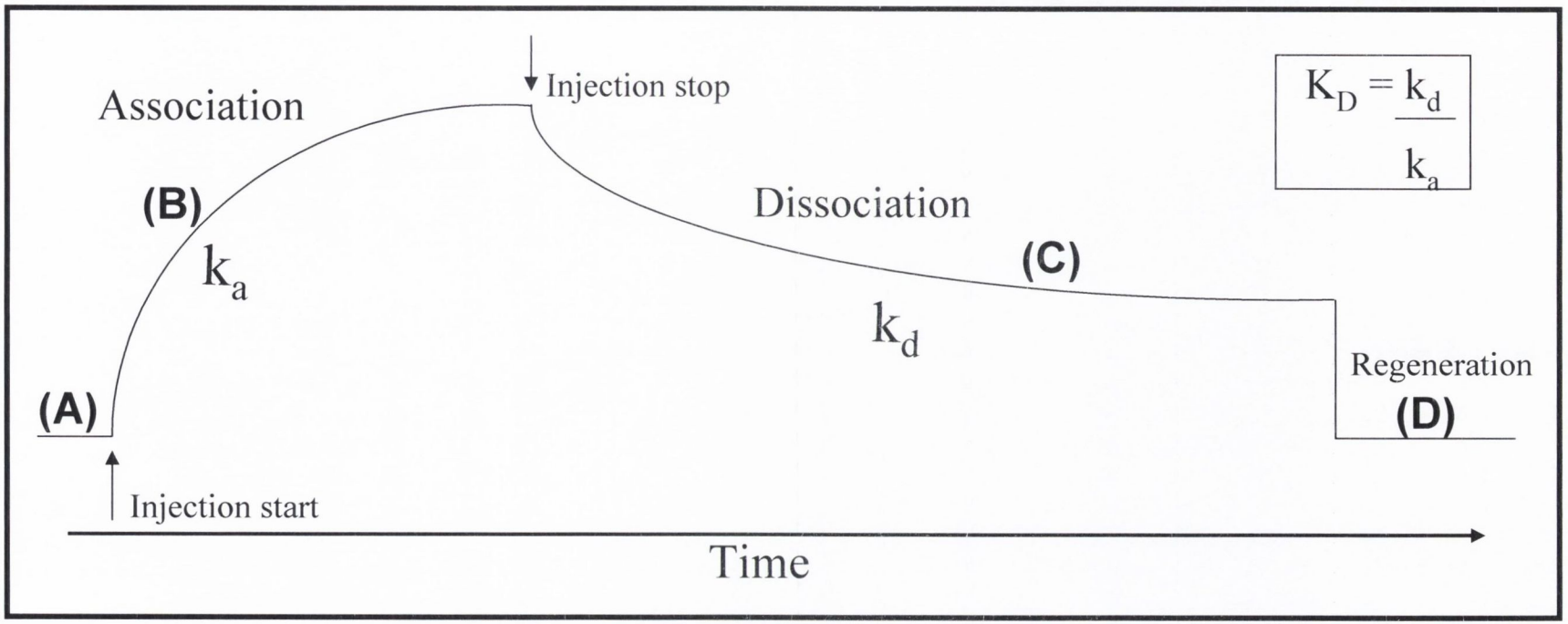

Figure 6.6 Biacore sensogram

(A) Buffer is passed over chip to establish baseline. (B) Injection of rAFnBPA protein causes a dose-dependent and saturable binding response. The rate of this association phase is termed k_a. (C) Buffer is passed over the system to remove unbound rAFnBPA and to investigate the stability of the complex formed between rAFnBPA and tropoelastin. The rate of the dissociation phase is termed k_d. (D) A regeneration buffer is passed over the chip to remove all rAFnBPA and return the system to baseline for the next cycle of a lower dilution of rAFnBPA. The final affinity constant K_D is calculated by k_d/k_a.

6.2 Results

6.2.1 rAFnBPA truncates bind to immobilised tropoelastin

6.2.1.1 rAFnBPA$_{37-511}$ binds to immobilised tropoelastin

Initial investigation of the interaction of FnBPA with tropoelastin in the laboratory of Prof. Weiss at the University of Sydney indicated that rAFnBPA$_{37-544}$ supported binding to the elastin monomer, tropoelastin. It was decided to study this interaction in more detail. Seven variant FnBPA proteins were taken to Prof Weiss' laboratory to compare their interactions with tropoelastin with that of rAFnBPA$_{37-544}$ (Figure 6.7). In this way, the roles of the C-terminal fibronectin-binding motif, the N1 subdomain and several amino acids located in the hydrophobic trench of FnBPA were investigated. Upon arrival in Sydney, these proteins were analysed by SDS-PAGE along with the recombinant human tropoelastin used in Biacore assays (Figure 6.8). All proteins were shown to be intact and of sufficient purity.

Following a more detailed molecular analysis of FnBPA (Pilka *et al.*, 2006; Schwarz-Linek *et al.*, 2003), it was noted that the recombinant protein used in SPR experiments described in Section 6.1 above contained a fibronectin-binding motif at its C-terminus. Indeed this protein supported binding to immobilised fibronectin in solid phase ELISA assays (Section 3.2.8). The true A domain was redefined to span residues 37-511. Recombinant protein rAFnBPA$_{37-511}$ was no longer able to bind fibronectin but retained the ability to bind immobilised fibrinogen and elastin (Figure 3.28). This protein was tested for its ability to bind immobilised human tropoelastin by SPR analysis. A strong dose-dependent association was observed along with little dissociation over the time measured until regeneration. The dissociation constant (K_D) of 127 ± 4 nM (Figure 6.9) is approximately 3-fold higher than the half maximum binding constant estimated for rAFnBPA$_{37-511}$ binding to immobilised elastin peptides by ELISA methods. The C-terminal residues 512-544 are therefore not involved in binding to tropoelastin. These data show that the true A domain of FnBPA is responsible for the binding of this protein to immobilised fibrinogen, elastin peptides and tropoelastin.

6.2.1.2 rAFnBPA$_{194-511}$ binds to immobilised tropoelastin

A further truncate, rAFnBPA$_{194-511}$, encompassing only subdomains N2 and N3 of region A was also able to bind to immobilised fibrinogen and elastin peptides with similar affinity to that of rAFnBPA$_{37-511}$ (Figure 3.28). This protein was also tested for binding to immobilised tropoelastin by SPR analysis and showed a dissociation constant of 146 ± 6 nM,

similar to that of rAFnBPA$_{37\text{-}511}$ (Figure 6.10). The K_D value of 146 ± 6 nM is approximately 3-fold higher than the half maximum binding constant estimated for rAFnBPA$_{194\text{-}511}$ binding to immobilised elastin peptides by ELISA methods. Both rAFnBPA$_{37\text{-}511}$ (N1N2N3) and rAFnBPA$_{194\text{-}511}$ (N2N3) recombinant proteins bound to tropoelastin in a dose-dependent manner with similar strong association and weak dissociation. This confirms previous data that the N1 subdomain of region A is not involved in ligand binding. These data show a five fold decrease in affinity for these constructs compared to experiments carried out with the initial rAFnBPA$_{37\text{-}544}$ protein, however all three proteins bind to tropoelastin in the low nanomolar range which indicates a significant biological interaction.

6.2.1.3 rAFnBPA$_{37\text{-}511}$ alanine-substituted proteins bind to immobilised tropoelastin

Any further truncation of rAFnBPA$_{194\text{-}511}$ would likely impinge on the predicted structural folds of this protein so a more precise approach was adopted to construct alanine-substituted variants of rAFnBPA$_{37\text{-}511}$. The A domain of FnBPA has sequence similarity to ClfA and binds to the same region of the γ chain of fibrinogen. A theoretical model of the N2N3 subdomains of FnBPA was generated based on the known crystal structure of ClfA (Deivanayagam *et al.*, 2002). The segment of fibrinogen to which this protein binds was docked *in silico* into the putative ligand-binding trench situated between N2 and N3. This model gave a detailed insight into the possible mechanism of fibrinogen binding and was used to predict residues in FnBPA that might be crucial in making contact with a ligand. Several residues were targeted for alanine substitution and resulting recombinant proteins were tested for fibrinogen and elastin peptide binding (Chapter 4). Some mutants had reduced affinity for elastin peptides with rAFnBPA$_{37\text{-}511}$ F306A and a double mutant, rAFnBPA$_{37\text{-}511}$ N304A/F306A, both showing a dramatic loss in elastin peptide binding. Five alanine-substituted proteins of rAFnBPA$_{37\text{-}511}$ were tested for their ability to bind to immobilised tropoelastin by Biacore. The proteins chosen contained substitutions which showed varying decreases in affinity for elastin peptides (R224A, L498A and N304A) and those which showed undetectable binding to immobilised elastin peptides by ELISA methods (F306A, N304A/F306A). The position of these residues in the putative ligand binding trench of rAFnBPA is indicated in Figure 6.11. Despite their inability to bind to immobilised elastin peptides, dissociation constants of 135 ± 7 nM and 171 ± 9 nM were obtained for proteins rAFnBPA$_{37\text{-}511}$ F306A (Figure 6.12) and rAFnBPA$_{37\text{-}511}$ N304A/F306A (Figure 6.13), respectively. This indicates that the amino acids that are involved in binding to elastin

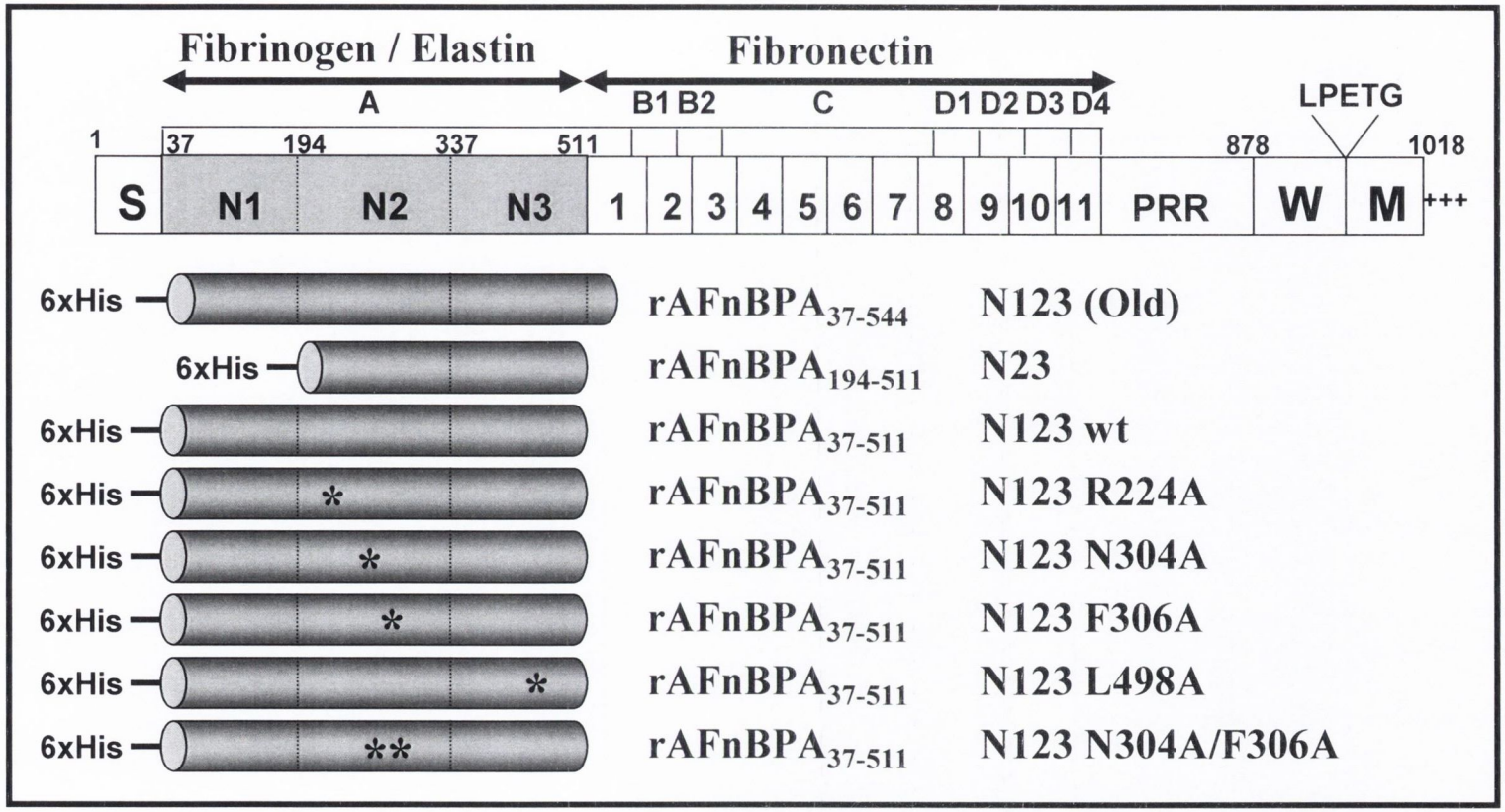

Figure 6.7 Structural organisation of FnBPA and recombinant truncated derivatives

The domain organisation of FnBPA is shown as previously described. Recombinant truncated derivatives used in Biacore assays are indicated below full-length protein. $rAFnBPA_{37\text{-}544}$ was initially used to assess the binding to immobilised tropoelastin. Further truncates, along with alanine-substituted variants of $rAFnBPA_{37\text{-}511}$ were used in subsequent analaysis.

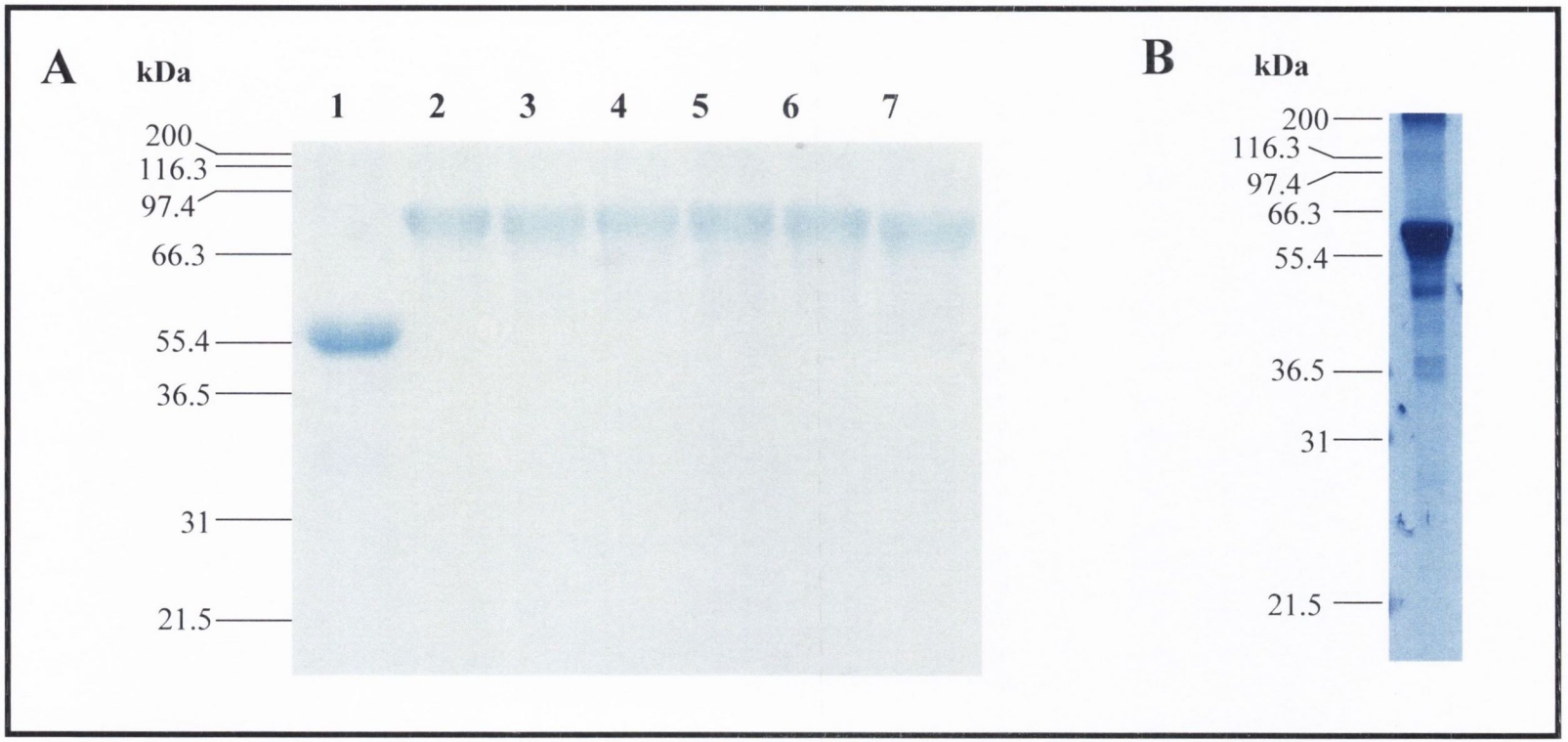

Figure 6.8 SDS PAGE analysis of rAFnBPA proteins and recombinant human tropoelastin

(A) 20 μM of $rAFnBPA_{194-511}$ (1), $rAFnBPA_{37-511}$ wild-type (2), R224A (3), N304A (4), F306A (5), L498A (6) and N304A/F306A (7) were analysed by SDS-PAGE and stained with GradiPure electrophoresis stain. (B) Recombinant human tropoelastin was analysed by SDS-PAGE and stained with GradiPure electrophoresis stain.

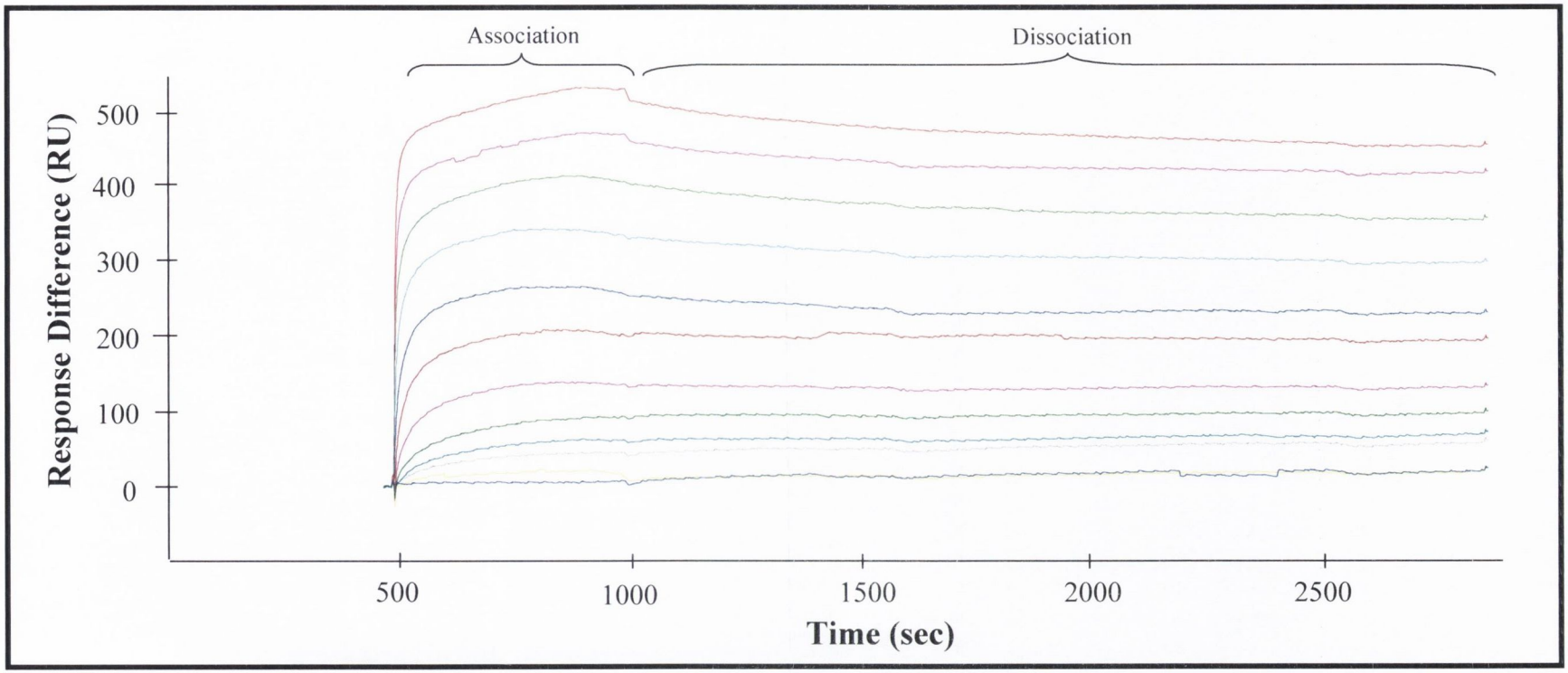

Figure 6.9 SPR analysis of rAFnBPA$_{37-511}$ wt binding to immobilised full-length tropoelastin at pH 7.0

Full-length human tropoelastin was immobilized on the surface of a CM5 sensor chip. rAFnBPA$_{37-511}$ wt was passed over the surface at concentrations ranging from 13 μM (topmost red trace) to 0 nM (bottommost blue trace). A strong interaction was observed between the proteins with little dissociation. The association and dissociation phase were fitted separately to yield k_a and k_d respectively, thus allowing K_D to be calculated. The sensogram shown is a representative of three independent experiments.

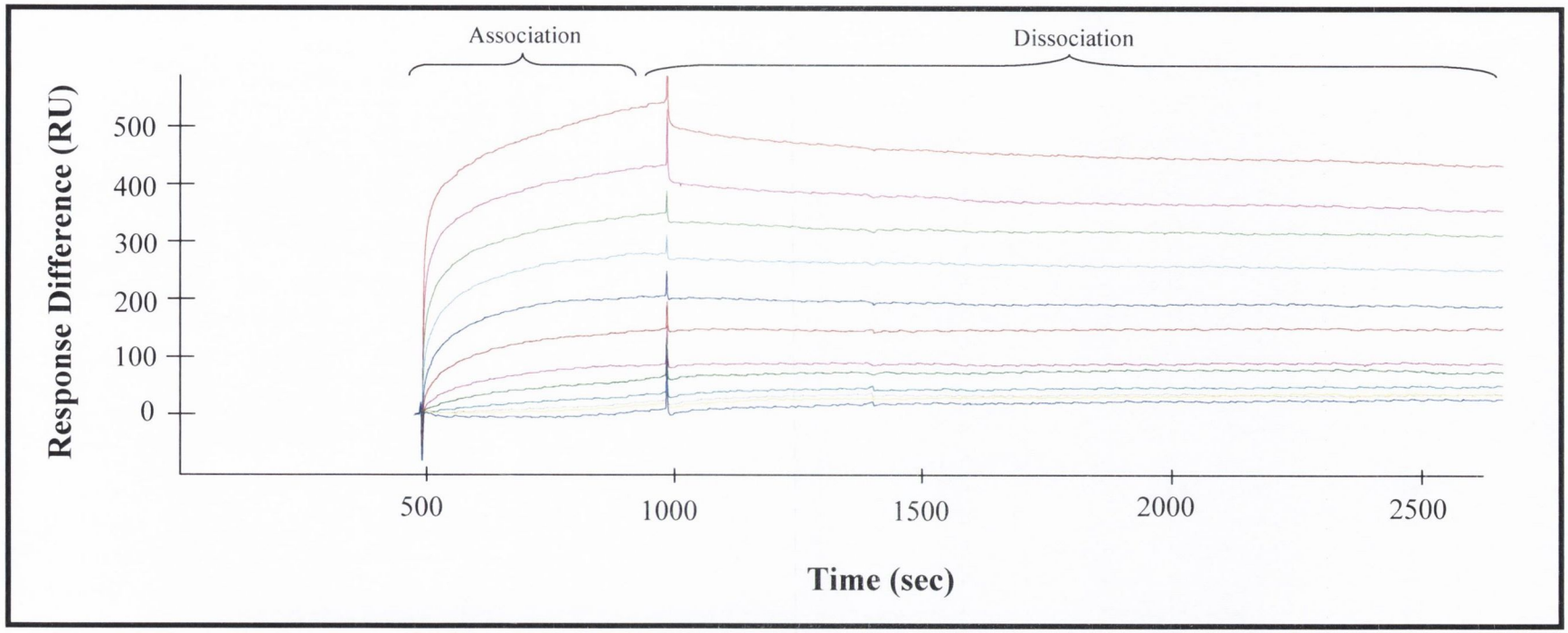

Figure 6.10 SPR analysis of rAFnBPA$_{194-511}$ wt binding to immobilised full-length tropoelastin at pH 7.0

Full-length human tropoelastin was immobilized on the surface of a CM5 sensor chip. rAFnBPA$_{194-511}$ wt was passed over the surface at concentrations ranging from 13 μM (topmost red trace) to 0 nM (bottommost blue trace). A strong interaction was observed between the proteins with little dissociation. The association and dissociation phase were fitted separately to yield k_a and k_d respectively, thus allowing K_D to be calculated. The sensogram shown is a representative of three independent experiments.

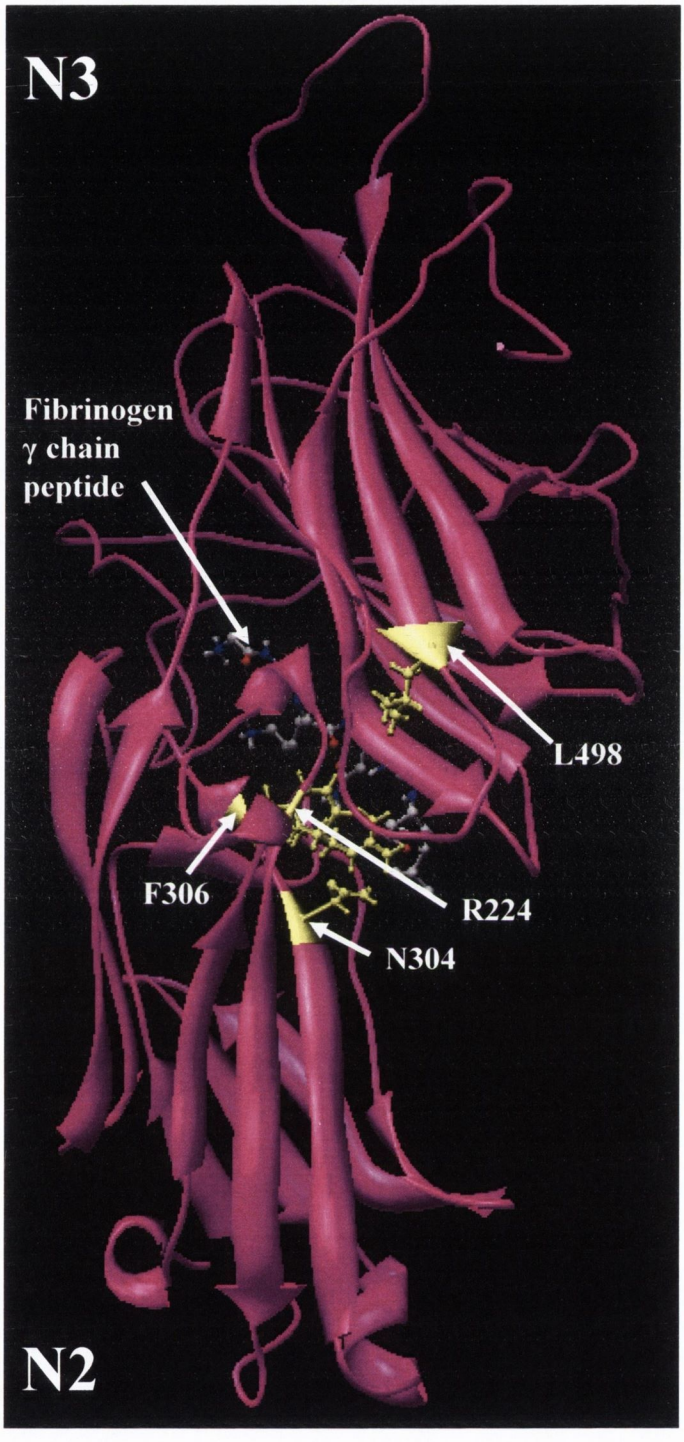

Figure 6.11 Site of amino acid substitutions of rAFnBPA

Predicted 3D structure of rAFnBPA$_{194\text{-}511}$ (N2N3), with the fibrinogen ligand (G_{404}AKQAGDV$_{411}$) docked into the trench between N2 and N3 of this structure. Amino acids R224, N304, F306 and L498 of FnBPA are shown in yellow with their side chains visible in ball and stick format.

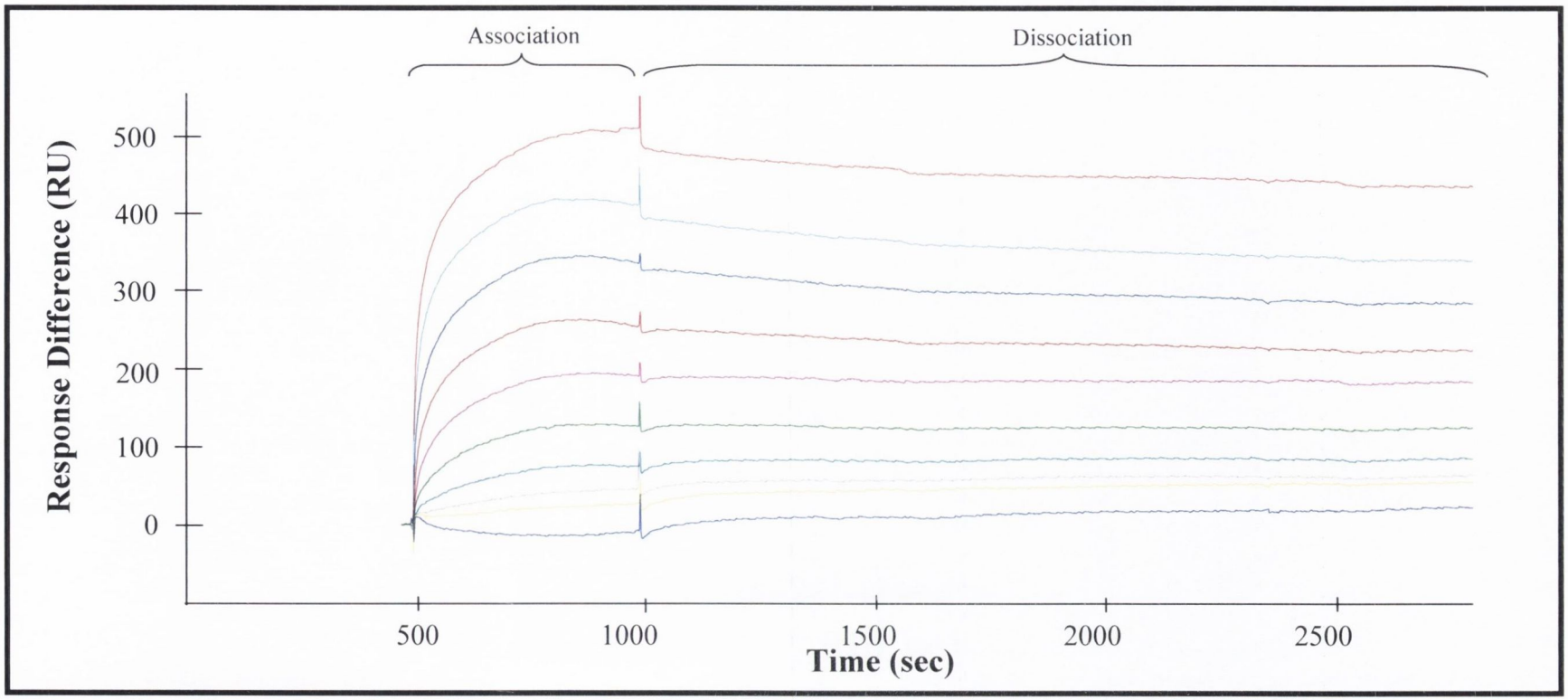

Figure 6.12 SPR analysis of rAFnBPA$_{37\text{-}511}$ F306A binding to immobilised full-length tropoelastin at pH 7.0

Full-length human tropoelastin was immobilized on the surface of a CM5 sensor chip. rAFnBPA$_{37\text{-}511}$ F306A was passed over the surface at concentrations ranging from 3.25 μM (topmost red trace) to 0 nM (bottommost blue trace). A strong interaction was observed between the proteins with little dissociation. The association and dissociation phase were fitted separately to yield k_a and k_d respectively, thus allowing K_D to be calculated. The sensogram shown is a representative of three independent experiments.

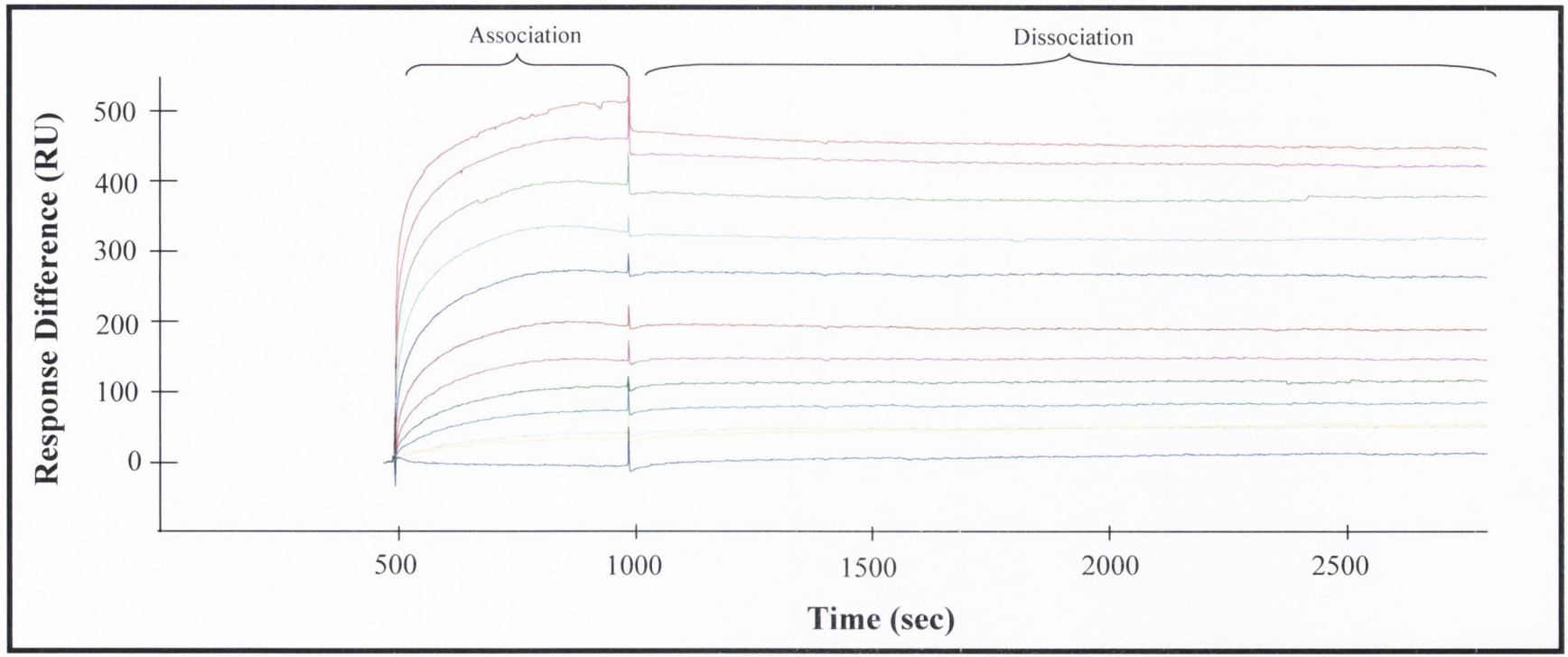

Figure 6.13 SPR analysis of rAFnBPA$_{37-511}$ N304A/F306A binding to immobilised full-length tropoelastin at pH 7.0

Full-length human tropoelastin was immobilized on the surface of a CM5 sensor chip. rAFnBPA$_{37-511}$ N304A/F306A was passed over the surface at concentrations ranging from 13 μM (topmost red trace) to 0 nM (bottommost blue trace). A strong interaction was observed between the proteins with little dissociation. The association and dissociation phase were fitted separately to yield k_a and k_d respectively, thus allowing K_D to be calculated. The sensogram shown is a representative of three independent experiments.

peptides are not involved in tropoelastin binding. Two other substituted proteins, rAFnBPA$_{37\text{-}511}$ R224A and rAFnBPA$_{37\text{-}511}$ L498A also showed no defect in tropoelastin binding, having K_Ds of 201 ± 10 nM (Figure 6.14) and 179 ± 9 nM, respectively (Figure 6.15). The k_a values for these proteins range from $9.53e^3$ to $1.45e^4$ with k_d values ranging from $1.29e^{-3}$ to $2.5e^{-3}$.

rAFnBPA$_{37\text{-}511}$ N304A showed a ~ 4.5-fold increased affinity for tropoelastin with a K_D of 27 ± 4 nM (Figure 6.16) which is in the same range as the K_D observed for the initial rAFnBPA$_{37\text{-}544}$ protein binding to tropoelastin. This increased affinity is due to the contribution of both an increased k_a and a decreased k_d to the final K_D value for this protein. The errors associated with both k_a and k_d of this interaction are quite large. If this increased affinity is reproducible, a corresponding increased affinity should be seen for the double mutant rAFnBPA$_{37\text{-}511}$ N304A/F306A. However this mutant does not have an increased affinity for tropoelastin. It is not likely that N304 is important in tropoelastin binding.

SPR analysis shows that all variant proteins of rAFnBPA bind to tropoelastin with the same or slightly increased affinity as rAFnBPA$_{37\text{-}511}$ (Table 6.1). All proteins tested showed a strong association with little or weak dissociation. The alanine substitution of residues situated around the hydrophobic trench therefore does not have any adverse affect on the interaction of this protein with immobilised human tropoelastin by Biacore.

6.2.2 Inhibition of rAFnBPA$_{37\text{-}511}$ binding to immobilised elastin peptides using soluble desmosine/isodesmosine

As mentioned in Section 6.1 above one of the major differences between elastin peptides and soluble tropoelastin is the presence of desmosine crosslinks in elastin peptides. To test whether the presence of these unique structure are vital in the interaction between rAFnBPA and elastin peptides, they were used in inhibition studies. An equimolar mixture of soluble desmosine and isodesmosine is commercially available. rAFnBPA$_{37\text{-}511}$ was preincubated with this mixture before being added to elastin-coated wells in an ELISA assay. A concentration of 25 μM resulted in >80% inhibition of rAFnBPA$_{37\text{-}511}$ binding to elastin peptide coated wells (Figure 6.17). This indicates that soluble desmosine/isodesmosine may bind into the hydrophobic trench thus preventing the interaction with elastin peptides. In agreement with this, inhibition was also observed for the binding of rAFnBPA$_{37\text{-}511}$ to fibrinogen although this inhibition was less potent. The higher affinity of rAFnBPA$_{37\text{-}511}$ for fibrinogen could result in the weaker inhibition seen with desmosine/isodesmosine.

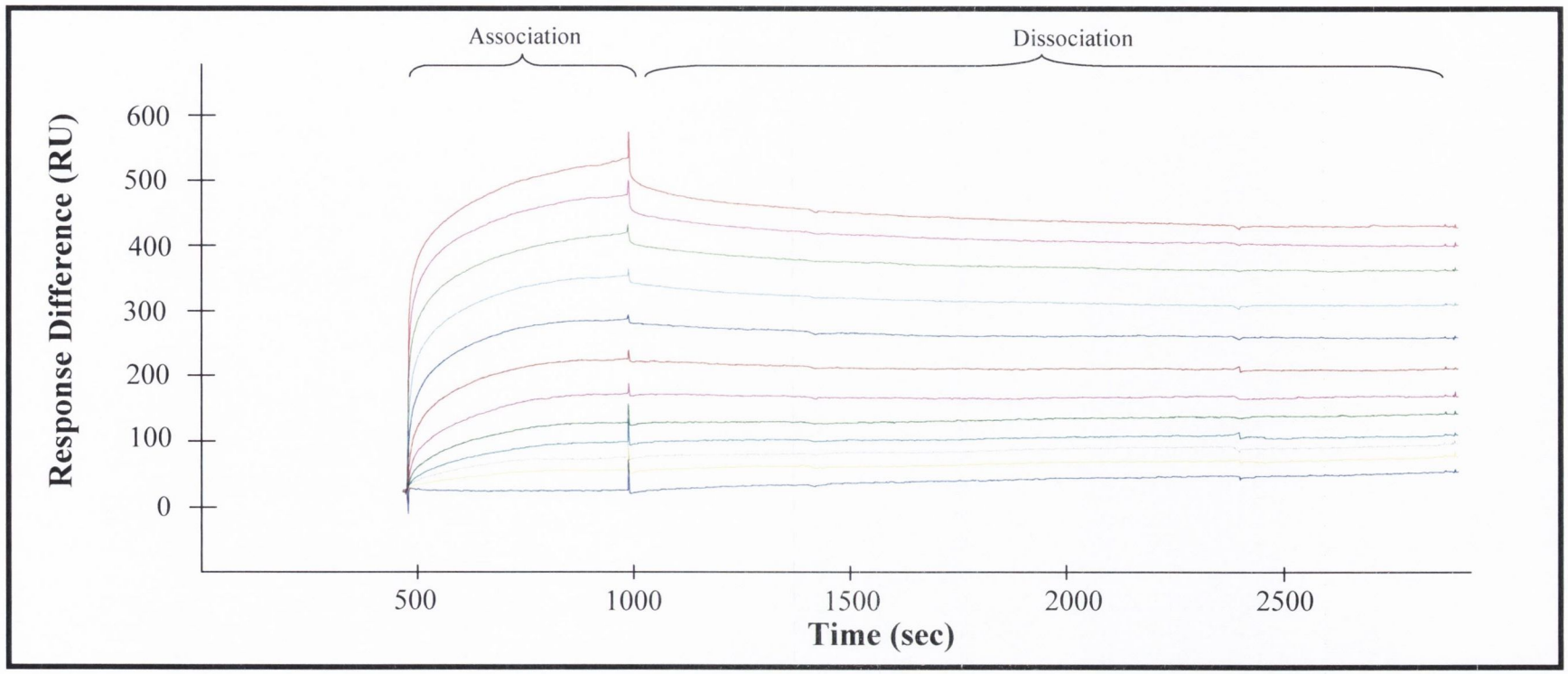

Figure 6.14 SPR analysis of rAFnBPA$_{37-511}$ R224A binding to immobilised full-length tropoelastin at pH 7.0

Full-length human tropoelastin was immobilized on the surface of a CM5 sensor chip. rAFnBPA$_{37-511}$ R224A was passed over the surface at concentrations ranging from 13 μM (topmost red trace) to 0 nM (bottommost blue trace). A strong interaction was observed between the proteins with little dissociation. The association and dissociation phase were fitted separately to yield k_a and k_d respectively, thus allowing K_D to be calculated. The sensogram shown is a representative of three independent experiments.

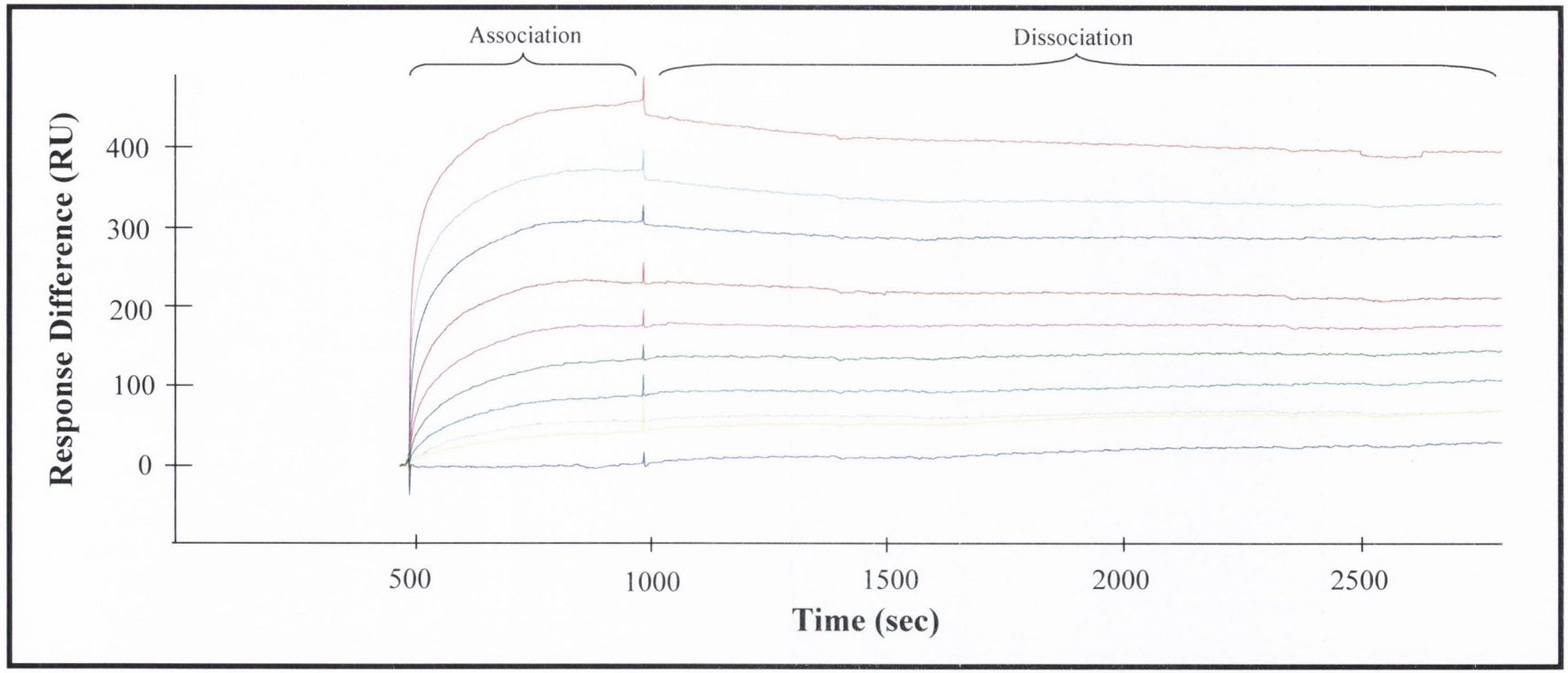

Figure 6.15 SPR analysis of rAFnBPA$_{37\text{-}511}$ L498A binding to immobilised full-length tropoelastin at pH 7.0

Full-length human tropoelastin was immobilized on the surface of a CM5 sensor chip. rAFnBPA$_{37\text{-}511}$ L498A was passed over the surface at concentrations ranging from 3.25 μM (topmost red trace) to 0 nM (bottommost blue trace). A strong interaction was observed between the proteins with little dissociation. The association and dissociation phase were fitted separately to yield k_a and k_d respectively, thus allowing K_D to be calculated. The sensogram shown is a representative of three independent experiments.

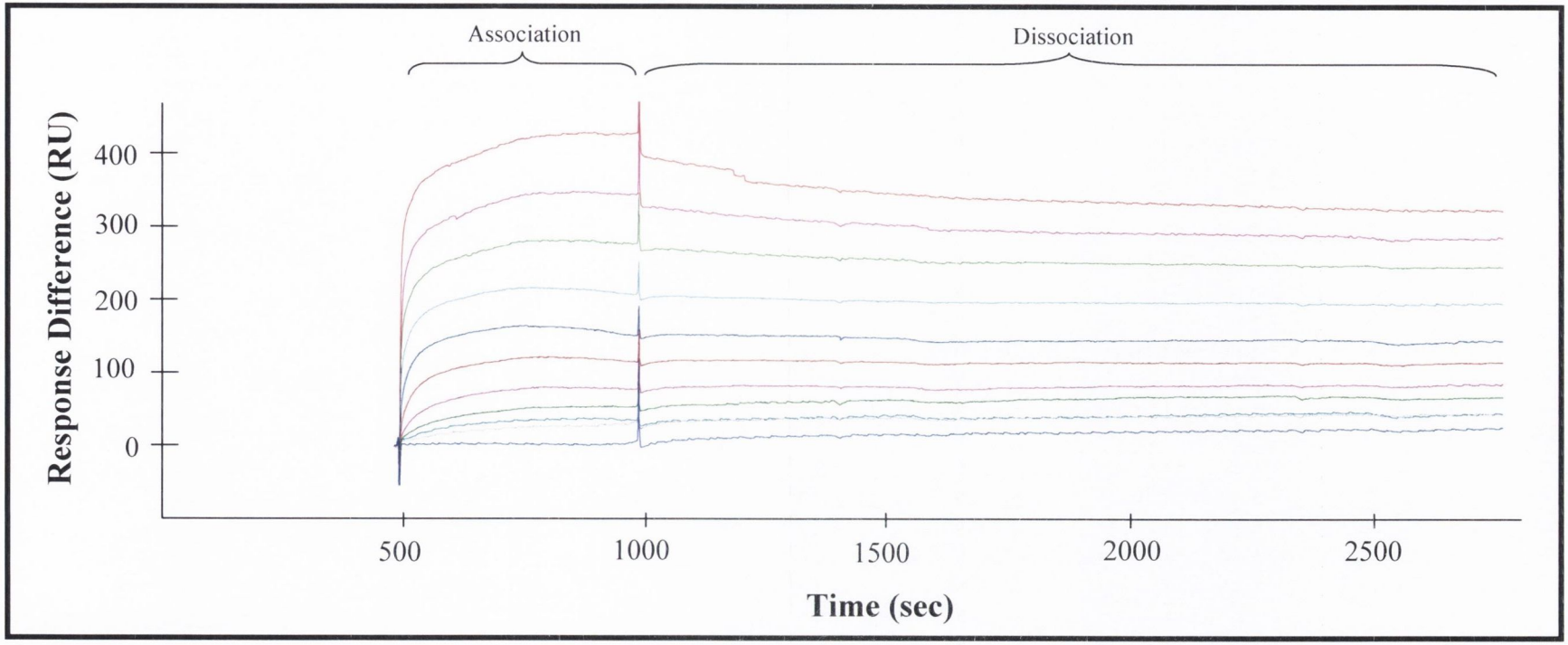

Figure 6.16 SPR analysis of rAFnBPA$_{37\text{-}511}$ N304A binding to immobilised full-length tropoelastin at pH 7.0

Full-length human tropoelastin was immobilized on the surface of a CM5 sensor chip. rAFnBPA$_{37\text{-}511}$ N304A was passed over the surface at concentrations ranging from 13 μM (topmost red trace) to 0 nM (bottommost blue trace). A strong interaction was observed between the proteins with little dissociation. The association and dissociation phase were fitted separately to yield k_a and k_d respectively, thus allowing K_D to be calculated. The sensogram shown is a representative of three independent experiments.

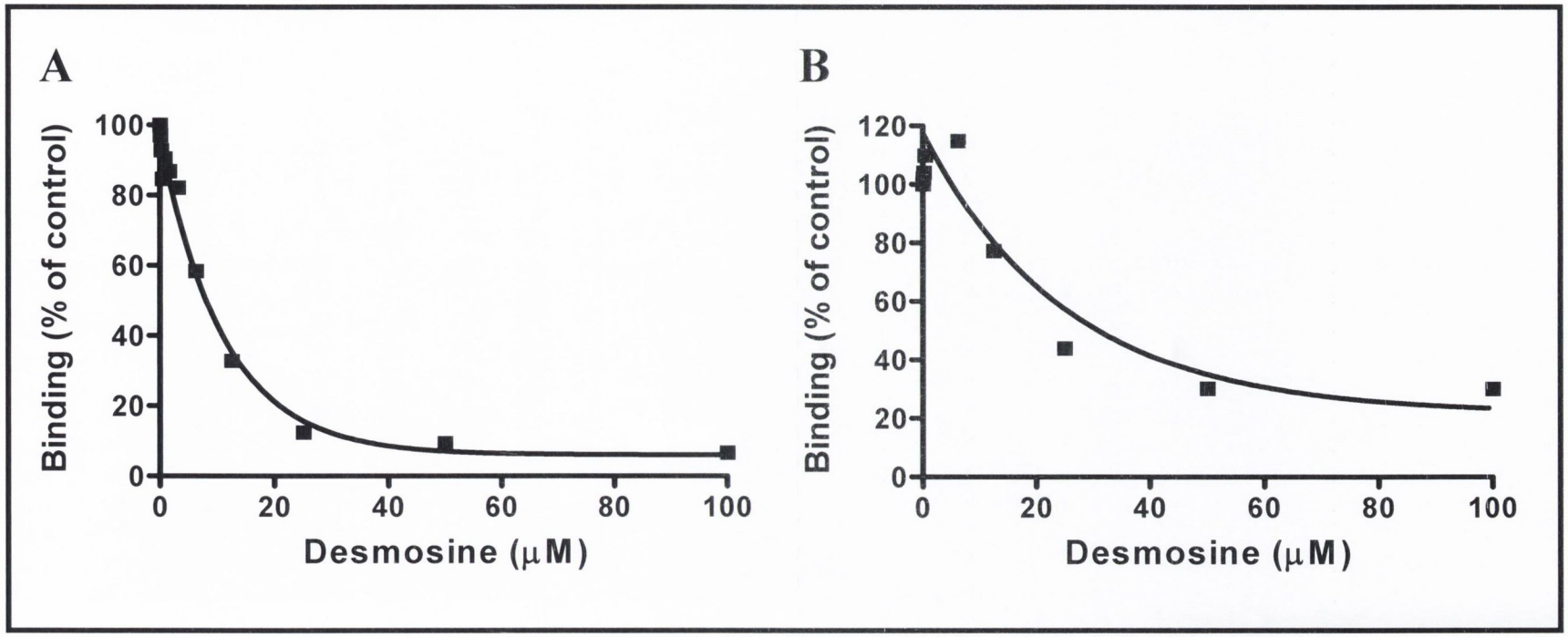

Figure 6.17 Inhibition of rAFnBPA$_{37-511}$ binding to immobilised elastin and fibrinogen using soluble desmsoine

Microtitre plates were coated with 10 μg/ml human aortic elastin (A) or fibrinogen (B). 0.1 μM (A) or 0.03 μM (B) of rAFnBPA$_{37-511}$ was preincubated with increasing amounts of soluble desmosine (100 μM – 0 μM) before being added to ligand-coated wells. Bound protein was detected with polyclonal anti-rAFnBPA antibodies and goat anti-rabbit HRP-conjugated antibodies followed by development with TMB substrate. Data points represent the mean of triplicate wells and are expressed as a percentage of control wells lacking inhibitor. This figure is representative of three independent experiments.

Protein	k_a (1/Ms)	SE k_a	χ^2 k_a	k_d (1/s)	SE k_d	χ^2 k_d	K_D (nM)	SE K_D
rAFnBPA$_{194-511}$	$1.07x10^4$	452	9.49	$1.47x10^{-3}$	$5.91x10^{-5}$	3.49	146	6
rAFnBPA$_{37-511}$								
Wild type	$1.34x10^4$	672	9.74	$1.42x10^{-3}$	$4.63x10^{-5}$	1.98	127	4
R224A	$9.74x10^3$	489	9.73	$1.79x10^{-3}$	$8.81x10^{-5}$	3.17	201	10
N304A	$2.13x10^4$	1120	9.49	$6.75x10^{-4}$	$8.7x10^{-5}$	2.52	27	4
F306A	$1.02x10^4$	457	9.64	$1.29x10^{-3}$	$6.58x10^{-5}$	2.36	135	7
L498A	$9.53x10^3$	530	9.81	$1.74x10^{-3}$	$8.4x10^{-5}$	2.74	179	9
N304A/F306A	$1.45x10^4$	319	9.76	$2.5x10^{-3}$	$1.32x10^{-4}$	1.65	171	9

Table 6.1 Binding of rAFnBPA constructs to immobilised tropoelastin

The rate association constant (k_a), the rate dissociation constant (k_d) and the equilibrium dissociation constant (K_D) of rAFnBPA constructs binding to full-length tropoelastin was calculated by curve fitting using BiaEvaluation 4.1. The standard error (S.E.) and goodness of the fit (χ^2) is also given.

6.3 Discussion

The adherence of $rAFnBPA_{37-544}$ to immobilised α-elastin peptides prompted an investigation to determine if $rAFnBPA_{37-544}$ could also interact with the elastin precursor, tropoelastin. Surface plasmon resonance analysis was performed by researchers in the laboratory of Prof. Weiss, University of Sydney, testing the binding of soluble rAFnBPA proteins to immobilised tropoelastin. $rAFnBPA_{37-544}$ bound strongly to full-length tropoelastin with a K_D of 28 ± 0.1 nM. In an attempt to narrow down the binding site within tropoelastin for rAFnBPA, three truncates of tropoelastin were tested. Binding to full-length tropoelastin was identical to that seen between $rAFnBPA_{37-544}$ and SHELN-18 with almost identical k_a and k_d and subsequent K_D values. Weaker binding to SHEL17-27 was observed while $rAFnBPA_{37-544}$ bound to SHEL27-C in a strong manner with slow dissociation but no curve fitting could be performed to generate reliable kinetic data. These results suggest that FnBPA interacts with tropoelastin at multiple sites. It is possible however that the N-terminus of tropoelastin contains the dominant binding region. Interaction with domains 17 to the C-terminus may support initial binding followed by sliding to the dominant binding region in the N-terminus to stabilize the interaction. It is worth noting however, that SHELN-18 is the longest tropoelastin fragment screened in this study and the stronger binding could be attributed to this. Analysis of binding to smaller tropoelastin fragments may help to narrow down the binding site for FnBPA within tropoelastin. This approach however has some disadvantages as further truncations of SHEL constructs will still contain short repetitive motifs that are present throughout the entire protein. It is also likely that secondary structure of these constructs will be lost.

Initial screening of the interaction between $rAFnBPA_{37-544}$ and tropoelastin revealed that a successful regeneration of the sensor chip surface could be achieved using a regeneration solution with high pH. This finding led to further investigation in which the binding was monitored at varying pH with the aim of determining the nature of the interaction. At pH below 11 an interaction was observed between the two proteins. At pH 11 and above no binding occurred. It is possible that this loss of binding is due to conformational changes induced by such a basic environment. However the pH dependent nature of the interaction is clear with binding occurring over a broad range of pH up to and including pH 10.6, which demonstrates a specific dose-dependent interaction. The binding profile of the two proteins at lower pHs can be explained by the charged states of each protein at different pHs. As

observed in the theoretical pH titration curve, tropoelastin undergoes a charge transition at pH 11, the same pH at which binding is eliminated. This indicates that the positively-charged lysines on tropoelastin may contribute to the interaction. As most of the lysines in tropoelastin exist in either KA or KP regions and are distributed throughout tropoelastin in alternating domains to facilitate crosslinking, this further explains the observation that binding occurs at multiple sites. At pH > 5, rAFnBPA$_{37\text{-}544}$ is negatively charged and is thus free to interact with the positively-charged lysines of tropoelastin. This result demonstrates that ionic interactions between positive regions on tropoelastin and negatively-charged regions of rAFnBPA$_{37\text{-}544}$ stabilize the binding between the proteins. These multiple surface-surface interactions promote dose-dependent binding by SPR and could indicate a mechanism to allow *S. aureus* to bind to human tropoelastin *in vivo*. As the binding between rAFnBPA and tropoelastin is likely to occur at multiple sites via a surface charge-charge interaction, numerous tropoelastin peptides of differing sequences are likely to bind making it difficult to define the exact binding site for FnBPA within tropoelastin.

To further define the binding site for tropoelastin within rAFnBPA, two truncates of rAFnBPA$_{37\text{-}544}$ were tested in this study for binding to immobilised tropoelastin by Biacore analysis. rAFnBPA$_{37\text{-}511}$ and rAFnBPA$_{194\text{-}511}$, representing subdomains N1N2N3 and N2N3, respectively, both bound to immobilised tropoelastin with similar affinities, demonstrating that the N1 subdomain is not required in binding this ligand. The investigation of the binding of rAFnBPA$_{37\text{-}511}$ to immobilised α-elastin peptides highlighted crucial residues within the putative ligand-binding trench of FnBPA. Substitution of these residues with alanine had a dramatic effect on elastin binding. In this study, recombinant alanine variants of rAFnBPA$_{37\text{-}511}$ were tested for binding to the tropoelastin monomer. rAFnBPA$_{37\text{-}511}$ bound to tropoelastin with a K_D of 127 ± 4 nM, a 4.5 fold decrease in affinity compared to that of rAFnBPA$_{37\text{-}544}$. This decrease in affinity of rAFnBPA$_{37\text{-}511}$ for full-length tropoelastin compared to that of rAFnBPA$_{37\text{-}544}$ may be explained by the possibility of further surface-surface interactions occurring with the larger protein spanning residues 37-544. The range of K_Ds observed for the alanine-substituted rAFnBPA$_{37\text{-}511}$ proteins, however did not differ significantly from that of rAFnBPA$_{37\text{-}511}$ wt. rAFnBPA$_{37\text{-}511}$ N304A had a ~5 fold decrease in K_D bringing it into the affinity range seen for that of rAFnBPA$_{37\text{-}544}$. This shows that residues located along the hydrophobic trench situated between N2 and N3 of region A of FnBPA that have important roles in the binding of fibrinogen and α-elastin peptides, are not involved in tropoelastin binding. The hypothesis that FnBPA binds to tropoelastin by a charge/surface interaction is

further supported by the fact that the alanine-substituted residues which are located in the interior of the FnBPA protein and whose side chains point into the hydrophobic trench, had no role in tropoelastin binding. The elastin peptides used in previous ELISA assays are a heterogeneous mix of digested fragments of aortic elastin prepared by hot oxalic acid treatment of human elastic tissue. This process likely exposes sites available for binding into the trench of rAFnBPA. These sites however, would not be exposed in intact recombinant tropoelastin. Thus FnBPA binds to tropoelastin and digested α-elastin peptides by distinct mechanisms.

It has already been shown by inhibition with the fibrinogen γ chain peptide and by alanine-substitution of residues such as N304 and F306 that elastin peptides bind to FnBPA by docking into the hydrophobic trench. It is conceivable that the desmosine crosslinks present in these peptides make vital contact with the residues lining the trench. In this way, preincubation of $rAFnBPA_{37\text{-}511}$ with soluble desmosine/isodesmosine structures may saturate the binding sites within the trench thereby blocking binding of both elastin peptides and fibrinogen. The higher concentration of desmosine/isodesmosine needed to inhibit binding to fibrinogen is indicative of the higher affinity rAFnBPA has for fibrinogen over elastin. Inhibition by steric hindrance cannot be ruled out but is thought unlikely as these unique amino acids are relatively small in size. Unsuccessful attempts were made to find a similar ringed structure to use in control inhibition studies which would be important to ascertain the specificity of the interaction. The inhibition of FnBPA binding to both ligands with desmosine/isodesmosine is further indication that elastin and fibrinogen bind to FnBPA in a similar manner.

This is the first demonstration that the A domain of FnBPA from *S. aureus* promotes binding to human tropoelastin. Investigation into this interaction using truncates of tropoelastin show a similar affinity of rAFnBPA for full-length tropoelastin as for SHELN-18 which may suggest that there is a dominant FnBPA binding site located in the N-terminus of tropoelastin. The pH dependent nature of the interaction indicates that the interaction is likely to occur by charge-charge contacts on the surfaces of both molecules. The alanine substitution of residues situated around the hydrophobic trench of rAFnBPA does not have any adverse affect on the interaction of this protein with immobilised human tropoelastin. This is in stark contrast to the interaction seen between rAFnBPA and α-elastin, which occurs by residues located along the hydrophobic trench between N2 and N3 of rAFnBPA (e.g. N304 and F306) making crucial contact with elastin peptides exposed by acidic digestion of elastic tissue. The

inhibition of rAFnBPA$_{37-511}$ binding to immobilised fibrinogen and elastin peptides with soluble desmosine/isodesmosine indicates that these structures may have a role in α-elastin interactions. Attempts to locate a similar aromatic compound to act as a negative control in these assays were in vain so it cannot be ruled out that steric hindrance caused the observed inhibition. It can be concluded that the mechanism of tropoelastin binding is distinct from that of elastin peptide binding.

The binding of *S. aureus* surface proteins to multiple ligands is widely recognized. FnBPA is indeed a multifunctional protein, binding diverse matrix proteins such as fibronectin, fibrinogen and elastin. *S. aureus* encounters elastin on its journey through blood vessel walls, traversing the extracellular space beneath the basement membrane of endothelial cells in tissue such as lung and around the synovial lining of various joints. During the course of an infection, both bacterial and host elastases are active. *S. aureus* is known to produce a cysteine protease, ScpB which degrades elastin tissue and is inhibited by α2-macroglobulin (Potempa *et al.*, 1988). It also produces a serine protease, SspA which inactivates α-1 proteinase inhibitor (α-1PI), a major factor which protects lungs from phagocytic proteases (Nowak and Miedzobrodzki, 1991). Thus, lung damage during *S. aureus* infection may partly depend on ScpB and SspA. In addition, *S. aureus* has been shown to induce the production of host matrix proteases in human dermal and synovial fibroblasts, both of which are located in elastin-rich tissue (Kanangat *et al.*, 2006). As *S. aureus* traverses the extracellular matrix during systemic infection, it many encounter different forms of elastic tissue due to the degradation of elastin induced by bacterial or host elastases and the subsequent repair of elastin tissue. Two methods of elastin repair have been described. The first was termed the salvage method, whereby elastin repair occurs by reincorporation of proteolytically damaged elastin peptides into the extracellular matrix, rendering it resistant to hot alkali solubilisation (Stone *et al.*, 1988). The second mechanism is *de novo* synthesis which involves a sequential process of enzymatic removal of damaged fibres followed by a localised upregulation of elastin mRNA levels and subsequent tropoelastin protein levels induced by the digested elastin fragments (Foster *et al.*, 1990). The degradation and subsequent repair processes during *S. aureus* infection may result in the exposure of a heterogeneous mix of elastin peptides and tropoelastin monomers, all of which *S. aureus* is capable of binding via FnBPA. The adaptability of this organism to diverse ligands may help to explain the persistent nature of some *S. aureus* infections.

Chapter 7

Discussion

7.1 Discussion

The colonisation of host tissue by *S. aureus* is an important factor in disease pathogenesis. *S. aureus* expresses on its cell surface a number of MSCRAMMs that promote the binding of the organism to components of the host's extracellular matrix and play an important role in bacterial virulence. *S. aureus* can infect elastin-rich tissues such as lung, skin, joints and heart valves. It is likely to encounter elastin on its journey through blood vessel walls, traversing the extracellular space beneath the basement membrane of endothelial cells in tissue such as lung and around the synovial lining of various joints. This is in contrast to fibrinogen-rich sites such as the bloodstream and the conditioned surface of biomaterials.

In this thesis the interaction of *S. aureus* with elastin and fibrinogen was examined. *S. aureus* strains expressing FnBPA were shown to adhere to immobilised elastin in a dose-dependent manner. A wild-type methicillin-sensitive strain of *S. aureus* adhered to immobilised elastin from human lung, human aorta and bovine ligament. Human aortic elastin promoted the strongest adherence and was used in subsequent binding assays. It has been shown previously that human aortic elastin dried onto the wells of microtitre plates behaves similarly to the native protein as anti-aortic elastin antibodies bound to immobilised elastin in a dose-dependent manner indicating that many epitopes from native elastin are present in immobilised peptides. Due to the functional redundancy of many *S. aureus* MSCRAMMs, *L. lactis* is an ideal surrogate host for the expression of *S. aureus* surface proteins. *L. lactis* expressing full-length FnBPA, FnBPB and FnBPA A domain bound to immobilised fibrinogen and elastin whereas wild-type *L. lactis* cells and cells expressing the BCD domains of FnBPA did not. This confirms previous results which suggested that the A domain of FnBPA is responsible for the elastin-binding phenotype of *S. aureus* (Roche *et al.*, 2004).

The A domains of FnBPA (rAFnBPA$_{37\text{-}544}$) and FnBPB (rAFnBPB$_{37\text{-}540}$) were purified in recombinant form and shown to bind specifically to immobilised fibrinogen and elastin in a dose-dependent manner. These proteins were also used to raise polyclonal antibodies in rabbits. Anti-rAFnBPA antibodies inhibited the adherence of bacteria expressing FnBPA to immobilised elastin. The binding of rAFnBPA$_{37\text{-}544}$ and rAFnBPB$_{37\text{-}540}$ to immobilised elastin was also inhibited by soluble elastin peptides, demonstrating the specificity of the interaction. The fibronectin-binding domains at the C-terminus of FnBPA have been studied in detail and 11 tandemly repeated binding domains were mapped between residues 512-874 (Schwarz-

Linek *et al.*, 2003). It was noted that a partial fibronectin-binding domain was located at the C-terminus of the recombinant FnBPA A domain protein used in early fibrinogen- and elastin-binding assays. This protein bound immobilised fibronectin which indicates that residues 512-544 are sufficient to interact with this ligand. The fibrinogen/elastin- and fibronectin-binding domains of FnBPA are very closely located at this junction, which could have implications in competitive ligand binding *in vivo*. The presence of the fibronectin-binding motifs at the C-terminus of the protein does not affect the binding of fibrinogen or elastin to FnBPA expressed on the cell surface. It is not fully understood, however if a single FnBPA molecule can bind to both fibronectin and fibrinogen/elastin simultaneously. It would be interesting to examine if preincubation of $rAFnBPA_{37\text{-}544}$ with fibrinogen could prevent this protein from binding to immobilised fibronectin. The binding of cell surface-expressed FnBPA to fibrinogen and fibronectin could occur at distinct phases in the infection process. Initial adherence to fibrinogen-coated surfaces could help to establish a focus of infection while the binding to the host cell integrin $\alpha_5\beta_1$ via fibronectin triggers the internalisation of bacteria which would be advantageous at later stages to aid in bacterial evasion of the immune system.

The revised A domain of FnBPA spanning residues 37-511 was expressed. This protein and an N2N3 truncate (residues 194-511) bound fibrinogen and elastin but not fibronectin. This indicates that, similar to ClfA and ClfB, the N1 subdomain is not required for ligand binding. The binding site for both fibrinogen and elastin was thus localised to residues 194-511 of FnBPA.

A 3D molecular model of the N2 and N3 domains of FnBPA was created based on the known crystal structure of ClfA which facilitated analysis of the binding sites for elastin and fibrinogen. To examine the role of the predicted latching strand in the proposed dock, lock and latch mechanism of ligand binding, residues were removed from the C-terminus of the N2N3 construct, $rAFnBPA_{194\text{-}511}$. Removal of two residues reduced the affinity for fibrinogen but not for elastin while a truncate $rAFnBPA_{194\text{-}498}$ lacking an additional ten residues did not bind detectably to either ligand. This shows the importance of the latching peptide and residues N-terminal to this involved in crossing over the ligand docked into the trench (hinge region). A further truncate, lacking the latching peptide, hinge region and β-trand G' of N3 was unable to bind either ligand. Similar to ClfA and ClfB, individual N2 and N3 subdomains, $rAFnBPA_{194\text{-}336}$ and $rAFnBPA_{337\text{-}511}$, were also unable to bind to immobilised fibrinogen or elastin. This is consistent with the requirement for the overall DEv-IgG fold to be maintained and indicates that both ligands bind to the same region of FnBPA possibly

involving the dock, lock and latch mechanism. This was further supported by the strong inhibition of adherence of *L. lactis* expressing FnBPA to elastin and fibrinogen by the monoclonal antibody 7C5 and the C-terminal fibrinogen γ chain peptide. The ability of the γ chain peptide of fibrinogen to block binding to elastin suggests that the two ligands are capable of docking into the same binding site. Competition between fibrinogen and elastin *in vivo* however, is unlikely to occur. The weaker binding of FnBPA for elastin compared to fibrinogen should not preclude a biologically significant interaction occurring in niches where the elastin is abundant and fibrinogen is absent.

In order to define further the ligand-binding sites in FnBPA, amino acid substitutions were created in the putative ligand-binding trench located between N2 and N3. The predicted 3D structure of N2N3 of FnBPA was used to identify residues of FnBPA that were within 3 Å of the docked fibrinogen ligand. In addition, residues were chosen for alteration based on their being in the equivalent position to residues of ClfA that were targeted for site-directed mutagenesis. Residue-altered rAFnBPA$_{37\text{-}511}$ recombinant proteins were purified and tested for binding to fibrinogen and elastin. The reduction in ligand binding seen with various substitutions can be correlated with their position around the hydrophobic trench and the predicted interactions of their side chains with residues of the fibrinogen peptide. The glycine residue at position 222 does not have a role to play in ligand binding whereas the substitution of another glycine, G497 does have an effect on ligand binding. This can be explained by G222 being located within the hydrophobic trench but it is some distance from the docked fibrinogen ligand. In contrast, G497 is located at the junction of the penultimate β-strand of N3 and the loop segment that most likely acts as the hinge that traverses the hydrophobic trench when the ligand is bound. This glycine residue could have a role in bending the hinge region over the fibrinogen ligand. The importance of the hydrophobic residue L498 might be its repositioning after the conformational change during latching and locking where it might stabilize the binding as occurs with Ile581 that is in a similar position in the ligand bound complex of SdrG (Ponnuraj *et al.*, 2003). Residues N304 and F306 were particularly important for binding both ligands and are predicted to be in close proximity to the side chain of D410 of the fibrinogen γ chain. They are located in equivalent positions to the crucial residues P336 and Y338 of ClfA (Deivanayagam *et al.*, 2002; Loughman *et al.*, 2005). This was confirmed by introducing N304A and F306A substitutions into FnBPA expressed on the surface of *L. lactis*. The importance of the ligand-binding trench was reinforced by the

reduced affinity exhibited by substitutions of several other residues. These data strongly suggest that both elastin and fibrinogen bind to the same region of FnBPA.

The precise interactions of FnBPA residues with a fibrinogen ligand will only be fully understood with a co-crystallised complex. Until that is achieved, it would be interesting to study the interaction of a series of alanine-substituted fibrinogen γ chain peptides with rAFnBPA. A panel of fibrinogen peptides, each containing alanine substitutions of sequential residues was generated in the laboratory of Prof. M. Hook to study the details of the interaction of this peptide with ClfA. Similar investigations with FnBPA could be carried out to understand the contacts made by residues such as N304 and F306 with fibrinogen. In addition, a direct comparison of the affinity of ClfA, FnBPA and FnBPB for the native fibrinogen γ chain peptide could be carried out. Isothermal titration calorimetry and fluorescence polarization are accurate techniques that could measure the precise affinity of an N2N3 construct of each MSCRAMM for their common γ chain ligand.

Elastin is a highly cross-linked polymer of tropoelastin. There is no obvious amino acid sequence similarity between tropoelastin and the C-terminus of the γ chain of fibrinogen. Without a crystallised complex of the ligands bound to FnBPA it is impossible to determine how two different proteins can binds to the same site. However the ability of a *S. aureus* surface protein to bind unrelated ligands is not without precedent as staphylococcal protein A binds to IgG, to von Willebrand factor (O'Seaghdha *et al.*, 2006) and to tumour necrosis factor receptor-1 (Gomez *et al.*, 2006). The α chain of fibrinogen (Ni Eidhin *et al.*, 1998) and the tail region of cytokeratin 10 both bind to the ClfB protein of *S. aureus*, most likely to the same region (Walsh *et al.*, 2004). Furthermore, as was demonstrated in the crystal structure of SdrG bound to a contaminating fibrinogen peptide, MSCRAMMs with variant IgG folds can accommodate linear peptides with a certain degree of flexibility (Ponnuraj *et al.*, 2003).

It has been reported that the *fnbA* and *fnbB* genes from 50 different strains representing the major MRSA clones found in Europe have undergone greater sequence divergence than genes encoding other surface proteins such as *clfA* and *clfB* (Kuhn *et al.*, 2006). The amino acid sequence of the A domain of FnBPA of strain P1 was shown here to be 73.5% identical to that of 8325-4. Interestingly the differences were not spread evenly. Despite having no role in fibrinogen or elastin binding, domain N1 was more highly conserved while domain N3 was the most divergent. Using the 3D model of the 8325-4 FnBPA A domain it is evident that the majority of variant residues are located on the surface of the protein. Residues identified by mutagenesis to be important in ligand binding were predominantly conserved. The

consequences of this sequence divergence were reduced ability of antibodies raised against the 8325-4 protein to bind to the P1 protein while retaining the ability to bind to both fibrinogen and elastin. A similar example of sequence variation has occurred with the coagulase protein of *S. aureus* allowing antigenic variation but conservation of function (Watanabe *et al.*, 2005). The binding of several monoclonal antibodies, raised against the A domain of FnBPA from strain 8325-4, to recombinant A domain of strain P1 was undetectable. This included the function-blocking monoclonal antibody, 7C5 which was shown to interact with the N2 subdomain of rAFnBPA (8325-4). This suggests that the ability of FnBPA to undergo antigenic variation while still retaining ligand-binding ability is very important during infection and the ability of two distinct forms of the protein to bind to both ligands further supports our contention that binding of fibrinogen and elastin occurs at the same site. Ongoing experiments in our laboratory have investigated FnBPA sequence variation in several clinical isolates of *S. aureus*. At least five distinct FnBPA types have emerged so far with extensive sequence variation predominantly occurring on the surface of the N2 and N3 subdomains (Loughman, A. and Foster, T. J., unpublished data). All variants have conserved G222, R224, N304, F306, F355, K357, G497 and L498 residues. It is proposed that each variant retains the ability to bind both fibrinogen and elastin.

Four staphylococcal proteins are known to bind to the extreme C-terminus of the γ chain of fibrinogen, namely ClfA, FnBPA, FnBPB and the ClfA homologue of *S. lugdunensis*, Fbl (Mitchell *et al.*, 2004). Only two of these proteins bind elastin. The hydrophobic trench of ClfA and FnBPA/B are sufficiently similar to accommodate the same region of fibrinogen, yet differ in their affinities for elastin. Residues known to be important in fibrinogen binding by ClfA are often functionally conserved in equivalent positions of FnBPA, e.g. Y338 and F306 of ClfA and FnBPA, respectively and V527 and L498 of ClfA and FnBPA, respectively. A systematic comparison of the residues of the trench regions of both proteins may identify key differences which would aid in the understanding of elastin binding by FnBPA/B and not ClfA. This approach would require the exact crystal structure of FnBPA to be known. Another important difference between FnBPA/B and ClfA/Fbl is the modular organisation of these proteins. The fibrinogen/elastin-binding domains of FnBPA and FnBPB are followed by fibronectin-binding motifs that adopt a structure only when bound to their ligand. In contrast, the fibrinogen-binding regions of ClfA and Fbl are followed by SD and SDSDSA repeats, respectively.

The model of FnBPA binding to fibrinogen/ elastin must be considered in context of the entire protein expressed on the surface of the bacterial cell. The presence of the fibronectin-binding repeats between the A domain and the cell wall do not hinder fibrinogen or elastin binding. However the binding of these repeats to the F1 modules of fibronectin may cause steric hindrance to the docking of fibrinogen or elastin into the hydrophobic trench between N2 and N3. The representation of the FnBP molecule in Figure 1.4 is misleading in the context of cell surface ligand binding. Upon fibrinogen or elastin docking, the latching peptide of N3 closes over the hydrophobic trench, undergoes β-strand complementation with the D and E strands of N2 before proceeding into the fibronectin-binding domains. N3 is positioned distal to the fibronectin-binding motifs at this stage with its latching strand traversing the N2 subdomain and linking it to the C-terminus of the molecule. The precise residues of the latching strand are unknown but the first fibronectin-binding motif begins at position 512. The location of the N1 domain also remains unknown for all staphylococcal proteins. However its presence is neither required nor hinders fibrinogen or elastin binding (Figure 7.1).

The elastin substrate used in *in vitro* binding assays is a partially degraded form of human aortic elastin that retains crosslinks but which has free N- and C-terminal peptides caused by chemical cleavage in hydrophilic domains. It is likely that these peptides bind into the hydrophobic trench in FnBPA. During infection it is possible that *S. aureus* encounters similar peptide fragments created by cleavage of host tissue by bacterial or host elastases. It has been shown previously that the elastin preparations used in binding assays are not contaminated with fibrinogen or fibronectin (Roche *et al.*, 2004), indicating the specificity of the FnBP-elastin interaction. Inhibition of rAFnBPA binding to immobilised elastin and fibrinogen was achieved using soluble desmosine/isodesmosine. It cannot be ruled out therefore, that these unique crosslinks contribute to the binding of FnBPA to elastin peptides. The adherence of rAFnBPA to immobilised α-elastin peptides prompted an investigation to determine if it could also interact with the elastin precursor, tropoelastin. It is interesting to note that, similar to rAFnBPA, the integrin αvβ3, which also contains a variant IgG fold (Deivanayagam *et al.*, 2002), binds to the C-terminus of the fibrinogen γ and α chains (Yokoyama *et al.*, 1999) and to tropoelastin (Rodgers and Weiss, 2004) among other ligands. Surface plasmon resonance analysis was performed testing the binding of soluble rAFnBPA proteins to immobilised tropoelastin. Previous results showed that $rAFnBPA_{37\text{-}544}$ bound to full-length tropoelastin and an N-terminal truncate (SHELN-18) with similar affinities. In

contrast, weaker binding occurred to tropoelastin truncates spanning domains 17-27 and domains 27-36. These results suggest that FnBPA interacts with tropoelastin at multiple sites. However dominant binding is likely to be localised to a region spanning the N-terminus to domain 18. It would be interesting to ascertain if FnBPA competes for the EbpS binding site on tropoelastin (domains 9 and 10). SHELN-18 is the longest tropoelastin fragment screened in this study and the stronger binding could be attributed to this. It is possible that a surface-surface interaction between the two proteins occurs rather than binding to a specific site. Previous results also indicated that the FnBPA-tropoelastin interaction was pH-dependent. Tropoelastin has a highly basic pI of 11. At pH > 5, rAFnBPA is negatively charged and is thus free to interact with the positively-charged lysines of tropoelastin. This result demonstrates that ionic interactions between positive regions on tropoelastin and negatively-charged regions of rAFnBPA stabilize the binding between the proteins. Smaller tropoelastin fragments may help to narrow down the binding site for FnBPA within tropoelastin. This approach however, has its disadvantages. Further truncations of SHEL constructs will still contain short motifs that are present throughout the entire protein. It is also likely that secondary structure of these constructs will be lost. Furthermore, as the FnBPA-tropoelastin interaction is proposed to occur at multiple sites via a surface charge-charge interaction, no one specific peptide is likely to bind. Instead, it is likely that various peptides of differing sequence but containing the required overall positive charge will interact with the FnBPA molecule.

Recombinant rAFnBPA$_{37\text{-}511}$ proteins with alanine substitutions were tested for binding to the tropoelastin monomer. All proteins tested bound to tropoelastin with similar affinities, including an N2N3 truncate of rAFnBPA which confirms this to be the minimum ligand-binding region. The binding of alanine-substituted proteins shows that residues located along the hydrophobic trench situated between N2 and N3 of region A of FnBPA that have important roles in the binding of fibrinogen and α-elastin peptides, are not involved in tropoelastin binding. The hypothesis that FnBPA binds to tropoelastin by a charge/surface interaction is further supported by the fact that the alanine-substituted residues which are located in the interior of the FnBPA protein and whose side chains point into the hydrophobic trench, had no role in tropoelastin binding. The elastin peptides used in previous ELISA assays are a heterogeneous mix of digested fragments of aortic elastin prepared by hot oxalic acid treatment of human elastic tissue. This process possibly exposes sites available for binding into the trench of rAFnBPA. These sites however, would not be exposed in intact

recombinant tropoelastin. Thus FnBPA binds to tropoelastin and digested α-elastin peptides by a distinct mechanism.

Endothelial cells, among others, synthesise and secrete tropoelastin. The direct interaction of *S. aureus* with endothelial cells has been known for some time (Tompkins *et al.*, 1990; Tompkins *et al.*, 1992). In addition, *S. aureus* binds to other elastin-synthesising cells such as fibroblasts and microvascular cells via bridging molecules such as fibronectin. The close proximity of bacteria to the surface of these cells provides opportunities to interact with the tropoelastin monomer on the host cell surface. Tropoelastin synthesis in fibroblast and endothelial cells is highest in foetal and infant development. *S. aureus* is a known pathogen of low birth weight neonates often causing tissue infections or even systemic sepsis. The high mortality of such infections has led to trials testing the efficacy of anti-staphylococcal IgG-based prophylactics (Bloom *et al.*, 2005). It is possible therefore that *S. aureus* interactions with secreted tropoelastin on these cells aids in the establishment of such infections. *S. aureus* encounters elastin on its journey through blood vessel walls, traversing the extracellular space beneath the basement membrane of endothelial cells in tissue such as lung and around the synovial lining of various joints. During the course of an infection, both bacterial and host elastases are active. *S. aureus* is known to produce proteases which aid in tissue destruction. The activity of these enzymes around the site of infection would lead to the presence of varying states of elastin tissue, in the process of being degraded or subsequently repaired by salvage or *de novo* synthesis methods. The elastin peptides produced are known chemoattractants, recruiting monocytes and neutrophils to the site of damage. The binding of *S. aureus* to these peptides may be a bacterial mechanism designed to inhibit this process and prevent an immune response. In any event, the elastin degradation process results in the exposure of a heterogeneous mixture of elastin peptides and tropoelastin monomers, all of which *S. aureus* is capable of binding via FnBPA. The adaptability of this organism may help to explain the persistent nature of some *S. aureus* infections.

References

Andrade, M.A., Ciccarelli, F.D., Perez-Iratxeta, C., and Bork, P. (2002) NEAT: a domain duplicated in genes near the components of a putative Fe^{3+} siderophore transporter from Gram-positive pathogenic bacteria. *Genome Biol* **3**: 47.1-47.5.

Arciola, C.R., Campoccia, D., Gamberini, S., Baldassarri, L., and Montanaro, L. (2005) Prevalence of *cna*, *fnbA* and *fnbB* adhesin genes among *Staphylococcus aureus* isolates from orthopedic infections associated to different types of implant. *FEMS Microbiol Lett* **246**: 81-86.

Armstrong-Esther, C.A. (1976) Carriage patterns of *Staphylococcus aureus* in a healthy non-hospital population of adults and children. *Ann Hum Biol* **3**: 221-227.

Arrecubieta, C., Asai, T., Bayern, M., Loughman, A., Fitzgerald, J.R., Shelton, C.E., Baron, H.M., Dang, N.C., Deng, M.C., Naka, Y., Foster, T.J., and Lowy, F.D. (2006) The role of *Staphylococcus aureus* adhesins in the pathogenesis of ventricular assist device-related infections. *J Infect Dis* **193**: 1109-1119.

Athanasopoulos, A.N., Economopoulou, M., Orlova, V.V., Sobke, A., Schneider, D., Weber, H., Augustin, H.G., Eming, S.A., Schubert, U., Linn, T., Nawroth, P.P., Hussain, M., Hammes, H.P., Herrmann, M., Preissner, K.T., and Chavakis, T. (2006) The extracellular adherence protein (Eap) of *Staphylococcus aureus* inhibits wound healing by interfering with host defense and repair mechanisms. *Blood* **107**: 2720-2727.

Baddour, L.M., Tayidi, M.M., Walker, E., McDevitt, D., and Foster, T.J. (1994) Virulence of coagulase-deficient mutants of *Staphylococcus aureus* in experimental endocarditis. *J Med Microbiol* **41**: 259-263.

Balwit, J.M., van Langevelde, P., Vann, J.M., and Proctor, R.A. (1994) Gentamicin-resistant menadione and hemin auxotrophic *Staphylococcus aureus* persist within cultured endothelial cells. *J Infect Dis* **170**: 1033-1037.

Banbula, A., Potempa, J., Travis, J., Fernandez-Catalan, C., Mann, K., Huber, R., Bode, W., and Medrano, F. (1998) Amino-acid sequence and three-dimensional structure of the *Staphylococcus aureus* metalloproteinase at 1.72 Å resolution. *Structure* **6**: 1185-1193.

Bashir, M.M., Indik, Z., Yeh, H., Ornstein-Goldstein, N., Rosenbloom, J.C., Abrams, W., Fazio, M., Uitto, J., and Rosenbloom, J. (1989) Characterization of the complete human elastin gene. Delineation of unusual features in the 5'-flanking region. *J Biol Chem* **264**: 8887-8891.

Bisaccia, F., Morelli, M.A., De Biasi, M., Traniello, S., Spisani, S., and Tamburro, A.M. (1994) Migration of monocytes in the presence of elastolytic fragments of elastin and

in synthetic derivates. Structure-activity relationships. *Int J Pept Protein Res* **44**: 332-341.

Blevins, J.S., Gillaspy, A.F., Rechtin, T.M., Hurlburt, B.K., and Smeltzer, M.S. (1999) The Staphylococcal accessory regulator (*sar*) represses transcription of the *Staphylococcus aureus* collagen adhesin gene (*cna*) in an *agr*-independent manner. *Mol Microbiol* **33**: 317-326.

Bloom, B., Schelonka, R., Kueser, T., Walker, W., Jung, E., Kaufman, D., Kesler, K., Roberson, D., Patti, J., and Hetherington, S. (2005) Multicenter study to assess safety and efficacy of INH-A21, a donor-selected human staphylococcal immunoglobulin, for prevention of nosocomial infections in very low birth weight infants. *Pediatr Infect Dis J* **24**: 858-866.

Boden, M.K., and Flock, J.I. (1992) Evidence for three different fibrinogen-binding proteins with unique properties from *Staphylococcus aureus* strain Newman. *Microb Pathog* **12**: 289-298.

Bone, R.C. (1994) Gram-positive organisms and sepsis. *Arch Intern Med* **154**: 26-34.

Bork, P., Downing, A.K., Kieffer, B., and Campbell, I.D. (1996) Structure and distribution of modules in extracellular proteins. *Q Rev Biophys* **29**: 119-167.

Boyd, C.D., Christiano, A.M., Pierce, R.A., Stolle, C.A., and Deak, S.B. (1991) Mammalian tropoelastin: multiple domains of the protein define an evolutionarily divergent amino acid sequence. *Matrix* **11**: 235-241.

Bozzini, S., Visai, L., Pignatti, P., Petersen, T.E., and Speziale, P. (1992) Multiple binding sites in fibronectin and the staphylococcal fibronectin receptor. *Eur J Biochem* **207**: 327-333.

Braverman, I.M., and Fonferko, E. (1982) Studies in cutaneous aging: I. The elastic fiber network. *J Invest Dermatol* **78**: 434-443.

Bressan, G.M., and Prockop, D.J. (1977) Synthesis of elastin in aortas from chick embryos. Conversion of newly secreted elastin to cross-linked elastin without apparent proteolysis of the molecule. *Biochemistry* **16**: 1406-1412.

Brogden, K.A. (2005) Antimicrobial peptides: pore formers or metabolic inhibitors in bacteria? *Nat Rev Microbiol* **3**: 238-250.

Brouillette, E., Lacasse, P., Shkreta, L., Belanger, J., Grondin, G., Diarra, M.S., Fournier, S., and Talbot, B.G. (2002) DNA immunization against the clumping factor A (ClfA) of *Staphylococcus aureus*. *Vaccine* **20**: 2348-2357.

Brown-Augsburger, P., Tisdale, C., Broekelmann, T., Sloan, C., and Mecham, R.P. (1995) Identification of an elastin cross-linking domain that joins three peptide chains. Possible role in nucleated assembly. *J Biol Chem* **270**: 17778-17783.

Calander, A.M., Jonsson, I.M., Kanth, A., Arvidsson, S., Shaw, L., Foster, S.J., and Tarkowski, A. (2004) Impact of staphylococcal protease expression on the outcome of infectious arthritis. *Microbes Infect* **6**: 202-206.

Casolini, F., Visai, L., Joh, D., Conaldi, P.G., Toniolo, A., Hook, M., and Speziale, P. (1998) Antibody response to fibronectin-binding adhesin FnbpA in patients with *Staphylococcus aureus* infections. *Infect Immun* **66**: 5433-5442.

Castiglione Morelli, M.A., Bisaccia, F., Spisani, S., De Biasi, M., Traniello, S., and Tamburro, A.M. (1997) Structure-activity relationships for some elastin-derived peptide chemoattractants. *J Pept Res* **49**: 492-499.

Chan, P.F., and Foster, S.J. (1998) Role of SarA in virulence determinant production and environmental signal transduction in *Staphylococcus aureus*. *J Bacteriol* **180**: 6232-6241.

Chavakis, T., Hussain, M., Kanse, S.M., Peters, G., Bretzel, R.G., Flock, J.I., Herrmann, M., and Preissner, K.T. (2002) *Staphylococcus aureus* extracellular adherence protein serves as anti-inflammatory factor by inhibiting the recruitment of host leukocytes. *Nat Med* **8**: 687-693.

Cheung, A.L., and Fischetti, V.A. (1990) The role of fibrinogen in staphylococcal adherence to catheters *in vitro*. *J Infect Dis* **161**: 1177-1186.

Clarke, A.W., (2006) Interactions of extracellular matrix proteins with tropoelastin. A thesis submitted for the degree of Doctor of Philosophy. University of Sydney, Australia.

Clarke, A.W., and Weiss, A.S. (2004) Microfibril-associated glycoprotein-1 binding to tropoelastin: multiple binding sites and the role of divalent cations. *Eur J Biochem* **271**: 3085-3090.

Clarke, A.W., Wise, S.G., Cain, S.A., Kielty, C.M., and Weiss, A.S. (2005) Coacervation is promoted by molecular interactions between the PF2 segment of fibrillin-1 and the domain 4 region of tropoelastin. *Biochemistry* **44**: 10271-10281.

Clarke, S.R., Wiltshire, M.D., and Foster, S.J. (2004) IsdA of *Staphylococcus aureus* is a broad spectrum, iron-regulated adhesin. *Mol Microbiol* **51**: 1509-1519.

Clarke, S.R., Brummell, K.J., Horsburgh, M.J., McDowell, P.W., Mohamad, S.A., Stapleton, M.R., Acevedo, J., Read, R.C., Day, N.P., Peacock, S.J., Mond, J.J., Kokai-Kun, J.F.,

and Foster, S.J. (2006) Identification of *in vivo*-expressed antigens of *Staphylococcus aureus* and their use in vaccinations for protection against nasal carriage. *J Infect Dis* **193**: 1098-1108.

Collins, L.V., Kristian, S.A., Weidenmaier, C., Faigle, M., Van Kessel, K.P., Van Strijp, J.A., Gotz, F., Neumeister, B., and Peschel, A. (2002) *Staphylococcus aureus* strains lacking D-alanine modifications of teichoic acids are highly susceptible to human neutrophil killing and are virulence attenuated in mice. *J Infect Dis* **186**: 214-219.

Cooper, J.E., and Feil, E.J. (2006) The phylogeny of *Staphylococcus aureus* - which genes make the best intra-species markers? *Microbiology* **152**: 1297-1305.

Corrigan, R.M., Rigby, D., Handley, P., and Foster, T.J. (2007) The role of *Staphylococcus aureus* surface protein SasG in adherence and biofilm formation. Manuscript submitted.

Cosgrove, S.E., Carroll, K.C., and Perl, T.M. (2004) *Staphylococcus aureus* with reduced susceptibility to vancomycin. *Clin Infect Dis* **39**: 539-545.

Coulter, S.N., Schwan, W.R., Ng, E.Y., Langhorne, M.H., Ritchie, H.D., Westbrock-Wadman, S., Hufnagle, W.O., Folger, K.R., Bayer, A.S., and Stover, C.K. (1998) *Staphylococcus aureus* genetic loci impacting growth and survival in multiple infection environments. *Mol Microbiol* **30**: 393-404.

Cox, B.A., Starcher, B.C., and Urry, D.W. (1973) Coacervation of alpha-elastin results in fiber formation. *Biochim Biophys Acta* **317**: 209-213.

Cui, J.C., Hu, D.L., Lin, Y.C., Qian, A.D., and Nakane, A. (2005) Immunization with glutathione S-transferase and mutant toxic shock syndrome toxin 1 fusion protein protects against *Staphylococcus aureus* infection. *FEMS Immunol Med Microbiol* **45**: 45-51.

Cunnion, K.M., Zhang, H.M., and Frank, M.M. (2003) Availability of complement bound to *Staphylococcus aureus* to interact with membrane complement receptors influences efficiency of phagocytosis. *Infect Immun* **71**: 656-662.

Damiano, V., Tsang, A., Kucich, U., Weinbaum, G., and Rosenbloom, J. (1981) Immuno electron microscopic studies on cells synthesizing elastin. *Connect Tissue Res* **8**: 185-188.

Davis, E.C., and Mecham, R.P. (1996) Selective degradation of accumulated secretory proteins in the endoplasmic reticulum. A possible clearance pathway for abnormal tropoelastin. *J Biol Chem* **271**: 3787-3794.

Davis, S.L., Gurusiddappa, S., McCrea, K.W., Perkins, S., and Hook, M. (2001) SdrG, a fibrinogen-binding bacterial adhesin of the microbial surface components recognizing adhesive matrix molecules subfamily from *Staphylococcus epidermidis*, targets the thrombin cleavage site in the B beta chain. *J Biol Chem* **276**: 27799-27805.

de Haas, C.J., Veldkamp, K.E., Peschel, A., Weerkamp, F., Van Wamel, W.J., Heezius, E.C., Poppelier, M.J., Van Kessel, K.P., and van Strijp, J.A. (2004) Chemotaxis inhibitory protein of *Staphylococcus aureus*, a bacterial antiinflammatory agent. *J Exp Med* **199**: 687-695.

de Ruyter, P.G., Kuipers, O.P., and de Vos, W.M. (1996) Controlled gene expression systems for *Lactococcus lactis* with the food-grade inducer nisin. *Appl Environ Microbiol* **62**: 3662-3667.

Debelle, L., and Alix, A.J. (1999) The structures of elastins and their function. *Biochimie* **81**: 981-994.

Deivanayagam, C.C., Wann, E.R., Chen, W., Carson, M., Rajashankar, K.R., Hook, M., and Narayana, S.V. (2002) A novel variant of the immunoglobulin fold in surface adhesins of *Staphylococcus aureus*: crystal structure of the fibrinogen-binding MSCRAMM, clumping factor A. *Embo J* **21**: 6660-6672.

Dinges, M.M., Orwin, P.M., and Schlievert, P.M. (2000) Exotoxins of *Staphylococcus aureus*. *Clin Microbiol Rev* **13**: 16-34.

Doolittle, R.F. (1984) Fibrinogen and fibrin. *Annu Rev Biochem* **53**: 195-229.

Downer, R. (2002) Molecular characterisation of the interaction between *Staphylococcus aureus* and elastin. A thesis submitted for the degree of Doctor of Philosophy. Trinity College, Dublin.

Downer, R., Roche, F., Park, P.W., Mecham, R.P., and Foster, T.J. (2002) The elastin-binding protein of *Staphylococcus aureus* (EbpS) is expressed at the cell surface as an integral membrane protein and not as a cell wall-associated protein. *J Biol Chem* **277**: 243-250.

Drapeau, G.R. (1978) Role of metalloprotease in activation of the precursor of staphylococcal protease. *J Bacteriol* **136**: 607-613.

Dryla, A., Gelbmann, D., von Gabain, A., and Nagy, E. (2003) Identification of a novel iron-regulated staphylococcal surface protein with haptoglobin-haemoglobin binding activity. *Mol Microbiol* **49**: 37-53.

Dryla, A., Prustomersky, S., Gelbmann, D., Hanner, M., Bettinger, E., Kocsis, B., Kustos, T., Henics, T., Meinke, A., and Nagy, E. (2005) Comparison of antibody repertoires

against *Staphylococcus aureus* in healthy individuals and in acutely infected patients. *Clin Diagn Lab Immunol* **12**: 387-398.

Dubick, M.A., Rucker, R.B., Cross, C.E., and Last, J.A. (1981) Elastin metabolism in rodent lung. *Biochim Biophys Acta* **672**: 303-306.

Dubin, G. (2003) Defense against own arms: staphylococcal cysteine proteases and their inhibitors. *Acta Biochim Pol* **50**: 715-724.

Dziewanowska, K., Patti, J.M., Deobald, C.F., Bayles, K.W., Trumble, W.R., and Bohach, G.A. (1999) Fibronectin-binding protein and host cell tyrosine kinase are required for internalization of *Staphylococcus aureus* by epithelial cells. *Infect Immun* **67**: 4673-4678.

Endl, J., Seidl, H.P., Fiedler, F., and Schleifer, K.H. (1983) Chemical composition and structure of cell wall teichoic acids of staphylococci. *Arch Microbiol* **135**: 215-223.

Enright, M.C., Day, N.P., Davies, C.E., Peacock, S.J., and Spratt, B.G. (2000) Multilocus sequence typing for characterization of methicillin-resistant and methicillin-susceptible clones of *Staphylococcus aureus*. *J Clin Microbiol* **38**: 1008-1015.

Farrell, D.H., Thiagarajan, P., Chung, D.W., and Davie, E.W. (1992) Role of fibrinogen alpha and gamma chain sites in platelet aggregation. *Proc Natl Acad Sci U S A* **89**: 10729-10732.

Fattom, A., Schneerson, R., Watson, D.C., Karakawa, W.W., Fitzgerald, D., Pastan, I., Li, X., Shiloach, J., Bryla, D.A., and Robbins, J.B. (1993) Laboratory and clinical evaluation of conjugate vaccines composed of *Staphylococcus aureus* type 5 and type 8 capsular polysaccharides bound to *Pseudomonas aeruginosa* recombinant exoprotein A. *Infect Immun* **61**: 1023-1032.

Fattom, A.I., Horwith, G., Fuller, S., Propst, M., and Naso, R. (2004) Development of StaphVAX, a polysaccharide conjugate vaccine against *S. aureus* infection: from the lab bench to phase III clinical trials. *Vaccine* **22**: 880-887.

Fazio, M.J., Mattei, M.G., Passage, E., Chu, M.L., Black, D., Solomon, E., Davidson, J.M., and Uitto, J. (1991) Human elastin gene: new evidence for localization to the long arm of chromosome 7. *Am J Hum Genet* **48**: 696-703.

Fischer, W., Mannsfeld, T., and Hagen, G. (1990) On the basic structure of poly(glycerophosphate) lipoteichoic acids. *Biochem Cell Biol* **68**: 33-43.

Fitzgerald, J.R., Sturdevant, D.E., Mackie, S.M., Gill, S.R., and Musser, J.M. (2001) Evolutionary genomics of *Staphylococcus aureus*: insights into the origin of

methicillin-resistant strains and the toxic shock syndrome epidemic. *Proc Natl Acad Sci U S A* **98**: 8821-8826.

Fitzgerald, J.R., Loughman, A., Keane, F., Brennan, M., Knobel, M., Higgins, J., Visai, L., Speziale, P., Cox, D., and Foster, T.J. (2006) Fibronectin-binding proteins of *Staphylococcus aureus* mediate activation of human platelets via fibrinogen and fibronectin bridges to integrin GPIIb/IIIa and IgG binding to the FcgammaRIIa receptor. *Mol Microbiol* **59**: 212-230.

Flock, J.I., Froman, G., Jonsson, K., Guss, B., Signas, C., Nilsson, B., Raucci, G., Hook, M., Wadstrom, T., and Lindberg, M. (1987) Cloning and expression of the gene for a fibronectin-binding protein from *Staphylococcus aureus*. *Embo J* **6**: 2351-2357.

Flock, J.I., Hienz, S.A., Heimdahl, A., and Schennings, T. (1996) Reconsideration of the role of fibronectin binding in endocarditis caused by *Staphylococcus aureus*. *Infect Immun* **64**: 1876-1878.

Foster, J.A., Rubin, L., Kagan, H.M., Franzblau, C., Bruenger, E., and Sandberg, L.B. (1974) Isolation and characterization of cross-linked peptides from elastin. *J Biol Chem* **249**: 6191-6196.

Foster, J.A., Rich, C.B., and Miller, M.F. (1990) Pulmonary fibroblasts: an *in vitro* model of emphysema. Regulation of elastin gene expression. *J Biol Chem* **265**: 15544-15549.

Foster, T.J. (2004) The *Staphylococcus aureus* "superbug". *J Clin Invest* **114**: 1693-1696.

Fowler, T., Wann, E.R., Joh, D., Johansson, S., Foster, T.J., and Hook, M. (2000) Cellular invasion by *Staphylococcus aureus* involves a fibronectin bridge between the bacterial fibronectin-binding MSCRAMMs and host cell beta1 integrins. *Eur J Cell Biol* **79**: 672-679.

Friedrich, R., Panizzi, P., Fuentes-Prior, P., Richter, K., Verhamme, I., Anderson, P.J., Kawabata, S., Huber, R., Bode, W., and Bock, P.E. (2003) Staphylocoagulase is a prototype for the mechanism of cofactor-induced zymogen activation. *Nature* **425**: 535-539.

Geisbrecht, B.V., Hamaoka, B.Y., Perman, B., Zemla, A., and Leahy, D.J. (2005) The crystal structures of EAP domains from *Staphylococcus aureus* reveal an unexpected homology to bacterial superantigens. *J Biol Chem* **280**: 17243-17250.

Ghuysen, J.M., and Strominger, J.L. (1963) Structure of the Cell Wall of *Staphylococcus aureus*, Strain Copenhagen. Ii. Separation and Structure of Disaccharides. *Biochemistry* **2**: 1119-1125.

Ghuysen, J.M., Tipper, D.J., and Strominger, J.L. (1965) Structure of the Cell Wall of *Staphylococcus aureus*, Strain Copenhagen. Iv. the Teichoic Acid-Glycopeptide Complex. *Biochemistry* **4**: 474-485.

Gillaspy, A.F., Patti, J.M., and Smeltzer, M.S. (1997) Transcriptional regulation of the *Staphylococcus aureus* collagen adhesion gene, *cna*. *Infect Immun* **65**: 1536-1540.

Gillaspy, A.F., Lee, C.Y., Sau, S., Cheung, A.L., and Smeltzer, M.S. (1998) Factors affecting the collagen-binding capacity of *Staphylococcus aureus*. *Infect Immun* **66**: 3170-3178.

Gillet, Y., Issartel, B., Vanhems, P., Fournet, J.C., Lina, G., Bes, M., Vandenesch, F., Piemont, Y., Brousse, N., Floret, D., and Etienne, J. (2002) Association between *Staphylococcus aureus* strains carrying gene for Panton-Valentine leukocidin and highly lethal necrotising pneumonia in young immunocompetent patients. *Lancet* **359**: 753-759.

Gomez, M.I., Lee, A., Reddy, B., Muir, A., Soong, G., Pitt, A., Cheung, A., and Prince, A. (2004) *Staphylococcus aureus* protein A induces airway epithelial inflammatory responses by activating TNFR-1. *Nat Med* **10**: 842-848.

Gomez, M.I., O'Seaghdha, M., Magargee, M., Foster, T.J., and Prince, A.S. (2006) *Staphylococcus aureus* protein A activates TNFR-1 signaling through conserved IgG binding domains. *J Biol Chem* **281**: 20190-20196.

Gomez, M.I., Seaghdha, M.O., and Prince, A.S. (2007) *Staphylococcus aureus* protein A activates TACE through EGFR-dependent signaling. *Embo J* **26**: 701-709.

Gosline, J.M. (1978) Hydrophobic interaction and a model for the elasticity of elastin. *Biopolymers* **17**: 677-695.

Gotte, L. (1977) Recent observations on the structure and composition of elastin. *Adv Exp Med Biol* **79**: 105-117.

Gouda, H., Shiraishi, M., Takahashi, H., Kato, K., Torigoe, H., Arata, Y., and Shimada, I. (1998) NMR study of the interaction between the B domain of staphylococcal protein A and the Fc portion of immunoglobulin G. *Biochemistry* **37**: 129-136.

Graille, M., Stura, E.A., Corper, A.L., Sutton, B.J., Taussig, M.J., Charbonnier, J.B., and Silverman, G.J. (2000) Crystal structure of a *Staphylococcus aureus* protein A domain complexed with the Fab fragment of a human IgM antibody: structural basis for recognition of B-cell receptors and superantigen activity. *Proc Natl Acad Sci U S A* **97**: 5399-5404.

Greene, C., McDevitt, D., Francois, P., Vaudaux, P.E., Lew, D.P., and Foster, T.J. (1995) Adhesion properties of mutants of *Staphylococcus aureus* defective in fibronectin-binding proteins and studies on the expression of *fnb* genes. *Mol Microbiol* **17**: 1143-1152.

Grosso, L.E., and Scott, M. (1993) PGAIPG, a repeated hexapeptide of bovine and human tropoelastin, is chemotactic for neutrophils and Lewis lung carcinoma cells. *Arch Biochem Biophys* **305**: 401-404.

Grundmeier, M., Hussain, M., Becker, P., Heilmann, C., Peters, G., and Sinha, B. (2004) Truncation of fibronectin-binding proteins in *Staphylococcus aureus* strain Newman leads to deficient adherence and host cell invasion due to loss of the cell wall anchor function. *Infect Immun* **72**: 7155-7163.

Haas, P.J., de Haas, C.J., Kleibeuker, W., Poppelier, M.J., van Kessel, K.P., Kruijtzer, J.A., Liskamp, R.M., and van Strijp, J.A. (2004) N-terminal residues of the chemotaxis inhibitory protein of *Staphylococcus aureus* are essential for blocking formylated peptide receptor but not C5a receptor. *J Immunol* **173**: 5704-5711.

Haas, P.J., de Haas, C.J., Poppelier, M.J., van Kessel, K.P., van Strijp, J.A., Dijkstra, K., Scheek, R.M., Fan, H., Kruijtzer, J.A., Liskamp, R.M., and Kemmink, J. (2005) The structure of the C5a receptor-blocking domain of chemotaxis inhibitory protein of *Staphylococcus aureus* is related to a group of immune evasive molecules. *J Mol Biol* **353**: 859-872.

Haggar, A., Hussain, M., Lonnies, H., Herrmann, M., Norrby-Teglund, A., and Flock, J.I. (2003) Extracellular adherence protein from *Staphylococcus aureus* enhances internalization into eukaryotic cells. *Infect Immun* **71**: 2310-2317.

Haggar, A., Shannon, O., Norrby-Teglund, A., and Flock, J.I. (2005) Dual effects of extracellular adherence protein from *Staphylococcus aureus* on peripheral blood mononuclear cells. *J Infect Dis* **192**: 210-217.

Hall, A.E., Domanski, P.J., Patel, P.R., Vernachio, J.H., Syribeys, P.J., Gorovits, E.L., Johnson, M.A., Ross, J.M., Hutchins, J.T., and Patti, J.M. (2003) Characterization of a protective monoclonal antibody recognizing *Staphylococcus aureus* MSCRAMM protein clumping factor A. *Infect Immun* **71**: 6864-6870.

Hammel, M., Ramyar, K.X., Spencer, C.T., and Geisbrecht, B.V. (2006) Crystallization and X-ray diffraction analysis of the complement component-3 (C3) inhibitory domain of

Efb from *Staphylococcus aureus*. *Acta Crystallograph Sect F Struct Biol Cryst Commun* **62**: 285-288.

Hancock, R.E. (2005) Mechanisms of action of newer antibiotics for Gram-positive pathogens. *Lancet Infect Dis* **5**: 209-218.

Hansen, U., Hussain, M., Villone, D., Herrmann, M., Robenek, H., Peters, G., Sinha, B., and Bruckner, P. (2006) The anchorless adhesin Eap (extracellular adherence protein) from *Staphylococcus aureus* selectively recognizes extracellular matrix aggregates but binds promiscuously to monomeric matrix macromolecules. *Matrix Biol* **25**: 252-260.

Hartford, O., Francois, P., Vaudaux, P., and Foster, T.J. (1997) The dipeptide repeat region of the fibrinogen-binding protein (clumping factor) is required for functional expression of the fibrinogen-binding domain on the *Staphylococcus aureus* cell surface. *Mol Microbiol* **25**: 1065-1076.

Hartford, O.M., Wann, E.R., Hook, M., and Foster, T.J. (2001) Identification of residues in the *Staphylococcus aureus* fibrinogen-binding MSCRAMM clumping factor A (ClfA) that are important for ligand binding. *J Biol Chem* **276**: 2466-2473.

Hartleib, J., Kohler, N., Dickinson, R.B., Chhatwal, G.S., Sixma, J.J., Hartford, O.M., Foster, T.J., Peters, G., Kehrel, B.E., and Herrmann, M. (2000) Protein A is the von Willebrand factor binding protein on *Staphylococcus aureus*. *Blood* **96**: 2149-2156.

Hawiger, J., Timmons, S., Kloczewiak, M., Strong, D.D., and Doolittle, R.F. (1982) Gamma and alpha chains of human fibrinogen possess sites reactive with human platelet receptors. *Proc Natl Acad Sci U S A* **79**: 2068-2071.

Hawiger, J., Kloczewiak, M., Timmons, S., Strong, D., and Doolittle, R.F. (1983) Interaction of fibrinogen with staphylococcal clumping factor and with platelets. *Ann N Y Acad Sci* **408**: 521-535.

Hemker, H.C., Bas, B.M., and Muller, A.D. (1975) Activation of a pro-enzyme by a stoichiometric reaction with another protein. The reaction between prothrombin and staphylocoagulase. *Biochim Biophys Acta* **379**: 180-188.

Herrick, S., Blanc-Brude, O., Gray, A., and Laurent, G. (1999) Fibrinogen. *Int J Biochem Cell Biol* **31**: 741-746.

Hetenyi, C., and van der Spoel, D. (2002) Efficient docking of peptides to proteins without prior knowledge of the binding site. *Protein Sci* **11**: 1729-1737.

Higgins, J. (2006) Studies of clumping factor A of *Staphylococcus aureus*. A thesis submitted for the degree of Doctor of Philosophy. Trinity College Dublin.

Higgins, J., Loughman, A., van Kessel, K.P., van Strijp, J.A., and Foster, T.J. (2006) Clumping factor A of *Staphylococcus aureus* inhibits phagocytosis by human polymorphonuclear leucocytes. *FEMS Microbiol Lett* **258**: 290-296.

Hillson, J.L., Karr, N.S., Oppliger, I.R., Mannik, M., and Sasso, E.H. (1993) The structural basis of germline-encoded VH3 immunoglobulin binding to staphylococcal protein A. *J Exp Med* **178**: 331-336.

Hinek, A., Jung, S., and Rutka, J.T. (1999) Cell surface aggregation of elastin receptor molecules caused by suramin amplified signals leading to proliferation of human glioma cells. *Acta Neuropathol (Berl)* **97**: 399-407.

Hochkeppel, H.K., Braun, D.G., Vischer, W., Imm, A., Sutter, S., Staeubli, U., Guggenheim, R., Kaplan, E.L., Boutonnier, A., and Fournier, J.M. (1987) Serotyping and electron microscopy studies of *Staphylococcus aureus* clinical isolates with monoclonal antibodies to capsular polysaccharide types 5 and 8. *J Clin Microbiol* **25**: 526-530.

Horsburgh, M.J., Ingham, E., and Foster, S.J. (2001) In *Staphylococcus aureus*, *fur* is an interactive regulator with PerR, contributes to virulence, and is necessary for oxidative stress resistance through positive regulation of catalase and iron homeostasis. *J Bacteriol* **183**: 468-475.

Houghton, A.M., Quintero, P.A., Perkins, D.L., Kobayashi, D.K., Kelley, D.G., Marconcini, L.A., Mecham, R.P., Senior, R.M., and Shapiro, S.D. (2006) Elastin fragments drive disease progression in a murine model of emphysema. *J Clin Invest* **116**: 753-759.

Houmard, J., and Drapeau, G.R. (1972) Staphylococcal protease: a proteolytic enzyme specific for glutamoyl bonds. *Proc Natl Acad Sci U S A* **69**: 3506-3509.

House-Pompeo, K., Xu, Y., Joh, D., Speziale, P., and Hook, M. (1996) Conformational changes in the fibronectin-binding MSCRAMMs are induced by ligand binding. *J Biol Chem* **271**: 1379-1384.

Hu, D.L., Omoe, K., Narita, K., Cui, J.C., Shinagawa, K., and Nakane, A. (2006) Intranasal vaccination with a double mutant of staphylococcal enterotoxin C provides protection against *Staphylococcus aureus* infection. *Microbes Infect* **8**: 2841-2848.

Hudson, M.C., Ramp, W.K., Nicholson, N.C., Williams, A.S., and Nousiainen, M.T. (1995) Internalization of *Staphylococcus aureus* by cultured osteoblasts. *Microb Pathog* **19**: 409-419.

Hussain, M., Haggar, A., Heilmann, C., Peters, G., Flock, J.I., and Herrmann, M. (2002) Insertional inactivation of Eap in *Staphylococcus aureus* strain Newman confers reduced staphylococcal binding to fibroblasts. *Infect Immun* **70**: 2933-2940.

Indik, Z., Yoon, K., Morrow, S.D., Cicila, G., Rosenbloom, J., Rosenbloom, J., and Ornstein-Goldstein, N. (1987) Structure of the 3' region of the human elastin gene: great abundance of Alu repetitive sequences and few coding sequences. *Connect Tissue Res* **16**: 197-211.

Jin, T., Bokarewa, M., Foster, T., Mitchell, J., Higgins, J., and Tarkowski, A. (2004) *Staphylococcus aureus* resists human defensins by production of staphylokinase, a novel bacterial evasion mechanism. *J Immunol* **172**: 1169-1176.

Jonsson, I.M., Mazmanian, S.K., Schneewind, O., Bremell, T., and Tarkowski, A. (2003) The role of *Staphylococcus aureus* sortase A and sortase B in murine arthritis. *Microbes Infect* **5**: 775-780.

Jonsson, K., Signas, C., Muller, H.P., and Lindberg, M. (1991) Two different genes encode fibronectin-binding proteins in *Staphylococcus aureus*. The complete nucleotide sequence and characterization of the second gene. *Eur J Biochem* **202**: 1041-1048.

Jonsson, P., Lindberg, M., Haraldsson, I., and Wadstrom, T. (1985) Virulence of *Staphylococcus aureus* in a mouse mastitis model: studies of alpha hemolysin, coagulase, and protein A as possible virulence determinants with protoplast fusion and gene cloning. *Infect Immun* **49**: 765-769.

Josefsson, E., McCrea, K.W., Ni Eidhin, D., O'Connell, D., Cox, J., Hook, M., and Foster, T.J. (1998) Three new members of the serine-aspartate repeat protein multigene family of *Staphylococcus aureus*. *Microbiology* **144**: 3387-3395.

Josefsson, E., Hartford, O., O'Brien, L., Patti, J.M., and Foster, T. (2001) Protection against experimental *Staphylococcus aureus* arthritis by vaccination with clumping factor A, a novel virulence determinant. *J Infect Dis* **184**: 1572-1580.

Kagan, H.M., and Sullivan, K.A. (1982) Lysyl oxidase: preparation and role in elastin biosynthesis. *Methods Enzymol* **82 Pt A**: 637-650.

Kagan, H.M., Vaccaro, C.A., Bronson, R.E., Tang, S.S., and Brody, J.S. (1986) Ultrastructural immunolocalization of lysyl oxidase in vascular connective tissue. *J Cell Biol* **103**: 1121-1128.

Kanangat, S., Postlethwaite, A., Hasty, K., Kang, A., Smeltzer, M., Appling, W., and Schaberg, D. (2006) Induction of multiple matrix metalloproteinases in human dermal

and synovial fibroblasts by *Staphylococcus aureus*: implications in the pathogenesis of septic arthritis and other soft tissue infections. *Arthritis Res Ther* **8**: R176.

Karlsson, A., Saravia-Otten, P., Tegmark, K., Morfeldt, E., and Arvidson, S. (2001) Decreased amounts of cell wall-associated protein A and fibronectin-binding proteins in *Staphylococcus aureus sarA* mutants due to up-regulation of extracellular proteases. *Infect Immun* **69**: 4742-4748.

Kawabata, S., Morita, T., Iwanaga, S., and Igarashi, H. (1985) Difference in enzymatic properties between alpha-thrombin-staphylocoagulase complex and free alpha-thrombin. *J Biochem (Tokyo)* **97**: 1073-1078.

Kawabata, S., Miyata, T., Morita, T., Miyata, T., Iwanaga, S., and Igarashi, H. (1986) The amino acid sequence of the procoagulant- and prothrombin-binding domain isolated from staphylocoagulase. *J Biol Chem* **261**: 527-531.

Kintarak, S., Whawell, S.A., Speight, P.M., Packer, S., and Nair, S.P. (2004) Internalization of *Staphylococcus aureus* by human keratinocytes. *Infect Immun* **72**: 5668-5675.

Kluytmans, J., van Belkum, A., and Verbrugh, H. (1997) Nasal carriage of *Staphylococcus aureus*: epidemiology, underlying mechanisms, and associated risks. *Clin Microbiol Rev* **10**: 505-520.

Kozel, B.A., Rongish, B.J., Czirok, A., Zach, J., Little, C.D., Davis, E.C., Knutsen, R.H., Wagenseil, J.E., Levy, M.A., and Mecham, R.P. (2006) Elastic fiber formation: a dynamic view of extracellular matrix assembly using timer reporters. *J Cell Physiol* **207**: 87-96.

Kuhn, G., Francioli, P., and Blanc, D.S. (2006) Evidence for clonal evolution among highly polymorphic genes in methicillin-resistant *Staphylococcus aureus*. *J Bacteriol* **188**: 169-178.

Kuipers, O.P., Beerthuyzen, M.M., Siezen, R.J., and De Vos, W.M. (1993) Characterization of the nisin gene cluster *nisABTCIPR* of *Lactococcus lactis*. Requirement of expression of the *nisA* and *nisI* genes for development of immunity. *Eur J Biochem* **216**: 281-291.

Kuklin, N.A., Clark, D.J., Secore, S., Cook, J., Cope, L.D., McNeely, T., Noble, L., Brown, M.J., Zorman, J.K., Wang, X.M., Pancari, G., Fan, H., Isett, K., Burgess, B., Bryan, J., Brownlow, M., George, H., Meinz, M., Liddell, M.E., Kelly, R., Schultz, L., Montgomery, D., Onishi, J., Losada, M., Martin, M., Ebert, T., Tan, C.Y., Schofield, T.L., Nagy, E., Meineke, A., Joyce, J.G., Kurtz, M.B., Caulfield, M.J., Jansen, K.U., McClements, W., and Anderson, A.S. (2006) A novel *Staphylococcus aureus* vaccine:

iron surface determinant B induces rapid antibody responses in rhesus macaques and specific increased survival in a murine *S. aureus* sepsis model. *Infect Immun* **74**: 2215-2223.

Kuroda, M., Ohta, T., Uchiyama, I., Baba, T., Yuzawa, H., Kobayashi, I., Cui, L., Oguchi, A., Aoki, K., Nagai, Y., Lian, J., Ito, T., Kanamori, M., Matsumaru, H., Maruyama, A., Murakami, H., Hosoyama, A., Mizutani-Ui, Y., Takahashi, N.K., Sawano, T., Inoue, R., Kaito, C., Sekimizu, K., Hirakawa, H., Kuhara, S., Goto, S., Yabuzaki, J., Kanehisa, M., Yamashita, A., Oshima, K., Furuya, K., Yoshino, C., Shiba, T., Hattori, M., Ogasawara, N., Hayashi, H., and Hiramatsu, K. (2001) Whole genome sequencing of meticillin-resistant *Staphylococcus aureus*. *Lancet* **357**: 1225-1240.

Kuusela, P., Vartio, T., Vuento, M., and Myhre, E.B. (1984) Binding sites for streptococci and staphylococci in fibronectin. *Infect Immun* **45**: 433-436.

Kuypers, J.M., and Proctor, R.A. (1989) Reduced adherence to traumatized rat heart valves by a low-fibronectin-binding mutant of *Staphylococcus aureus*. *Infect Immun* **57**: 2306-2312.

Labandeira-Rey, M., Couzon, F., Boisset, S., Brown, E.L., Bes, M., Benito, Y., Barbu, E.M., Vazquez, V., Hook, M., Etienne, J., Vandenesch, F., and Bowden, M.G. (2007) *Staphylococcus aureus* Panton Valentine Leukocidin Causes Necrotizing Pneumonia. *Science*.

Laemmli, U.K. (1970) Cleavage of structural proteins during the assembly of the head of bacteriophage T4. *Nature* **227**: 680-685.

Larsson, A., Peng, S., Persson, H., Rosenbloom, J., Abrams, W.R., Wassberg, E., Thelin, S., Sletten, K., Gerwins, P., and Westermark, P. (2006) Lactadherin binds to elastin-a starting point for medin amyloid formation? *Amyloid* **13**: 78-85.

Lau, Y.K., Gobin, A.M., and West, J.L. (2006) Overexpression of lysyl oxidase to increase matrix crosslinking and improve tissue strength in dermal wound healing. *Ann Biomed Eng* **34**: 1239-1246.

Lee, J.C., Park, J.S., Shepherd, S.E., Carey, V., and Fattom, A. (1997) Protective efficacy of antibodies to the *Staphylococcus aureus* type 5 capsular polysaccharide in a modified model of endocarditis in rats. *Infect Immun* **65**: 4146-4151.

Lee, L.Y., Hook, M., Haviland, D., Wetsel, R.A., Yonter, E.O., Syribeys, P., Vernachio, J., and Brown, E.L. (2004a) Inhibition of complement activation by a secreted *Staphylococcus aureus* protein. *J Infect Dis* **190**: 571-579.

Lee, L.Y., Liang, X., Hook, M., and Brown, E.L. (2004b) Identification and characterization of the C3 binding domain of the *Staphylococcus aureus* extracellular fibrinogen-binding protein (Efb). *J Biol Chem* **279**: 50710-50716.

Lewis, L.A., Li, K., Bharosay, M., Cannella, M., Jorgenson, V., Thomas, R., Pena, D., Velez, M., Pereira, B., and Sassine, A. (1990) Characterization of gentamicin-resistant respiratory-deficient (res-) variant strains of *Staphylococcus aureus*. *Microbiol Immunol* **34**: 587-605.

Llewelyn, M., and Cohen, J. (2002) Superantigens: microbial agents that corrupt immunity. *Lancet Infect Dis* **2**: 156-162.

Loughman, A. (2005) Platelet activation by *Staphylococcus aureus*. A thesis submitted for the degree of Doctor of Philosophy. Trinity College, Dublin.

Loughman, A., Fitzgerald, J.R., Brennan, M.P., Higgins, J., Downer, R., Cox, D., and Foster, T.J. (2005) Roles for fibrinogen, immunoglobulin and complement in platelet activation promoted by *Staphylococcus aureus* clumping factor A. *Mol Microbiol* **57**: 804-818.

Lowy, F.D. (1998) *Staphylococcus aureus* infections. *N Engl J Med* **339**: 520-532.

Ludwig, W., Seewaldt, E., Kilpper-Balz, R., Schleifer, K.H., Magrum, L., Woese, C.R., Fox, G.E., and Stackebrandt, E. (1985) The phylogenetic position of *Streptococcus* and *Enterococcus*. *J Gen Microbiol* **131**: 543-551.

Mariani, T.J., Reed, J.J., and Shapiro, S.D. (2002) Expression profiling of the developing mouse lung: insights into the establishment of the extracellular matrix. *Am J Respir Cell Mol Biol* **26**: 541-548.

Marrack, P., and Kappler, J. (1990) The staphylococcal enterotoxins and their relatives. *Science* **248**: 1066.

Marraffini, L.A., Ton-That, H., Zong, Y., Narayana, S.V., and Schneewind, O. (2004) Anchoring of surface proteins to the cell wall of *Staphylococcus aureus*. A conserved arginine residue is required for efficient catalysis of sortase A. *J Biol Chem* **279**: 37763-37770.

Martin, S.L., Vrhovski, B., and Weiss, A.S. (1995) Total synthesis and expression in *Escherichia coli* of a gene encoding human tropoelastin. *Gene* **154**: 159-166.

Massey, R.C., Kantzanou, M.N., Fowler, T., Day, N.P., Schofield, K., Wann, E.R., Berendt, A.R., Hook, M., and Peacock, S.J. (2001) Fibronectin-binding protein A of

Staphylococcus aureus has multiple, substituting, binding regions that mediate adherence to fibronectin and invasion of endothelial cells. *Cell Microbiol* **3**: 839-851.

Massimi, I., Park, E., Rice, K., Muller-Esterl, W., Sauder, D., and McGavin, M.J. (2002) Identification of a novel maturation mechanism and restricted substrate specificity for the SspB cysteine protease of *Staphylococcus aureus*. *J Biol Chem* **277**: 41770-41777.

Mazmanian, S.K., Liu, G., Ton-That, H., and Schneewind, O. (1999) *Staphylococcus aureus* sortase, an enzyme that anchors surface proteins to the cell wall. *Science* **285**: 760-763.

Mazmanian, S.K., Liu, G., Jensen, E.R., Lenoy, E., and Schneewind, O. (2000) *Staphylococcus aureus* sortase mutants defective in the display of surface proteins and in the pathogenesis of animal infections. *Proc Natl Acad Sci U S A* **97**: 5510-5515.

Mazmanian, S.K., Ton-That, H., Su, K., and Schneewind, O. (2002) An iron-regulated sortase anchors a class of surface protein during *Staphylococcus aureus* pathogenesis. *Proc Natl Acad Sci U S A* **99**: 2293-2298.

Mazmanian, S.K., Skaar, E.P., Gaspar, A.H., Humayun, M., Gornicki, P., Jelenska, J., Joachmiak, A., Missiakas, D.M., and Schneewind, O. (2003) Passage of heme-iron across the envelope of *Staphylococcus aureus*. *Science* **299**: 906-909.

McAleese, F.M., Walsh, E.J., Sieprawska, M., Potempa, J., and Foster, T.J. (2001) Loss of clumping factor B fibrinogen-binding activity by *Staphylococcus aureus* involves cessation of transcription, shedding and cleavage by metalloprotease. *J Biol Chem* **276**: 29969-29978.

McCrea, K.W., Hartford, O., Davis, S., Eidhin, D.N., Lina, G., Speziale, P., Foster, T.J., and Hook, M. (2000) The serine-aspartate repeat (Sdr) protein family in *Staphylococcus epidermidis*. *Microbiology* **146**: 1535-1546.

McDevitt, D., Francois, P., Vaudaux, P., and Foster, T.J. (1994) Molecular characterization of the clumping factor (fibrinogen receptor) of *Staphylococcus aureus*. *Mol Microbiol* **11**: 237-248.

McDevitt, D., and Foster, T.J. (1995) Variation in the size of the repeat region of the fibrinogen receptor (clumping factor) of *Staphylococcus aureus* strains. *Microbiology* **141**: 937-943.

McDevitt, D., Francois, P., Vaudaux, P., and Foster, T.J. (1995) Identification of the ligand-binding domain of the surface-located fibrinogen receptor (clumping factor) of *Staphylococcus aureus*. *Mol Microbiol* **16**: 895-907.

McDevitt, D., Nanavaty, T., House-Pompeo, K., Bell, E., Turner, N., McIntire, L., Foster, T., and Hook, M. (1997) Characterization of the interaction between the *Staphylococcus aureus* clumping factor (ClfA) and fibrinogen. *Eur J Biochem* **247**: 416-424.

McGavin, M.J., Zahradka, C., Rice, K., and Scott, J.E. (1997) Modification of the *Staphylococcus aureus* fibronectin-binding phenotype by V8 protease. *Infect Immun* **65**: 2621-2628.

Miajlovic, H., Loughman, A., Cox, D., and Foster, T.J. (2007) Both complement- and fibrinogen-dependent mechanisms contribute to platelet activation mediated by *Staphylococcus aureus* Clumping factor B. Manuscript submitted.

Mitchell, J. (2004) Molecular analysis of surface proteins of staphylococci. A thesis submitted for the degree of Doctor of Philosophy. Trinity College, Dublin.

Mitchell, J., Tristan, A., and Foster, T.J. (2004) Characterization of the fibrinogen-binding surface protein Fbl of *Staphylococcus lugdunensis*. *Microbiology* **150**: 3831-3841.

Moks, T., Abrahmsen, L., Nilsson, B., Hellman, U., Sjoquist, J., and Uhlen, M. (1986) Staphylococcal protein A consists of five IgG-binding domains. *Eur J Biochem* **156**: 637-643.

Mongodin, E., Bajolet, O., Cutrona, J., Bonnet, N., Dupuit, F., Puchelle, E., and de Bentzmann, S. (2002) Fibronectin-binding proteins of *Staphylococcus aureus* are involved in adherence to human airway epithelium. *Infect Immun* **70**: 620-630.

Moreillon, P., Entenza, J.M., Francioli, P., McDevitt, D., Foster, T.J., Francois, P., and Vaudaux, P. (1995) Role of *Staphylococcus aureus* coagulase and clumping factor in pathogenesis of experimental endocarditis. *Infect Immun* **63**: 4738-4743.

Moroney, S.M., Heller, L.C., Arbuckle, J., Talavera, M., and Widen, R.H. (2006) Staphylococcal Cassette Chromosome mec (SCCmec) and Panton-Valentine Leukocidin Characterization of Methicillin-Resistant *Staphylococcus aureus* Clones. *J Clin Microbiol.*

Morrissey, J.A., Cockayne, A., Hammacott, J., Bishop, K., Denman-Johnson, A., Hill, P.J., and Williams, P. (2002) Conservation, surface exposure, and *in vivo* expression of the Frp family of iron-regulated cell wall proteins in *Staphylococcus aureus*. *Infect Immun* **70**: 2399-2407.

Naik, M.T., Suree, N., Ilangovan, U., Liew, C.K., Thieu, W., Campbell, D.O., Clemens, J.J., Jung, M.E., and Clubb, R.T. (2006) *Staphylococcus aureus* Sortase A transpeptidase.

Calcium promotes sorting signal binding by altering the mobility and structure of an active site loop. *J Biol Chem* **281**: 1817-1826.

Navarre, W.W., Ton-That, H., Faull, K.F., and Schneewind, O. (1998) Anchor structure of staphylococcal surface proteins. II. C-terminal structure of muramidase and amidase-solubilized surface protein. *J Biol Chem* **273**: 29135-29142.

Nguyen, T., Ghebrehiwet, B., and Peerschke, E.I. (2000) *Staphylococcus aureus* protein A recognizes platelet gC1qR/p33: a novel mechanism for staphylococcal interactions with platelets. *Infect Immun* **68**: 2061-2068.

Ni Eidhin, D., Perkins, S., Francois, P., Vaudaux, P., Hook, M., and Foster, T.J. (1998) Clumping factor B (ClfB), a new surface-located fibrinogen-binding adhesin of *Staphylococcus aureus*. *Mol Microbiol* **30**: 245-257.

Nilsson, I.M., Lee, J.C., Bremell, T., Ryden, C., and Tarkowski, A. (1997) The role of staphylococcal polysaccharide microcapsule expression in septicemia and septic arthritis. *Infect Immun* **65**: 4216-4221.

Nilsson, I.M., Patti, J.M., Bremell, T., Hook, M., and Tarkowski, A. (1998) Vaccination with a recombinant fragment of collagen adhesin provides protection against *Staphylococcus aureus*-mediated septic death. *J Clin Invest* **101**: 2640-2649.

Novick, R. (1967) Properties of a cryptic high-frequency transducing phage in *Staphylococcus aureus*. *Virology* **33**: 155-166.

Nowak, D., and Miedzobrodzki, J. (1991) Serine proteinase from *Staphylococcus aureus* enhances elastin degradation by elastases in the presence of human alpha-1-proteinase inhibitor. *Antonie Van Leeuwenhoek* **59**: 109-114.

O'Brien, L., Kerrigan, S.W., Kaw, G., Hogan, M., Penades, J., Litt, D., Fitzgerald, D.J., Foster, T.J., and Cox, D. (2002a) Multiple mechanisms for the activation of human platelet aggregation by *Staphylococcus aureus*: roles for the clumping factors ClfA and ClfB, the serine-aspartate repeat protein SdrE and protein A. *Mol Microbiol* **44**: 1033-1044.

O'Brien, L.M., Walsh, E.J., Massey, R.C., Peacock, S.J., and Foster, T.J. (2002b) *Staphylococcus aureus* clumping factor B (ClfB) promotes adherence to human type I cytokeratin 10: implications for nasal colonization. *Cell Microbiol* **4**: 759-770.

O'Connell, D.P., Nanavaty, T., McDevitt, D., Gurusiddappa, S., Hook, M., and Foster, T.J. (1998) The fibrinogen-binding MSCRAMM (clumping factor) of *Staphylococcus aureus* has a Ca^{2+}-dependent inhibitory site. *J Biol Chem* **273**: 6821-6829.

O'Riordan, K., and Lee, J.C. (2004) *Staphylococcus aureus* capsular polysaccharides. *Clin Microbiol Rev* **17**: 218-234.

O'Seaghdha, M., van Schooten, C.J., Kerrigan, S.W., Emsley, J., Silverman, G.J., Cox, D., Lenting, P.J., and Foster, T.J. (2006) *Staphylococcus aureus* protein A binding to von Willebrand factor A1 domain is mediated by conserved IgG binding regions. *Febs J* **273**: 4831-4841.

Ogawa, S.K., Yurberg, E.R., Hatcher, V.B., Levitt, M.A., and Lowy, F.D. (1985) Bacterial adherence to human endothelial cells *in vitro*. *Infect Immun* **50**: 218-224.

Owen, P. (1985) Crossed Immunoelectrophoresis in the study of outer membrane antigens. In Enterobacterial surface antigens: Methods for molecular characterisation. Amsterdam: Elsevier Science Publishers B.V.

Palma, M., Nozohoor, S., Schennings, T., Heimdahl, A., and Flock, J.I. (1996) Lack of the extracellular 19-kilodalton fibrinogen-binding protein from *Staphylococcus aureus* decreases virulence in experimental wound infection. *Infect Immun* **64**: 5284-5289.

Palma, M., Wade, D., Flock, M., and Flock, J.I. (1998) Multiple binding sites in the interaction between an extracellular fibrinogen-binding protein from *Staphylococcus aureus* and fibrinogen. *J Biol Chem* **273**: 13177-13181.

Palma, M., Haggar, A., and Flock, J.I. (1999) Adherence of *Staphylococcus aureus* is enhanced by an endogenous secreted protein with broad binding activity. *J Bacteriol* **181**: 2840-2845.

Palma, M., Shannon, O., Quezada, H.C., Berg, A., and Flock, J.I. (2001) Extracellular fibrinogen-binding protein, Efb, from *Staphylococcus aureus* blocks platelet aggregation due to its binding to the alpha-chain. *J Biol Chem* **276**: 31691-31697.

Palmqvist, N., Foster, T., Tarkowski, A., and Josefsson, E. (2002) Protein A is a virulence factor in *Staphylococcus aureus* arthritis and septic death. *Microb Pathog* **33**: 239-249.

Palmqvist, N., Foster, T., Fitzgerald, J.R., Josefsson, E., and Tarkowski, A. (2005) Fibronectin-binding proteins and fibrinogen-binding clumping factors play distinct roles in staphylococcal arthritis and systemic inflammation. *J Infect Dis* **191**: 791-798.

Park, P.W., Roberts, D.D., Grosso, L.E., Parks, W.C., Rosenbloom, J., Abrams, W.R., and Mecham, R.P. (1991) Binding of elastin to *Staphylococcus aureus*. *J Biol Chem* **266**: 23399-23406.

Park, P.W., Rosenbloom, J., Abrams, W.R., and Mecham, R.P. (1996) Molecular cloning and expression of the gene for elastin-binding protein (*ebpS*) in *Staphylococcus aureus*. *J Biol Chem* **271**: 15803-15809.

Park, P.W., Broekelmann, T.J., Mecham, B.R., and Mecham, R.P. (1999) Characterization of the elastin-binding domain in the cell-surface 25-kDa elastin-binding protein of *Staphylococcus aureus* (EbpS). *J Biol Chem* **274**: 2845-2850.

Parks, W.C., Secrist, H., Wu, L.C., and Mecham, R.P. (1988) Developmental regulation of tropoelastin isoforms. *J Biol Chem* **263**: 4416-4423.

Partridge, S.M., and Davis, H.F. (1955) The chemistry of connective tissues. 3. Composition of the soluble proteins derived from elastin. *Biochem J* **61**: 21-30.

Partridge, S.M., Davis, H.F., and Adair, G.S. (1955) The chemistry of connective tissues. 2. Soluble proteins derived from partial hydrolysis of elastin. *Biochem J* **61**: 11-21.

Pasquali-Ronchetti, I., and Baccarani-Contri, M. (1997) Elastic fiber during development and aging. *Microsc Res Tech* **38**: 428-435.

Patel, A., Fine, B., Sandig, M., and Mequanint, K. (2006) Elastin biosynthesis: The missing link in tissue-engineered blood vessels. *Cardiovasc Res* **71**: 40-49.

Patel, A.H., Nowlan, P., Weavers, E.D., and Foster, T. (1987) Virulence of protein A-deficient and alpha-toxin-deficient mutants of *Staphylococcus aureus* isolated by allele replacement. *Infect Immun* **55**: 3103-3110.

Patti, J.M., Boles, J.O., and Hook, M. (1993) Identification and biochemical characterization of the ligand-binding domain of the collagen adhesin from *Staphylococcus aureus*. *Biochemistry* **32**: 11428-11435.

Patti, J.M., Bremell, T., Krajewska-Pietrasik, D., Abdelnour, A., Tarkowski, A., Ryden, C., and Hook, M. (1994) The *Staphylococcus aureus* collagen adhesin is a virulence determinant in experimental septic arthritis. *Infect Immun* **62**: 152-161.

Patti, J.M. (2004) A humanized monoclonal antibody targeting *Staphylococcus aureus*. *Vaccine* **22**: S39-43.

Peacock, S.J., Foster, T.J., Cameron, B.J., and Berendt, A.R. (1999) Bacterial fibronectin-binding proteins and endothelial cell surface fibronectin mediate adherence of *Staphylococcus aureus* to resting human endothelial cells. *Microbiology* **145**: 3477-3486.

Peacock, S.J., Day, N.P., Thomas, M.G., Berendt, A.R., and Foster, T.J. (2000) Clinical isolates of *Staphylococcus aureus* exhibit diversity in *fnb* genes and adhesion to human fibronectin. *J Infect* **41**: 23-31.

Peacock, S.J., Moore, C.E., Justice, A., Kantzanou, M., Story, L., Mackie, K., O'Neill, G., and Day, N.P. (2002) Virulent combinations of adhesin and toxin genes in natural populations of *Staphylococcus aureus*. *Infect Immun* **70**: 4987-4996.

Perkins, S., Walsh, E.J., Deivanayagam, C.C., Narayana, S.V., Foster, T.J., and Hook, M. (2001) Structural organization of the fibrinogen-binding region of the clumping factor B MSCRAMM of *Staphylococcus aureus*. *J Biol Chem* **276**: 44721-44728.

Perry, A.M., Ton-That, H., Mazmanian, S.K., and Schneewind, O. (2002) Anchoring of surface proteins to the cell wall of *Staphylococcus aureus*. III. Lipid II is an *in vivo* peptidoglycan substrate for sortase-catalyzed surface protein anchoring. *J Biol Chem* **277**: 16241-16248.

Peschel, A., Otto, M., Jack, R.W., Kalbacher, H., Jung, G., and Gotz, F. (1999) Inactivation of the *dlt* operon in *Staphylococcus aureus* confers sensitivity to defensins, protegrins, and other antimicrobial peptides. *J Biol Chem* **274**: 8405-8410.

Peschel, A., Jack, R.W., Otto, M., Collins, L.V., Staubitz, P., Nicholson, G., Kalbacher, H., Nieuwenhuizen, W.F., Jung, G., Tarkowski, A., van Kessel, K.P., and van Strijp, J.A. (2001) *Staphylococcus aureus* resistance to human defensins and evasion of neutrophil killing via the novel virulence factor MprF is based on modification of membrane lipids with l-lysine. *J Exp Med* **193**: 1067-1076.

Pierce, R.A., Moore, C.H., and Arikan, M.C. (2006) Positive transcriptional regulatory element located within exon 1 of elastin gene. *Am J Physiol Lung Cell Mol Physiol* **291**: L391-399.

Pilka, E.S., Werner, J.M., Schwarz-Linek, U., Pickford, A.R., Meenan, N.A., Campbell, I.D., and Potts, J.R. (2006) Structural insight into binding of *Staphylococcus aureus* to human fibronectin. *FEBS Lett* **580**: 273-277.

Pilpa, R.M., Fadeev, E.A., Villareal, V.A., Wong, M.L., Phillips, M., and Clubb, R.T. (2006) Solution structure of the NEAT (NEAr Transporter) domain from IsdH/HarA: the human hemoglobin receptor in *Staphylococcus aureus*. *J Mol Biol* **360**: 435-447.

Ponnuraj, K., Bowden, M.G., Davis, S., Gurusiddappa, S., Moore, D., Choe, D., Xu, Y., Hook, M., and Narayana, S.V. (2003) A "dock, lock, and latch" structural model for a staphylococcal adhesin binding to fibrinogen. *Cell* **115**: 217-228.

Postma, B., Poppelier, M.J., van Galen, J.C., Prossnitz, E.R., van Strijp, J.A., de Haas, C.J., and van Kessel, K.P. (2004) Chemotaxis inhibitory protein of *Staphylococcus aureus* binds specifically to the C5a and formylated peptide receptor. *J Immunol* **172**: 6994-7001.

Postma, B., Kleibeuker, W., Poppelier, M.J., Boonstra, M., Van Kessel, K.P., Van Strijp, J.A., and de Haas, C.J. (2005) Residues 10-18 within the C5a receptor N-terminus compose a binding domain for chemotaxis inhibitory protein of *Staphylococcus aureus*. *J Biol Chem* **280**: 2020-2027.

Potempa, J., Watorek, W., and Travis, J. (1986) The inactivation of human plasma alpha 1-proteinase inhibitor by proteinases from *Staphylococcus aureus*. *J Biol Chem* **261**: 14330-14334.

Potempa, J., Dubin, A., Korzus, G., and Travis, J. (1988) Degradation of elastin by a cysteine proteinase from *Staphylococcus aureus*. *J Biol Chem* **263**: 2664-2667.

Potts, J.R., and Campbell, I.D. (1994) Fibronectin structure and assembly. *Curr Opin Cell Biol* **6**: 648-655.

Prasad, L., Leduc, Y., Hayakawa, K., and Delbaere, L.T. (2004) The structure of a universally employed enzyme: V8 protease from *Staphylococcus aureus*. *Acta Crystallogr D Biol Crystallogr* **60**: 256-259.

Prevost, G., Cribier, B., Couppie, P., Petiau, P., Supersac, G., Finck-Barbancon, V., Monteil, H., and Piemont, Y. (1995) Panton-Valentine leucocidin and gamma-hemolysin from *Staphylococcus aureus* ATCC 49775 are encoded by distinct genetic loci and have different biological activities. *Infect Immun* **63**: 4121-4129.

Proctor, R.A., van Langevelde, P., Kristjansson, M., Maslow, J.N., and Arbeit, R.D. (1995) Persistent and relapsing infections associated with small-colony variants of *Staphylococcus aureus*. *Clin Infect Dis* **20**: 95-102.

Proctor, R.A., and Peters, G. (1998) Small colony variants in staphylococcal infections: diagnostic and therapeutic implications. *Clin Infect Dis* **27**: 419-422.

Proft, T., and Fraser, J.D. (2003) Bacterial superantigens. *Clin Exp Immunol* **133**: 299-306.

Prokesova, L., Porwit-Bobr, Z., Baran, K., Potempa, J., Pospisil, M., and John, C. (1991) Effect of metalloproteinase from *Staphylococcus aureus* on *in vitro* stimulation of human lymphocytes. *Immunol Lett* **27**: 225-230.

Prokesova, L., Potuznikova, B., Potempa, J., Zikan, J., Radl, J., Hachova, L., Baran, K., Porwit-Bobr, Z., and John, C. (1992) Cleavage of human immunoglobulins by serine proteinase from *Staphylococcus aureus*. *Immunol Lett* **31**: 259-265.

Que, Y.A., Francois, P., Haefliger, J.A., Entenza, J.M., Vaudaux, P., and Moreillon, P. (2001) Reassessing the role of *Staphylococcus aureus* clumping factor and fibronectin-binding protein by expression in *Lactococcus lactis*. *Infect Immun* **69**: 6296-6302.

Que, Y.A., Haefliger, J.A., Piroth, L., Francois, P., Widmer, E., Entenza, J.M., Sinha, B., Herrmann, M., Francioli, P., Vaudaux, P., and Moreillon, P. (2005) Fibrinogen and fibronectin binding cooperate for valve infection and invasion in *Staphylococcus aureus* experimental endocarditis. *J Exp Med* **201**: 1627-1635.

Raibaud, S., Schwarz-Linek, U., Kim, J.H., Jenkins, H.T., Baines, E.R., Gurusiddappa, S., Hook, M., and Potts, J.R. (2005) *Borrelia burgdorferi* binds fibronectin through a tandem beta-zipper, a common mechanism of fibronectin binding in staphylococci, streptococci, and spirochetes. *J Biol Chem* **280**: 18803-18809.

Reiser, K., McCormick, R.J., and Rucker, R.B. (1992) Enzymatic and nonenzymatic cross-linking of collagen and elastin. *Faseb J* **6**: 2439-2449.

Rhem, M.N., Lech, E.M., Patti, J.M., McDevitt, D., Hook, M., Jones, D.B., and Wilhelmus, K.R. (2000) The collagen-binding adhesin is a virulence factor in *Staphylococcus aureus* keratitis. *Infect Immun* **68**: 3776-3779.

Rice, K., Huesca, M., Vaz, D., and McGavin, M.J. (2001a) Variance in fibronectin binding and *fnb* locus polymorphisms in *Staphylococcus aureus*: identification of antigenic variation in a fibronectin-binding protein adhesin of the epidemic CMRSA-1 strain of methicillin-resistant *S. aureus*. *Infect Immun* **69**: 3791-3799.

Rice, K., Peralta, R., Bast, D., de Azavedo, J., and McGavin, M.J. (2001b) Description of staphylococcal serine protease (*ssp*) operon in *Staphylococcus aureus* and nonpolar inactivation of *sspA*-encoded serine protease. *Infect Immun* **69**: 159-169.

Rich, R.L., Demeler, B., Ashby, K., Deivanayagam, C.C., Petrich, J.W., Patti, J.M., Narayana, S.V., and Hook, M. (1998) Domain structure of the *Staphylococcus aureus* collagen adhesin. *Biochemistry* **37**: 15423-15433.

Roche, F.M., Massey, R., Peacock, S.J., Day, N.P., Visai, L., Speziale, P., Lam, A., Pallen, M., and Foster, T.J. (2003a) Characterization of novel LPXTG-containing proteins of *Staphylococcus aureus* identified from genome sequences. *Microbiology* **149**: 643-654.

Roche, F.M., Meehan, M., and Foster, T.J. (2003b) The *Staphylococcus aureus* surface protein SasG and its homologues promote bacterial adherence to human desquamated nasal epithelial cells. *Microbiology* **149**: 2759-2767.

Roche, F.M., Downer, R., Keane, F., Speziale, P., Park, P.W., and Foster, T.J. (2004) The N-terminal A domain of fibronectin-binding proteins A and B promotes adhesion of *Staphylococcus aureus* to elastin. *J Biol Chem* **279**: 38433-38440.

Rodgers, U.R., and Weiss, A.S. (2004) Integrin alpha v beta 3 binds a unique non-RGD site near the C-terminus of human tropoelastin. *Biochimie* **86**: 173-178.

Rollof, J., and Normark, S. (1992) *In vivo* processing of *Staphylococcus aureus* lipase. *J Bacteriol* **174**: 1844-1847.

Rooijakkers, S.H., Ruyken, M., Roos, A., Daha, M.R., Presanis, J.S., Sim, R.B., van Wamel, W.J., van Kessel, K.P., and van Strijp, J.A. (2005) Immune evasion by a staphylococcal complement inhibitor that acts on C3 convertases. *Nat Immunol* **6**: 920-927.

Rooijakkers, S.H., Ruyken, M., van Roon, J., van Kessel, K.P., van Strijp, J.A., and van Wamel, W.J. (2006) Early expression of SCIN and CHIPS drives instant immune evasion by *Staphylococcus aureus*. *Cell Microbiol* **8**: 1282-1293.

Rosenbloom, J. (1982) Elastin: biosynthesis, structure, degradation and role in disease processes. *Connect Tissue Res* **10**: 73-91.

Rosenbloom, J., Bashir, M., Yeh, H., Rosenbloom, J., Ornstein-Goldstein, N., Fazio, M., Kahari, V.M., and Uitto, J. (1991) Regulation of elastin gene expression. *Ann N Y Acad Sci* **624**: 116-136.

Rucker, R.B. (1982) Isolation of soluble elastin from copper-deficient chick aorta. *Methods Enzymol* **82**: 650-657.

Rucker, R.B., and Dubick, M.A. (1984) Elastin metabolism and chemistry: potential roles in lung development and structure. *Environ Health Perspect* **55**: 179-191.

Rzychon, M., Sabat, A., Kosowska, K., Potempa, J., and Dubin, A. (2003) Staphostatins: an expanding new group of proteinase inhibitors with a unique specificity for the regulation of staphopains, *Staphylococcus spp.* cysteine proteinases. *Mol Microbiol* **49**: 1051-1066.

Sabat, A., Kosowska, K., Poulsen, K., Kasprowicz, A., Sekowska, A., van Den Burg, B., Travis, J., and Potempa, J. (2000) Two allelic forms of the aureolysin gene (*aur*) within *Staphylococcus aureus*. *Infect Immun* **68**: 973-976.

Sabat, A., Melles, D.C., Martirosian, G., Grundmann, H., van Belkum, A., and Hryniewicz, W. (2006) Distribution of the serine-aspartate repeat protein-encoding *sdr* genes among nasal-carriage and invasive *Staphylococcus aureus* strains. *J Clin Microbiol* **44**: 1135-1138.

Said-Salim, B., Mathema, B., and Kreiswirth, B.N. (2003) Community-acquired methicillin-resistant *Staphylococcus aureus*: an emerging pathogen. *Infect Control Hosp Epidemiol* **24**: 451-455.

Sambrook, J., Fritsch, E. F. and Maniatis, T. (1989) Molecular cloning: a laboratory manual, 2nd Ed. Cold Spring Harbor, NY.

Sandberg, L.B., and Wolt, T.B. (1982) Production and isolation of soluble elastin from copper-deficient swine. *Methods Enzymol* **82 Pt A**: 657-665.

Saravia-Otten, P., Muller, H.P., and Arvidson, S. (1997) Transcription of *Staphylococcus aureus* fibronectin-binding protein genes is negatively regulated by *agr* and an *agr*-independent mechanism. *J Bacteriol* **179**: 5259-5263.

Savolainen, K., Paulin, L., Westerlund-Wikstrom, B., Foster, T.J., Korhonen, T.K., and Kuusela, P. (2001) Expression of *pls*, a gene closely associated with the *mecA* gene of methicillin-resistant *Staphylococcus aureus*, prevents bacterial adhesion *in vitro*. *Infect Immun* **69**: 3013-3020.

Sawai, T., Tomono, K., Yanagihara, K., Yamamoto, Y., Kaku, M., Hirakata, Y., Koga, H., Tashiro, T., and Kohno, S. (1997) Role of coagulase in a murine model of hematogenous pulmonary infection induced by intravenous injection of *Staphylococcus aureus* enmeshed in agar beads. *Infect Immun* **65**: 466-471.

Schaffer, A.C., Solinga, R.M., Cocchiaro, J., Portoles, M., Kiser, K.B., Risley, A., Randall, S.M., Valtulina, V., Speziale, P., Walsh, E., Foster, T., and Lee, J.C. (2006) Immunization with *Staphylococcus aureus* clumping factor B, a major determinant in nasal carriage, reduces nasal colonization in a murine model. *Infect Immun* **74**: 2145-2153.

Schleifer, K.H., and Kandler, O. (1972) Peptidoglycan types of bacterial cell walls and their taxonomic implications. *Bacteriol Rev* **36**: 407-477.

Schleifer, K.H., and Kroppenstedt, R.M. (1990) Chemical and molecular classification of staphylococci. *Soc Appl Bacteriol Symp Ser* **19**: 9S-24S.

Schneewind, O., Mihaylova-Petkov, D., and Model, P. (1993) Cell wall sorting signals in surface proteins of gram-positive bacteria. *Embo J* **12**: 4803-4811.

Schroder, A., Kland, R., Peschel, A., von Eiff, C., and Aepfelbacher, M. (2006a) Live cell imaging of phagosome maturation in *Staphylococcus aureus* infected human endothelial cells: small colony variants are able to survive in lysosomes. *Med Microbiol Immunol (Berl)* **195**: 185-194.

Schroder, A., Schroder, B., Roppenser, B., Linder, S., Sinha, B., Fassler, R., and Aepfelbacher, M. (2006b) *Staphylococcus aureus* fibronectin-binding protein-A induces motile attachment sites and complex actin remodeling in living endothelial cells. *Mol Biol Cell* **17**: 5198-5210.

Schwarz-Linek, U., Werner, J.M., Pickford, A.R., Gurusiddappa, S., Kim, J.H., Pilka, E.S., Briggs, J.A., Gough, T.S., Hook, M., Campbell, I.D., and Potts, J.R. (2003) Pathogenic bacteria attach to human fibronectin through a tandem beta-zipper. *Nature* **423**: 177-181.

Sephel, G.C., Buckley, A., and Davidson, J.M. (1987) Developmental initiation of elastin gene expression by human fetal skin fibroblasts. *J Invest Dermatol* **88**: 732-735.

Shannon, O., and Flock, J.I. (2004) Extracellular fibrinogen-binding protein, Efb, from *Staphylococcus aureus* binds to platelets and inhibits platelet aggregation. *Thromb Haemost* **91**: 779-789.

Shannon, O., Uekotter, A., and Flock, J.I. (2005) Extracellular fibrinogen-binding protein, Efb, from *Staphylococcus aureus* as an antiplatelet agent *in vivo*. *Thromb Haemost* **93**: 927-931.

Shannon, O., Uekotter, A., and Flock, J.I. (2006) The neutralizing effects of hyperimmune antibodies against extracellular fibrinogen-binding protein, Efb, from *Staphylococcus aureus*. *Scand J Immunol* **63**: 184-190.

Shapiro, S.D. (1994) Elastolytic metalloproteinases produced by human mononuclear phagocytes. Potential roles in destructive lung disease. *Am J Respir Crit Care Med* **150**: S160-164.

Sharp, K.H., Schneider, S., Cockayne, A., and Paoli, M. (2007) Crystal structure of the heme-IsdC complex, the central conduit of the Isd iron/heme uptake system in *Staphylococcus aureus*. *J Biol Chem*.

Shaw, L., Golonka, E., Potempa, J., and Foster, S.J. (2004) The role and regulation of the extracellular proteases of *Staphylococcus aureus*. *Microbiology* **150**: 217-228.

Shaw, L.N., Golonka, E., Szmyd, G., Foster, S.J., Travis, J., and Potempa, J. (2005) Cytoplasmic control of premature activation of a secreted protease zymogen: deletion

of staphostatin B (SspC) in *Staphylococcus aureus* 8325-4 yields a profound pleiotropic phenotype. *J Bacteriol* **187**: 1751-1762.

Sherertz, R.J., Carruth, W.A., Hampton, A.A., Byron, M.P., and Solomon, D.D. (1993) Efficacy of antibiotic-coated catheters in preventing subcutaneous *Staphylococcus aureus* infection in rabbits. *J Infect Dis* **167**: 98-106.

Siboo, I.R., Chambers, H.F., and Sullam, P.M. (2005) Role of SraP, a Serine-Rich Surface Protein of *Staphylococcus aureus*, in binding to human platelets. *Infect Immun* **73**: 2273-2280.

Sieprawska-Lupa, M., Mydel, P., Krawczyk, K., Wojcik, K., Puklo, M., Lupa, B., Suder, P., Silberring, J., Reed, M., Pohl, J., Shafer, W., McAleese, F., Foster, T., Travis, J., and Potempa, J. (2004) Degradation of human antimicrobial peptide LL-37 by *Staphylococcus aureus*-derived proteinases. *Antimicrob Agents Chemother* **48**: 4673-4679.

Signas, C., Raucci, G., Jonsson, K., Lindgren, P.E., Anantharamaiah, G.M., Hook, M., and Lindberg, M. (1989) Nucleotide sequence of the gene for a fibronectin-binding protein from *Staphylococcus aureus*: use of this peptide sequence in the synthesis of biologically active peptides. *Proc Natl Acad Sci U S A* **86**: 699-703.

Sinha, B., Francois, P.P., Nusse, O., Foti, M., Hartford, O.M., Vaudaux, P., Foster, T.J., Lew, D.P., Herrmann, M., and Krause, K.H. (1999) Fibronectin-binding protein acts as *Staphylococcus aureus* invasin via fibronectin bridging to integrin alpha5beta1. *Cell Microbiol* **1**: 101-117.

Sinha, B., Francois, P., Que, Y.A., Hussain, M., Heilmann, C., Moreillon, P., Lew, D., Krause, K.H., Peters, G., and Herrmann, M. (2000) Heterologously expressed *Staphylococcus aureus* fibronectin-binding proteins are sufficient for invasion of host cells. *Infect Immun* **68**: 6871-6878.

Sjodahl, J. (1977) Repetitive sequences in protein A from *Staphylococcus aureus*. Arrangement of five regions within the protein, four being highly homologous and Fc-binding. *Eur J Biochem* **73**: 343-351.

Skaar, E.P., and Schneewind, O. (2004) Iron-regulated surface determinants (Isd) of *Staphylococcus aureus*: stealing iron from heme. *Microbes Infect* **6**: 390-397.

Snodgrass, J.L., Mohamed, N., Ross, J.M., Sau, S., Lee, C.Y., and Smeltzer, M.S. (1999) Functional analysis of the *Staphylococcus aureus* collagen adhesin B domain. *Infect Immun* **67**: 3952-3959.

Stackebrandt, E., and Teuber, M. (1988) Molecular taxonomy and phylogenetic position of lactic acid bacteria. *Biochimie* **70**: 317-324.

Starcher, B.C., and Galione, M.J. (1976) Purification and comparison of elastins from different animal species. *Anal Biochem* **74**: 441-447.

Stone, P.J., Franzblau, C., and Kagan, H.M. (1982) Proteolysis of insoluble elastin. *Methods Enzymol* **82**: 588-605.

Stone, P.J., Morris, S.M., Martin, B.M., McMahon, M.P., Faris, B., and Franzblau, C. (1988) Repair of protease-damaged elastin in neonatal rat aortic smooth muscle cell cultures. *J Clin Invest* **82**: 1644-1654.

Stranger-Jones, Y.K., Bae, T., and Schneewind, O. (2006) Vaccine assembly from surface proteins of *Staphylococcus aureus*. *Proc Natl Acad Sci U S A* **103**: 16942-16947.

Switalski, L.M., Speziale, P., and Hook, M. (1989) Isolation and characterization of a putative collagen receptor from *Staphylococcus aureus* strain Cowan 1. *J Biol Chem* **264**: 21080-21086.

Switalski, L.M., Patti, J.M., Butcher, W., Gristina, A.G., Speziale, P., and Hook, M. (1993) A collagen receptor on *Staphylococcus aureus* strains isolated from patients with septic arthritis mediates adhesion to cartilage. *Mol Microbiol* **7**: 99-107.

Symersky, J., Patti, J.M., Carson, M., House-Pompeo, K., Teale, M., Moore, D., Jin, L., Schneider, A., DeLucas, L.J., Hook, M., and Narayana, S.V. (1997) Structure of the collagen-binding domain from a *Staphylococcus aureus* adhesin. *Nat Struct Biol* **4**: 833-838.

Takamatsu, D., Bensing, B.A., and Sullam, P.M. (2004) Four proteins encoded in the *gspB-secY2A2* operon of *Streptococcus gordonii* mediate the intracellular glycosylation of the platelet-binding protein GspB. *J Bacteriol* **186**: 7100-7111.

Tamburro, A.M., Guantieri, V., Daga-Gordini, D., and Abatangelo, G. (1977) Conformational transitions of alpha-elastin. *Biochim Biophys Acta* **492**: 370-376.

Taylor, J.M., and Heinrichs, D.E. (2002) Transferrin binding in *Staphylococcus aureus*: involvement of a cell wall-anchored protein. *Mol Microbiol* **43**: 1603-1614.

Thakker, M., Park, J.S., Carey, V., and Lee, J.C. (1998) *Staphylococcus aureus* serotype 5 capsular polysaccharide is antiphagocytic and enhances bacterial virulence in a murine bacteremia model. *Infect Immun* **66**: 5183-5189.

Tipper, D.J., and Strominger, J.L. (1965) Mechanism of action of penicillins: a proposal based on their structural similarity to acyl-D-alanyl-D-alanine. *Proc Natl Acad Sci U S A* **54**: 1133-1141.

Tompkins, D.C., Hatcher, V.B., Patel, D., Orr, G.A., Higgins, L.L., and Lowy, F.D. (1990) A human endothelial cell membrane protein that binds *Staphylococcus aureus in vitro*. *J Clin Invest* **85**: 1248-1254.

Tompkins, D.C., Blackwell, L.J., Hatcher, V.B., Elliott, D.A., O'Hagan-Sotsky, C., and Lowy, F.D. (1992) *Staphylococcus aureus* proteins that bind to human endothelial cells. *Infect Immun* **60**: 965-969.

Ton-That, H., Liu, G., Mazmanian, S.K., Faull, K.F., and Schneewind, O. (1999) Purification and characterization of sortase, the transpeptidase that cleaves surface proteins of *Staphylococcus aureus* at the LPXTG motif. *Proc Natl Acad Sci U S A* **96**: 12424-12429.

Ton-That, H., Mazmanian, S.K., Faull, K.F., and Schneewind, O. (2000) Anchoring of surface proteins to the cell wall of *Staphylococcus aureus*. Sortase catalyzed *in vitro* transpeptidation reaction using LPXTG peptide and NH(2)-Gly(3) substrates. *J Biol Chem* **275**: 9876-9881.

Toonkool, P., Jensen, S.A., Maxwell, A.L., and Weiss, A.S. (2001) Hydrophobic domains of human tropoelastin interact in a context-dependent manner. *J Biol Chem* **276**: 44575-44580.

Torres, V.J., Pishchany, G., Humayun, M., Schneewind, O., and Skaar, E.P. (2006) *Staphylococcus aureus* IsdB is a hemoglobin receptor required for heme iron utilization. *J Bacteriol* **188**: 8421-8429.

Tung, H., Guss, B., Hellman, U., Persson, L., Rubin, K., and Ryden, C. (2000) A bone sialoprotein-binding protein from *Staphylococcus aureus*: a member of the staphylococcal Sdr family. *Biochem J* **345**: 611-619.

Uhlen, M., Guss, B., Nilsson, B., Gatenbeck, S., Philipson, L., and Lindberg, M. (1984) Complete sequence of the staphylococcal gene encoding protein A. A gene evolved through multiple duplications. *J Biol Chem* **259**: 1695-1702.

Uitto, J. (1979) Biochemistry of the elastic fibers in normal connective tissues and its alterations in diseases. *J Invest Dermatol* **72**: 1-10.

Urry, D.W., Luan, C.H., and Peng, S.Q. (1995) Molecular biophysics of elastin structure, function and pathology. *Ciba Found Symp* **192**: 4-30.

van Wamel, W.J., Rooijakkers, S.H., Ruyken, M., van Kessel, K.P., and van Strijp, J.A. (2006) The innate immune modulators staphylococcal complement inhibitor and chemotaxis inhibitory protein of *Staphylococcus aureus* are located on beta-hemolysin-converting bacteriophages. *J Bacteriol* **188**: 1310-1315.

Vandenesch, F., Kornblum, J., and Novick, R.P. (1991) A temporal signal, independent of *agr*, is required for *hla* but not *spa* transcription in *Staphylococcus aureus*. *J Bacteriol* **173**: 6313-6320.

Vann, J.M., and Proctor, R.A. (1988) Cytotoxic effects of ingested *Staphylococcus aureus* on bovine endothelial cells: role of *S. aureus* alpha-hemolysin. *Microb Pathog* **4**: 443-453.

Vaudaux, P., Francois, P., Bisognano, C., Kelley, W.L., Lew, D.P., Schrenzel, J., Proctor, R.A., McNamara, P.J., Peters, G., and Von Eiff, C. (2002) Increased expression of clumping factor and fibronectin-binding proteins by *hemB* mutants of *Staphylococcus aureus* expressing small colony variant phenotypes. *Infect Immun* **70**: 5428-5437.

Veldkamp, K.E., Heezius, H.C., Verhoef, J., van Strijp, J.A., and van Kessel, K.P. (2000) Modulation of neutrophil chemokine receptors by *Staphylococcus aureus* supernate. *Infect Immun* **68**: 5908-5913.

Vermeiren, C.L., Pluym, M., Mack, J., Heinrichs, D.E., and Stillman, M.J. (2006) Characterization of the heme binding properties of *Staphylococcus aureus* IsdA. *Biochemistry* **45**: 12867-12875.

Vernachio, J., Bayer, A.S., Le, T., Chai, Y.L., Prater, B., Schneider, A., Ames, B., Syribeys, P., Robbins, J., and Patti, J.M. (2003) Anti-clumping factor A immunoglobulin reduces the duration of methicillin-resistant *Staphylococcus aureus* bacteremia in an experimental model of infective endocarditis. *Antimicrob Agents Chemother* **47**: 3400-3406.

Vesga, O., Groeschel, M.C., Otten, M.F., Brar, D.W., Vann, J.M., and Proctor, R.A. (1996) *Staphylococcus aureus* small colony variants are induced by the endothelial cell intracellular milieu. *J Infect Dis* **173**: 739-742.

von Eiff, C., Bettin, D., Proctor, R.A., Rolauffs, B., Lindner, N., Winkelmann, W., and Peters, G. (1997a) Recovery of small colony variants of *Staphylococcus aureus* following gentamicin bead placement for osteomyelitis. *Clin Infect Dis* **25**: 1250-1251.

von Eiff, C., Heilmann, C., Proctor, R.A., Woltz, C., Peters, G., and Gotz, F. (1997b) A site-directed *Staphylococcus aureus hemB* mutant is a small-colony variant which persists intracellularly. *J Bacteriol* **179**: 4706-4712.

von Eiff, C., Becker, K., Machka, K., Stammer, H., and Peters, G. (2001a) Nasal carriage as a source of *Staphylococcus aureus* bacteremia. Study Group. *N Engl J Med* **344**: 11-16.

von Eiff, C., Becker, K., Metze, D., Lubritz, G., Hockmann, J., Schwarz, T., and Peters, G. (2001b) Intracellular persistence of *Staphylococcus aureus* small-colony variants within keratinocytes: a cause for antibiotic treatment failure in a patient with darier's disease. *Clin Infect Dis* **32**: 1643-1647.

Vrhovski, B., Jensen, S., and Weiss, A.S. (1997) Coacervation characteristics of recombinant human tropoelastin. *Eur J Biochem* **250**: 92-98.

Vrhovski, B., and Weiss, A.S. (1998) Biochemistry of tropoelastin. *Eur J Biochem* **258**: 1-18.

Wachi, H., Seyama, Y., Yamashita, S., Suganami, H., Uemura, Y., Okamoto, K., Yamada, H., and Tajima, S. (1995) Stimulation of cell proliferation and autoregulation of elastin expression by elastin peptide VPGVG in cultured chick vascular smooth muscle cells. *FEBS Lett* **368**: 215-219.

Wade, D., Palma, M., Lofving-Arvholm, I., Sallberg, M., Silberring, J., and Flock, J.I. (1998) Identification of functional domains in Efb, a fibrinogen-binding protein of *Staphylococcus aureus*. *Biochem Biophys Res Commun* **248**: 690-695.

Walsh, E.J., O'Brien, L.M., Liang, X., Hook, M., and Foster, T.J. (2004) Clumping factor B, a fibrinogen-binding MSCRAMM (microbial surface components recognizing adhesive matrix molecules) adhesin of *Staphylococcus aureus*, also binds to the tail region of type I cytokeratin 10. *J Biol Chem* **279**: 50691-50699.

Wann, E.R., Gurusiddappa, S., and Hook, M. (2000) The fibronectin-binding MSCRAMM FnbpA of *Staphylococcus aureus* is a bifunctional protein that also binds to fibrinogen. *J Biol Chem* **275**: 13863-13871.

Ward, J.B. (1981) Teichoic and teichuronic acids: biosynthesis, assembly, and location. *Microbiol Rev* **45**: 211-243.

Watanabe, S., Ito, T., Takeuchi, F., Endo, M., Okuno, E., and Hiramatsu, K. (2005) Structural comparison of ten serotypes of staphylocoagulases in *Staphylococcus aureus*. *J Bacteriol* **187**: 3698-3707.

Weidenmaier, C., Kokai-Kun, J.F., Kristian, S.A., Chanturiya, T., Kalbacher, H., Gross, M., Nicholson, G., Neumeister, B., Mond, J.J., and Peschel, A. (2004) Role of teichoic acids in *Staphylococcus aureus* nasal colonization, a major risk factor in nosocomial infections. *Nat Med* **10**: 243-245.

Weidenmaier, C., Peschel, A., Xiong, Y.Q., Kristian, S.A., Dietz, K., Yeaman, M.R., and Bayer, A.S. (2005) Lack of wall teichoic acids in *Staphylococcus aureus* leads to reduced interactions with endothelial cells and to attenuated virulence in a rabbit model of endocarditis. *J Infect Dis* **191**: 1771-1777.

Wells, J.M., Wilson, P.W., and Le Page, R.W. (1993) Improved cloning vectors and transformation procedure for *Lactococcus lactis*. *J Appl Bacteriol* **74**: 629-636.

Wendel, D.P., Taylor, D.G., Albertine, K.H., Keating, M.T., and Li, D.Y. (2000) Impaired distal airway development in mice lacking elastin. *Am J Respir Cell Mol Biol* **23**: 320-326.

Werb, Z., Banda, M.J., McKerrow, J.H., and Sandhaus, R.A. (1982) Elastases and elastin degradation. *J Invest Dermatol* **79**: 154s-159s.

Wertheim, H.F., Vos, M.C., Ott, A., van Belkum, A., Voss, A., Kluytmans, J.A., van Keulen, P.H., Vandenbroucke-Grauls, C.M., Meester, M.H., and Verbrugh, H.A. (2004) Risk and outcome of nosocomial *Staphylococcus aureus* bacteraemia in nasal carriers versus non-carriers. *Lancet* **364**: 703-705.

Wladyka, B., Puzia, K., and Dubin, A. (2005) Efficient co-expression of a recombinant staphopain A and its inhibitor staphostatin A in *Escherichia coli*. *Biochem J* **385**: 181-187.

Wolz, C., McDevitt, D., Foster, T.J., and Cheung, A.L. (1996) Influence of *agr* on fibrinogen binding in *Staphylococcus aureus* Newman. *Infect Immun* **64**: 3142-3147.

Wu, W.J., Vrhovski, B., and Weiss, A.S. (1999) Glycosaminoglycans mediate the coacervation of human tropoelastin through dominant charge interactions involving lysine side chains. *J Biol Chem* **274**: 21719-21724.

Xie, C., Alcaide, P., Geisbrecht, B.V., Schneider, D., Herrmann, M., Preissner, K.T., Luscinskas, F.W., and Chavakis, T. (2006) Suppression of experimental autoimmune encephalomyelitis by extracellular adherence protein of *Staphylococcus aureus*. *J Exp Med* **203**: 985-994.

Xu, Y., Rivas, J.M., Brown, E.L., Liang, X., and Hook, M. (2004) Virulence potential of the staphylococcal adhesin CNA in experimental arthritis is determined by its affinity for collagen. *J Infect Dis* **189**: 2323-2333.

Yokoyama, K., Zhang, X.P., Medved, L., and Takada, Y. (1999) Specific binding of integrin alpha v beta 3 to the fibrinogen gamma and alpha E chain C-terminal domains. *Biochemistry* **38**: 5872-5877.

Zhang, L., Jacobsson, K., Vasi, J., Lindberg, M., and Frykberg, L. (1998) A second IgG-binding protein in *Staphylococcus aureus*. *Microbiology* **144**: 985-991.

Zhang, L., Jacobsson, K., Strom, K., Lindberg, M., and Frykberg, L. (1999) *Staphylococcus aureus* expresses a cell surface protein that binds both IgG and beta2-glycoprotein I. *Microbiology* **145**: 177-183.

Zhang, L., Rosander, A., Jacobsson, K., Lindberg, M., and Frykberg, L. (2000) Expression of staphylococcal protein Sbi is induced by human IgG. *FEMS Immunol Med Microbiol* **28**: 211-218.

Zhou, H., Xiong, Z.Y., Li, H.P., Zheng, Y.L., and Jiang, Y.Q. (2006) An immunogenicity study of a newly fusion protein Cna-FnBP vaccinated against *Staphylococcus aureus* infections in a mice model. *Vaccine* **24**: 4830-4837.

Zong, Y., Bice, T.W., Ton-That, H., Schneewind, O., and Narayana, S.V. (2004a) Crystal structures of *Staphylococcus aureus* sortase A and its substrate complex. *J Biol Chem* **279**: 31383-31389.

Zong, Y., Mazmanian, S.K., Schneewind, O., and Narayana, S.V. (2004b) The structure of sortase B, a cysteine transpeptidase that tethers surface protein to the *Staphylococcus aureus* cell wall. *Structure* **12**: 105-112.